รายงานวิจัยฉบับสมบูรณ์

Amino acid-containing copolymers for coating on magnetic nanoparticles: From fundamental knowledge to medical applications

พอลิเมอร์ร่วมที่มีอะมิโนแอซิดในโครงสร้างเพื่อเคลือบอนุภาคนาโนแม่เหล็ก: จากความรู้พื้นฐานสู่การประยุกต์ใช้ทางการแพทย์

โดย รองศาสตราจารย์ ดร. เมธา รัตนากรพิทักษ์ และคณะ

พฤษภาคม 2562

สัญญาเลขที่ RSA5980002

รายงานวิจัยฉบับสมบูรณ์

พอลิเมอร์ร่วมที่มีอะมิโนแอซิดในโครงสร้างเพื่อเคลือบอนุภาคนาโนแม่เหล็ก: จากความรู้พื้นฐานสู่การประยุกต์ใช้ทางการแพทย์

คณะผู้วิจัย	สังกัด
1. รองศาสตราจารย์ ดร.เมธา รัตนากรพิทักษ์	มหาวิทยาลัยนเรศวร
2. ศาสตราจารย์ ดร.ธีรยุทธ วิไลวัลย์	จุฬาลงกรณ์มหาวิทยาลัย
3. ผู้ช่วยศาสตราจารย์ ดร.อุทัย วิชัย	มหาวิทยาลัยนเรศวร
4. ผู้ช่วยศาสตราจารย์ ดร.บุญจิรา รัตนากรพิทักษ์	มหาวิทยาลัยนเรศวร
5. ผู้ช่วยศาสตราจารย์ ดร.มลิวรรณ นาคขุนทด	มหาวิทยาลัยนเรศวร
6. นางสาวสุดารัตน์ ขัดสาย	มหาวิทยาลัยนเรศวร
7. นางสาวนันทิยา ดีบุบผา	มหาวิทยาลัยนเรศวร
8. นางสาวสุจิตรา แป้นแก้ว	มหาวิทยาลัยนเรศวร
9. นางสาวยิ่งรัก พรายอินทร์	มหาวิทยาลัยนเรศวร
10. นายบัณฑิต ทองอ่อน	มหาวิทยาลัยนเรศวร
11. นางสาวศิรประภา มีรอด	มหาวิทยาลัยนเรศวร

สนับสนุนโดยสำนักงานกองทุนสนับสนุนการวิจัย

(ความเห็นในรายงานนี้เป็นของผู้วิจัย สกว. ไม่จำเป็นต้องเห็นด้วยเสมอไป)

กิตติกรรมประกาศ

งานวิจัยนี้ได้รับการสนับสนุนทุนวิจัยจากสำนักงานกองทุนสนับสนุนงานวิจัย (สกว.) ร่วมกับมหาวิทยาลัยนเรศวร ประจำปี 2559-2562 สัญญาเลขที่ RSA5980002 ข้าพเจ้าขอขอบคุณนักวิจัยร่วมทุกท่านที่มีส่วนร่วมในการวิเคราะห์และวิจารณ์ผลการทดลอง ได้แก่ ศาสตราจารย์ ดร.ธีรยุทธ วิไลวัลย์ จากภาควิชาเคมี คณะวิทยาศาสตร์ จุฬาลงกรณ์มหาวิทยาลัย ผู้ช่วยศาสตราจารย์ ดร.อุทัย วิชัย และ ผู้ช่วยศาสตราจารย์ ดร.บุญจิรา รัตนากรพิทักษ์ จากภาควิชาเคมี คณะวิทยาศาสตร์ มหาวิทยาลัยนเรศวร ผู้ช่วยศาสตราจารย์ ดร.มลิวรรณ นาคขุนทด จากภาควิชาชีววิทยา คณะวิทยาศาสตร์ มหาวิทยาลัยนเรศวร Prof.Dr.Véronique Montembault, Dr.Sagrario Pascua และ Prof.Dr.Laurent Fontaine จาก Université du Maine ประเทศฝรั่งเศส และขอขอบคุณนิสิตปริญญาโทและปริญญาเอกทุกท่านที่มีส่วนสำคัญในการทำงานวิจัยนี้ ได้แก่ นางสาวนันทิยา ดีบุบผา นางสาวสุดารัตน์ ขัดสาย นางสาวสุจิตรา แป้นแก้ว นางสาวยิ่งรัก พรายอินทร์ นายบัณฑิต ทองอ่อน และ นางสาวศิรประภา มีรอด ที่มีส่วนร่วมในผลงานวิจัยนี้ สุดท้ายนี้ข้าพเจ้าขอขอบคุณทุนการศึกษานิสิตปริญญาโทและปริญญาเอก ได้แก่ ทุนจากโครงการปริญญาเอกกาญจนาภิเษก (คปก.) และทุนเรียนดีวิทยาศาสตร์แห่งประเทศไทย จากโครงการพัฒนากำลังคนด้านวิทยาศาสตร์ (SAST)

Abstract (บทคัดย่อ)

Project Code : RSA5980002

Project Title : Amino acid-containing copolymers for coating on magnetic nanoparticles: From fundamental knowledge to medical applications

ชื่อโครงการ : พอลิเมอร์ร่วมที่มีอะมิโนแอซิดในโครงสร้างเพื่อเคลือบอนุภาคนาโนแม่เหล็ก: จากความรู้พื้นฐานสู่การประยุกต์ใช้ทางการแพทย์

ชื่อนักวิจัย : รองศาสตราจารย์ ดร.เมธา รัตนากรพิทักษ์

ภาควิชาเคมี คณะวิทยาศาสตร์ มหาวิทยาลัยนเรศวร

E-mail Address : methar@nu.ac.th

ระยะเวลาโครงการ : มิถุนายน 2559- มีนาคม 2562

Abstract

This work focuses on the surface modification of magnetite nanoparticle (MNP) with amino acid-containing polymers and/or stimuli-responsive polymers and their applications. These novel polymers containing amino acid-derived polymers and/or stimuli-responsive polymers can provide a viable route to the production of tailored materials with unique intelligent properties for various bio-medical applications, such as drug controlled release and biocompatible materials. The functional polymers were synthesized *via* various methods, e.g. reversible addition–fragmentation chain transfer (RAFT) polymerization and conventional radical polymerization and then coated on MNP surface. Three different types of amino acid-derive monomers are of interest in this work; 1) azlactone monomer (Chapter II), 2) thiolactone monomer (Chapter III) and 3) N-acryloyl glycine (NAG) monomer (Chapter IV). These monomers contain polymerizable groups (acryloyl groups) and reactive functional groups (heterocyclic or carboxylate groups) for further coupling with other biomolecules. In addition to the amino acid-derived polymers, the polymers may contain other stimuli-responsive polymers, such as thermo-responsive poly(N-isopropylacrylamide) (PNIPAAm) (Chapter V) and pH-responsive poly(acrylic acid) (PAA)(Chapter VI). Therefore, it is expected that the knowledge obtained from this work will be useful for further development in advanced applications in nanoscience and nanotechnology.

Keyword: magnetite, nanoparticle, functional polymer, amino acid, controlled release

บทคัดย่อ

งานวิจัยนี้ศึกษาการดัดแปรพื้นผิวอนุภาคนาโนแมกนีไทท์ (MNP) ด้วยพอลิเมอร์ที่มีส่วนประกอบเป็นกรดอะมิโนและ/หรือพอลิเมอร์ที่มีสมบัติการตอบสนองต่อสิ่งกระตุ้นภายนอกและการประยุกต์ใช้งาน โดยพอลิเมอร์เหล่านี้จะสามารถใช้ในการออกแบบการสังเคราะห์เป็นพอลิเมอร์ร่วม (copolymer) ได้หลายหลายแนวทางและทำให้ได้สมบัติพอลิเมอร์ที่มีความหลากหลายและจำเพาะเจาะจงสำหรับการประยุกต์ใช้ทางการแพทย์ได้ เช่น การควบคุมการปลดปล่อยยาหรือสารชีวโมเลกุล การใช้เป็นวัสดุชีวภาพ เป็นต้น การสังเคราะห์ฟังก์ชันนอลพอลิเมอร์ในงานวิจัยนี้มีหลายแนวทาง ได้แก่ การใช้ปฏิกิริยาพอลิเมอไรเซชันแบบรีเวอสซิเบิลแอดดิชันแฟรกเมนเตชันเชนทรานสเฟอร์ (RAFT) และปฏิกิริยาพอลิเมอไรเซชันแบบอนุมูลอิสระดั้งเดิม เป็นต้น ตัวอย่างโมโนเมอร์ที่ใช้ในงานวิจัยนี้ ได้แก่ 1) แอซแลคโตนโมโนเมอร์ (รายละเอียดในบทที่ 2), 2) ไธโอแลคโตนโมโนเมอร์ (รายละเอียดในบทที่ 3), 3) เอ็นอะคริโลอิลไกลซีนโมโนเมอร์ (รายละเอียดในบทที่ 4) โดยโมโนเมอร์เหล่านี้ได้มีการออกแบบเพื่อให้มีหมู่ที่สามารถเกิดปฏิกิริยาพอลิเมอไรเซชันได้ (หมู่อะคริโลอิล) และมีหมู่ที่ว่องไวต่อการเกิดปฏิกิริยากับสารชีวโมเลกุลเพื่อเกิดพันธะโควาเลนต์ได้ (หมู่เฮทเทอโรไซคลิกหรือหมู่คาร์บอกซิเลท) นอกจากนี้ ในงานวิจัยยังศึกษาการเคลือบอนุภาคนาโนแมกนีไทท์ด้วยพอลิเมอร์ที่มีสมบัติการตอบสนองต่อสิ่งกระตุ้นภายนอก เช่น พอลิเอ็นไอโซโพรพิลอะคริลาไมด์ (PNIPAAm) ซึ่งเป็นพอลิเมอร์ที่ตอบสนองต่อการเปลี่ยนแปลงอุณหภูมิ (รายละเอียดในบทที่ 5) และ พอลิอะคริลิกแอซิด (PAA) ซึ่งเป็นพอลิเมอร์ที่ตอบสนองต่อการเปลี่ยนสภาวะกรดเบส (รายละเอียดในบทที่ 6) ดังนั้น ความรู้ที่ได้รับจากงานวิจัยนี้คาดว่าจะเป็นประโยชน์ในการศึกษาและการพัฒนาการดัดแปรพื้นผิวอนุภาคนาโนแมกนีไทท์เพื่อการประยุกต์ใช้งานขั้นสูงทางด้านนาโนวิทยาศาสตร์และนาโนเทคโนโลยีต่อไป

คำสำคัญ : แมกนีไทท์, อนุภาคนาโน, พอลิเมอร์ที่มีฟังก์ชัน, กรดอะมิโน, การควบคุมการปลดปล่อย

หน้าสรุปโครงการ (Executive Summary)

ทุนพัฒนานักวิจัย ประจำปี 2559-2562

รหัสโครงการ RSA5980002

---

1. ชื่อโครงการ

พอลิเมอร์ร่วมที่มีอะมิโนแอซิดในโครงสร้างเพื่อเคลือบอนุภาคนาโนแม่เหล็ก: จากความรู้พื้นฐานสู่การประยุกต์ใช้ทางการแพทย์

Amino acid-containing copolymers for coating on magnetic nanoparticles: From fundamental knowledge to medical applications

2. ชื่อหัวหน้าโครงการ หน่วยงานที่สังกัด ที่อยู่ หมายเลขโทรศัพท์ โทรสาร และ e-mail

ผู้หัวหน้าโครงการ นายเมธา รัตนากรพิทักษ์ Mr. Metha Rutnakornpituk

หน่วยงานที่สังกัด ภาควิชาเคมี คณะวิทยาศาสตร์ มหาวิทยาลัยนเรศวร อ.เมือง จ. พิษณุโลก

โทรศัพท์ 055-963464 โทรสาร 055-963401

e-mail: methar@nu.ac.th โทรศัพท์มือถือ 086-589-3736

3. Research filed : Synthesis of copolymer and surface modification of nanoparticle

Keywords : magnetite, nanoparticle, functional polymer, amino acid, controlled release

4. Budget 1,500,000 baht

5. Duration 3 years

6. Research problem and its significance

Magnetite nanoparticle (MNP) has markedly been of scientific and technological interest in the present day because of its magnetically guidable and nanoscale-related properties. The potential applications of MNP include magnetic resonance imaging (MRI) enhancement, drug delivery, magnetic separation and diagnosis of biological molecules such as DNA and antibodies. It is usually stabilized either by charge repulsion of electrical surface or steric repulsion of long-chain polymeric surfactants grafted on surfaces to prevent particle aggregation, resulting in the loss of nano-scale related properties. Many previous works focused on coating the particles with polymers

using various approaches, such as physical adsorption of polymers on its surfaces, emulsion polymerization in the presence of MNP and the so-called “grafting to” and “grafting from” strategies. In addition, coating the particles with polymers also improves particle dispersibility in the media and biocompatibility, which are minimum requirements for uses in biomedical applications. Furthermore, the polymers on MNP surface also provide a platform for incorporation of various biological functional molecules.

In this research, surface modification of MNP with many functional polymers, including amino acid-containing polymers, pH-responsive polymers and thermo-responsive polymers and its applications were focused. Amino acid-derived monomers have been intensively studied during the last decade because they may create new non biological macromolecules with biomimetic structures and properties. Importantly, amino acid-derived monomers as well as their corresponding polymer structures are increasingly available for designing the additional functional groups. The copolymers containing amino acid-based polymers and/or stimuli-responsive polymers can provide a viable route to the production of tailored materials with unique intelligent properties for various biological and medicinal applications, such as controlled release and biocompatible materials.

In this work, the functional copolymers were synthesized *via* various methods, e.g. reversible addition–fragmentation chain transfer (RAFT) polymerization and conventional radical polymerization and then coated on MNP surface. Three different types of amino acid-derive monomers are of interest in this work; 1) azlactone monomer (Chapter 1), 2) thiolactone monomer (Chapter 2) and 3) N-acryloyl glycine (NAG) monomer (Chapter 3). These monomers contain polymerizable groups (acryloyl groups) and reactive functional groups (heterocyclic or carboxylate groups) for further coupling with other biomolecules. In addition to the amino acid-derived polymers, the polymer may contain other stimuli-responsive polymers, such as thermo-responsive poly(N-isopropylacrylamide) (PNIPAAm) (Chapter 4) and pH-responsive poly(acrylic acid) (PAA)(Chapter 5).

7. Research Objectives

1. To design and synthesize the functional polymers containing amino acid-derived monomers and/or stimuli-responsive polymers to coat on MNP surface

2. To use the MNP coated with functional polymers in biomedical applications, such as to immobilize and to control the release of entrapped entities on the particle surface

8. Research methodology and brief results

The experimental section in this project was divided into 3 steps:

1) Synthesis of MNP and surface functionalization with functional groups,

2) Synthesis of functional polymers on MNP surface and

3) Applications of polymer-coated MNP

Step 1: Synthesis of MNP and surface functionalization with functional groups

MNP was synthesized *via* the co-precipitation of Fe^{2+} and Fe^{3+} salts in an aqueous basic solution. Surface functionalization of bare MNP with functional groups such as amino groups and acrylamide groups was performed to get the MNP surface ready for “grafting from” or “grafting to” polymerizations.

Step 2 and 3: Synthesis of functional polymers on MNP surface and their applications

The details of the surface functionalization of MNP with functional polymers and their applications are following;

Recyclable magnetic nanocluster crosslinked with poly(ethylene oxide)-block-poly(2-vinyl-4,4-dimethylazlactone) copolymer for adsorption with antibody (details in Chapter II)

Surface modification of MNP with poly(ethylene oxide)-*block*-poly(2-vinyl-4,4-dimethylazlactone) (PEO-*b*-PVDM) diblock copolymers and its application as recyclable magnetic nano-support for adsorption with antibody were studied. PEO-*b*-PVDM copolymers were first synthesized *via* a RAFT polymerization using PEO chain-transfer agent as a macromolecular chain transfer agent to mediate the RAFT polymerization of VDM. They were then grafted on amino-functionalized MNP by coupling with some azlactone rings of the PVDM block to form magnetic

nanoclusters with tunable cluster size. The nanocluster size could be tuned by adjusting the chain length of the PVDM block. The nanoclusters were successfully used as efficient and recyclable nano-supports for adsorption with anti-rabbit IgG antibody. They retained higher than 95% adsorption of the antibody during eight adsorption-separation-desorption cycles, indicating the potential feasibility in using this novel hybrid nanocluster as recyclable support in cell separation applications.

Effect of alkyl chain lengths on the assemblies of magnetic nanoparticles coated with multi-functional thiolactone-containing copolymer (details in Chapter III)

Synthesis of MNP coated with poly(N,N-diethylaminoethyl methacrylate)-*b*-poly(N-isopropyl acrylamide-*st*-thiolactone acrylamide) (PDEAEMA-*b*-P(NIPAAm-*st*-TlaAm) copolymer and its use in controlled drug release and bio-conjugation were studied. TlaAm units in the copolymer were ring-opened with various alkyl amines to form thiol groups (-SH), followed by thiol-ene coupling reactions with acrylamide-coated MNP and then quaternized to obtain cationic copolymer-MNP assemblies (the size < 200 nm/cluster). The use of alkyl amines having various chain lengths (e.g. 1-propylamine, 1-octylamine or 1-dodecylamine) in the nucleophilic ring-opening reactions of the thiolactone rings affected their magnetic separation ability, water dispersibility and release rate of doxorubicin model drug. In all cases, when increasing the temperature, they showed a thermo-responsive behavior as indicated by the decrease in hydrodynamic size and the accelerated drug release rate. These copolymer-MNP assemblies could be used as a novel platform with thermal-triggering controlled drug release and capability for adsorption with any negatively charged biomolecules.

Multi-responsive poly(N-acryloyl glycine)-based nanocomposite and its drug release characteristics (details in Chapter IV)

pH- and thermo-responsive nanocomposite composing of poly(*N*-acryloyl glycine) (PNAG) matrix and MNP was synthesized and then used for drug controlled release application. The effects of crosslinkers, e.g. ethylenediamine and *tris*(2-aminoethyl)amine, and their concentrations (1 and 10 mol%) on the size, magnetic separation ability and water dispersibility of the nanocomposite

were investigated. The nanocomposite crosslinked with *tris*(2-aminoethyl)amine (size ranging between 50 and 150 nm in diameter) can be rapidly separated by a magnet while maintaining its good dispersibility in water. It can respond to the pH and temperature change as indicated by the changes in its zeta potential and hydrodynamic size. From the in vitro release study, theophylline as a model drug was rapidly released when the pH changed from neutral to acidic/basic conditions or when increasing the temperature from 10 °C to 37 °C. This novel nanocomposite showed a potential application as a magnetically guidable vehicle for drug controlled release with pH- and thermo-triggered mechanism.

Controlled magnetite nanoclustering in the presence of glycidyl-functionalized thermo-responsive poly(*N-isopropylacrylamide*) *(details in Chapter V)*

Glycidyl-functionalized poly(*N*-isopropylacrylamide) (PNIPAAm), synthesized *via* RAFT polymerization, was used for controlling degree of nanoclustering of MNP. The polymer was grafted onto MNP *via* the ring-opening reaction between glycidyl groups at the PNIPAAm chain terminal and amino groups on the MNP surface to obtain thermo-responsive MNP nanocluster. Hydrodynamic size (D_h) and colloidal stability of the nanocluster, corresponding to the degree of nanoclustering reaction, can be regulated either by adjusting the ratio of MNP to the polymer in the reaction or by introducing glycidyl groups to the polymers. The size of the nanocluster ranged between 20 and 150 nm in diameter with about 10-120 particles/cluster. Thermogravimetric analysis (TGA) and vibrating sample magnetometry (VSM) were used to confirm the presence of the polymer in the nanocluster. A study showing indomethacin controlled release of these MNP nanoclusters was also performed. This stable nanocluster with magnetically guidable properties might be potentially used for entrapment of other bio-entities or therapeutic drugs with temperature-responsive properties for controlled release applications.

Reusable magnetic nanocluster coated with poly(acrylic acid) and its adsorption with antibody and antigen (details in Chapter VI)

Synthesis of negatively charged magnetite nanocluster grafted with poly(acrylic acid) (PAA) and its application as reusable nano-supports for adsorption with antibody and antigen were presented herein. It was facilely prepared *via* a free radical polymerization of PAA in the presence of functionalized MNP to obtain highly negative charged nanocluster with high magnetic

responsiveness, good dispersibility and stability in water. According to transmission electron microscopy, size of the nanocluster ranged between 200 and 500 nm without large aggregation visually observed in water. Hydrodynamic size of the nanocluster consistently increased as increasing pH of the dispersion, indicating its pH-responsive properties due to the repulsion of anionic carboxylate groups in the structure. This nanocluster was successfully used as an efficient and reusable support for adsorption with anti-horseradish peroxidase antibody. It preserved higher than 97% adsorption ability of the antibody after eight reusing cycles, signifying the potential of this novel nanocluster as a reusable support in magnetic separation applications of other bioentities.

9. Conclusions

This works focused on the synthesis and design of amino acid-containing polymers and/or stimuli-responsive polymer, their coating on MNP surface and their medical-related applications. The functional polymers grafted on MNP surface were synthesized through either “grafting to” or “grafting from” strategies using various polymerization mechanisms, such as RAFT polymerization (Chapter II, III and V) and conventional radical polymerization (Chapter IV and VI). The novelty of this project came from the synthesis of new types of (co)polymers grafted on MNP surface, such as (co)polymers between azlactone-containing polymer and PEO (Chapter II), thiolactone-containing polymer and PNIPAAm (Chapter III) and PNIPAAm containing glycidyl units (Chapter V). In addition, the polymer structure on MNP surface was also designed such that it can readily react and crosslink with the functional groups on MNP surface in a controllable fashion. Effect of the change in solution temperature and/or pH on the entrapment and loading efficiencies and also on releasing profiles of the entrapped entities were studied (Chapter III, IV, V and VI). It was found that releasing rate of entrapped entities in the functional polymeric shell of MNP can be tuned when temperature or pH of its environment change. There are five international publications from this work. The authors hope that the results from this work can be extended and used for advanced science and technology.

LIST OF CONTENTS

Chapter I

Introduction

Research problem and its significance

Magnetite nanoparticle (MNP) has markedly been of scientific and technological interest in the present day because of its magnetically guidable and nanoscale-related properties. The potential applications of MNP include magnetic resonance imaging (MRI) enhancement, drug delivery, magnetic separation and diagnosis of biological molecules such as DNA and antibodies. It is usually stabilized either by charge repulsion of electrical surface or steric repulsion of long-chain polymeric surfactants grafted on surfaces to prevent particle aggregation, resulting in the loss of nano-scale related properties. Many previous works focused on coating the particles with polymers using various approaches, such as physical adsorption of polymers on its surfaces, emulsion polymerization in the presence of MNP and the so-called "grafting to" and "grafting from" strategies. In addition, coating the particles with polymers also improves particle dispersibility in the media and biocompatibility, which are minimum requirements for uses in biomedical applications. Furthermore, the polymers on MNP surface also provide a platform for incorporation of various biological functional molecules.

In this research, surface modification of MNP with many functional polymers, including amino acid-containing polymers, pH-responsive polymers and thermo-responsive polymers and its applications have been focused. Amino acid-derived monomers have been intensively studied during the last decade because they may create new non-biological macromolecules with biomimetic structures and properties. Importantly, amino acid-derived monomers as well as their corresponding polymer structures are increasingly available for designing the additional functional groups. The copolymers containing amino acid-based polymers and/or stimuli-responsive polymers can provide a viable route to the production of tailored materials with unique intelligent properties for various biological and medicinal applications, such as controlled release and biocompatible materials.

In this work, the functional polymers were synthesized *via* various methods, e.g. reversible addition–fragmentation chain transfer (RAFT) polymerization and conventional radical polymerization and then coated on MNP surface. Three different types of amino acid-derive monomers were of interest in this work; 1) azlactone monomer (Chapter 1), 2)

thiolactone monomer (Chapter 2) and 3) N-acryloyl glycine (NAG) monomer (Chapter 3). These monomers contain polymerizable groups (acryloyl groups) and reactive functional groups (heterocyclic or carboxylate groups) for further coupling with other biomolecules. In addition to the amino acid-derived polymers, the polymers may contain other stimuli-responsive polymers, such as thermo-responsive poly(N-isopropylacrylamide) (PNIPAAm) (Chapter 4) and pH-responsive poly(acrylic acid) (PAA)(Chapter 5).

Research objectives

1. To design and synthesize the functional polymers containing amino acid-derived monomers and/or stimuli-responsive polymers to coat on MNP surface

2. To use the MNP coated with functional polymers in biomedical applications, such as to immobilize and to control the release of entrapped entities on the particle surface

Therefore, the content of this report comprises 5 chapters as following,

Chapter II: Recyclable magnetic nanocluster crosslinked with poly(ethylene oxide)-*block*-poly(2-vinyl-4,4-dimethylazlactone) copolymer for adsorption with antibody

Chapter III: Effect of alkyl chain lengths on the assemblies of magnetic nanoparticles coated with multi-functional thiolactone-containing copolymer

Chapter IV: Multi-responsive poly(*N*-acryloyl glycine)-based nanocomposite and its drug release characteristics

Chapter V: Controlled magnetite nanoclustering in the presence of glycidyl-functionalized thermo-responsive poly*(*N-isopropylacrylamide*)*

Chapter VI: Reusable magnetic nanocluster coated with poly(acrylic acid) and its adsorption with antibody and antigen

Chapter II

Recyclable magnetic nanocluster crosslinked with poly(ethylene oxide)-*block*-poly(2-vinyl-4,4-dimethylazlactone) copolymer for adsorption with antibody

Abstract

Surface modification of magnetic nanoparticle (MNP) with poly(ethylene oxide)-*block*-poly(2-vinyl-4,4-dimethylazlactone) (PEO-*b*-PVDM) diblock copolymers and its application as recyclable magnetic nano-support for adsorption with antibody were reported herein. PEO-*b*-PVDM copolymers were first synthesized *via* a reversible addition-fragmentation chain-transfer (RAFT) polymerization using poly(ethylene oxide) chain-transfer agent as a macromolecular chain transfer agent to mediate the RAFT polymerization of VDM. They were then grafted on amino-functionalized MNP by coupling with some azlactone rings of the PVDM block to form magnetic nanoclusters with tunable cluster size. The nanocluster size could be tuned by adjusting the chain length of the PVDM block. The nanoclusters were successfully used as efficient and recyclable nano-supports for adsorption with anti-rabbit IgG antibody. They retained higher than 95% adsorption of the antibody during eight adsorption-separation-desorption cycles, indicating the potential feasibility in using this novel hybrid nanocluster as recyclable support in cell separation applications.

Keywords: magnetite; nanocluster; azlactone; RAFT; antibody; adsorption

1. Introduction

Magnetic nanoparticles (MNPs) have potential applications in a wide range of biomedical areas, such as hyperthermia treatment of tumor [1], contrast enhancement agents in magnetic resonance imaging (MRI) [2], immunoassay magnetic marker [3], site-specific drug delivery system [4] and magnetic separation [5]. However, there are limitations in applying external magnetic field to MNPs in biomedical uses because unmodified MNPs are not stable in physiological fluids, leading to their aggregation in aqueous dispersion due to attractive forces, e.g. dipole-dipole interaction and magnetic force [6]. Therefore, surface modification of MNPs is a crucial requirement to use these particles as biomedical materials. One of the most common useful methods for surface modification is grafting polymers onto the particle surface, not only to protect the particle against aggregation, but also to provide a platform for further surface functionalization.

In general, there are two approaches for attachment of polymers to particle surface, including the so-called "grafting-from" and "grafting-onto" strategies [7-10]. The "grafting-from" strategy involves the growth of polymer from particle surface [7, 8], while in the "grafting-onto" strategy, a pre-synthesized polymer is first prepared in solution and then grafted onto particle surface [9, 10]. The combination of these two strategies with controlled radical polymerization (CRP) techniques, such as atom transfer radical polymerization (ATRP) and reversible addition-fragmentation chain transfer (RAFT) polymerization, has been widely used to prepare well-defined polymers coated onto MNP surface [11-14]. RAFT polymerization is one of several types of CRP techniques that produce polymers with controllable molecular weights and narrow polydispersity indices (PDIs). Moreover, RAFT polymerization is applicable to a wide range of vinyl monomers without using metal catalysts. It can also be performed under mild condition reactions in various reaction systems, including aqueous solution, organic solvents, suspensions, emulsions and ionic liquids [15-23].

Another limitation of applications of MNPs in biomedical applications is the low magnetic sensitivity of single nanoparticles, resulting in difficulties concerning their targeted delivery of MNPs by using a permanent magnetic field. The particle size should be sufficiently large in order to yield high magnetization. However, the particles are unstable when their size is too large due to attractive forced among the particles, leading to macroscopic aggregation and thus loss in nano-scale related properties. Controllable formation of nanoclustering is another potential approach to enhance magnetic sensitivity of

MNPs. High saturation magnetization of these magnetic nanoclusters is essential to efficiently separate them from dispersions or localize them to a target-organ.

In the present day, many works have reported the use of MNPs for separation of bio-entities such as DNA, RNA and proteins [24, 25, 5]. In addition, the potential of specific antibody-conjugated MNP for cell separation [26] and magnetic marker [3] was extensively studied. For example, Puertas et al. [27] have recently reported the synthesis of carboxylated MNP for ionic adsorption with antibodies through their richest positive charged regions. The adsorption of antibodies was applicable at the pH lower than its isoelectric point and the antibodies could be easily eluted by increasing the ionic strength and/or changing the net charge of the antibodies by changing the solution pH. Moreover, Xu et al. [26] have also synthesized antibody-conjugated MNPs for use as a platform to separate circulating tumor cells (CTCs) from fresh whole blood. MNPs having reactive carboxyl groups were conjugated with antibody against human epithelial growth factor receptor 2 (anti-HER2) through an amidation reaction. The particle was then used to isolate HER2 from human breast cancer cell line SK-BR3. It was found that the capture of the HER2 was obtained only when the MNP was conjugated with the specific antibody.

In this work, we used the "grafting-onto" strategy to modify MNP surface with poly(ethylene oxide)-*block*-poly(2-vinyl-4,4-dimethylazlactone) (PEO-*b*-PVDM) copolymers to form magnetic nanoclusters with tunable cluster size. The copolymers were synthesized *via* RAFT polymerization to produce well-defined diblock structures with controlled PVDM block lengths. PEO allows the particles to well disperse in aqueous medium and some azlactone rings in the PVDM block serve as reactive electrophilic sites for further coupling with amino groups grafted on MNP surface. It was hypothesized that the chain length of the reactive PVDM block should somewhat influence the nanoclustering formation, which essentially affected its magnetic properties and water dispersibility. Degree of nanoclustering and magnetic sensitivity of the MNP clusters were optimized such that water dispersible nanoclusters with high magnetic separation efficiency were obtained. In this study, the efficiency of the magnetic nanoclusters for separation of anti-rabbit IgG antibody from the dispersion and their recycling ability were also determined (Scheme 1).

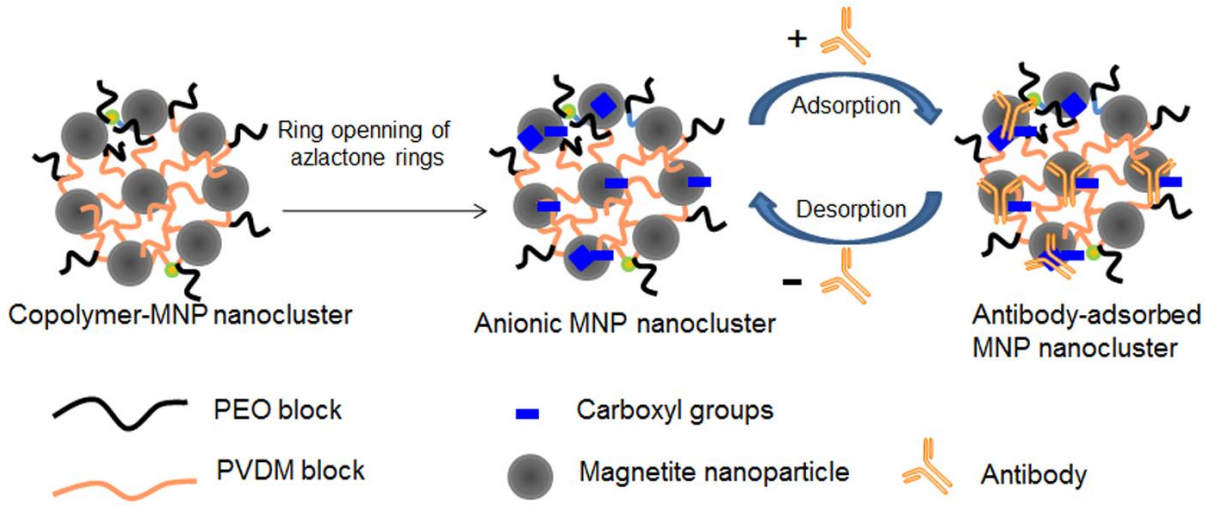

Scheme 1. Schematic illustration of PEO-*b*-PVDM diblock copolymer-MNP nanocluster for antibody adsorption and its recycling

2. Experimental

2.1 Materials

Unless otherwise noted, all reagents were used without further purification: iron (III) acetylacetonate ($Fe(acac)_3$, 99.9%, Acros), benzyl alcohol (98%, Unilab), oleic acid (90%, Fluka), (3-aminopropyl)triethoxysilane (APS, 99%, Sigma-Aldrich), triethylamine (TEA, ≥ 99%, Sigma-Aldrich), 4,4'-azobis(4-cyanovaleric acid) (ACVA, ≥ 98%, Aldrich), anti-rabbit IgG (antibody produced in goat, Sigma-Aldrich), IgG from rabbit serum (Sigma-Aldrich), anti-IgG-HRP (anti-rabbit IgG (whole molecule)-peroxidase (Sigma-Aldrich), 10% BSA diluents (KPL), ABTS® Peroxidase Substrate (KPL), Bradford reagent (Sigma), bovine gamma globulin (BGG, Thermo Scientific) and 2-(*N*-morpholino)ethanesulfonic acid (MES, 99%, Acros). 2-Dodecylsulfanylthiocarbonylsulfanyl-2-methylpropionic acid (DMP) [28], poly(ethylene oxide) chain transfer agent (PEO-CTA) [29] and 2-vinyl-4,4-dimethylazlactone (VDM) [30] were synthesized following the reported procedures. Pure water was obtained from a Millipore Direct Q system. 1,4-Dioxane (99.8%, Sigma-Aldrich), *n*-hexane (95%, Acros), *N*,*N*-dimethylformamide (DMF, 99.8%, Aldrich), toluene (99.8%, Sigma-Aldrich), ethanol (≥ 99.5%, Sigma-Aldrich), and dichloromethane (CH_2Cl_2, ≥ 99.5 %, Sigma-Aldrich) were used as received.

2.2 Characterization

Fourier transform infrared (FTIR) spectroscopy was performed on a Perkin-Elmer Model 1600 Series FTIR Spectrophotometer. The solid samples were mixed with KBr to form pellets. Nuclear magnetic resonance (NMR) spectra were performed on a 400 MHz Bruker NMR spectrometer for ^{1}H NMR (400 MHz). Chemical shifts are reported in ppm relative to deuterated solvent resonances. Molar masses and molar mass distributions were determined *via* size exclusion chromatography (SEC) operating at 35^{o}C on a system equipped with a Spectra System AS1000 autosampler with a guard column (Polymer Laboratories, PL gel 5 µm guard, 50 × 7.5 mm) followed by two columns (Polymer Laboratories, two PL gel 5 µm Mixed–D columns, 2 × 300 × 7.5 mm) and a refractive index detector (SpectraSystem RI-150). Polystyrene standards (580-483 × 10^{3} g.mol^{-1}) were used to calibrate the SEC. Transmission electron microscopy (TEM) was performed on a Philips Tecnai 12 operated at 120 kV equipped with a Gatan model 782 CCD camera. Thermogravimetric analysis (TGA) was performed on SDTA 851 Mettler-Toledo at the temperature ranging between 25 and 600^{o}C at a heating rate of 20^{o}C/min under oxygen atmosphere. Vibrating sample magnetometer (VSM) measurements were performed at room temperature using a Standard 7403 Series, Lakeshore vibrating sample magnetometer. Hydrodynamic diameter (D_h) and zeta potential of the particles were measured *via* a photo correlation spectroscopy (PCS) using NanoZS4700 nanoseries Malvern instrument. The sample dispersions were sonicated for 30 min before the measurements at 25^{o}C without filtration. The ability of antibody adsorption to MNP was investigated with an ultraviolet-visible (UV-vis) spectrophotometer on Perkin Elmer model Lamda 20 at λ = 595 nm.

2.3 Synthesis and properties of copolymers-MNP nanoclusters

2.3.1 Synthesis of PEO-*b*-PVDM diblock copolymers by RAFT polymerization (Scheme 2)

An example of the synthesis of PEO-*b*-PVDM block copolymer using a molar ratio of $[VDM]_0$:$[PEO\text{-}CTA]_0$:$[ACVA]_0$ equal to 100:1:0.2 molar ratio is herein explained. VDM (0.74 g, 5.34 x 10^{-3} mol), PEO-CTA (0.126 g, 5.34 x 10^{-5} mol), ACVA (3 mg, 1.07 x 10^{-5} mol), 1,4-dioxane (3.0 mL) and DMF (0.2 mL) used as an internal reference were added to a Schlenk tube equipped with a stir bar. The mixture was deoxygenated by bubbling argon for 30 min. The solution was then immersed in an oil bath thermostated at 70^{o}C for 4 h to allow

the polymerization to occur. Conversion of VDM was determined to be 41% by ^{1}H NMR spectroscopy by comparing the integration area value of the vinylic protons of VDM at 5.93 ppm with the integration area value of the CH proton of DMF at 8.01 ppm. After precipitation in *n*-hexane, the polymer was dried *in vacuo* at room temperature for 12 h to yield a yellow powder product. The final polymer was analyzed by SEC, FT-IR spectroscopy and ^{1}H NMR spectroscopy. $\overline{M_n}_{,SEC}$ = 8800 g.mol^{-1}, PDI = 1.09. FTIR (ν, cm^{-1}): $\nu_{(C\text{-}O\text{-}C;\ azlactone)}$ = 1201, $\nu_{(C=N;\ azlactone)}$ = 1699 and $\nu_{(C=O;\ azlactone)}$ = 1817. ^{1}H NMR (400 MHz, $CDCl_3$, δ (ppm)): 0.86 (CH_3-$(CH_2)_{10}$-CH_2-S-), 1.40 (-OCO-(C(C**H**$_3)_2$-N=), 1.80-2.80 (-CH_2-CH)$_n$, 3.38 (C**H**$_3$O(CH_2-CH_2O)$_{44}$-) and 3.65 (CH_3O(C**H**$_2$-C**H**$_2$O)$_{44}$-C**H**$_2$$CH_2$-OC(O)C($CH_3)_2$-).

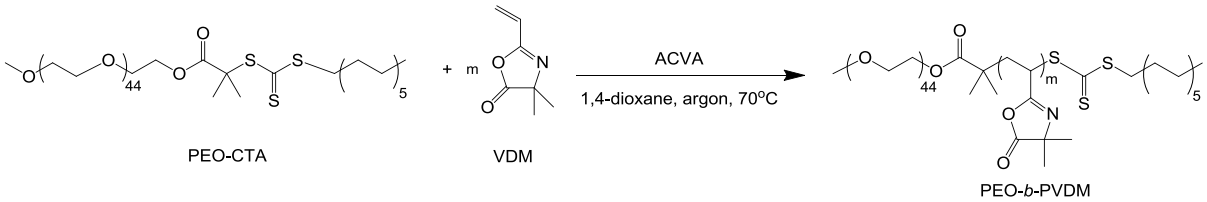

Scheme 2. Synthesis of PEO-*b*-PVDM diblock copolymers by RAFT polymerization

2.3.2 Synthesis of (3-aminopropyl)triethoxysilane-grafted MNP (APS-grafted MNP)

Amino-grafted MNPs were synthesized through a three-step process: (1) synthesis of MNP core, (2) grafting of oleic acid onto the MNP and (3) a ligand exchange reaction with APS. First, a thermal decomposition of Fe(acac)$_3$ (5 g, 14.05 mmol) in benzyl alcohol (90 mL) was performed at 180°C for 48 h to obtain MNP core. The particle was magnetically separated from the dispersion and washed with ethanol and CH_2Cl_2 repetitively to remove benzyl alcohol and then dried *in vacuo*. Oleic acid (4 mL) was then dropped to a MNP-toluene dispersion (0.8 g of MNPs in 30 mL of toluene) previously sonicated, to form oleic acid-grafted MNPs. APS (0.6 g, 2.71 x 10^{-3} mol) was then added to the oleic acid-grafted MNP dispersed in toluene (0.8 g of the MNP in 30 mL of toluene) containing 2 M TEA (5 mL) to form APS-grafted MNPs. After stirring for 24 h, the particles were precipitated in ethanol and washed with toluene to remove oleic acid and ungrafted APS from the dispersion. FTIR (ν, cm^{-1}): $\nu_{(Fe\text{-}O)}$ = 586, $\nu_{(Si\text{-}O\ stretching)}$ = 1103-1079, $\nu_{(CH3\ stretching)}$ = 2974-2886 and $\nu_{(N\text{-}H\ stretching)}$ = 3363.

2.3.3 Formation of PEO-*b*-PVDM copolymers-MNP nanoclusters (Scheme 3)

APS-grafted MNP (100 mg) was dispersed in 10 mL 1,4-dioxane by sonication. Then, a PEO-*b*-PVDM diblock copolymer solution (100 mg of the copolymer in 10 mL of 1,4-dioxane) was added to the APS-grafted MNP dispersion under stirring at room temperature for 12 h. The copolymer-MNP nanocluster was magnetically separated from the dispersion and washed with 1,4-dioxane. This process was repeatedly performed to remove ungrafted copolymer from the MNP nanocluster. The copolymer-MNP nanocluster was then dried *in vacuo* at room temperature for 12 h.

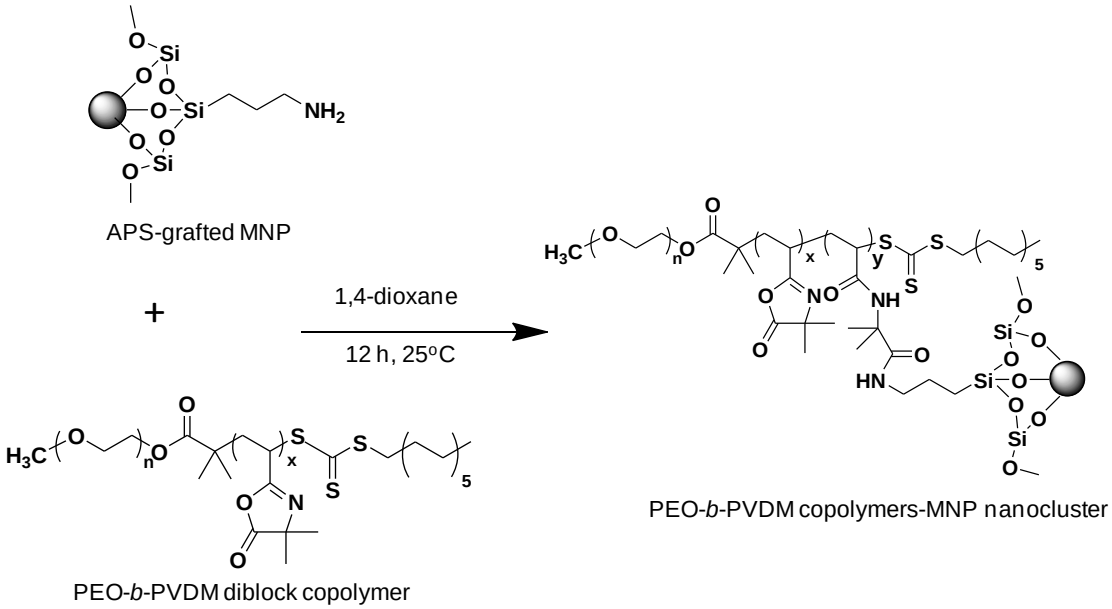

Scheme 3. Synthesis of PEO-*b*-PVDM copolymers-MNP nanocluster

2.3.4 Study in adsorption percentage of the copolymer-MNP nanoclusters with antibody

The copolymer-MNP nanocluster was first dispersed in water for 12 h to form carboxylated-enriched nanocluster due to the ring-opening reaction of the remaining azlactone rings in the copolymer on particle surface. After drying process, 10 mg of the copolymer-MNP nanoclusters were incubated in 1 mL of 10 mM MES pH 6 solution containing anti-rabbit IgG antibody for 2 h at room temperature. The Bradford assay [31] was used to determine antibody adsorption percentage of the particles with antibody. The protein concentration of all samples was determined using a calibration curve of BGG as a protein standard (in the Supporting Information). The copolymer-MNP nanoclusters after adsorption with antibody were separated from the supernatant using an external magnet and characterized *via* FTIR, VSM and TGA (see the supporting information). The absorption at

595 nm of the antibody solution before and after adsorption process was measured using the Bradford assay. The adsorption percentage of the antibody on the nanoclusters can be directly calculated using the following equation:

Adsorption percentage = [(A-B)/A] x100 (1)

where A is the initial concentration of antibody and B is the concentration of antibody in the supernatant at time *t* (non-adsorbed antibody).

2.3.5 Determination of recycling ability of the PEO-*b*-PVDM copolymer-MNP nanoclusters in adsorption with anti-rabbit IgG antibody

Copolymer-MNP nanoclusters adsorbed with anti-rabbit IgG antibody were thoroughly washed with 1 mL of a washing solution to desorb the antibody on the nanocluster surface. Desorption percentage of the antibody on the nanoclusters was determined using the Bradford assay and calculated from the following equation:

Desorption percentage = (C/B) x 100 (2)

where C is the concentration of desorbed antibody and B is the concentration of adsorbed antibody. The adsorption-separation-desorption process was performed repeatedly to determine the recycling efficiency of the nanoclusters as illustrated in Scheme 4.

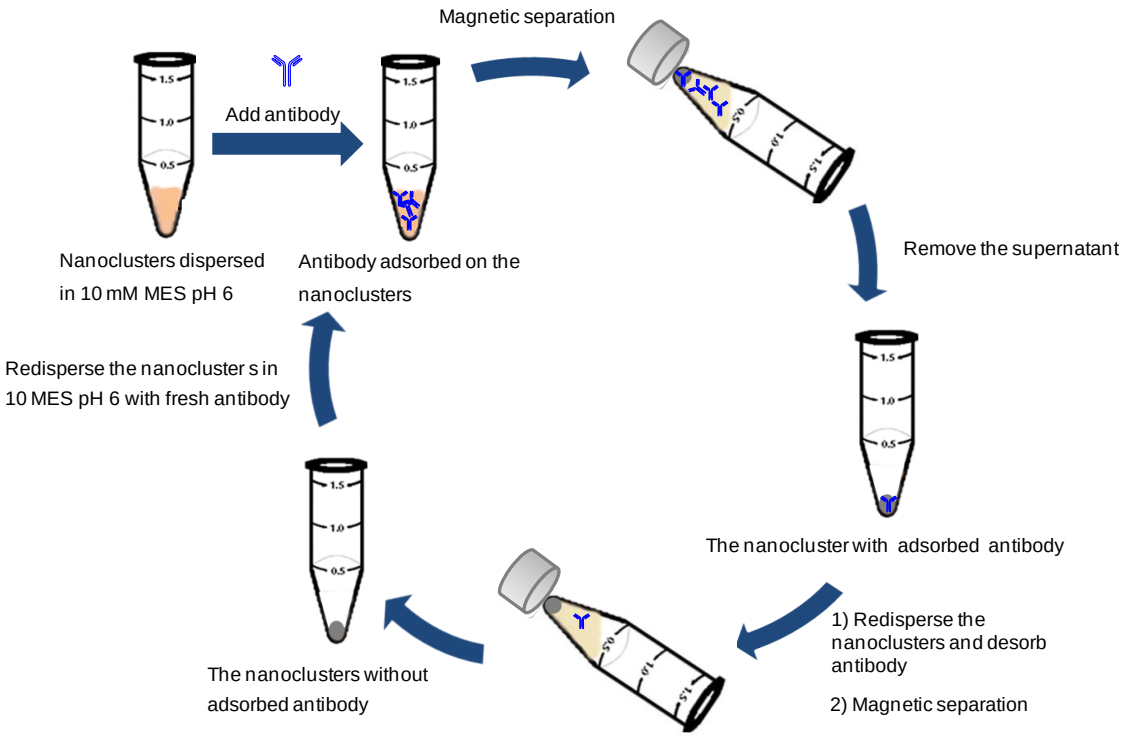

Scheme 4. Schematic illustration of an adsorption-separation-desorption cycle of the recyclable copolymer-MNP nanocluster in adsorption with antibody (anti-rabbit-IgG)

2.3.6 Antigen recognition capacity study of antibody-adsorbed magnetic nanoclusters

After antibody adsorption procedure, the remaining carboxyl groups of magnetic nanoclusters were blocked with 1 mL of 1% BSA in 10 mM MES pH 6 at 25^{o}C for 16 h. MNP nanoclusters were then washed with 10 mM MES pH 6 to remove an excess BSA. To detect the antigen recognition capacity of antibody-adsorbed MNP nanoclusters, an indirect detection method was used. First, 1 mL of 400 ppm of primary antigen (2.00 times molar excess) in 10 mM MES pH 6 was added into anti rabbit-IgG antibody-adsorbed MNP nanoclusters and incubated for 30 min. After washing the particles with 10 mM MES pH 6, they were incubated with 1 mL of 400 ppm of anti rabbit-HRP antibody for another 30 additional min. The presence of antigen on the particle surface was visualized by adding 1 mL of ABTS-H_2O_2 solution into 10 µl of the MNP nanocluster dispersion.

3. Results and discussion

3.1 Synthesis of PEO-*b*-PVDM diblock copolymers by RAFT polymerization

PEO-*b*-PVDM copolymers-MNP nanoclusters were obtained by the reaction between primary amine groups coated on MNPs surface and azlactone groups within the backbone of PEO-*b*-PVDM diblock copolymers *via* a ring-opening reaction (Scheme 3). In the first step, PEO-*b*-PVDM diblock copolymers were synthesized using PEO-CTA as the macromolecular chain transfer agent to mediate the RAFT polymerization of VDM in the presence of ACVA used as initiator in 1,4-dioxane at 70°C. The characteristics of the copolymers having three different PVDM block lengths are shown in Table 1. Theoretical number-average molecular weights ($\overline{M_n}_{,th}$) calculated from the monomer conversion increased as increasing the PVDM block length and this result is in good agreement with SEC results (Table 1). Figure 1 shows that SEC traces of PEO-*b*-PVDM diblock copolymers shift to earlier retention times with respect to the SEC trace of PEO-CTA maintaining low polydispersity indices (PDIs ≤ 1.10). This result shows that the copolymerization is well controlled leading to well-defined diblock copolymer structures.

Table 1. Diblock copolymers based on PEO and VDM synthesized by RAFT polymerization at 70°C in 1,4-dioxane: experimental conditions and characterizations

Run	Copolymer[a]	$[VDM]_0$: $[PEO\text{-}CTA]_0$: $[ACVA]_0$	Reaction time (h)	VDM conv.[b] (%)	$\overline{M_n}_{,th}$[c] (g/mol)	$\overline{M_n}_{,SEC}$[d] (g/mol)	PDI[d]
1	PEO_{44}-*b*-$PVDM_{21}$	25:1:0.2	4	84	5277	7400	1.04
2	PEO_{44}-*b*-$PVDM_{41}$	100:1:0.2	4	41	8060	8800	1.09
3	PEO_{44}-*b*-$PVDM_{84}$	100:1:0.2	8	84	14083	14500	1.06

[a]The number of monomer units determined by ^{1}H NMR spectroscopy. [b] VDM conversion determined by ^{1}H NMR spectroscopy by comparing the integration area value of the vinylic protons of VDM at 5.93 ppm with the integration area value of the CH proton of DMF at 8.01 ppm. [c] $\overline{M_n}_{,th} = \overline{M_n}_{,NMR\ of\ PEO\text{-}CTA} + (([VDM]_0/[PEO\text{-}CTA]_0) \times VDM_{conv.} \times M_{VDM})$. [d]Determined by SEC in THF using polystyrene standard.

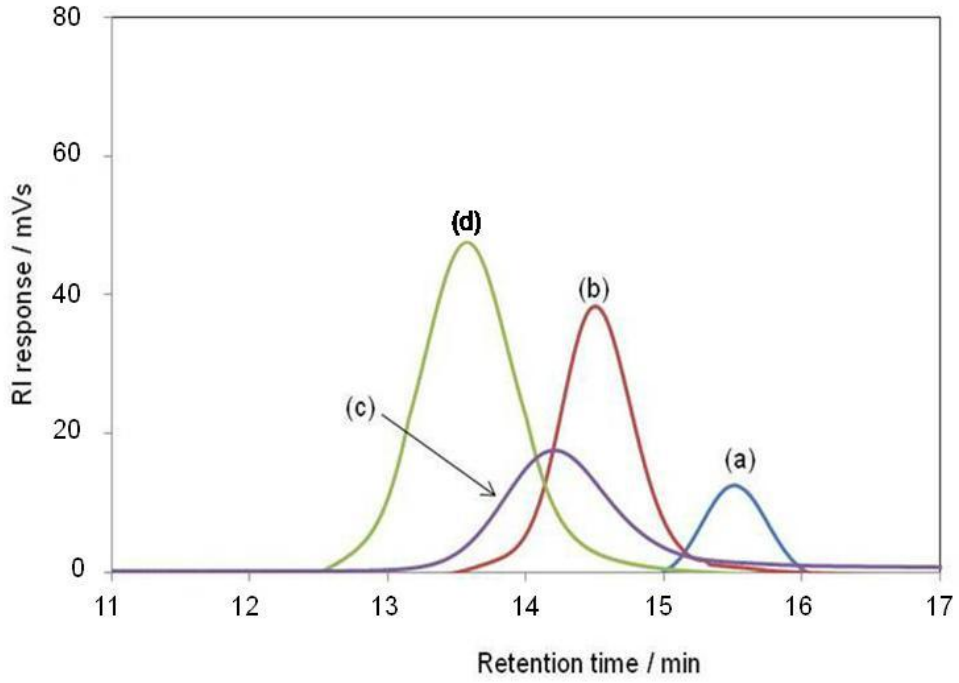

Figure 1. Overlay SEC traces of (a) PEO_{44}-CTA, (b) PEO_{44}-*b*-$PVDM_{21}$ copolymer (Run 1, Table 1), (c) PEO_{44}-*b*-$PVDM_{41}$ copolymer (Run 2, Table 1) and (d) PEO_{44}-*b*-$PVDM_{84}$ copolymer (Run 3, Table 1).

^{1}H NMR spectrum (Figure 2A) of the PEO_{44}-*b*-$PVDM_{41}$ copolymer (Run 2, Table 1) shows the presence of signals at 3.38 ppm ($CH_3O(CH_2\text{-}CH_2O)_{44}$-, labeled *a*) and at 3.65 ppm ($CH_3O(CH_2\text{-}CH_2O)_{44}\text{-}CH_2CH_2\text{-}OC(O)C(CH_3)_2$-, labeled *b*), which are characteristics of the PEO block and the presence of a signal at 1.40 ppm (-OCO-($C(CH_3)_2$-N=, labeled *c*), which is characteristic of PVDM block. The other two block copolymers show similar ^{1}H NMR patterns to that of PEO_{44}-*b*-$PVDM_{41}$ block copolymer with different integration ratios of signals labeled *b* and *c*, depending on the block lengths of each copolymer. Moreover, the FTIR spectrum (Figure 2B) of the PEO_{44}-*b*-$PVDM_{41}$ copolymer shows the characteristic bands of the azlactone rings at 1817 cm^{-1} ($\nu_{C=O}$), at 1699 cm^{-1}($\nu_{C=N}$) and at 1201 cm^{-1} ($\nu_{C\text{-}O\text{-}C}$).

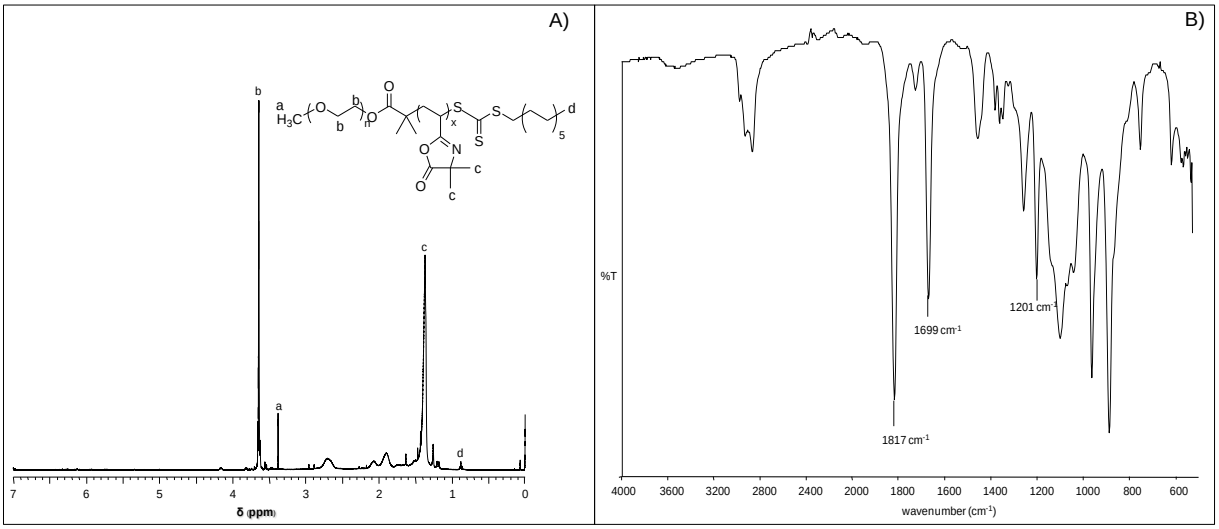

Figure 2. A) ^{1}H NMR spectrum of the PEO_{44}-*b*-$PVDM_{41}$ block copolymer (Run 2, Table 1) in $CDCl_3$ and B) FTIR spectrum of the PEO_{44}-*b*-$PVDM_{41}$ block copolymer.

3.2 Formation of PEO-*b*-PVDM copolymers-MNP nanoclusters

PEO-*b*-PVDM copolymers-MNP nanoclusters were obtained by reaction between amino groups grafted onto the surface of APS-grafted MNPs with azlactone rings of PVDM block of copolymers in 1,4-dioxane at room temperature. Resulting copolymers-MNP nanoclusters were characterized by TGA and FTIR spectroscopy. TGA technique was used to calculate the percentage of organic layers bound onto MNPs. It was assumed that the percent weight loss was attributed to the weight of organic components and the residual weight was due to completely oxidized iron oxide in the form of magnetite. It was found that APS content in the nanoclusters was about 2.2% and the copolymers in the nanoclusters were in the range of 8.4-11.9% (Figure 3).

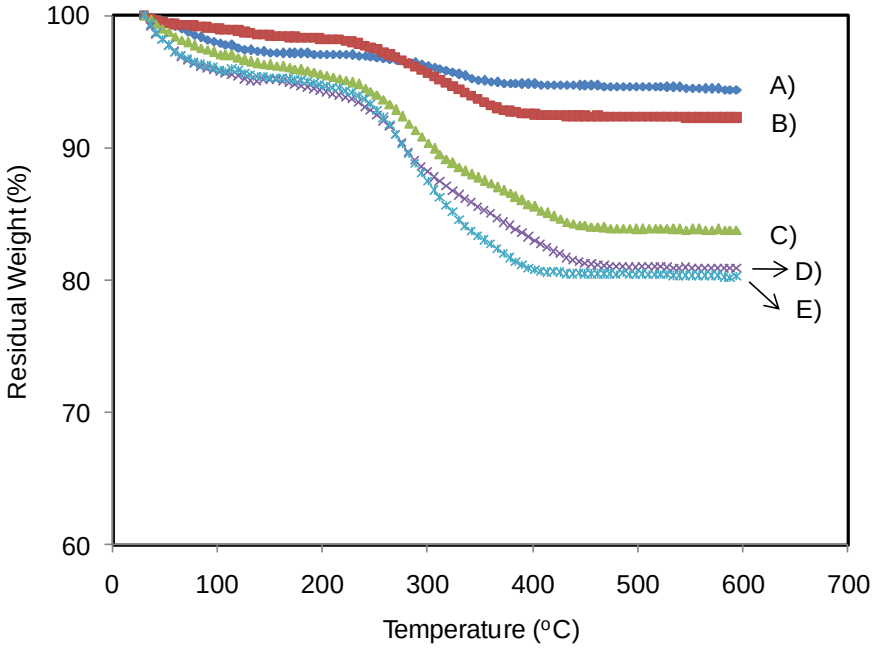

Figure 3. TGA thermograms of A) bare MNPs, B) APS-grafted MNPs, C) PEO_{44}-*b*-$PVDM_{21}$-MNP nanoclusters, D) PEO_{44}-*b*-$PVDM_{41}$-MNP nanoclusters and E) PEO_{44}-*b*-$PVDM_{84}$-MNP nanoclusters.

The FTIR spectrum of PEO_{44}-*b*-$PVDM_{41}$-MNP nanoclusters exhibits the left over C=O characteristic band of the azlactone ring at 1819 cm^{-1} after the coupling reaction (Figure 4), indicating the availability of some azlactone rings for further hydrolysis with water to form the MNP containing carboxylated-enriched surface for ionic adsorption with antibody in the next step.

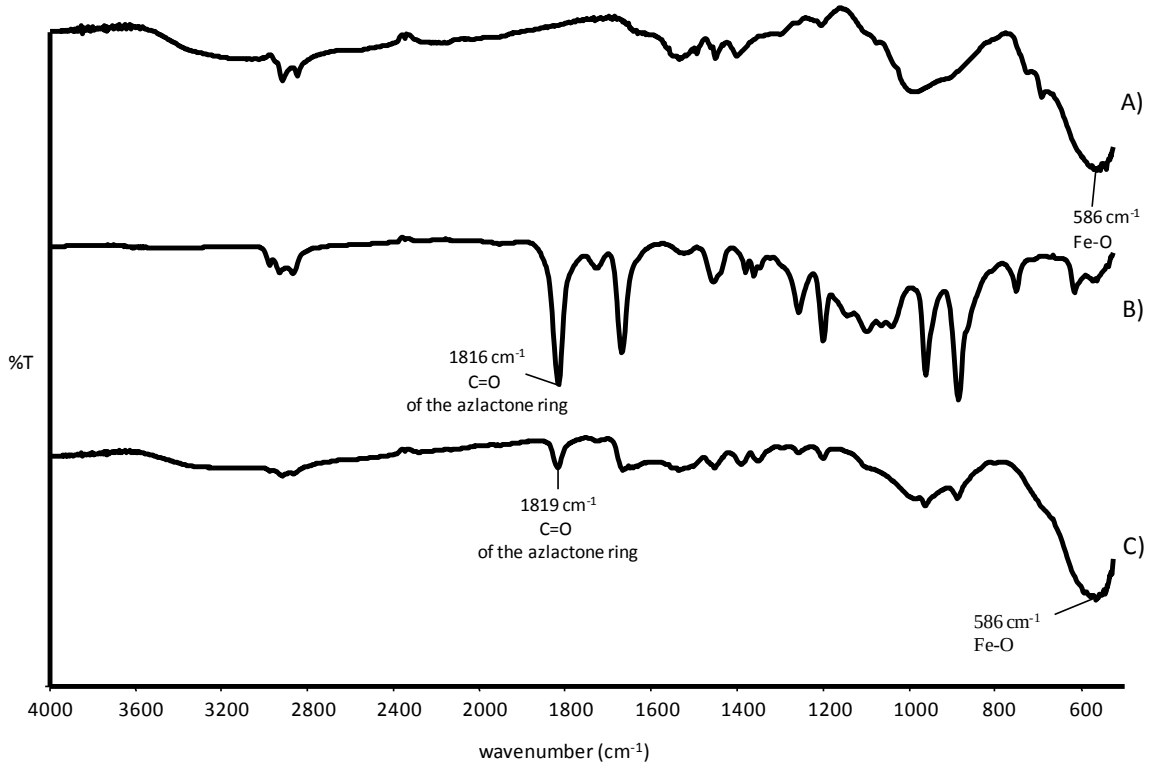

Figure 4. FTIR spectra of A) APS-grafted MNPs, B) PEO_{44}-*b*-$PVDM_{41}$ block copolymers and C) PEO_{44}-*b*-$PVDM_{41}$-MNP nanoclusters.

TEM images of APS-grafted MNPs and MNP nanoclusters coated with PEO-*b*-PVDM block copolymers containing different PVDM chain lengths are shown in Figure 5. It was found that large aggregations of the particles were observed for APS-grafted MNPs (Figure 5A). After PEO-*b*-PVDM block copolymer coating, the particle dispersibility was obviously improved due to hydrophilic PEO coating on its surface. In addition, the existence of carboxylic acid groups arising from the ring-opening reaction of azlactone rings in the PVDM block after exposure in water might also enhance water dispersibility of the particles. The ring-opening reaction between azlactone rings in the PVDM block of the copolymers and amino groups grafted on MNP surface led to the formation of the nanoclusters (Scheme 3). The size of these nanoclusters increased from 20 to 150 nm with increasing the PVDM chain lengths: approximately 10, 50 and 100 particles/cluster were obtained for PEO_{44}-*b*-$PVDM_{21}$, PEO_{44}-*b*-$PVDM_{41}$ and PEO_{44}-*b*-$PVDM_{84}$ block copolymers, respectively (Figure 5B, 5C and 5D). Increasing reactive azlactone groups in the PVDM block by increasing the PVDM length increased numbers of the MNP participating in the nanoclustering, indicating that the

size of these nanoclusters can be controlled by adjusting the number of reactive azlactone rings in the block copolymers.

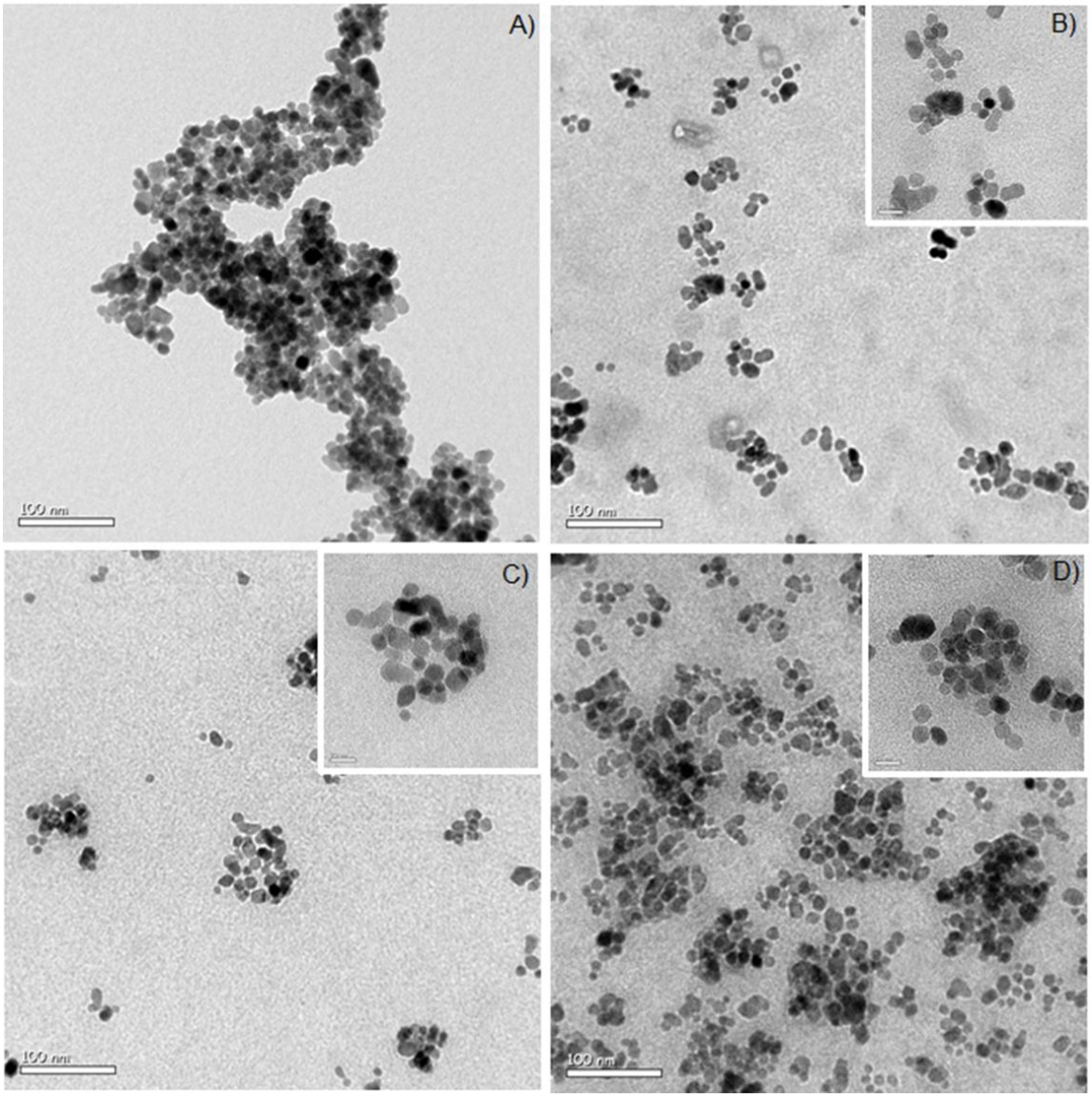

Figure 5. TEM images of A) APS-grafted MNPs, B) PEO_{44}-*b*-$PVDM_{21}$-MNP nanoclusters, C) PEO_{44}-*b*-$PVDM_{41}$-MNP nanoclusters and D) PEO_{44}-*b*-$PVDM_{84}$-MNP nanoclusters. All TEM samples were prepared from aqueous dispersions. The expansion of some nanoclusters is shown in the inset.

Hydrodynamic diameter (D_h) of APS-grafted MNP estimated by PCS was significantly larger than those of the MNPs coated with PEO-*b*-PVDM block copolymers, indicating the improvement in water dispersibility of the particles after copolymer coating

(Table 2) and are in good agreement with TEM results. Increasing PVDM block lengths in the copolymers led to the increase in D_h (97-166 nm) as ascertained by the TEM results. In addition, hydrodynamic size distributions of the copolymers-MNP nanoclusters were narrow as compared to that of APS-grafted MNP as a result of polymer coating and thus improving their water dispersibility. Zeta potential values of the nanoclusters were increased significantly after copolymer coating (-27.2 to -33.9 mV) due to the ring-opening of PVDM units in the copolymers, resulting in the formation of the nanoclusters with carboxylated-enriched surface. The negative charge of the carboxylated-coated nanoclusters was essential for magnetic separation of antibody through ionic adsorption mechanism in the next step.

Table 2. Hydrodynamic diameter (D_h), size distribution and zeta potential of the nanoclusters dispersed in 10 mM MES pH 6 solutions

Run	Samples	D_h (nm)	Zeta potential (mV)
1	APS-coated MNP	984.1	-3.5
2	PEO_{44}-*b*-$PVDM_{21}$-MNP nanoclusters	96.7	-27.2
3	PEO_{44}-*b*-$PVDM_{41}$-MNP nanoclusters	117.5	-28.3
4	PEO_{44}-*b*-$PVDM_{84}$- MNP nanoclusters	166.1	-33.9

Magnetic properties of bare MNP, APS-grafted MNP and MNP nanoclusters coated with PEO-*b*-PVDM block copolymers containing different PVDM chain lengths are shown in Figure 6. Saturation magnetizations (M_s) of MNP nanoclusters ranged between 33 and 42 emu/g and these numbers were lower than their MNP precursors. This was attributed to the presence of organic components in the structure, leading to the lower percentage of magnetite content in the nanoclusters. Although there was some degree of MNP nanoclustering, these particles exhibited superparamagnetism evidenced by the absence of magnetic remanence and coercivity in the *M*-*H* curves.

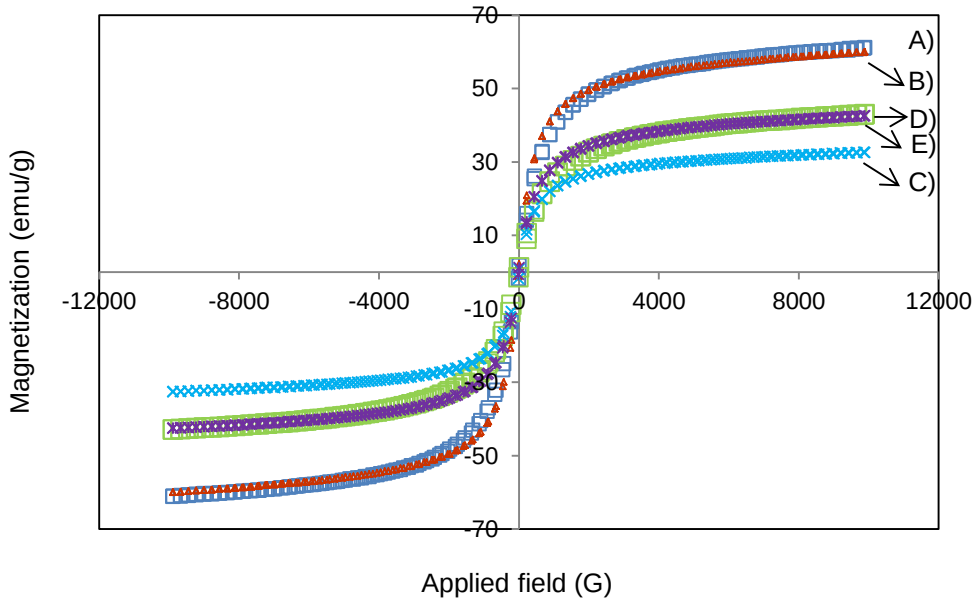

Figure 6. *M-H* curves of A) bare MNPs, B) APS-grafted MNPs, C) PEO_{44}-*b*-$PVDM_{21}$-MNP nanoclusters, D) PEO_{44}-*b*-$PVDM_{41}$-MNP nanoclusters and E) PEO_{44}-*b*-$PVDM_{84}$-MNP nanoclusters.

3.3 Adsorption percentage and recycling studies of the copolymer-MNP nanoclusters with antibody

To use them in antibody adsorption application, copolymers-MNP nanoclusters having carboxylated-enriched surface are desirable for ionic adsorption between negatively charged MNP and positive moiety in anti-rabbit IgG antibody. Residual azlactone rings on the MNP surface were thus hydrolyzed to form nanoclusters with negatively charged surface due to carboxylated groups coating before adsorption experiments. Nanoclusters having four different cluster sizes as shown in Table 2 were used as nano-solid supports in antibody adsorption experiments. It was found that APS-coated MNP was not dispersible in 10 mM MES pH 6 solution due to the absence of polymer coating on its surface. On the other hand, the nanoclusters grafted with carboxylated-functionalized PEO_{44}-*b*-$PVDM_{21}$ and PEO_{44}-*b*-$PVDM_{41}$ copolymers were well dispersible in the media but not completely separated from the media using an external magnet. Traces of MNP in the supernatant after magnetic separation and/or ultracentrifugation could therefore interfere with Bradford assay [27]. The presence of single nanoparticles or magnetic clusters with small size, hypothetically having

low magnetic sensitivity, resulted in difficulty in removal from the dispersion [32]. A compromise between good water dispersibility and magnetic sensitivity of MNP is crucial for use as a nano-solid support. Therefore, the nanoclusters grafted with these two copolymers were unable to be used as supports for antibody adsorption. Interestingly, nanoclusters grafted with PEO_{44}-*b*-$PVDM_{84}$ copolymer with D_h of 166 nm exhibited good dispersibility in the media and, more importantly, they facilitated separation by an external magnet without traces of MNP in the dispersion resulting in an absence of interference with Bradford assay. Therefore, the carboxylated-functionalized PEO_{44}-*b*-$PVDM_{84}$ copolymer-coated MNP nanoclusters were then subjected to the adsorption experiments with anti-rabbit-IgG antibody.

Adsorption percentage of the copolymer-MNP nanoclusters with anti-rabbit-IgG antibody was investigated after removing an excess antibody from the mixture. Figure 7 shows that 200 ppm was the maximum concentration of antibody that can be used for binding on nanocluster surface. Increasing antibody concentration to 300 and 400 ppm resulted in the existence of non-adsorbed antibody in the dispersion. Therefore, 200 ppm antibody loading in 10 mg of PEO_{44}-*b*-$PVDM_{84}$-MNP nanoclusters will be used for further experiments. In addition, the M_s from VSM and the percent weight residual from TGA techniques of the antibody-adsorbed nanoclusters showed slight decreases as compared to those before the adsorption, implying that there was some antibody adsorbed on the complexes.

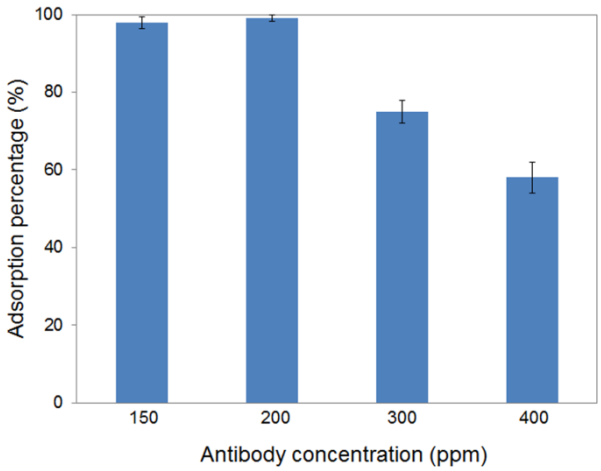

Figure 7. Adsorption percentages of PEO_{44}-*b*-$PVDM_{84}$-MNP nanoclusters for ionic adsorption with anti-rabbit IgG antibody (Adsorption percentage = [(A-B)/A] x100, where A is the initial concentration of antibody and B is the concentration of antibody in the supernatant at time *t* (non-adsorbed antibody)).

Because these nanoclusters possess magnetically guidable properties, which are great advantages in facilitating recycling process, the recycling ability of the copolymer-MNP nanoclusters was thus investigated. After 2 h adsorption of antibody, the nanoclusters were separated from dispersion using a permanent magnet. To prove the recycling concept, desorption of anti-rabbit IgG from nanocluster surface was examined by testing different washing solutions. The amount of antibody in supernatant after adsorption-desorption processes were quantitatively determined using Bradford assay and the desorption percentage was determined using the Equation (2). NaCl salt solutions at concentrations 300 mM, 1.0 and 2.5 M at pH 7, as well as 1.0 M NaCl solution at pH 12 were used for this purpose. These salt solutions at pH 7 were unable to desorb anti-rabbit IgG antibody from the nanocluster surface probably because the solution pH was in the range of isoelectric point (pI) of the antibody (6-9) [33]. The antibody can also be desorbed by changing the global net charge of the antibody by shifting the solution pH [27]. 1.0 M NaCl solution with pH 12 exhibited a complete removal of the antibody from the surface due to the suppression in ionic adsorption between carboxylated nanoclusters and the antibody as opposed to the case when the pH is in the pI range of the antibody. Therefore, 1 M NaCl pH 12 solution was used as the washing solution to investigate the adsorption recycling ability of the nanoclusters.

Figure 8 shows the adsorption percentage of the nanoclusters with the antibody in each cycle. After each adsorption-separation process, the concentration of adsorbed antibody and desorbed antibody from each cycle was determined using Bradford assay. The results showed that the particles retained a higher than 96% adsorption of the antibody for eight adsorption-separation-desorption cycles, indicating the potential feasibility in using this novel hybrid nanocluster as recyclable support in cell separation applications.

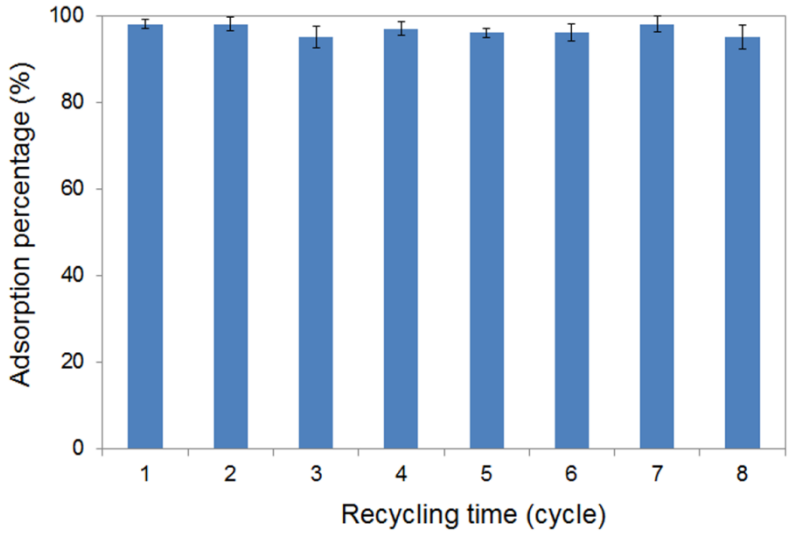

Figure 8. Recycling efficiency of PEO_{44}-*b*-$PVDM_{84}$-MNP nanoclusters in the ionic adsorption of anti-rabbit IgG antibody after 8-recycling process**.**

3.4 Antigen recognition capacity study of antibody-adsorbed magnetic nanoclusters

The antigen recognition capacity of antibody-adsorbed MNP nanoclusters was determined from the development of a green-blue color product after the oxidation with ABTS, when reacted with horseradish peroxidase (HRP) labeled conjugates. Therefore, anti-rabbit IgG-adsorbed MNP nanoclusters were first immobilized with an IgG antigen, followed by anti-rabbit IgG-HRP as a secondary antibody for color development when reacted with ABTS. It was found that anti-rabbit IgG-adsorbed MNP nanoclusters exhibited the changing of color from light green to blue after the oxidation with ABTS (Figure 9D), indicating the conjugation of IgG antigen with anti-rabbit IgG adsorbed on the nanocluster surface. The MNP nanoclusters without anti-rabbit IgG-HRP as the secondary antibody (Figure 9E), without IgG antigen (Figure 9F) and without anti-rabbit IgG (Figure 9G) were used as control dispersions. These dispersions showed negative results as their solution color did not change upon the oxidation with ABTS. The dispersion media (10 mM MES pH 6) (Figure 9A) and those with 1% BSA as a blocking reagent (Figure 9B) were also testified to evaluate the negative results of the control solutions. In addition, the solution of anti-rabbit IgG-HRP as the secondary antibody (without MNP nanoclusters) was also used in the testing to evaluate the color change (positive result) due to the reaction between HRP and ABTS (Figure 9C). It should be also noted that the MNP nanoclusters after eight recycling process also showed a

positive result as illustrated in Figure 9D. Therefore, these experiments confirm that the antigen recognition of the antibody-adsorbed MNP nanoclusters was preserved. These MNP nanoclusters could be used as a recyclable magnetic marker to immobilize with other specific antibody-antigen conjugates.

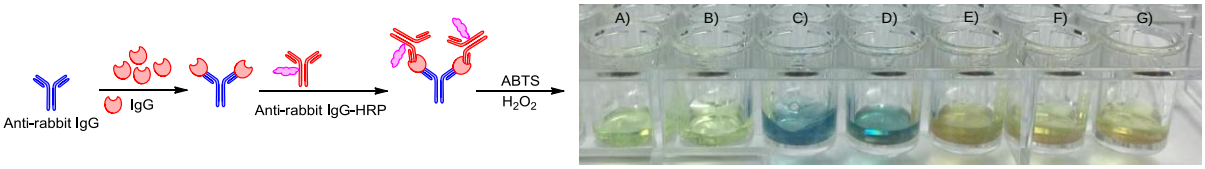

Figure 9. Scheme showing the indirect method used to visualize the antigen recognition capability; A) 10 mM MES pH 6, B) 1% BSA in 10 mM MES pH 6, C) anti-rabbit IgG-HRP, D) anti-rabbit IgG-adsorbed MNP nanoclusters immobilized with IgG and anti-rabbit IgG-HRP, E) anti-rabbit IgG-adsorbed MNP nanoclusters immobilized with IgG, F) anti-rabbit IgG-adsorbed MNP nanoclusters without IgG (blocked with BSA) and G) MNP nanoclusters**.**

4. Conclusions

Surface modification of MNPs with well-defined PEO-*b*-PVDM diblock copolymers using "grafting-onto" strategy to form magnetic nanoclusters was described. The nanocluster size could be tuned by adjusting the amount of reactive azlactone rings in the PVDM block to obtain a controllable size below 150 nm. The obtained nanoclusters were well dispersed in water, have good magnetic sensitivity and negatively charged surface. These properties are required to use these particles in magnetic separation applications. The good magnetic sensitivity of the nanoclusters allowed facile manipulation using magnetic separation. Moreover, their negatively charged surface provided adsorption capability with positively charged bio-entities. These novel magnetic nanoclusters were successfully used as efficient and recyclable nano-solid supports for adsorption with anti-rabbit IgG antibody for at least 8-recycling process. The preliminary studies in the adsorption of the nanoclusters with IgG antigen were also demonstrated. The purity of the antigen after the adsorption and their efficiency for use in real sample separation are warranted for further exploration. These magnetic nanoclusters might be advantageous for use as nano-solid supports for efficient and

facile separation of other positively charged molecules, especially antibody-antigen conjugates.

References

[1] D.H. Kim, S.H. Lee, K H. Im, K.N. Kim, K.M. Kim, I.B. Shim, et al. Curr. Appl. Phys. 6, Suppl.1 (2006) 242-246.

[2] R.Y. Hong, B. Feng, L.L. Chen, G.H. Liu, H.Z. Li, Y. Zheng et al. Biochem. Eng. J. 42 (2008) 290-300.

[3] J.M. Moon, B.S. Kim, Y.S. Choi, J.O. Lee, T. Nakahara and K. Yoshinaga. Macromol. Res. 18 (2010) 793-799.

[4] Q. Yuan, R. Venkatasubramanian, S. Hein and R.D.K. Misra**.** Acta Biomater. 4 (2008) 1024-1037.

[5] F. Xu, J. H. Geiger, G. L. Baker, M.L. Bruening. Langmuir 27 (2011) 3106-3112.

[6] D.K. Kim, Y. Zhang, W. Voit, K.V. Rao, M. Muhammed. J. Magn. Magn. Mater. 225 (2001) 30-36.

[7] Y. Shen, W. Guo, L. Qi, J. Qiao, F. Wang, L. Mao. J. Mater. Chem. B. 1 (2013) 2260-2267.

[8] Y. Prai-in, K. Tankanya, B. Rutnakornpituk, U. Wichai, V. Montembault, S. Pascual, et al. Polymer 53 (2012) 113-120.

[9] T.T.T. N'Guyen, H. T. T. Duong, J. Basuki, V. Montembault, S. Pascual, C. Guibert, et al. Angew. Chem. Int. Ed. 52 (2013) 14152-14156.

[10] J.S. Basuki, H.T.T. Duong, A. Macmillan, R. Whan, C. Boyer, T.P. Davis. Macromolecules 46 (2013) 7043-7054.

[11] Y. Zhou, S. Wang, B. Ding, Z. Yang. Chem. Eng. J. 138 (2008) 578-585.

[12] N. Pothayee, S. Balasubramaniam, R.M. Davis, J.S. Riffle, M.R.J. Carroll, R.C. Woodward, et al. Polymer 52 (2011) 1356-1366.

[13] H. Wang, W. Luo, J. Chen. J. Mater. Sci. 47 (2012) 5918-5925.

[14] A. Aqil, S. Vasseur, E. Duguet, C. Passirani, J. P. Benoît, A. Roch, et al. Eur. Polym. J. 44 (2008) 3191-3199.

[15] C.L. McCormick, A.B. Lowe. Acc. Chem. Res. 37 (2004) 312-325.

[16] H. Mori, H. Iwaya, T. Endo. React. Funct. Polym. 67 (2007) 916-927.

[17] X. Zhang, J. Rieger**,** B. Charleux. Polym. Chem. 3 (2012) 1502-1509.

[18] C.N. Urbani, H.N. Nguyen, M.J. Monteiro. Aust. J. Chem. 59 (2006) 728-732.

[19] S. Puttick, D.J. Irvine, P. Licence, K.J. Thurecht. J. Mater. Chem. 19 (2009) 2679-2682.

[20] S. Pascual, T. Blin, P.J. Saikia, M. Thomas, P. Gosselin, L. Fontaine. J. Polym. Sci. A Polym. Chem. 48 (2010) 5053-5062.

[21] M.E. Levere, H.T. Ho, S. Pascual, L. Fontaine. Polym. Chem. 2 (2011) 2878-2887.

[22] H.T. Ho, M. E. Levere, D. Fournier, V. Montembault, S. Pascual, L. Fontaine. Aust. J. Chem. 65 (2012) 970-977.

[23] H.T. Ho, M.E. Levere, S. Pascual, V. Montembault, N. Casse, A. Caruso, et al. Polym. Chem. 4 (2013) 675-685.

[24] T. Theppaleak, B. Rutnakornpituk, U. Wichai, T. Vilaivan, M. Rutnakornpituk. J. Biomed. Nanotech. 9 (2013) 1509-1520.

[25] T.R. Sarkar, J. Irudayaraj. Anal. Biochem. 379 (2008) 130-132.

[26] H. Xu, Z.P. Aguilar, L. Yang, M. Kuang, H. Duan, Y. Xiong, et al. Biomaterials 32 (2011) 9758-9765.

[27] S. Puertas , P. Batalla , M. Moros , E. Polo , P. del Pino , J.M. Guisan, et al. ACS Nano 5 (2011) 4521-4528.

[28] J.T. Lai, D. Filla, R. Shea. Macromolecules 35 (2002) 6754-6756.

[29] Y. He, T.P. Lodge. Chem. Commun. 26 (2007) 2732-2734.

[30] L.D. Taylor, H.S. Kolesinski, A.C. Mehta, L. Locatell, P.S. Larson. Makromol. Chem. Rapid Comm. 3 (1982) 779-782.

[31] M.M. Bradford. Anal. Biochem. 72 (1976) 248-254.

[32] H. Amiri, M. Mahmoudi, A. Lascialfari. Nanoscale 3 (2011) 1022-1030.

[33] M.A. Clauss, R.K. Jain. Cancer Res. 50 (1990) 3487-3492.

Supporting information

Part 1. Synthesis of 2-vinyl-4,4-dimethylazlactone (VDM) monomer

(A) Synthesis of *N*-acryloyl-2-methylalanine (Figure S1)

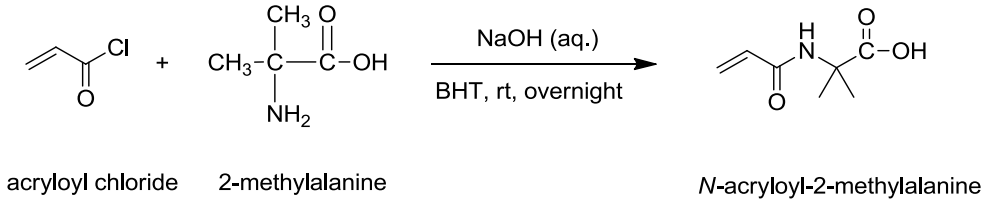

Figure S1. Synthesis of *N*- acryloyl-2-methylalanine

2-methylalanine (5.6966 g, 5.52 x 10^{-2} mol, 1 eq.) was added into a sodium hydroxide aqueous solution (4.416 g, 11.04 x 10^{-2} mol, 2 eq. in 15 mL water) in the presence of BHT (0.0552 g, 2.5051 x 10^{-4} mol) as polymerization inhibitor at 0-10^{o}C, followed by an addition of acryloyl chloride (5 mL, 5.52 x 10^{-2} mol, 1 eq.). After 12 h stirring, conc. HCl (6.81 mL, 6.90 x 10^{-2}mol, 1.25 eq.) was added into the solution, which was kept at 10^{o}C. The mixture was continuously stirred for another 30 min to form white solid, which was filtered, washed with water and dried. Yield: 69-72%. ^{1}H NMR (400 MHz, DMSO-*d6*) δ_H: 1.37 (s, 6H, ($C(CH_3)_2$), 5.58 (dd, 1H, CH_2=CH [trans]), 6.03 (dd, 1H CH_2=CH [cis]), 6.25 (dd, 1H, CH_2=CH), 8.26 (s, 1H, NH), 12.16 (s, 1H, COOH).^{13}C NMR (400 MHz, DMSO-*d6*) δ_C: 25.1 ($C(\mathbf{C}H_3)_2$), 55.0 (-$\mathbf{C}(CH_3)_2$-), 125.3 ($\mathbf{C}H_2$=CH), 131.8 (CH_2=$\mathbf{C}$H), 164.0 (COOH), 175.5 (NH-C=O). FTIR (ATR): 3337 cm^{-1} (N-H stretching), 1707 cm^{-1} (C=O of carboxylic acid), 1647 cm^{-1} (C=O stretching of amide), 1599 cm^{-1} (C=C stretching), 1551 cm^{-1} (N-H bending). HRMS: theoretical m/z = 157.1672 g.mol^{-1} $[M+H]^+$, experimental m/z = 158.0817 g.mol^{-1} $[M+H]^+$.

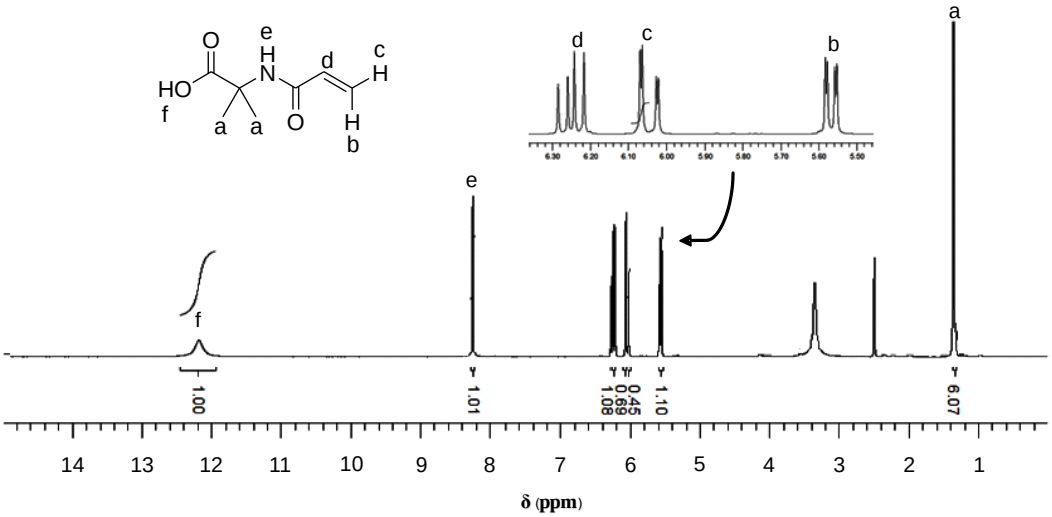

Figure S2. [1]H NMR spectrum of *N*-acryloyl-2-methylalanine in DMSO-*d6*

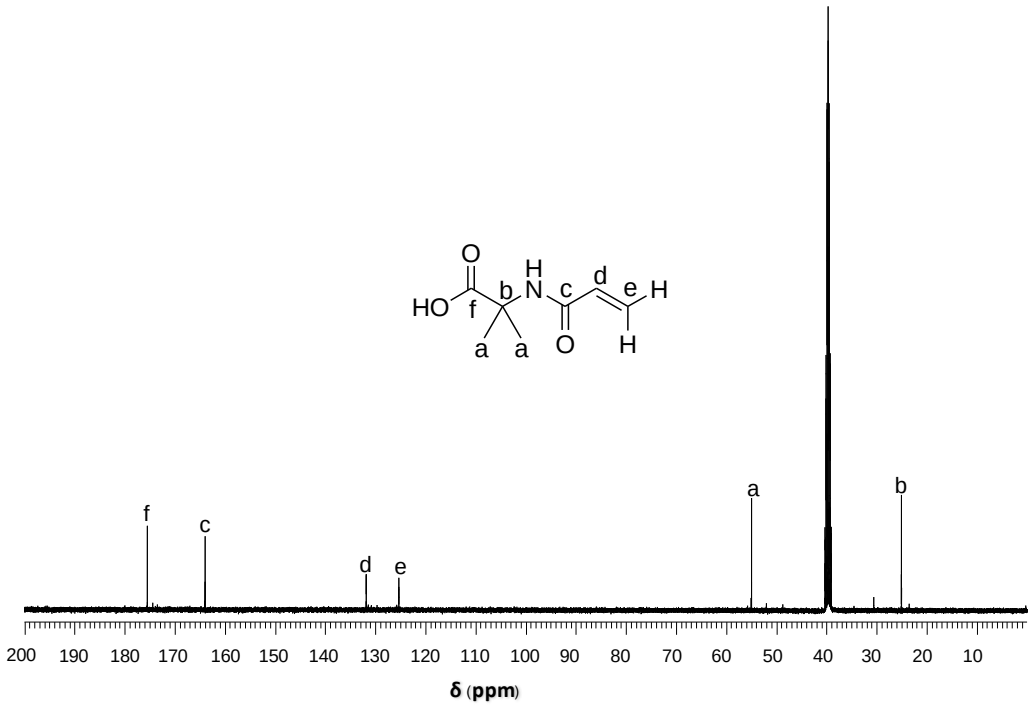

Figure S3. [13]C NMR spectrum of *N*-acryloyl-2-methylalanine in DMSO-*d6*

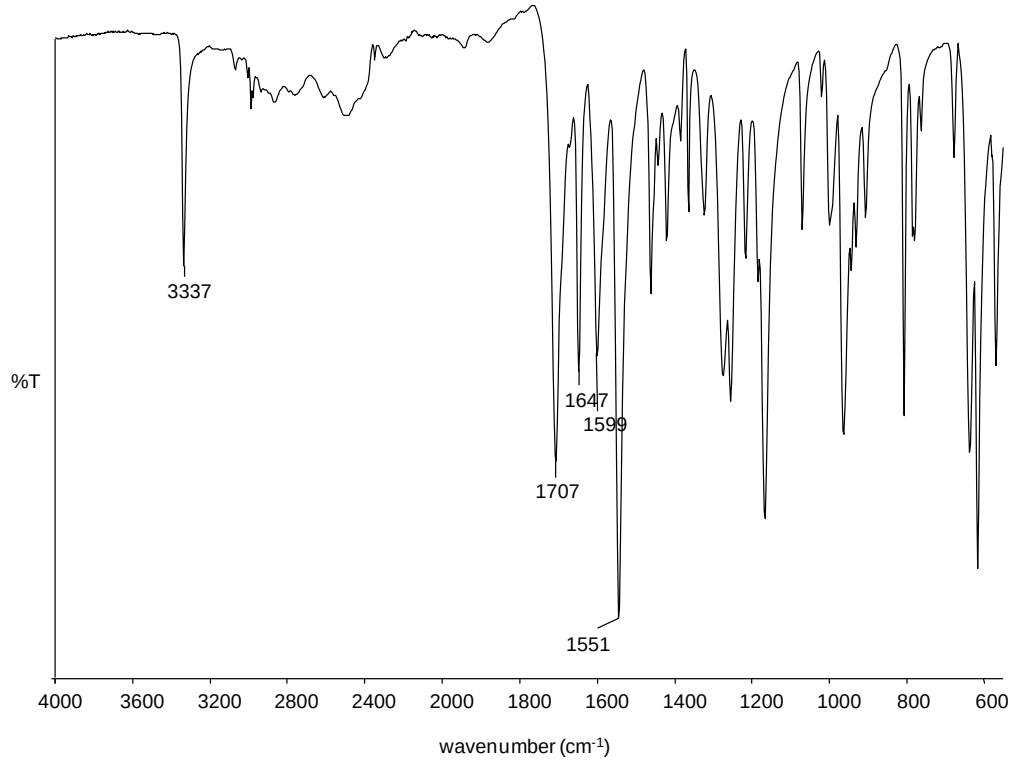

Figure S4. FTIR spectrum of *N*-acryloyl-2-methylalanine

(B) Cyclization of *N*-acryloyl-2-methylalanine to form VDM cyclic (Figure S5)

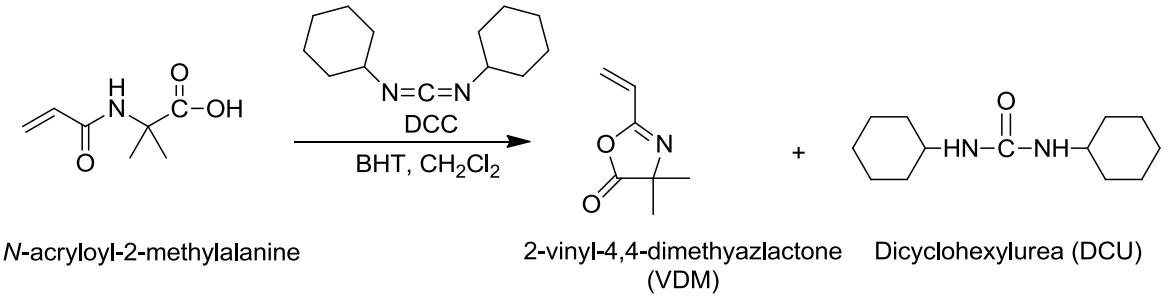

Figure S5. Synthesis of VDM monomer

N-acryloyl-2-methylalanine (5.00 g, 3.18 x 10^{-2} mol) and BHT (0.0549 g, 2.4912 x 10^{-4} mol) in CH_2Cl_2 (30 mL) was stirred at 0^{o}C under argon atmosphere to form colloidal dispersion. DCC solution (7.21 g, 6.37 x 10^{-3} mol in 40 mL CH_2Cl_2) was then added to the mixture with continuously stirring. After 12 h reaction, the solid dicyclohexyl urea by-product was filtered off and the filtrate was evaporated to remove CH_2Cl_2. The VDM product

was purified by distillation under reduced pressure to give a colorless mobile liquid. Yield: 60%. ^{1}H NMR (400 MHz, $CDCl_3$) δ_H: 1.47 (s, 6H, (-C(C**H**$_3$)$_2$-), 5.93 (dd, 1H, C**H**$_2$=CH [trans]), 6.25 (dd, 1H, C**H**$_2$=CH [cis]), 6.27 (dd, 1H, CH_2=C**H**). ^{13}C NMR (400 MHz, DMSO-*d6*) δ_C: 25.5 (-(C(**C**H_3)$_2$-), 66.6 (-(**C**$(CH_3)_2$-), 124.7 (**C**H_2=CH), 129.6 (CH_2=**C**H), 154.7 (-C=N-) and 181.3 (-C=O). FTIR: 1822 cm^{-1} (C=O stretching), 1668 cm^{-1} (C=N stretching), 1204 cm^{-1} (C-O-C stretching). HRMS: theoretical m/z = 139.1519 g.mol^{-1} $[M+H]^+$, experimental m/z = 140.0712 g.mol^{-1} $[M+H]^+$.

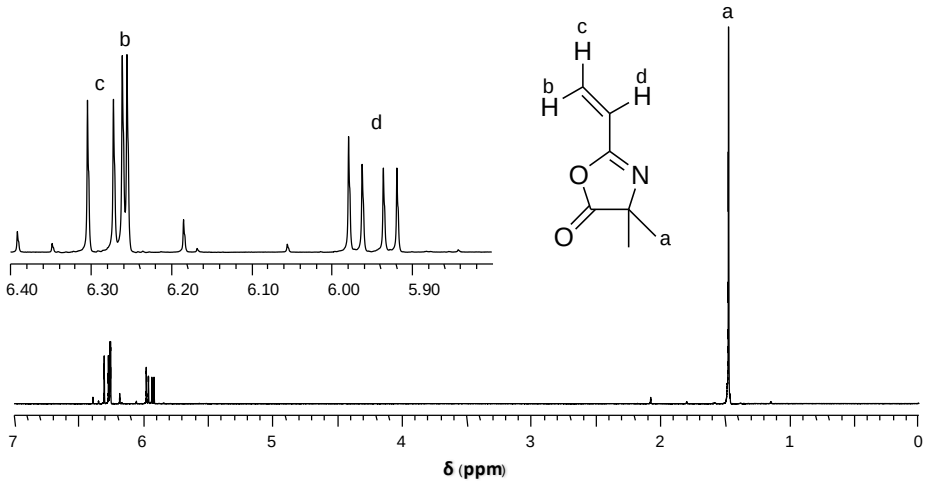

Figure S6. ^{1}H NMR spectrum of the VDM in $CDCl_3$

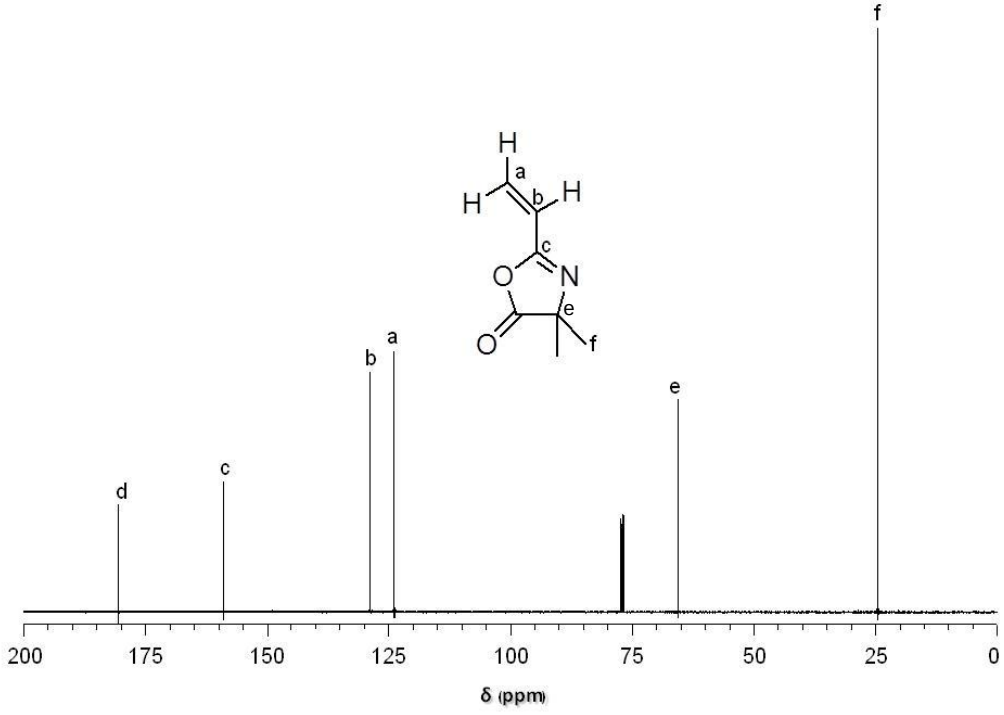

Figure S7. ^{13}C NMR spectrum of the VDM in $CDCl_3$

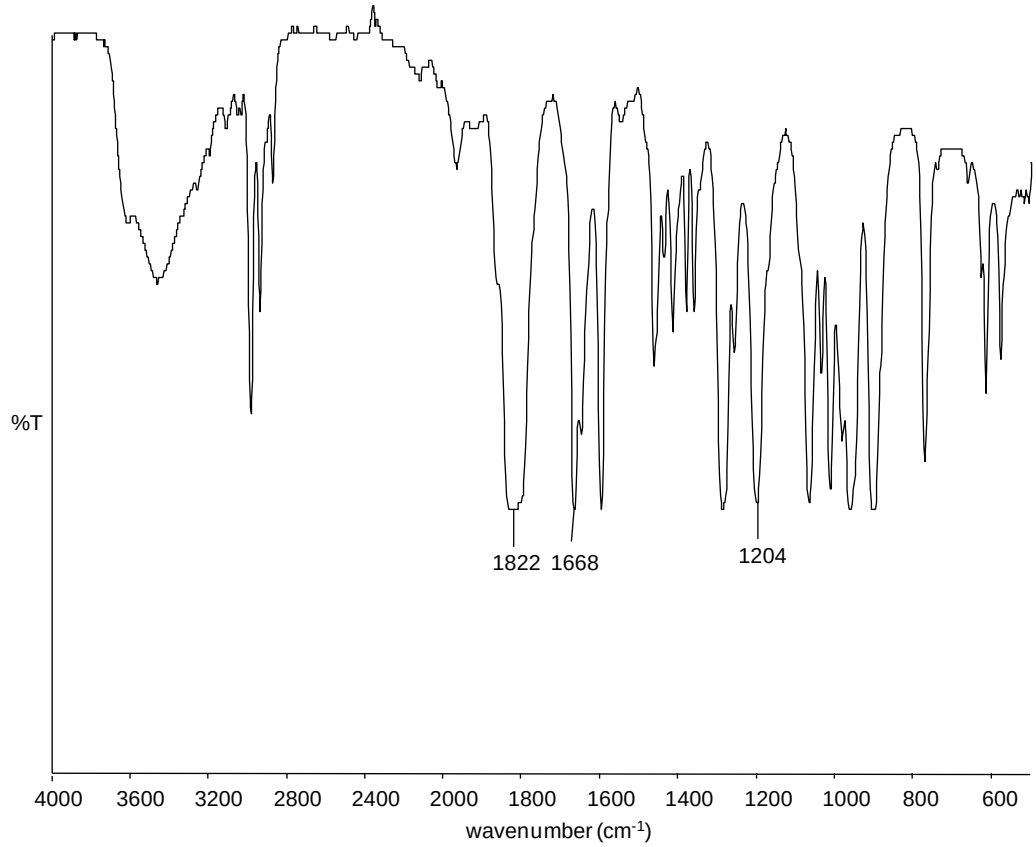

Figure S8. FTIR spectrum of VDM

Part 2. Synthesis of the poly(ethylene oxide) macromolecular chain transfer agent (PEO-CTA)

(A) Synthesis of *S*-1-dodecyl-*S*'-(*α,α*'-dimethyl-*α*"-acetic acid)trithiocarbonate (DMT)

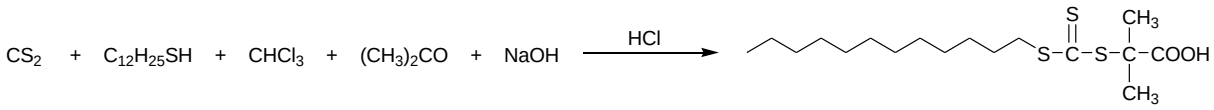

Figure S9. Synthesis of S-1-dodecyl-S'-(α,α'-dimethyl-α''-acetic acid)trithiocarbonate.

1-Dodecanethiol (20.24 g, 0.1 mol), acetone (48.06 g, 8.26 x 10^{-1} mol) and Aliquot 336 (tricaprylylmethylammonium chloride, 1.62 g, 4.00 x 10^{-3} mol) were mixed in a round bottomed flask cooled to 10^{o}C under nitrogen flow. Sodium hydroxide solution (50%) (4.20 g, 1.05 x 10^{-1}mol) was slowly added for 20 min. During this time, the solution color changed from colorless solution to white slurry. The reaction was continuously stirred for 15 min followed by dropwise addition of carbon disulfide (7.61 g, 1.00 x 10^{-1}mol) dissolved in

acetone (10.02 g, 1.73 x 10^{-1}mol). The reaction mixture was set at 40^{o}C and stirred for 1 h before cooling to ambient temperature. During this time, the solution color turned red. Chloroform (11.91 g, 1.50 x 10^{-1}mol) was added to the mixture, followed by dropwise addition of 50% sodium hydroxide solution (40.00 g, 5.00 x 10^{-1}mol) over 30 min. After stirring overnight, water (150 mL) was added to the frozen mixture, followed by addition of concentrated HCl (40 mL) to obtain a pH 1 solution. An excess of acetone was removed from the mixture by nitrogen flow. It was observed that the resultant solid mixture was precipitated out from the mixture after removal of acetone. The solid was collected with a Buchner funnel and then stirred in 250 mL of 2-propanol to dissolve the resultant product. The undissolved solid (by-product) was filtered off and the 2-propanol solution was concentrated to dryness to obtain the product. The crude product was recrystallized from cold hexanes to yield yellow crystalline solid. Yield 65%. ^{1}H NMR (400 MHz, $CDCl_3$) δ_H: 0.88 (t, 3H, CH_3), 1.26 (m, 20H, $(CH_2)_{10}$), 1.70 (s, 6H, $C(CH_3)_2$), 3.28 (t, 2H, CH_2). FTIR (ATR): 1718 cm^{-1} (C=O), 1070 cm^{-1} (C-S).

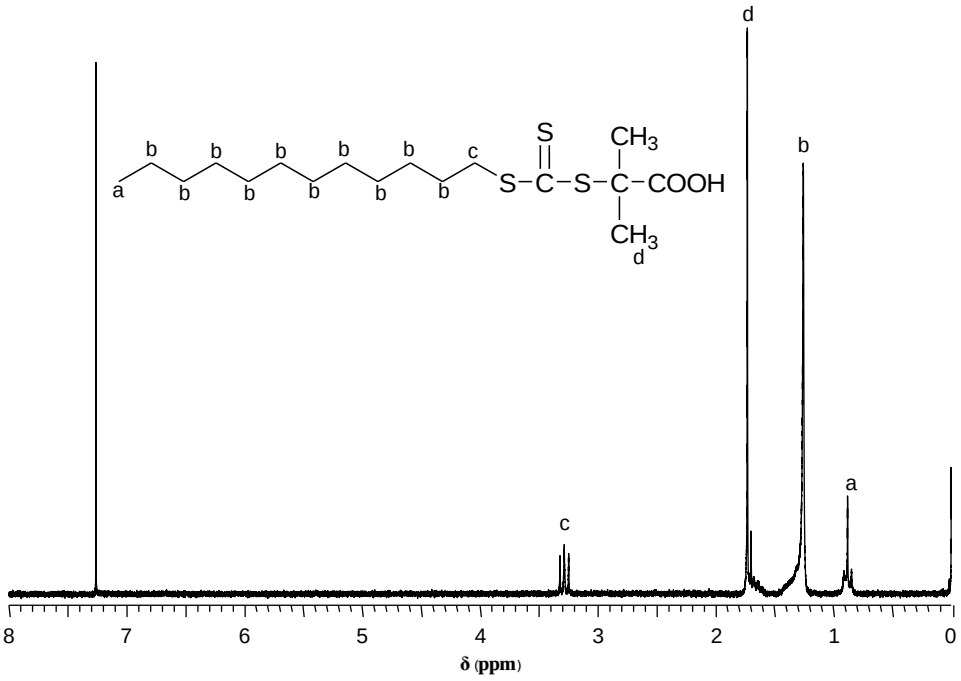

Figure S10. ^{1}H NMR spectrum of S-1-dodecyl-S$^{'}$-(α,α$^{'}$-dimethyl-α$^{''}$-acetic acid) trithiocarbonate in $CDCl_3$

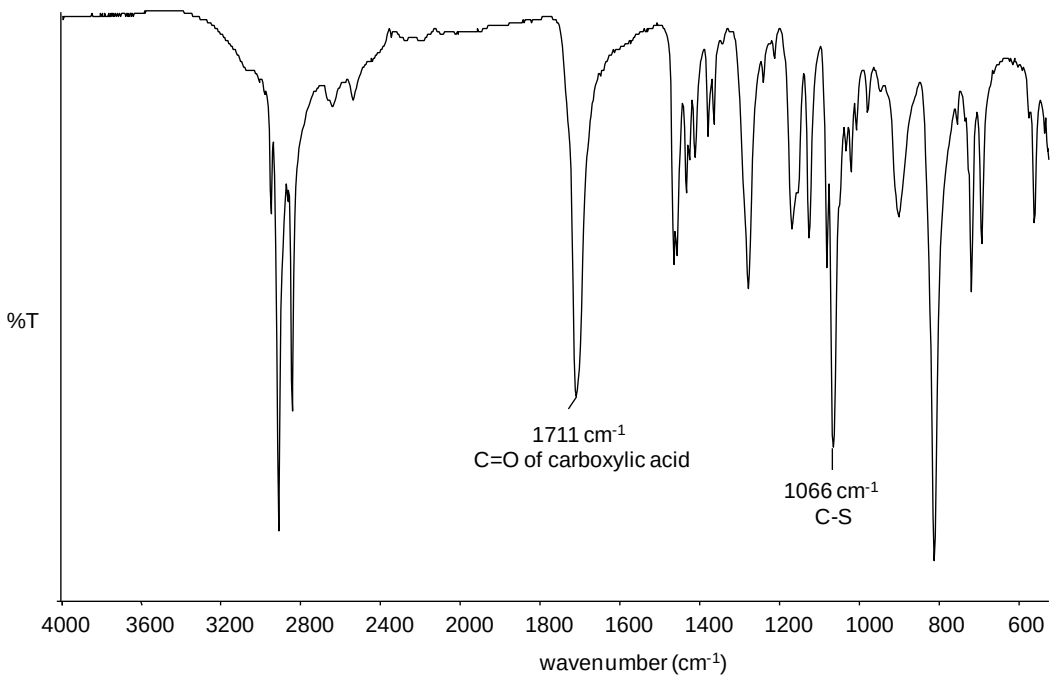

Figure S11.FTIR spectrum of S-1-dodecyl-S'-(α,α'-dimethyl-α''-acetic acid)trithiocarbonate

(B) Coupling reaction between poly(ethylene oxide) (PEO) and *S*-1-dodecyl-*S'*-(*α,α'*-dimethyl-*α"*-acetic acid)trithiocarbonate (DMT) to obtain PEO-CTA

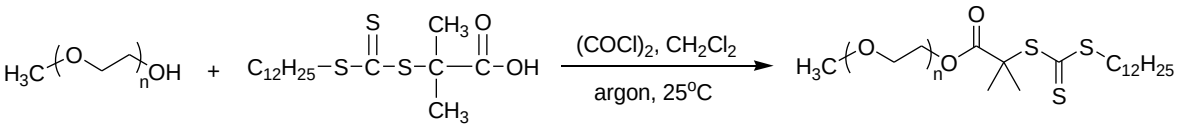

Figure S12. Synthesis of PEO-CTA

Oxalyl chloride (0.68 mL, 7.86 x 10^{-3} mol) and *S*-1-dodecyl-*S'*-(*α,α'*-dimethyl-*α"*-acetic acid)trithiocarbonate (0.54 g, 1.48 x 10^{-3} mol) were added in dried CH_2Cl_2 (5.0 mL). The reaction mixture was refluxed with stirring under argon atmosphere at 25^{o}C until gas evolution ceased (3 h). After removal of the excess reagents *in vacuo,* dried CH_2Cl_2 (15 mL) and PEO (1.50 g, 7.5 x 10^{-4} mol) were added into the residue. The reaction was continuously stirred for 24 h under argon atmosphere at 25^{o}C. The resultant product was precipitated from the mixture by addition of n-hexane in the solution. The product was filtrated and dried in a

vacuum oven to give a yellow solid. Yield: 75.31 %. ^{1}H NMR (400 MHz, $CDCl_3$) δ_H: 0.88 (t, 3H,-CH_2-C**H**$_3$)**,** 1.25 (20H, CH_3-(C**H**$_2$)$_{10}$-CH_2-S), 1.70 (s, 6H, -C(C**H**$_3$)$_2$-S-C(S)-S-), 3.26 (t, 2H, -S-C(S)-C**H**$_2$-CH_2-), 3.39 (s, 3H, C**H**$_3$O(CH_2-CH_2-O$_{44}$-), 3.65 (m, CH_3O(C**H**$_2$-C**H**$_2$O)$_{44}$), 4.25 (t, 2H,-C**H**$_2$-OC(O)-C(CH_3)$_2$-S-C(S)-S-). The functionalization yield was 99.34 %, determined by ^{1}H NMR from the relative intensity of the chemical shift at *δ = 4.25 ppm* (t, 2H,-C**H**$_2$-OC(O)-C(CH_3)$_2$-S-C(S)-S-) and *δ = 0.88 ppm* (t, 3H,-CH_2-C**H**$_3$).

The functionalization yield

= [Integration area at *4.25 ppm*/(2 protons)]/ [Integration area at *0.88 ppm*/(3 protons)] x 100

= [(2/2)/(3.02/3)] x 100

= 99.34%

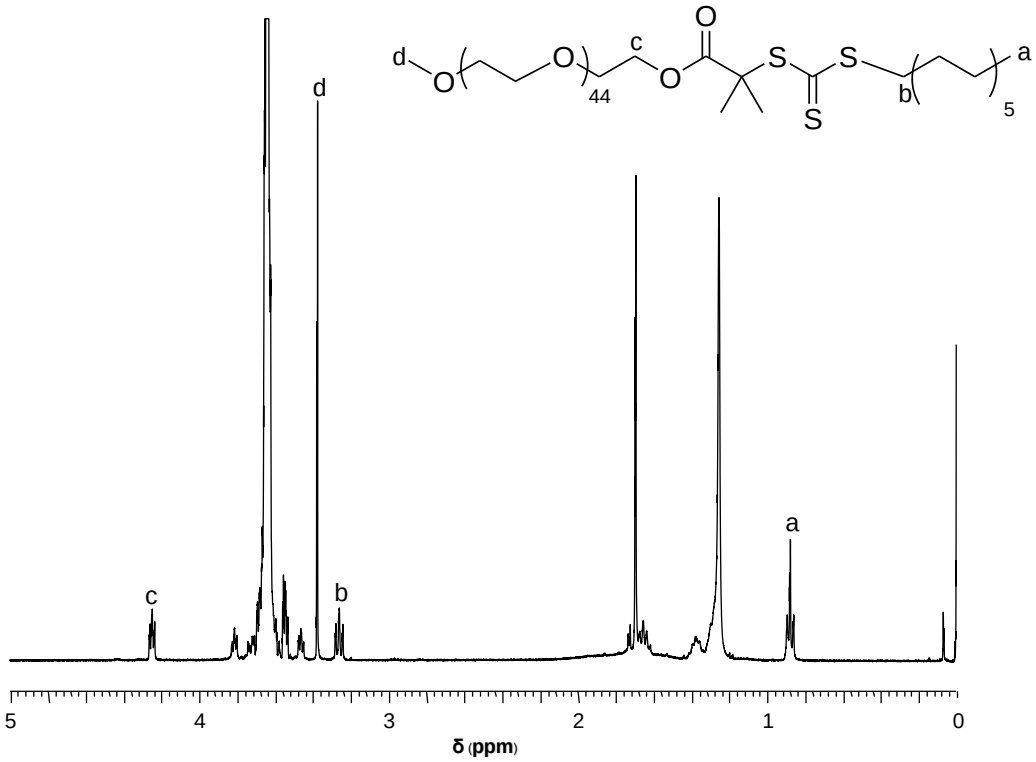

Figure S13.^{1}H NMR spectrum of PEO-CTA in $CDCl_3$

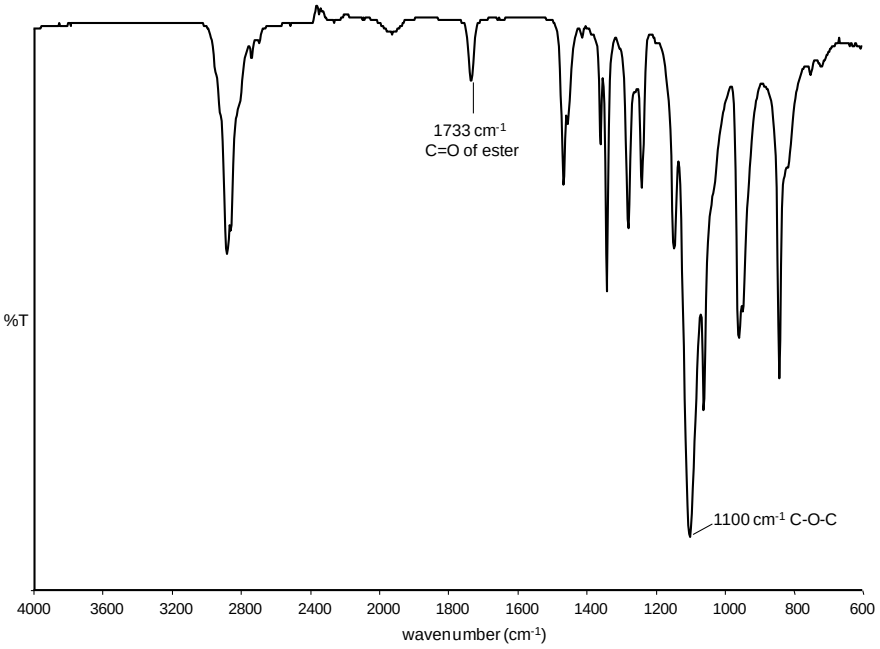

Figure S14. FTIR spectrum of PEO-CTA

Part 3. Study in adsorption percentages of the copolymer-MNP nanoclusters with antibody

(A) Characterizations of the copolymer-MNP nanoclusters adsorbed with anti-rabbit-IgG antibody

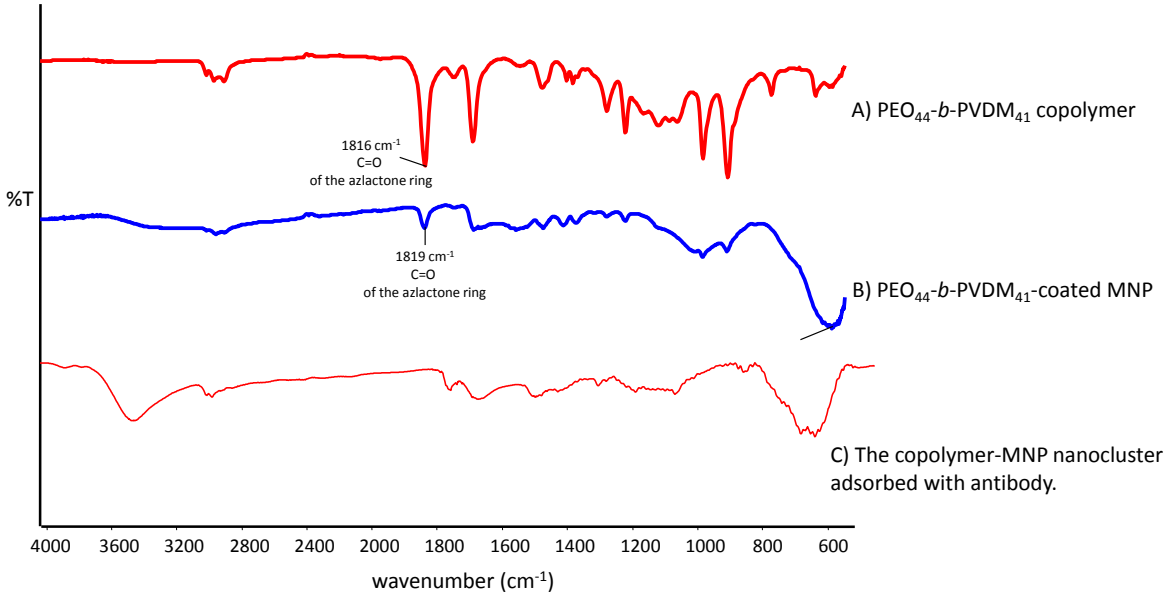

Figure S15. FTIR spectra of A) PEO_{44}-*b*-$PVDM_{41}$ copolymers, B) PEO_{44}-*b*-$PVDM_{41}$-MNP nanoclusters and C) the copolymer-MNP nanocluster adsorbed with antibody.

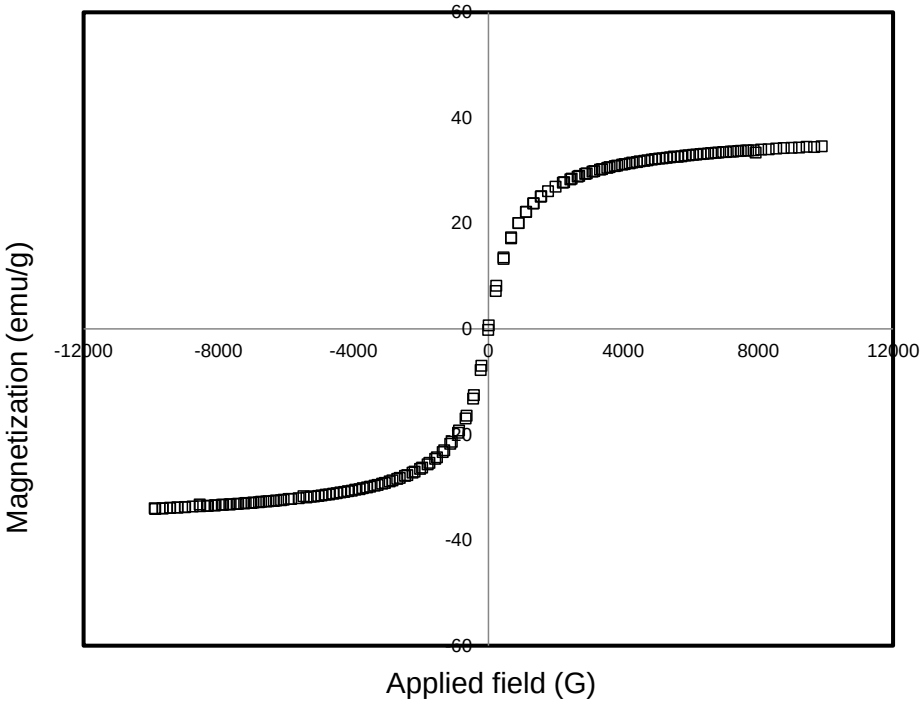

Figure S16. *M-H* curve of PEO_{44}-*b*-$PVDM_{41}$ copolymer-MNP nanocluster adsorbed with antibody.

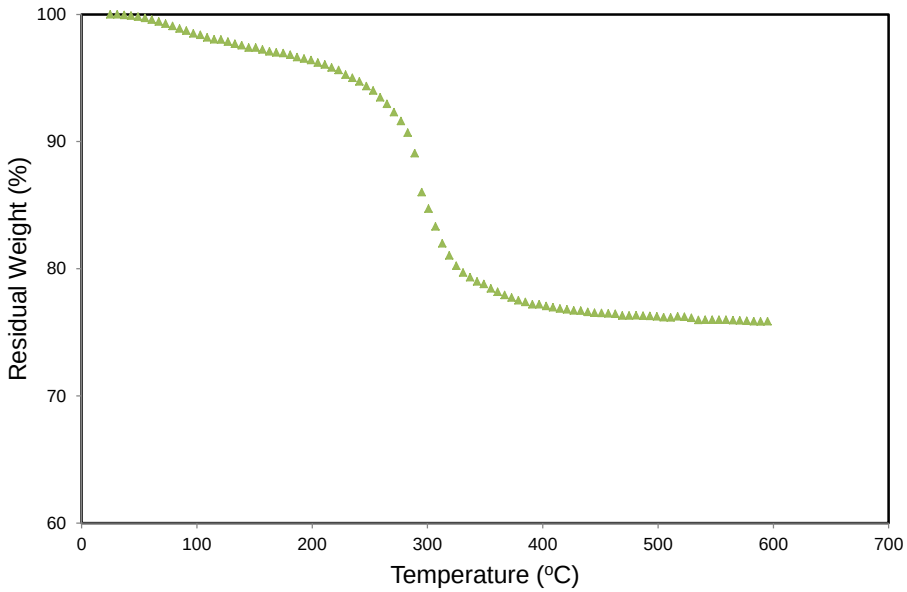

Figure S17. The TGA thermogram of PEO_{44}-*b*-$PVDM_{41}$ copolymer-MNP nanocluster adsorbed with antibody.

(B) Calibration curve of BGG

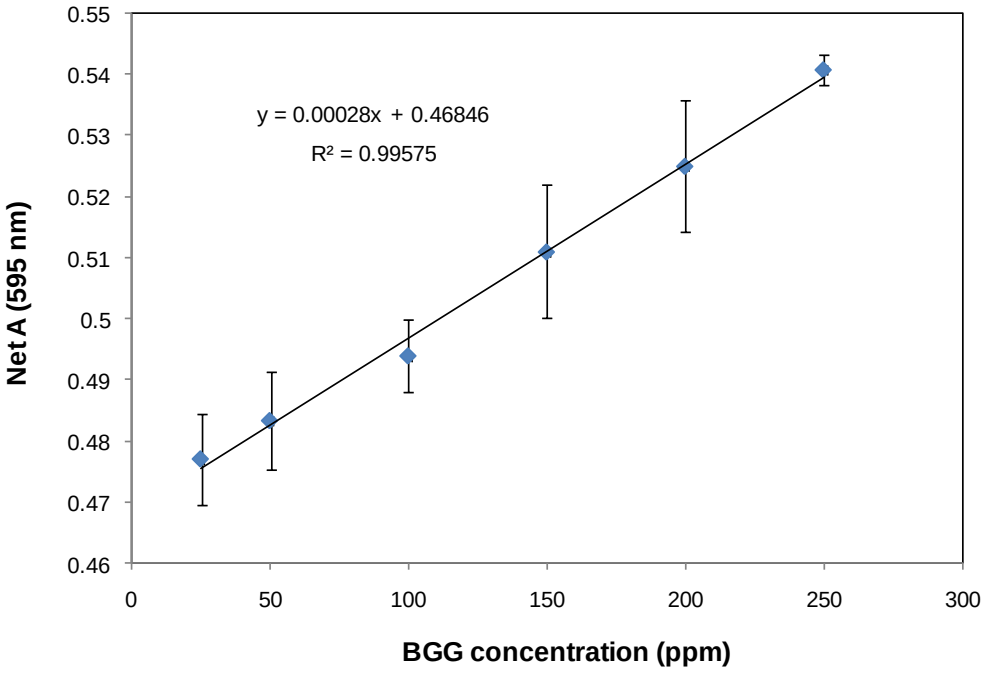

Figure S18. The calibration curve of BGG

Part 4. FTIR spectrum of bare MNP

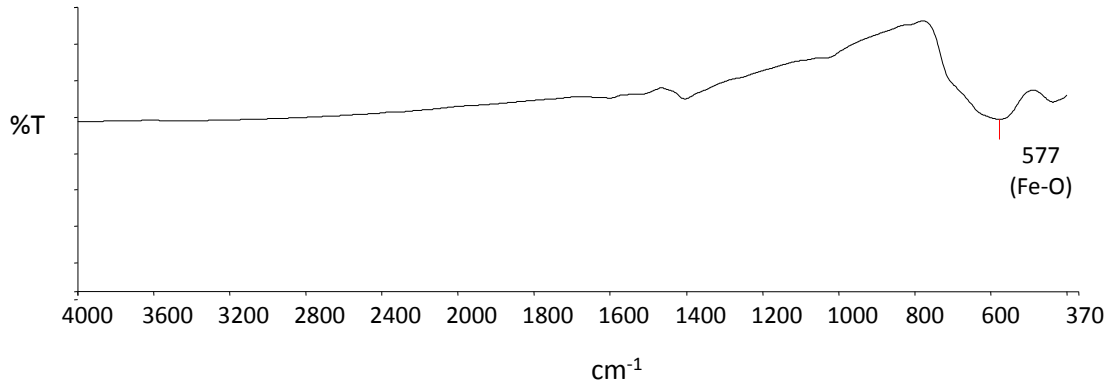

Part 5. TEM images of the nanoclusters before and after coating with the copolymers

TEM images of PEO_{44}-*b*-$PVDM_{21}$-MNP nanoclusters

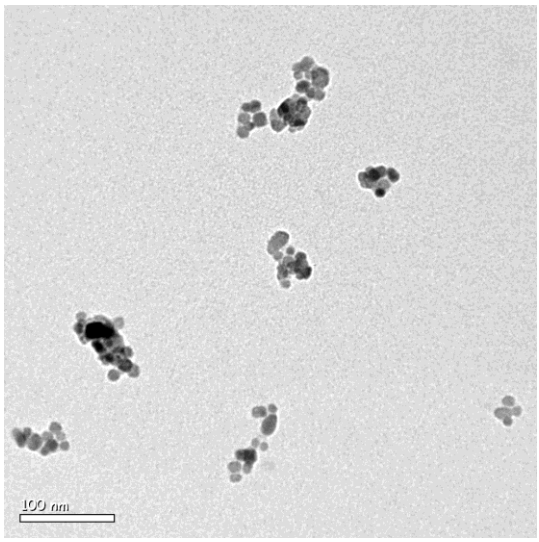

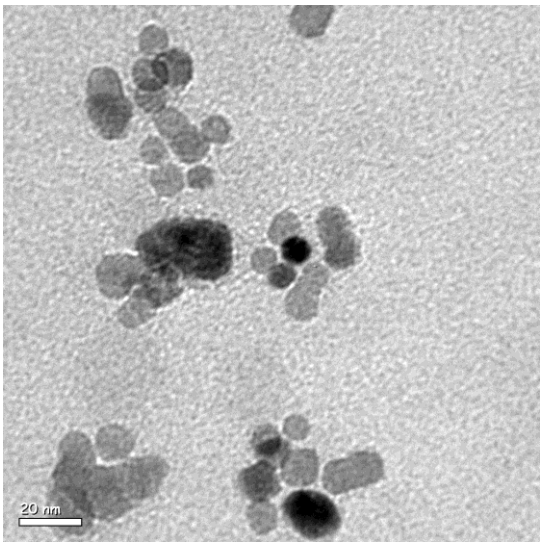

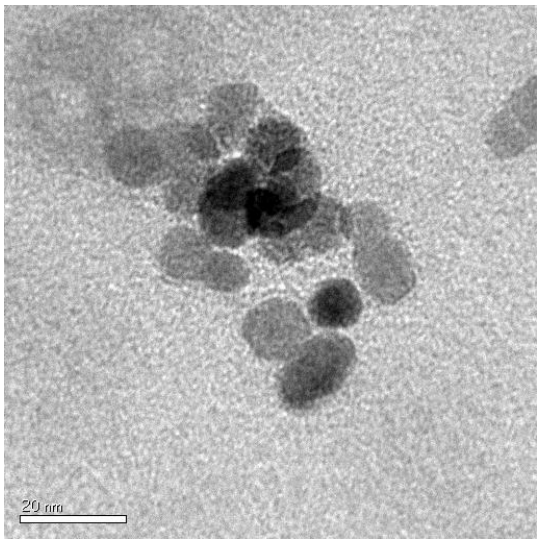

TEM images of PEO_{44}-*b*-$PVDM_{41}$-MNP nanoclusters

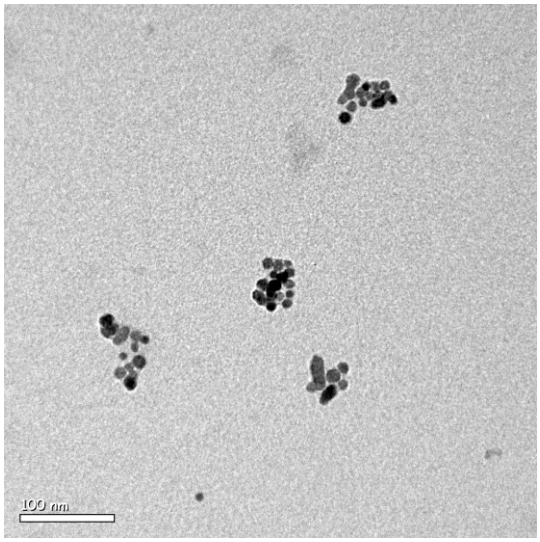

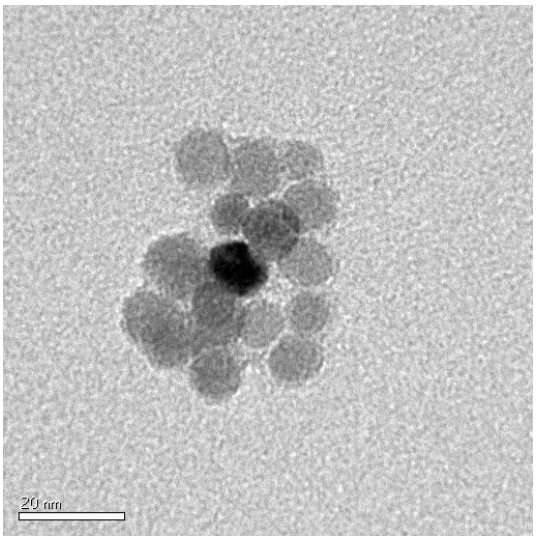

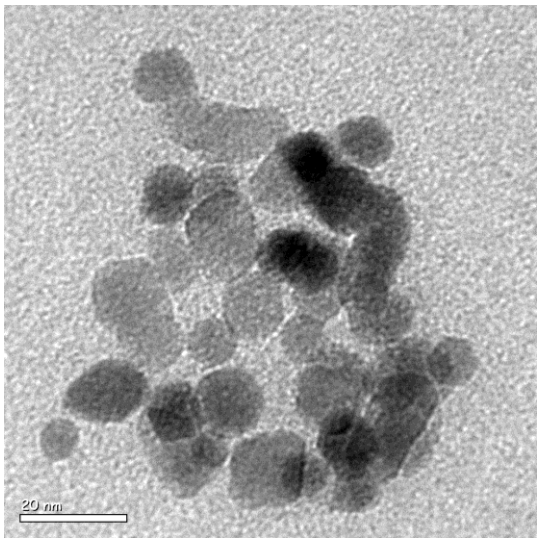

TEM images of PEO_{44}-*b*-$PVDM_{84}$-MNP nanoclusters

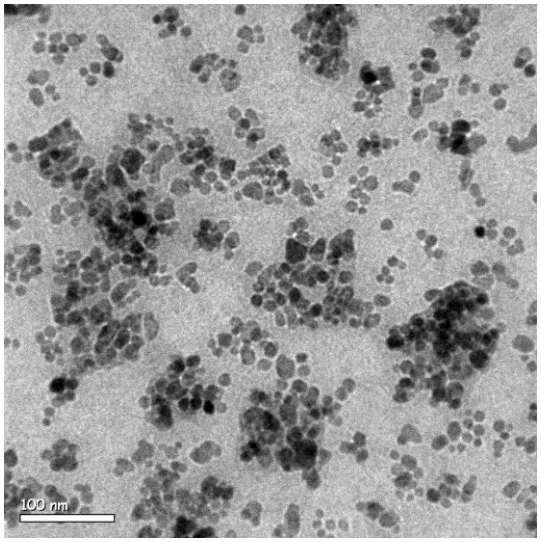

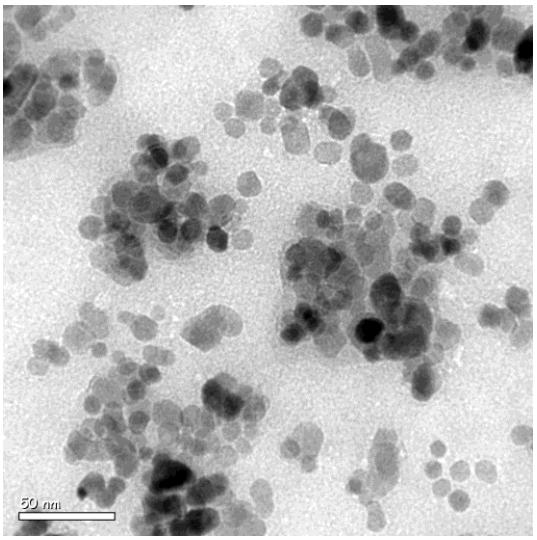

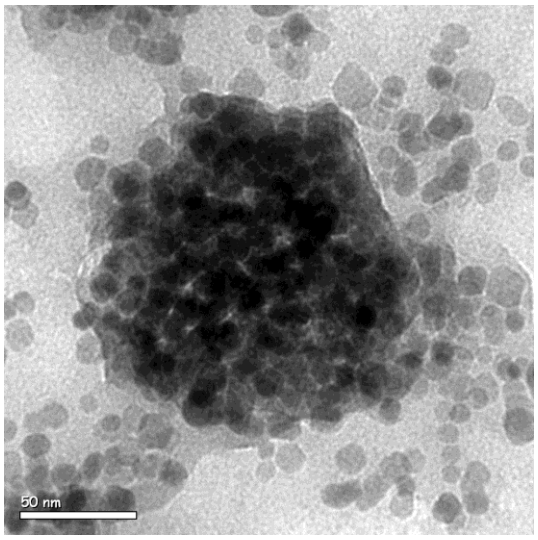

TEM images of the particles before grafting with the copolymers

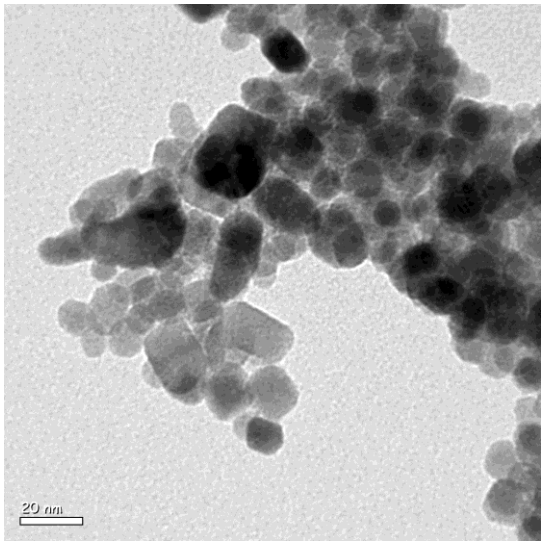

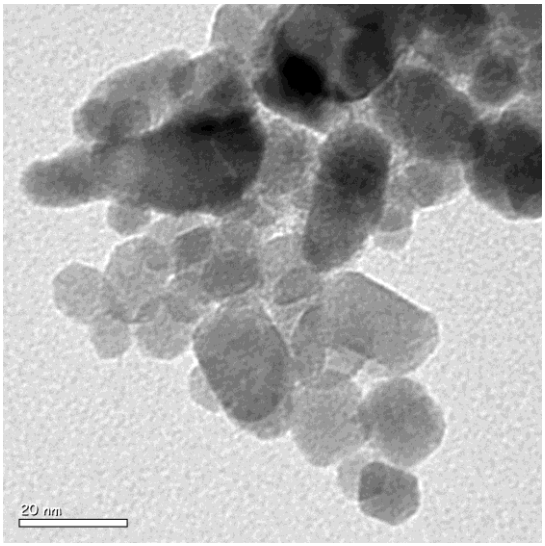

Chapter III

Effect of alkyl chain lengths on the assemblies of magnetic nanoparticles coated with multi-functional thiolactone-containing copolymer

Abstract

This work presents the synthesis of magnetite nanoparticle (MNP) coated with poly(N,N-diethylaminoethyl methacrylate)-*b*-poly(N-isopropyl acrylamide-*st*-thiolactone acrylamide) (PDEAEMA-*b*-P(NIPAAm-*st*-TlaAm) copolymer and its use in controlled drug release and bio-conjugation. TlaAm units in the copolymer were ring-opened with various alkyl amines to form thiol groups (-SH), followed by thiol-ene coupling reactions with acrylamide-coated MNP and then quaternized to obtain cationic copolymer-MNP assemblies (the size < 200 nm/cluster). The use of alkyl amines having various chain lengths (e.g. 1-propylamine, 1-octylamine or 1-dodecylamine) in the nucleophilic ring-opening reactions of the thiolactone rings affected their magnetic separation ability, water dispersibility and release rate of doxorubicin model drug. In all cases, when increasing the temperature, they showed a thermo-responsive behavior as indicated by the decrease in hydrodynamic size and the accelerated drug release rate. These copolymer-MNP assemblies could be used as a novel platform with thermal-triggering controlled drug release and capability for adsorption with any negatively charged biomolecules.

Keywords: magnetic, nanoparticle, assembly, thiolactone, thermo-responsive

Introduction

In recent years, magnetite nanoparticle (MNP) has extensively attracted interest owing to their superparamagnetic properties and their potential applications in various fields. Incorporation of MNP into various organic nano-assemblies has been investigated by features of their intriguing biomedical applications, such as remotely controlled drug release, magnetically guidable drug delivery (Sahoo et al. 2013; Wang et al. 2013; Li et al. 2006), magnetic resonance imaging (MRI) (Mahmoud et al. 1999; Hu et al. 2013), and hyperthermia cancer treatment delivery (Qu et al. 2014; Chen et al. 2015; Singh et al. 2014). However, it tends to aggregate to each other mainly owing to dipole-dipole and magnetic attractive forces, leading the loss in nano-scale related properties and a decrease in the surface area/volume ratio (Lim et al. 2013). Grafting long-chain polymers onto MNP surface is currently one of the promising approaches to realize its dispersibility in the media due to charge repulsion of ionic surface or steric repulsion of long chain surfactant (Chen et al. 2012; Mekkapat et al. 2013). In addition, this polymeric coating can also serve as a platform for conjugation of biomolecules of interest on the MNP surface (Leung et al. 2013; Machida et al. 2014; Prabha and Raj 2016; Ulbrich et al. 2016).

Many works have now extensively reported in the MNP polymeric coating accomplished either *via* "grafting from" or "grafting to" strategies (Qin et al. 2004; Wang et al. 2008) with controlled radical polymerization (CRP) techniques. CRP technique produces well controllable polymer architecture on particle surface because it can control molecular weight, polydispersity, functionality and composition distribution of polymers (Braunecker and Matyjaszewski 2007). Three general techniques of CRP include nitroxide-mediated polymerization (NMP) (Sciannamea et al. 2008), atom transfer radical polymerization (ATRP) (Matyjaszewski 2012; Huang et al. 2017), reversible addition fragmentation chain transfer polymerization (RAFT) (Moad et al. 2008; Hill et al. 2015). Being of our particular interest, RAFT as opposed to other CRP techniques can be performed in various kinds of solvent, wide range of temperature, no need of metals used for polymerization and large range of monomer classes (Willcock and O'Reilly 2010).

This present work reports the synthesis of a multifunctional copolymer *via* RAFT for coating onto the surface of MNP and its use in drug controlled release and bio-conjugation. This copolymer was well designed to have multi-functions including; 1) thermo-responsive poly(N-isopropylacrylamide) (PNIPAAm) serving as a drug reservoir with a temperature-

triggering mechanism, 2) thiolactone moiety for covalent grafting with MNP surface and tuning degree of hydrophobicity of the copolymer, and 3) positively charged poly(N,N-diethylamino-2-ethylmethacrylate) (PDEAEMA) for improving its water dispersibility and ionic adsorption with anionic bio-entities. PNIPAAm responded to the change of the environmental temperature due to the phase separation when crossing its lower critical solution temperature (LCST = 30-34 °C) (Gandhi et al. 2015). When raising the temperature above its LCST, the copolymer was in the collapse state due to the formation of the intramolecular hydrogen bonding among the polymer chains. In contrast, it swelled at the temperature below its LCST owing to the intermolecular hydrogen bonding between water molecules and polymer chains (Du et al. 2010; Bischofberger and Trappe 2015; Patil and Wadgaonkar 2017; Rodkate and Rutnakornpituk 2016; Meerod et al. 2015).

The reactions involving thiol chemistry has now gain a great attention because thiols (-SH) are highly reactive nucleophiles for the reactions with epoxide, alkyl halides, and double or triple bonds (Espeel and Du Prez 2015; Stamenovi et al. 2011). However, the applications of thiols are rather limited because they have a short shelf life due to the oxidation reaction resulting in disulfide formation (Espeel et al. 2012). A promising approach to overcome this limitation is to use a reactive thiolactone, a cyclic thioester, as a latent thiol functional group. This reaction involves a ring-opening reaction of thiolactone moieties to obtain thiol functionality (-SH), subsequently reacting with electrophiles for the second modification in one-pot reaction (Espeel and Du Prez 2015; Chen et al. 2014; Reinicke et al. 2013; Espeel et al. 2011). Many works from Du Prez's research group have reported the use of thiolactone for the double modification purpose (Espeel and Du Prez 2015; Stamenovi et al. 2011; Espeel et al. 2012; Chen et al. 2014; Reinicke et al. 2013; Espeel et al. 2011).

In this report, we describe a synthesis of a thermo-responsive multifunctional diblock copolymer containing thiolactone acrylamide (TlaAm) units for coating on MNP surface and its use for drug controlled release and bio-conjugation applications. PDEAEMA synthesized *via* RAFT polymerization was used as a macro chain transfer agent (CTA) for a chain extension of PNIPAAm-*st*-PTlAm second block. PTlAm units were ring opened by alkyl amines to form thiol groups, which were subsequently reacted with the acrylamide-coated MNP to obtain the copolymer-coated particle. PDEAEMA block was then quaternized to obtain cationic MNP to improve the water dispersibility of the particle and for ionic adsorption with negative bio-entities. The effect of alkyl chain lengths (C3, C8 and C12) on

the assemblies of the copolymer-coated MNP, affecting their water dispersibility and magnetic separation ability, was investigated. Moreover, the temperature change and the effect of alkyl chain lengths on the rate of the drug release (doxorubicin as a model drug) were also studied (Fig. 1).

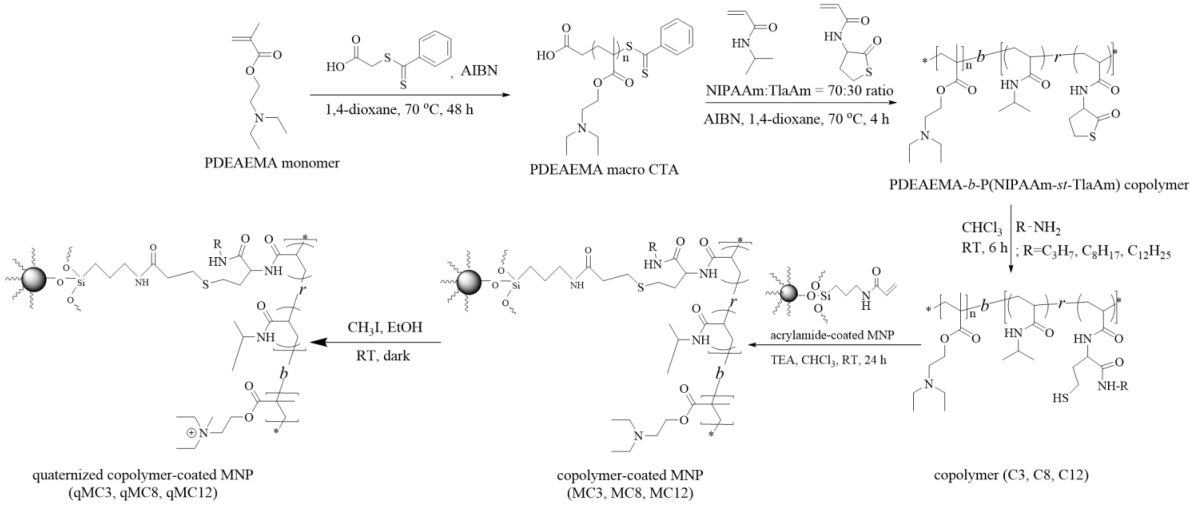

Fig. 1 Synthetic scheme of the copolymer-coated MNP (MC) and its quaternization (qMC)

Experimental

Materials

Unless otherwise stated, the reagents were used without purification: iron(III) acetylacetonate ($Fe(acac)_3$, 99%, Acros), aminopropyltriethoxysilane (APTES, 99%, Acros), *D,L*-homocysteine thiolactone hydrochloride (99%, Acros), oleic acid (Carlo Erba), (3-aminopropyl) triethoxysilane (APTES, 99%, Acros), triethylamine (TEA, 97%, Carlo Erba), 2,2'-azobis(2-methylpropionitrile) (AIBN, 98%, Sigma-Aldrich), s-(thiobenzoyl) thioglycolic acid as a chain transfer agent (99%, Aldrich), 2-(diethylamino) ethyl methacrylate (DEAEMA, 99% stabilized, Acros), and *N*-isopropylacrylamide (NIPAAm, 99%, Acros) were used as received. Acryloyl chloride was synthesized prior to use *via* a chloride exchange reaction between acrylic acid (98%, Acros) and benzoyl chloride (99%, Acros) to obtain a colorless liquid with 60% yield. 1-Propylamine (99%, Sigma-Aldrich), 1-octylamine (99%, Merck), 1-dodecylamine (98%, Acros) and iodomethane (2.0 M in tert-butyl methyl ether, Sigma-Aldrich) were used as received. Doxorubicin hydrochloride (DOX, 2 mg/ml, Pharmachemie BV) were used as received.

Synthesis of N-thiolactone acrylamide (TlaAm) monomer (Reinicke et al. 2013)

To the mixture of *D,L*-homocysteine thiolactone hydrochloride (7.05 g, 45.6 mmol) in a H_2O/1,4-dioxane solution (100 ml), $NaHCO_3$ (19.20 g, 227.9 mmol) was added and stirred for 30 min in an ice bath. Acryloyl chloride (8.3 g, 91.2 mmol) was then added dropwise and stirred at room temperature overnight. After the reaction completed, brine (100 ml) was added into the solution, followed by extracting with ethyl acetate (3×200 ml) to obtain TlaAm in an organic layer. Finally, TlaAm monomer was purified by recrystallization from CH_2Cl_2 and then dried *in vacuo*.

Synthesis of acrylamide-coated MNP

MNP was synthesized *via* a thermal decomposition method of $Fe(acac)_3$ (5 g, 14.1 mmol) in 90 ml benzyl alcohol at 180 °C for 48 h. Then, the particle was magnetically separated and washed with ethanol and then chloroform. Oleic acid (4 ml) was slowly added to the MNP-toluene dispersion (30 ml) with sonication to form oleic acid-coated MNP, followed by an addition of APTES (4 ml) containing TEA (2 ml) to form amino-coated MNP. After stirring for 24 h, the particles were precipitated in ethanol and washed with toluene. After re-dispersing the particles (0.1 g) in a NaOH solution (6.72 mmol in 10 ml DI), acryloyl chloride (3.36 g, 37.1 mmol) was then added to the dispersion and stirred for 24 h. The product was magnetically separated, repeatedly washed with water and then stored in the form of dispersions in THF (0.1 g MNP/1 ml).

Synthesis of PDEAEMA macro chain transfer agent (PDEAEMA macro CTA)

DEAEMA monomer (1.9361 g, 10.4 mmol), S-(thiobenzoyl) thioglycolic acid (31.7 mg, 0.1 mmol) as CTA and AIBN initiator (4.9 mg, 0.03 mmol) ($[DEAEMA]_0$:[CTA]:[AIBN] molar ratio of 70:1:0.2, respectively) were dissolved in 1,4-dioxane (7 ml) under N_2 atmosphere with stirring for 30 min. The RAFT polymerization was performed for 48 h at 70 °C to obtain *c*a.50% monomer conversion with $\overline{M_n}$ of PDEAEMA about 6,700 g/mol (Supplementary material Fig. S1). The polymerization was ceased by cooling at room temperature in air. The PDEAEMA macro CTA was purified by dialysis in methanol and dried *in vacuo*.

Synthesis of PDEAEMA-b-P(NIPAAm-st-TlaAm) block copolymer

PDEAEMA macro CTA (0.06 mmol), NIPAAm (4.24 mmol), TlaAm (1.82 mmol) and AIBN initiator (0.01 mmol) ($[NIPAAm]_0$:$[TlaAm]_0$:[PDEAEMA macro CTA]:[AIBN] molar ratio of 70:30:1:0.2, respectively) was dissolved in 1,4-dioxane (8.5 ml) under N_2 atmosphere with stirring for 30 min. The RAFT polymerization was performed at 70 °C for 4 h to obtain *ca*.50% NIPAAm conversion and 30% TlaAm conversion with $\overline{M_n}$ of the copolymer about 12,200 g/mol (Supplementary material Fig. S2). The polymerization was stopped by cooling at room temperature with air. The copolymer was purified by dialysis in methanol and dried *in vacuo*.

Synthesis of the copolymer-coated MNP by a double modification of PDEAEMA-b-P(NIPAAm-st-TlaAm) copolymer

The copolymer (0.16 mmol of TlaAm unit) was dissolved in chloroform (5 ml) followed by an addition of primary alkylamines (0.32 mmol, 2:1 molar ratio of alkyl amine to TlaAm unit), e.g. 1-propylamine, 1-octylamine and 1-dodecylamine, to obtain the C3, C8 and C12 copolymers, respectively. The solution was then mixed with the acrylamide-coated MNP (100 mg) and TEA (0.1 ml) and stirred for 24 h under N_2 gas. The copolymer-coated MNP was magnetically separated and washed with chloroform and designated as MC3, MC8 and MC12, respectively.

Quaternization of PDEAEMA in the copolymer-coated MNP

The copolymer-coated MNP (1.76 mmol of DEAEMA units) was re-dispersed in ethanol (40 ml), followed by dropwise addition of 2M CH_3I solution (1.76 mmol). The mixture was stirred for 20 h in dark at room temperature. The quaternized products (qMC3, qMC8 and qMC12) were magnetically separated and washed with THF to remove an excess of CH_3I, followed by drying *in vacuo* to obtain black powder.

In vitro release studies of entrapped DOX from the copolymer-coated MNP

The drug solution (2 mg/ml of DOX) was added dropwise into the quaternized MNP dispersions (10 mg/2 ml in DI water) with stirring at 15 ^oC for 3 h. The DOX-entrapped MNP was separated from an excess DOX by magnetic separation for 30 min and washed with DI water for 4 times. The dispersion of DOX-entrapped MNP (10 mg in 3 mL DI water) was

placed in a water bath at 25 °C (below LCST of PNIPAAm) for 1 h and then temperature was increased to 45 °C (above LCST of PNIPAAm) for another 80 min. During the experiment, 0.2 ml of the dispersions was withdrawn from the release media at a pre-determined time until the released drug reached the equilibrium (the total time points ranging between 12 and 15). After 30-min magnetic separation, the concentrations of the released drug in the supernatant at a given time were determined *via* UV-visible spectrophotometry at λ= 480 nm and % drug release was calculated from the following equation;

$$\%\ \text{drug released} = \frac{\text{Weight of released drug at a given time}}{\text{Weight of the entrapped drug in the MNP}} \text{ x } 100$$

where the weight of the entrapped drug in the MNP was determined from the amount of the drug at the maximum point of the release profile combined with those remaining in the particles. To dissolve the remaining drug from the MNP, DI water (3 ml) was added to the particles and then the mixture was heated at 50 ^{o}C for 1 h. After 30-min magnetic separation, the drug concentration in the supernatant was then determined *via* UV-visible spectrophotometry. The drug entrapment efficiency was calculated from the following equation;

$$\text{Entrapment efficiency (\%EE)} = \frac{\text{weight of the entrapped drug in the MNP}}{\text{weight of the loaded drug}} \text{ x } 100$$

Characterization

FTIR spectrophotometry was operated on a Perkin–Elmer Model 1600 Series FTIR spectrophotometer. ^{1}H NMR spectroscopy was performed on a 400 MHz Bruker NMR spectrometer using DMSO-d_6 or $CDCl_3$ as solvents. The hydrodynamic diameter (D_h) and zeta potential of the particles were measured by PCS using NanoZS4700 nanoseries Malvern instrument. The sample dispersions were sonicated for 1 h before each measurement without filtration. The TEM images were conducted using a Philips Tecnai 12 operated at 120 kV equipped with Gatan model 782 CCD camera. The particles were re-dispersed in water and then sonicated before deposition on a TEM grid. TGA was performed on Mettler-Toledo's SDTA 851 at the temperature ranging between 50 and 800 °C and a heating rate of 20 °C/min under oxygen atmosphere. Magnetic properties of the particles were measured at room

temperature using a Standard 7403 Series, Lakeshore vibrating sample magnetometer (VSM). UV-visible spectrophotometry was performed on microplate reader at λ = 480 nm.

Results and Discussion

This work focused on the surface modification of MNP with multi-functional PDEAEMA-*b*-P(NIPAAm-*st*-TlaAm) copolymer to obtain magnetic nanocluster with thermo-responsive properties for drug controlled release application. The copolymer was synthesized *via* RAFT polymerization to control architecture and the molecular weight of the block copolymer. PDEAEMA macro CTA was first synthesized, followed by the extension of P(NIPAAm-*st*-TlaAm) second block from PDEAEMA first block. It was envisioned that the quaternized PDEAEMA could form the corona, while P(NIPAAm-*st*-TlaAm) block self-assembled to be a core in aqueous media. (Supplementary material Fig. S3). PTlaAm in the P(NIPAAm-*st*-TlaAm) allowed for a double modification for 1) adjustment of the degree of the hydrophobicity of the polymeric core and 2) immobilization of the polymer on MNP surface. This P(NIPAAm-*st*-TlaAm) core was also used for entrapment of a therapeutic drug with a thermo-triggering release mechanism owing to the existence of PNIPAAm in the structure. In addition, an optimal degree of hydrophilicity/hydrophobicity of the copolymer might be necessary for controlled release of the entrapped drug. Therefore, three different alkyl chain lengths (C3, C8 and C12) were used for tuning the degree of the hydrophobicity of the copolymer coated on the particle surface.

Synthesis and characterization of the copolymer-coated MNP

^{1}H NMR spectra of the purified products from each step were shown in Fig. 2. The signals corresponding to the methylene protons of PDEAEMA macro CTA (1.8-1.9 ppm) indicated the polymerization of PDEAEMA (Fig. 2A). This macro CTA was then used for the propagation of NIPAAm and TlaAm monomers. The new signals at δ 1.1 and 3.6 ppm of the NIPAAm units and at δ 3.2 and 4.7 ppm of TlaAm units indicated the propagation of both monomers from PDEAEMA macro CTA (Fig. 2B). After the ring-opening reactions of thiolactone units with various alkylamines (1-propylamine, 1-octylamine and 1-dodecylamine), the strong signals of the protons of alkyl groups appeared in the range of δ 0.9- 1.4 ppm (Fig. 2C, 2D, and 2E). In good agreement with this result, the disappearance of TlaAm signals at δ 3.3-3.4 ppm (signal *k* in Fig. 2B) and δ 4.7 (signal *i* in Fig. 2B), indicating the successful ring-opening reactions of thiolactone moiety in the copolymers. In addition,

the results from FTIR were also in good agreement with those obtained from ^{1}H NMR (Supplementary material Fig. S4).

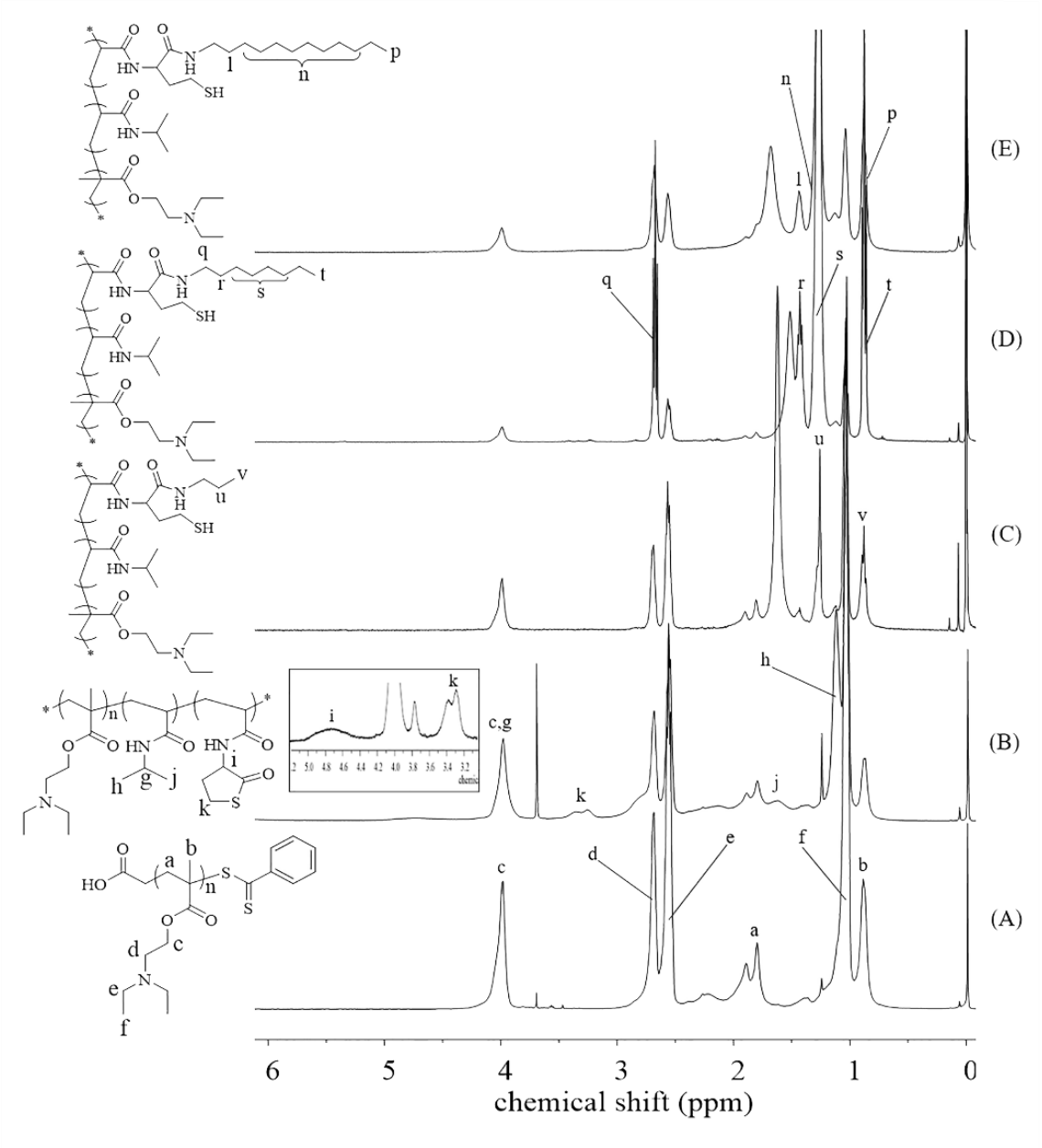

Fig. 2 ^{1}H NMR spectra of (A) PDEAEMA macro CTA, (B) PDEAEMA-*b*-P(NIPAAm-*st*-TlaAm) copolymers before the ring-opening reaction, and after the ring-opening reactions with (C) 1-propylamine, (D) 1-octylamine, and (E) 1-dodecylamine

After the ring-opening reaction of thiolactone rings in the copolymers with alkylamines to form thiol groups (-SH), the acrylamide-coated MNP was subsequently added to the mixture allowing for the thiol-ene reaction (Lowe 2010). The proposed thiol-ene

reaction mechanism between the acrylamide on the MNP surface and thiol groups (-SH) of the copolymer is shown in Fig. 3. Figure 4 shows FTIR spectra of the acrylamide-coated MNP and the MNP coated with the copolymers after the thiol-ene reaction. The signal at 590 cm^{-1} corresponding to Fe-O bond in the MNP appeared in every sample (Fig. 4). Fig. 4B-4D show the characteristic adsorption signals of C=O stretching (1730 cm^{-1}), C-O stretching (1260 cm^{-1}) of carboxyl groups and C-C stretching (800 cm^{-1}) of the copolymer, signifying the existence of the copolymer on the particle surface through the thiol-ene reaction.

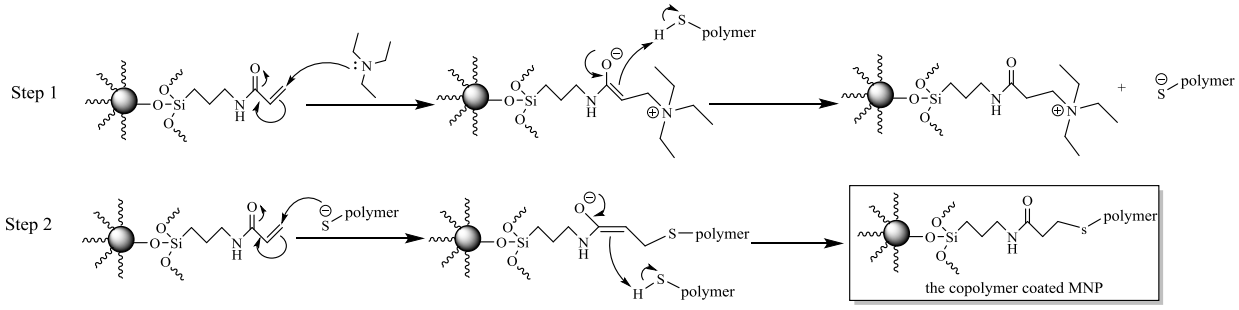

Fig. 3 The thiol-ene reaction mechanism between the acrylamide groups on the MNP surface and thiol groups of the copolymer

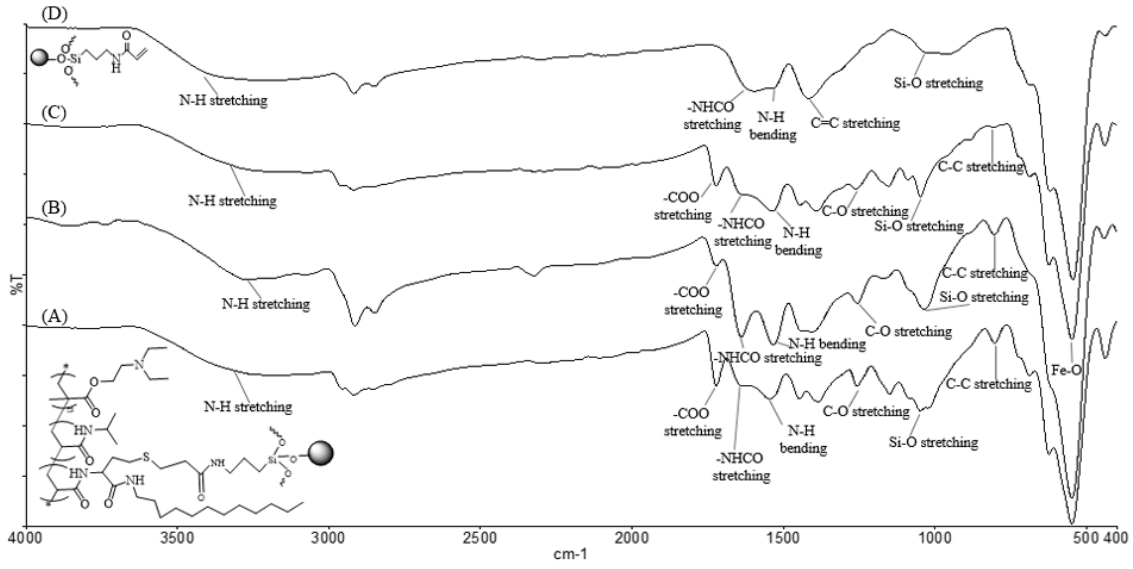

Fig. 4 FTIR spectra of (A) acrylamide-coated MNP, (B) MC3, (C) MC8, and (D) MC12

To study the organic/inorganic composition of the copoymer-coated MNP, TGA was used to determine the weight loss at 800 ^{o}C (Fig. 5A). It was hypothesized that the residue weight was the weight of iron oxide from oxidized MNP, while the loss weight was the organic conponents in the copolymer-MNP assemblies. The decrease of the residual weight

in the samples corresponded to the increase in the organic contents in the MNP. It was found that there was about 12% organic content in acrylamide-coated MNP, while after coating with the copolymer, there were 26%, 28% and 41% of the polymers in MC12, MC8 and MC3, respectively, signifying that MC3 had higher degree of alkyl substitution as compared to the other two. This was rationalized that the short alkyl chain length in the C3 copolymer might have less steric hindrance in the particle coating step, resulting in the better accessibility of the particles to react with the copolymers and thus higher amounts of the copolymers on the particles.

VSM technique was used to determine magnetic properties of the MNP before and after the copolymer coating (Fig. 5B). They well responded to an applied magnet and showed superparamagnetic behavior due to the absence of the coercitivity (H_c) and remanence (M_r) upon removal of an external magnetic field. The saturation magnetization (M_s) decreased from 58 emu/g of acrylamide-coated MNP to 56 emu/g of MC12, 54 emu/g of the MC8 and 31 emu/g of MC3, due to the presence of non-magnetic copolymer on the particle surface and thus the drop of their magnetic responsiveness. The decrease in the net magnetization corresponded well to the increase of the copolymers coated on the particles observed in TGA.

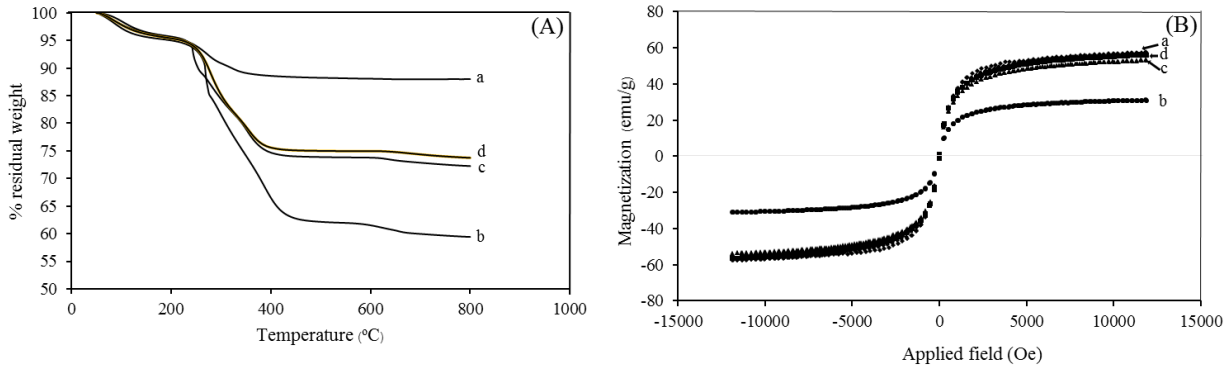

Fig. 5 (A) TGA thermograms and (B) *M-H* curves of (a) acrylamide-coated MNP, (b) MC3, (c) MC8 and (d) MC12

The copolymer-coated MNP was then quaternized to improve the particle dispersibility in water. Zeta potentials of the particle both before (MC3, MC8 and MC12) and after quaternization (qMC3, qMC8, and qMC12) were studied using PCS (Table 1). The zeta potentials of acrylamide-coated MNP before and after quaternization did not change because there was no copolymer coated on the MNP surface. After the copolymer coating, their zeta potential values of all copolymers significantly increased from 0 to 16-28 mV after quaternizations, owing to the formation of permanent positive charges of quaternary

ammonium groups in the copolymer-coated MNP. It should be noted that these positive charges might facilitate the particles to be well dispersible in an aqueous media, which was necessary for the use in drug controlled release applications discussed later in this report.

In addition, the preliminary studies in the use of the cationic MNP for ionic adsorption with negative bio-entities were also investigated. DNA tagged with 6-carboxytetramethyl rhodamine (TAMRA-5'-TACCACCATTC-3') was selected as a model compound to proof the idea of ionic adsorption capability of the particles. qMC12 (2 mg) as a representative was dispersed in 0.4 μM DNA solution (2 ml) and then stirred for 2 h, followed by magnetic separation. It was found that the concentrations of DNA in the solutions significantly decreased from 0.42 μM to 0.05 μM (Supplementary materials Fig. S5), indicating that the MNP can be used as a cationic platform for adsorption with DNA through the electrostatic interaction.

Table 1 Zeta potential values and hydrodynamic size (D_h) of the copolymer-coated MNP

Types of MNP	Zeta potential [mV]		D_h of quaternized particles [nm]	
	Before quaternization	After quaternization	at 25 °C	at 45 °C
Acrylamide-coated MNP	-15.3 ± 0.5	-15.3 ± 0.5	564 ± 63	506 ± 52
MC3	0	28.4 ± 1.0	1068 ± 197	396 ± 58
MC8	0	16.2 ± 0.6	836 ± 214	372 ± 103
MC12	0	26.3 ± 0.8	1426 ± 218	295 ± 0

Representative TEM images of acrylamide-coated MNP and the quaternized copolymer-coated MNP (qMC) prepared from aqueous dispersions are shown in Fig. 6. Acrylamide-coated MNP showed macroscopic aggregation due to the lack of polymer coating resulting in the particles with poor water dispersibility (Fig. 6A). After coating with the copolymer and then quaternization, formation of the nanoclusters with the size below 200

nm/cluster was observed (Fig. 6B-6D). They showed good dispersibility in water without noticeable aggregation after standing for 2 h (Fig. 7A). After 75 h, the qMC3 dispersion exhibited some aggregation, while those of qMC8 and qMC12 were insignificant. This was attributed to the higher degree of alkyl substitution of 1-propylamine in the copolymer due to less steric hindrance as compared to those of 1-octyl and 1-dodecylamines, resulting in the higher degree of hydrophobicity of the copolymer and consequently aggregating in water. The TGA result discussed above also supported this assumption that there was higher amount of the copolymer in qMC3, which might result in the higher degree of hydrophobicity as compared to qMC8 and qMC12.

The particle dispersibility in water shown Fig. 7A was in good agreement with their magnetic separation ability in water. After 5 min of magnetic separation, qMC3 can be completely separated while there were some dispersible particles remaining in qMC8 and qMC12 dispersions (Fig. 7B). Importantly, the completely separated ability of particles from the dispersion with an assistance of a magnet was necessary for the determination of the drug controlled release discussed later in this work.

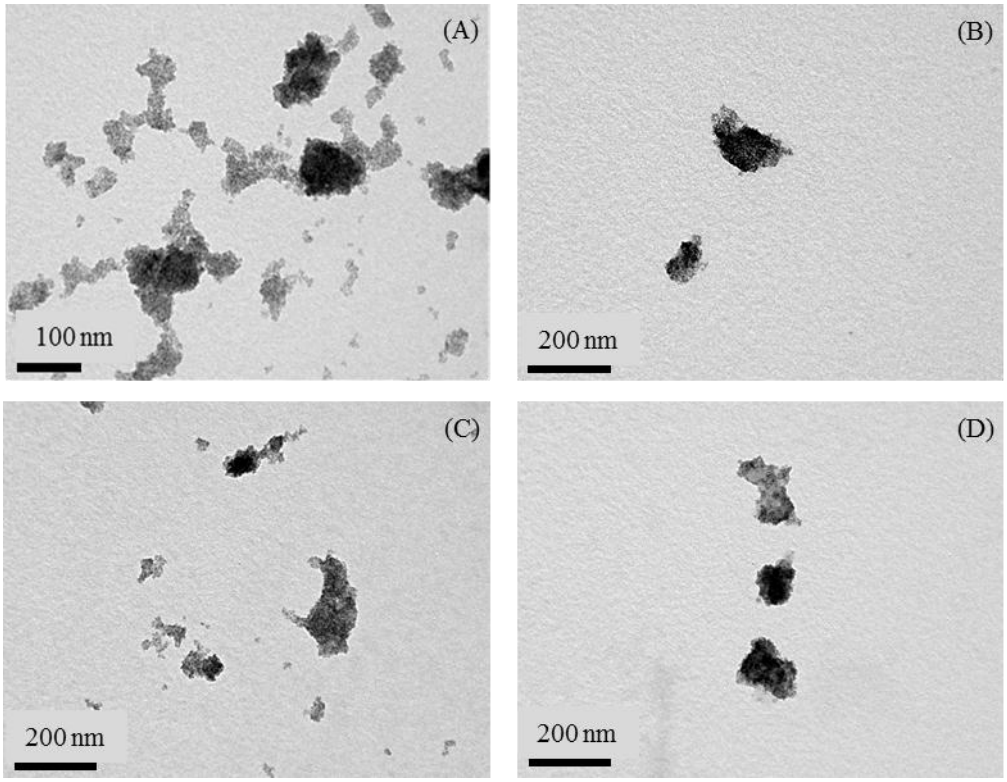

Fig. 6 TEM images of (A) acrylamide-coated MNP, (B) qMC3, (C) qMC8 and (D) qMC12 prepared from aqueous dispersions

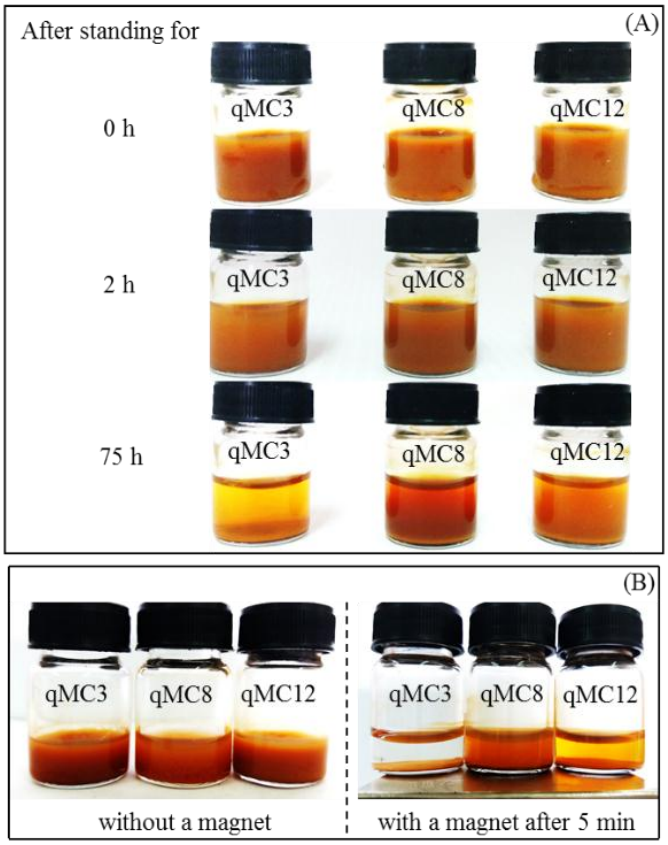

Fig. 7 (A) Water dispersibility and (B) magnetic separation ability of qMC3, qMC8 and qMC12

Because the copolymer coated on the particles in this work comprised thermo-responsive moieties of PNIPAAm and PDEAEMA, the effect of the change in the temperature on their D_h was investigated. The experimental temperatures were set at 25 ^oC and 45 ^oC, which crosses their critical solution temperature (LCST of PNIPAAm = 30-34 ^oC and LCST of PDEAEMA = 31 ^oC) (Gandhi et al. 2015; Maeda et al. 2004). It was found that, in all cases, D_h of the particle coated with the copolymers at 45 ^oC was smaller than those at 25 ^oC (Table 1). The copolymers collapsed at the temperature above its critical solution temperature, resulting in the shrinkage of the nanocluster and thus the decrease in their D_h. It should be noted that the shrinkage of the copolymer when heated to 45 ^oC would be utilized as a triggering mechanism for drug controlled release discussed in the later section.

In vitro release studies of entrapped DOX from the copolymer-coated MNP triggered by the temperature change

DOX, known as a chemotherapy medication used to treat cancer, was used as a model drug for entrapment in and then release from the copolymer-coated MNP. It was hypothesized that DOX was entrapped in the copolymer-coated particles due to the hydrogen bonding of DOX molecules with the copolymer. %EE of qMC3 was *ca*.5.4%, while those of qMC8 and qMC12 ranged between 10.3% and 10.8%. The two-fold lower percentage of qMC3 as compared to those of the other two samples was probably due to the higher degree of hydrophobicity in qMC3 (higher degree of alkyl substitution), which might result in less entrapment of DOX on the particles.

DOX release studies were performed at 25 ^{o}C with a step-wise increase in the temperature to 45 ^{o}C after the equilibrium (Fig. 8). In all cases, the release of DOX from the particle at 25 ^{o}C reached their equilibrium within 40 min and they were held at this temperature for 1 h to ensure the equilibrium. Generally, when the temperature of dispersion is increased above room temperature, the preloaded drug should mainly be released *via* a diffusion mechanism [Liu et al. 2010]. In this work, when increasing the temperature to 45 ^{o}C (above LCST of PNIPAAm), all samples (qMC3, qMC8 and qMC12) showed the same trend of the drug release. The increment of DOX release upon increasing the temperature was mainly attributed to "a diffusion mechanism". Interestingly, qMC8 and qMC12 showed the faster rate of DOX release with additional release of *ca*.8-10% and reached the equilibrium within 40 min. This accelerated release rate was attributed to "a squeezing mechanism" due to the collapse of PNIPAAm chains at above its LCST [Trongsatitkul and Budhlall 2013]. However, the release rate of DOX in qMC3 seemed to be retarded at the beginning of the elevated temperature and it was then slowly released afterward with additional DOX release of *ca.*11%. The higher degree of hydrophobicity in qMC3 discussed above might inhibit the squeezing behavior of PNIPAAm in the copolymer, which thus initially retarded the release of the entrapped drug from the particles at the elevated temperature (Fig. 9).

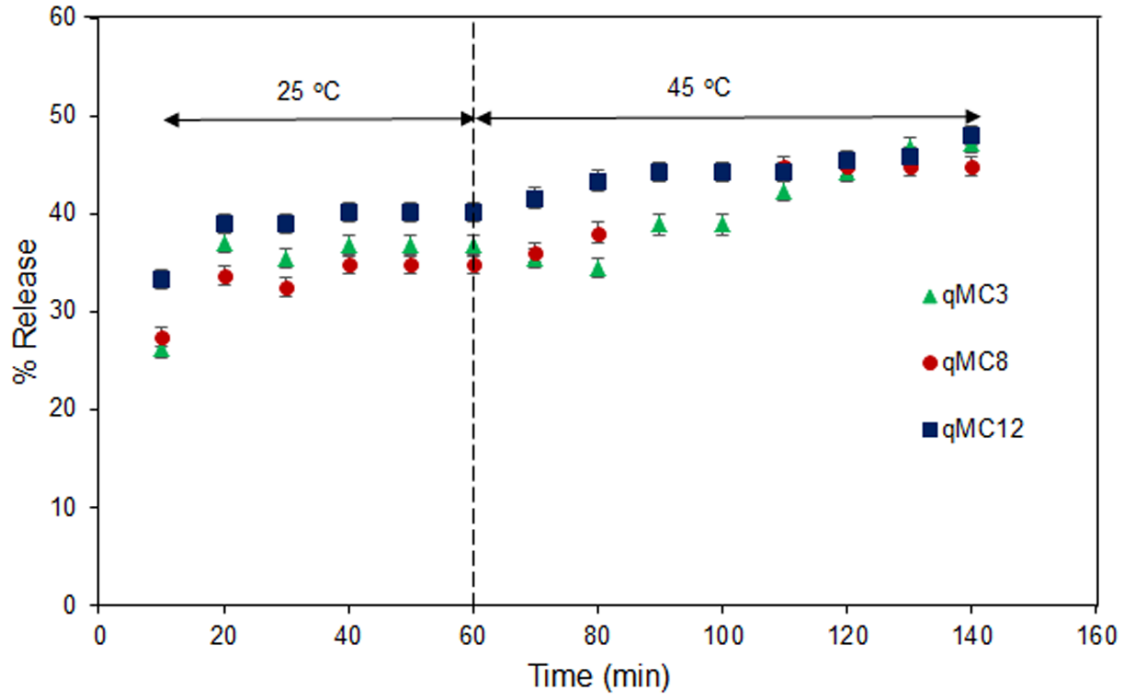

Fig. 8 DOX release profiles of the copolymer-coated MNP (qMC3, qMC6 and qMC12)

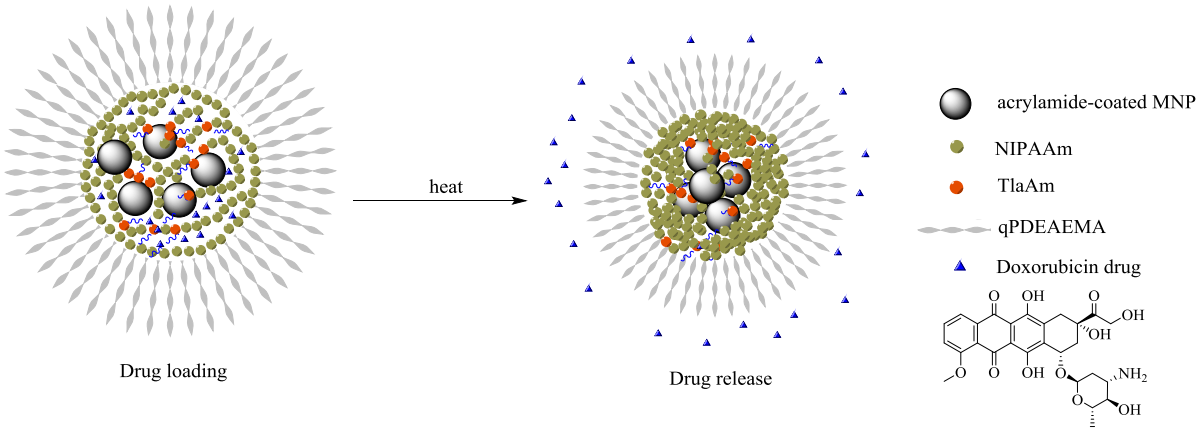

Fig. 9 The proposed mechanism of DOX release from the copolymer-coated MNP

Conclusions

We herein reported the multi-responsive MNP modified with cationic PDEAEMA-*b*-P(NIPAAm-*st*-TlaAm) copolymer and its potential applications in controlled drug release and bio-conjugation. Degree of hydrophobicity of the copolymers coated on surface of particle can be tuned by using various alkyl chain lengths in thiolactone ring-opening reaction and this can influence the particle self-assemblies in water (e.g. D_h, dispersibility, nano-aggregation) and the drug release rate. These particles exhibited the temperature responsive

behavior, which can be used as a triggering mechanism for controlled release of DOX. These versatile copolymer-MNP assemblies showed an enormous potential for use as a smart platform with thermal-triggering controlled drug release system and for conjugation with any negatively charged bio-entities.

References

Bischofberger I and Trappe V (2015) New aspects in the phase behaviour of poly-N-isopropyl acrylamide: systematic temperature dependent shrinking of PNiPAM assemblies well beyond the LCST. Sci Rep 5:15520–15529

Braunecker WA and Matyjaszewski K (2007) Controlled/living radical polymerization: features, developments, and perspectives. Prog Polym Sci 32:93–146

Chen J-T, Ahmed M, Liu Q, Narain R (2012) Synthesis of cationic magnetic nanoparticles and evaluation of their gene delivery efficacy in Hep G2 cells. J Biomed Mater Res A 100A:2342–2347

Chen L, Zhang H, Li L, Yang Y, Liu X, Xu B (2015) Thermoresponsive hollow magnetic microspheres with hyperthermia and controlled release properties. J Appl Polym Sci 132:42617

Chen Y, Espeel P, Reinicke S, Du Prez FE, Stenzel MH (2014) Control of glycopolymer nanoparticle morphology by a one-pot, double modification procedure using thiolactones. Macromol Rapid Commun 35:1128–1134

Du H, Wickramasinghe R, Qian X (2010) Effects of salt on the lower critical solution temperature of poly (N-isopropylacrylamide). J Phys Chem 114:16594–16604

Espeel P and Du Prez FE (2015) One-pot multi-step reactions based on thiolactone chemistry: A powerful synthetic tool in polymer science. Eur Polym J 6:247–272

Espeel P, Goethals F, Du Prez FE (2011) One-pot multistep reactions based on thiolactones: extending the realm of thiol-ene chemistry in polymer synthesis. J Am Chem Soc 133:1678–1681

Espeel P, Goethals F, Stamenovi MM, Petton L, Du Prez FE (2012) Double modular modification of thiolactone-containing polymers: towards polythiols and derived structures. Polym Chem 3:1007–1015

Gandhi A, Paul A, Sen OS, Sen KK (2015) Studies on thermoresponsive polymers: Phase behaviour, drug delivery and biomedical applications. Asian J Pharm Sci 10:99–107

Hill MR, Carmean R N, Sumerlin B S (2015) Expanding the scope of RAFT polymerization: recent advances and new horizons. Macromolecules 48:5459-5469

Hu Y, Meng L, Niu L, Lu Q (2013) Highly cross-linked and biocompatible polyphosphazene-coated superparamagnetic Fe_3O_4 nanoparticles for magnetic resonance imaging. Langmuir 29:9156-9163

Huang L, Liu M, Mao L, Xu D, Wan Q, Zeng G, Shi Y, Wen Y, Zhang X, Wei Y (2017) Preparation and controlled drug delivery applications of mesoporous silica polymer nanocomposites through the visible light induced surface-initiated ATRP. Appl Surf Sci 412:571–577

Leung KCF, Lee S, Wong C, Chak C, Lai JMY, Zhu X, Wang YJ, Wang YXJ, Cheng CHK (2013) Nanoparticle–DNA–polymer composites for hepatocellular carcinoma cell labeling, sensing, and magnetic resonance imaging. Methods 64:315–321

Li Y, Zhang X, Cheng H, Kim G, Cheng S, Zhuo R (2006) Novel stimuli-responsive micelle self-assembled from Y-Shaped P(U-Y-NIPAAm) copolymer for drug delivery. Biomacromolecules 7:2956-2960

Lim J, Yeap SP, Che HX, Low SC (2013) Characterization of magnetic nanoparticle by dynamic light scattering. Nanoscale Res Lett 8:381-394

Liu P, Luo Q, Guan Y, Zhang Y (2010) Drug release kinetics from monolayer films of glucose-sensitive microgel. Polymer 51:2668-2675

Lowe AB (2010) Thiol-ene ‘‘click’’ reactions and recent applications in polymer and materials synthesis. Polym Chem 1:17-36

Machida N, Inoue Y, Ishihara K (2014) Phospholipid polymer-coverd magnetic nanoparticles for tracking intracellular molecular reaction. Trans Mat Res Soc Japan 39:427–430

Maeda Y and Mochiduki H (2004) Hydration changes during thermosensitive association of a block copolymer consisting of LCST and UCST blocks. Macromol Rapid Commun 25:1330–1334

Mahmoud WE, Bronstein LM, Al-Hazmi F, Al-Noaiser F, Al-Ghamdi AA (2013) Development of Fe/Fe_3O_4 core-shell nanocubes as a promising magnetic resonance imaging contrast agent. Langmuir 29:13095-13101

Matyjaszewski K (2012) Atom transfer radical polymerization (ATRP): current status and future perspectives. Macromolecules 45:4015-4039

Meerod S, Rutnakornpituk B, Wichai U, Rutnakornpituk M (2015) Hydrophilic magnetic nanoclusters with thermo-responsive properties and their drug controlled release. J Magn Magn Mater 392:83–90

Mekkapat S, Thong-On B, Rutnakornpituk B, Wichai U, Rutnakornpituk M (2013) Magnetic core–bilayer shell complex of magnetite nanoparticle stabilized with mPEG–polyester amphiphilic block copolymer. J Nanopart Res 15:2051–2062

Moad G, Rizzardo E, Thang SH (2008) Radical Addition Fragmentation Chemistry in Polymer Synthesis. Polymer 49:1079–1131

Patil SS and Wadgaonkar PP (2017) Temperature and pH dual stimuli responsive PCL-*b*-PNIPAAm block copolymer assemblies and the cargo release studies. J Polym Sci A Polym Chem 55:1383–1396

Prabha G and Raj V (2016) Preparation and characterization of polymer nanocomposites coated magnetic nanoparticles for drug delivery applications. J Magn Magn Mater 408:26–34

Qin S, Qin D, Ford WT, Resasco DE, Herrera JE (2004) Functionalization of single-walled carbon nanotubes with polystyrene *via* grafting to and grafting from methods. Macromolecules 37:752–757

Qu Y, Li J, Ren J, Leng J, Lin C, Shi D (2014) Enhanced magnetic fluid hyperthermia by micellar magnetic nanoclusters composed of $Mn_xZn_{1-x}Fe_2O_4$ nanoparticles for induced tumor cell apoptosis. ACS Appl Mater Interfaces 6:16867-16879

Reinicke S, Espeel P, Stamenović MM, Du Prez FE (2013) One-pot double modification of P(NIPAAm): a tool for designing tailor-made multiresponsive polymers. ACS Macro Lett 2:539–543

Rodkate N and Rutnakornpituk M (2016) Multi-responsive magnetic microsphere of poly(N-isopropylacrylamide)/carboxymethylchitosan hydrogel for drug controlled release. Carbohydr Polym 151:251–259

Sahoo B, Devi KSP, Banerjee R, Maiti TK, Pramanik P, Dhara D (2013) Thermal and pH responsive polymer-tethered multifunctional magnetic nanoparticles for targeted delivery of anticancer drug. ACS Appl Mater Interfaces 5:3884-3893

Sciannamea V, Je´roˆme R, Detrembleur C (2008) In-situ nitroxide-mediated radical polymerization (NMP) processes: their understanding and optimization. Chem Rev 108:1104-1126

Singh LP, Srivastava SK, Mishra R, Ningthoujam RS (2014) Multifunctional hybrid nanomaterials from water dispersible CaF_2:Eu^{3+}, Mn^{2+} and Fe_3O_4 for luminescence and hyperthermia application. J Phys Chem C 118:18087-18096

Stamenovi MM, Espeel P, Van Camp V, Du Prez FE (2011) Norbornenyl-based RAFT agents for the preparation of functional polymers *via* thiol-ene chemistry. Macromolecules 44:5619-5630

Trongsatitkul T and Budhlall BM (2013) Microgels or microcapsules? Role of morphology on the release kinetics of thermoresponsive PNIPAm-co-PEGMa hydrogels. Polym. Chem 4: 1502-1516

Ulbrich K, Holá K, Šubr V, Bakandritsos A, Tuček J, Zbořil R (2016) Targeted drug delivery with polymers and magnetic nanoparticles: covalent and noncovalent approaches, release control, and clinical studies. Chem. Rev 116:5338–5431

Wang B, Li B, Zhao B, Li CY (2008) Amphiphilic janus gold nanoparticles *via* combining "solid-state grafting-to" and "grafting-from" methods. J Am Chem Soc 130:11594–11595

Wang C, Xu H, Liang C, Liu Y, Li Z, Yang G, et al (2013) Iron oxide @ polypyrrole nanoparticles as a multifunctional drug carrier for remotely controlled cancer therapy with synergistic antitumor effect. ACS nano 7:6782-6795

Willcock H and O'Reilly RK (2010) End group removal and modification of RAFT polymers. Polym Chem 1:149–157

Supplementary Material

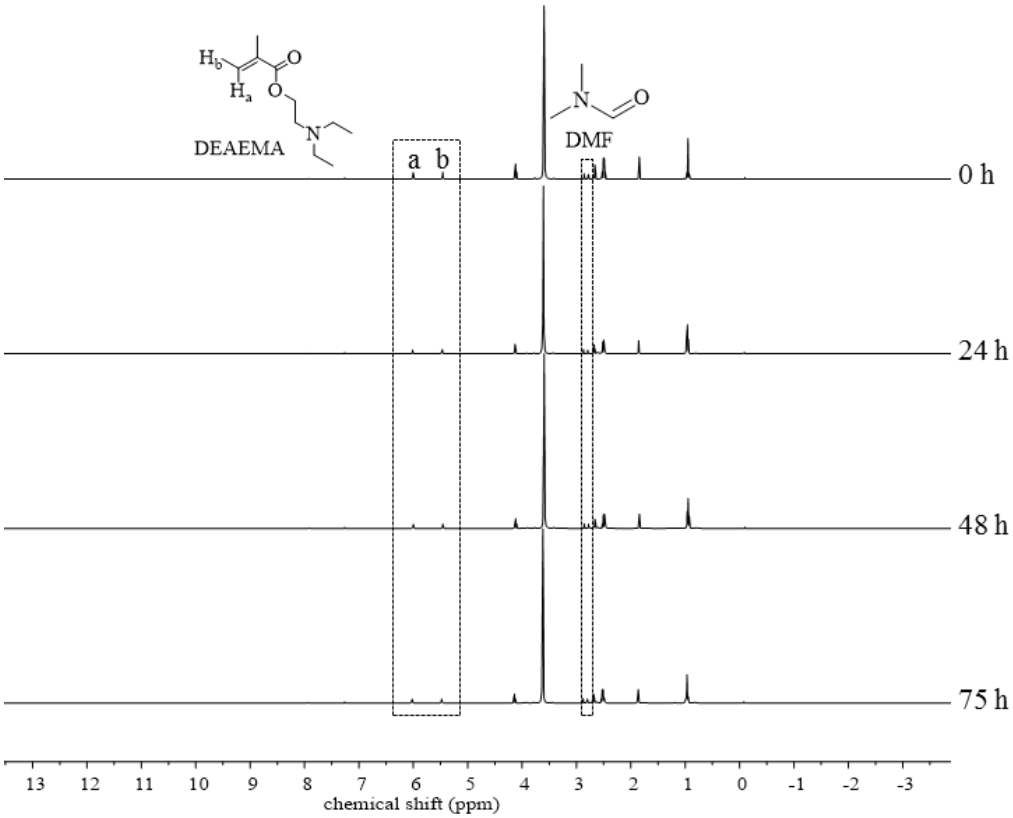

Figure S1 Monitoring the monomers conversions *via* ^{1}H NMR spectroscopy during RAFT of DEAEMA using DMF as an internal standard

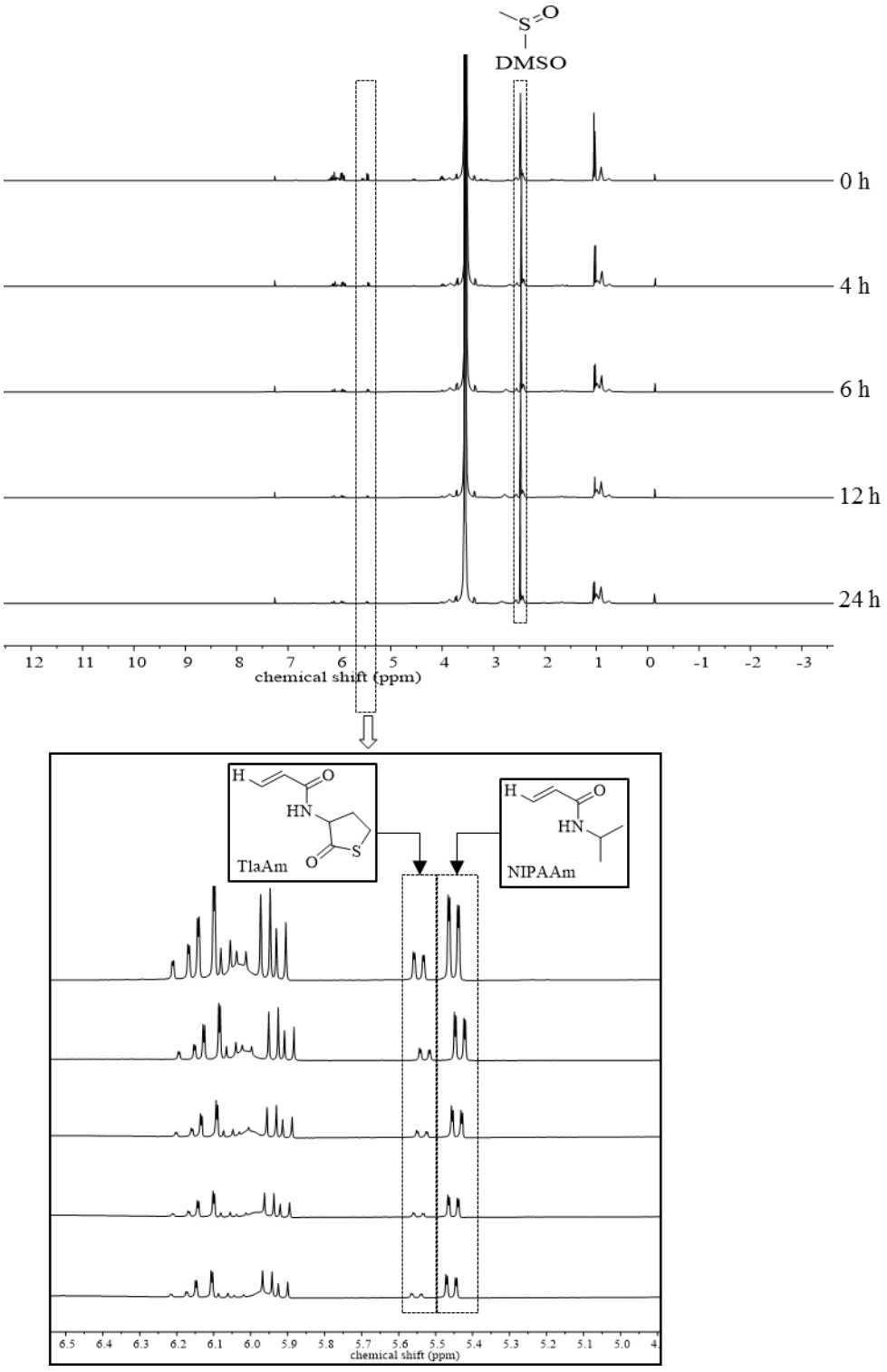

Figure S2 Monitoring the monomers conversions of PDEAEMA-*b*-P(NIPAAm-*st*-TlaAm) *via* ^{1}H NMR spectroscopy during RAFT using DMF as an internal standard

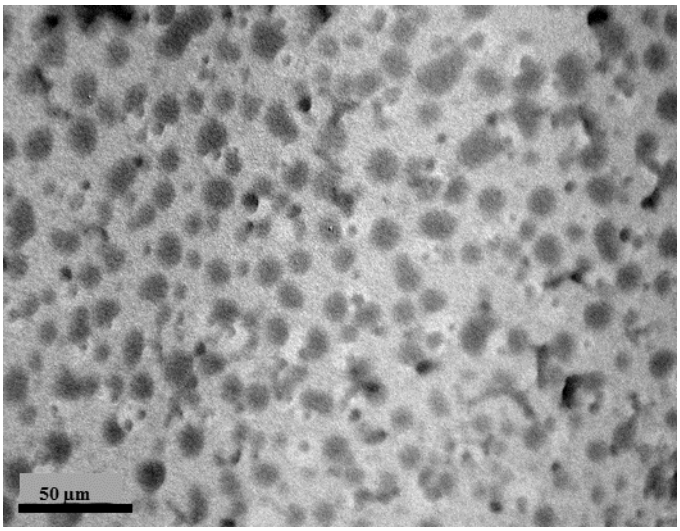

Figure S3 A TEM image of quaternized C12 copolymer showing the self-assemble behavior. The TEM sample was prepared from the copolymer aqueous dispersion.

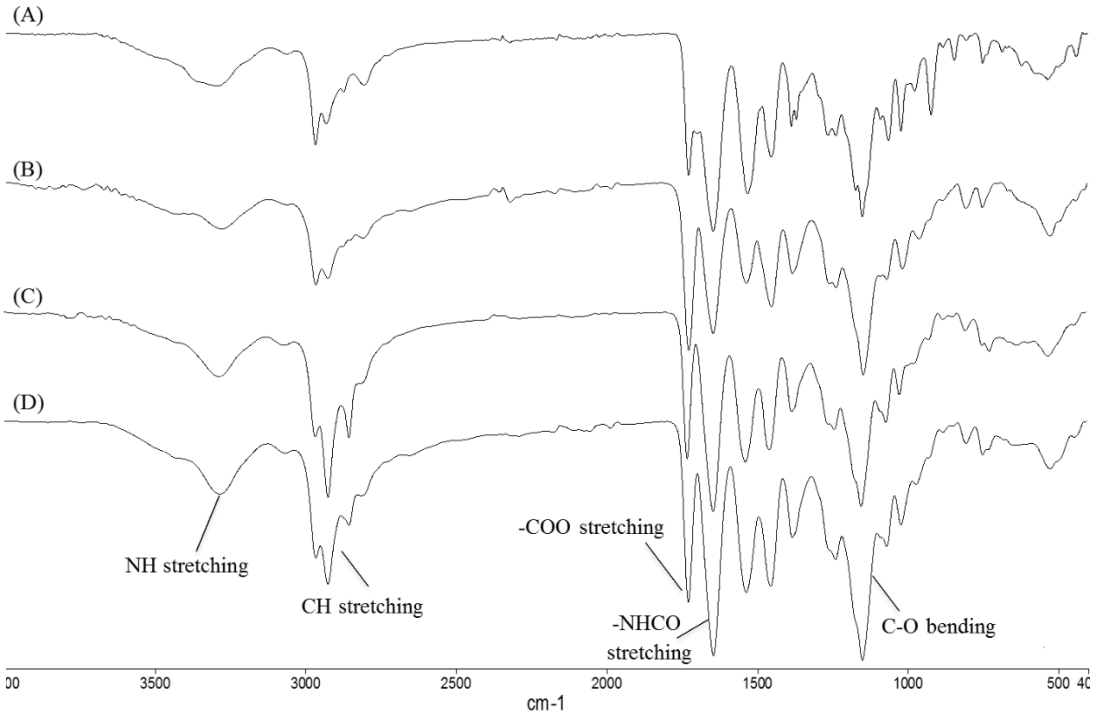

Figure S4 FTIR spectra of (A) PDEAEMA-*b*-P(NIPAAm-*st*-TlaAm) copolymers before the ring-opening reaction, and after the ring-opening reactions with (B) 1-propylamine, (C) 1-octylamine, and (D) 1-dodecylamine

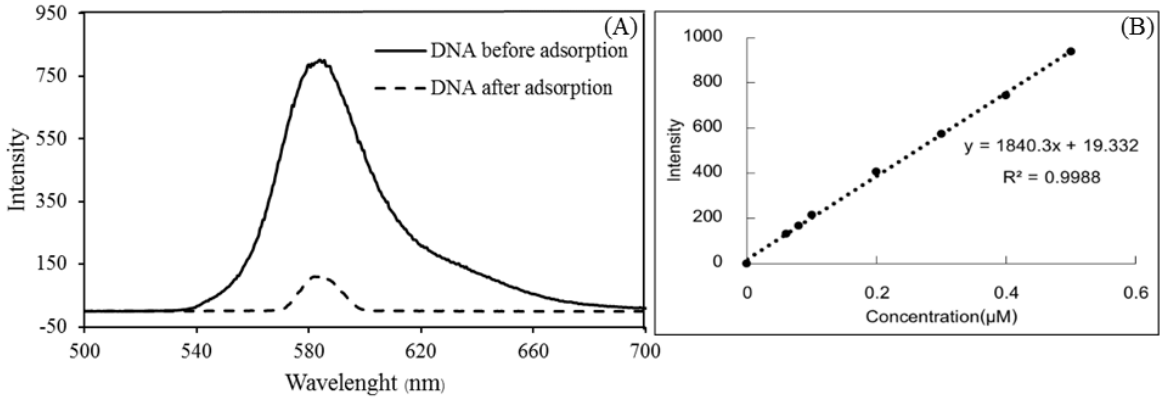

Figure S5 (A) Fluorescence spectra of the DNA solutions before and after adsorption with qMC12 and (B) a standard calibration curve of the DNA solutions (TAMRA-5'-TACCACCATTC-3')

Chapter IV

Multi-responsive poly(*N*-acryloyl glycine)-based nanocomposite and its drug release characteristics

Abstract

pH- and thermo-responsive nanocomposite composing of poly(*N*-acryloyl glycine) (PNAG) matrix and magnetite nanoparticle (MNP) was synthesized and then used for drug controlled release application. The effects of crosslinkers, e.g. ethylenediamine and *tris*(2-aminoethyl)amine, and their concentrations (1 and 10 mol%) on the size, magnetic separation ability and water dispersibility of the nanocomposite were investigated. The nanocomposite crosslinked with *tris*(2-aminoethyl)amine (size ranging between 50 and 150 nm in diameter) can be rapidly separated by a magnet while maintaining its good dispersibility in water. It can respond to the pH and temperature change as indicated by the changes in its zeta potential and hydrodynamic size. From the in vitro release study, theophylline as a model drug was rapidly released when the pH changed from neutral to acidic/basic conditions or when increasing the temperature from 10 °C to 37 °C. This novel nanocomposite showed a potential application as a magnetically guidable vehicle for drug controlled release with pH- and thermo-triggered mechanism.

Keywords: Poly(*N*-acryloyl glycine); Magnetite nanoparticle; Nanocomposite; Drug controlled release; pH- and thermos-responsive

1. Introduction

Magnetite nanoparticle (MNP) has attracted great attention in recent years in biomedical and biotechnological applications [1-5] owing to its magnetically guidable properties [2], high surface area-to-volume ratio [4], high saturation magnetization [6-7], low toxicity and high biocompatibility [8]. These intriguing properties make MNP as an ideal candidate for use in various biomedical fields such as drug delivery [5], diagnostics, therapeutics [2,9-10] and magnetic separation [11-13].

In the magnetic separation application, MNP should have high magnetic responsiveness, so that it should abruptly respond to a magnet and completely remove un-adsorbed entities after decanting [14-15]. Formation of nanocomposite containing multi-particles of MNP embedded in polymer matrix was another promising approach to enhance magnetic sensitivity while maintaining its good dispersibility in the media. When individual unique properties of both MNP and polymer matrix were combined, multi-functional nanocomposite serving as a platform for further conjugation with desirable bio-entities can be obtained [16-17]. Thus, this hybrid-nanocomposite has been particularly used in biological field such as drug delivery system [18-19], controlled release [16,20,23], and magnetic separation [1-13]. Previous works have reported the synthesis of MNP-polymer nanocomposite having both good magnetic separation ability and good water dispersibility for drug controlled release [4,16] and for conjugation with bio-entities [17,24].

Interestingly, polymer matrix having external stimuli-responsive properties in nanocomposite can be used as a handle in controlled release applications [25-29]. Previous works have presented the use of MNP coated with pH- and thermo-responsive polymers as a handle for triggered mechanisms for drug controlled release [28]. Among the pH- and thermo-responsive polymers, poly(*N*-acryloyl glycine) (PNAG) is of particular interest in this research because it can be facilely synthesized *via* a free radical polymerization of *N*-acryloyl glycine monomer in aqueous solutions [12,30]. H-bonding network of carboxyl groups (-COOH) and amide groups (-CONH-) in PNAG chains with water molecules plays a crucial role in its pH- and temperature-responsive properties [31].

In a basic pH condition, the carboxylate groups (COO^-) of PNAG should be formed, resulting in the enhancement in water swelling due to negative charge repulsion among the chains. On the other hand, when the polymer was protonated in an acidic pH condition, its collapsed structure should be formed [32]. PNAG also showed thermo-responsive properties when its environmental temperature changed due to H-bonding of amide bonds in the chains

with water molecules [33,34], similarly to the case of the amino acid-derived polymers, such as poly(*N*-acryloyl glycinamide) (PNAGA) [35], poly(acrylamide) (PAAm) and poly(acrylic acid) (PAA) [36,37,38]. However, the study in upper critical solution temperature (UCST) of PNAG homopolymer has never been reported, while those of PNAG-containing copolymer were very limited [39]. At the temperature below the UCST, PNAG should be stabilized by intramolecular H-bonding, resulting in the formation of solid hydrogels. At the temperature above its UCST, it can reversibly turn into fluid state because the intramolecular H-bonding is diminished and the simultaneous formation of intermolecular H-bonding between water molecules and chains of polymer [35].

This work reports the synthesis of MNP nanocomposite coated with pH/thermo-responsive PNAG and its use in drug controlled release. Modification of MNP surface with PNAG was first prepared *via* a free radical polymerization, followed by a crosslinking reaction. Different types and concentrations of the crosslinkers (1 mol% and 10 mol% of *tris*(2-aminoethyl)amine or ethylenediamine) were used in the crosslinking in an attempt to tune the reaction condition to gain the nanocomposite with good water dispersibility and high magnetic separation ability. The effect of the crosslinking condition of the nanocomposite on the controlled release of theophylline as a model drug was also investigated. It was rationalized that PNAG can serve as a reservoir of the drug with both pH- and temperature-triggered drug release mechanisms (Fig. 1). The effects of pH (pH 2.0, pH 7.4, and pH 11.0) and temperature (10 °C and 37 °C) on its drug release rate were also herein investigated.

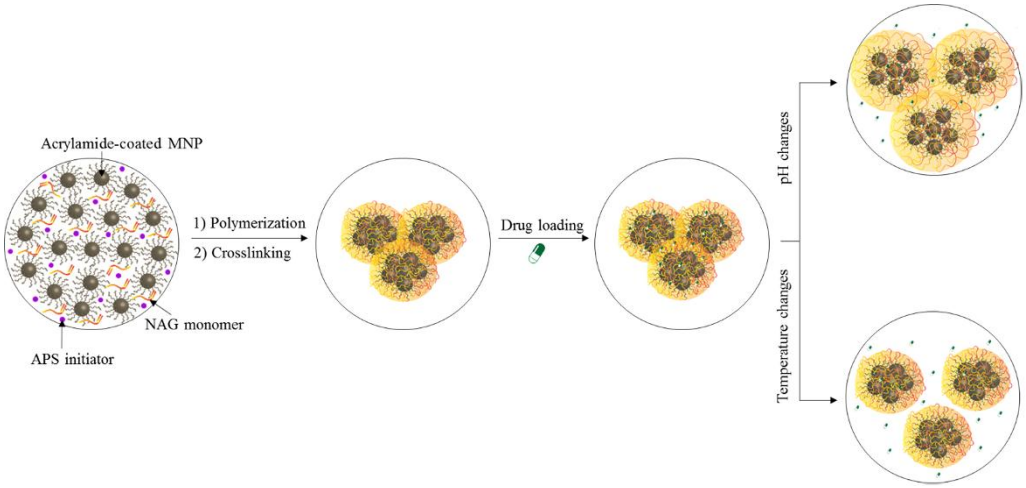

Fig. 1 Schematic preparation of PNAG-coated MNP nanocomposite for drug controlled release applications

2. Experimental

2.1 Materials

Ammonium hydroxide (NH_4OH) (28-30%, J.T. Baker), *N*-(3-dimethylaminopropyl)-*N*′-ethylcarbodiimide hydrochloride (EDC.HCl) (GL Biochem Shanghai Ltd.), ethylenediamine (Carlo Erba), glycine (AR grade), iron(II) chloride tetrahydrate ($FeCl_2.4H_2O$) (99%, Acros organic), iron(III) chloride ($FeCl_3$) (98%, Acros), oleic acid (Carlo Erba), ammonium persulfate (APS) (98%, Carlo Erba), (3-aminopropyl) triethoxysilane (APTES) (99%, Acros), triethylamine (TEA) (97%, Carlo Erba), theophylline anhydrous (≥99%, Sigma Aldrich), and *tris*(2-aminoethyl)amine (96%, Sigma Aldrich) were used as received. Acryloyl chloride was prepared *via* a chloride exchange reaction between benzoyl chloride (Acros, 99%) and acrylic acid (98%, Acros) at 75 °C to obtain a colorless liquid with 60% yield.

2.2 Characterization

Fourier transform infrared spectrometry (FTIR) was conducted on a Perkin–Elmer Model 1600 Series FTIR Spectrometer. ^{1}H NMR spectroscopy was characterized *via* a 400 MHz Bruker NMR spectrometer. Transmission electron microscopy (TEM) was conducted on Philips Tecnai 12 operated at 120 kV. The dispersion of the particle in water was dropped on a carbon-coated copper grid at room temperature without filtration. Zeta potential and hydrodynamic size (D_h) of the particle were determined on NanoZS4700 nanoseries Malvern photocorrelation spectrometer (PCS). Magnetic properties were characterized *via* a Standard 7403 Series, Lakeshore vibrating sample magnetometer (VSM). UV-visible spectrophotometry was conducted on Analytik-Jena AG specord 200 plus UV-Vis Spectrophotometer at λ = 272 nm.

2.3 Preparation of *N*-acryloyl glycine (NAG) monomer

Glycine (61.8 mmol, 4.64 g) was dissolved in a NaOH aqueous solution (123.6 mmol, 4.95 g). An acryloyl chloride solution in tetrahydrofuran (61.8 mmol, 5.0 mL) was added into the solution and then stirred at 0 °C for 3 h. The mixture was washed with diethyl ether and then aqueous solution layer was adjusted to a pH 2 solution with conc.HCl. The extraction with ethyl acetate was carried out and then organic layer was dried with anh.Na_2SO_4, filtered

and evaporated *in vacuo*. Finally, white solid as a product was obtained: 2.41 g, 30% yield; ^{1}H NMR (400 MHz, D_2O): δ 4.08 ppm (*s*, 2H), 5.82-5.84 (*dd*, 1H), and 6.24-6.39 (*dd* and *t*, 2H).

2.4 Preparation of acrylamide-coated MNP

30%NH_4OH solution (5.0 mL) was added into a solution mixture of $FeCl_2.4H_2O$ (2.1 mmol, 0.83 g) and $FeCl_3$ (2.5 mmol, 0.50 g) with stirring at 25 °C for 30 min. After separated and washed with distilled water, an oleic acid solution (1.0 mL) in toluene (9.0 mL) was added into the MNP dispersion and then stirred at 25 °C for 30 min. Oleic acid-coated MNP was precipitated in acetone, separated by a magnet and then re-dispersed in toluene (10.0 mL). TEA (13.6 mmol, 1.0 mL) and APTES (11.9 mmol, 2.5 mL) were then added to the dispersion with stirring at 25 °C under N_2 for 24 h to obtain amino-coated MNP.

After magnetic separation, washing and evaporation until dryness, amino-coated MNP (0.05 g) was then dispersed in a NaOH solution (1.50 g) by ultrasonication. An acryloyl chloride (49.5 mmol, 5.0 mL) was slowly added into the MNP dispersion at 0 °C in an ice bath for 1 h, and then the mixture was continuously stirred at 25 °C for 24 h. After a reaction completed, the particle was separated by a magnet and then repeatedly washed with distilled water and stored in the dispersion form (0.02 g MNP/mL H_2O).

2.5 Preparation of PNAG-coated MNP nanocomposite

NAG monomer (0.25 g, 1.94 mmol) was dissolved in distilled water (20.0 mL), followed by an addition of a dispersion of acrylamide-coated MNP (0.05 g MNP in 25.0 mL distilled water). An APS radical initiator solution (10% in distilled water, 0.04 mmol) was injected into the mixture and the reaction was set allowed for 2 h at 70 °C under N_2 gas to obtain PNAG-coated MNP nanocomposite.). After magnetic separation and washing with distilled water to remove the unreacted monomers and uncoated polymer chains, the nanocomposite was then dried *in vacuo*. In the crosslinking reaction, the dispersion of the nanocomposite (0.05 g nanocomposite in 50.0 mL distilled water) was added with EDC.HCl (5% in distilled water) as a coupling agent and stirred at 25 °C 1 h. After magnetic separation, the nanocomposite was re-dispersed in the crosslinker solutions (1 or 10 mol% of ethylenediamine or *tris*(2-aminoethyl)amine in a pH 11 buffer solution) and then stirred for 1 h. After the crosslinking reaction, the MNP nanocomposite was rinsed with distilled water with the use of a magnet to wash the unreacted crosslinking agents and then dried *in vacuo*.

2.6 The release studies of entrapped theophylline from the MNP nanocomposite

The dispersion of the MNP nanocomposite (5 mg of the MNP nanocomposite in 1.0 mL aqueous dispersion) was dropwise added with a theophylline solution (1.0 mL, 10 mg/mL in distilled water). After stirring for 3 h at 40 °C, the drug-loaded MNP nanocomposite was removed from an excess drug using an external magnet. In the *in vitro* release study, the theophylline-entrapped MNP nanocomposite (5 mg of the MNP nanocomposite) was dispersed in 5.0 mL buffer solutions (pH 2.0, pH 7.4 or pH 11.0). The dispersion was placed into a water bath at 10 °C or 37 °C. At a predetermined time interval, 100 µL of sample dispersion was withdrawn from the release media. After each sampling, the nanocomposite was magnetically separated and then the supernatant was analyzed *via* UV–Visible spectrophotometer at 272 nm wavelength. Percent release (%) was estimated from the following equation;

$$\text{Percent release (\%)} = \frac{\text{Weight of the release drug at a given time}}{\text{Weight of the drug entrapped in the MNP nanocomposite}} \times \times 100 \quad (1)$$

To determine drug entrapment efficiency (EE) and drug loading efficiency (DLE), the weight of theophylline entrapped in the MNP nanocomposite was determined from the amount of the drug at the maximum point of the release profile combined with those remaining in the particles. The nanocomposite was extracted with a 0.1 M HCl solution to dissolve the left over drug and then analyzed *via* UV–Visible spectrophotometer. Therefore, EE and DLE were defined from the following equations:

$$\text{EE (\%)} = \frac{\text{Weight of the drug entrapped in the MNP nanocomposite}}{\text{Weight of the loaded drug}} \times 100 \quad (2)$$

$$\text{DLE (\%)} = \frac{\text{Weight of the drug entrapped in the MNP nanocomposite}}{\text{Weight of the MNP nanocomposite}} \times 100 \quad (3)$$

3. Results and Discussion

In this work, PNAG-coated MNP was first synthesized *via* a free radical polymerization to form water dispersible magnetic nanocomposite. In addition to steric stabilization, PNAG also provided electrostatic repulsion stabilization to the nanocomposite due to the presence of carboxylate groups. Additional crosslinking of the MNP nanocomposite was conducted to obtain those with good magnetic separation ability while retaining its good water dispersibility. Two different crosslinkers (ehtylenediamine and *tris*(2-aminoethyl)amine) were used in this work to study the effect of the crosslinkers and their concentrations on D_h, water dispersibility and magnetic separation ability of the MNP nanocomposite. pH- and thermo-responsive properties of PNAG coated on its surface provided dual triggering mechanisms for drug release. In this report, in vitro release profile of theophylline entrapped on the nanocomposite was investigated as a function of pH (2.0 7.4 and 11.0) and temperature (10 °C and 37 °C).

3.1 Characterization of the MNP nanocomposite

FTIR spectra of the particles before and after coating with PNAG are displayed in Fig. 2. The spectrum of acrylamide-coated MNP shows the weak signals of NHC=O stretching (1539 and 1625 cm^{-1}), N-H stretching (3232 cm^{-1}) and also those of MNP core at 551 cm^{-1} (Fe-O stretching) (Fig. 2A). Once the nanocomposite was formed by coating MNP with PNAG, the peaks attributed to C-O stretching (1221 cm^{-1}), NHC=O stretching (1550 and 1633 cm^{-1}), C=O stretching (1722 cm^{-1}) and N-H stretching (3301 cm^{-1}) were observed (Fig. 2C). These signals corresponded well to those of PNAG homopolymer (Fig. 2B), indicating the presence of PNAG coated on the MNP nanocomposite.

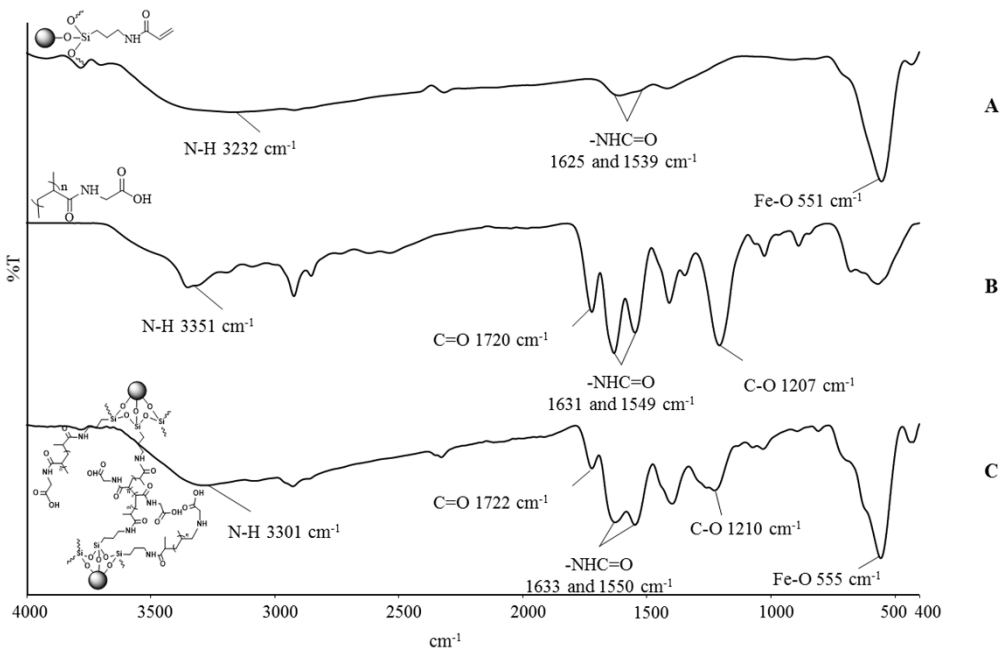

Fig. 2 FTIR spectra of (A) acrylamide-coated MNP, (B) PNAG homo-polymer and (C) PNAG-coated MNP nanocomposite

3.2 Effect of crosslinking reactions on the properties of the MNP nanocomposite

Ethylenediamine and *tris*(2-aminoethyl)amine with two different concentrations (1 and 10 mol%) were used as the crosslinkers in the nanocomposite. The goal of this work was to obtain the MNP nanocomposite with good magnetic separation ability while retaining its good water stability; the conditions in the crosslinking reactions (type of crosslinkers and concentrations) were thus optimized. Zeta potentials and D_h of the nanocomposites were investigated using PCS technique (Fig. 3).

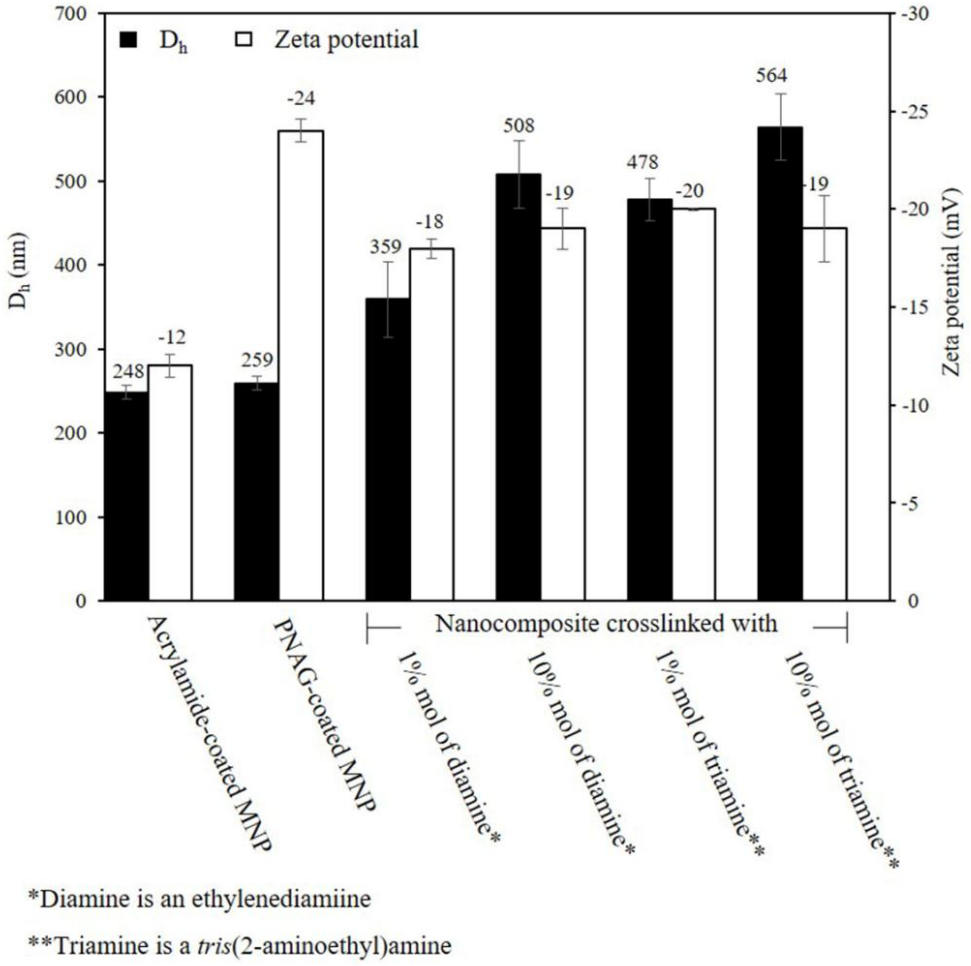

Fig. 3 D_h and zeta potential values of (a) acrylamide-coated MNP, (b) the MNP nanocomposite (before crosslinking), the MNP nanocomposites after crosslinking with (c) 1 mol% and (d) 10 mol% of ethylenediamine, and (e) 1 mol% and (f) 10 mol% of *tris*(2-aminoethyl)amine

As compared to acrylamide-coated MNP, PNAG-coated MNP nanocomposite did not show an increase in D_h while its zeta potential values significantly increased from -12 to -24 mV, and this was probably due to the existence of anionic carboxylate groups from PNAG. This result well corresponded to those observed from the conductometric titration shown in supporting information. After the crosslinking reactions, D_h of all samples significantly increased while its zeta potential values decreased. The coupling reactions between the carboxyl groups of PNAG coated on the particles and the amino groups of the crosslinkers induced the nano-aggregation of the individual particles, resulting in the formation of nanocomposite having multiple particles embedded and a slight drop in the degree of negative charge. The increase in the crosslinker concentration from 1% to 10% also promoted

the formation of the crosslinked nanocomposite as indicated by the enlarged D_h. Interestingly, the use of *tris*(2-aminoethyl)amine seemed to enhance the degree of crosslinking as compared to those of ethylenediamine (at the same crosslinker concentrations), probably due to the higher number of the equivalent reactive amines in the reactions (Fig. 4).

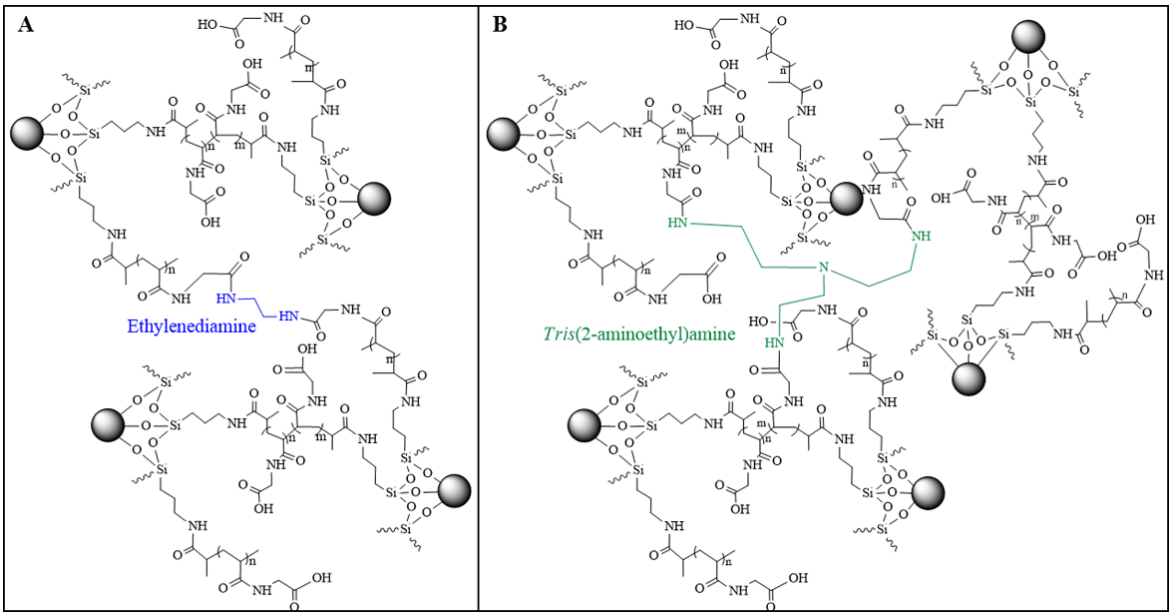

Fig. 4 The proposed mechanism of the crosslinking amidations of PNAG-coated MNP with (A) ethylenediamine and (B) *tris*(2-aminoethyl)amine

The size and the size distribution of the MNP nanocomposite in each step of the reactions were also observed *via* TEM (Fig. 5). Acrylamide-coated MNP exhibited aggregation of the particles without the formation of nanoclusters owing to the lack of polymer coating (Fig. 5A). When MNP surface was coated with PNAG, the particles showed an improvement in water dispersibility without significant aggregation (Figure 5B). After the crosslinking, the cluster feature of the nanocomposite with the size ca. 50-150 nm in diameter was observed (Fig. 5C-5F) and this corresponded to those observed in PCS results. However, there was no apparent difference in the size and the size distribution of the nanocomposite between those crosslinked with ethylenediamine and *tris*(2-aminoethyl)amine or with different concentrations.

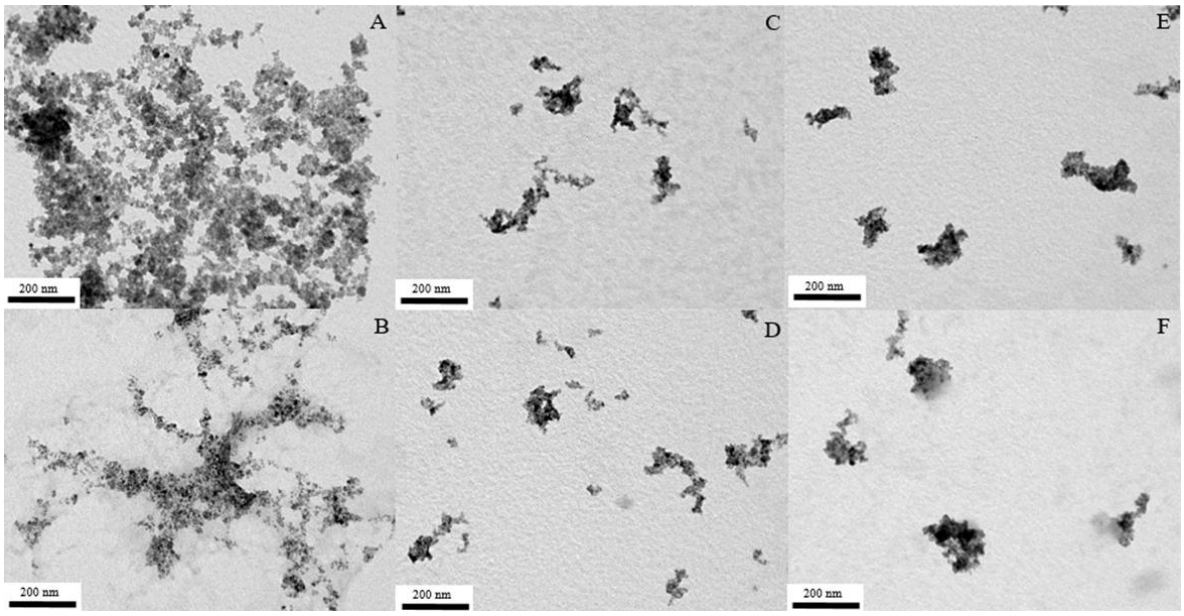

Fig. 5 TEM of (A) acrylamide-coated MNP, (B) the MNP nanocomposite (before crosslinking), the MNP nanocomposite after crosslinking with (C) 1 mol% and (D) 10 mol% of ethylenediamine, and (E) 1 mol% and (F) 10 mol% of *tris*(2-aminoethyl)amine

Water dispersibility, stability and magnetic separation ability of the particles in each step of the reactions were investigated. Acrylamide-coated MNP aggregated within a few minutes after the preparation due to a lack of polymeric stabilization. After coating with PNAG, the particles were well stabilized through both steric and electrostatic repulsion mechanisms, resulting in the stable MNP dispersions with insignificant aggregation even after 24 h of the preparation. However, they cannot be completely separated after applying with a magnet for 5 min, which would be troublesome when employed for magnetic separation applications. The crosslinking of these nanocomposites was conducted in an attempt to enhance the magnetic separation ability, while retaining its good water stability. *Tris*(2-aminoethyl)amine and ethylenediamine with two different concentrations (1 mol% and 10 mol%) were used as additional crosslinkers. According to the results in Table 1, the nanocomposites after crosslinking showed a fair dispersibility in water after 24 h standing with a slight aggregation. This was probably due to the formation of the nanoclusters with a larger size, which corresponded well to the results observed from PCS technique discussed above. These nanocomposites can be separated within 5 min due to the increase in its size, resulting in an improved response to a magnet. Interestingly, as compared to the others, those crosslinked with 10 mol% *tris*(2-aminoethyl)amine can be completely separated from the

dispersion and it would be used as a representative for other studies, e.g. magnetic properties, drug entrapment and controlled release studies.

Table 1 The effect of crosslinking agents and their concentrations on water dispersibility and magnetic separation ability

Acrylamide-coated MNP (no PNAG coating)	PNAG coating (before crosslinking)	After crosslinking with			
		1 mol% of diamine*	10 mol% of diamine*	1 mol% of triamine**	10 mol% of triamine**
At initial time					
					
Dispersibility in water					
After 24 h					
					
Magnetic separation ability					
After 5 min					
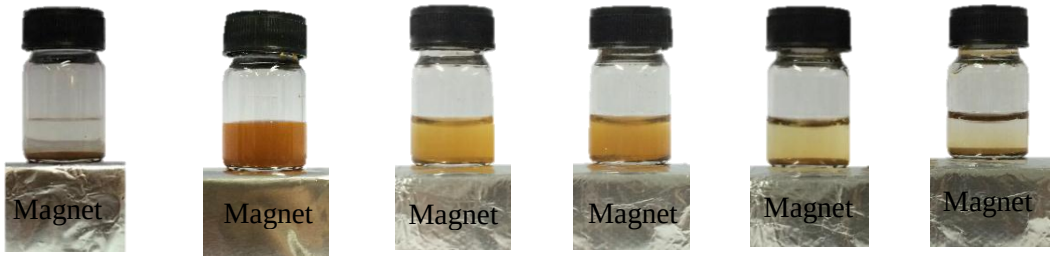					

* Diamine is ethylenediamine.

** Triamine is *tris*(2-aminoethyl)amine

3.3 Multi-responsive properties of the MNP nanocomposite as a function of magnetic field, dispersion pH and temperature

Magnetic properties of acrylamide-coated MNP and PNAG-coated MNP nanocomposites before and after crosslinking with 10 mol% of *tris*(2-aminoethyl)amine were determined *via* VSM technique. It was found that, the saturation magnetization (M_s) of the particles decreased from 68 emu/g to 40 emu/g after coating with PNAG due to the presence of non-magnetic organic polymer in the nano-composite (Fig. 6). After the crosslinking reaction, its M_s value increased to 50 emu/g and this was probably owing to the formation of MNP nanoclusters, leading to the increase in the magnetic sensitivity [15].

To confirm pH-responsive properties of the crosslinked MNP nanocomposite, its D_h was determined in pH 2.0, 7.4 and 11.0 buffer solutions. It was found that D_h in pH 2.0 cannot be measured due to macro-aggregation of the particles (indicated by an arrow in the inset in Fig. 7A). This was probably because PNAG was in the COOH form, resulting in the lack of anionic charged repulsion. In addition, its D_h increased from 617 nm to 1011 nm when the pH changed from pH 7.4 to pH 11.0 and this was attributed to presence of negatively charged repulsion of $-COO^-$ from PNAG chains, resulting the swelling of the nanocomposite. The change of D_h as a function of dispersion pH corresponded to the pK_a value of PNAG (pK_a 3.2) in term of the protonated/deprotonated forms of the carboxyl groups[40]. D_h of the MNP nanocomposite was then investigated at 10 °C and 37 °C in pH 7.4 buffer solutions. D_h significantly dropped from 685 nm to 260 nm when the temperature was decreased from 10 °C to 37 °C (Fig. 7B). It was rationalized that a number of the crosslinked MNP nanocomposites might be in the agglomerated form at 10 °C due to the H-bonding among each nanocomposite. At 37 °C, the nano-composite might be separated from each other due to the predominant interaction between PNAG on the nanocomposite surface and water molecules.

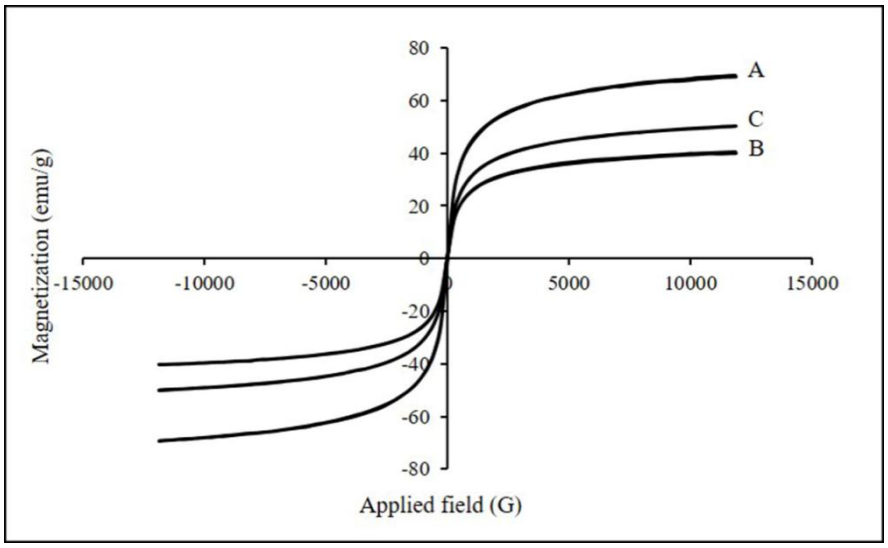

Fig. 6 M-H curves of (A) acrylamide-coated MNP, (B) the MNP nanocomposite (before crosslinking) and (C) the MNP nanocomposites after crosslinking with 10 mol% of *tris*(2-aminoethyl)amine

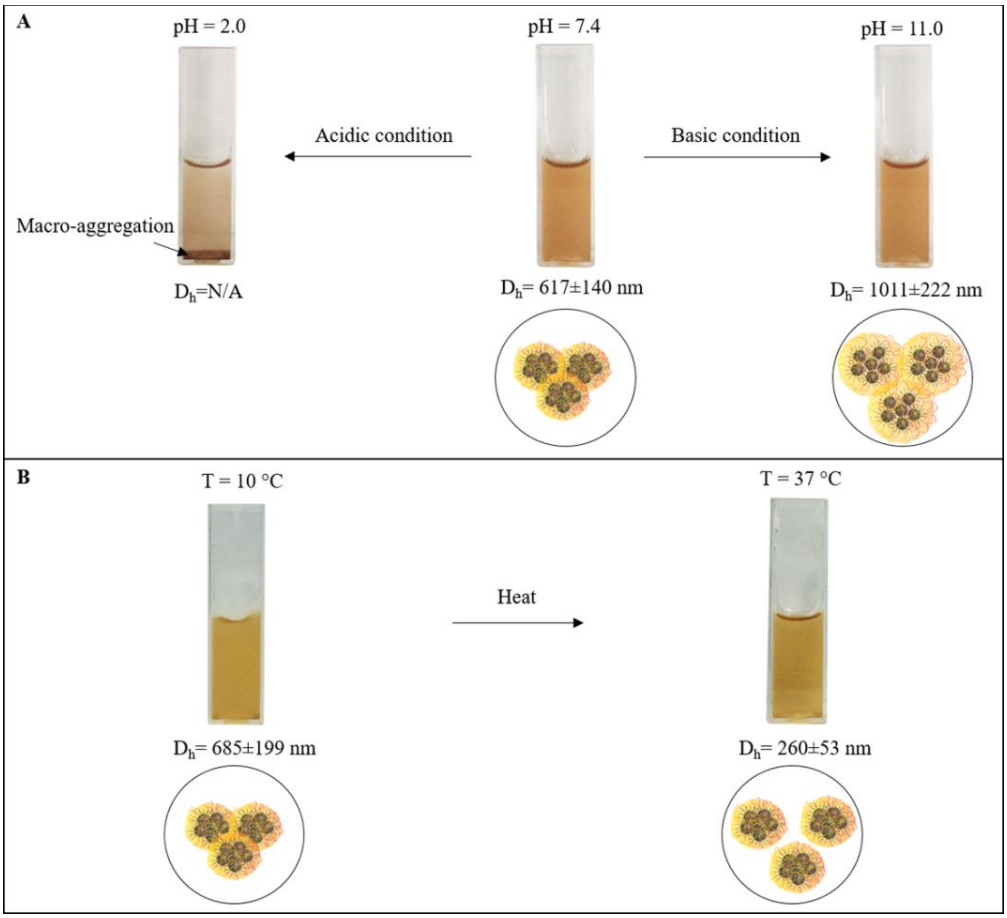

Fig 7. (A) pH- and (B) thermo-responsive properties of the MNP nanocomposite after crosslinking with 10 mol% of *tris*(2-aminoethyl)amine

3.4 Drug release behavior

A show case of the MNP nanocomposite for a drug controlled release application was also carried out in this work. Theophylline, a methylxanthine drug used in therapy for respiratory diseases, was selected as a model drug because it can be quantified *via* UV-vis spectrophotometry and possesses the amino groups in the structure. The protonation/deprotonation of the amino groups in theophylline leads to ionic adsorption/repulsion interactions with the carboxyl groups of PNAG, resulting in the drug release triggered by the change of the dispersion pH.

EE and DLE of the MNP nanocomposite crosslinked with 10 mol% of *tris*(2-aminoethyl)amine were first investigated. EE and DLE of the nanocomposite were 22-35% and 45-69%, respectively, depending on the pH and temperature of the dispersions. The effect of pH- and temperature changes on the theophylline release rate from the MNP nanocomposite was then studied. The theophylline release studies were performed using stepwise pH changes from pH 7.4 to pH 2.0 and from pH 7.4 to pH 11.0 (Fig. 8A and 8B). It should be noted that pK_a of PNAG was about 3.2 [40] and that of theophylline was 8.8 [41,42]. It was found that the drug was rapidly released when the pH changed from neutral to acidic/basic conditions. This was attributed to the negatively charged repulsion of the deprotonated forms of PNAG ($-COO^-$) on the particle surface and theophylline in the basic condition (Fig. 9A). Similarly, the positively charged repulsion of the protonated forms of these two components (-COOH of PNAG and $\equiv NH^+$ of theophylline) was rationalized for the abrupt release of the drug in the case of acidic condition.

The effect of the temperature change on the theophylline release behavior was also studied using a stepwise temperature change from 10 °C to 37 °C (Fig. 8C). There was about 12% of the drug released at 10 °C and it was rapidly released for 92% when heated to 37 °C. The abrupt release of the drug from the nanocomposite was attributed to the separation of the agglomerated nanocomposites at high temperature as indicated by the decrease in D_h (Fig. 9B).

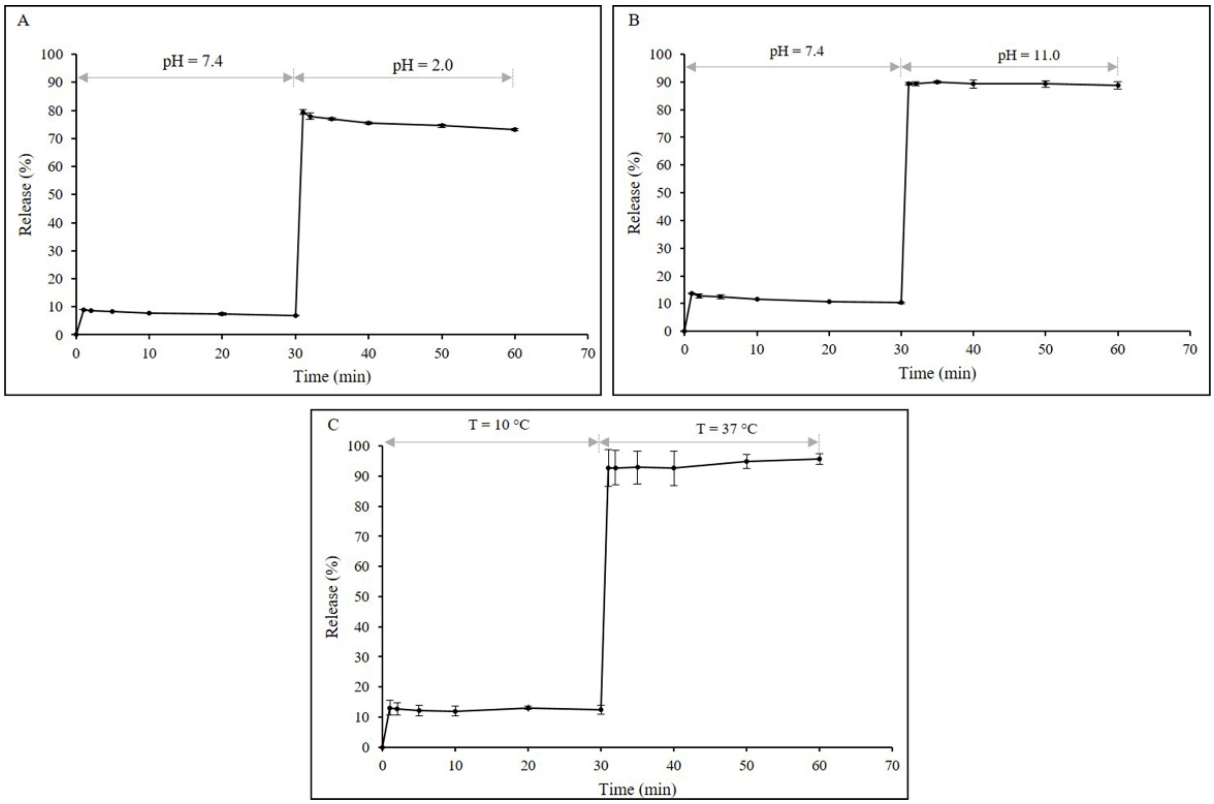

Fig. 8 (A), (B) The effect of pH and (C) temperature on the theophylline release profiles from the MNP nanocomposite crosslinking with 10 mol% of *tris*(2-aminoethyl)amine

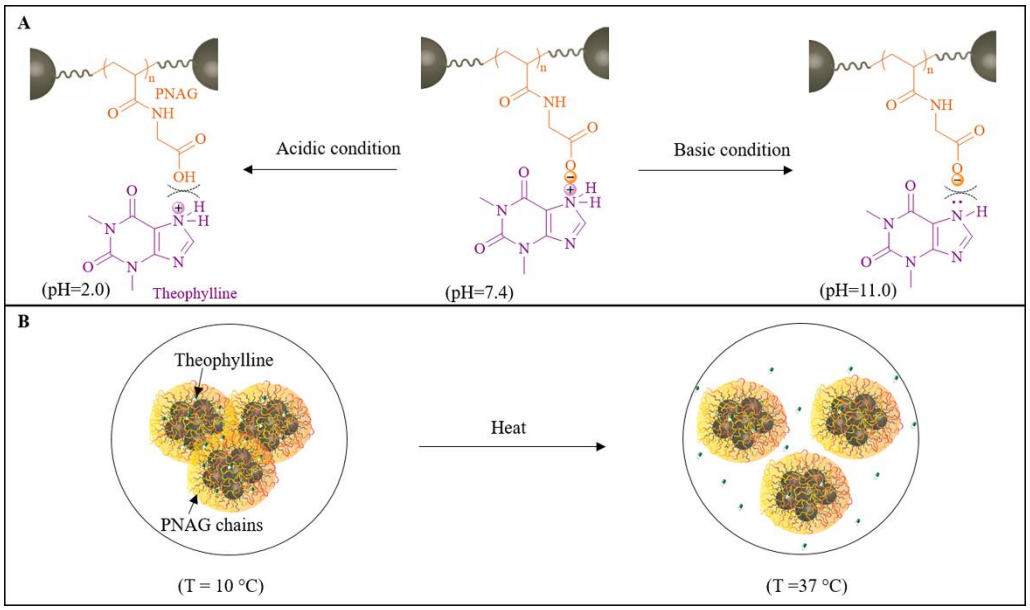

Fig. 9 Proposed mechanisms of the theophylline release from the MNP nanocomposite triggered with (A) pH and (B) temperature changes

4. Conclusions

This work presented the preparation of pH- and thermo-responsive nanocomposite based on PNAG matrix and MNP and its application in drug controlled release. The MNP nanocomposite having good magnetic separation ability and water stability was obtained by tuning the types and concentrations of the crosslinkers. It exhibited dual-responsive properties as indicated by the change in its zeta potential and D_h when the environmental pH and temperature were changed. In addition, this novel nanocomposite was also demonstrated for use as a magnetically guidable vehicle for theophylline controlled release with pH- and thermo- triggered mechanisms.

References

[1] Muñoz-Bonilla A, Sánchez-Marcos J, Herrasti P. Conducting Polymer Hybrids. In: Kumar V, Kalia S, Swart HC, editors. Springer Series on Polymer and Composite Materials. Switzerland: Springer International Publishing AG; 2017. p. 45-80.

[2] Estelrich J, Escribano E, Queralt J, Busquets MA. Iron oxide nanoparticles for magnetically-guided and magnetically-responsive drug delivery. Int J Mol Sci. 2015;16:8070-8101.

[3] Willard MA, Kurihara LK, Carpenter EE, Calvin S, Harris VG. Chemically prepared magnetic nanoparticles. Int Mater Rev. 2013;49:125-170.

[4] Thong-On B, Rutnakornpituk M. Controlled magnetite nanoclustering in the presence of glycidyl-functionalized thermo-responsive poly(*N*-isopropylacrylamide). Eur Polym J. 2016;85:519-531.

[5] Bucak S, Yavuzturk B, Demir A. Magnetic Nanoparticles: Synthesis, surface modifications and application in drug delivery. 2012. DOI: 10.5772/52115.

[6] Petcharoen K, Sirivat A. Synthesis and characterization of magnetite nanoparticles *via* the chemical co-precipitation method. Mater Sci Eng, B. 2012;177:421- 427.

[7] Hetti M, Wei Q, Pohl R, Casperson R, Bartusch M, Neu V, Pospiech D, Voit B. Magnetite core-shell nanoparticles in nondestructive flaw detection of polymeric materials. ACS Appl Mater Interfaces. 2016;8:28208-28215.

[8] Xiao L, Li J, Brougham DF, Fox EK, Feliu N, Bushmelev A, Schmidt A, Mertens N, Kiessling F, Valldor M, Fadeel B, Mathur S. Water-soluble superparamagnetic

magnetite nanoparticles with biocompatible coating for enhanced magnetic resonance imaging. ACS Nano. 2011;5:6315-6324.

[9] Reddy NN, Mohan YM, Varaprasad K, Ravindra S, Joy PA, Raju KM. Magnetic and electric responsive hydrogel-magnetic nanocomposites for drug-delivery application. J Appl Polym Sci. 2011;122: 1364-1375.

[10] Panja S, Saha B, Ghosh SK, Chattopadhyay S. Synthesis of novel four armed PE-PCL grafted superparamagnetic and biocompatible nanoparticles. Langmuir. 2013;29:12530-12540.

[11] Pourjavadi A, Abedin-Moghanaki A, Nasseri SA. A new functionalized magnetic nanocomposite of poly(methylacrylate) for the efficient removal of anionic dyes from aqueous media. RSC Adv. 2016;6:7982-7989.

[12] Ringeard J-M, Griesmar P, Caplain E, Michiel M, Serfaty S, Huerou J-YL, Marinkova D, Yotova L. Design of poly(*N*-acryloylglycine) materials for incorporation of microorganisms. J Appl Polym Sci. 2013;130:835-841.

[13] Medeiros SF, Santos AM, Fessi H, Elaissari A. Stimuli-responsive magnetic particles for biomedical applications. Int J Pharm. 2011;403:139-161.

[14] Ge J, Hu Y, Biasini M, Beyermann WP, Yin Y. Superparamagnetic magnetite colloidal nanocrystal clusters. Angew Chem Int Ed Engl. 2007;46:4342-4345.

[15] Luo B, Xu S, Luo A, Wang W-R, Wang S-L, Guo J, Lin Y, Zhao D-Y, Wang C-C. Mesoporous biocompatible and acid-degradable magnetic colloidal nanocrystal clusters with sustainable stability and high hydrophobic drug loading capacity. ACS Nano. 2011;5:1428-35.

[16] Meerod S, Rutnakornpituk B, Wichai U, Rutnakornpituk M. Hydrophilic magnetic nanoclusters with thermo-responsive properties and their drug controlled release. J Magn Magn Mater. 2015;392:83-90.

[17] Khadsai S, Rutnakornpituk B, Vilaivan T, Nakkuntod M, Rutnakornpituk M. Anionic magnetite nanoparticle conjugated with pyrrolidinyl peptide nucleic acid for DNA base discrimination. J Nanopart Res. 2016;18:9.

[18] Oka C, Ushimaru K, Horiishi N, Tsuge T, Kitamoto Y. Core-shell composite particles composed of biodegradable polymer particles and magnetic iron oxide nanoparticles for targeted drug delivery. J Magn Magn Mater. 2015;381:278-284.

[19] Merino S, Martín C, Kostarelos K, Prato M, Vázquez E. Nanocomposite hydrogels: 3D polymer-nanoparticle synergies for on-demand drug delivery. ACS Nano. 2015;9: 4686-4697.

[20] Davaran S, Alimirzalu S, Nejati-Koshki K, Nasrabadi HT, Akbarzadeh A, Khandaghi AA, Abbasian M, Alimohammadi S. Physicochemical characteristics of Fe_3O_4 magnetic nanocomposites based on poly(*N*-isopropylacrylamide) for anti-cancer drug delivery. Asian Pac J Cancer Prev. 2014;15:49-54.

[21] Xu SS, Wu J, Jiang W. Synthesis and characterisation of a pH-sensitive magnetic nanocomposite for controlled delivery of doxorubicin. J Microencapsul. 2015;32:533-537.

[22] Habibi D, Kaamyabi S, Amini MM. Doxorubicin poly *N*-vinylpyrrolidone and poly *N*-isopropylacrylamide-*co*-*N*-vinylpyrrolidone coated magnetic nanoparticles. Appl Surf Sci. 2014;320:301-308.

[23] Dutta S, Parida S, Maiti C, Banerjee R, Mandal M, Dhara D. Polymer grafted magnetic nanoparticles for delivery of anticancer drug at lower pH and elevated temperature. J Colloid Interface Sci. 2016;467:70-80.

[24] Prai-In Y, Boonthip C, Rutnakornpituk B, Wichai U, Montembault V, Pascual S, Fontaine L, Rutnakornpituk M. Recyclable magnetic nanocluster crosslinked with poly(ethylene oxide)-*block*-poly(2-vinyl-4,4-dimethylazlactone) copolymer for adsorption with antibody. Mater Sci Eng C Mater Biol Appl. 2016;67:285-93.

[25] Li F, Sun J, Zhu H, Wen X, Lin C, Shi D. Preparation and characterization novel polymer-coated magnetic nanoparticles as carriers for doxorubicin. Colloids Surf B Biointerfaces. 2011;88(1):58-62.

[26] Koppolu B, Rahimi M, Nattama S, Wadajkar A, Nguyen KT. Development of multiple-layer polymeric particles for targeted and controlled drug delivery. Nanomedicine. 2010;6: 355-361.

[27] Theamdee P, Traiphol R, Rutnakornpituk B, Wichai U, Rutnakornpituk M. Surface modification of magnetite nanoparticle with azobenzene-containing water dispersible polymer. J Nanopart. Res. 2011;13:4463-4477.

[28] Kurd K, Khandagi AA, Davaran S, Akbarzadeh A. Cisplatin release from dual-responsive magnetic nanocomposites. Artif Cells Nanomed Biotechnol. 2016;44:1031-1039.

[29] Rodkate N, Rutnakornpituk M. Multi-responsive magnetic microsphere of poly(*N*-isopropylacrylamide)/carboxymethylchitosan hydrogel for drug controlled release. Carbohydr Polym. 2016;151:251-259.

[30] El-Sherbiny IM, Lins RJ, Abdel-Bary EM, Harding DRK. Preparation, characterization, swelling and *in vitro* drug release behaviour of poly(*N*-acryloylglycine-chitosan) interpolymeric pH and thermally-responsive hydrogels. Eur Polym J. 2005;41:2584-2591.

[31] Deng K, Li Q, Bai L, Gou Y, Dong L, Huang C, et al. A pH/thermo-responsive injectable hydrogel system based on poly(*N*-acryloylglycine) as a drug carrier. Iran Polym J. 2011;20:185-194.

[32] Rzaev ZMO, Dinçer S, Pişkin E. Functional copolymers of *N*-isopropylacrylamide for bioengineering applications. Prog Polym Sci. 2007;32:534-595.

[33] Sun W, An Z, Wu P. UCST or LCST? composition-dependent thermoresponsive behavior of poly(*N*-acryloylglycinamide-*co*-diacetone acrylamide). Macromolecules. 2017;50:2175-2182.

[34] Seuring J, Agarwal S. Polymers with upper critical solution temperature in aqueous solution. Macromol Rapid Commun. 2012;33:1898-1920.

[35] Seuring J, Bayer FM, Huber K, Agarwal S. Upper critical solution temperature of poly(*N*-acryloyl glycinamide) in water: A concealed property. Macromolecules. 2012;45:374-384.

[36] Pineda-Contreras BA, Schmalz H, Agarwal S. pH dependent thermoresponsive behavior of acrylamide-acrylonitrile UCST-type copolymers in aqueous media. Polym Chem. 2016;7:1979-86.

[37] Gandhi A, Paul A, Sen SO, Sen KK. Studies on thermoresponsive polymers: Phase behaviour, drug delivery and biomedical applications. Asian J Pharm. Sci. 2015;10:99-107.

[38] Ward MA, Georgiou TK. Thermoresponsive polymers for biomedical applications. Polymers. 2011;3:1215-1242.

[39] Zhang Y, Chen S, Pang M, Zhang W. Synthesis and micellization of a multi-stimuli responsive block copolymer based on spiropyran. Polym Chem. 2016;7:6880-6884.

[40] Deng KL, Zhong HB, Tian T, Gou Y, Li Q, Dong LR. Drug release behavior of a pH/temperature sensitive calcium alginate/poly(*N*-acryloylglycine) bead with core-shelled structure. Express Polym Lett. 2010;4:773-780.

[41] Elouzi AA, Abeid F, Almegrhe M, El-Baseir M. Acidic beverage and the bioavailability of theophylline. J Chem Pharm Res. 2012;4:3454-3459.

[42] Shalaeva M, Kenseth J, Lombardo F, Bastin A. Measurement of dissociation constants (pK_a values) of organic compounds by multiplexed capillary electrophoresis using aqueous and cosolvent buffers. J Pharm Sci. 2008;97:2581-2606.

Supporting information

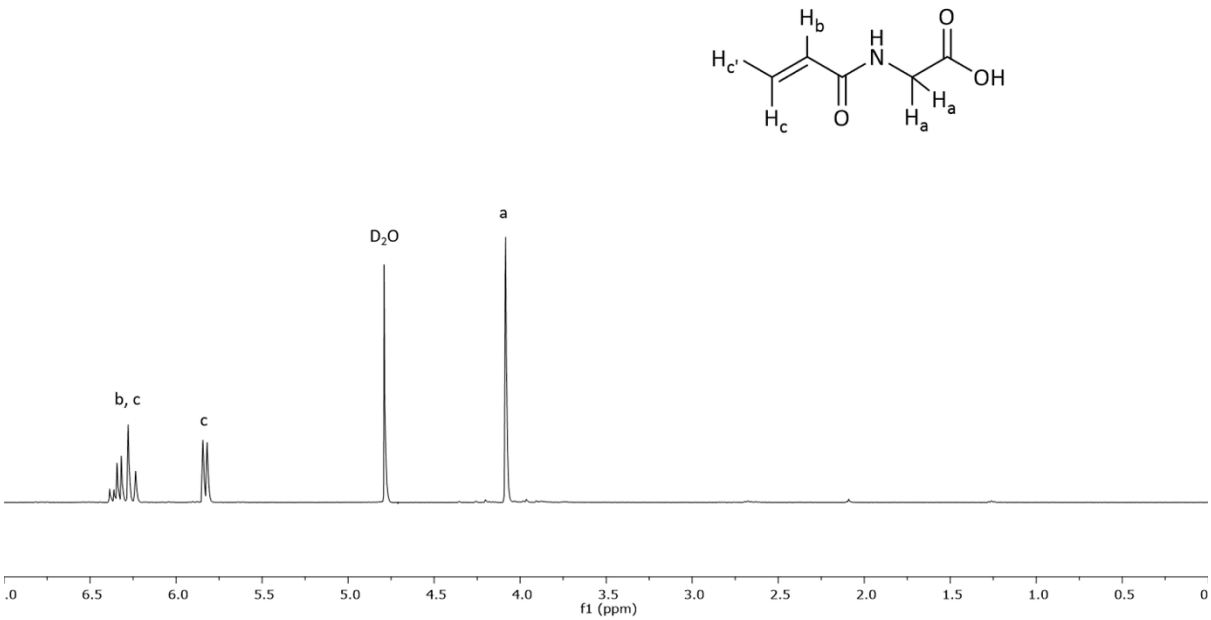

Fig. S1 ^{1}H NMR spectrum of NAG monomer

Calculations of the grafting density of carboxyl groups on PNAG-coated MNP after dispersing in water

The amounts of carboxyl groups presenting on the MNP surface were quantitatively determined by a conductometric titration. The conductometric titration curve of the reaction between NaOH and HCl having a V-shape (Blank) shows (Fig. 1A). During the titration, the reaction that takes place in the titration vessel is following:

$$Na^+ + OH^- \xrightarrow{H^+ \; Cl^-} H_2O + Cl^- + Na^+$$

In the region I, before the end point, OH^- is removed from the solution by reaction with H^+, and Cl^- is added to the solution. The conductance of the solution decreases prior to the end point. After the end point (region II), no OH^- is available to react, and the conductance of the solution increases as a result of the additional of H^+ and Cl^-.

In the case of the titration of HCl with -COOH groups on the particle surface, the conductrometric titration curve exhibits three regions (Fig. 1B). Before the titration of -

COOH groups on the particle surface, the -COOH coated on the particle surface was dispersed in an excess of NaOH solution. Thus, the reaction that takes place in the vessel is following:

$$-COO^- + OH^- \xrightarrow{Na^+ \quad OH^-} -COO^- + Na^+ + H_2O \quad Na^+OH^-_{excess}$$

In the region I of the titration, because basicity of excess OH^- in the solution is stronger than that of $-COO^-$, the OH^- in the solution was first neutralized when HCl was titrated.

$$Na^+_{excess} + OH^-_{excess} \xrightarrow{H^+ \quad Cl^-} H_2O + Na^+ + Cl^-$$

In the region II, when the OH^- in the solution was completely neutralized, the H^+ ions reacted with the $-COO^-$ groups on the MNP surface. After the COO^- groups on the MNP surface were completely reacted with H^+ ions, the solution conductivity sharply increase due to the excess of OH^- and Na^+ (region III). The measurement of the amounts of -COOH groups on the surface of the polymer-coated MNP was estimated from the following equation:

$$\text{Carboxylic acid} = \frac{M\Delta V}{m}$$

$$= \frac{0.005 \text{ mol/L} \times (1.6 \times 10^{-3} \text{ L})}{2 \times 10^{-3} \text{ g}}$$

$$= 4.0 \text{ mmol/g}$$

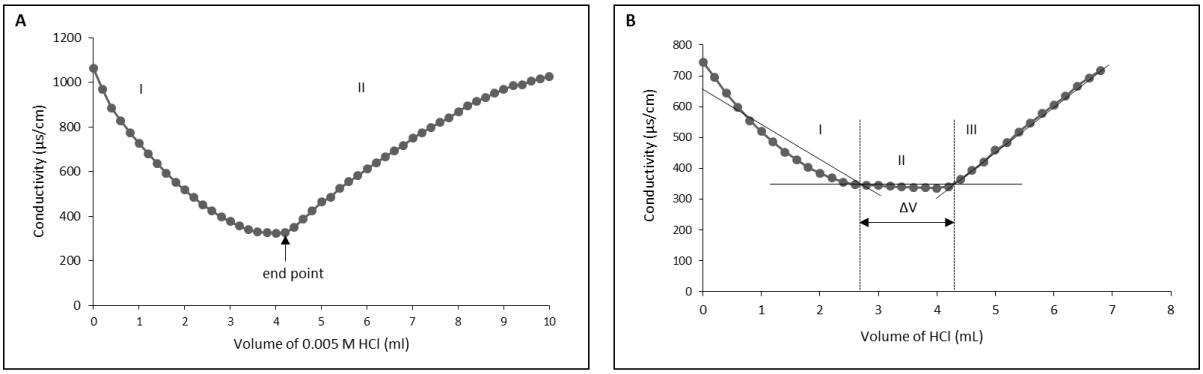

Fig. S2 Examples of the conductometric titration curves, (A) the titration curve of HCl with NaOH and (B) the titration curve of HCl with carboxyl groups on the PNAG-coated MNP surface

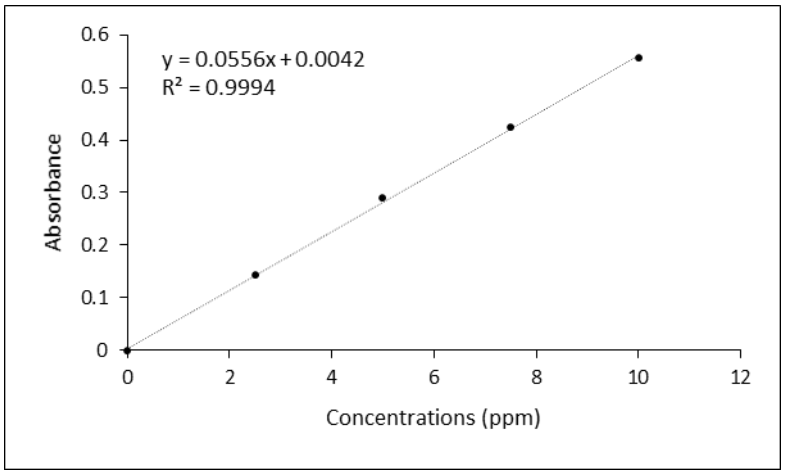

Fig. S3 The calibration curve of theophylline standard with various concentration solution at pH 2.0

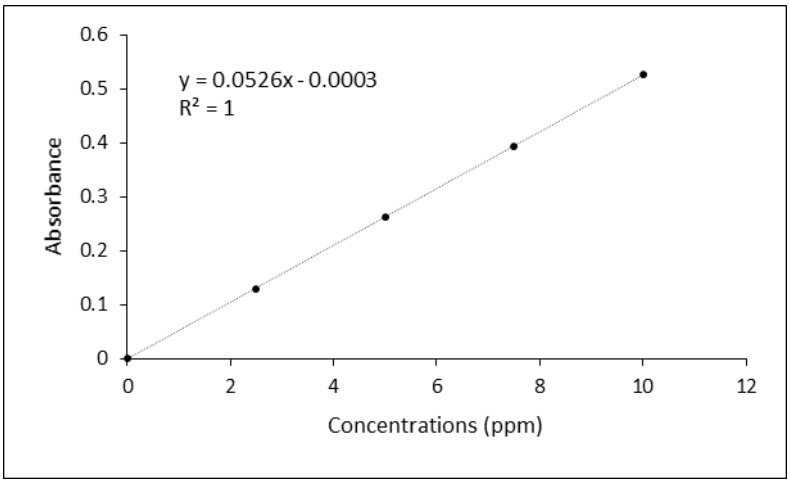

Fig. S4 The calibration curve of theophylline standard with various concentration solution at pH 7.4

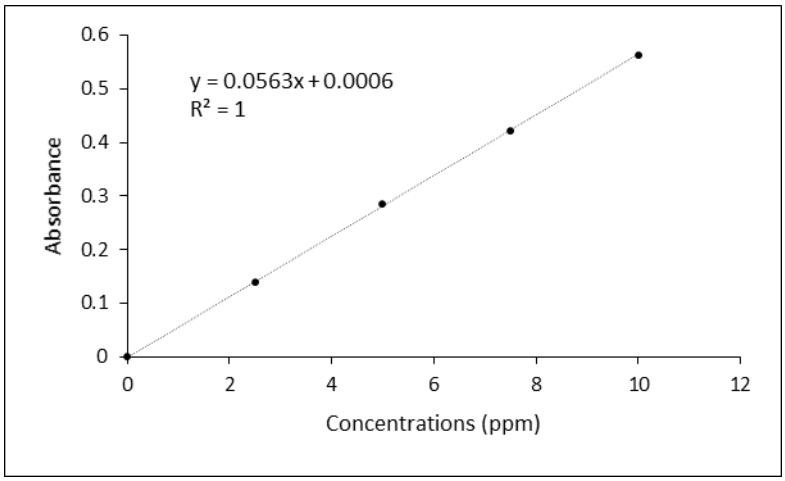

Fig. S5 The calibration curve of theophylline standard with various concentration solution at pH 11.0

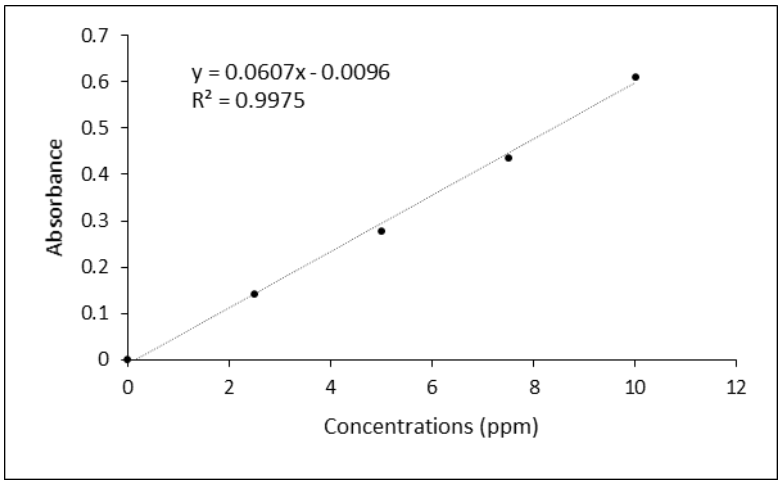

Fig. S6 The calibration curve of theophylline standard with various concentration solution at 0.1 M HCl

Chapter V

Controlled magnetite nanoclustering in the presence of glycidyl-functionalized thermo-responsive poly(*N*-isopropylacrylamide)

Abstract

Glycidyl-functionalized poly(*N*-isopropylacrylamide) (PNIPAAm), synthesized *via* a reversible addition-fragmentation transfer polymerization (RAFT), was used for controlling degree of nanoclustering of magnetite nanoparticle (MNP). The polymer was grafted onto MNP *via* the ring-opening reaction between glycidyl groups at the PNIPAAm chain terminal and amino groups on the MNP surface to obtain thermo-responsive MNP nanocluster. Hydrodynamic size (D_h) and colloidal stability of the nanocluster, corresponding to the degree of nanoclustering reaction, can be regulated either by adjusting the ratio of MNP to the polymer in the reaction or by introducing glycidyl groups to the polymers. The size of the nanocluster ranged between 20 and 150 nm in diameter with about 10-120 particles/cluster. Thermogravimetric analysis (TGA) and vibrating sample magnetometry (VSM) were used to confirm the presence of the polymer in the nanocluster. A study showing indomethacin controlled release of these MNP nanoclusters was also performed. This stable nanocluster with magnetically guidable properties might be potentially used for entrapment of other bio-entities or therapeutic drugs with temperature-responsive properties for controlled release applications.

Keywords: magnetite; nanoparticle; nanocluster; poly(*N*-isopropylacrylamide); thermo-responsive

1. Introduction

In recent years, much attention has been paid in the study in magnetite nanoparticle (MNP) particularly in developing facile and efficient synthetic approaches to control its size, magnetic properties and chemical reactivity. Because of its high surface area-to-volume ratio, many attempts have been made in conjugating bioentities such as deoxyribonucleic acid (DNA) [1, 2], peptide nucleic acid (PNA) [3, 4], protein [5, 6], amino acid [7] and antibodies [8, 9], on the surface for potential uses in biomedical applications. Due to strong inter-particle attractive interactions such as Van der Waals force and magnetic force, they tended to agglomerate to form uncontrollable aggregate, resulting in the loss in nanoscale-related properties [10] and thus limiting its biomedical applications [11]. Coating the particle with long chain polymer is one of a promising approach to prevent the particle aggregation through a steric stabilization mechanism, resulting in improvement in stability and dispersibility in the media. In addition, the polymer coated on the particle surface also served as a platform for conjugation with functional biomolecules [12, 13].

Many applications, such as controlled drug delivery and magnetic separation of cells and antibodies, take advantages of magnetically guidable properties of MNP. In these applications, drug-conjugated or bioentity-conjugated MNP should have good magnetic responsiveness, so that they can rapidly respond to an external magnetic field. One of the promising approaches in enhancing magnetic responsiveness of MNP without the formation of macroscopic particle aggregation was to assemble them into the form of nanocluster. MNP nanocluster is composed of many interconnected single particles of ≈3-20 nm in size and minor amount of organic components [14]. Unlike micron-sized particles, formation of MNP nanocluster significantly increased magnetic responsiveness [15, 16] as opposed to individual MNP and also maintained its dispersibility and stability in the media [17, 18]. Importantly, its superparamagnetic properties should also be maintained as long as individual MNP core can be distinguished from each other after nanocluster formation, meaning that there was no one polycrystalline particle but a nanocluster with distinguishable particles smaller than 20 nm [19]. Controlling the degree of MNP nanoclustering with reasonable size will result in the nanocluster with good magnetic responsiveness, good dispersibility and stability in the media. Many approaches have been investigated in controlling the formation of MNP nanocluster such as physical or physicochemical interaction between pre-synthesized MNP and polymer particle [16, 20], *in-situ* polymerization of monomers in the presence of MNP [21-23] and *in-situ* precipitation of MNP in the presence of polymer microsphere [24, 25].

The study in the synthesis of MNP nanocluster coated with responsive polymers was rather limited [26, 27]. In this work, preparation of MNP nanocluster coated with poly(*N*-isopropylacrylamide)(PNIPAAm) is presented. PNIPAAm functionalized with glycidyl methacrylate (GMA) was first synthesized *via* Reversible Addition Fragmentation Chain Transfer (RAFT) polymerization and then grafted onto MNP surface. RAFT polymerization, one of several types of controlled radical polymerization (CRP) techniques, was used in this work because it can produce polymers with controllable molecular weights and narrow polydispersity indices (PDIs) and can be performed under mild condition reactions in various reaction systems without using metal catalysts [28]. PNIPAAm is the most studied thermo-responsive polymer owing to its physiologically relevant transition temperature and relative insensitivity to pH and salt content [29]. It has a lower critical solution temperature (LCST) at 32°C, which is close to that of human body [30]. Below its LCST, PNIPAAm is well soluble in water due to the formation of hydrogen bonding of the chains with water molecules, resulting in the formation of a swollen state. When increasing the temperature above its LCST, PNIPAAm deswells to a collapsed state due to the formation of hydrogen bondings among the polymer chains. This process is generally reversible, making the polymer to behave as an on-off system when the temperature is changed across the LCST. Syntheses of the copolymers containing PNIPAAm have been widely reported [31-35]. However, the studies in surface modification of MNP with PNIPAAm-containing copolymers are rather limited [36, 37].

In this report, PNIPAAm was first synthesized *via* RAFT polymerization, followed by the functionalization with GMA units at the chain terminal. The chemical structures and functional groups of the synthesized PNIPAAm were characterized *via* proton nuclear magnetic resonance spectroscopy (^{1}H NMR) and fourier transform infrared spectroscopy (FTIR), respectively. It was then grafted to MNP through the ring-opening reaction of the glycidyl groups at the chain terminal with amino groups grafted on MNP surface and essentially induced the formation of MNP nanocluster. Transmission electron microscopy (TEM) was conducted to determine the nanocluster size and photocorrelation spectroscopy (PCS) was performed to determine hydrodynamic size (D_h) and LCST of the nanoclusters. The effects of MNP-to-polymer ratio used in the reactions and the number of GMA units in the polymer on D_h and colloidal stability of the nanocluster were also investigated. Magnetic properties of the nanoclusters were investigated *via* vibrating sample magnetometry (VSM). The composition of MNP-polymer nanocluster was also determined *via* thermogravimetric

analysis (TGA). In addition, a case study showing the drug controlled release application of these MNP nanoclusters was also investigated.

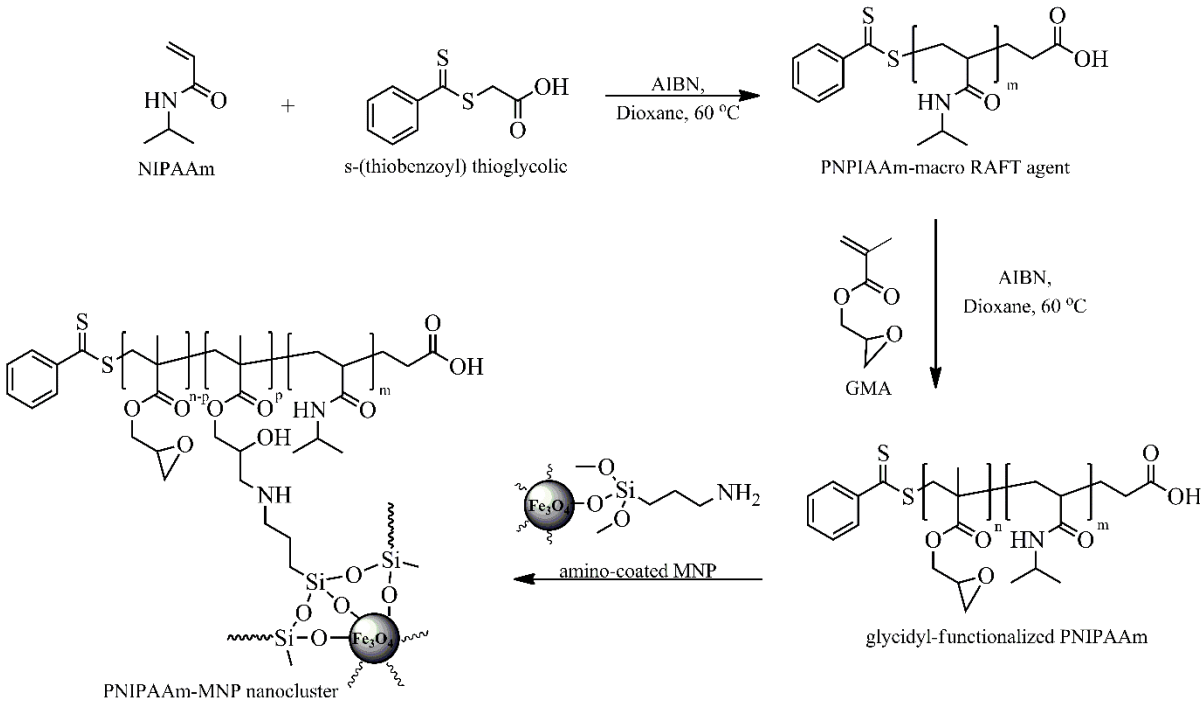

Figure 1 Schematic representation for controlled nanoclustering of MNP with glycidyl-functionalized PNIPAAm

2. Experimental

2.1 Materials

Unless otherwise stated, all reagents were used without further purification: iron (III) acetylacetonate ($Fe(acac)_3$) (Acros, 99.9%), benzyl alcohol (Unilab, 98%), oleic acid (Fluka), triethylamine (Carto Erba, 97%), 3-aminopropyl triethoxysilane (APS)(Acros, 99%), glycidyl methacrylate (GMA) (Sigma-Aldrich, 97%), 2,2′-azobis (2-methylpropionitrile) (AIBN) (Sigma-Aldrich, 98%), *S*-(thiobenzoyl)thioglycolic acid (Sigma-Aldrich, 99%). *N*-isopropylacrylamide (NIPAAm) (Acros, 99%) was recrystallized twice in hexane before polymerization.

2.2 Synthesis

2.2.1 Synthesis of PNIPAAm macro RAFT agents

In a round bottom flask, NIPAAm (10 g, 88.370 mmol), S-(thiobenzoyl) thioglycolic acid RAFT agent (0.0924 g, 0.435 mmol) and an AIBN initiator (0.0182 g, 0.110 mmol) were dissolved in 50 mL of 1,4-dioxane under N_2 atmosphere with stirring for 30 min. RAFT polymerization of PNIPAAm was allowed for 48 h at 60°C to achieve 60% monomer conversion. The mixture was then diluted with 1,4-dioxane to 100 mL and cooled to room temperature. The polymer was then purified by precipitation in diethyl ether and dried *in vacuo*. Purified PNIPAAm macro RAFT agents were subsequently used for the synthesis of glycidyl-functionalized PNIPAAm.

2.2.2 Synthesis of glycidyl-functionalized PNIPAAm (PNIPAAm-GMA)

A procedure similar to aforementioned polymerization was used for the synthesis of PNIPAAm-GMA with the use of PNIPAAm macro RAFT agent. An example described here is for the synthesis of PNIPAAm-GMA with 8 repeating units of GMA (PNIPAAm-GMA_8). PNIPAAm-GMA with 18 repeating units of GMA (PNIPAAm-GMA_{18}) was synthesized using the similar procedure with appropriate amounts of GMA loaded. GMA (0.16 mL, 1.173 mmol), PNIPAAm macro RAFT agent (1.00 g, 0.077 mmol) and AIBN initiator (3.0 mg, 0.018 mmol) were dissolved in 1,4-dioxane (30 mL) with N_2 purging for 30 min. The reaction was set under N_2 atmosphere at 60°C for 48 h to achieve about 60% reaction conversion. After the reaction, the product was purified by precipitation in methanol and dried *in vacuo*.

2.2.3 Synthesis of amino-coated MNP

MNP was synthesized *via* a thermal decomposition of $Fe(acac)_3$ (5 g, 14.05 mmol) in benzyl alcohol (90 mL) at 180°C for 48 h under N_2 atmosphere. After the reaction, the precipitant was removed from the mixture using an applied magnetic field and repetitively washed with ethanol and then CH_2Cl_2. The resultant product was obtained as fine black powder after drying under reduced pressure. Oleic acid (4 ml) was then added to the MNP dispersion (0.6 g MNP in 30 ml toluene) with sonication for 3 h under N_2 atmosphere. MNP aggregate was removed from the oleic acid-coated MNP by centrifugation at 5000 rpm for 15 min. To prepare amino-coated MNP, APS (1 ml, 4.517 mmol) was added to a mixture of oleic acid-coated MNP (0.1 g) and TEA (0.01 ml, 0.075 mmol) in dried toluene (6 ml). The dispersion was sonicated for 4 h at room temperature under N_2 atmosphere. Amino-coated

MNP was retrieved using a magnet, washed twice with ethanol and toluene and finally dried *in vacuo*.

2.2.4 Synthesis of MNP-polymer nanoclusters

The polymer solution (0.001-10 mg in 1 mL of DI water) was added dropwise to amino-coated MNP dispersion (1 mg MNP in 2 mL pH 10-aqueous solution). The mixture was stirred at 65°C for 12 h under N_2 atmosphere. The product was isolated using a magnet, washed twice with DI water and acetone and then dried *in vacuo*.

2.3 Characterization

2.3.1 Characterization of the polymers and nanoparticles

^{1}H NMR spectra were performed on a 400 MHz Br.uker NMR spectrometer using $CDCl_3$ as a solvent. FTIR was performed on a Perkin-Elmer Model 1600 Series FTIR Spectrophotometer in the wavenumber range of 4,000-400 cm^{-1}. The samples were mixed and pressed with KBr to form disc samples. TEM was performed on Philips Tecnai 12, operated at 120 kV equipped with Gatan model 782 CCD camera. MNP dispersions in water were directly cast onto carbon-coated copper grids and allowed to slowly evaporate at room temperature. Magnetic properties of the particles were measured at room temperature using a Standard 7403 Series, Lakeshore vibrating sample magnetometer. Magnetic moment of each sample was investigated over a range of ± 10000 G of applied magnetic fields using 30 min sweep time. TGA was performed on SDTA 851 Mettler-Toledo at the temperature ranging between 25 and 600°C at a heating rate of 20°C/min under oxygen atmosphere. Hydrodynamic size (D_h) of the particles was measured by PCS using NanoZS4700 nanoseries Malvern instrument.

2.3.2 Determination of indomethacin entrapment (EE) and loading efficiency (DLE) of the polymer-coated MNP nanoclusters

The indomethacin solution (1 mL, 5 mg/mL in ethanol) was added dropwise with stirring to an aqueous dispersion of the nanoclusters (3 mL, 5 mg of MNP nanocluster). The mixture was stirred at 20 ˚C for 120 min. The weight of the entrapped drug in the complex was determined from the difference of the weights of the loaded drug and the excess of the drug remaining dispersible in the solution. After centrifugation to remove agglomerated particles, the drug concentration in the supernatant, reflecting the amount of the entrapped drug in the MNP nanoclusters, was determined using UV–Visible spectrophotometer at λ_{max} = 320 nm. EE and DLE were calculated from the following equations:

$$\text{Entrapment efficiency (EE)} = \frac{\text{Weight of the entrapped drug in the MNP nanocluster}}{\text{Weight of the loaded drug}} \text{ x100} \quad (1)$$

$$\text{Drug loading efficiency (DLE)} = \frac{\text{Weight of the entrapped drug in the MNP nanocluster}}{\text{Weight of the MNP nanocluster}} \text{ x100} \quad (2)$$

2.3.3 The cumulative release studies of entrapped indomethacin from the polymer-coated MNP nanoclusters

Indomethacin-loaded MNP nanoclusters (5 mg of MNP nanocluster) were dispersed in a 2 mL phosphate buffer solution (PBS) (pH 7.4). The dispersion of indomethacin-loaded MNP nanoclusters was placed in a water bath at 20 ˚C (below LCST) or 45 ˚C (above LCST). At a predetermined time interval, 200 µL aliquots of the dispersions were withdrawn from the release media and 200 µL of PBS (pH 7.4) was replaced. After separation of the MNP nanoclusters using an external magnet, the concentrations of the released drug in the supernatant were determined *via* UV–Visible spectrophotometer at λ_{max} = 320 nm.

$$\text{Cumulative release} = \frac{\text{weight of released drug at a given time}}{\text{Weight of the entrapped drug in the MNP nanocluster}} \text{ x100} \quad (3)$$

3. Results and Discussion

The main objective of this work is to control degree of nanoclustering of MNP using glycidyl-functionalized PNIPAAm (PNIPAAm-GMA) *via* a "grafting onto" approach. PNIPAAm-GMA was first synthesized *via* a RAFT polymerization by a sequential addition of NIPAAm monomer and then GMA monomer to form reactive glycidyl-functionalized PNIPAAm. It was envisioned that reactive amino groups on the particle surface can readily open the epoxy rings in PNIPAAm-GMA and then induce MNP nanoclustering due to the presence of multi-functional groups on MNP surface and also in the polymer structure. PNIPAAm-GMA_8 and PNIPAAm-GMA_{18} (Table 1) were used in MNP nanoclustering reactions to investigate the effect of numbers of GMA on D_h, dispersibility and stability of MNP nanocluster in aqueous dispersions. In addition, effect of the polymer concentrations used in the nanoclustering reaction on D_h was also determined.

Synthesis of glycidyl-functionalized PNIPAAm (PNIPAAm-GMA)

PNIPAAm macro RAFT agent was synthesized *via* a RAFT polymerization of NIPAAm using S-(thiobenzoyl)thioglycolic acid as a chain-transfer agent. In Figure 2A, the

presence of the signals at 1.5 ppm (peak *d*) and 2.0 ppm (peak *c*) corresponding to methylene and methine protons, respectively, indicated the formation of PNIPAAm. In addition, the C<u>H</u>$_3$ signals at 1.1 ppm (peak *a*) and C<u>H</u> signals at 3.85 ppm (peak *b*) of the repeating units without the signals of vinyl groups of NIPAAm monomers (5.6, 6.0 and 6.2 ppm of C<u>H</u>$_2$=C<u>H</u>-) also signified the formation of the PNIPAAm macro RAFT agent. The molecular weight ($\overline{M_n}$) of the polymer calculated from the reaction conversion (64% conversion) was about 11,000 g/mol corresponding to 122 NIPAAm repeating units. This polymer was then used as a macro RAFT agent for further functionalization with GMA to obtain PNIPAAm with different numbers of glycidyl units.

Figure 2B shows an example of ^{1}H NMR spectrum of PNIPAAm-GMA$_{18}$. The signals of glycidyl groups, such as 2.6, 2.8 and 3.2 ppm (peak *i*, *j* and *h*) of epoxy rings and 4.3 ppm (peak *g*) of methylene protons adjacent to the ester groups, were observed indicating the formation of PNIPAAm-GMA. According to the reaction conversion (60%), PNIPAAm with two different numbers of GMA units (8 and 18 units) was obtained, and the polymer was thus designated as PNIPAAm-GMA$_8$ and PNIPAAm-GMA$_{18}$, respectively (Table 1). ^{1}H NMR spectrum of PNIPAAm-GMA$_8$ is similar to that of Figure 2B and shown in the supporting information.

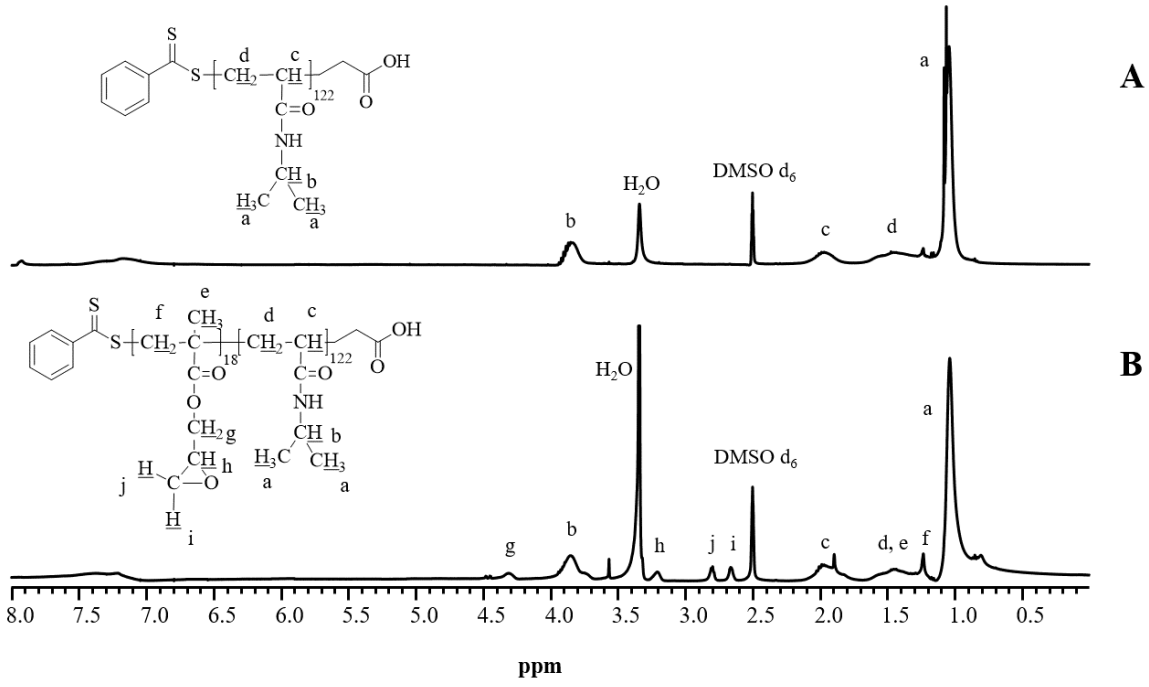

Figure 2 ^{1}H NMR spectra of A) PNIPAAm macro RAFT agent and B) PNIPAAm-GMA$_{18}$ (solvent : DMSO D$_6$)

From the results in Table 1, both $\overline{M_n}$, GPC and $\overline{M_n}$, 1H NMR of the polymers gradually increased when increasing the numbers of GMA units (8 and 18 repeating units) in PNIPAAm chains. In all cases, the $\overline{M_n}$, GPC values were slightly higher than $\overline{M_n}$, 1H NMR and their PDIs were in the range of 1.24-1.41.

Table 1 RAFT polymerizations of PNIPAAm and PNIPAAm-GMA

Polymer name	[1][Monomer]:[RAFT]:[AIBN]	Conversion (%) after 48 h	[2] $\overline{M_n}$ 1H NMR (g/mol)	$\overline{M_n}$ GPC (g/mol)	PDI
PNIPAAm	[200]:[1]:[0.25]	64	11000	13000	1.30
PNIPAAm-GMA_8	[15]:[1]:[0.25]	60	12000	14000	1.24
PNIPAAm-GMA_{18}	[30]:[1]:[0.25]	61	14000	16000	1.41

[1] The monomers are NIPAAm or GMA

[2] $\overline{M_n}$, 1H NMR $= \frac{[\text{monomer}]}{[\text{RAFT agent}]} \times \%\text{conversion} \times \text{molecular weight of monomer}$

In good agreement with ^{1}H NMR, FTIR spectrum of PNIPAM shows N-H stretching at 3437 cm^{-1} and the characteristic signals of amide groups at 1647 cm^{-1} and 1550 cm^{-1} ((O=C)-N-H)(Figure 3A). After functionalization of PNIPAAm with glycidyl groups, FTIR spectrum shows the characteristic signals of epoxy rings of GMA at 841 cm^{-1} and 909 cm^{-1} (Figure 3B) [38, 39]. In addition, the signals at 1730 cm^{-1} ((C=O)-O) and 1173 cm^{-1} (C-O) also indicated the presence of ester linkages of GMA units in the polymer chains.

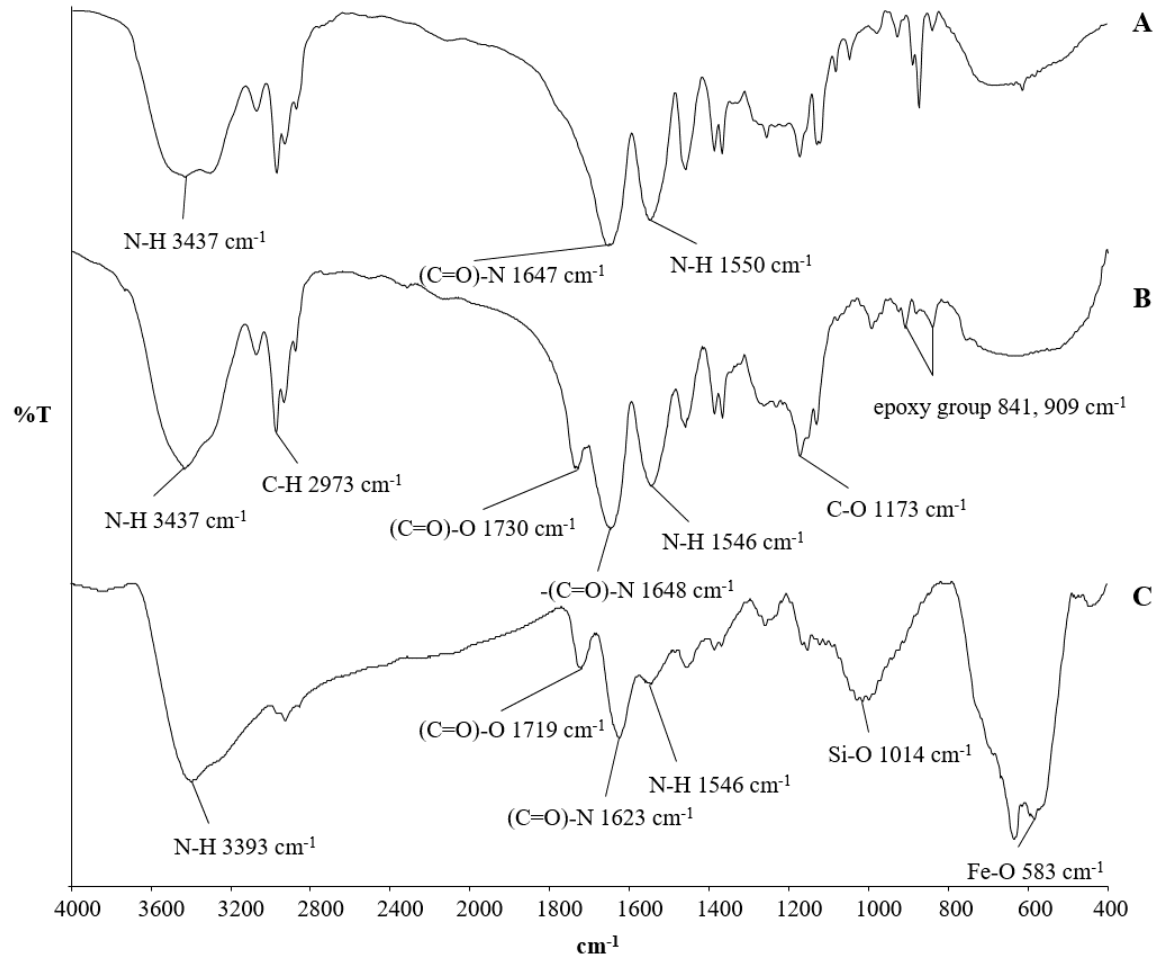

Figure 3 FTIR spectra of A) PNIPAAm, B) PNIPAAm-GMA_{18} and C) MNP-PNIPAAm-GMA_{18} nanocluster

Synthesis of MNP-PNIPAAm-GMA nanocluster

FTIR spectrum of the amino-coated MNP shows the signals at 998 cm^{-1} (Si-O stretching), 1537 cm^{-1} (N-H bending), 3369 cm^{-1} (N-H stretching) and 583 cm^{-1} (Fe-O) of the MNP core (in the supporting information). To form the nanocluster, glycidyl-functionalized PNIPAAm solutions in water having various polymer concentrations were added to the amino-coated MNP dispersions in basic condition (pH 10) and the reaction was set at 65°C for 12 h. Epoxy functional groups of PNIPAAm-GMA can readily react with amino groups on MNP surface *via* a ring-opening reaction. FTIR spectrum of the nanocluster shows characteristic signals of both MNP core at 583 cm^{-1} (Fe-O stretching) and PNIPAAm-GMA at 1719 cm^{-1} ((C=O)-O stretching of glycidyl groups), 3393 cm^{-1} (N-H stretching), 1623 cm^{-1} and 1548 cm^{-1} ((O=C)-N-H of the amide groups) (Figure 3C). In addition, the characteristic

peaks of the epoxy groups (841 $cm^{-1}$and 909 cm^{-1}) disappeared after the MNP nanoclustering due to the ring-opening reactions of glycidyl units.

D_h of the polymers including PNIPAAm, PNIPAAm-GMA_8 and PNIPAAm-GMA_{18} (without MNPs) and those of MNP-polymers nanoclusters were investigated as a function of the polymer concentrations *via* PCS (Figure 4A). Without MNP, D_h tended to consistently increase when increasing polymer concentrations from 0.001 to 10 mg/ml. Interestingly, PNIPAAm-GMA_{18} showed significantly larger D_h (up to 820 nm at 10 mg/ml polymer concentration) than those of the other two polymers (PNIPAAm and PNIPAAm-GMA_8). This result suggested that PNIPAAm-GMA_{18} might have some polymer agglomeration in water due to the relatively long hydrophobic GMA segments in the structure.

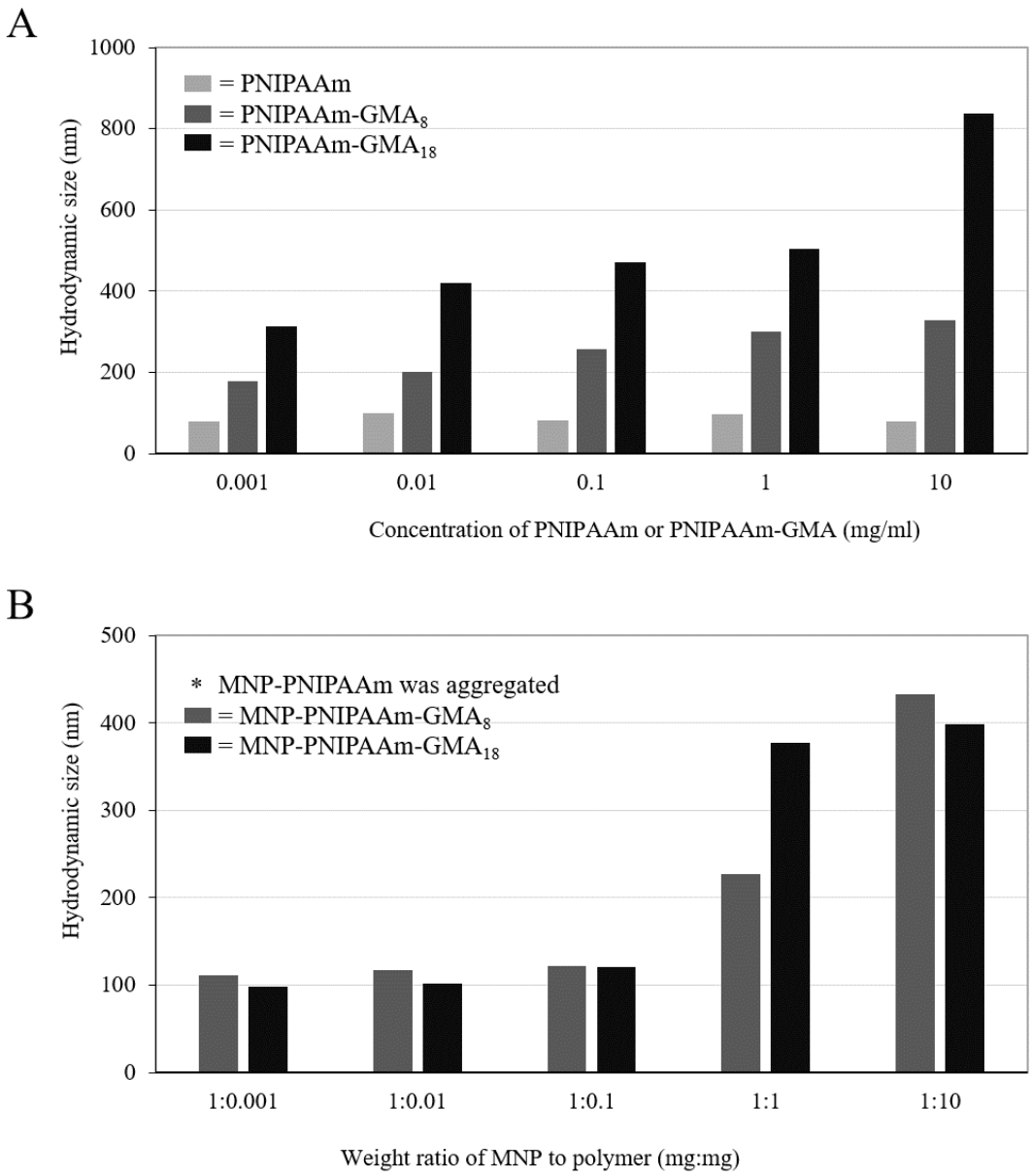

Figure 4 (A) D_h of PNIPAAm and PNIPAAm-GMA (without MNP) and (B) D_h of MNP nanocluster grafted with PNIPAAm or PNIPAAm-GMA in various polymer concentrations. 1 mg MNP in 1 ml polymer solution was used in these reactions.

After the naoclustering reaction, ungrafted polymer was removed from the MNP dispersion *via* a magnetic separation and washing process. MNP-polymer nanocluster was then redispersed in water and its D_h was investigated as a function of the polymer concentration (Figure 4B). MNP-PNIPAAm (without GMA unit) apparently aggregated, regardless of the ratio of MNP to the polymer used, due to the absence of glycidyl group in the polymer chain for covalent coating on the MNP surface, and thus its D_h did not measured.

The presence of glycidyl groups in PNIPAAm-GMA provided covalent bonding of the polymers with MNP *via* ring-opening reactions, resulting in the improved dispersibility of the particles in water due to the polymer coating. D_h tended to increase (from 100 nm to 400 nm) when the ratio of the polymer in the reactions increased and this was attributed to the formation of MNP nanoclustering. In addition, it should be mentioned that D_h of these MNP nanoclusters seemed to be smaller than those of their corresponding polymers at the same polymer concentrations (Figure 4A), signifying the formation of nanoclustering between the MNP and the functionalized polymers. The proposed mechanism of the formation of the nanoclusters is shown in Figure 5. Because MNP coated with multifunctional groups of primary amino groups, these particles can serve as nano-crosslinkers and thus induced the formation of MNP nanoclusters, which were evidenced by TEM technique. These results implied that D_h of the nanoclusters, reflecting the degree of nanoclustering reactions, can be regulated either by adjusting the ratio of the polymers to MNP in the reactions or by introducing GMA units to the polymers.

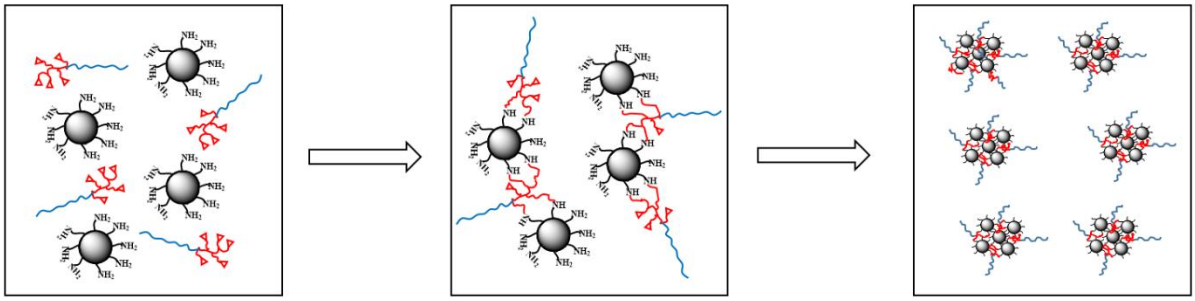

Figure 5 Schematic mechanism of the formation of MNP-PNIPAAm nanoclusters

TEM images of amino-coated MNP and the nanoclusters using 1:0.1 and 1:10 ratio of MNP to PNIPAAm-GMA_{18} are shown in Figure 6. These particles were dispersed in water and directly cast on copper grids for the TEM sample preparation. Before the reactions between MNP and the polymers, amino-coated MNP showed large aggregate of the particles without nanoclusters due to the lack of polymeric stabilization to the particles (Figure 6A). When introducing amino-coated MNP into PNIPAAm-GMA_{18} solutions, MNP nanoclusters were thoroughly observed in TEM images (Figure 6B and 6C). The size of these nanoclusters ranged between 20 and 150 nm in diameter with about 10-120 particles/cluster. These TEM results supported the proposed mechanism of MNP nanoclustering shown in Figure 5. TEM images of the MNP nanoclusters grafted with PNIPAAm-GMA_8 exhibit the formation of the

nanoclusters similarly to those of PNIPAAm-GMA_{18} without significant difference in their size (in the supporting information).

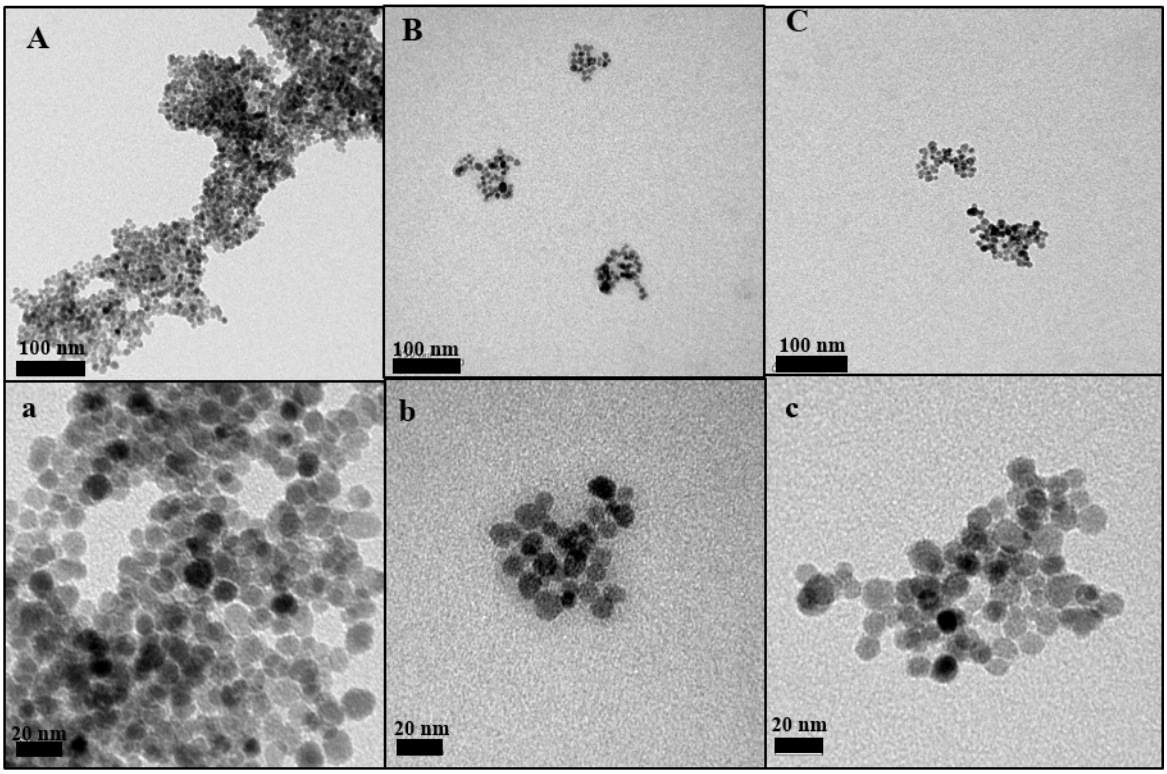

Figure 6 Representative TEM images of MNP before and after nanoclustering reactions dispersed from water. (A, a) amino-coated MNP, (B, b) MNP-PNIPAAm-GMA_{18} nanocluster with MNP:polymer ratio of 1:0.1 and (C, c) MNP-PNIPAAm-GMA_{18} nanocluster with MNP:polymer ratio of 1:10

It should be noted that a compromise between colloidal stability in water and magnetic responsiveness of the nanoclusters is crucial for use in magnetic separation applications. It was hypothesized that the formation of MNP nanoclusters with a controllable degree of clustering should retain its nano-scale related properties but having sufficient magnetic responsiveness. Therefore, the stability in water and magnetic responsiveness of the MNP nanoclusters coated with PNIPAAm-GMA_8 or PNIPAAm-GMA_{18} were investigated. This experiment was performed with the use of MNP:PNIPAAm-GMA ratio of 1:10 because PCS results indicated that there was some degree of MNP-polymer nanoclustering as opposed to those having 1:0.1 MNP:polymer (Figure 4B). Therefore, 1:10 ratio of MNP to the polymers would be focused for the studies in the effect of the number of GMA units

(PNIPAAm-GMA_8 and PNIPAAm-GMA_{18}) on the particle stability, magnetic responsiveness and thermo-responsive properties.

The MNP nanoclusters coated with PNIPAAm-GMA_8 or PNIPAAm-GMA_{18} showed a good dispersibility in water without aggregation after 3 days and some slight aggregation after 7 days of the preparations (Figure 7a and 7b), while those coated with PNIPAAm (without GMA units) exhibited macroscopic aggregation within 30 min (Figure 7c). This result confirmed the reactions between GMA units in the polymers and the amino groups on the particle surface, resulting in the polymer coating and thus improved dispersibility in water.

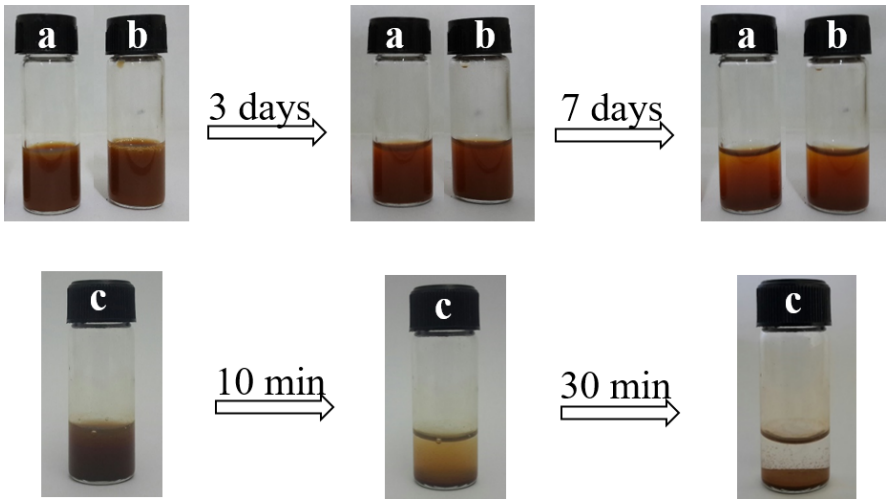

Figure 7 Water dispersibility of MNP nanoclusters coated with (a) PNIPAAm-GMA_8, (b) PNIPAAm-GMA_{18} and (c) PNIPAAm,

Colloidal stability of MNP nanoclusters coated with the polymers in water when subjected to an applied magnetic field was investigated. The particles coated with PNIPAAm-GMA were able to be completely separated from the dispersions within 120 min with an assistance of a permanent magnet (Figure 8a and 8b). This was attributed to the formation of MNP nanoclusters, resulting in an improvement in magnetic responsiveness. It should be mentioned that individual MNP cannot be magnetically separated from its carrier fluid because the particle and the solvent can move as a whole [40]. When PNIPAAm (without GMA) was used instead of PNIPAAm-GMA, the particles were magnetically separated from the dispersion within 3 min (Figure 8c). The much shorter separation time was again attributed to the large aggregation of the particles due to a lack of polymer coating, which was in good agreement with the PCS and water dispersibility results. These results

indicated that coating the polymers on MNP is necessary in order to obtain stable nanoclusters with ability to be separated from their dispersions. However, the magnetic responsiveness and water dispersibility of the nanoclusters coated with PNIPAAm-GMA_8 and PNIPAAm-GMA_{18} were not different from each other.

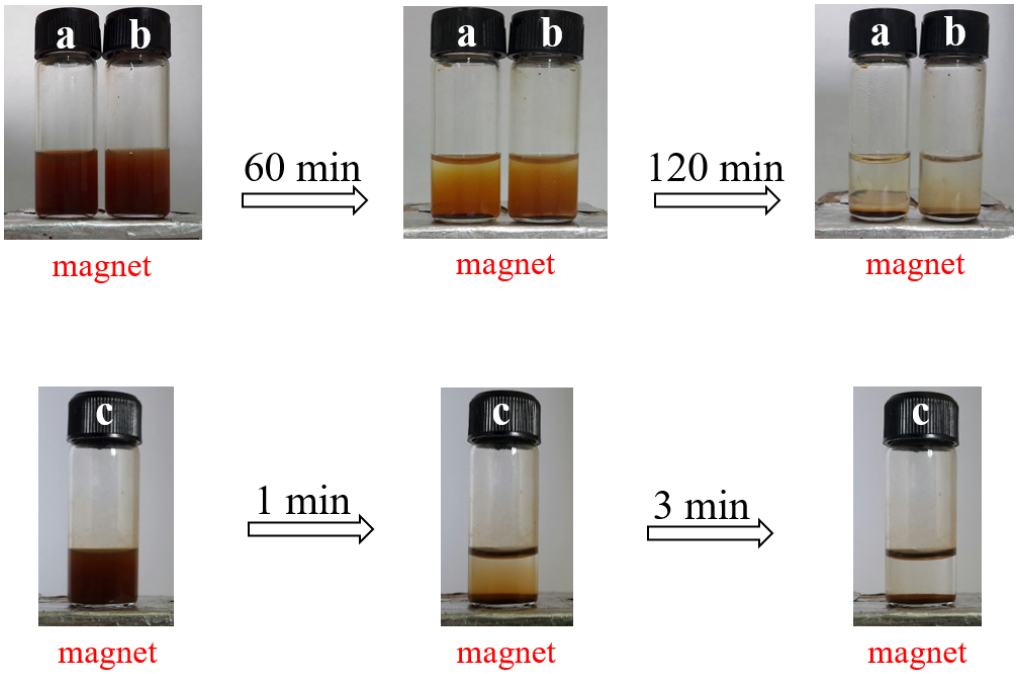

Figure 8 Magnetic separation in water of MNP nanoclusters coated with (a) PNIPAAm-GMA_8, (b) PNIPAAm-GMA_{18} and (c) PNIPAAm,

Percentage of organic components in the nanoclusters was determined *via* TGA technique. It was assumed that the percent weight loss was attributed to the weight of organic components and the residual weight was those of iron oxide in the nanoclusters (Figure 9A). The organic component in amino-coated MNP (without the polymer) was about 5%, while those in MNP-polymer nanoclusters were about 37% and 47%, depending on the type of the polymer (PNIPAAm-GMA_8 or PNIPAAm-GMA_{18}) used in the nanoclustering reactions. The MNP nanoclusters coated with the polymers with higher number of GMA units (PNIPAAm-GMA_{18}) showed higher percentage of the organic component in the structure.

The results from VSM experiments were also in good agreement with those from TGA. The nanoclusters having low MNP contents (high organic components) exhibited low magnetic responsiveness, as indicated by the low saturation magnetization (M_s) in the *M-H*

curves (Figure 9B). These nanoclusters showed superparamagnetic behavior as indicated by the absence of coercivity and remanence when there was no applied magnetic field.

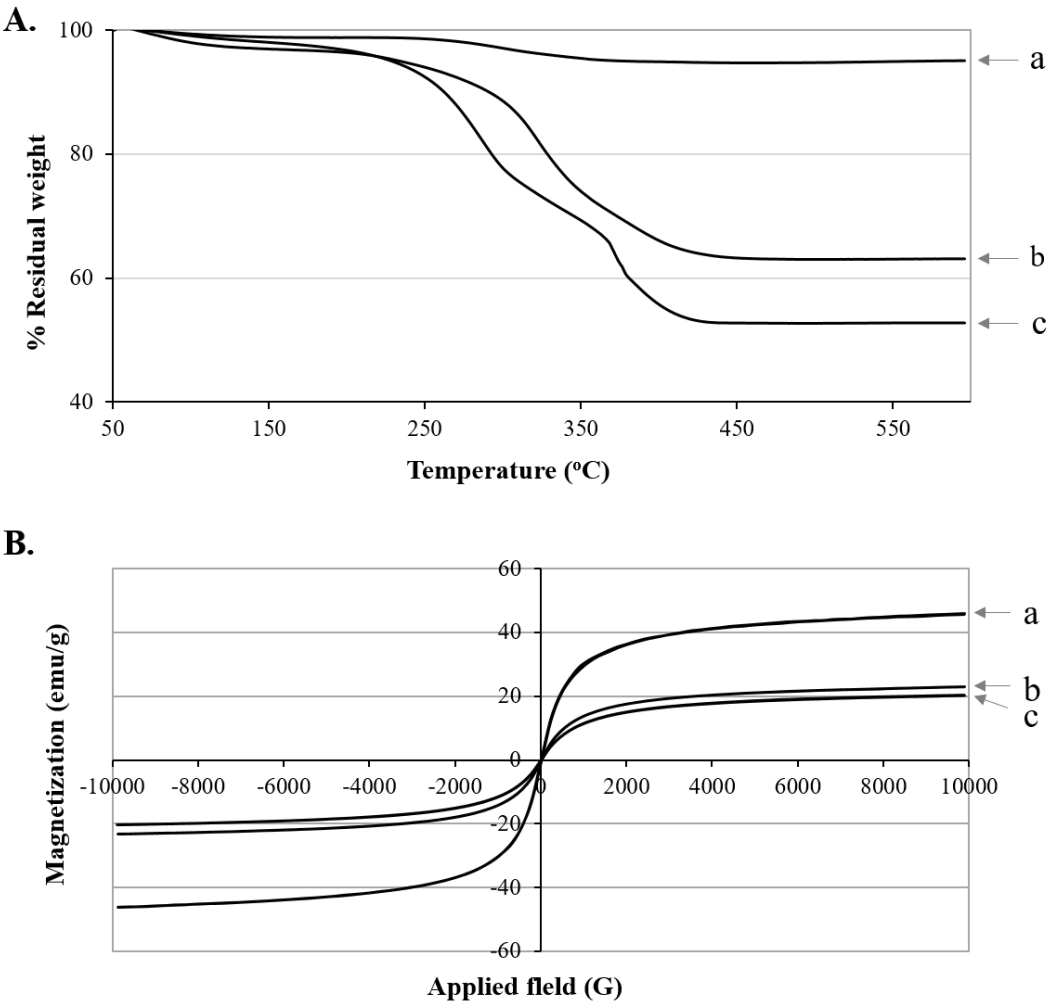

Figure 9 A) TGA thermograms and B) *M-H* curves of (a) amino-coated MNP, (b) MNP-PNIPAAm-GMA_8 and (c) MNP-PNIPAAm-GMA_{18} , when 1:10 ratio of MNP to the polymer was used in the nanoclustering reactions.

Figure 10 shows D_h of MNP nanoclusters coated with PNIPAAm-GMA_8 and PNIPAAm-GMA_{18} as a function of dispersion temperature. D_h values did not significantly change at the temperature below 34°C and drastically increased at the temperature between 34 °C and 40°C, indicating the LCST of the MNP nanoclusters of 34°C for both samples. The observed LCST was slightly higher than those of PNIPAAm homopolymer (32°) [41] and this was attributed to the existence of GMA moiety in the structure, resulting in the formation of hydroxyl groups in the structure after the ring-opening reactions. The increase in LCST of

PNIPAAm due to the presence of hydrophilic components in the polymer structure has been previously reported [31].

At the temperature above the LCST (34°C), PNIPAAm in the nanoclusters became more hydrophobic due to hydrogen bonding among the polymer chains, leading to the enhancement in the particle agglomeration in water and thus increasing their D_h. These results well corresponded to their aggregation when standing at the temperature above the LCST for 30 min (the inset in Figure 10). They can be re-dispersible at the temperature below the LCST and this behavior was reversible. When considering the effect of the number of GMA units in the polymer chains on D_h of the nanoclusters, the increase in GMA units further improved their water swellability due to the increased formation of hydrophilic hydroxyl groups as indicated by the larger D_h at the temperature above the LCST.

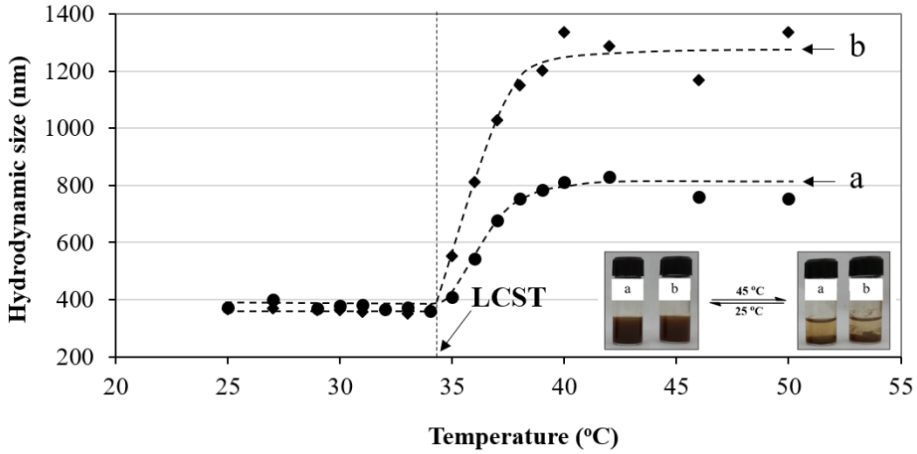

Figure 10 D_h of MNP nanoclusters coated with (a) PNIPAAm-GMA_8 and (b) PNIPAAm-GMA_{18} as a function of temperatures, when 1:10 ratio of MNP to the polymers was used in the nanoclustering reactions.

A case study showing the drug controlled release application of these MNP nanoclusters was also performed. EE and DLE of the nanoclusters were first investigated. It was found that EE and DLE of the nanoclusters were rather high (45-48% of EE and 75-85% of DLE). Indomethacin release profiles of the MNP nanoclusters coated with PNIPAAm-GMA_8 and PNIPAAm-GMA_{18} in PBS (pH 7.4) at the temperature below (20 °C) and above (45 °C) its LCST were then investigated. In all cases, indomethacin releases from the samples reached their equilibrium within 30 min.

In the case of MNP nanoclusters coated with PNIPAAm-GMA_8, 74% indomethacin was released at the temperature above its LCST (44°C), while 44% indomethacin released

when the temperature was below its LSCT (20 ˚C). The significantly higher percent drug release (*ca*. 30%) at the temperature above its LCST was owing to the squeezing mechanism of the collapsed PNIPAAm coated on the MNP nanoclusters at 45°C (Figure 11A), resulting in an increased amount of indomethacin being released. A similar result was also observed when the nanoclusters coated with PNIPAAm-GMA_{18} were used in the experiment (Figure 11B). However, less difference in the indomethacin being released of (*ca*.5%) when the temperature passed the LCST in this case was attributed to the presence of higher hydrophilic hydroxyl groups after the ring-opening reaction as discussed in PCS results (Figure 10). As a result, loosely packed structure of PNIPAAm-GMA_{18} on the particles was formed and influenced the shrinkage of PNIPAAm and the release of the entrapped indomethacin.

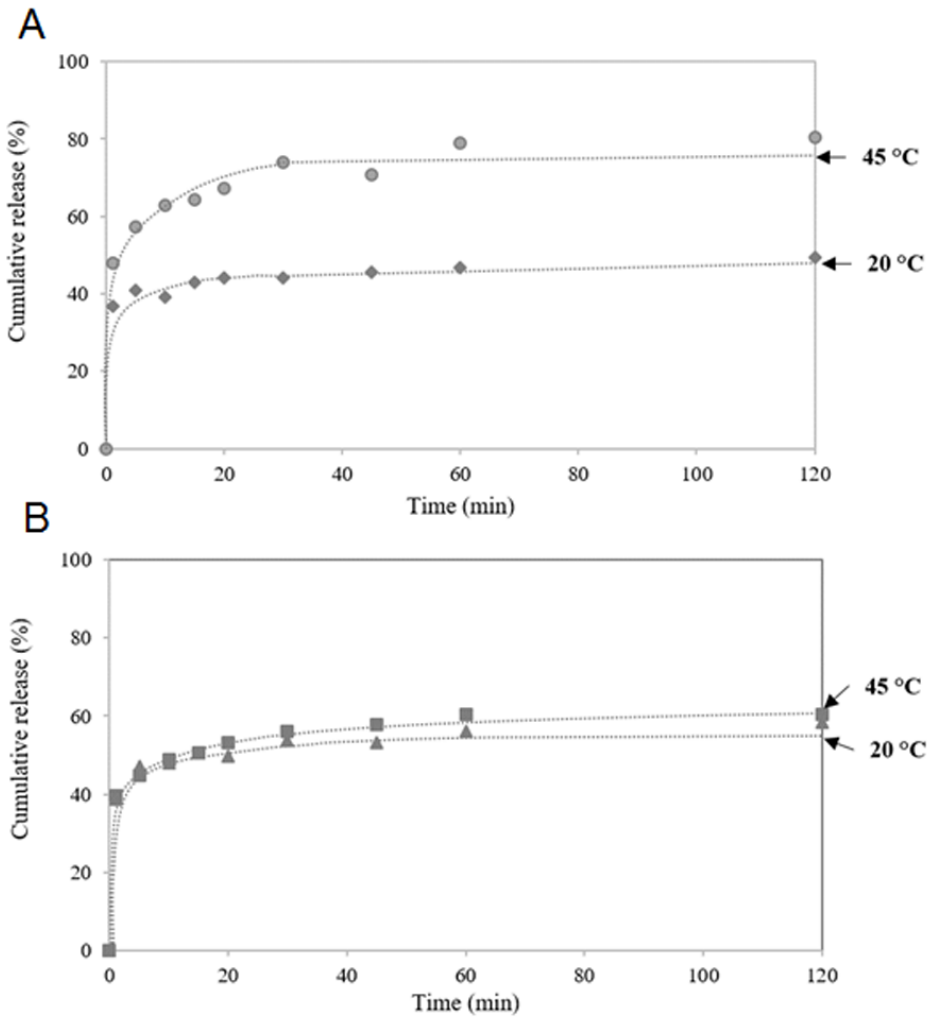

Figure 11 Indomethacin release profiles of MNP nanoclusters coated with (A) PNIPAAm-GMA_8 and (B) PNIPAAm-GMA_{18} at 20 ˚C and 45 ˚C.

4. Conclusions

Controlled nanoclustering of MNP using PNIPAAm-GMA *via* a "grafting onto" approach was presented in this work. PNIPAAm provided thermo-responsive properties to the nanolcusters while GMA units allowed for the formation of nanocluster structure through the glycidyl ring-opening reactions. RAFT polymerization was used to control the molecular weight of PNIPAAm and the number of GMA units in the polymer. The particles with good colloidal stability in water with good magnetic responsiveness were much desirable. The degree of nanoclustering can be controlled either by tuning the ratio of MNP to the polymers in the reactions or by introducing GMA units to the polymer. Increasing the ratio of the polymer to MNP in the reaction seemed to increase D_h and improved their water dispersibility. The temperature change crossing its LCST can be used as a triggering mechanism for controlled release of entrapped drugs on the nanoclusters. These novel MNP nanoclusters with thermo-responsive properties, good magnetic sensitivity and good water dispersibility might be good candidates for advanced technologies such as controlled release applications.

References

[1] Yiu HHP, McBain SC, Lethbridge ZAD, Lees MR, Dobson J. Preparation and characterization of polyethylenimine-coated Fe_3O_4-MCM-48 nanocomposite particles as a novel agent for magnet-assisted transfection. J Biomed Mater Res A. 2010;92A(1):386-392.

[2] Chorny M, Polyak B, Alferiev IS, Walsh K, Friedman G, Levy RJ. Magnetically driven plasmid DNA delivery with biodegradable polymeric nanoparticles. The FASEB Journal. 2007;21(10):2510-2519.

[3] Theppaleak T, Rutnakornpituk B, Wichai U, Vilaivan T, Rutnakornpituk M. Magnetite nanoparticle with positively charged surface for immobilization of peptide nucleic acid and deoxyribonucleic acid. J Biomed Nanotechnol. 2013;9(9):1509-1520.

[4] Theppaleak T, Rutnakornpituk M, Wichai U, Vilaivan T, Rutnakornpituk B. Anion-exchanged nanosolid support of magnetic nanoparticle in combination with PNA probes for DNA sequence analysis. J Nanopart Res. 2013;15(12).

[5] Bayrakci M, Gezici O, Bas SZ, Ozmen M, Maltas E. Novel humic acid-bonded magnetite nanoparticles for protein immobilization. Materials Science and Engineering: C. 2014;42:546-552.

[6] Jiang W, Lai K, Wu Y, Gu Z. Protein corona on magnetite nanoparticles and internalization of nanoparticle–protein complexes into healthy and cancer cells. Arch Pharmacal Res. 2013;37(1):129-141.
[7] Karamipour S, Sadjadi MS, Farhadyar N. Fabrication and spectroscopic studies of folic acid-conjugated Fe_3O_4@Au core–shell for targeted drug delivery application. Spectrochimica Acta Part A: Molecular and Biomolecular Spectroscopy. 2015;148:146-155.
[8] Li TJ, Huang CC, Ruan PW, Chuang KY, Huang KJ, Shieh DB, et al. In vivo anti-cancer efficacy of magnetite nanocrystal - based system using locoregional hyperthermia combined with 5-fluorouracil chemotherapy. Biomaterials. 2013;34(32):7873-7883.
[9] Zhang Y, Kohler N, Zhang M. Surface modification of superparamagnetic magnetite nanoparticles and their intracellular uptake. Biomaterials. 2002;23(7):1553-1561.
[10] Dong H, Huang J, Koepsel RR, Ye P, Russell AJ, Matyjaszewski K. Recyclable antibacterial magnetic nanoparticles grafted with quaternized poly(2-(dimethylamino)ethyl methacrylate) brushes. Biomacromolecules. 2011;12(4):1305-1311.
[11] Yang X, Chen L, Han B, Yang X, Duan H. Preparation of magnetite and tumor dual-targeting hollow polymer microspheres with pH-sensitivity for anticancer drug-carriers. Polymer. 2010;51(12):2533-2539.
[12] Rossi LM, Quach AD, Rosenzweig Z. Glucose oxidase-magnetite nanoparticle bioconjugate for glucose sensing. Anal Bioanal Chem. 2004;380(4):606-613.
[13] Reynolds AF, Hilt JZ. Poly(n-isopropylacrylamide)-based hydrogel coatings on magnetite nanoparticles via atom transfer radical polymerization. Nanotechnology. 2008;19(17):175101.
[14] Sun S, Zeng H, Robinson DB, Raoux S, Rice PM, Wang SX, et al. Monodisperse MFe_2O_4 (M = Fe, Co, Mn) Nanoparticles. J Am Chem Soc. 2004;126(1):273-279.
[15] Luo B, Xu S, Luo A, Wang WR, Wang SL, Guo J, et al. Mesoporous biocompatible and acid-degradable magnetic colloidal nanocrystal clusters with sustainable stability and high hydrophobic drug loading capacity. ACS Nano. 2011;5(2):1428-1435.
[16] Amiri H, Mahmoudi M, Lascialfari A. Superparamagnetic colloidal nanocrystal clusters coated with polyethylene glycol fumarate: a possible novel theranostic agent. Nanoscale. 2011;3(3):1022-1030.
[17] Ge J, Hu Y, Biasini M, Beyermann WP, Yin Y. Superparamagnetic magnetite colloidal nanocrystal clusters. Angew Chem Int Ed. 2007;46(23):4342-4345.

[18] Gao J, Ran X, Shi C, Cheng H, Cheng T, Su Y. One-step solvothermal synthesis of highly water-soluble, negatively charged superparamagnetic Fe_3O_4 colloidal nanocrystal clusters. Nanoscale. 2013;5(15):7026-7033.
[19] Berret J-F, Schonbeck N, Gazeau F, El Kharrat D, Sandre O, Vacher A, et al. Controlled clustering of superparamagnetic nanoparticles using block copolymers: design of new contrast agents for magnetic resonance imaging. J Am Chem Soc. 2006;128(5):1755-1761.
[20] Dou J, Zhang Q, Jian L, Gu J. Magnetic nanoparticles encapsulated latexes prepared with photo-initiated miniemulsion polymerization. Colloid Polym Sci. 2010;288(18):1751-1756.
[21] Fan T, Li M, Wu X, Li M, Wu Y. Preparation of thermoresponsive and pH-sensitivity polymer magnetic hydrogel nanospheres as anticancer drug carriers. Colloids Surf B Biointerfaces. 2011;88(2):593-600.
[22] Khan A, El-Toni AM, Alhoshan M. Preparation of thermo-responsive hydrogel-coated magnetic nanoparticles. Mater Lett. 2012;89:12-15.
[23] Meerod S, Rutnakornpituk B, Wichai U, Rutnakornpituk M. Hydrophilic magnetic nanoclusters with thermo-responsive properties and their drug controlled release. J Magn Magn Mater. 2015;392:83-90.
[24] Yoon KY, Kotsmar C, Ingram DR, Huh C, Bryant SL, Milner TE, et al. Stabilization of superparamagnetic iron oxide nanoclusters in concentrated brine with cross-linked polymer shells. Langmuir. 2011;27(17):10962-10969.
[25] Chaleawlert-umpon S, Pimpha N. Morphology-controlled magnetite nanoclusters via polyethyleneimine-mediated solvothermal process. Mater Chem Phys. 2012;135(1):1-5.
[26] Isojima T, Lattuada M, Vander Sande JB, Hatton TA. Reversible clustering of pH- and temperature-responsive janus magnetic nanoparticles. ACS Nano. 2008;2(9):1799-1806.
[27] Wakamatsu H, Yamamoto K, Nakao A, Aoyagi T. Preparation and characterization of temperature-responsive magnetite nanoparticles conjugated with N-isopropylacrylamide-based functional copolymer. J Magn Magn Mater. 2006;302(2):327-333.
[28] Micic N, Young A, Rosselgong J, Hornung C. Scale-up of the reversible addition-fragmentation chain transfer (RAFT) polymerization using continuous flow processing. Processes. 2014;2(1):58-70.
[29] Wei W, Hu X, Qi X, Yu H, Liu Y, Li J, et al. A novel thermo-responsive hydrogel based on salecan and poly(N-isopropylacrylamide): Synthesis and characterization. Colloids Surf B Biointerfaces. 2015;125:1-11.

[30] Abandansari HS, Aghaghafari E, Nabid MR, Niknejad H. Preparation of injectable and thermoresponsive hydrogel based on penta-block copolymer with improved sol stability and mechanical properties. Polymer. 2013;54(4):1329-1340.
[31] Théato P, Zentel R. α,ω-Functionalized poly-N-isopropylacrylamides: controlling the surface activity for vesicle adsorption by temperature. J Colloid Interface Sci. 2003;268(1):258-262.
[32] Constantin M, Cristea M, Ascenzi P, Fundueanu G. Lower critical solution temperature versus volume phase transition temperature in thermoresponsive drug delivery systems. Express Polym Lett. 2011;5(10):839-848.
[33] Eeckman F, Moës AJ, Amighi K. Synthesis and characterization of thermosensitive copolymers for oral controlled drug delivery. Eur Polym J. 2004;40(4):873-881.
[34] Rwei SP, Chuang YY, Way TF, Chiang WY. Thermosensitive copolymer synthesized by controlled living radical polymerization: Phase behavior of diblock copolymers of poly(N-isopropyl acrylamide) families. J Appl Polym Sci. 2016;133(13):43224-43231.
[35] Zeighamian V, Darabi M, Akbarzadeh A, Rahmati-Yamchi M, Zarghami N, Badrzadeh F, et al. PNIPAAm-MAA nanoparticles as delivery vehicles for curcumin against MCF-7 breast cancer cells. Artificial Cells, Nanomedicine, and Biotechnology. 2016;44(2):735-742.
[36] Yamamoto K, Matsukuma D, Nanasetani K, Aoyagi T. Effective surface modification by stimuli-responsive polymers onto the magnetite nanoparticles by layer-by-layer method. Appl Surf Sci. 2008;255(2):384-387.
[37] Lien YH, Wu TM. Preparation and characterization of thermosensitive polymers grafted onto silica-coated iron oxide nanoparticles. J Colloid Interface Sci. 2008;326(2):517-521.
[38] Li P, Xu R, Wang W, Li X, Xu Z, Yeung KWK, et al. Thermosensitive poly(N-isopropylacrylamide-co-glycidyl methacrylate) microgels for controlled drug release. Colloids Surf B Biointerfaces. 2013;101(0):251-255.
[39] Tang Y, Liu L, Wu J, Duan J. Synthesis and self-assembly of thermo/pH-responsive double hydrophilic brush–coil copolymer with poly(l-glutamic acid) side chains. J Colloid Interface Sci. 2013;397(0):24-31.
[40] Sondjaja R, Alan Hatton T, Tam MKC. Clustering of magnetic nanoparticles using a double hydrophilic block copolymer, poly(ethylene oxide)-b-poly(acrylic acid). J Magn Magn Mater. 2009;321(16):2393-2397.
[41] Chin H-Y, Wang D, Schwartz DK. Dynamic molecular behavior on thermoresponsive polymer brushes. Macromolecules. 2015;48(13):4562-4571.

Supporting information

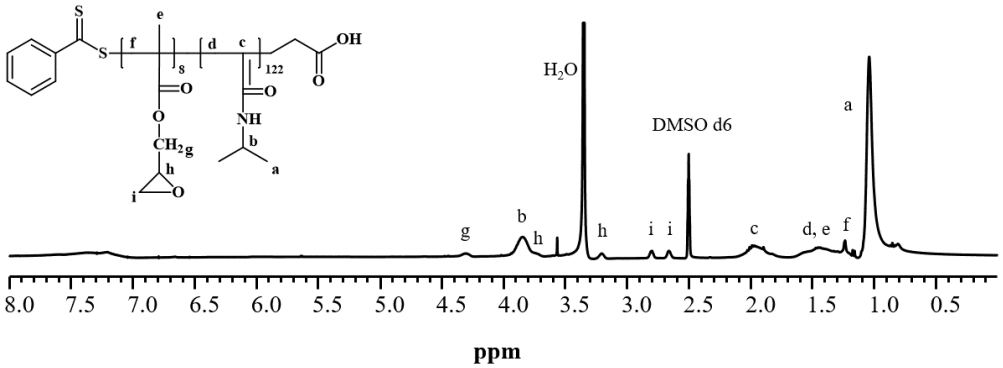

Figure S1. ^{1}H NMR spectrum of PNIPAAm-GMA$_8$

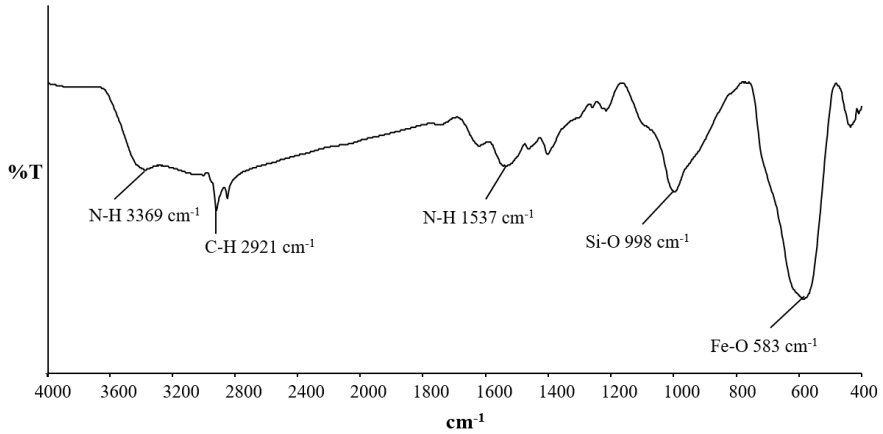

Figure S2 FTIR spectra of amino-coated MNP

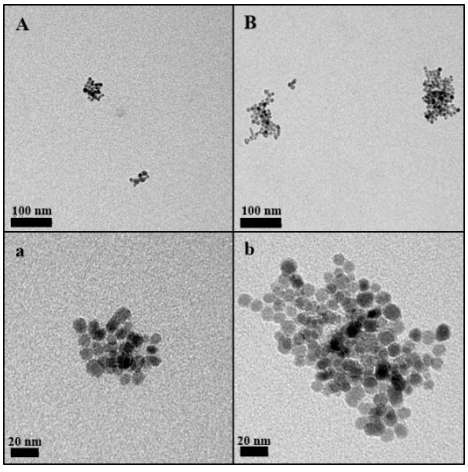

Figure S3 TEM images of MNP nanoclustering dispersed from water. (A, a) MNP-PNIPAAm-GMA$_8$ nanocluster with MNP:polymer ratio of 1:0.1 and (B, b) MNP-PNIPAAm-GMA$_8$ nanocluster with MNP:polymer ratio of 1:10

Chapter VI

Reusable magnetic nanocluster coated with poly(acrylic acid) and its adsorption with antibody and antigen

Abstract

Synthesis of negatively charged magnetite nanocluster grafted with poly(acrylic acid) (PAA) and its application as reusable nano-supports for adsorption with antibody and antigen were presented herein. It was facilely prepared *via* a free radical polymerization of PAA in the presence of functionalized magnetite nanoparticle (MNP) to obtain highly negative charged nanocluster with high magnetic responsiveness, good dispersibility and stability in water. According to transmission electron microscopy, size of the nanocluster ranged between 200 and 500 nm without large aggregation visually observed in water. Hydrodynamic size of the nanocluster consistently increased as increasing pH of the dispersion, indicating its pH-responsive properties due to the repulsion of anionic carboxylate groups in the structure. This nanocluster was successfully used as an efficient and reusable support for adsorption with anti-horseradish peroxidase antibody. It preserved higher than 97% adsorption ability of the antibody after eight reusing cycles, signifying the potential of this novel nanocluster as a reusable support in magnetic separation applications of other bioentities.

Keywords: magnetite; nanocluster; adsorption; reusable; antibody; antigen

1. Introduction

Magnetite nanoparticle (MNP) has recently shown a great potential for use in biotechnology due to its ability to get close to biological entities such as cells, viruses, proteins, and genes with heating ability when exposed to magnetic field [1]. However, bare MNP without surface modification is not practically used in these applications because it is not stable in physiological fluids. This will result in particle agglomeration in aqueous media due to many attractive forces, such as magnetic and dipole-dipole attractions [2]. Therefore, the challenge for the preparation of stable magnetic fluids is to prevent agglomeration during the nanoparticle synthesis process. The promising methods to prevent particle agglomeration include the use of electrostatic and steric stabilizers. Long chain and/or charged polymers were usually coated on MNP surface to provide steric and/or charge repulsion stabilization mechanisms to improve its stability and dispersibility in media, and also serve as a platform for conjugation with functional bioentities [3-5].

Many research works have presented the application of MNP for magnetic separation of bio-entities such as DNA [6-7], RNA [8] and proteins [9], particularly in specific conjugation with antibody for magnetic separation [10-12] and marker [13]. For example, antibody-conjugated MNP was used as a nanosolid support for separation of circulating tumor cells from fresh whole blood [10]. Carboxyl-coated MNP was demonstrated for use as a dual functional nanosupport for: 1) separation of messenger RNA from mammalian cells and 2) extraction of the supercoiled form of plasmid DNA from agarose gel [14]. The application of carboxylated-coated MNP for ionic adsorption with antibody using its positively charged surface has been previously reported [15]. The adsorption of antibody was suitable for application at the pH below its isoelectric point and the antibody was effectively desorbed by increasing the ionic strength or by altering the net charge of the antibody by adjusting pH of the solution.

However, weak magnetic responsiveness of well dispersible MNP might be a main limitation in magnetic separation and targeting delivery applications [16-17]. To increase magnetic sensitivity of MNP, the particle size should be suitably large to produce high magnetic responsiveness. Nonetheless, the particle is not stable when its size is too large owing to particle attractive forces, yielding an unstable colloidal dispersion of the particle that can rapidly agglomerate to each other [18-19]. Formation of MNP nanocluster in a controllable fashion is a promising approach to improve its magnetic responsiveness.

MNP nanocluster comprises many interconnected single particles (≈3-20 nm in diameter) and minor amount of organic content [20]. Formation of MNP nanocluster with a proper size gave rise to those with good dispersibility and stability in the media [21-22], and also good magnetic responsiveness [16, 23]. Also, its superparamagnetic properties should also be retained as long as each MNP core can be distinguishable from each other after nanoclustering reaction [24]. Many researchers have investigated in controlling the formation of MNP nanocluster via many approaches, e.g. physicochemical or physical interaction between pre-synthesized MNP and polymer particle [23, 25], an *in-situ* precipitation of MNP in the presence of polymeric microsphere [26-27] and an *in-situ* polymerization of monomers in the presence of functional MNP [28-30].

From our previous works, attempts have been made for preparing magnetic nanocluster via an *in situ* precipitation of MNP in the presence of presynthesized functional polymers. Water dispersible MNP nanocluster prepared via a ring-opening reaction of poly(ethylene oxide)-*block*-poly(2-vinyl-4,4-dimethylazlactone) (PEO-*b*-PVDM) diblock copolymers was used as a reusable magnetic solid support for antibody adsorption [31]. It showed high adsorption ability (>95%) with anti-rabbit IgG antibody even after eight adsorption-separation-desorption cycles. Other functional polymers used for controlling degree of MNP nanoclustering, e.g. diacrylate-terminated polydimethylsiloxane (PDMA)/disiloxane [32] and glycidyl-functionalized poly(N-isopropyl acrylamide) (PNIPAAm) [33], have also been demonstrated with some potential applications such as drug controlled release. An *in situ* polymerization of thermo-responsive PNIPAAm in the presence of acrylamide-coated MNP has been reported as a facile method for preparing magnetic nanocluster for temperature-triggered drug control release applications [28].

In the present report, a radical polymerization of poly(acrylic acid) (PAA) in the presence of functionalized MNP to obtain anionic magnetic nanocluster for adsorption with antibody and antigen is reported (Fig. 1). The loading ratio of acrylic acid monomer and MNP in the polymerization was varied such that water dispersible nanocluster with good magnetic sensitivity was gained. PAA was of great interest in this work because it can provide good water dispersibility to the particles due to both electrostatic and steric repulsion mechanisms. In addition, anionic PAA on the nanocluster surface also allowed for electrostatic adsorption with positively charged bioentities; antibody and antigen produced from rabbits were used as representatives in the present report. Adsorption ability and reusing efficiency of the anionic MNP nanocluster with the antibody were also investigated.

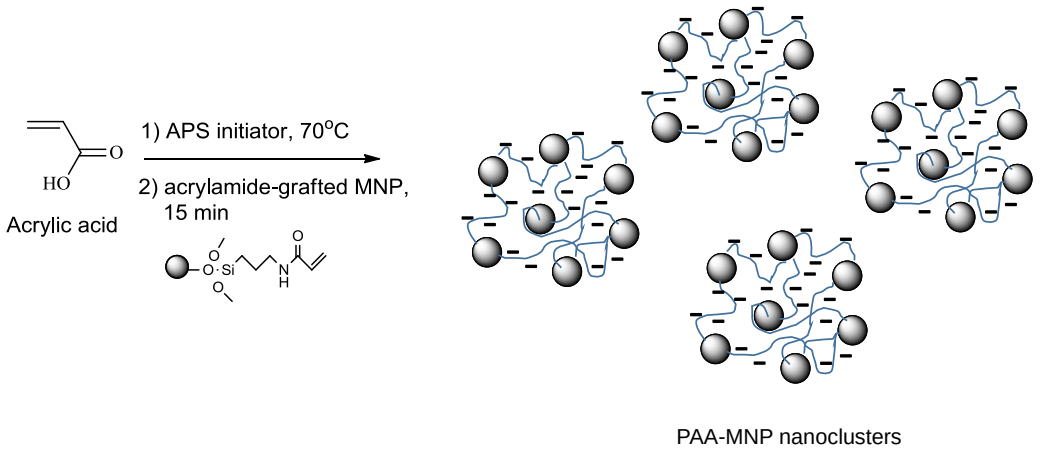

Fig. 1 Synthesis of PAA-MNP nanocluster *via* a free radical polymerization in the presence of acrylamide-functionalized MNP

2. Experimental

2.1 Materials

Unless otherwise indicated, all reagents were used without purification: Iron (III) chloride anhydrous ($FeCl_3$, 98%, Acros), iron (II) chloride tetrahydrate ($FeCl_2.4H_2O$, 99 %, Acros organic), oleic acid (68%, Carlo Erba), (3-aminopropyl)trimethoxysilane (APTES,98%, Acros), ammonium persulfate (APS, 98%, Carlo Erba), ammonium hydroxide (NH_4OH, 28-30%, J.T. Baker) and triethylamine (TEA, 97 %, Carlo Erba). Acrylic acid (99.5%, Acros) was distilled under reduced pressure. Acryloyl chloride was synthesized *via* a coupling reaction between acrylic acid and benzoyl chloride (99%, Acros) at 75˚C to give a colorless liquid with *ca.* 60-65% yield. Anti-peroxidase-antibody produced in rabbit (anti-HRP), peroxidase from horseradish (HRP), 10% BSA diluents (KPL), ABTS® peroxidase substrate (KPL), Bradford reagent (Sigma), bovine gamma globulin (BGG, Thermo Scientific) and 2-(*N*-morpholino)ethanesulfonic acid (MES, 99%, Acros) were used as received.

2.2 Characterization

Fourier transform infrared spectrophotometry (FTIR) was conducted on a Perkin-Elmer Model 1600 Series FTIR Spectrophotometer. TEM was performed on a Philips Tecnai12 TEM operated at 120 kV with Gatan CCD camera (model 782). Aqueous dispersion was cast on carbon-coated copper grids. Photocorrelation spectroscopy was performed on NanoZS4700 nanoseries Malvern instrument. Dispersing media (water) was filtered through

nylon syringe filters (0.2 µm pore size) prior to use. The dispersion was sonicated for *ca.*20 min before each experiment. Thermogravimetric analysis (TGA) was conducted on TGA/DSC1 Mettler-Toledo using a 20^{o}C/min heating rate under O_2 atmosphere. Vibrating sample magnetometry (VSM) were measured at room temperature using a Standard 7403 Series, Lakeshore. The ability of antibody adsorption and desorption to nanocluster was investigated *via* a Synergy HT, Biotek microplate reader using UV-Visible wavelength (λ_{max}) at 595 nm.

2.3 Synthesis of acrylamide-grafted MNP as a crosslinker

Synthesis of acrylamide-grafted MNP has previously been reported [28]. Briefly, MNP was synthesized *via* a co-precipitation of $FeCl_3$ (0.83 g in 10 mL deionized water) and $FeCl_2.4H_2O$ (0.5 g in 10 mL deionized water) in 25% NH_4OH (10 mL) solutions. After the purification process, oleic acid (2 mL) was added to MNP-toluene dispersion (0.4 g of MNP in 15 mL of toluene) with sonication to form oleic acid-grafted MNP. APTES (0.3 g, 1.36 x 10^{-3} mol) was then added to the MNP dispersion (0.4 g of the MNP in 15 mL of toluene) containing 2 M TEA (2.5 mL) to form amino-grafted MNP. After 24 h stirring, the particles were repeatedly precipitated in ethanol and washed with toluene. After re-dispersing the particles (0.05 g) in a 7.5 M NaOH solution (5 ml), acryloyl chloride (2.0 mL, 0.022 mol) was slowly added to the dispersion at 0 ◦C in an ice-water bath. After stirring for 24 h, the product was magnetically separated, repetitively washed with water and then kept in the form of aqueous dispersions with 0.01 g of the MNP/mL water.

2.4 Synthesis of PAA-MNP nanocluster

PAA100-MNP nanocluster and PAA300-MNP nanocluster were synthesized *via* a free radical polymerization using 1 mole equivalent of APS as an initiator with 100 and 300 mole equivalent of AA, respectively. First, APS solution (0.002 g, 8.76×10^{-5} mole in 0.05 mL deionized water) was added into AA solutions (0.068 g, 8.76×10^{-3} mole of AA for PAA100 and 0.210 g, 2.61×10^{-2} mole of AA for PAA300 in 5 mL deionized water). The polymerization was performed at 70°C under N_2 atmosphere for 30 min. Acrylamide-grafted MNP dispersion (0.01 g MNPs, 0.5 mL water) was slowly dropped to the mixture and it was stirred for another 10 min to form PAA-MNP nanocluster. It was repeatedly washed with water with an assistance of a magnet to remove unreacted monomer and ungrafted polymer chain from the nanocluster.

2.5 Studies in adsorption efficiency of PAA-MNP nanocluster with anti-HRP antibody

PAA-MNP nanocluster (10 mg) was incubated in 10 mM MES pH 5 solution (1 mL) containing 400 ppm anti-HRP antibody for 2 h. The Bradford assay was used as an indirect method to study the antibody adsorption efficiency. The protein concentrations of all samples were investigated using a calibration curve of BGG as a protein standard. After adsorption with anti-HRP antibody, PAA-MNP nanocluster was separated from the supernatant using a permanent magnet. The absorption at 595 nm of the antibody solution before and after adsorption was determined using the Bradford assay. Adsorption efficiency was calculated from the amount of the antibody adsorbed on the nanocluster (in the unit of mg antibody/mg MNP) (Fig. 2). So, it was calculated from this equation;

$$\text{Adsorption efficiency} = [(A\text{-}B)/A] \times 100 \quad \ldots\ldots(1)$$

where A is the loaded amount of anti-HRP antibody and B is the amount of anti-HRP antibody remaining in the supernatant.

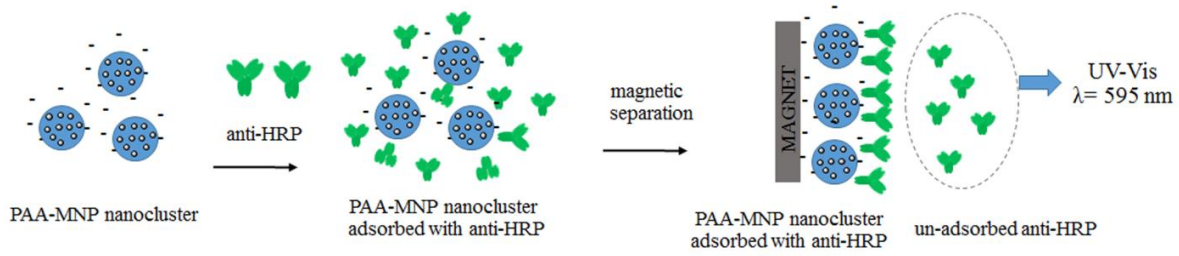

Fig.2 A schematic representation of PAA-MNP nanoclusters for adsorption with anti-HRP antibody

2.6 Studies in reusing efficiency of PAA-MNP nanocluster in adsorption with anti-HRP antibody

PAA-MNP nanocluster (10 mg) was mixed with anti-HRP antibody in a 10 M MES buffer pH 5 solution (1 mL). The nanocluster adsorbed with anti-HRP was magnetically separated with a magnet and excess anti-HRP in the solution was decanted. Anti-HRP on the nanocluster surface was then desorbed by repeatedly washing with 2 M NaCl solution with pH 12. The amount of the antibody after desorption was investigated using the Bradford assay described above. Desorption efficiency was estimated from this equation:

Desorption efficiency = $(C/B) \times 100$……..…(2)

where C is the amount of desorbed anti-HRP antibody and B is the amount of adsorbed anti-HRP antibody.

The anti-HRP-free nanocluster was then retrieved from the mixture using a permanent magnet. The adsorption-desorption process was performed repetitively to study the reusing efficiency in adsorption with anti-HRP antibody of the nanocluster as illustrated in Fig. 3.

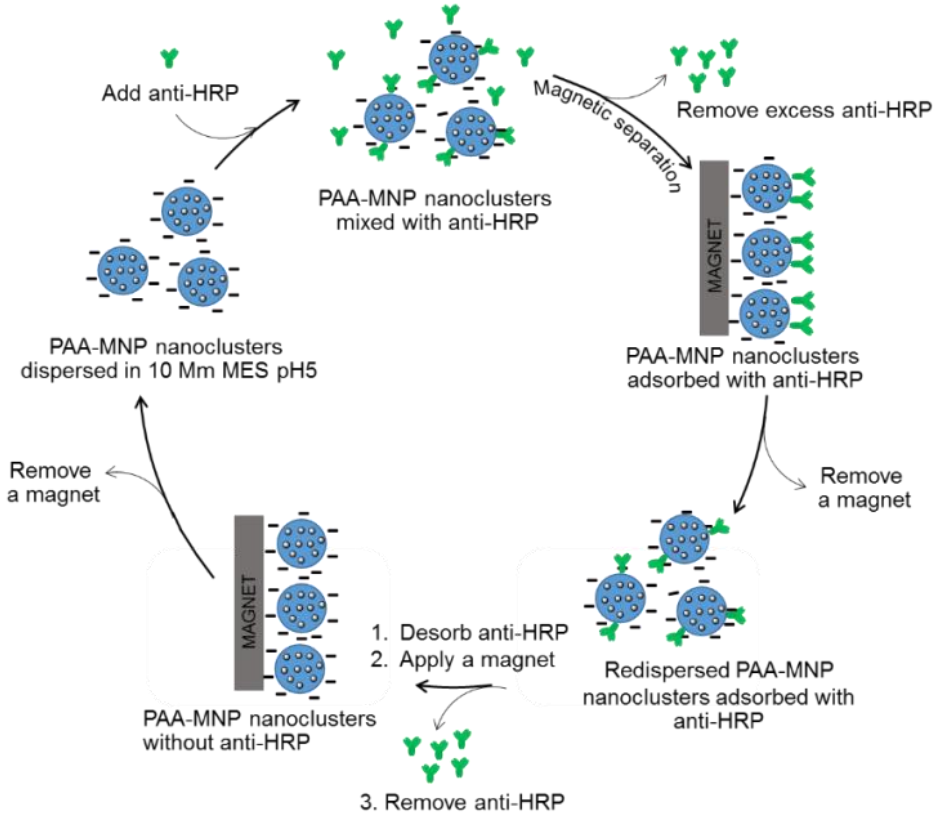

Fig. 3 Illustration of an adsorption- desorption cycle of PAA-MNP nanocluster in the adsorption with anti-HRP antibody

2.7 Studies in capacity for antigen recognition of PAA-MNP nanocluster adsorbed with antibody

After adsorption with antibody, the residue carboxyl groups of PAA-MNP nanocluster were blocked with 1 mL of 1% BSA in 10 mM MES pH 7 at 25^{o}C for 16 h. The nanocluster was then washed with 10 mM MES pH 6 to remove excess BSA. An indirect detection method was employed to determine the antigen recognition capacity of the nanocluster adsorbed with antibody. First, 1 mL of 400 ppm of HRP antigen in a 10 mM MES pH 7 solution was added

into anti-HRP antibody-adsorbed nanocluster and incubated for 30 min. The nanocluster was repeatedly washed with a 10 mM MES pH 7 solution. The existence of antigen on the particle surface was apparently observed by an addition of 1 mL of ABTS-H_2O_2 solution into 10 µL of the nanocluster dispersion. UV absorbance at the wavelength of 414 nm of the mixtures was then measured.

3. Results and Discussion

The objective of this work was to synthesize negatively charged magnetic nanocluster *via* a facile single-step free radical polymerization of PAA in the presence of functionalized MNP to obtain the nanocluster having high antibody adsorption ability. The ratio of AA monomer to the MNP was fine-tuned such that the nanocluster with good water dispersibility, good magnetic responsiveness and high negatively charged surface was obtained. This nanocluster with negatively charged surface was demonstrated for use as magnetic nanosupport for adsorption with anti-HRP antibody and its adsorption ability was also investigated. In addition, reusing efficiency of the nanocluster in adsorption with anti-HRP antibody and its antigen recognition capacity were also studied.

To prepare PAA-MNP nanocluster, acrylamide-coated MNP was first synthesized *via* a coupling reaction between amino groups coated on MNP surface and acryloyl chloride. This functionalized MNP can serve as active nanocrosslinker during a free radical polymerization of AA and thus induced MNP nanoclustering due to the presence of multi-functional acrylamide groups on the particle surface (Fig. 1). It was envisioned that PAA homopolymer might also be formed during the polymerization in competition with the formation of PAA-MNP nanocluster. The PAA homopolymer was then removed from the nanocluster *via* repetitive magnetic separation and washing processes.

TEM images of oleic acid-coated MNP, PAA100-MNP and PAA300-MNP nanocluster are shown in Fig. 4. TEM samples of oleic acid-coated MNP were prepared from toluene dispersion while those of both PAA-MNP nanocluster samples were prepared from pH 7 aqueous dispersion. Oleic acid-coated MNP was spherical in shape with the size of 8-10 nm in diameter without any sign of nanoclustering (Fig. 4A). After the polymerization, formation of MNP nanocluster was thoroughly observed from TEM images (Fig. 4B and 4C). These TEM images supported the proposed mechanism of the formation of PAA-MNP nanocluster illustrated in Fig. 1. The size of PAA100-MNP nanocluster ranged between 200 to 300 nm in diameter, while those of PAA300-MNP nanocluster was broader and slightly

larger (200-500 nm in diameter). The slightly larger size of PAA300-MNP nanocluster was attributed to the relatively higher amounts of PAA in PAA300-MNP nanocluster to react with the reactive MNP in the clustering reaction.

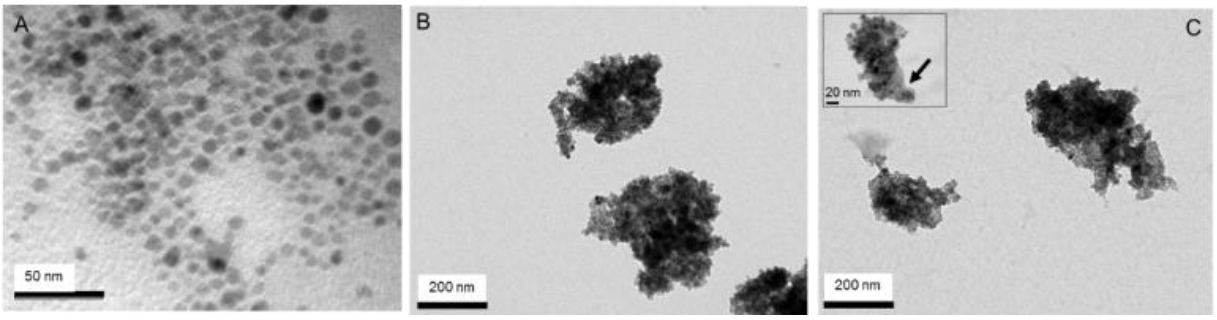

Fig. 4 TEM images of (A) oleic acid-coated MNP (B) PAA100-MNP nanocluster (C) PAA300-MNP nanocluster. The arrow in the inset in Fig. 4C indicates the presence of PAA coated on the nanocluster surface.

FTIR spectra of the samples from each step of the reactions are shown in Fig. 5. The spectrum of amino-grafted MNP exhibits the signals of amino-coated silica layer at 3369 cm^{-1} (N-H stretching) and 998 cm^{-1} (Si-O stretching) and that of MNP core at 571 cm^{-1} (Fe-O stretching) (Fig. 5A). After functionalization with acrylamide groups, FTIR spectrum exhibits characteristic signals of amide stretching bands at 1650 cm^{-1} and 1560 cm^{-1} (Fig. 5B). After the polymerization and nanoclustering reactions, the spectrum of PAA-MNP nanocluster shows characteristic signals of O=CO stretching (1709 cm^{-1}) and O-H stretching bands (3392 cm^{-1}) of carboxylic acid groups, signifying the presence of PAA units in its structure (Fig. 5C).

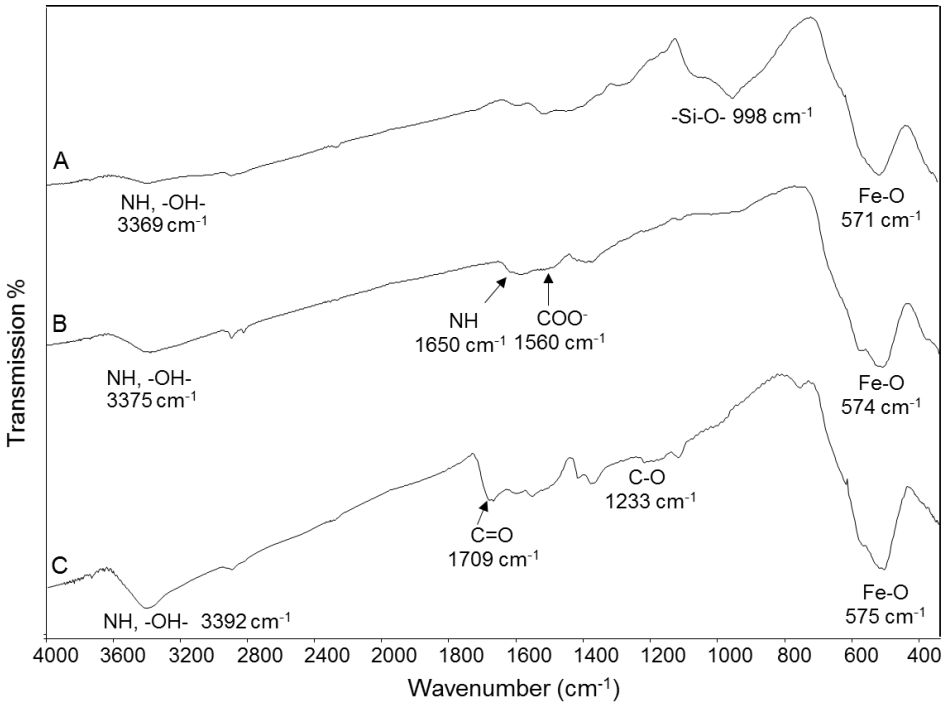

Fig. 5 FTIR spectra of (A) amino-grafted MNP, (B) acrylamide-grafted MNP and (C) PAA100-MNP nanocluster

Zeta potential values of the nanocluster as a function of dispersion pH are shown in the Fig. 6A. The presence of ionizable carboxylic acid groups of PAA in the structure should make them a polyelectrolyte in aqueous dispersion. In addition to functioning as both electrostatic and steric stabilizers, the polyelectrolyte PAA also provided advantageous pH-responsive properties to the nanocluster due to its large electrostatic potentials (pK_a of acrylic acid is 4.25) [34]. The results in Fig. 6 suggested that this nanocluster was pH responsive. Zeta potential values of these nanocluster in water continuously decreased with increasing the dispersion pH and became highly negatively charged in basic pH. This was attributed to the formation of protonated carboxylic acid groups (–COOH) and deprotonated carboxylate groups ($–COO^-$) depending on the solution pH. Fig. 6A indicated that the isoelectric point (PI) of these particles was about pH of 2.5. This number was about two orders of magnitude lower than pK_a of acrylic acid (pK_a of acrylic acid was 4.25) [34]. The polymeric nature of PAA may decrease the pK_a by one or more unit due to the potential electrostatic repulsion of many adjacent carboxylate groups. It should be noted that, at pH 7, the surface charge of the nanocluster was highly negative (-35 mV), which was necessary for magnetic separation of antibody via an electrostatic adsorption mechanism later discussed in this work.

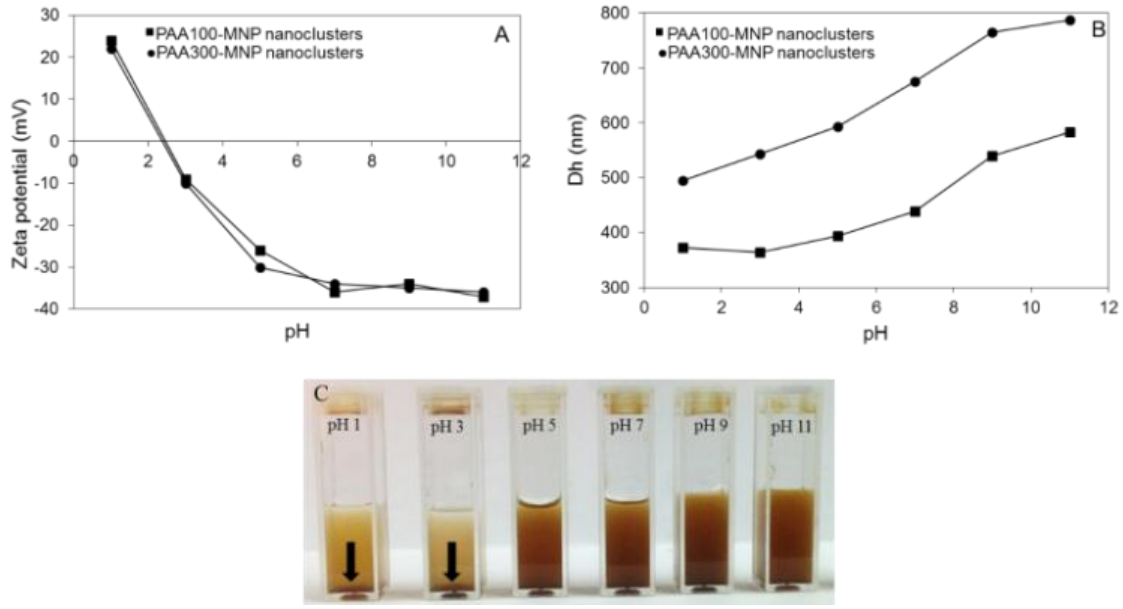

Fig. 6 (A) Zeta potential of PAA100-MNP and PAA300-MNP nanocluster, (B) D_h of PAA100- MNP and PAA300-MNP nanocluster as a function of dispersion pH and (C) appearance of PAA100-MNP nanocluster dispersed in water in various pH. The arrows in Fig. 6C indicate the aggregation of the nanocluster in pH 1 and pH 3 dispersions after 1 h of the preparation.

D_h of the nanocluster was studied as a function of solution pH (Fig. 6B). It was found that D_h increased as increasing pH of the dispersion. At pH below its PI, PAA chain in the nanocluster was in a protonated form (-COOH), making it having no or less electrostatic repulsion among the chains and eventually shrink. Increasing pH of the dispersion above its PI further increased the degree of negative charge of the nanocluster, resulting in the enhancement in polymer swelling and thus increasing its D_h. This explanation agreed well with the zeta potential plots as a function of pH discussed in Fig. 6A. In addition, pH-responsive properties of the nanocluster were also evidenced by its dispersibility and stability as a function of pH in water (Fig. 6C). The nanocluster apparently aggregated in pH 1-pH 3 dispersions and was stable and well dispersible in pH 5-pH 11 dispersions due to the existence of additional electrostatic repulsion stabilization.

Effect of PAA compositions on D_h of the nanocluster was also investigated (Fig. 6B). PAA300-MNP nanocluster showed higher D_h values than that of PAA100-MNP nanocluster at the same dispersion pH. This was attributed to the higher amount of PAA in PAA300-MNP nanocluster, resulting in the higher degree of water swelling and higher D_h. The result

also supported the slightly larger size of PAA300-MNP nanocluster observed in TEM images (Fig. 4).

To determine the composition of PAA grafted in the MNP nanocluster, TGA was performed to measure its weight loss at 600^{o}C (Fig. 7). It should be noted that the ungrafted species, including PAA homopolymer and residue monomer, were removed from the MNP nanocluster *via* repetative washing-magnetic separating process. It was assumed that the residue weight was the weight of iron oxide from MNP core remaining at 600 ^{o}C; the weight loss was attributed to the organic PAA content in the nanocluster. It was found that PAA content in PAA100-MNP nanocluster was 9 % (Fig. 7B) and those in PAA300-MNP nanocluster was about 14 % (Fig. 7C). This result corresponded well with the high D_h and the high degree of water swelling of PAA300-MNP nanocluster observed in the PCS experiment due to the high percentage of PAA in the structure as compared to PAA100-MNP nanocluster.

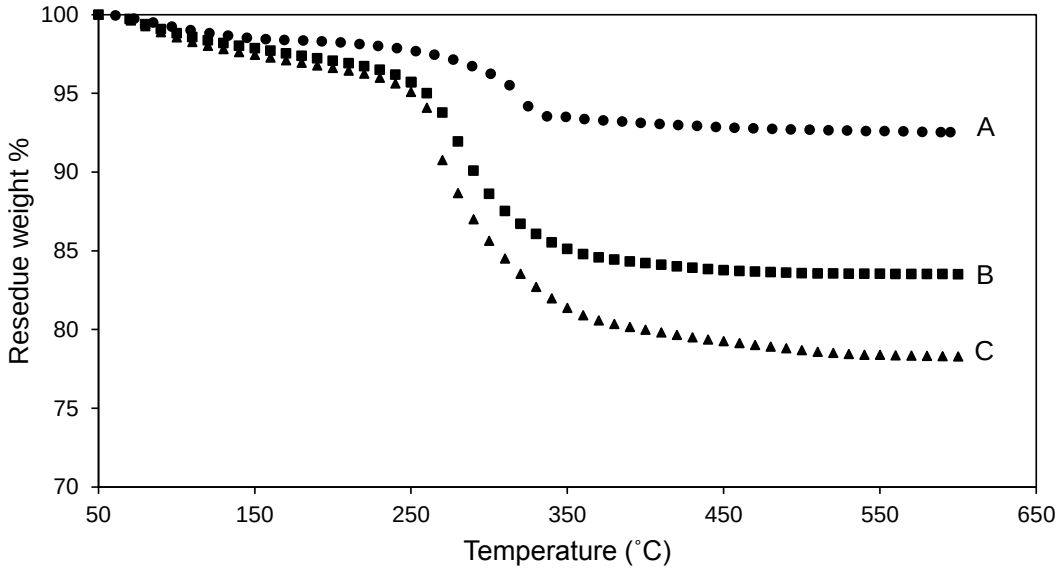

Fig. 7 TGA thermograms of (A) bare MNP, (B) PAA100-MNP nanocluster and (C) PAA300-MNP nanocluster

Magnetic properties of bare MNP, PAA100-MNP nanocluster and PAA300-MNP nanocluster were investigated *via* VSM technique (Fig. 8). Saturation magnetizations (M_s) decreased from 62 emu/g of bare MNP to 22-40 emu/g of the nanocluster. This was again attributed to the presence of non-magnetic PAA in the structure, resulting in the lowered percentage of magnetite content in the nanocluster. PAA300-MNP nanocluster showed a lower saturation magnetization (M_s) value than the other due to the higher PAA content in the

structure. This result was in good agreement with that observed from the TGA experiment, indicating higher PAA content in PAA300-MNP nanocluster than the other sample. Even though there was some drop of the M_s value due to the presence of PAA in the structure, it was still well responsive to an applied magnetic field as shown in the inset in Fig. 8. The picture illustrated PAA100-MNP nanocluster dispersed in DI water and a magnetically assisted separation. Without an external magnetic field, the colloidal dispersion was brown in color and homogeneous without any sign of precipitation. When a magentic field was applied, the nanocluster was enriched, leading to transparent dispersion. The dispersing-magnetically separating process of the nanocluster was reversible for a number of cycles without any sign of precipitation when stored at room temprature. It should be mentioned that this dispersing-magnetically separating behavior was not observed in well dispersible individual MNP [35]. In addition, this nanocluster still retained its superparamagnetic properties evidenced by the lack of coercitivity and remanence after removing the magnetic field.

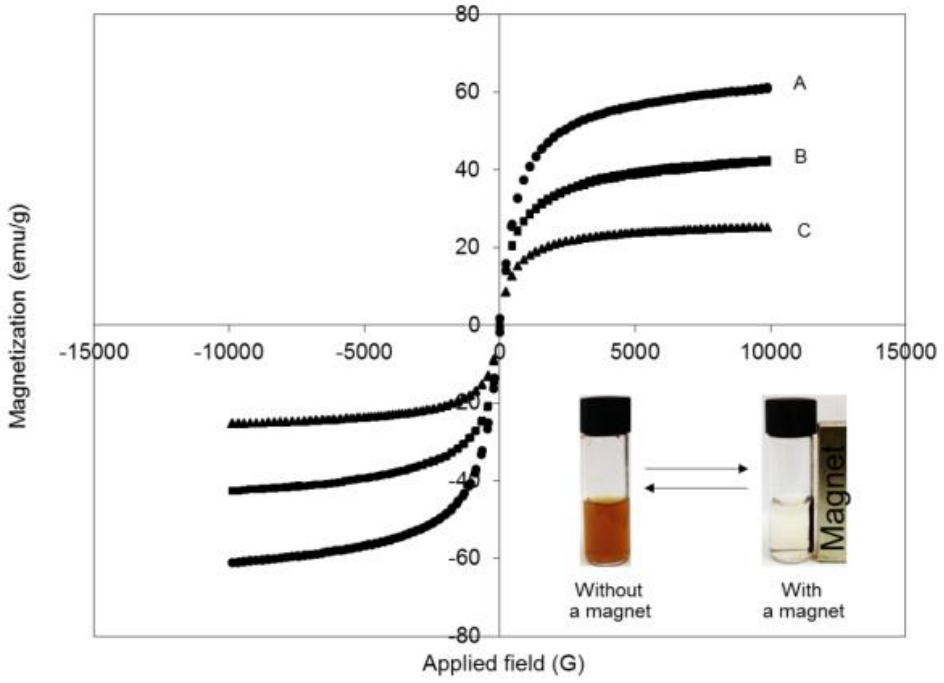

Fig. 8 Magnetization curves of (A) bare MNP, (B) PAA100-MNP nanocluster (C) PAA300-MNP nanocluster. The inset shows the capturing of PAA100-MNP nanocluster with a magnet.

To employ this in antibody adsorption applications, PAA-MNP nanocluster having carboxylated-enriched surface was desired for adsorption between the anionic nanocluster

and positively charged anti-HRP, and it shall be then used for the studies in antigen recognition capacity (Fig. 9). In the antibody adsorption experiment, PAA100-MNP nanocluster was chosen as a representative because it exhibied higher magnetic responsiveness than those of PAA300-MNP nanocluster evidenced *via* VSM technique. In addition, PAA100-MNP nanocluster also showed better stability as it was well dispersible in water without any sign of precipitation even after 24 h of preparation.

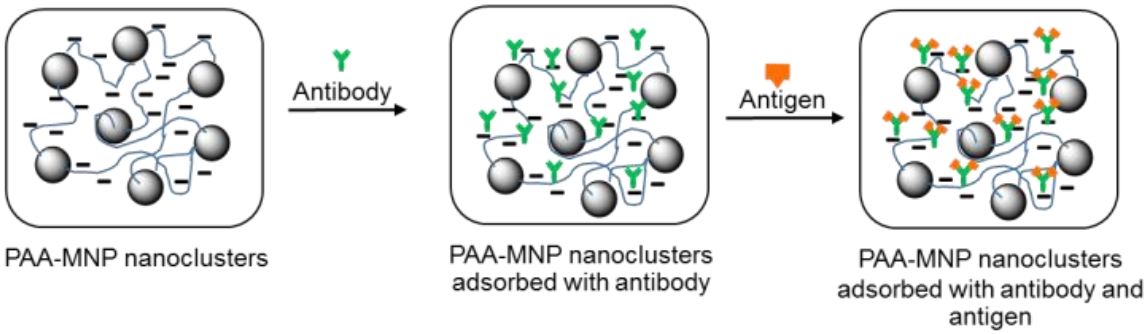

Fig. 9 Schematic illustration of PAA-MNP nanocluster adsorbed with antibody and antigen

To determine the antibody adsorption ability of the nanocluster, various concentrations of anti-HRP antibody were loaded to PAA-MNP nanocluster (10 mg) in 1 mL of 10 mM MES pH 5 solutions. It was found that the maximum concentration of the antibody that can bind on the nanocluster surface while retaining 100% adsorption efficiency was 400 ppm (Fig. 10). Increasing the antibody concentrations from 400 ppm to 500-1000 ppm resulted in the remaining of un-adsorbed antibody in the dispersions. Hence, 400 ppm antibody loaded in 10 mg of PAA-MNP nanocluster would be used for the following experiments.

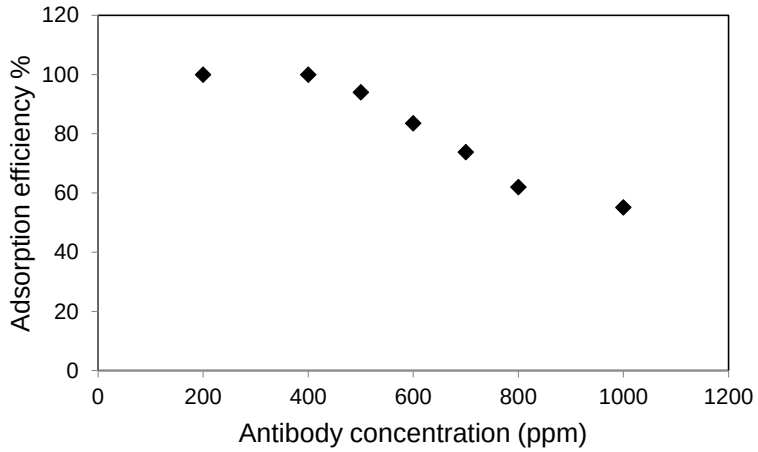

Fig. 10 Adsorption efficiency of PAA100-MNP nanocluster with anti-HRP antibody as a function of the antibody concentrations

Fig. 11 shows the reusing efficiency of PAA100-MNP nanocluster for the adsorption with anti-HRP antibody after eight reusing processes. After each adsorption-separation process, the concentrations of adsorbed and desorbed antibody from each cycle were investigated using the Bradford assay. The result indicated that the nanocluster preserved higher than 97% adsorption ability of the antibody for eight reusing cycles, signifying the capability of this novel nanocluster as reusable solid support in magnetic separation application of bioentities.

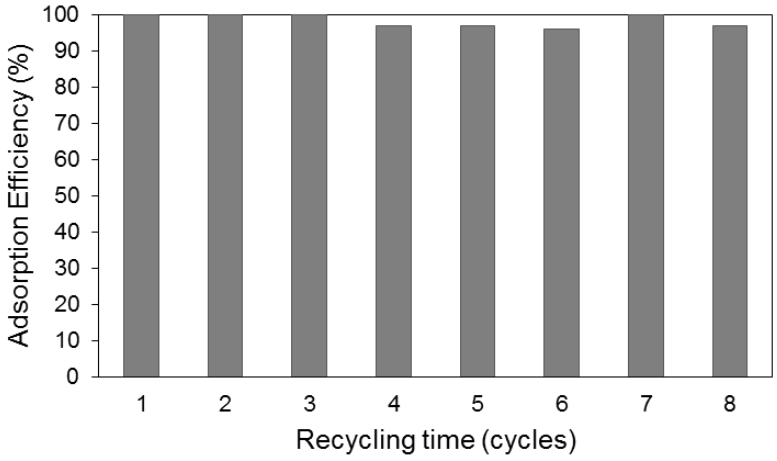

Fig. 11 Adsorption efficiency of PAA100-MNP nanocluster with anti-HRP antibody after eight reusing processes

The capacity of the antigen recognition of the nanocluster adsorbed with antibody was observed from the change to a greenish color product after the oxidation with an ABTS

oxidizing agent, once it was reacted with horseradish peroxidase (HRP) labeled conjugates. Hence, the nanocluster adsorbed with anti-HRP was conjugated with HRP for color development once reacted with ABTS. PAA100-MNP nanocluster adsorbed with anti-HRP and HRP exhibited the color changing from light green to blue once oxidized with ABTS (Fig. 12G), signifying the positive result owing to the conjugation of HRP with anti-HRP on the nanocluster surface. The nanocluster without anti-HRP and HRP (Fig. 12D) and those solely adsorbed with anti-HRP (without HRP)(Figure 12E) were used as the controls. These dispersions showed no changes in the color development after oxidized with ABTS. Other control dispersions including the pH 7 MES buffer solution (the dispersing media)(Fig. 12A), those with 1% BSA (a blocking reagent) (Fig. 12B), anti-HRP (Fig. 12C) and ABTS (Fig. 12H) were also investigated to confirm their negative results. Moreover, the solution of HRP antigen (without MNP nanocluster) was also tested to confirm the color change (positive testing) owing to the reaction of HRP with ABTS (Fig. 12F). More importantly, after eight reusing processes, the nanocluster adsorbed with anti-HRP and HRP showed the color change (the positive result) after an addition with ABTS, indicating that the antigen recognition of the MNP nanocluster adsorbed with antibody was still preserved even after repeatedly used. These results signified that the nanocluster shall be used as reusable magnetic support for immobilization with other conjugates such as aptamers and their target molecules.

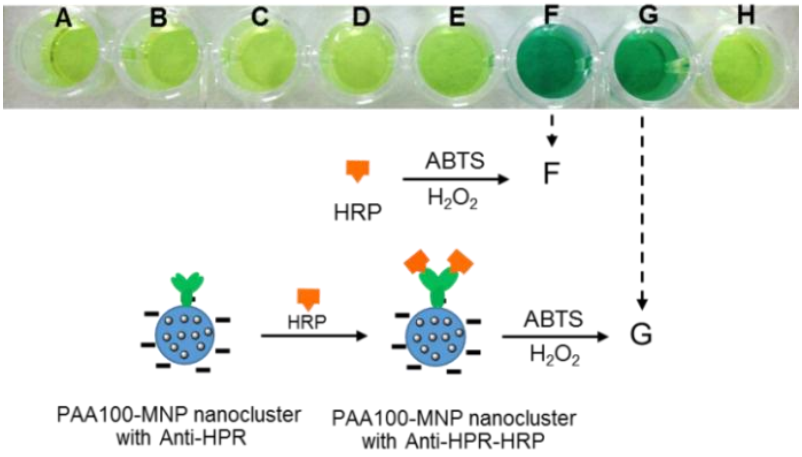

Fig. 12 Visualization of the antigen recognition capability using an indirect method. Appearance of the samples after an addition with ABTS oxidizing agent; A) 10 mM MES buffer pH7, B) 1% BSA in 10 mM MES buffer pH7, C) anti-HRP, D) the nanocluster without anti-HRP and HRP, E) the nanocluster adsorbed with anti-HRP, F) HRP antigen (the positive control), G) the nanocluster adsorbed with anti-HRP and HRP (the sample) and H) ABTS

4. Conclusions

Magnetite nanocluster grafted with PAA was synthesized *via* a free radical polymerization in the presence of MNP to obtain the nanocluster with highly negative charge, high magnetic responsiveness, good dispersibility and good stability in water. D_h of the nanocluster changed in response to the change in the dispersion pH, indicating its pH-responsive behavior. The degree of nanoclustering was optimized such that its good dispersibility and stability in neutral water were obtained while maintaining its good magnetic sensitivity, which was essential for facile manipulation in magnetic separation applications. In addition, its anionic surface also served as adsorbed platform with positivelt charged bio-molecules. In this work, this novel magnetic nanocluster was effectively used as reusable support for adsorption with anti-HRP for at least eight cycles. This magnetic nanocluster shall be beneficial for use as a support for efficient and facile separation of any positively charged bio-entities.

References

[1] Tartaj P, Morales MD, Veintemillas-Verdaguer S, González-Carreño T, Serna CJ (2002) The preparation of magnetic nanoparticles for applications in biomedicine. J Phys D: Appl Phys 36:182–197

[2] Dong H, Huang J, Koepsel RR, Ye P, Russell AJ, Matyjaszewski K (2011) Recyclable antibacterial magnetic nanoparticles grafted with quaternized poly(2-(dimethylamino) ethyl methacrylate) brushes. Biomacromolecules, 12:1305-1311

[3] Frimpong RA, Hilt JZ (2008) Poly(n-isopropylacrylamide)-based hydrogel coatings on magnetite nanoparticles via atom transfer radical polymerization. Nanotechnology, 19:175101-175107

[4] Khadsai S, Rutnakornpituk B, Vilaivan T, Nakkuntod M, Rutnakornpituk M (2016) Anionic magnetite nanoparticle conjugated with pyrrolidinyl peptide nucleic acid for DNA base discrimination. J Nanopart Res 18:263-277

[5] Rutnakornpituk M, Puangsin N, Theamdee P, Rutnakornpituk B, Wichai U (2011) Poly(acrylic acid)-grafted magnetic nanoparticle for conjugation with folic acid. Polymer 52:987-995

[6] Theppaleak T, Rutnakornpituk B, Wichai U, Vilaivan T, Rutnakornpituk M (2013) Magnetite nanoparticle with positively charged surface for immobilization of peptide nucleic acid and deoxyribonucleic acid. J Biomed Nanotech 9:1509-1520

[7] Theamdee P, Rutnakornpituk B, Wichai U, Rutnakornpituk M (2014) Recyclable magnetic nanoparticle grafted with pH-responsive polymer for adsorption with DNA. J Nanopart Res 16:2494-2506

[8] Xiong L, Bi J, Tang Y, Qiao SZ (2016) Magnetic core–shell silica nanoparticles with large radial mesopores for siRNA delivery. Small 12:4735-4742

[9] Iype T, Thomas J, Mohan S, Johnson KK, George LE, Ambattu LA, Bhati A, Ailsworth K, Menon B, Rayabandlad SM, Jesudasan RA, Santhosh S, Ramchand CN (2017) A novel method for immobilization of proteins via entrapment of magnetic nanoparticles through epoxy cross-linking. Anal Biochem 519:42-50

[10] Xu H, Aguilar ZP, Yang L, Kuang M, Duan H, Xiong Y, Wei H, Wang A (2011) Antibody conjugated magnetic iron oxide nanoparticles for cancer cell separation in fresh whole blood. Biomaterials 32:9758-9765

[11] Yim C, Lee H, Lee S, Jeon S (2017) One-step immobilization of antibodies on ZIF-8/Fe_3O_4 hybrid nanoparticles for the immunoassay of Staphylococcus aureus. RSC Advances 7:1418-1422

[12] Ortega GA, Zuaznabar-Gardona JC, Morales-Tarre O, Reguera E (2016) Immobilization of dengue specific IgM antibodies on magnetite nanoparticles by using facile conjugation strategies. RSC Advances 6:98457-98465

[13] Moon JM, Kim BS, Choi YS, Lee JO, Nakahara T, Yoshinaga K (2010) Preparation of polymer-coated magnetite fine particles for immunoassay magnetic marker. Macromol Res 18:793-799

[14] Sarkar TR, Irudayaraj J (2008) Carboxyl-coated magnetic nanoparticles for mRNA isolation and extraction of supercoiled plasmid DNA. Anal Biochem 379:130-132

[15] Puertas S, Batalla P, Moros M, Polo E, del Pino P, Guisan JM, Grazú V, de la Fuente JM (2011) Taking advantage of unspecific interactions to produce highly active magnetic nanoparticle-antibody conjugates. *ACS Nano* 5:4521-4528

[16] Luo B, Xu S, Luo A, Wang WR, Wang SL, Guo J, Lin Y, Zhao DY, Wang CC (2011) Mesoporous biocompatible and acid-degradable magnetic colloidal nanocrystal clusters with sustainable stability and high hydrophobic drug loading capacity. ACS Nano 5:1428–1435

[17] Sun Q, Kandalam AK, Wang Q, Jena P, Kawazoe Y, Marquez M (2006) Effect of Au coating on the magnetic and structural properties of Fe nanoclusters for use in biomedical applications: A density-functional theory study. Phys Rev B 73:134409

[18] Amiri H, Mahmoudi M, Lascialfari A (2011) Superparamagnetic colloidal nanocrystal clusters coated with polyethylene glycol fumarate: a possible novel theranostic agent. Nanoscale 3:1022–1030

[19] Mahmoudi M, Simchi A, Imani M, Stroeve P, Sohrabi A (2010) Templated growth of superparamagnetic iron oxide nanoparticles by temperature programming in the presence of poly(vinyl alcohol). Thin Solid Films 518:4281–4289

[20] Sun S, Zeng H, Robinson DB, Raoux S, Rice PM, Wang SX, Li G (2004) Monodisperse MFe_2O_4 (M = Fe, Co, Mn) Nanoparticles. J Am Chem Soc 126:273-279

[21] Ge J, Hu Y, Biasini M, Beyermann WP, Yin Y (2007) Superparamagnetic magnetite colloidal nanocrystal clusters. Angew Chem Int Ed 46:4342-4345

[22] Gao J, Ran X, Shi C, Cheng H, Cheng T, Su Y (2013) One-step solvothermal synthesis of highly water-soluble, negatively charged superparamagnetic Fe_3O_4 colloidal nanocrystal clusters. Nanoscale 5:7026-7033 (2013)

[23] Amiri H, Mahmoudi M, Lascialfari A (2011) Superparamagnetic colloidal nanocrystal clusters coated with polyethylene glycol fumarate: a possible novel theranostic agent. Nanoscale 3:1022–1030

[24] Berret JF, Schonbeck N, Gazeau F, Kharrat DE, Sandre O, Vacher A, Airiau M (2006) Controlled clustering of superparamagnetic nanoparticles using block copolymers: Design of new contrast agents for magnetic resonance imaging. J Am Chem Soc 128:1755-1761

[25] Dou J, Zhang Q, Jian L, Gu J (2010) Magnetic nanoparticles encapsulated latexes prepared with photo-initiated miniemulsion polymerization. Colloid Polym Sci 288:1751–1756

[26] Fan T, Li M, Wu X, Li M, Wu Y (2011) Preparation of thermoresponsive and pH-sensitivity polymer magnetic hydrogel nanospheres as anticancer drug carriers. Colloids Surf B 88:593-600

[27] Khan A, El-Toni AM, Alhoshan M (2012) Preparation of thermo-responsive hydrogel-coated magnetic nanoparticles. Mater Lett 89:12-15

[28] Meerod S, Rutnakornpituk B, Wichai U, Rutnakornpituk M (2015) Hydrophilic magnetic nanoclusters with thermo-responsive properties and their drug controlled release. J Magn Magn Mater 392:83-90

[29] Yoon KY, Kotsmar C, Ingram DH, Huh C, Bryant SL, Milner TE, Johnston KP (2011) Stabilization of superparamagnetic iron oxide nanoclusters in concentrated brine with cross-linked polymer shells. Langmuir 27:10962-10969

[30] Chaleawlert-umpon S, Pimpha N (2012) Morphology-controlled magnetite nanoclusters via polyethyleneimine-mediated solvothermal process. Mater Chem Phys 135:1–5

[31] Prai-In Y, Boonthip C, Rutnakornpituk B, Wichai U, Montembault V, Pascual S, Fontaine L, Rutnakornpituk M (2016) Recyclable magnetic nanocluster crosslinked with poly(ethylene oxide)-block-poly(2-vinyl-4,4-dimethylazlactone) copolymer for adsorption with antibody. Mater Sci Eng C 67:285-293

[32] Thong-On B, Rutnakornpituk B, Wichai U, Rutnakornpituk M (2015) Controlled nanoclustering of magnetic nanoparticles using telechelic polysiloxane and disiloxane. J Nanopart Res 17:261-274

[33] Thong-On B, Rutnakornpituk M (2016) Controlled magnetite nanoclustering in the presence of glycidyl-functionalized thermo-responsive poly(N-isopropylacrylamide). Eur Polym J 85:519-531

[34] Tjipangandjara KF, Somasundaran P (1992) Effects of the conformation of poly acrylic acid on the dispersion-flocculation of alumina and kaolinite fines. Adv Powder Technol 3:119-127

[35] Chen K, Zhu Y, Li L, Lu Y, Guo X (2010) Recyclable spherical polyelectrolyte brushes containing magnetic nanoparticles in core. Macromol Rapid Commun 31:1440-1443

Supporting Information

1) A calibration curve of BGG

The calibration curve of BGG was investigated using UV–Visible spectrophotometer measurement at λ_{max} = 595 nm.

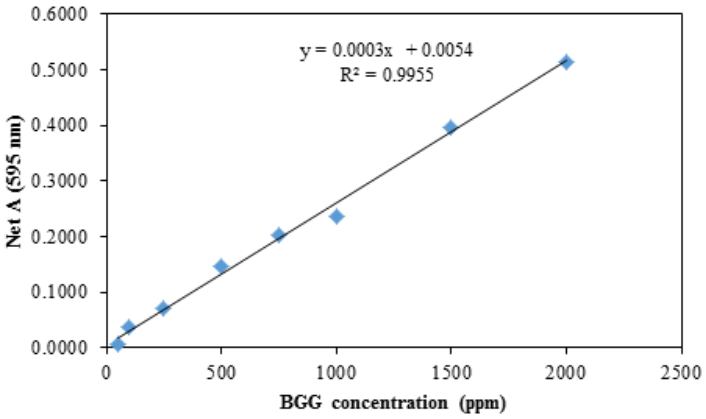

Figure S1 A calibration curve of BGG

2) The conductometric titration curves

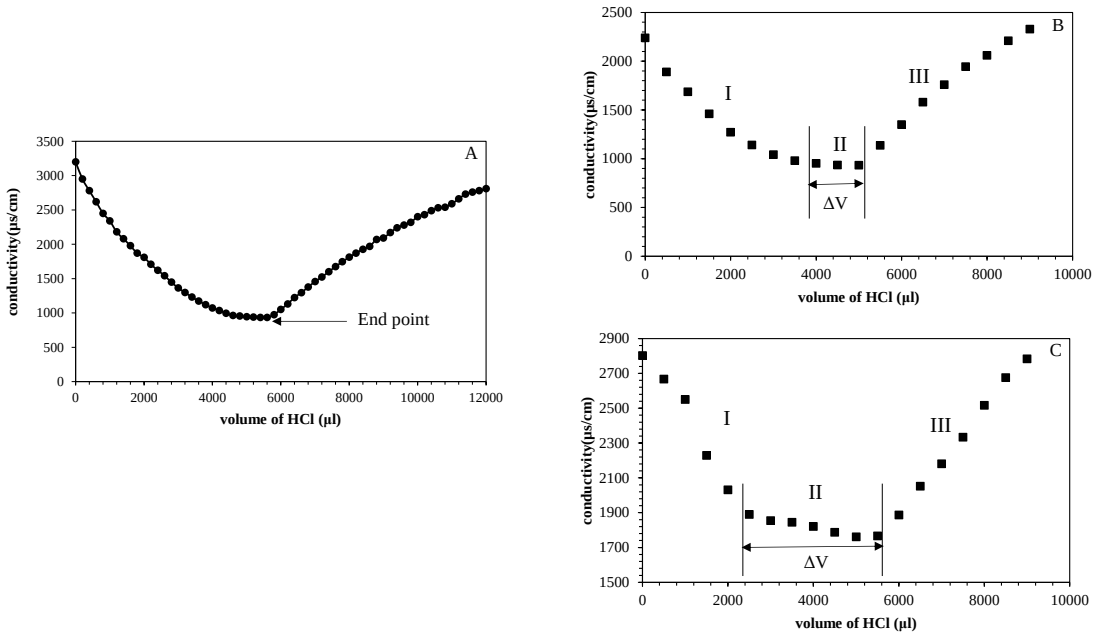

Figure S2 The conductometric titration curves, A) the titration curve of HCl with NaOH, and the titration curves of HCl with carboxyl groups (COO^-) on (B) the PAA100-MNP nanoclusters and (C) PAA300-MNP nanoclusters

Calculations

1. Calculations of the grafting density of carboxyl groups on poly(AA)100-MNP nanoclusters after dispersing in water

The amounts of carboxyl groups presenting on the particle surface were quantitatively determined by a conductometric titration. Figure 41A shows the conductometric titration curve of the reaction between NaOH and HCl having a V-shape (Blank). During the titration, the reaction that takes place in the titration vessel is following:

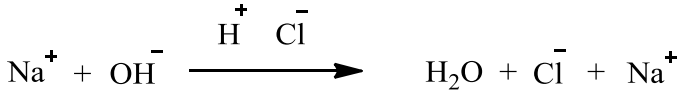

In the region I, before the end point, OH^- is removed from the solution by reaction with H^+, and Cl^- is added to the solution. The conductance of the solution decreases prior to the end point. After the end point (region II), no OH^- is available to react, and the conductance of the solution increases as a result of the additional of H^+ and Cl^-.

In the case of the titration of HCl with –COOH groups on the MNP nanocluster, the conductrometric titration curve exhibits three regions (Figure 40B and 40C). Before the titration of –COOH groups on the MNP nanocluster, the –COOH grafted on the MNP nanocluster was dispersed in an excess of NaOH solution. Thus, the reaction that takes place in the vessel is following:

In the region I of the titration, because basicity of excess OH- in the solution is stronger than that of $–COO^-$, the OH^- in the solution was first neutralized when HCl was titrated.

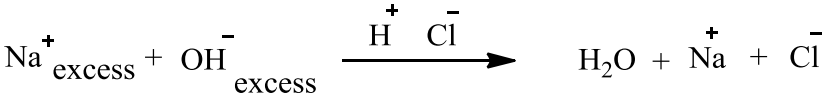

In the region II, when the OH- in the solution was completely neutralized, the H+ ions reacted with the COO^- groups on the MNP surface. After the COO^- groups on the MNP surface were completely reacted with H^+ ions, the solution conductivity sharply increase due to the excess of H^+ and Na^+ (region III). The measurement of the amounts of –COOH groups on the surface of the polymer-grafted MNP was estimated from the following equation:

$$\text{Carboxylic acid} = \frac{M\,\Delta V}{m}$$

$$= \frac{0.005\ \text{mol/L} \times (1000 \times 10^{-6})\text{L}}{0.001\text{g}}$$

$$= 5\ \text{mmol/g}$$

Where, *V* is the consumption volume of HCl solution in the second region (region II) of the conductometric titration (L) *M* is the molar concentration of polyelectrolyte (mol/L). In this calculation, example is the poly(AA)100-MNP nanoclusters.

2. Calculations of the grafting density of carboxyl groups on poly(AA)300-MNP nanoclusters after dispersing in water

$$\text{Carboxylic acid} = \frac{M\,\Delta V}{m}$$

$$= \frac{0.005\ \text{mol/L} \times (3000 \times 10^{-6})\text{L}}{0.001\text{g}}$$

$$= 15\ \text{mmol/g}$$

3) The ability of antibody adsorption onto the pol(AA)-grafted MNP nanoclusters

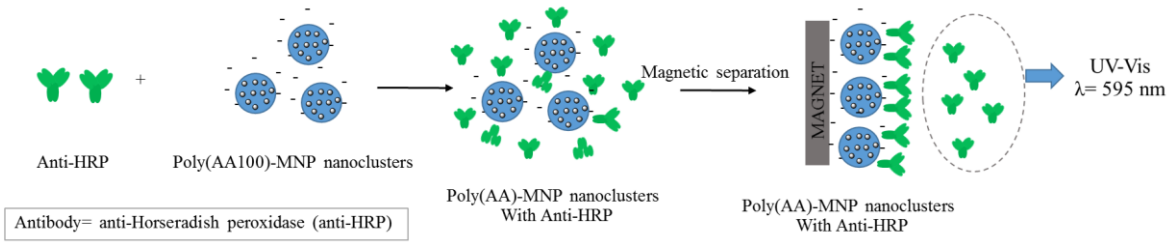

Figure S3 A schematic representation of poly(AA)-MNP nanoclusters in adsorption with anti-HRP antibody

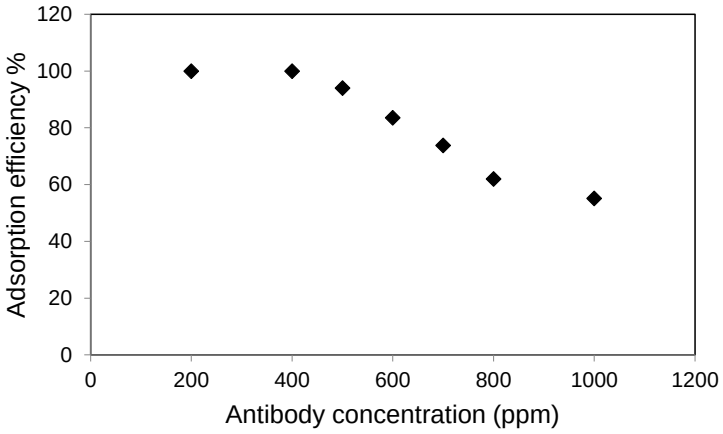

Figure S4 Adsorption efficiency of PAA100-MNP nanoclusters for ionic adsorption with anti-HRP antibody (Adsorption efficiency = [(A-B)/A] x100, where A is the loaded concentration of antibody and B is the concentration of adsorbed antibody)

RESEARCH OUTPUT

1. 5 International publications
2. 13 International presentations
3. 3 National presentations
4. 2 Invited oral presentations
5. 5 Awards
6. 5 International/national collaborations
7. การนำผลงานวิจัยไปใช้ประโยชน์และการผลิตนักวิจัย

1) 5 International publications

1.1) Y. Prai-In, C. Boonthip, B. Rutnakornpituk, U. Wichai, V. Montembault, S. Pascual, L. Fontaine* and M. Rutnakornpituk*, “Recyclable magnetic nanocluster crosslinked with poly(ethylene oxide)-block-poly(2-vinyl-4,4-dimethylazlactone) copolymer for adsorption with antibody”, *Materials Science & Engineering C* (2016) 67, 285-293 (IF 5.085, year 2017)

1.2) S. Paenkaew and M. Rutnakornpituk* Effect of alkyl chain lengths on the assemblies of magnetic nanoparticles coated with multi-functional thiolactone-containing copolymer, *Journal of Nanoparticle Research* (2018) 20, 193-204 (IF 2.127, year 2017)

1.3) N. Deepuppha, S. Khadsai, B. Rutnakornpituk, U. Wichai and M. Rutnakornpituk*, Multi-responsive poly(*N*-acryloyl glycine)-based nanocomposite and its drug release characteristics, Journal of Nanomaterials (2019) Volume 2019, Article ID 8252036, 12 pages (IF 2.207, year 2017)

1.4) B. Thong-On, M. Rutnakornpituk*, Controlled magnetite nanoclustering in the presence of glycidyl-functionalized thermo-responsive poly(N-isopropylacrylamide), *European Polymer Journal* (2016), 85, 519-531 (IF 3.741, year 2017)

1.5) S. Meerod, N. Deepuppha, B .Rutnakornpituk, M. Rutnakornpituk*, Reusable magnetic nanocluster coated with poly(acrylic acid) and its adsorption with antibody and antigen, .*Journal of Applied Polymer Science*, (2018) 135, 46160 (10 pages)(IF 1.901, year 2017)

2) 13 International presentations

2.1) Multi-functional copolymer for coating on magnetite nanoparticle for use in bioconjugation, Sujitra Paenkaew, Metha Rutnakornpituk, The 4th edition of Nanotech France 2018 International Conference and Exhibition, 27-29 June, 2018, Paris, France: Pôle Universitaire Léonard de Vinci

2.2) Anionic magnetite nanoparticle conjugated with peptide nucleic acid for pre-concentration of real DNA, Sudarat Khadsai, Noppadol Seeja, Metha Rutnakornpituk, Tirayut Vilaivan, Maliwan Nakkuntod, Waroon Suwankitti, Boonjira Rutnakornpituk, The 4th edition of Nanotech France 2018 International Conference and Exhibition, 27-29 June, 2018, Paris, France: Pôle Universitaire Léonard de Vinci

2.3) Multi-functional copolymer-coated nanocluster and its drug controlled release application, Sujitra Pankaew and Metha Rutnakornpituk, Universal Academic Cluster International Autumn Conference in Tokyo, Oral, 11-13 October 2017, Tokyo, Japan

2.4) Multi-functional copolymer-coated magnetic nanoparticle and its drug controlled release, Sujitra Pankaew and Metha Rutnakornpituk, The First Materials Research Society of Thailand International Conference (1st MRS Thailand International Conference), Poster, 31 October-3 November 2017, Convention Center, The Empress Hotel, Chiang Mai, Thailand

2.5) Multi-responsive poly(N-acryloyl glycine)-based nanocomposite and its controlled release application, Nunthiya Deepuppha, Sudarat Khadsai, Boonjira Rutnakornpituk and Metha Rutnakornpituk, The First Materials Research Society of Thailand International Conference (1st MRS Thailand International Conference), Poster, 31 October-3 November 2017, Convention Center, The Empress Hotel, Chiang Mai, Thailand

2.6) Anionic magnetite nanoparticle conjugated with pyrrolidinyl PNA for real DNA pre-concentration, Sudarat Khadsai, Boonjira Rutnakornpituk, Tirayut Vilaivan, Maliwan Nakkuntod, and Metha Rutnakornpituk, The First Materials Research Society of

Thailand International Conference (1st MRS Thailand International Conference), Poster, 31 October-3 November 2017, Convention Center, The Empress Hotel, Chiang Mai, Thailand

2.7) Magnetite nanocluster coated with thiolactone-containing copolymer: effect of alkyl substitution on magnetic separation ability and water dispersibility, Sujitra Pankaew and Metha Rutnakornpituk, The 7th International Polymer Conference of Thailand (PCT7), Oral, 1-2 June, 2017, Amari Water Gate Hotel, Bangkok, Thailand

2.8) Multi-responsive nanocomposite and its controlled release application, Nunthiya Deepuppha, Sudarat Khadsai and Metha Rutnakornpituk, The 7th International Polymer Conference of Thailand (PCT7), Poster, 1-2 June, 2017, Amari Water Gate Hotel, Bangkok, Thailand

2.9) Magnetic nanoparticle coated with multi-responsive copolymer containing thiolactone acrylamide, Sujittra Paenkaew and Metha Rutnakornpituk, Pure and Applied Chemistry International Conference (PACCON2017), 2-3 February 2017, Bangkok, Thailand

2.10) PNA-conjugated magnetic nanocluster for real DNA pre-concentration, Metha Rutnakornpituk, Sudarat Khadsai, Boonjira Rutnakornpituk, Maliwan Nakkuntod, Tirayut Vilaivan, The 11th International Polymer Conference (IPC2016), 13-16 December 2016, Fukuoka, Japan

2.11) Poly(acrylic acid)-grafted magnetite nanocluster conjugated with pyrollidinyl peptide nucleic acid for DNA base discrimination, Noppadol Seeja, Tirayut Vilaivan, Metha Rutnakornpituk, Boonjira Rutnakornpituk, The 6th International Polymer Conference of Thailand (PCT6), June 30th-July 1st, 2016, Patumwan Princess Hotel, Bangkok, Thailand

2.12) Synthesis of magnetic nanoparticle grafted with thermo-responsive polymer containing thiolactone acrylamide moiety, Sujitra Pankeaw and Metha Rutnakornpituk, The 6th International Polymer Conference of Thailand (PCT6), June 30th-July 1st, 2016, Patumwan Princess Hotel, Bangkok, Thailand

2.13) Dual-responsive poly(*N*-acryloyl glycine)-containing copolymer for coating on magnetic nanoparticle**,** Nunthiya Deepuppha, Sudarat Khadsai and Metha Rutnakornpituk' The 6th International Polymer Conference of Thailand (PCT6), June 30th - July 1st, 2016, Patumwan Princess Hotel, Bangkok, Thailand

2.1) Multi-functional copolymer for coating on magnetite nanoparticle for use in bioconjugation, Sujitra Paenkaew, Metha Rutnakornpituk, The 4th edition of Nanotech France 2018 International Conference and Exhibition, 27-29 June, 2018, Paris, France: Pôle Universitaire Léonard de Vinci

14:30 - 14:45	Multi-scale assessment of soot using electron microscopy: applications on soot from bench-scale fire of polymers **G. Okyay**, S. Bellayer, F. Samyn, M. Jimenez and S. Bourbigot	**Dr. Gizem Okyay**, University of Lille, **France**
14:45 - 15:00	Investigation of the spin-orbit coupling effect of intrinsic and p-type 2D MoS2 by spectroscopic ellipsometry **B. Song**, H. Gu, Y-T. Ho, M. Fang and S. Liu	**Mr. Baokun Song**, Huazhong University of Science & Tech., **China**
15:00 - 15:15	Optical properties of Pb0.865La0.09(Zr0.65Ti0.35)O3 thin films studied by spectroscopic ellipsometry **H.Gu**, M.Li, C. Huang and S. Liu	**Dr. Honggang Gu**, Huazhong University of Science & Tech., **China**
15:15 - 15:30	Determination of the monolayer coverage of silica particles **A. La Rosa**, G. Durand, M. Alvarez, T. Justet and Alan Taylor	**Mr. Angelo La Rosa**, London South Bank University, **UK**
15:30 - 15:45	Friction Reduction on Anodized Alumina by Deposition of Ti Nanolayers **T. Matijošius**, L. Staišiūnas and S. Asadauskas	**Mr. Tadas Matijošius**, Center for Physical Sciences and Technology, **Lithuania**
15:45 - 16:00	Porous PDMS / CNF Nanocomposites for Sensing Applications W. Luo, **M.C. Saha** and Y. Liu	**Prof. Mrinal Saha**, University of Oklahoma, **USA**
16:00 - 16:30	**Coffee Break / Posters Session I**	**Coffee Break Area**
16:30 - 16:45	Tuning the electronic response of MoS2 by pressure induction **R. Torres-Cavanillas**, M. Morant-Giner, G. Escorcia, J. Dugay, M. Galbiati, S. Tatay, M. Giménez-Márquez, A. Forment-Aliaga, E. Coronado.	**Mr. Ramón Torres-Cavanillas**, Univesity of Valencia, **Spain**
16:45 - 17:00	Solution-processable inorganic hole injection layer to improve the performance of quantum-dot light-emitting diodes **S.J. Kang**	**Prof. Seong Jun Kang**, Kyung Hee University, **Rep. of Korea**
17:00 - 17:15	Highly Conductive, Mechanically Robust Ion Gels Based on Co-polymers and their Electrochemical Applications **H.C. Moon**	**Prof. Hong Chul Moon**, University of Seoul, **Rep. of Korea**
17:15 - 17:30	Enhancement in thermoelectric properties of Te-embedded Bi2Te3 by stong phonon scattering at interface **K. Jeong**, H. Choi, J. Chae, H. Park, J. Baeck, T. Hyeon Kim, J.Y. Song, J. Park, K-H. Jeong and M-H. Cho	**Dr. Kwangsik Jeong**, Yonsei University, **Rep. of Korea**
17:30 - 17:45	Multi-functional copolymer for coating on magnetite nanoparticle for use in bioconjugation **S. Paenkaew** and M. Rutnakornpituk	**Ms. Sujittra Paenkaew**, Naresuan University, **Thailand**

The 4th edition of Nanotech France 2018 International Conference and Exhibition. Paris, France: Pôle Universitaire Léonard de Vinci

(Oral presentation)

Multi-functional copolymer for coating on magnetite nanoparticle for use in bioconjugation

Sujittra Paenkaew and Metha Rutnakornpituk *

Department of Chemistry and Center of Excellence in Biomaterials, Faculty of Science, Naresuan University, Phitsanulok, 65000 Thailand.

Abstract:

Surface modification of magnetite nanoparticle (MNP) with a multi-functional copolymer and its bioconjugation is presented herein. This copolymer was designed to possess multi-functions including 1) thermo-responsive poly(*N*-isopropyl acrylamide) (PNIPAAm) serving as a drug reservoir and for drug controlled release, 2) thiolactone moiety for covalent grafting onto MNP surface and also inducing the formation of MNP nanoclusters and 3) cationic poly(diethylaminoethyl methacrylate) (PDEAEMA) for improving its water dispersibility and for ionic adsorption with DNA. Fourier Transform Infrared Spectrophotometry (FTIR) results signified the existence of the copolymer in MNP nanoclusters. The copolymer-coated nanoclusters showed the significant increase in zeta potential from +16 mV to +28 mV after quaternization. This significantly improved dispersibility of the particle in an aqueous media and it was thus used as a cationic platform for adsorption with DNA through the electrostatic interaction. Thermo-responsive PNIPAAm coated in the nanoclusters collapsed at the temperature above its critical solution temperature, resulting in the shrinkage of the nanoclusters and thus eventually decreasing their hydrodynamic size (D_h). The shrinkage of the copolymer when heated to 45 °C would be utilized as a triggering mechanism for drug controlled release application. It was also found that the use of alkyl amines having various chain lengths (R-NH_2; where R is alkyl groups having C3, C8 and C12) in the nucleophilic ring-opening reactions of the thiolactone rings affected their magnetic separation ability, water dispersibility and release rate of doxorubicin model drug. These versatile copolymer-coated nanoclusters showed a great potential for use as a smart platform for bioconjugation and drug controlled release application.

Keywords: magnetite nanoparticle, multi-functional copolymer, thermo-responsiveness, drug controlled release**.**

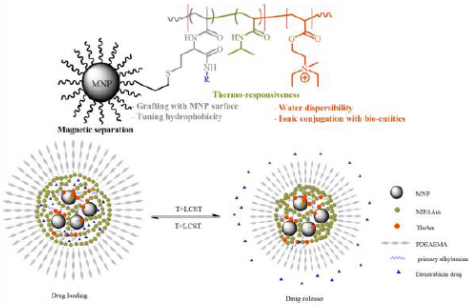

Figure 1: Illustrating the surface modification of magnetite nanoparticle (MNP) coated with the multi-functional copolymer and its use in controlled drug release.

References:

1. Espeel, P., Du Prez, F. E. (2015) One-pot multi-step reactions based on thiolactone chemistry: a powerful synthetic tool in polymer science, *Eur. Polym. J.*, 6, 2247–272.
2. Meerod, S., Rutnakornpituk, B., Wichai, U., Rutnakornpituk, M. (2015), Hydrophilic magnetic nanoclusters with thermo-responsive properties and their drug controlled release, *J. Magn. Magn. Mater.*, 392, 83–90.

2.2) Anionic magnetite nanoparticle conjugated with peptide nucleic acid for pre-concentration of real DNA, Sudarat Khadsai, Noppadol Seeja, Metha Rutnakornpituk, Tirayut Vilaivan, Maliwan Nakkuntod, Waroon Suwankitti, Boonjira Rutnakornpituk, The 4th edition of Nanotech France 2018 International Conference and Exhibition, 27-29 June, 2018, Paris, France: Pôle Universitaire Léonard de Vinci

The 4th edition of Nanotech France 2018 International Conference and Exhibition. Paris, France: Pôle Universitaire Léonard de Vinci

(Oral presentation)

Poly(*N*-acryloyl glycine)-grafted magnetite nanoparticle conjugated with pyrrolidinyl peptide nucleic acid for selective enrichment of trace DNA samples

Sudarat Khadsai[1], Noppadol Seeja[1], Metha Rutnakornpituk[1], Tirayut Vilaivan[2], Maliwan Nakkuntod[3], Waroon Suwankitti[3], Boonjira Rutnakornpituk[1,4*]

[1]Department of Chemistry and Center of Excellence in Biomaterials, Faculty of Science, Naresuan University, Phitsanulok 65000, Thailand
[2]Organic Synthesis Research Unit, Department of Chemistry, Faculty of Science; Chulalongkorn University, Patumwan, Bangkok 10330, Thailand
[3]Department of Biology, Faculty of Science, Naresuan University, Phitsanulok 65000 Thailand
[4]The Center of Excellence for Innovation in Chemistry, Naresuan University, Phitsanulok, 65000, Thailand

Abstract

Poly(*N*-acryloyl glycine) (PNAG)-grafted magnetite nanoparticle (MNP) was used as magnetic support for real deoxyribonucleic acid (DNA) preconcentration using pyrrolidinyl peptide nucleic acid (PNA) as a probe. The PNAG-grafted MNP was covalently conjugated with streptavidin, followed by immobilization with biotin-conjugated PNA via specific interaction between biotin and streptavidin. The particles with the size of 300-400 nm were well dispersible in water, had a good response to a magnet and had the capacity of 373 pmol PNA/mg MNP. The probe on the particle can discriminate between non-complementary and complementary DNA using fluorophore-tagged DNA as a model. Also, the particles were used for precontration of zein genes of maize in fresh produce and eight cereal products as real samples. After the desorption of the DNA adsorbed on the particle and then amplification with Polymerase Chain Reaction (PCR) technique, gel electrophoresis indicated that only the real samples having zein gene of maize can be adsorbed on the PNA-functionalized MNP, indicating the high specificity between PNA and complementary DNA. This PNA-functionalized MNP might be effectively used as nano-solid supports for DNA enrichment in real samples.

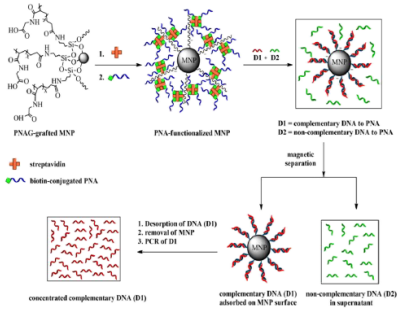

Keywords: magnetite, nanoparticle, nano-solid supports, pyrrolidinyl peptide nucleic acid, PNA probe, real deoxyribonucleic acid, enrichment, pre-concentration

References:

1. Theppaleak, T., Rutnakornpituk, B., Wichai, U., Vilaivan, T., Rutnakornpituk, M. (2013), *J. Biomed. Nanotech.,* 9, 1509-1520.
2. Khadsai, S., Rutnakornpituk, B., Vilaivan, T., Nakkuntod, M., Rutnakornpituk, M. (2016), *J. Nanopart. Res.,* 18(263), 1-15

2.3) Multi-functional copolymer-coated nanocluster and its drug controlled release application, Sujitra Pankaew and Metha Rutnakornpituk, Universal Academic Cluster International Autumn Conference in Tokyo, Oral, 11-13 October 2017, Tokyo, Japan

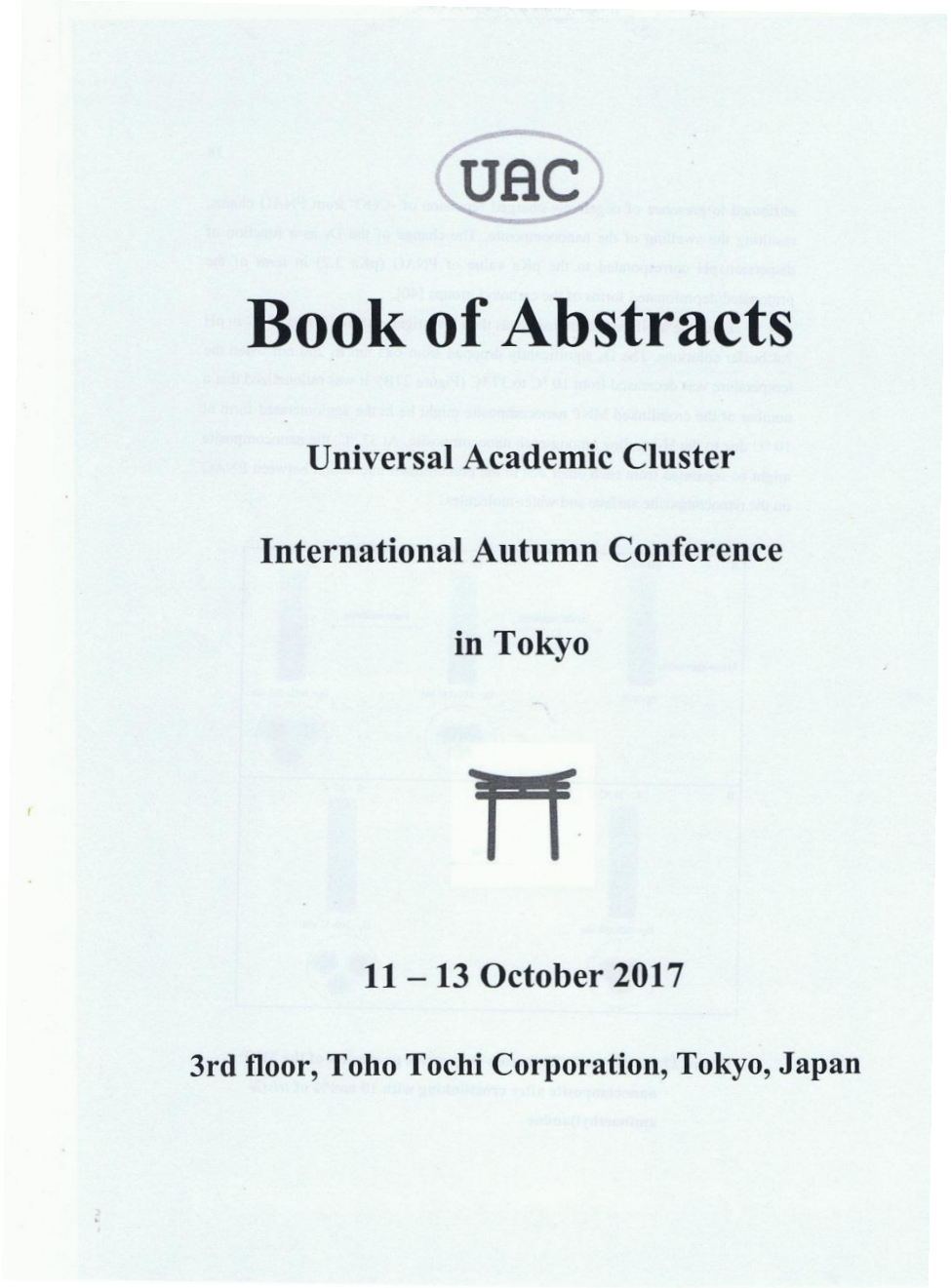
UAC

Book of Abstracts

Universal Academic Cluster

International Autumn Conference

in Tokyo

11 – 13 October 2017

3rd floor, Toho Tochi Corporation, Tokyo, Japan

10 Universal Academic Cluster International Autumn Conference in Tokyo, 11-13 October 2017

Multi-functional copolymer-coated nanocluster and its drug controlled release application

Sujittra Paenkaew and Metha Rutnakornpituk

Department of Chemistry and Center of Excellence in Biomaterials, Faculty of Science, Naresuan University, Phitsanulok, 65000 Thailand.

Abstract

This work presents the synthesis of magnetite nanoparticle (MNP) coated with a multi-functional copolymer containing thiolactone acrylamide (TlaAm) and its use in controlled drug release. TlaAm units in the copolymer were ring-opened with various alkyl amines (e.g. 1-propylamine, 1-octylamine or 1-dodecylamine) to form thiol groups (-SH), followed by a thiol-ene coupling reaction with acrylamide-coated MNP and then quaternized to obtain cationic copolymer-MNP nanoclusters having various degrees of hydrophobicity. It was found that the MNP nanoclusters having different chain lengths of alkyl groups exhibited differences in magnetic separation ability, water dispersibility and release rate of doxorubicin model drug. Moreover, all copolymer-coated MNPs showed a thermo-responsive behavior as their hydrodynamic size (D_h) decreased when increasing the temperature of the dispersions due to the shrinkage of PNIPAAm moiety. These copolymer-MNP nanoclusters could be used as a platform with thermal-triggering controlled drug release.

2.4) Multi-functional copolymer-coated magnetic nanoparticle and its drug controlled release, Sujitra Pankaew and Metha Rutnakornpituk, The First Materials Research Society of Thailand International Conference (1st MRS Thailand International Conference), Poster, 31 October-3 November 2017, Convention Center, The Empress Hotel, Chiang Mai, Thailand

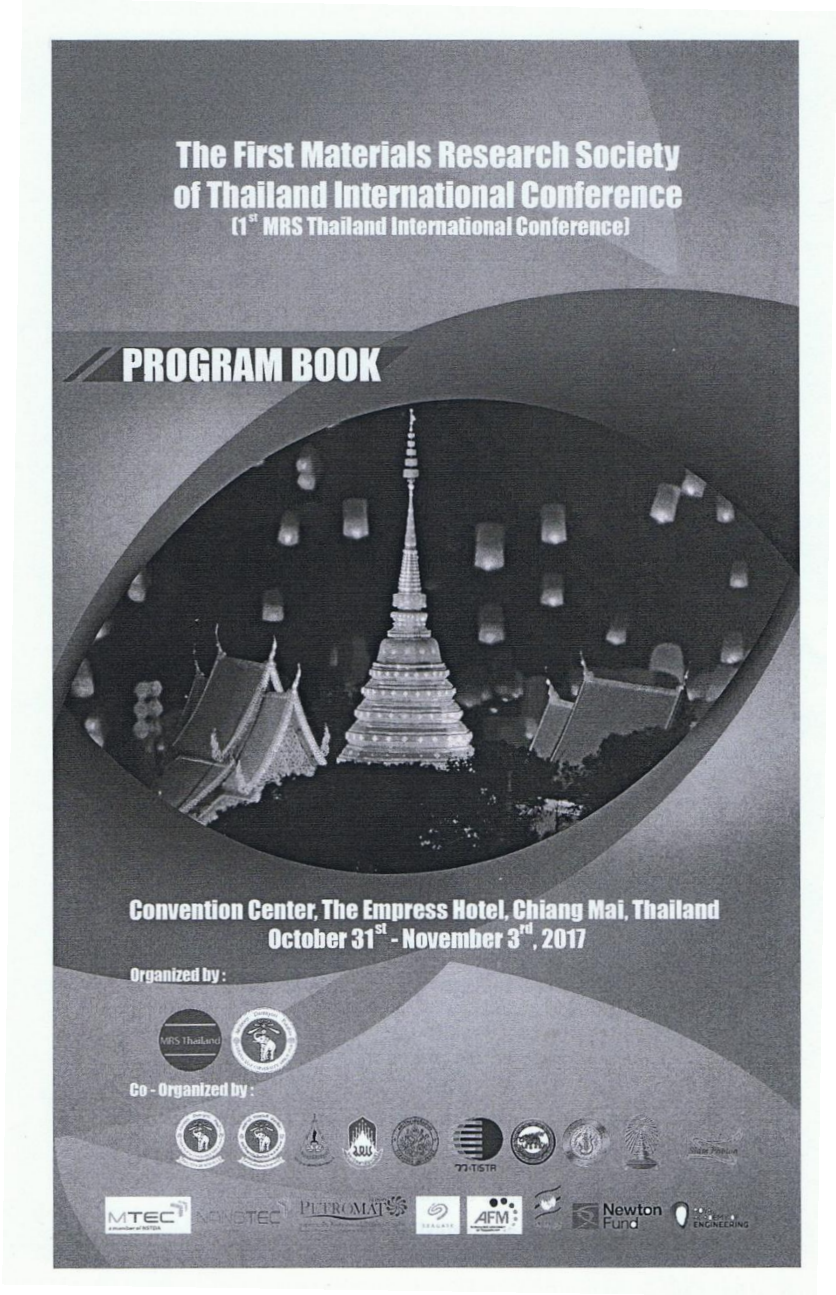

S6-P8	**Concentration Effect of Ferrofluids in Ferrogels on Their Magnetic and Magneto-elasticity Behaviors** Sunaryono, Muchlis Fajar Hidayat, Chusnana Insjaf Yogihati, Ahmad Taufiq, Nandang Mufti, Retno Rahmawati, and Markus Diantoro
S6-P9	**Thermally assisted domain wall motion driven by spin torque** P. Wongsasueb, P. Chureemart and J. Chureemart
S6-P10	**Surface Investigation on Annealing Effects of IrMn Thin Films** Kanogkwan Sawaengsai, Sakuntam Sanorpim, Sukkaneste Tungasmita, Duangamol Tungasmita, Kunpot Mopoung and Laddawan Supadee
S6-P11	**Synthesis of Superparamagnetic Iron Oxide Nanoparticles (SPION) for biomedical applications** Wid Meksiriwattana and Kanlaya Prapainop
S6-P12	**Structural, Magnetic, and Antibacterial Performances of Magnetite Ferrofluids Templated by PEG-20.000** Ahmad Taufiq, Fitri Nur Ikasari, Hendra Susanto, Endang Suarsini, Sunaryono, Nurul Hidayat, Arif Hidayat, Nandang Mufti, Abdulloh Fuad and Markus Diantoro
S6-P13	**Synthesis and physical properties of delafossite $CuBO_2$ transparent conducting oxide** Sornamol Traiphop and Teerasak Kamwanna
S6-P14	**Optical, Magnetic and Electronic Properties of Sb_xCuCrO_2 Transparent Conducting Oxide** Chutarat Yonchai and Teerasak Kamwanna
S6-P15	**Effect of Nickel Ferrite Addition on Characteristics of Nanostructured Nickel Ferrite/Hydroxyapatite Ceramic** Pattarinee Klumdoung and Piyapong Pankaew
S6-P16	**Synthesis, characterization and magnetic properties of Cu-doped Co_3O_4** Jessada Khajonrit, Chaturon Nettonglang and Santi Maensiri
S6-P17	**"Smart" multi-functional copolymer-coated magnetic nanoparticle and its applications for bioconjugation and drug controlled release** Sujittra Paenkaew and Metha Rutnakornpituk
S6-P18	**Multi-responsive poly(N-acryloyl glycine)-based nanocomposite and its controlled release application** Nunthiya Deepuppha, Sudarat Khadsai, Boonjira Rutnakornpituk and Metha Rutnakornpituk
S6-P19	**Anionic magnetite nanoparticle conjugated with pyrrolidinyl PNA for real DNA pre-concentration** Sudarat Khadsai, Boonjira Rutnakornpituk, Tirayut Vilaivan, Maliwan Nakkuntod and Metha Rutnakornpituk

Poster Session

The First Materials Research Society of Thailand International Conference
(1st MRS Thailand International Conference)
October 31 – November 3, 2017
The Empress Convention Center, Chiang Mai, Thailand

"Smart" multi-functional copolymer-coated magnetic nanoparticle and its applications for bioconjugation and drug controlled release

Sujittra Paenkaew and Metha Rutnakornpituk *
Department of Chemistry and Center of Excellence in Biomaterials, Faculty of Science, Naresuan University, Phitsanulok, 65000 Thailand.
Phone: 66-5596-3464, Fax: 66-5596-3401

*E-mail: methar@nu.ac.th

Abstract

Synthesis of magnetic nanoparticle (MNP) coated with a multi-functional polymer, poly(N,N-diethylaminoethyl methacrylate)-*b*-poly(N-isopropyl acrylamide-*st*-thiolactone acrylamide) copolymer (PDEAEMA-*b*-P(NIPAAm-*st*-TlaAm)), and its drug controlled release are herein presented. This copolymer was well designed to have multi-functions including thermo-responsive PNIPAAm serving as a drug reservoir with a temperature-triggering mechanism, thiolactone moiety for covalent grafting with MNP surface and tuning degree of hydrophobicity of the copolymer. In addition, the positively charged PDEAEMA can improve its water dispersibility and serve as a platform for ionic adsorption with anionic bio-entities such as DNA. It was found that the degree of hydrophobicity of the copolymers coated on surface of particle can be tuned by using various alkyl chain lengths in thiolactone ring-opening reaction. This can influence the particle self-assemblies in water (e.g. D_h, dispersibility, nano-aggregation) and the release rate of doxorubicin model drug. When increasing the dispersion temperature, the particles showed a thermo-responsive behavior as indicated by the decrease in hydrodynamic size and the accelerated drug release rate. These versatile copolymer-MNP assemblies showed a great potential for use as a smart platform with thermal-triggering controlled drug release system and for conjugation with any negatively charged bio-entities.

Keywords: poly(N-acryloyl glycine); nanocomposites; pH- and thermo-responsive polymer; drug release

2.5) Multi-responsive poly(N-acryloyl glycine)-based nanocomposite and its controlled release application, Nunthiya Deepuppha, Sudarat Khadsai, Boonjira Rutnakornpituk and Metha Rutnakornpituk, The First Materials Research Society of Thailand International Conference (1st MRS Thailand International Conference), Poster, 31 October-3 November 2017, Convention Center, The Empress Hotel, Chiang Mai, Thailand

The First Materials Research Society of Thailand International Conference
(1st MRS Thailand International Conference)
October 31 – November 3, 2017
The Empress Convention Center, Chiang Mai, Thailand

Multi-responsive poly(*N*-acryloyl glycine)-based nanocomposite and its controlled release application

Nunthiya Deepuppha, Sudarat Khadsai, Boonjira Rutnakornpituk and Metha Rutnakornpituk*

Department of Chemistry and Center of Excellence in Biomaterials, Faculty of Science, Naresuan University, Phitsanulok, 65000 Thailand.
Phone: 66-5596-3464, Fax: 66-5596-3401

*E-mail: methar@nu.ac.th

Abstract

Magnetic nanocomposite coated with pH- and thermo-responsive poly(*N*-acryloyl glycine)(PNAG) was prepared via a one pot-free radical polymerization, followed by a crosslinking reaction. Two types of the crosslinkers (ethylenediamine and *tris*(2-aminoethyl)amine) with two different concentrations (1 and 10 mol%) were used in an attempt to tune the size, magnetic separation ability and water dispersibility of the nanocomposite. It was found that the nanocomposite crosslinked with *tris*(2-aminoethyl)amine can be rapidly separated by a magnet while maintaining its good dispersibility in water. The release profiles of theophylline as a model drug from the nanocomposite were investigated as a function of pH (2.0 7.4 and 11.0) and temperature (10 ˚C and 37 ˚C) of the dispersions. The drug was rapidly released when the dispersion pH changed from neutral to acidic/basic conditions or when increasing the temperature from 10 ˚C to 37 ˚C. This nanocomposite showed a great potential for use as a magnetically guidable vehicle for thermo- and pH-triggered drug controlled release applications.

Keywords: poly(N-acryloyl glycine); nanocomposites; pH- and thermo-responsive polymer; drug release

2.6) Anionic magnetite nanoparticle conjugated with pyrrolidinyl PNA for real DNA pre-concentration, Sudarat Khadsai, Boonjira Rutnakornpituk, Tirayut Vilaivan, Maliwan Nakkuntod, and Metha Rutnakornpituk, The First Materials Research Society of Thailand International Conference (1st MRS Thailand International Conference), Poster, 31 October-3 November 2017, Convention Center, The Empress Hotel, Chiang Mai, Thailand

The First Materials Research Society of Thailand International Conference
(1st MRS Thailand International Conference)
October 31 – November 3, 2017
The Empress Convention Center, Chiang Mai, Thailand

Anionic magnetite nanoparticle conjugated with pyrrolidinyl PNA for real DNA pre-concentration

Sudarat Khadsai[a], Boonjira Rutnakornpituk[a], Tirayut Vilaivan[b], Maliwan Nakkuntod[c], and Metha Rutnakornpituk[a,*]

[a]*Department of Chemistry and Center of Excellence in Biomaterials, Faculty of Science, Naresuan University, Phitsanulok 65000, Thailand.*
[b]*Department of Chemistry, Organic Synthesis Research Unit, Faculty of Science, Chulalongkorn University, Patumwan, Bangkok 10330, Thailand,*
[c]*Department of Biology, Faculty of Science, Naresuan University, Phitsanulok 65000, Thailand.*

*E-mail: methar@nu.ac.th

Abstract

Magnetite nanoparticles (MNPs) were surface modified with anionic poly(*N*-acryloyl glycine) (PNAG) and then streptavidin for specific interaction with biotin-conjugated pyrrolidinyl peptide nucleic acid (PNA). Hydrodynamic size (D_h) of PNAG-grafted MNPs varied from 334 to 496 nm depending on the loading ratio of the MNP to NAG in the reaction. UV-visible and fluorescence spectrophotometries were used to confirm the successful of streptavidin and PNA on the MNPs. It was found that approximately 291 pmol of the PNA/mg MNP was immobilized on the particle surface. The PNA-functionalized MNPs were effectively used as solid supports for DNA base discrimination to differentiate between fully complementary and non-complementary/single-base mismatch DNA using the PNA probe. These novel particles were also used for pre-concentration of zein gene of maize in fresh produce and cereal products as real DNA samples. After desorption of the real DNA adsorbed on the particles and then amplification with Polymerase Chain Reaction (PCR) technique and gel electrophoresis indicated the existence of the zein gene of maize on the particles.

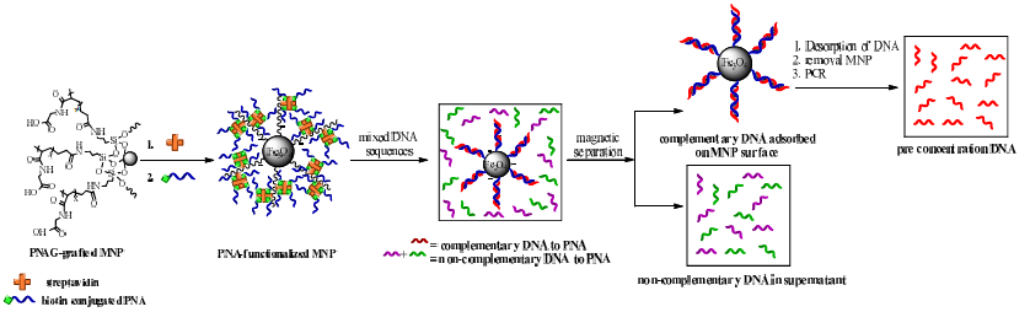

Keywords: Magnetite, Nanoparticle, PNA probe, real DNA, Base discrimination, Pre-concentration

2.7) Magnetite nanocluster coated with thiolactone-containing copolymer: effect of alkyl substitution on magnetic separation ability and water dispersibility, Sujitra Pankaew and Metha Rutnakornpituk, The 7th International Polymer Conference of Thailand (PCT7), Oral, 1-2 June, 2017, Amari Water Gate Hotel, Bangkok, Thailand

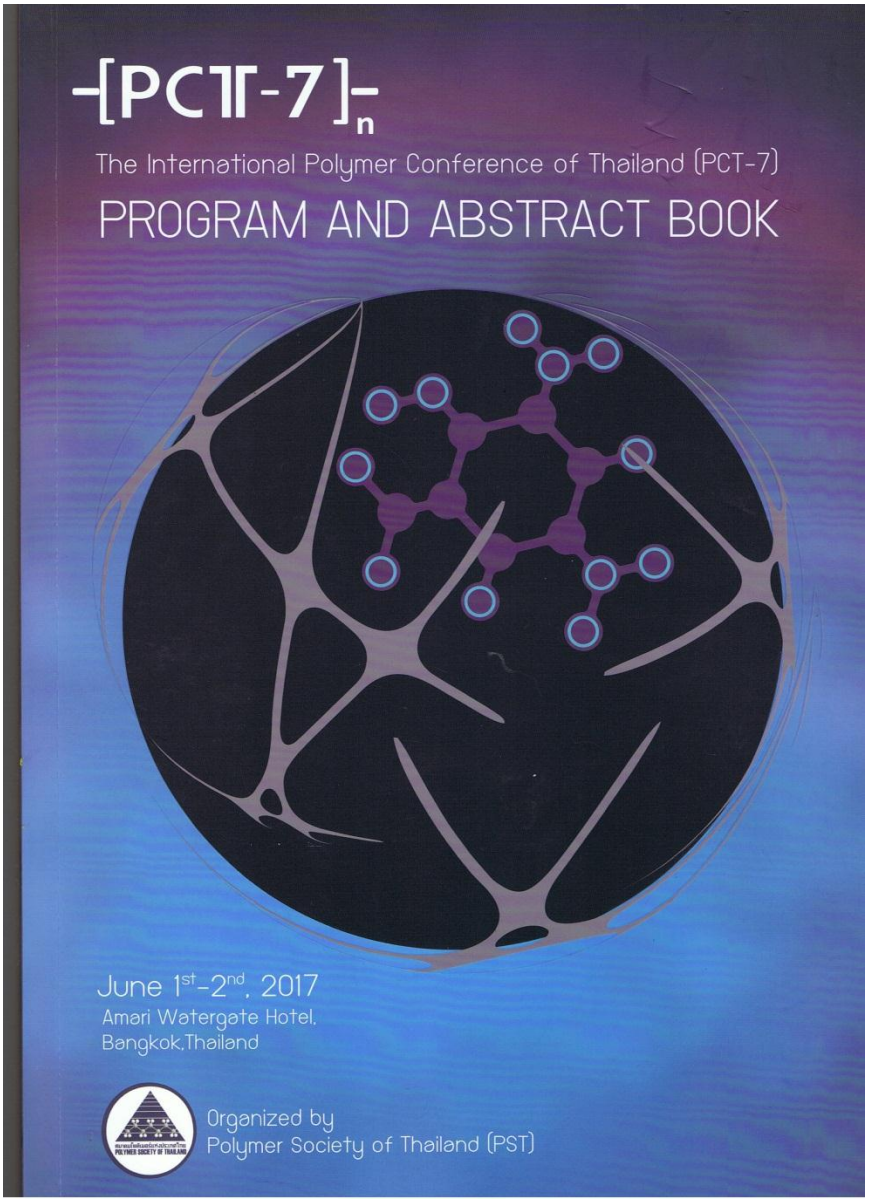

-[PCTF-7]-

FUNC-O1 (14:00-14:15)	**Encapsulation of heat storage material in poly(methyl methacrylate-co-divinylbenzene) shell by microsuspension iodine transfer polymerization (ms ITP)** ***Siriluk Namwong***, *Masayoshi Okubo, Amorn Chaiyasat and Preeyaporn Chaiyasat* Chulalongkorn University
FUNC-O2 (14:15-14:30)	**Synthesis of responsive polymer/corrosion inhibitor conjugates** ***Farzad Seidi***, *Daniel Crespy* Vidyasirimedhi Institute of Science and Technology
FUNC-O3 (14:30-14:45)	**Temperature-Responsive Properties of Poly(PEGMA) Hydrogel Thin Films** ***Ekkachai Martwong***, *and Yvette Tran* PSL Research University
FUNC-O4 (14:45-15:00)	**Preparation of biomaterials by colloid-electrospinning** ***Ratchapol Jenjob***, *Kusuma Thongchaivetcharat, Arjaree Jobdeedamrong, and Daniel Crespy* Vidyasirimedhi Institute of Science and Technology
Session	**Advanced and Functional Polymers (2)**
Date/Time/Room	**Thursday, June 1st, 2017/ 15.30-16:45/ Banglampoo (6th floor)**
Session Chair	***Assoc. Prof. Metha Rutnakornpituk***
FUNC-KN2 (Keynote Lecture) (15:30-16:00)	**Fabrication of Curable Poly(lactic acid-*co*-glycidyl methacrylate) Copolymers and their Use in Various Cosmetic and Biomedical Applications** ***Assoc. Prof. Pakorn Opaprakasit*** Thammasat University
FUNC-O5 (16:00-16:15)	**Starch-*g*-PLA for compatible PLA/TPS blends and its application as external stimuli responsive fiber** ***Nathapol Chinvirojsatian***, *Autchara Pangon, and Suwabun Chirachanchai* Chulalongkorn University
FUNC-O6 (16:15-16:30)	**Development of Poly(Methyl Methacrylate) Products with Superhydrophobic Surfaces** ***Nithiwit Sriprasert***, *Preeyaporn Chaiyasat, Amorn Chaiyasat, Mantana Opaprakasit, Atitsa Petchsuk, and Pakorn Opaprakasit* Thammasat University
FUNC-O7 (16:30-16:45)	**Magnetite nanocluster coated with thiolactone-containing copolymer: effect of alkyl substitution on magnetic separation ability and water dispersibility** ***Sujittra Paenkaew*** *and Metha Rutnakornpituk* Naresuan University
FUNC-O8 (16:45-17:00)	**A feasibility of developing transparent barrier coating for dye sensitized solar cells from polymer composites based on PVDC/PU reinforced with cellulose nanocrystals** ***Kitti Yuwawech***, *Chutimar Deetuam and Jatuphorn Wootthikanokkhan* King Mongkut's University of Technology (KMUTT)

FUNC-O7

Magnetite nanocluster coated with thiolactone-containing copolymer: effect of alkyl substitution on magnetic separation ability and water dispersibility

Sujittra Paenkaew and Metha Rutnakornpituk *
Department of Chemistry and Center of Excellence in Biomaterials, Faculty of Science, Naresuan University, Phitsanulok, 65000 Thailand.
Phone: 66-5596-3464, Fax: 66-5596-3401, *E-mail: methar@nu.ac.th

Abstract

Synthesis of a novel functional polymer, poly(N,N-diethylaminoethyl methacrylate)-*b*-poly(N-isopropyl acrylamide-*st*-thiolactone acrylamide) copolymer (PDEAEMA-*b*-P(NIPAAm-*st*-TlaAm( ), and its coating on magnetite nanoparticle (MNP) are presented. TlaAm units in the copolymer were ring-opened with alkyl amines to form thiol groups (-SH), followed by thiol-ene coupling reactions with acrylamide-coated MNP to obtain the MNP nanocluster. The goal of this work was to obtain the nanocluster that can be rapidly separated by a magnet while maintaining its good water dispersibility. Therefore, 1-propylamine, 1-octylamine and 1-dodecylamine were used in the ring-opening reactions (to form C3-MNP, C8-MNP and C12-MNP, respectively) to investigate the effect of degree of hydrophobicity due to various chain lengths of the alkyl groups on their magnetic separation ability and water dispersibility. It was found that C3-MNP, as compared to C8-MNP and C12-MNP, showed a good response to a magnet upon magnetic separation with good dispersing stability in water after 24 h of the synthesis. Interestingly, all copolymer-coated MNPs showed a thermo-responsive behavior as their hydrodynamic size (D_h) decreased when increasing the temperature of the dispersions due to the shrinkage of PNIPAAm moiety. This novel copolymer-MNP hybrid might be efficiently used as a vehicle in drug controlled release applications.

Keywords: Magnetite, Nanoparticle, Block copolymer; thermo-responsiveness

2.8) Multi-responsive nanocomposite and its controlled release application, Nunthiya Deepuppha, Sudarat Khadsai and Metha Rutnakornpituk, The 7th International Polymer Conference of Thailand (PCT7), Poster, 1-2 June, 2017, Amari Water Gate Hotel, Bangkok, Thailand

BIOP-P21	**Porous semi-IPN hydrogel scaffold based on silk sericin and poly(2-hydroxyethyl methacrylate): Effect of cross-linker loading** ***Sukhonthamat Sonjan***, *Sararat Mahasaranon, Gareth M. Ross and Sukunya Ross* Naresuan University
BIOP-P22	**Design and characterization of seeds coated by hydrophilic and hydrophobic films for longer shelf life and greater germination** ***Sukunya Ross***, *Sararat Mahasaranon, Gareth M. Ross, Suphannika Intanon and Bunyarit Sinkangam* Naresuan University
BIOP-P23	**Preparation of Acetylated Cellulose for PLA/Acetylated Cellulose Biocomposite** ***Thana Boonnak*** *and Kawee Srikulkit* Chulalongkorn University
Biomedical Polymers (BMED)	
BMED-P1	**Multi-responsive nanocomposites and their controlled release application** ***Nunthiya Deepuppha***, *Sudarat Khadsai and Metha Rutnakornpituk* Naresuan University
BMED-P2	**Synthesis and Characterization of Quaternized Cellulose incorporated into Poly (lactic acid-co-glycidyl methacrylate) Microbeads** ***Narumon Jongmanwattana***, *Kittiwut Kasemwong, and Pakorn Opaprakasit* Sirindhorn International Institute of Technology (SIIT)
BMED-P3	**Preparation of Water-In-Oil-In-Water Double Emulsions Stabilized by Chitosan/Sodium Carboxymethyl Cellulose Complex** ***Nopparat Viriyakitpattana*** *and Panya Sunintaboon* Mahidol University
BMED-P4	**Self-Assembly of DNA-Based Biomaterials** ***Pitchaya Pakornpadungsit,*** *Thridsawan Prasopdee and Wirasak Smitthipong* Kasetsart University
BMED-P5	**Development of Drug Controlled-Released Materials Employing Polylactide Copolymers** ***Nichaporn Wongsirojkul***, *Atitsa Petchsuk, Paiboon Sreearunothai and Pakorn Opaprakasit* Thammasat University
BMED-P6	**Green Synthesis of Multifunctional Gold Nanoparticles using DOTA-Bombesin Conjugated Water-soluble Chitosan and Radiolysis Method** ***Theeranan Tangthong*** *and Wanvimol Pasanphan* Kasetsart University
BMED-P7	**Porous hydrogel wound dressing incorporated with natural products (honey and sericin) for enhanced healing** ***Thanyaporn Pinthong***, *Sukunya Ross, Sararat Mahasaranon and Gareth M Ross1* Naresuan University

BMED-P1

Multi-responsive nanocomposites and their controlled release application

Nunthiya Deepuppha, Sudarat Khadsai and Metha Rutnakornpituk *
Department of Chemistry and the Center of Excellence in Biomaterials, Faculty of Science, Naresuan University, Phitsanulok, 65000 Thailand. Phone 66-5596-3464, Fax 66-5596-3401,
E-mail: methar@nu.ac.th

Abstract

Thermo- and pH-responsive nanocomposite based on poly(*N*-acryloylglycine) (PNAG) and magnetite nanoparticles (MNP) was synthesized *via* a free radical polymerization and then crosslinked. The effect of cross-linking agents, e.g. ethylenediamine and *tris*(2-aminoethyl)amine, on the size, magnetic separation ability and water dispersibility of the nanocomposite was investigated. The nanocomposite was characterized *via* transmission electron microscopy (TEM) to investigate their particle size and size distribution. It was found that the nanocomposite crosslinked with *tris*(2-aminoethyl)amine have the size of 200-300 nm in diameter and can be rapidly separated by a magnet while maintaining a good dispersibility in water. The preliminary study in responsive release of the entrapped theophylline as a model drug from the nanocomposite was determined. This novel nanocomposite might be efficiently used as a magnetically guidable nano-vehicle for thermo- and pH-triggered drug controlled release applications.

Keywords: Nanocomposite poly*(N*-acryloylglycine) magnetite nanoparticle thermo- and pH-responsive polymer

2.9) Magnetic nanoparticle coated with multi-responsive copolymer containing thiolactone acrylamide, Sujittra Paenkaew and Metha Rutnakornpituk, Pure and Applied Chemistry International Conference (PACCON2017), 2-3 February 2017, Bangkok, Thailand

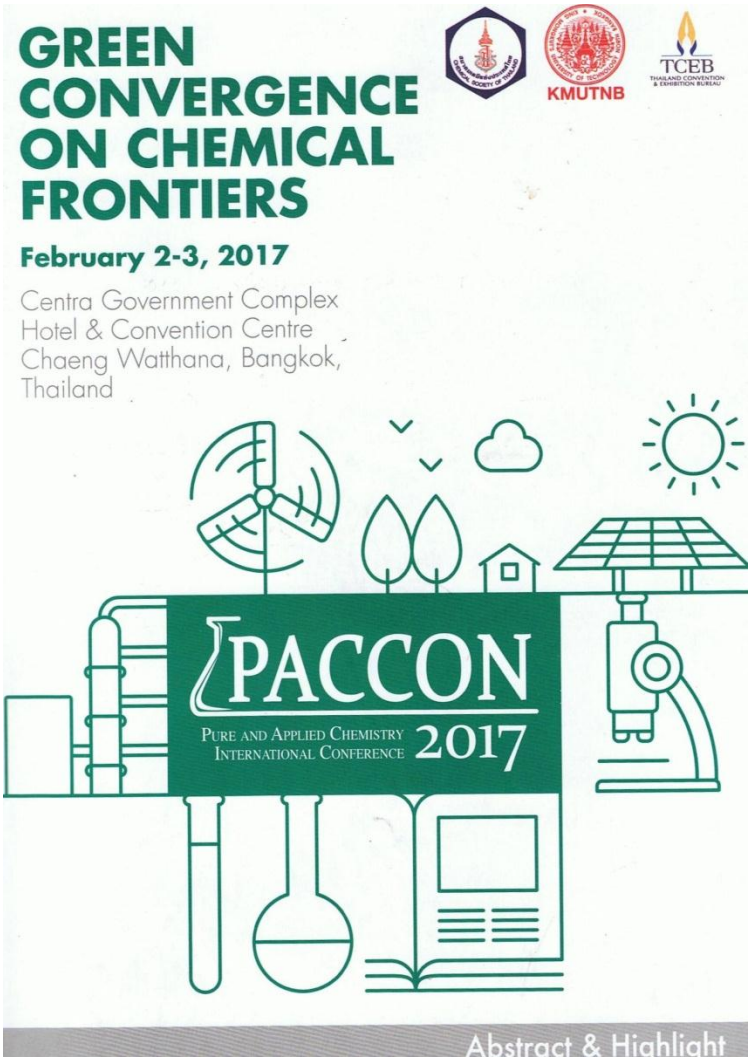

PO -P- 051	**Magnetic nanoparticle coated with multi-responsive copolymer containing thiolactone acrylamide**	

Sujittra Paenkaew and Metha Rutnakornpituk *

Department of Chemistry and Center of Excellence in Biomaterials, Faculty of Science, Naresuan University, Thailand

*e-mail: methar@nu.ac.th

- PDEAEMA-*b*-P(NIPAAm-*st*-TlaAm) copolymer that was synthesized *via* RAFT polymerization was ring-opened with alkyl amines to form thiol groups (-SH), followed by the thiol-ene coupling reactions with acrylamide-grafted MNP.
- FT-IR, TEM, and PCS were performed to confirm the copolymer-grafted MNP having surface.
- The effect of degree of hydrophobicity from various chain lengths of alkyl groups on the aggregation, water dispersibility and morphology of the copolymer-coated MNP.

Keywords: Block copolymer; Nanoparticle; Thermosensitive

2.10) PNA-conjugated magnetic nanocluster for real DNA pre-concentration, Metha Rutnakornpituk, Sudarat Khadsai, Boonjira Rutnakornpituk, Maliwan Nakkuntod, Tirayut Vilaivan, The 11th International Polymer Conference (IPC2016), 13-16 December 2016, Fukuoka, Japan

The 11th SPSJ International Polymer Conference (IPC2016)
"The cutting edge in polymer science & technology and the next milestone"
Fukuoka, JAPAN December 13-16, 2016

August 12, 2016

Doctor Metha Rutnakornpituk
Department of Chemistry and
Center of Excellence in Biomaterials
Faculty of Science
Naresuan University

The 11th SPSJ International Polymer Conference (IPC 2016)
"The cutting edge in polymer science & technology and the next milestone"
December 13-16, 2016; Fukuoka, Japan

Dear Doctor Metha Rutnakornpituk:

Thank you very much for your interest in attending IPC2016. This is to acknowledge receipt of your application to IPC2016

Registration No.:1320
Presentation style: Oral presentation
Session: S-4 Frontiers in Biomedical Polymers and Nanomedicines
Paper title: PNA-conjugated magnetic nanocluster for real DNA pre-concentration

It is also our pleasure to inform you of details of your presentation at a later date. Please note that a tight budget does not allow us to support you financially. We look forward to meeting you and your presentation in IPC 2016.

Sincerely yours,

Kazuo SAKURAI
Chair, Program Committee, IPC 2016
Professor, Department of Chemistry and Biochemistry,
Faculty of Environmental Engineering
The University of Kitakyushu

IPC2016 Secretariat
The Society of Polymer Science, Japan
Shintomicho Bldg. 3-10-9 Irifune, Chuo-ku, Tokyo 104-0042 JAPAN
E-mail: ipc2016@spsj.or.jp Fax: +81-3-5540-3737

PNA-conjugated magnetic nanocluster for real DNA pre-concentration

[1]Metha Rutnakornpituk*, [1]Sudarat Khadsai, [1]Boonjira Rutnakornpituk, [2]Maliwan Nakkuntod, [3]Tirayut Vilaivan

[1]Department of Chemistry and Center of Excellence in Biomaterials, Faculty of Science, Naresuan University, Phitsanulok 65000, Thailand

[2]Department of Biology, Faculty of Science, Naresuan University, Phitsanulok 65000 Thailand

[3]Organic Synthesis Research Unit, Department of Chemistry; Faculty of Science; Chulalongkorn University, Patumwan, Bangkok 10330, Thailand

Phone: +66 55 3464 Fax: +66 55 3401 *E-mail: methar@nu.ac.th

Introduction

Magnetite nanoparticle (MNP) has presently been of scientific and technological interest because of its magnetically guidable and nanoscale-related properties. In this work, anionic poly(*N*-acryloyl glycine) (PNAG)-grafted magnetite nanocluster (MNC) was used as a support for pre-concentration of real DNA using pyrrolidinyl peptide nucleic acid (PNA) as a probe. PNAG-grafted MNC was covalently conjugated with streptavidin, followed by functionalization with biotin-conjugated PNA *via* specific biotin-streptavidin interaction.

Results and Discussion

The synthesized PNAG-grafted MNC with size of 200-400 nm were well dispersible in water, had a good response to a magnet and had the capacity of 373 pmol PNA/mg MNP. The PNA probe on the particles can differentiate between complementary and non-complementary DNA using fluorophore-tagged DNA as a model. The particles were also used for pre-concentration of zein gene in maize as a real DNA sample. After desorption of the DNA adsorbed on the particles and then amplification with Polymerase Chain Reaction (PCR) technique, UV-visible spectrophotometry and gel electrophoresis indicated the existence of the zein gene on the particles.

Taking advantages of the high stability and high specificity between pyrrolidinyl PNA and DNA, this anionic MNP might be greatly advantageous for use as magnetic nano-supports for various future technologies, such as diagnostics of genetic diseases and pre-concentration of real DNA samples.

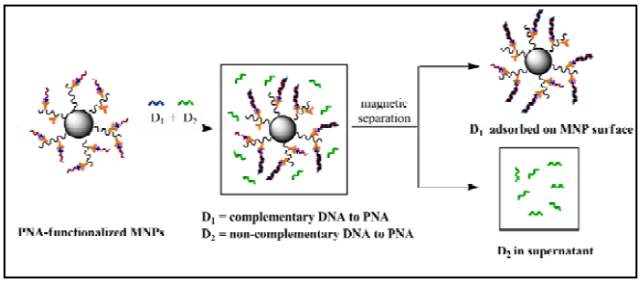

Figure 1. Pre-concentration of DNA using PNAG-grafted MNP functionalized with PNA probe

References Stubinitzky,C. Vilaivan,T. Wagenknecht,H.A. *Org.Biomol.Chem.* **2014**, *12*, 3586.

2.11) Poly(acrylic acid)-grafted magnetite nanocluster conjugated with pyrollidinyl peptide nucleic acid for DNA base discrimination, Noppadol Seeja, Tirayut Vilaivan, Metha Rutnakornpituk, Boonjira Rutnakornpituk, The 6th International Polymer Conference of Thailand (PCT6), June 30th-July 1st, 2016, Patumwan Princess Hotel, Bangkok, Thailand

SMART-P3

Poly(acrylic acid)-grafted magnetite nanocluster conjugated with pyrollidinyl peptide nucleic acid for DNA base discrimination

Nonpadol Seeja[1], Tirayut Vilaivan[2], Metha Rutnakornpituk[1], Boonjira Rutnakornpituk[1]*
[1]Department of Chemistry and Center of Excellence in Biomaterials, Faculty of Science, Naresuan University, Phitsanulok, 65000 Thailand
[2]Organic Synthesis Research Unit, Department of Chemistry, Faculty of Science, Chulalongkorn University, Phayathai Road, Patumwan, Bangkok 10330 Thailand, *E-mail: boonjirab@nu.ac.th

Abstract

This work focuses on the synthesis of poly(acrylic acid)(PAA)-grafted magnetite nanocluster (MNC) conjugated with pyrollidinyl peptide nucleic acid (PNA) as a probe for deoxyribose nucleic acid (DNA) base discrimination. To prepare the MNC, acrylamide-functionalized magnetite nanoparticles were co-polymerized with acrylic acid monomers in the presence of ammonium persulfate, a radical initiator, to form anionic MNC, followed by a covalent coupling with the PNA. The PNA-functionalized MNC was well dispersible in pH 7 phosphate buffer solutions. Transmission electron microscopy (TEM) indicated that the size of the MNC ranged between 200 to 300 nm in diameter. Due to the presence of ionizable carboxylic acid groups of PAA in the structure, the MNC showed responsive properties to the change of the dispersion pH. From UV-Visible spectrophotometry technique, the functionalized amounts of the PNA were 0.184 nmol/mg MNC. The PNA probe on the MNC can differentiate between fully complementary, completely mismatch and single-base mismatch DNA using fluorophore-tagged DNA as a model with the loading capacity of 0.074 nmol DNA/mg MNC. This novel anionic MNC with the PNA probe might be potentially applicable for use as a magnetically guidable tool for pre-concentration of DNA mixtures and a promising method for testing genetic modification.

Keywords: magnetite nanoparticle / peptide nucleic acid / poly(acrylic acid)

2.12) Synthesis of magnetic nanoparticle grafted with thermo-responsive polymer containing thiolactone acrylamide moiety, Sujitra Pankeaw and Metha Rutnakornpituk, The 6th International Polymer Conference of Thailand (PCT6), June 30th-July 1st, 2016, Patumwan Princess Hotel, Bangkok, Thailand

SMART-P1

Synthesis of magnetic nanoparticle grafted with thermo-responsive polymer containing thiolactone acrylamide moiety

Sujittra Paenkaew and Metha Rutnakornpituk *
Department of Chemistry and Center of Excellence in Biomaterials, Faculty of Science, Naresuan University, Phitsanulok, 65000 Thailand.
Phone: +66-5596-3464, Fax: +66-5596-3401, *E-mail: methar@nu.ac.th

Abstract
In this work, synthesis and characterization of magnetite nanoparticle (MNP) grafted with thermo-responsive functional diblock copolymer containing thiolactone acrylamide moiety are reported. The copolymer of poly(2- (diethylamino) ethyl methacrylate)-*b*-poly(*N*-isopropylacrylamide-*st*-thiolactone acrylamide) (PDEAEMA-*b*-P(NIPAAm- *st*-TlaAm)) was synthesized *via* reversible addition fragmentation chain transfer (RAFT) polymerization using a PDEAEMA macro chain transfer agent (CTA) to mediate the polymerization of statistical NIPAAm-TlaAm block. The TlaAm units were ring-opened with 1-alkylamine to form thiol groups (-SH), followed by the thiol-ene coupling reactions with acrylamide-grafted MNP. PDEAEMA block in the copolymer was subsequently quaternized with CH_3I to provide good water dispersibility to the copolymer-grafted MNP. The copolymer was characterized using proton nuclear magnetic resonance (^{1}H NMR) and Fourier transform infrared spectroscopies (FTIR). The copolymer-grafted MNP was analyzed *via* FTIR, photon correlation spectroscopy (PCS), transmission electron microscopy (TEM). This novel polymer-MNP hybrid might be efficiently used in drug controlled release application and it will be warranted for future studies.

Keywords: magnetite; nanoparticle; RAFT polymerization

2.13) Dual-responsive poly(*N*-acryloyl glycine)-containing copolymer for coating on magnetic nanoparticle**,** Nunthiya Deepuppha, Sudarat Khadsai and Metha Rutnakornpituk' The 6th International Polymer Conference of Thailand (PCT6), June 30th - July 1st, 2016, Patumwan Princess Hotel, Bangkok, Thailand

---

SMART-P2

Dual-responsive poly(N-acryloyl glycine)-containing copolymer for coating on magnetic nanoparticle

Nunthiya Deepuppha, Sudarat Khadsai and Metha Rutnakornpituk *
Department of Chemistry and Center of Excellence in Biomaterials, Faculty of Science, Naresuan University, Phitsanulok, 65000 Thailand. Phone: 66-5596-3464, Fax: 66-5596-3401.
E-mail: methar@nu.ac.th

Abstract
Thermo- and pH-responsive methoxy poly(ethylene glycol)-*b*-poly(*N*-acryloyl glycine) (mPEG-*b*-PNAG) copolymer was synthesized via reversible addition-fragmentation chain-transfer polymerization (RAFT) and was used for coating on magnetite nanoparticle (MNP). mPEG macro chain transfer agent (mPEG-CTA) was used to mediate RAFT of NAG monomers to produce mPEG-*b*-PNAG copolymer with controlled molecular weight and polydispersity index (PDI). The copolymer was used for coupling with amino functional groups grafted on MNP surface to form water dispersible thermo- and pH responsive magnetic nanocluster. The polymer-MNP hybrid was characterized via photocorrelation spectroscopy (PCS) to determine their hydrodynamic size (Dh) and transmission electron microscopy (TEM) to investigate their particle size and size distribution. This novel polymer-MNP hybrid might be applicable for use as a magnetically guidable vehicle for thermo- and pH-triggered drug controlled release applications.

Keywords: poly(*N*-acryloylglycine) RAFT magnetite nanoparticle Thermo- and pH-responsive copolymer

3) 3 National presentations

3.1) Nunthiya Deepuppha, Sudarat Khadsai, Boonjira Rutnakornpituk and Metha Rutnakornpituk, Synthesis of multi-responsive crosslinked magnetic nanocomposite (Oral presentation and Proceeding), 9th Science Research Conference, 25-26 May 2017, Burapha University, Chonburi, Thailand

3.2) Metha Rutnakornpituk and Bandit Thong-On, Controlled magnetite nanoclustering in the presence of glycidyl-functionalized thermo-responsive poly(N-isopropylacrylamide), (Poster) การประชุมใหญ่โครงการส่งเสริมการวิจัยในอุดมศึกษา ครั้งที่ 5 (The Fifth Higher Education Research Promotion Congress (HERP CONGRESS V) 2-4 มีนาคม 2560, ณ มหาวิทยาลัยราชภัฏอุดรธานี

3.3) Noppadol Seeja, Tirayut Vilaivan, Metha Rutnakornpituk, Uthai Wichai, Boonjira Rutnakornpituk, Magnetite nanoparticles grafted poly (acrylic acid) conjugated with Peptide Nucleic Acid (PNA) for biomedical applications (Oral presentation and Proceeding) The 8th National Science Research Conference (การประชุมวิชาการระดับชาติ วิทยาศาสตร์วิจัย ครั้งที่ 8) 30-31 May 2016, มหาวิทยาลัยพะเยา

3.1) Nunthiya Deepuppha, Sudarat Khadsai, Boonjira Rutnakornpituk and Metha Rutnakornpituk, Synthesis of multi-responsive crosslinked magnetic nanocomposite (Oral presentation and Proceeding), 9th Science Research Conference, 25-26 May 2017, Burapha University, Chonburi, Thailand

การประชุมวิชาการระดับชาติ "วิทยาศาสตร์วิจัย" ครั้งที่ 9

CH-O-025

การสังเคราะห์นาโนคอมโพสิตแม่เหล็กที่ตอบสนองต่อสิ่งกระตุ้นหลากหลายที่มีการเชื่อมโยงระหว่างโมเลกุล

Synthesis of multi-responsive crosslinked magnetic nanocomposite

นันทิยา ดีบุบผา, สุดารัตน์ ขัดสาย, บุญจิรา รัตนากรพิทักษ์, และ เมธา รัตนากรพิทักษ์*

Nunthiya Deepuppha, Sudarat Khadsai, Boonjira Rutnakornpituk and Metha Rutnakornpituk*

ภาควิชาเคมี และสถานวิจัยเพื่อความเป็นเลิศทางวิชาการด้านวัสดุชีวภาพ คณะวิทยาศาสตร์ มหาวิทยาลัยนเรศวร อ.เมือง จ.พิษณุโลก 65000 โทรศัพท์ +66 5596 3464

บทคัดย่อ

งานวิจัยนี้ศึกษาการสังเคราะห์อนุภาคนาโนคอมโพสิตของอนุภาคนาโนแมกนีไทต์และพอลิเอ็นอะคริโลอิลไกลซีนด้วยปฏิกิริยาการพอลิเมอไรเซชันแบบอนุมูลอิสระและการเชื่อมโยงระหว่างโมเลกุล และศึกษาผลของการใช้ตัวเชื่อมโยงระหว่างโมเลกุลต่อการเกิดนาโนคอมโพสิตของอนุภาค จากผลการทดลองพบว่าอนุภาคนาโนคอมโพสิตมีขนาดไฮโดรไดนามิก (D_h) อยู่ในช่วง 300-600 นาโนเมตร เมื่อทำการพิสูจน์เอกลักษณ์ด้วยเทคนิคกล้องจุลทรรศน์อิเล็กตรอนแบบส่งผ่าน (transmission electron microscopy, TEM) พบว่าอนุภาคนาโนคอมโพสิตมีการกระจายตัวที่ดีและมีขนาดอยู่ในช่วง 200-300 นาโนเมตร ซึ่งอนุภาคนาโนคอมโพสิตที่ได้จากงานวิจัยนี้อาจนำไปประยุกต์ใช้เป็นวัสดุในการควบคุมการปลดปล่อยยาที่สามารถตอบสนองต่อการเปลี่ยนแปลงอุณหภูมิและสภาวะกรดเบสได้

คำสำคัญ : พอลิเอ็นอะคริโลอิลไกลซีน/ นาโนคอมโพสิต/ อนุภาคนาโนแมกนีไทต์

Abstract

Nanocomposite based on poly(*N*-acryloylglycine) (PNAG) and magnetite nanoparticles (MNP) was synthesized via a free radical polymerization and crosslinking. The effect of crosslinkers on the formation of nanocomposite was investigated. It was found that the hydrodynamic diameters (D_h) of the nanocomposite ranged from 300 nm to 600 nm. Transmission electron microscopy (TEM) indicated that the nanocomposite as well dispersible in water with the diameter of 200-300 nm. This novel nanocomposite might be applicable for use as a magnetically guidable vehicle for thermo- and pH-triggered drug controlled release applications.

Keywords : poly(*N*-acryloylglycine)/ nanocomposite/ magnetite nanoparticle

*Corresponding author. E-mail : methar@nu.ac.th

รายงานสืบเนื่องจากการประชุมวิชาการ "วิทยาศาสตร์วิจัย" ครั้งที่ 9

การสังเคราะห์นาโนคอมโพสิตแม่เหล็กที่ตอบสนองต่อสิ่งกระตุ้นหลากหลายที่มีการเชื่อมโยงระหว่างโมเลกุล

Synthesis of multi-responsive crosslinked magnetic nanocomposite

นันทิยา ดีบุบผา, สุดารัตน์ ขัดสาย, บุญจิรา รัตนากรพิทักษ์ และ เมธา รัตนากรพิทักษ์*

Nunthiya Deepuppha, Sudarat Khadsai, Boonjira Rutnakompituk and Metha Rutnakompituk*

ภาควิชาเคมี และสถาบันวิจัยเพื่อความเป็นเลิศทางวิชาการด้านวัสดุชีวภาพ คณะวิทยาศาสตร์ มหาวิทยาลัยนเรศวร อ.เมือง จ.พิษณุโลก 65000 โทรศัพท์ +66 5596 3464

บทคัดย่อ

งานวิจัยนี้ศึกษาการสังเคราะห์อนุภาคนาโนคอมโพสิตของอนุภาคนาโนแมกนีไทต์และพอลิเอ็นอะคริโลอิลไกลซีนด้วยปฏิกิริยาการพอลิเมอไรเซชันแบบอนุมูลอิสระและการเชื่อมโยงระหว่างโมเลกุล และศึกษาผลของการใช้ตัวเชื่อมโยงระหว่างโมเลกุลต่อการเกิดนาโนคอมโพสิตของอนุภาค จากผลการทดลองพบว่าอนุภาคนาโนคอมโพสิตมีขนาดไฮโดรไดนามิก (D_h) อยู่ในช่วง 300-600 นาโนเมตร เมื่อทำการพิสูจน์เอกลักษณ์ด้วยเทคนิคกล้องจุลทรรศน์อิเล็กตรอนแบบส่งผ่าน (transmission electron microscopy, TEM) พบว่าอนุภาคนาโนคอมโพสิตมีการกระจายตัวที่ดีและมีขนาดอยู่ในช่วง 200-300 นาโนเมตร ซึ่งอนุภาคนาโนคอมโพสิตที่ได้จากงานวิจัยนี้อาจนำไปประยุกต์ใช้เป็นวัสดุในการควบคุมการปลดปล่อยยาที่สามารถตอบสนองต่อการเปลี่ยนแปลงอุณหภูมิและสภาวะกรดเบสได้

คำสำคัญ : พอลิเอ็นอะคริโลอิลไกลซีน/ นาโนคอมโพสิต/ อนุภาคนาโนแมกนีไทต์

Abstract

Nanocomposite based on poly(*N*-acryloylglycine) (PNAG) and magnetite nanoparticles (MNP) was synthesized via a free radical polymerization and crosslinking. The effect of crosslinkers on the formation of nanocomposite was investigated. It was found that the hydrodynamic diameters (D_h) of the nanocomposite ranged from 300 nm to 600 nm. Transmission electron microscopy (TEM) indicated that the nanocomposite as well dispersible in water with the diameter of 200-300 nm. This novel nanocomposite might be applicable for use as a magnetically guidable vehicle for thermo- and pH-triggered drug controlled release applications.

Keywords : poly(*N*-acryloylglycine)/ nanocomposite/ magnetite nanoparticle

*Corresponding author. E-mail : methar@nu.ac.th

1. บทนำ

ปัจจุบันวัสดุนาโนคอมโพสิตได้รับความสนใจอย่างกว้างขวางทั้งทางด้านวิทยาศาสตร์และเทคโนโลยี เนื่องจากวัสดุดังกล่าวมีประสิทธิภาพสูงกว่าวัสดุแบบดั้งเดิมและสามารถประยุกต์ใช้งานในหลายด้าน ทั้งทางด้านชีวภาพและอุตสาหกรรม (Li, S.-2010) เช่น การใช้เป็นวัสดุควบคุมการปลดปล่อยยา (Davaran, S.- 2014) วัสดุทางทันตกรรม (Khurshid, Z.-2015) และวัสดุทางวิศวกรรมเนื้อเยื่อ (Sultana, N.-2015) โดยเฉพาะอย่างยิ่งการประยุกต์ใช้ในระบบขนส่งยาหรือการควบคุมการปลดปล่อยยานั้นได้รับความสนใจอย่างมากในด้านการแพทย์และเภสัชกรรม ซึ่งวัสดุดังกล่าวจำเป็นต้องมีกลไกในการควบคุมการปลดปล่อยและไม่เป็นพิษต่อร่างกาย วัสดุผสมของพอลิเมอร์และอนุภาคนาโนเป็นหนึ่งทางเลือกที่น่าสนใจในการเตรียมระบบขนส่งยา ซึ่งมีหลายงานวิจัยที่มุ่งเน้นที่อนุภาคนาโนแมกนีไทต์ (magnetite nanoparticle, MNP) เนื่องจากอนุภาคดังกล่าวมีความเป็นพิษต่ำ (toxicity) และมีความเข้ากันได้กับเนื้อเยื่อในร่างกาย (biocompatibility) สามารถตอบสนองต่อสนามแม่เหล็กภายนอกได้ (Petcharoen, K.-2012) การเคลือบพอลิเมอร์บนพื้นผิวอนุภาคนาโนแมกนีไทต์สามารถช่วยลดความเป็นพิษที่อาจเกิดจากอนุภาค (Davaran, S.-2014) และยังช่วยให้อนุภาคมีการกระจายตัวในน้ำที่ดีขึ้น ทั้งนี้การใช้พอลิเมอร์ที่สามารถตอบสนองต่อสิ่งเร้าภายนอก ยังสามารถใช้เป็นกลไกในการควบคุมการปลดปล่อยยาผ่านพฤติกรรมการตอบสนองดังกล่าวได้ โดยในงานวิจัยนี้สนใจศึกษาการใช้พอลิเอ็นอะคริโรอิลไกลซีน (poly(*N*-acryloylglycine), PNAG) เพื่อเคลือบบนอนุภาคนาโนแมกนีไทต์ เนื่องจาก PNAG เป็นพอลิเมอร์ที่สามารถตอบสนองต่อการเปลี่ยนแปลงอุณหภูมิและสภาวะกรดเบส ทั้งนี้ยังสามารถละลายได้ดีในน้ำ (Kuilin, D.-2011)

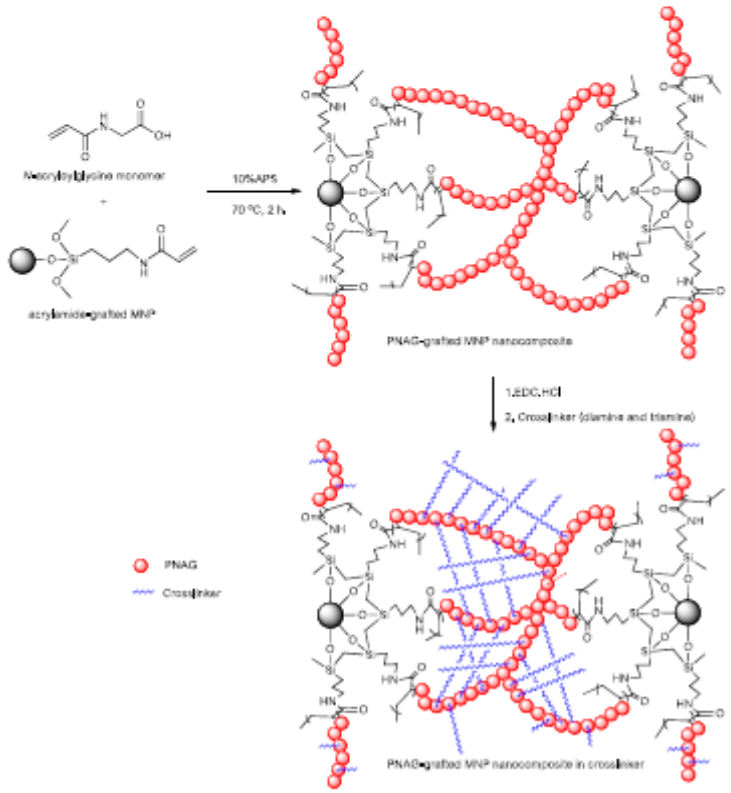

รูปที่ 1 การสังเคราะห์นาโนคอมโพสิตของพอลิเอ็นอะคริโลอิลไกลซีนและอนุภาคแมกนีไทต์และการเกิดนาโนคอมโพสิต

ดังนั้นงานวิจัยนี้จึงสนใจที่จะศึกษาการสังเคราะห์นาโนคอมโพสิตซึ่งประกอบด้วยอนุภาคนาโนแมกนีไทต์และพอลิเอ็นอะคริโลอิลไกลซีน (PNAG-grafted MNP nanocomposite) และเกิดปฏิกิริยาการเชื่อมโยงระหว่างโมเลกุล (รูปที่ 1) โดยศึกษาผลของชนิดและความเข้มข้นของตัวเชื่อมโยงระหว่างโมเลกุล ต่อการเกิดนาโนคอมโพสิตของอนุภาค พร้อมทั้งศึกษาขนาดและการกระจายตัวในน้ำของอนุภาคดังกล่าว ซึ่งอนุภาคนาโนคอมโพสิตที่ได้จากงานวิจัยนี้อาจนำไปประยุกต์ใช้เป็นวัสดุในการควบคุมการปลดปล่อยยาที่สามารถตอบสนองต่อการเปลี่ยนแปลงอุณหภูมิและสภาวะกรดเบสได้

2. วิธีการทดลอง

การสังเคราะห์นาโนคอมโพสิตของอนุภาคนาโนแมกนีไทต์และพอลิเอ็นอะคริโลอิลไกลซีน แบ่งออกเป็น 2 ขั้นตอนดังนี้

2.1 การสังเคราะห์อนุภาคนาโนแมกนีไทต์และปฏิกิริยาการตรึงหมู่อะคริลาไมด์บนพื้นผิวอนุภาคนาโนแมกนีไทต์ (acylamide-grafted MNP)

อนุภาคนาโนแมกนีไทต์สังเคราะห์ด้วยวิธีการตกตะกอนร่วม (co-precipitation) ซึ่งเป็นการทำปฏิกิริยาระหว่างเฟอร์รัสคลอไรด์เตตระไฮเดรต ($FeCl_2.4H_2O$) และเฟอร์ริกคลอไรด์ ($FeCl_3$) ภายใต้สภาวะสารละลายเบสแอมโมเนียมไฮดรอกไซด์ คนเป็นเวลา 30 นาที ที่อุณหภูมิห้อง แล้วแยกอนุภาคที่มีคุณสมบัติในการตอบสนองต่อแม่เหล็กได้ออกโดยใช้แม่เหล็กภายนอก จากนั้นเคลือบอนุภาคด้วยโอเลอิกแอซิด (oleic acid) เพื่อป้องกันการเกาะกลุ่มของอนุภาค (aggregation) ตรึงหมู่อะมิโนลงบนพื้นผิวอนุภาคโดยใช้ 3-aminopropyl trimethoxysilane (APTES) ในสภาวะสารละลายเบสของไตรเอทิลามีน (triethylamine, TEA) เป็นเวลา 24 ชั่วโมง ภายใต้สภาวะแก๊สไนโตรเจน จากนั้นแยกอนุภาคที่พื้นผิวตรึงด้วยหมู่อะมิโนออกด้วยแม่เหล็กภายนอก แล้วล้างอนุภาคด้วยเอทานอลเพื่อกำจัด APTES ที่ไม่เกิดปฏิกิริยาออก

จากนั้นทำปฏิกิริยาการตรึงหมู่อะคริลาไมด์บนพื้นผิวอนุภาคนาโนแมกนีไทต์ด้วยอะคริโรอิลคลอไรด์ โดยการทำปฏิกิริยากับอนุภาคที่พื้นผิวตรึงด้วยหมู่อะมิโนภายใต้สภาวะสารละลายเบสของโซเดียมไฮดรอกไซด์เป็นเวลา 24 ชั่วโมง ที่อุณหภูมิห้อง หลังสิ้นสุดการเกิดปฏิกิริยาแยกอนุภาคที่พื้นผิวตรึงด้วยหมู่อะคริลาไมด์ออกด้วยแม่เหล็กภายนอก แล้วล้างอนุภาคด้วยน้ำเพื่อกำจัดอะคริโรอิลคลอไรด์ที่ไม่เกิดปฏิกิริยา

2.2 การสังเคราะห์นาโนคอมโพสิตของอนุภาคนาโนแมกนีไทต์และพอลิเอ็นอะคริโลอิลไกลซีน

ทำการสังเคราะห์นาโนคอมโพสิต โดยปฏิกิริยาพอลิเมอไรเซชันของอนุภาคที่พื้นผิวตรึงด้วยหมู่อะคริลาไมด์และเอ็นอะคริโรอิลไกลซีนมอนอเมอร์ โดยอาศัยแอมโมเนียมเปอร์ซัลเฟตทำหน้าที่เป็นตัวเริ่มต้นปฏิกิริยา ทำปฏิกิริยาที่อุณหภูมิ 70 องศาเซลเซียส เป็นเวลา 2 ชั่วโมง เมื่อปฏิกิริยาเกิดสมบูรณ์ทำการแยกอนุภาคออกด้วยแม่เหล็กภายนอก แล้วล้างอนุภาคด้วยน้ำเพื่อกำจัดมอนอเมอร์ที่ไม่เกิดปฏิกิริยาและสายโซ่ของพอลิเมอร์ที่ไม่ถูกตรึงบนอนุภาค

หลังจากนั้นนำนาโนคอมโพสิตที่ได้มาทำการสังเคราะห์ต่อเป็นนาโนคอมโพสิต โดยเกิดปฏิกิริยาคู่ควบ (coupling reaction) ของหมู่คาร์บอกซิลิกของพอลิเอ็นอะคริโลอิลไกลซีนโดยใช้ *N*-(3-dimethylaminopropyl)-*N'*-ethylcarbodiimide hydrochloride (EDC.HCl) ทำหน้าที่เป็นตัวคู่ควบ (coupling agent) ทำปฏิกิริยาที่อุณหภูมิห้องเป็นเวลา 1 ชั่วโมง จากนั้นทำการเชื่อมโยงระหว่างโมเลกุล (crosslinking) ต่อภายใต้สภาวะเบสโดยใช้ ethylenediamine (diamine) และ *tris*-(2-aminoethyl)amine (triamine) ทำหน้าที่เป็นตัวเชื่อมโยงระหว่างโมเลกุล (crosslinker) ทำ

ปฏิกิริยาที่อุณหภูมิห้องเป็นเวลา 1 ชั่วโมง เมื่อปฏิกิริยาเกิดสมบูรณ์ทำแยกอนุภาคนาโนคอมโพสิตออกด้วยแม่เหล็กภายนอก แล้วทำการล้างอนุภาคด้วยน้ำเพื่อกำจัดตัวเชื่อมโยงที่ไม่เกิดปฏิกิริยา

3. ผลการทดลองและอภิปรายผลการทดลอง

3.1 การวิเคราะห์และพิสูจน์เอกลักษณ์นาโนคอมโพสิตของอนุภาคนาโนแมกนีไทต์และพอลิเอ็นอะคริโลอิลไกลซีน

จากการวิเคราะห์และพิสูจน์เอกลักษณ์นาโนคอมโพสิตด้วยเทคนิคเทคนิคอินฟราเรดสเปคโตรสโคปี (fourier transform infrared spectrometer, FTIR) พบสัญญาณการสั่นของ Fe-O stretching (555 cm^{-1}) ซึ่งสอดคล้องกับสัญญาณของอนุภาคที่พื้นผิวตริงด้วยหมู่อะคริลาไมด์และสัญญาณการสั่นของ N-H stretching (3301 cm^{-1}) C-N stretching (2439 cm^{-1} C=O stretching (1722 cm^{-1}) NHC=O stretching (1550 และ 1633 cm^{-1}) และ C-O stretching (1221 cm^{-1}) ซึ่งสอดคล้องกับสัญญาณของพอลิเอ็นอะคริโอิลไกลซีน ดังแสดงในรูปที่ 2

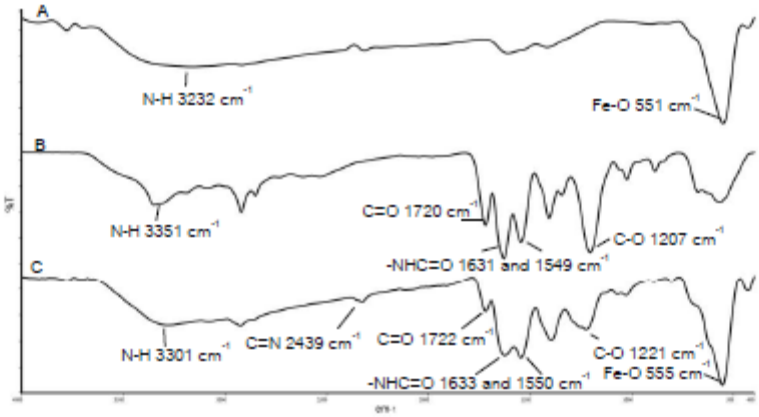

รูปที่ 2 สเปกตรัม FTIR ของอนุภาคที่พื้นผิวตริงด้วยหมู่อะคริลาไมด์ (A), พอลิเอ็นอะคริโอิลไกลซีน (B) และนาโนคอมโพสิต (C)

3.2 การศึกษาผลการใช้ตัวเชื่อมโยงระหว่างโมเลกุลต่อการเกิดนาโนคอมโพสิตและการกระจายตัวของอนุภาคนาโนแมกนีไทต์

ในงานวิจัยนี้ได้ทำการศึกษาผลของการเชื่อมโยงระหว่างโมเลกุลสองชนิดได้แก่ ethylenediamine (diamine) และ *tris*-(2-aminoethyl)amine (triamine) ต่อการเกิดนาโนคอมโพสิตและการกระจายตัวของอนุภาค โดยควบคุมความเข้มข้นของตัวเชื่อมโยงแต่ละชนิดที่ใช้เป็น 1% โดยโมลและ 10% โดยโมล รูปที่ 3 แสดงขนาดไฮโดรไดนามิก (D_h) โดยการวิเคราะห์ด้วยเทคนิควัดการกระเพื่อมของความเข้มแสง (photo correlation spectroscopy, PCS) ของอนุภาคนาโนแมกนีไทต์ (ก่อนการเคลือบด้วย PNAG) นาโนคอมโพสิต (หลังการเคลือบด้วย PNAG) และนาโนคอมโพสิต (หลังการเชื่อมโยงระหว่างโมเลกุล) จากผลการทดลองพบว่าเมื่อมีการเชื่อมโยงระหว่างโมเลกุลแล้วอนุภาคมีขนาดใหญ่ขึ้น เนื่องจากมีการเหนี่ยวนำเชื่อมโยงของหลายอนุภาครวมกลุ่มเป็นคอมโพสิตขนาดนาโนเมตร นอกจากนี้ยังพบว่าเมื่อความเข้มข้นของตัวเชื่อมโยงเพิ่มมากขึ้นจาก 1% โดยโมลเป็น 10% โดยโมล ทำให้ขนาดไฮโดรไดนามิกของอนุภาคเพิ่มขึ้น ทั้งนี้เนื่องมาจากการมีหมู่เอมีนของตัวเชื่อมโยงที่ใช้ในการทำปฏิกิริยาการเชื่อมโยงตาข่ายมากขึ้น จึงทำให้ขนาดของนาโนคอม

โพสิตเพิ่มมากขึ้น นอกจากนี้เมื่อมีการเปลี่ยนชนิดของตัวเชื่อมโยงที่ใช้จาก diamine ไปเป็น triamine ที่ความเข้มข้นเดียวกัน พบว่ามีขนาดไฮโดรไดนามิกของอนุภาคเพิ่มมากขึ้น ทั้งนี้อธิบายได้ในทำนองเดียวกัน กล่าวคือ triamine มีจำนวนของหมู่เอมีนที่ใช้ในการเกิดปฏิกิริยาการเชื่อมโยงตาข่ายมากกว่า diamine จึงส่งผลให้นาโนคอมโพสิตที่ได้มีขนาดใหญ่กว่า

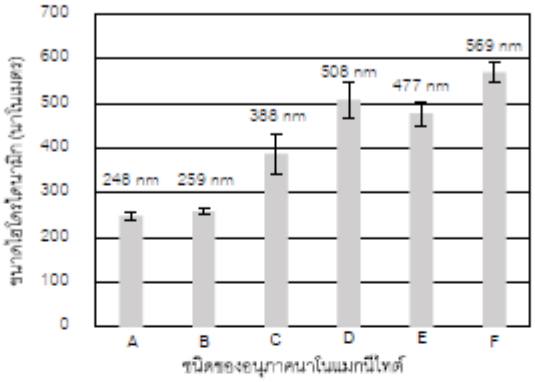

รูปที่ 3 ขนาดไฮโดรไดนามิก (D_h) ของอนุภาคที่พื้นผิวตรึงด้วยหมู่อะคริลาไมด์ (A), นาโนคอมโพสิตของอนุภาคนาโนแมกนีไทต์และพอลิเอ็นอะคริโลอิลไกลซีน (ก่อนการเชื่อมโยงตาข่าย) (B), นาโนคอมโพสิตที่เชื่อมตาข่ายด้วย 1%diamine (C), 10%diamine (D), 1%triamine (E) และ 10%triamine (F)

จากภาพถ่ายจากกล้องจุลทรรศน์อิเล็กตรอนแบบส่องผ่านพบว่าอนุภาคที่ไม่ได้เกิดปฏิกิริยาการเชื่อมโยงระหว่างโมเลกุลจะเกิดการกระจายตัวของอนุภาคไม่เป็นกลุ่มก้อน ซึ่งทำให้ยากต่อการแยกด้วยแม่เหล็กภายนอก และเมื่อวัดเส้นผ่านศูนย์กลางเฉลี่ยของอนุภาคมีขนาดเฉลี่ยเท่ากับ 110±11(A) นาโนเมตร และเมื่อทำปฏิกิริยาการเชื่อมโยงระหว่างโมเลกุลของอนุภาคเป็นนาโนคอมโพสิตจะทำให้อนุภาคดังกล่าวเกิดการเกาะกลุ่มกันเป็นก้อนซึ่งทำให้สามารถแยกด้วยแม่เหล็กภายนอกได้ ทั้งนี้ยังมีขนาดเฉลี่ยเท่ากับ 210±76(B) 235±47(C) 260±112(D) และ 290±11(E) นาโนเมตร ซึ่งใหญ่กว่าอนุภาคก่อนเกิดการเชื่อมโยงระหว่างโมเลกุล ซึ่งภาพถ่ายนี้สอดคล้องกับผลการทดลองการวัดขนาดไฮโดรไดนามิก (D_h) ของอนุภาค (เทคนิค PCS) ดังแสดงในรูปที่ 3

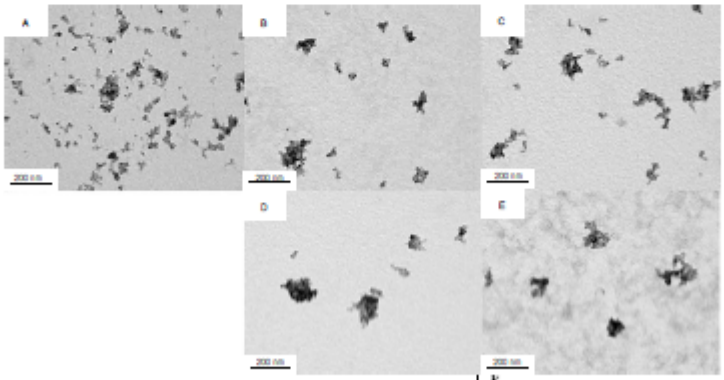

รูปที่ 4 ภาพถ่ายจากกล้องจุลทรรศน์อิเล็กตรอนแบบส่องผ่านของอนุภาคที่พื้นผิวตรึงด้วยหมู่อะคริลาไมด์ (A), นาโนคอมโพสิตที่เชื่อมตาข่ายด้วย 1%diamine (B), 10%diamine (C), 1%triamine (D) และ 10%triamine (E)

4. สรุปผลการทดลอง

นาโนคอมโพสิตของอนุภาคนาโนแมกนีไทต์และพอลิเอ็นอะคริโลอิลไกลซีนสามารถสังเคราะห์ได้จากปฏิกิริยาพอลิเมอไรเซชันและเชื่อมโยงระหว่างโมเลกุล และจากการศึกษาผลของตัวเชื่อมโยงระหว่างโมเลกุลสองชนิดคือ diamine และ triamine ต่อการเกิดนาโนคอมโพสิตของอนุภาคพบว่าเมื่อเพิ่มความเข้มข้นตัวเชื่อมโยงจะส่งผลให้อนุภาคมีขนาดเพิ่มขึ้น และการใช้ตัวเชื่อมโยงเป็น triamine จะส่งผลให้อนุภาคมีขนาดเพิ่มขึ้นเช่นเดียวกัน ซึ่งเมื่อพิจารณาขนาดไฮโดรไดนามิกของอนุภาคพบอยู่ในช่วง 300-600 นาโนเมตร และจากการศึกษาขนาดและการกระจายตัวของอนุภาคด้วยเทคนิคกล้องจุลทรรศน์อิเล็กตรอนแบบส่องผ่าน พบว่าอนุภาคนาโนคอมโพสิตมีการกระจายตัวที่ดีและมีขนาดอยู่ในช่วง 200-300 นาโนเมตร ซึ่งคาดว่าอนุภาคนาโนคอมโพสิตนี้อาจนำไปประยุกต์ใช้เป็นวัสดุในการควบคุมการปลดปล่อยยาที่สามารถตอบสนองต่อการเปลี่ยนแปลงอุณหภูมิและสภาวะกรดเบสได้ซึ่งจะต้องมีการศึกษาต่อไป

5. กิตติกรรมประกาศ

งานวิจัยนี้ได้รับการสนับสนุนจากสำนักงานกองทุนสนับสนุนงานวิจัย (สกว.) (RSA5980002) และโครงการพัฒนากำลังคนด้านวิทยาศาสตร์ทุนเรียนดีวิทยาศาสตร์แห่งประเทศไทย

6. เอกสารอ้างอิง

Davaran, S., Alimirzalu, S., Nejati-Koshki, K., Nasrabadi, H. T., Akbarzadeh, A., Khandaghi, A. A., et al. (2014). Physicochemical characteristics of Fe_3O_4 magnetic nanocomposites based on poly(N-isopropylacrylamide) for anti-cancer drug delivery. *Asian Pacific Journal of Cancer Prevention, 15 (1)*, 49-54.

Deng, K., Li, Q., Bai, L., Gou, Y., Dong, L., Huang, C., et al. (2011). A pH/Thermo-responsive injectable hydrogel system based on poly(*N*-acryloylglycine) as a drug carrier. *Iranian Polymer Journal, 20*, 185-194.

Khurshid, Z., Zafar, M., Qasim, S., Shahab, S., Naseem, M. and AbuReqaiba, A. (2015). Advances in nanotechnology for restorative dentistry. *Materials, 8*, 717-731.

Li, S., Meng Lin, M. M., Toprak, M. S., Kim, D. K. and Muhammed, M. (2010). Nanocomposites of polymer and inorganic nanoparticles for optical and magnetic applications, *Nano Reviews, 1*, 5214 - DOI: 10.3402/nano.v1i0.5214.

Petcharoen, K. and Sirivat, A. (2012). Synthesis and characterization of magnetite nanoparticles via the chemical co-precipitation method. *Materials Science and Engineering: B, 177*, 421-427.

Sultana, N., Mokhtar, M., Hassan, M. H., Jin, R. M., Roozbahani, F. and Khan, T.H. (2015) Chitosan-based nanocomposite scaffolds for tissue engineering applications. *Materials and Manufacturing Processes, 30*, 273–278.

3.2) Metha Rutnakornpituk and Bandit Thong-On, Controlled magnetite nanoclustering in the presence of glycidyl-functionalized thermo-responsive poly(N-isopropylacrylamide), (Poster) การประชุมใหญ่โครงการส่งเสริมการวิจัยในอุดมศึกษา ครั้งที่ 5 (The Fifth Higher Education Research Promotion Congress (HERP CONGRESS V) 2-4 มีนาคม 2560, ณ มหาวิทยาลัยราชภัฏอุดรธานี

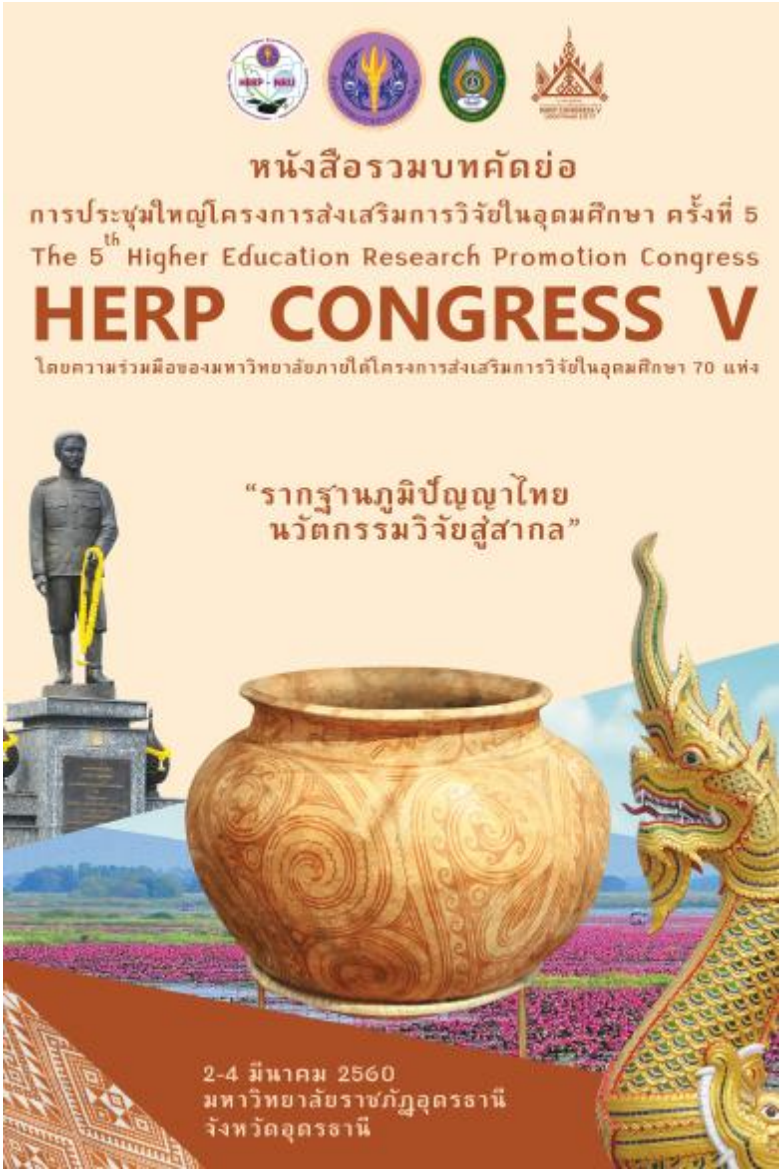

มหาวิทยาลัยนเรศวร

รหัส	หัวหน้าโครงการ	บทคัดย่อ
20U-039	ผศ.ดร.เกรียงศักดิ์ เตมีย์	การแสดงภาพ 3 มิติและการส่งผ่านด้วยกระจกสะท้อนคอนจูเกต วงแหวน แพนด้า
20U-040	อ.ดร.แกร์เร็ธ ไมเคิล รอส	ระบบไฮโดรเจลชนิดใหม่จากผลิตภัณฑ์ธรรมชาติที่สามารถช่วยในการฟื้นฟูบาดแผล
20U-041	Dr.Kyle V Lopin	Low-cost Open Source Single Chip Potentiostat for Electrochemical Experiments
20U-042	อ.ดร ณัฐนันท์ หงษ์ศรีจันทร์	การศึกษาลักษณะการเสื่อมสภาพการทำงานของทีเซลล์ในระหว่างการติดพยาธิใบไม้ตับแบบเรื้อรังและมะเร็งท่อน้ำดี
20U-043	อ.ดร.ทนงศักดิ์ โนไชยา	การพัฒนาผงฝุ่นซิลิกาควบแน่นเพื่อเป็นวัสดุประสานสำหรับการใช้งานในคอนกรีตบริเวณพื้นที่คลอไรด์สูง
20U-044	รศ.ดร.ธีระชัย บงการณ์	ผลของการเติม CuO ต่อการก่อเกิดเฟส โครงสร้างจุลภาค สมบัติทางไฟฟ้าและแม่เหล็กของเซรามิก $(Ba_{0.85}Ca_{0.15})(Ti_{0.90}Zr_{0.10})O_3$
20U-045	ผศ.ดร.ปนัดดา จันทร์เนย	การแสดงออกของโปรตีนและยีนต้านอนุมูลอิสระในข้าวที่ปลูกในดินที่มีแคดเมียม
20U-046	ผศ.ดร.ปาจรีย์ ทองสนิท	โครงการผลกระทบของการสะสมของกรดต่อแร่ธาตุโลหะหนักในดินในสภาพภูมิอากาศเปลี่ยนแปลง
20U-047	อ.ดร.พงษ์ธร จุฬพันธ์ทอง	การประยุกต์ใช้วัสดุกากอุตสาหกรรมเพื่อพัฒนาคอนกรีตป้องกันกัมมันตรังสี
20U-048	รศ.ดร.เมธา รัตนากรพิทักษ์	Controlled magnetite nanoclustering in the presence of glycidyl-functionalized thermo-responsive poly (*N*-isopropylacrylamide)

Controlled magnetite nanoclustering in the presence of glycidyl-functionalized thermo-responsive poly(*N*-isopropylacrylamide)

Metha Rutnakornpituk* and Bandit Thong-On

Department of Chemistry and Center of Excellence in Biomaterials, Faculty of Science, Naresuan University

Glycidyl-functionalized poly(*N*-isopropylacrylamide) (PNIPAAm), synthesized *via* a reversible addition-fragmentation transfer polymerization (RAFT), was used for controlling degree of nanoclustering of magnetite nanoparticle (MNP). The polymer was grafted onto MNP *via* the ring-opening reaction between glycidyl groups at the PNIPAAm chain terminal and amino groups on the MNP surface to obtain thermo-responsive MNP nanocluster. Hydrodynamic size (D_h) and colloidal stability of the nanocluster, corresponding to the degree of nanoclustering reaction, can be regulated either by adjusting the ratio of MNP to the polymer in the reaction or by introducing glycidyl groups to the polymers. The size of the nanocluster ranged between 20 and 150 nm in diameter with about 10-120 particles/cluster. Thermogravimetric analysis (TGA) and vibrating sample magnetometry (VSM) were used to confirm the presence of the polymer in the nanocluster. A study showing indomethacin controlled release of these MNP nanoclusters was also performed. This stable nanocluster with magnetically guidable properties might be potentially used for entrapment of other bio-entities or therapeutic drugs with temperature-responsive properties for controlled release applications.

Keywords magnetite, nanoparticle, nanocluster, poly(*N*-isopropylacrylamide), thermo-responsive

3.3) Noppadol Seeja, Tirayut Vilaivan, Metha Rutnakornpituk, Uthai Wichai, Boonjira Rutnakornpituk, Magnetite nanoparticles grafted poly (acrylic acid) conjugated with Peptide Nucleic Acid (PNA) for biomedical applications (Oral presentation and Proceeding) The 8th National Science Research Conference (การประชุมวิชาการระดับชาติ วิทยาศาสตร์วิจัย ครั้งที่ 8) 30-31 May 2016, มหาวิทยาลัยพะเยา

วันจันทร์ที่ 30 พฤษภาคม 2559

Parallel Sessions 2 ห้องที่ 2 หัวข้อกลุ่ม เคมีวัสดุศาสตร์

เวลา 14.00 น.–15.20 น. ห้อง PKY7 อาคารเรียนรวม มหาวิทยาลัยพะเยา

ลำดับ	เวลา	รหัส	หัวข้อเรื่อง	ชื่อ-สกุล
1	14.00–14.20	CH–O–05	การวางระบบก๊าซชีวภาพให้มีประสิทธิ์ของชุดต้นแบบขนาดเล็ก	ผศ.ดร.วิชิตร อุดอ้าย
2	14.20–14.40	CH–O–06	อนุภาคนาโนแมกนีไทท์ที่มีการติดหมู่พอลิอะไคลิคแอซิดบนพื้นผิวสำหรับการดึงเพปไทด์นิวคลีอิกแอซิดเพื่อประยุกต์ใช้ในทางการแพทย์	นายนภดล สีจัะ
3	14.40–15.00	CH–O–07	ผลของโครงสร้างต่อพฤติกรรมการเข้าจับกันด้วยตัวเองและการเปลี่ยนสี ของพอลิไดอะเซตทิลีน	น.ส.ชนิดา ชนันทอง
4	15.00–15.20	CH–O–08	การศึกษาเคมีพื้นผิวด้วยการวัดค่ามุมสัมผัสด้วยเครื่องวัดมุมสัมผัสอย่างง่ายและราคาถูก	นายจารุเดช รักพงษ์

การประชุมวิชาการระดับชาติ "วิทยาศาสตร์วิจัย" ครั้งที่ 8

CH-O-06

อนุภาคนาโนแมกนีไทท์ที่มีการติดหมู่พอลิอะไครลิก แอซิด บนพื้นผิวสำหรับการตรึงเพปไทด์นิวคลีอิก แอซิดเพื่อประยุกต์ใช้ในทางการแพทย์

Magnetite nanoparticles grafted poly (acrylic acid) conjugated with Peptide Nucleic Acid (PNA) for biomedical applications

นาตล สีจ๊ะ[1], ธีรยุทธ วิไลวัลย์[2], เมธา รัตนากรพิทักษ์[1], อุทัย วิชัย[1], บุญจิรา รัตนากรพิทักษ์[1]*

Nopadol Seeja[1], Tirayut Villaivan[2], Metha Rutnakornpituk[1], Uthai Wichai[1], Boonjira Rutnakornpituk[1]*

[1] *ภาควิชาเคมี และศูนย์ความเป็นเลิศทางด้านวัสดุชีวภาพ คณะวิทยาศาสตร์ มหาวิทยาลัยนเรศวร, พิษณุโลก 65000*

[2] *ภาควิชาเคมี คณะวิทยาศาสตร์ จุฬาลงกรณ์มหาวิทยาลัย, ถนนพญาไท, ปทุมวัน, กรุงเทพ 10330*

บทคัดย่อ

งานวิจัยนี้เป็นการศึกษาการดัดแปร พื้นผิวอนุภาคนาโนแมกนีไทท์ให้มีประจุลบด้วยพอลิอะไครลิก แอซิด (Poly(N-acrylic acid) ด้วยวิธีการสังเคราะห์พอลิเมอร์โดยผ่านอนุมูลอิสระ เพื่อนำมาใช้มาตรึงกับพีเอ็นเอใหม่ชนิดพิร์โรลิดินิลพีเอ็นเอเพื่อประยุกต์ใช้ในทางการแพทย์ต่อไปในอนาคต ทั้งนี้เนื่องจากพิร์โรลิดินิลพีเอ็นเอสามารถเกิดสารประกอบเชิงซ้อนที่มีความเสถียรมากกับดีเอ็นเอและแสดงสมบัติการจับยึดกับดีเอ็นเออย่างจำเพาะเจาะจงสูง โดยการจดจำคู่เบสแบบเดียวกับวัตสัน-ครีก เช่นเดียวกับดีเอ็นเอธรรมชาติ จากนั้นทำการศึกษาหมู่ฟังก์ชั่นของพอลิอะไครลิก แอซิด ด้วยเทคนิคฟูรูเรียทรานส์ฟอร์ม อินฟาเรดสเปกโตรเมตรี จากการศึกษาการตรึงเบต้า-พิร์โรลิดินิลพีเอ็นเอลงบนอนุภาคด้วยเทคนิค ยูวี-วิสิเบิล สเปกโตรโฟโตเมตรี พบว่าปริมาณของเบต้า-พิร์โรลิดินิลพีเอ็นเอที่ถูกตรึงบนอนุภาคคิดเป็น 0.173 ไมโครโมลต่อมิลลิกรัมของอนุภาคนาโนแมกนีไทต์ และคาดว่าอนุภาคที่ถูกตรึงด้วยเบต้า-พิร์โรลิดินิลพีเอ็นเอนี้สามารถนำมาประยุกต์ใช้ในทางการแพทย์ได้อย่างมีประสิทธิภาพต่อไป

คำสำคัญ : อนุภาคนาโนแมกนีไทท์, พิร์โรลิดินิลเปปไทด์นิวคลีอิกแอซิด, พอลิอะไครลิก แอซิด

Abstract

In this work, the surface modification of magnetite nanoparticles (MNPs) with the polyacrylic acid was prepared via a radical polymerization to form anionic magnetic nanoclusters. They were then conjugated with the pyrolidinyl PNA for further using in the biomedical applications. The pyrolidinyl PNA system showed a strong binding affinity and high sequence specificity with DNA via Watson-Crick base pairing rule. The functional group of polyacrylic acid on the magnetite nanoparticle was determined by FT-IR spectrometry technique. From the studies of the amount for PNA immobilization via UV-VIS spectrophotometry technique, it was found that the amount of pyrolidinyl PNA on the magnetite nanoparticle was 0.173 μmol/mg of magnetite. This biocompatible hybrid magnetite nanoparticle with pyrolidinyl PNA might further use in the biomedical applications.

Keywords: magnetite nanoparticle, peptide nucleic acid, poly(acrylic acid)

***Corresponding author. E-mail:** boonjirab@nu.ac.th


Proceedings
การประชุมวิชาการระดับชาติ
"วิทยาศาสตร์วิจัย"
ครั้งที่ 8
Science and Technology to Innovation
SCIENCE
RESEARCH
CONFERENCE
8th
30-31 พฤษภาคม 2559
คณะวิทยาศาสตร์ มหาวิทยาลัยพะเยา
ISBN : 978-616-7820-37-8

Proceedings The 8th Science Research Conference. 30-31 May 2016. University of Phayao.

อนุภาคนาโนแมกนีไทท์ที่มีการติดหมู่พอลิอะไครลิก แอซิดบนพื้นผิวสำหรับการตรึงเพปไทด์นิวคลีอิก แอซิดเพื่อประยุกต์ใช้ในทางการแพทย์

Magnetite nanoparticles grafted poly (acrylic acid) conjugated with Peptide Nucleic Acid (PNA) for biomedical applications

นภดล สีจ๊ะ[1], ธีรยุทธ วิไลวัลย์[2], เมธา รัตนากรพิทักษ์[1], อุทัย วิชัย[1], บุญจิรา รัตนากรพิทักษ์[1]*

Noppadol Seeja[1], Tirayut Vilaivan[2], Metha Rutnakornpituk[1], Uthai Wichai[1], Boonjira Rutnakornpituk[1]*

[1] *ภาควิชาเคมี และศูนย์ความเป็นเลิศทางด้านวัสดุชีวภาพ คณะวิทยาศาสตร์ มหาวิทยาลัยนเรศวร, พิษณุโลก 65000*

[2] *ภาควิชาเคมี คณะวิทยาศาสตร์ จุฬาลงกรณ์มหาวิทยาลัย, ถนนพญาไท, ปทุมวัน, กรุงเทพ 10330*

บทคัดย่อ

งานวิจัยนี้เป็นการศึกษาการดัดแปร พื้นผิวอนุภาคนาโนแมกนีไทท์ให้มีประจุลบด้วยพอลิอะไครลิก แอซิด (Poly(N-acrylic acid) ด้วยวิธีการสังเคราะห์พอลิเมอร์โดยผ่านอนุมูลอิสระ เพื่อนำมาใช้มาตรึงกับพีเอ็นเอใหม่ชนิดพิร์โรลิดินิลพีเอ็นเอเพื่อประยุกต์ใช้ในทางการแพทย์ต่อไปในอนาคต ทั้งนี้เนื่องจากพิร์โรลิดินิลพีเอ็นเอสามารถเกิดสารประกอบเชิงซ้อนที่มีความเสถียรมากกับดีเอ็นเอและแสดงสมบัติการจับยึดกับดีเอ็นเออย่างจำเพาะเจาะจงสูง โดยการจดจำคู่เบสแบบเดียวกับวัตสัน-คริก เช่นเดียวกับดีเอ็นเอธรรมชาติ จากนั้นทำการศึกษาหมู่ฟังก์ชั่นของพอลิอะไครลิก แอซิด ด้วยเทคนิคฟรูเรียทรานส์ฟอร์ม อินฟาเรดสเปกโตรเมตรี จากการศึกษาการตรึงเบต้า-พิร์โรลิดินิลพีเอ็นเอลงบนอนุภาคด้วยเทคนิค ยูวี-วิสิเบิล สเปกโตรโฟโตเมตรี พบว่าปริมาณของเบต้า-พิร์โรลิดินิลพีเอ็นเอที่ถูกตรึงบนอนุภาคคิดเป็น 0.184 นาโนโมลต่อมิลลิกรัมของอนุภาคนาโนแมกนีไทท์ และคาดว่าอนุภาคที่ถูกตรึงด้วยเบต้า-พิร์โรลิดินิลพีเอ็นเอนี้สามารถนำมาประยุกต์ใช้ในทางการแพทย์ได้อย่างมีประสิทธิภาพต่อไป

คำสำคัญ : อนุภาคนาโนแมกนีไทท์ / พิร์โรลิดินิลเปปไทด์นิวคลีอิกแอซิด / พอลิอะไครลิก แอซิด

Abstract

In this work, the surface modification of magnetite nanoparticles (MNPs) with the polyacrylic acid was prepared via a radical polymerization to form anionic magnetic nanoclusters. They were then conjugated with the pyrolidinyl PNA for further using in the biomedical applications. The pyrolidinyl PNA system showed a strong binding affinity and high sequence specificity with DNA via Watson-Crick base pairing rule. The functional group of polyacrylic acid on the magnetite nanoparticle was determined by FT-IR spectrometry technique. From the studies of the amount for PNA immobilization via UV-VIS spectrophotometry technique, it was found that the amount of pyrolidinyl PNA on the magnetite nanoparticle was 0.184 nmol/mg of magnetite. This biocompatible hybrid magnetite nanoparticle with pyrolidinyl PNA might further use in the biomedical applications.

Keywords: magnetite nanoparticle / peptide nucleic acid / poly(acrylic acid)

***Corresponding author. E-mail:** boonjirab@nu.ac.th

Proceedings The 8th Science Research Conference. 30-31 May 2016. University of Phayao.

1. บทนำ

อนุภาคนาโนแมกนีไทท์ (magnetite nanoparticles, MNP) เป็นสารประกอบของเหล็กออกไซด์ที่มีขนาดเล็กระดับนาโน และมีสมบัติการตอบสนองต่อสนามแม่เหล็กภายนอก นอกจากนี้ยังไม่เป็นสารพิษ มีความแข็งแรงทนทาน [1] จึงทำให้ในปัจจุบันการศึกษาเกี่ยวกับอนุภาคนาโนแมกนีไทท์ (MNP) กำลังได้รับความสนใจจากนักวิจัยอย่างแพร่หลายเช่น การพัฒนาวัสดุทางอิเล็คโทรนิค แผ่นเก็บข้อมูลแม่เหล็กและการประยุกต์ใช้ทางการแพทย์ จากงานวิจัยที่ผ่านมาได้มีการศึกษาการใช้สารชีวโมเลกุลเช่น DNA อะมิโน แอซิด หรือ เปปไทด์ ตรึงบนพื้นผิวอนุภาคนาโนแมกนีไทท์มาประยุกต์ใช้ในทางการแพทย์กันอย่างมากมายเช่นนำมาใช้เป็นอนุภาคในการตรวจสอบลำดับเบสของ DNA หรือใช้เป็นอนุภาคในการทำให้ DNA หรือเปปไทด์บริสุทธิ์ขึ้น [2,3,4] ทั้งนี้เนื่องจากอนุภาคนาโนแมกนีไทท์ มีพื้นที่ผิวมากซึ่งเหมาะสำหรับการตรึงสารชีวโมเลกุลบนพื้นผิวอนุภาค นอกจากนี้ยังอาศัยประโยชน์จากสมบัติความเป็นแม่เหล็กของอนุภาคโดยการแยกอนุภาคนาโนแมกนีไทท์ที่มีการตรึงสารเหล่านี้ออกมาโดยใช้สนามแม่เหล็กจากภายนอก จึงทำให้การแยกอนุภาคออกจากสารละลายได้ง่ายขึ้น งานวิจัยนี้จึงสนใจที่จะนำเอาข้อดีของอนุภาคนาโนแมกนีไทท์มามาประยุกต์ใช้ในทางการแพทย์เช่นนำมาใช้เป็นอนุภาคในการตรวจสอบลำดับเบสของ DNA และจากความสำเร็จของงานวิจัยของกลุ่มศาสตราจารย์ ดร. ธีรยุทธ วิไลวัลย์ และคณะ [5, 6] ในการพัฒนาพีเอ็นเอระบบใหม่ที่ชื่อว่า พิร์โรลิดินิล เพปไทด์นิวคลีอิกแอซิด (pyrolidinyl PNA) ที่ประกอบด้วยวงแหวนพิโรลิดีนที่มีนิวคลีโอเบสต่ออยู่และมีสะพานเชื่อมเป็นกรดบีตาอะมิโนชนิด (1S,2S)-aminocyclopentanecarboxylic acid (ss-ACPC PNA) ดังรูปที่ 1 โดยพีเอ็นเอดังกล่าวสามารถเกิดสารประกอบเชิงซ้อนลูกผสมระหว่างพีเอ็นเอ-ดีเอ็นเอ (hybridized PNA-DNA complex) ที่มีเสถียรภาพและความจำเพาะเจาะจงสูง ซึ่งมีความเสถียรมากกว่าสารประกอบเชิงซ้อนระหว่างดีเอ็นเอกับดีเอ็นเอตามธรรมชาติโดยการจดจำคู่เบสแบบเดียวกับวัตสัน-คริก เช่นเดียวกับดีเอ็นเอธรรมชาติ นอกจากนี้พีเอ็นเอยังเสถียรต่อเอนไซม์นิวคลีเอสและโปรตีเอสจึงเชื่อได้ว่าพีเอ็นเอน่าจะเสถียรในร่างกายของสิ่งมีชีวิต ดังนั้นในงานวิจัยนี้ได้เลือก pyrolidinyl PNA มาใช้ร่วมกับอนุภาคนาโนแมกนีไทท์เพื่อประยุกต์ใช้ในทางการแพทย์ต่อไปในอนาคต โดยจะทำการดัดแปรพื้นผิวอนุภาคนาโนแมกนีไทท์ให้มีประจุลบด้วยพอลิอะไครลิก แอซิด (Poly(N-acrylic acid) เพื่อนำมาใช้มาตรึงกับ pyrolidinyl PNA ด้วยพันธะโควาเลนต์ (covalent bond) ในสภาวะที่เหมาะสมเพื่อประยุกต์ใช้ในทางการแพทย์เช่นนำมาใช้เป็นอนุภาคในการตรวจสอบลำดับเบสของ DNA ต่อไป และสามารถวิเคราะห์การดัดแปรพื้นผิวอนุภาคนาโนแมกนีไทท์ด้วยพอลิอะไครลิก แอซิด (Polyacrylic acid) และการตรึง pyrolidinyl PNA กับอนุภาคนาโนแมกนีไทท์ด้วยเทคนิคต่างๆ เช่น ฟูเรียทรานส์ฟอร์ม อินฟาเรดสเปกโตรเมตรี (FT-IR spectrometry), ยูวี-วิสิเบิลสเปกโตรโฟโตเมตรี (UV-Vis spectrophotometer), โฟโตคอรีเรชันสเปกโตรสโคปี (Photo correlation spectroscopy ,PCS) และ การไทเทรตโดยการวัดค่าการนำไฟฟ้า (conductometric titration) เป็นต้น

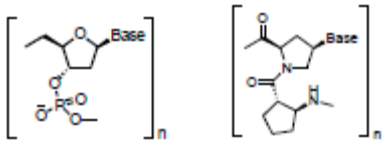

DNA ss-ACPC PNA

รูปที่ 1 โครงสร้างของ DNA และ ss-ACPC PNA

2. วิธีการทดลอง

2.1 การสังเคราะห์และดัดแปรพื้นผิวอนุภาคนาโนแมกนีไทท์ ด้วยพอลิอะไครลิก แอซิด แสดงดังรูปที่ 2 แบ่งออกเป็น 4 ขั้นตอนดังนี้

2.1.1 การสังเคราะห์อนุภาคนาโนแมกนีไทท์ด้วยเทคนิคการตกตะกอนร่วม (Co-Precipitation) โดยการทำปฏิกิริยาระหว่างเฟอรัสคลอไรด์ ($FeCl_2$) และเฟอริคคลอไรด์ ($FeCl_3$) ในสภาวะที่เป็นเบส เป็นเวลา 30 นาที ที่อุณหภูมิห้อง และพิสูจน์เอกลักษณ์ของอนุภาคด้วยเทคนิค FT-IR spectrometry จากนั้นทำการเคลือบ Oleic acid บนอนุภาคเพื่อเสถียรอนุภาคไม่ให้เกิดเกาะกลุ่มเป็นตะกอนใหญ่ (aggregation) และทำการพิสูจน์เอกลักษณ์ของอนุภาคด้วย FT-IR spectrometry

2.1.2 การตรึง 3-aminopropyl trimethoxysilane (APTES) บนอนุภาคนาโนแมกนีไทท์ โดยการนำอนุภาคนาโนแมกนีไทท์ที่เสถียรด้วย Oleic acid มาทำปฏิกิริยากับ Aminopropyl triethoxysilane (APTES) ในสภาวะที่เป็นเบส เป็นเวลา 24 ชั่วโมง ภายใต้สภาวะก๊าซไนโตรเจนที่อุณหภูมิห้องและทำการพิสูจน์เอกลักษณ์ของอนุภาคด้วย FT-IR spectrometry

2.1.3 การตรึงหมู่ Acrylamide บนอนุภาคนาโนแมกนีไทท์ โดยการนำอนุภาคนาโนแมกนีไทท์ที่ถูกตรึงด้วย APTES มาทำปฏิกิริยากับ Acryloyl chloride ที่อุณหภูมิ 0 °C เป็นเวลา 2 ชั่วโมงและทำปฏิกิริยาต่อที่อุณหภูมิห้องเป็นเวลา 24 ชมหลังสิ้นสุดปฏิกิริยาทำการแยกอนุภาคออกแล้วล้างด้วยน้ำปราศจากไอออน (DI water) ทำให้แห้งและพิสูจน์เอกลักษณ์ของอนุภาคด้วย FT-IR spectrometry

2.1.4 การตรึงพอลิเมอร์ ชนิด พอลิอะไครลิก แอซิด (PAA) ลงบนพื้นผิวอนุภาค โดยขั้นแรกจะเป็นการนำ พอลิอะไครลิก แอซิด มาทำปฏิกิริยากับ Ammonium Persulphate (APS) ที่อุณหภูมิ 70 °C เป็นเวลา 30 นาที หลังจากนั้นเติม Acrylamide-coated MNPs ทำการพอลิเมอไรซ์เป็นเวลา 10 นาที จากนั้นล้างอนุภาคด้วยน้ำ DI ทำให้แห้งและพิสูจน์เอกลักษณ์ด้วย FT-IR spectrometry และ การวิเคราะห์ค่าความต่างศักย์พื้นผิว (zeta potential) ด้วย Photo correlation spectroscopy

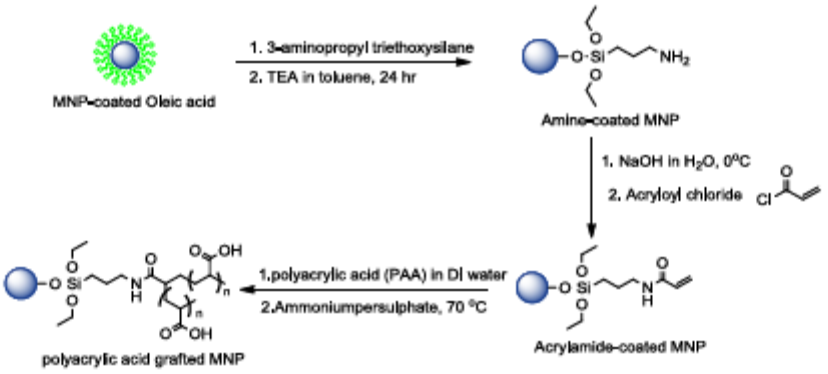

รูปที่ 2 การสังเคราะห์และดัดแปรพื้นผิวอนุภาคนาโนแมกนีไทท์ด้วยพอลิอะไครลิก แอซิด

2.2 การตรึง pyrrolidinyl PNA ลงบนพื้นผิวอนุภาคที่ถูกเคลือบด้วยพอลิเมอร์ชนิด พอลิอะไครลิก แอซิด ดังรูปที่ 3 โดย pyrrolidinyl PNA ที่ใช้ในงานวิจัยนี้มีลำดับเบสดังนี้ Ac-CGA GGA TGG CG-Lys-NH_2 โดยแบ่งออกเป็น 2 ขั้นตอนโดยขั้นแรกทำการเปลี่ยนหมู่ฟังก์ชันคาร์บอกซิลิคที่ถูกตรึงลงบนพื้นผิวของอนุภาคนาโนแมกนีไทท์ให้ว่องไวต่อการเกิดปฏิกิริยา โดยใช้ EDC-HCl ใน MES บัฟเฟอร์และขั้นตอนที่สองเป็นการนำอนุภาคนาโนแมกนีไทท์เปลี่ยนหมู่ฟังก์ชันคาร์บอกซิลิคแล้วมาทำปฏิกิริยาต่อกับ pyrrolidinyl PNA ในฟอสเฟตบัฟเฟอร์ pH 10 เป็นเวลา 12 ชั่วโมง หลังจากนั้นนำสารละลาย pyrrolidinyl PNA ที่ได้ก่อนตรึงและหลังตรึงลงบนอนุภาคมาวัดค่าการดูดกลืนแสงที่ความยาวคลื่น 260 นาโนเมตรด้วย UV-Vis spectrophotometer เพื่อหาปริมาณ pyrrolidinyl PNA โดยการเทียบกับกราฟมาตรฐานของสารละลาย pyrrolidinyl PNA และคำณวนหาปริมาณ pyrrolidinyl PNA ที่ถูกตรึงลงบนอนุภาคโดยใช้สมการที่ (1)

ปริมาณ PNA ที่ตรึงบนอนุภาค = ปริมาณ PNA ก่อนตรึง – ปริมาณ PNA ที่เหลือในสารละลาย (1)

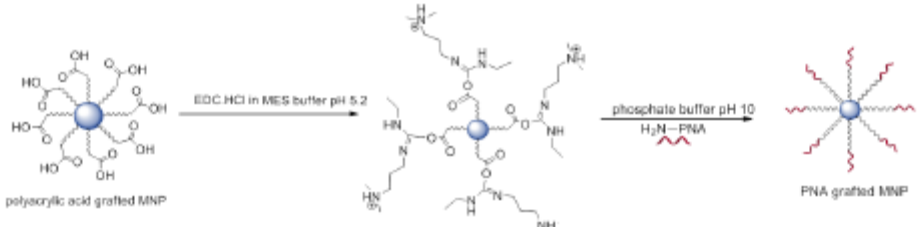

รูปที่ 3 การตรึง pyrrolidinyl PNA ลงบนพื้นผิวอนุภาคที่ถูกเคลือบด้วยพอลิเมอร์ชนิด พอลิอะไครลิก แอซิด

3. ผลและอภิปรายผลการทดลอง

3.1 การตรวจสอบเอกลักษณ์ของอนุภาคนาโนแมกนีไทท์ที่สังเคราะห์ในแต่ละขั้นตอนด้วย FT-IR spectrometry

เมื่อนำเอาอนุภาคนาโนแมกนีไทท์ที่สังเคราะห์ได้ในแต่ละขั้นตอนที่ประกอบไปด้วยการสังเคราะห์อนุภาคนาโนแมกนีไทท์ โดยวิธีการตกตะกอนร่วม (A) การตรึง 3-aminopropyl trimethoxysilane (MNP-APTES) บนอนุภาคนาโนแมกนีไทท์(B) การตรึงหมู่ Acrylamide บนอนุภาคนาโนแมกนีไทท์ (C) การตรึงพอลิเมอร์ ชนิด polyacrylic acid ลงบนพื้นผิวอนุภาคนาโนแมกนีไทท์ (D) มาทำการพิสูจน์เอกลักษณ์ด้วย FT-IR spectrometry พบว่าได้สเปคตรัม FT-IR ดังรูปที่ 4

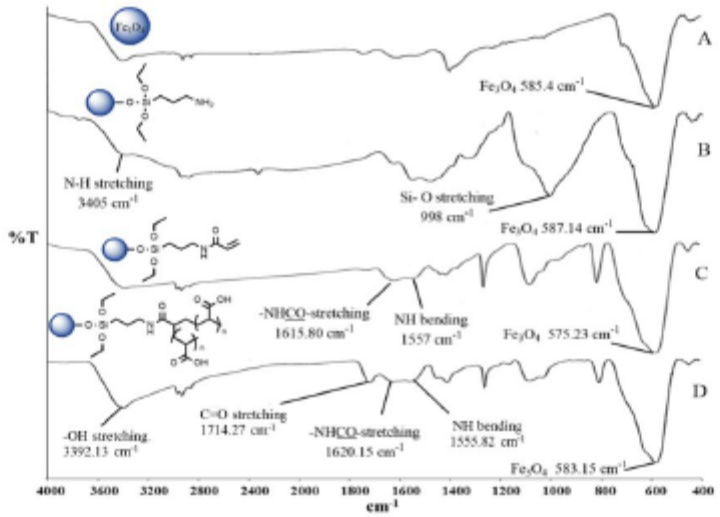

รูปที่ 4 FT-IR สเปคตรา ของ A) Fe_3O_4 , B) APTES-coated Fe_3O_4 , C) Acrylamide coated Fe_3O_4และ D) Polyacrylic acid-grafted Fe_3O_4

จาก FT-IR สเปคตราของอนุภาคนาโนแมกนีไทท์ที่สังเคราะห์ได้ในแต่ละขั้นตอนพบว่าในสเปคตัม A จะพบ สัญญาณ Fe-O ของสารประกอบเหล็กออกไซด์ที่ตำแหน่ง 585.4 cm^{-1} ซึ่งเป็นลักษณะเฉพาะของอนุภาคนาโนแมกนีไทท์ สเปคตรัม B พบสัญญาณของหมู่ฟังก์ชันเอมีนของ APTES คือ NH stretching (3405 cm^{-1}) และ Si-O stretching (998.16 cm^{-1}) แสดงถึงการมี หมู่ APTES อยู่บนพื้นผิวอนุภาค สเปคตรัม C พบสัญญาณของหมู่คาร์บอนิลของหมู่เอไมด์ของ Acrylamide -NH-CO- stretching ที่ 1615.8 cm^{-1} และ N-H bending ที่ 1557 cm^{-1} ซึ่งแสดงให้เห็นถึงการมี หมู่ Acrylamide อยู่บนพื้นผิวอนุภาค และสเปคตรัม D จะพบสัญญาณของหมู่คาร์บอนิล (C=O stretching) ของหมู่คาร์บอกซิลิค แอซิดของพอลิอะไครลิกที่ 1714 cm^{-1} และ พบสัญญาณของหมู่ไฮดรอกซีของหมู่คาร์บอกซิลิค แอซิดที่ 3392 cm^{-1} ซึ่งแสดงให้เห็นถึงการมีพอลิอะไครลิก แอซิด อยู่บนอนุภาคนาโนแมกนีไทท์

3.2 การวิเคราะห์ค่าความต่างศักย์พื้นผิว (zeta potential) อนุภาคที่เคลือบด้วยพอลิเมอร์ชนิด พอลิอะไครลิก แอซิดด้วย Photo correlation spectroscopy เนื่องจากพอลิอะไครลิก แอซิดเป็นพอลิเมอร์ที่สามารถตอบสนองต่อการเปลี่ยนแปลงของค่าพีเอช จากผลของการมีหมู่คาร์บอกซิลิคอยู่บนสายโซ่ จึงได้ทำการศึกษาหาค่าความเป็นประจบของอนุภาคนาโนแมกนีไทท์ที่ pH ต่างๆ เพื่อพิสูจน์คุณสมบัติของพอลิเมอร์โดยใช้ Photo correlation spectroscopy แสดงผลดังตารางที่ 1

ตารางที่ 1 ค่าความต่างศักย์พื้นผิว ของอนุภาคนาโนแม็กนีไทท์ที่ถูกเคลือบพอลิอะไครลิกแอซิด ที่ pH ต่างๆ

Zeta potential			
pH	ค่าความเป็นประจุ (mV)	pH	ค่าความเป็นประจุ (mV)
2	0.77	7	-41.4
4	-29.1	8	-44.3
6	-39	10	-47.7

จากตารางพบว่าเมื่อมีค่า pH สูงขึ้นทำให้ประจุลบบนพื้นผิวของอนุภาคนาโนแมกนีไทท์มีแนวโน้มที่มากขึ้น ทั้งนี้เนื่องจากเมื่อค่า pH สูงขึ้นจะทำให้โปรตอนของหมู่คาร์บอกซิลิกแอซิดของ พอลิอะไครลิก แอซิด ถูกดีโปรโตเนตเกิดเป็นหมู่คาร์บอกซิเลตซึ่งเป็นประจุลบได้มาก จึงทำให้ที่พื้นผิวของอนุภาคมีความเป็นลบมากขึ้นซึ่งแสดงให้เห็นว่าบนอนุภาคนาโนแมกนีไทท์มีพอลิเมอร์ชนิด พอลิอะไครลิก แอซิดอยู่และ

นอกจากนี้จากผลการทดลองสามารถบอกได้ว่าหมู่ฟังก์ชันของพอลิเมอร์ชนิดพอลิอะไครลิก แอซิด ที่ถูกดัดแปรบนพื้นผิวอนุภาคนาโนแมกนีไทท์สามารถตอบสนองต่อการเปลี่ยนแปลงของ pH ได้อีกด้วย

3. 3 การศึกษาการตรึง pyrolidinyl PNA ลงบนอนุภาคที่ดัดแปรด้วยพอลิเมอร์ชนิดพอลิอะไครลิก แอซิด ด้วย UV-Vis spectrophotometer

การยืนยันการการตรึง pyrolidinyl PNA ลงบนอนุภาคด้วยเทคนิคไทเทรตโดยการวัดค่าการนำไฟฟ้า

หลังจากที่ทำการดัดแปรพื้นผิวของอนุภาคนาโนแมกนีไทท์ด้วยพอลิเมอร์ชนิดพอลิอะไครลิก แอซิดแล้ว อนุภาคนาโนแมกนีไทท์ที่ได้จะนำมาทำการตรึงด้วยกับ pyrolidinyl PNA ด้วยพันธะโควาเลนต์ (covalent bond) ในสภาวะที่เหมาะสมเพื่อนำมาประยุกต์ใช้ประโยชน์ทางการแพทย์ต่อไป โดยในการศึกษาปริมาณของ pyrolidinyl PNA บนอนุภาคจะใช้ UV-Vis spectrophotometer โดยการวัดค่าการดูดกลืนแสงที่ 260 นาโนเมตร ของ สารละลาย pyrolidinyl PNA ทั้งก่อนและหลังทำการตรึงลงบนอนุภาคนาโนแม็กนีไทท์ที่ จากผลการศึกษาพบว่าค่าการดูดกลืนแสงของสารละลาย pyrolidinyl PNA หลังทำการตรึงลงบนอนุภาคนาโนแม็กนีไทท์ลดลงดังแสดงในรูปที่ 5 ซึ่งแสดงให้เห็นว่า pyrolidinyl PNA ถูกตรึงลงบนอนุภาค หลังจากนั้นนำค่าการดูดกลืนแสงที่ได้มาทำการหาปริมาณของพีเอ็นเอโดยเทียบกับกราฟมาตรฐานของพีเอ็นเอจากผลการคำนวณหาปริมาณ pyrolidinyl PNA ที่ถูกตรึงลงบนอนุภาคพบว่าปริมาณของ pyrolidinyl PNA ที่ถูกตรึงบนอนุภาคคิดเป็น 0.184 นาโนโมลต่อมิลลิกรัมของอนุภาคนาโนแมกนีไทท์

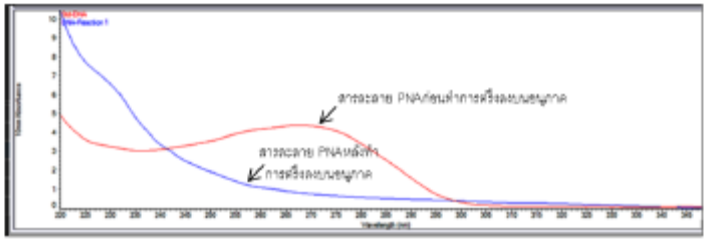

รูปที่ 5 สเปกตรัมการดูดกลืนแสงของ สารละลายของ pyrolidinyl PNA ก่อนและหลังทำการตรึงลงบนอนุภาค

3.3.1 การยืนยันการการตรึง pyrolidinyl PNA ลงบนอนุภาคด้วยเทคนิคไทเทรตโดยการวัดค่าการนำไฟฟ้า

เพื่อทำการยืนยันการการตรึง pyrolidinyl PNA ลงบนอนุภาคจึงได้ทำการศึกษาค่าการเปลี่ยนแปลงประจุของพอลิอะไครลิก แอซิดบนพื้นผิวของอนุภาคนาโนแมกนีไทท์ก่อนและหลังการตรึงด้วย pyrolidinyl PNA ด้วยเทคนิคการไทเทรตโดยการวัดค่าการนำไฟฟ้า ผลการทดลองที่ได้แสดงดังรูปที่ 6

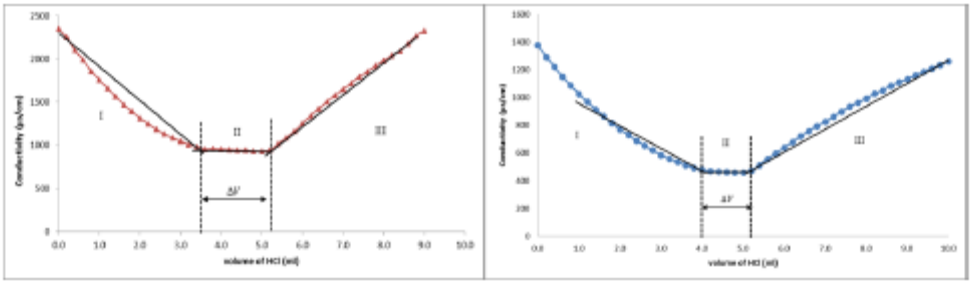

A B

รูปที่ 6 การไทเทรตโดยการวัดค่าการนำไฟฟ้าของอนุภาคนาโนแม็กนีไทท์ก่อน (A) และหลัง (B) การตรึงด้วย pyrolidinyl PNA

จากรูปนำค่าΔV (L) ที่ใช้ในบริเวณ II มาคำณวนหาปริมาณของหมู่คาร์บอกซิลิคบนอนุภาคได้ดังสมการที่ (2)

$$\text{Carboxylic acid} = \frac{M\Delta V}{m} \qquad (2)$$

โดย M = ความเข้มข้นของ HCl ที่ใช้คือ 0.005 โมลาร์ และ m = น้ำหนักของอนุภาคนาโนแมกนีไทท์ (g)

จากการคำนวณค่าที่ได้พบว่าปริมาณของหมู่คาร์บอกซิลิคบนอนุภาคนาโนแม็กนีไทท์ที่ถูกตรึงด้วยพอลิอะไครลิก แอซิด (ก่อนตรึง pyrolidinyl PNA) เท่ากับ 4.25 mmol/g ของอนุภาคและปริมาณของหมู่คาร์บอกซิลิคบนอนุภาคโนแม็กนีไทท์ที่ถูกตรึงด้วย pyrolidinyl PNA เท่ากับ 3.00 mmol/g ของอนุภาคแสดงให้เห็นถึงการลดลงของหมู่คาร์บอกซิลิคบนอนุภาคเกิดจากมีการถูกตรึงด้วย pyrolidinyl PNA บนอนุภาคอนุภาคนาโนแม็กนีไทท์นั่นเอง

4. สรุปผลการทดลอง

การสังเคราะห์อนุภาคนาโนแมกนีไทท์ให้มีประจุลบด้วยพอลิอะไครลิก แอซิด (Polyacrylic acid) นี้ สามารถยืนยันการตรึงพอลิอะไคลิค แอซิด บนพื้นผิวอนุภาคด้วย FT-IR spectrometry พบว่าแสดงหมู่ฟังก์ชันที่เป็นลักษณะเฉพาะของพอลิอะไครลิก แอซิดบนอนุภาคนาโนแมกนีไทท์ ในการศึกษาการตรึง pyrrolidinyl PNA ด้วย UV-Vis spectrophotometer พบว่า pyrolidinyl PNA สามารถถูกตรึงลงบนอนุภาคโดยดูได้จากค่าการดูดกลืนแสงของ pyrolidinyl PNA หลังทำการตรึงลงบนอนุภาคที่ลดลง และจากการไทเทรตโดยวัดค่าการนำไฟฟ้าเพื่อหาความปริมาณของหมู่คาร์บอกซิลิค แอซิดพบว่าเมื่อทำการตรึง pyrolidinyl PNA บนอนุภาคทำให้ปริมาณของหมู่คาร์บอกซิลิค แอซิดบนอนุภาคลดลง ซึ่งแสดงให้เห็นว่า pyrolidinyl PNA ถูกตรึงบนอนุภาคนาโนแมกนีไทท์ได้ จากอนุภาคที่ถูกตรึงด้วย pyrolidinyl PNA และด้วยความสามารถในการจับยึดกับดีเอ็นเอได้อย่างแข็งแรง และมีความจำเพาะเจาะจงสูงของพีเอ็นเอระบบนี้ คาดว่าอนุภาคที่ได้นี้สามารถนำมาประยุกต์ใช้ประโยชน์ทางการแพทย์ได้เช่นใช้เป็นอนุภาคสำหรับการตรวจสอบลำดับเบสของดีเอ็นเอได้ซึ่งจะต้องทำการศึกษาต่อไป

5. กิตติกรรมประกาศ

งานวิจัยนี้ได้รับการสนับสนุนจากทุนศาสตราจารย์วิจัยดีเด่น (สกว.)

6. เอกสารอ้างอิง

Pankhurst, Q. A., Counolly, J. and Dobson, J. (2003).Application of magnetic nanoparticles in biomedicine.167-181.

Palecek, E., and Fojta, M. (2007). Magnetic beads as versatile tools for electrochemical DNA and protein biosensing, *Talanta*, 74, 276–290.

Lee, HJ., Jang, KS., Jang, S., et al. (2010). Poly(amino acid)s micelle-mediated assembly of magnetite nanoparticles for ultra-sensitive long-term MR imaging of tumors. *Chem Commun*. 46, 3559-3561.

Chiang, CL., Sung, CS., Chen, CY. (2006). Application of silica–magnetite nanocomposites to the isolation of ultrapure plasmid DNA from bacterial cells. *J Magn Magn Mater*. 305, 483-490.

Suparpprom, C., Srisuwannaket, C., Sangvanich, P. and Vilaivan, T. (2005). Synthesis and oligodeoxynucleotide binding properties of pyrrolidinyl peptide nucleic acids bearing prolyl-2-aminocyclopentanecarboxylic acid, *Tetrahedron Lett*, 46, 283-2837.

Vilaivan, T. and Srisuwannaket, C. (2006). Hybridization of pyrrolidinyl peptide nucleic acids and DNA: selectivity, base-pairing specificity, and direction of binding. *Org Lett*. 8, 1897-1900.

4) 2 Invited oral presentations

4.1) The workshop on “Natural Product-Based Drug Discovery for Aging Society” at Faculty of Pharmaceutical Sciences, Naresuan University, 6 December, 2018, Title: Functional polymer-coated magnetic nanoparticle and its bio-conjugation and drug controlled release applications

4.2) The seminar at Aston University, Birmingham, UK, 19 May, 2016, Surface decoration of magnetic nanoparticle with functional polymers and biomolecules: Synthesis and applications

4.1) The workshop on “Natural Product-Based Drug Discovery for Aging Society” at Faculty of Pharmaceutical Sciences, Naresuan University, 6 December, 2018, Title: Functional polymer-coated magnetic nanoparticle and its bio-conjugation and drug controlled release applications

Faculty of Pharmaceutical Sciences
Naresuan University
Phitsanulok, Thailand 65000 Tel: 66-5596-3730 Fax: 66-5596-3731

31st October 2018

Dear Associate Professor Dr. Metha Rutnakornpituk

I would like to invite you to give a 20 minute-lecture in the workshop on “Natural Product-Based Drug Discovery for Aging Society” which will be held at Faculty of Pharmaceutical Sciences, Naresuan University on 6 December, 2018 under the international collaborative project on “Discovery and Generation of New Medicinal Chemical Entities Based on Bioactive Natural Products for Aging Society” supported by The Thai Research Fund (TRF) and National Natural Science Foundation of China (NSFC). Please kindly send an abstract of your presentation to me within 5th November 2018.

Your acceptance of my invitation will be greatly appreciated.

I am looking forward to hearing from you,

Yours sincerely,

Kornkanok Ingkaninan

Associate Professor Dr. Kornkanok Ingkaninan
Bioscreening Lab
Department of Pharmaceutical Chemistry and Pharmacognosy
Faculty of Pharmaceutical Sciences
Naresuan University
Phitsanulok 65000, Thailand

THE 2nd NSFC-TRF

COLLABORATIVE PROJECT MEETING

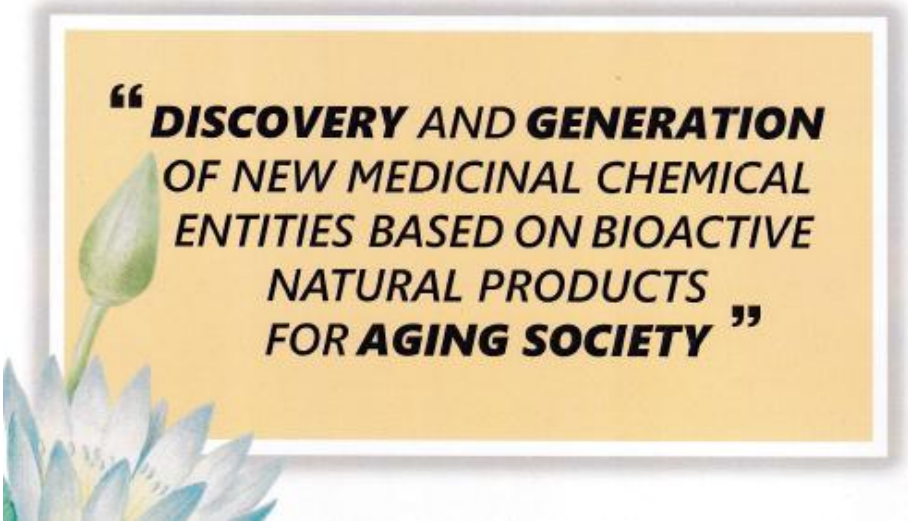

PROGRAM

2nd NSFC-TRF collaborative project meeting
"Discovery and Generation of New Medicinal Chemical Entities Based on Bioactive Natural Products for Aging Society"
December 6, 2018. Chayanupap 2 Room

Time	Topic	Speaker
09.00 - 09.15	Opening ceremony	Honorary Prof. Dr. Kanchana Ngourungsi President of Naresuan University
09.15 - 09.45	*Chairpersons: Assoc. Prof. Dr. Kornkanok Ingkaninan* *Prof. Dr. Jian-Xin Li* Medicinal-space investigation of sinomenine, an economically available alkaloid from traditional Chinese medicine	Prof. Dr. Zhu-Jun Yao (Nanjing University)
09.45 - 10.05	Cytotoxic merosesquiterpenes from the sponge *Spongia sp.*	Assoc. Prof. Dr. Anuchit Plubrukarn (Prince of Songkla University)
10.05 - 10.25	Genome mining and biosynthesis of microbial natural products	Prof. Dr. Hui Ming Ge (Nanjing University)
10.25 - 10.40	Coffee break	
10.40 - 11.00	*Chairpersons: Prof. Dr. Zhu-Jun Yao* *Assoc. Prof. Dr. Anuchit Plubrukarn* Functional polymer-coated magnetic nanoparticle and its bioconjugation and drug controlled release applications	Assoc. Prof. Dr. Metha Rutnakornpituk (Naresuan University)
11.00 - 11.20	Enantioselective total synthesis of (+)-Plumisclerin A	Dr. Ming Gao (Nanjing University)
11.20 - 11.50	Development of an at-line fractionation LC/QTOF-MS/MS method with rapid biochemical-identification for isolation of natural steroid 5 alpha-reductase inhibitors in *Impatiens balsamina* Linn.	Dr. Jukkarin Srivilai (University of Phayao)
11.50 - 13.00	Lunch	
13.00 - 13.30	*Chairpersons: Prof. Dr. Hui Ming Ge* *Dr. Sudaporn Wongwan* Research and development of natural products from Thai biodiversity	Assoc. Prof. Dr. Kornkanok Ingkaninan (Naresuan University)
13.30 - 13.50	Isolation of phosphodiesterase 5 inhibitors from water lily (*Nymphaea pubescens* Willd.)	Asst. Prof. Dr. Nungruthai Suphrom (Naresuan University)
13.50 - 14.10	At-line microfractionation of PDE5 radiometric based assay coupled to QTOF LC/MS for the early identification of active compounds from *Derris scandens*	Dr. Prapapan Temkitthawon (Naresuan University)

Functional polymer-coated magnetic nanoparticle and its bioconjugation and drug controlled release applications

Metha Rutnakornpituk

Department of Chemistry and Center of Excellence in Biomaterials, Faculty of Science,
Naresuan University, Phitsanulok 65000, Thailand
methar@nu.ac.th

Our research works have recently focused on coating magnetic nanoparticles (MNP) with functional polymers using various approaches, such as physical adsorption of polymers on its surfaces, emulsion polymerization in the presence of MNP and the so-called "grafting to" and "grafting from" strategies. Coating these particles with polymers also improves particle dispersibility in the media and biocompatibility, which are minimum requirements for uses in biomedical applications. Furthermore, the polymers on MNP surface also provide a platform for incorporation of various biological functional molecules.

Recently, we have focused on surface modification of MNP with various functional polymers and also investigated its biomedical-related applications, such as drug controlled release and bioconjugation (DNA, antibody, antigen and drug molecules). The functional polymers that attracted our interest in this work include; 1) amino acid-derived polymers, e.g. azlactone-based polymer and thiolactone-based polymer and 2) stimuli-responsive polymers, e.g. poly(N-isopropyl acrylamide) and poly(acrylic acid).

Amino acid-derived polymers have been widely studied during the last decade because they may create new non biological macromolecules with biomimetic structures and properties. In addition to that, stimuli-responsive polymers have also been of our great interest in this work because they can provide triggering mechanisms for release of entrapped drugs. Such characteristics and the potential applications of these functional polymers have motivated us to design and develop tailored materials with unique intelligent properties *via* assorted polymerization techniques. These functional polymers coated on MNP surface thus show a great potential for use in various biological and medicinal applications, such as drug controlled release *via* thermo-chemotherapy against cancer, bio-chemical sensing and biocompatible materials.

1. Paenkaew, S., Rutnakornpituk, M. (2018) Effect of alkyl chain lengths on the assemblies of magnetic nanoparticles coated with multi-functional thiolactone-containing copolymer. J. Nanopart. Res., 20: 193-204.
2. Khadsai, S., Seeja, N., Deepuppha, N., Rutnakornpituk, M., Vilaivan, T., Nakkuntod, M., Rutnakornpituk, B. (2018) Poly(acrylic acid)-grafted magnetite nanoparticle conjugated withpyrrolidinyl peptide nucleic acid for specific adsorption with real DNA. Colloids Surf. B Biointerfaces, 165: 243–251
3. Meerod, S., Deepuppha, N., Rutnakornpituk, B., Rutnakornpituk, M. (2018) Reusable magnetic nanocluster coated with poly(acrylic acid) and its adsorption with antibody and antigen. J. App. Polym. Sci., 135: 46160.
4. Thong-On, B., Rutnakornpituk, M. (2016) Controlled magnetite nanoclustering in the presence of glycidyl-functionalized thermo-responsive poly(Nisopropylacrylamide). Euro. Polym. J., 85: 519-531.
5. Prai-In, Y., Boonthip, C., Rutnakornpituk, B., Wichai, U., Montembault, V., Pascual, S., Fontaine, L., Rutnakornpituk, M. (2016) Recyclable magnetic nanocluster crosslinked with poly(ethylene oxide)-block-poly(2-vinyl-4,4-dimethylazlactone) copolymer for adsorption with antibody. Mater. Sci. Eng. C 67: 285-293.

Metha Rutnakornpituk, Khon Kaen U. (B.Sc. 1996), Virginia Tech, USA (Ph.D. 2002, Prof. JS Riffle), Visiting Fellow, U. du Maine, France (Prof. L. Fontaine). TRF Research Scholar (2003-present). Assoc Prof., Naresuan University (2009-present). Research fields: Synthesis of block copolymers *via* controlled radical polymerization (e.g. ATRP, RAFT) and living anionic polymerization, surface modification of nanoparticle.

4.2) The seminar at Aston University, Birmingham, UK, 19 May, 2016, Surface decoration of magnetic nanoparticle with functional polymers and biomolecules: Synthesis and applications

Surface decoration of magnetic nanoparticle with functional polymers and biomolecules: Synthesis and applications

Assoc.Prof.Dr.Metha Rutnakornpituk

Department of Chemistry and Center of Excellence in Biomaterials, Faculty of Science, Naresuan University, Phitsanulok, 65000 Thailand, e-mail: methar@nu.ac.th

Surface decoration of magnetite nanoparticle (MNP) has recently attracted a great attention in biomedical applications. In this work, various approaches for decoration of MNP surface with functional polymers and/or biomolecules will be presented. After the polymer coating, the MNP with desirable properties such as high magnetic responsiveness, biocompatibility, water dispersibility and containing interactive functions on their surface was obtained. Some controlled radical polymerizations (CRP) such ATRP and RAFT were also employed for the MNP surface functionalization. In this presentation, conjugation of some biomolecules such as DNA, peptide nucleic acid (PNA), antibody and drugs on to the MNP surface will be described.

5) 5 Awards

5.1) รางวัลผลงานวิจัยเด่น สกว. จาก สำนักงานกองทุนสนับสนุนการวิจัย (สกว.) ประจำปี 2560 เรื่อง นวัตกรรมสารเลียนแบบสารพันธุกรรมและการประยุกต์ใช้ (เป็นผู้ร่วมวิจัยในงานวิจัยของ ศาสตราจารย์ ดร.ธีรยุทธ วิไลวัลย์)

5.2) ผลงานระดับดีเยี่ยมแบบโปสเตอร์ จากงานประชุมประจำปี สกอ ปี 2560 ณ มหาวิทยาลัยราชภัฏอุดรธานี

5.3) รางวัลนักวิจัยดีเด่น ด้านการวิจัยเชิงวิชาการพื้นฐาน ของมหาวิทยาลัยนเรศวรประจำปี 2559

5.4) นางสาวนันทิยา ดีบุบผาและนายวสวัตติ์ อินทรานุสรณ์ ได้รับรางวัลการนำเสนอผลงานวิจัยแบบบรรยายยอดเยี่ยม จากงานประชุมวิชาการ 9th Science Research Conference, 25-26 May 2017, Burapha University, Chonburi, Thailand

5.5) นางสาวสุดารัตน์ ขัดสาย ได้รางวัลการนำเสนอผลงานวิจัยแบบโปสเตอร์ยอดเยี่ยมจาก The First Materials Research Society of Thailand International Conference (1st MRS Thailand International Conference), Poster, 31 October-3 November 2017, Convention Center, The Empress Hotel, Chiang Mai, Thailand

5.1) รางวัลผลงานวิจัยเด่น สกว. จาก สำนักงานกองทุนสนับสนุนการวิจัย (สกว.) ประจำปี 2560 เรื่อง นวัตกรรมสารเลียนแบบสารพันธุกรรมและการประยุกต์ใช้ (เป็นผู้ร่วมวิจัยในงานวิจัยของ ศาสตราจารย์ ดร.ธีรยุทธ วิไลวัลย์)

สำนักงานกองทุนสนับสนุนการวิจัย (สกว.)

ประกาศเกียรติคุณฉบับนี้ให้ไว้เพื่อแสดงว่า

ผลงานวิจัยเรื่อง

นวัตกรรมสารเลียนแบบสารพันธุกรรมและการประยุกต์ใช้

โดย

รองศาสตราจารย์ ดร.เมธา รัตนากรพิทักษ์

นักวิจัย

ได้รับเลือกเป็นผลงานวิจัยเด่นประจำปี พ.ศ. ๒๕๖๐

ให้ไว้ ณ วันที่ ๒๓ พฤษภาคม พ.ศ. ๒๕๖๑

ศาสตราจารย์นายแพทย์ สุทธิพันธ์ จิตพิมลมาศ

ผู้อำนวยการสำนักงานกองทุนสนับสนุนการวิจัย

5.2) ผลงานระดับดีเยี่ยมแบบโปสเตอร์ จากงานประชุมประจำปี สกอ ปี 2560 ณ มหาวิทยาลัยราชภัฏอุดรธานี

สำนักงานคณะกรรมการการอุดมศึกษา

โดยสำนักบริหารโครงการส่งเสริมการวิจัยในอุดมศึกษาและพัฒนามหาวิทยาลัยวิจัยแห่งชาติ

เกียรติบัตรฉบับนี้ให้ไว้เพื่อแสดงว่า

รศ. ดร.เมธา รัตนากรพิทักษ์

มหาวิทยาลัยนเรศวร

เป็นผู้ได้รับรางวัลผลงานวิจัยดีมาก

ในการประชุมใหญ่โครงการส่งเสริมการวิจัยในอุดมศึกษา ครั้งที่ ๕ (HERP CONGRESS V)

ระหว่างวันที่ ๒-๔ มีนาคม พุทธศักราช ๒๕๖๐

ขอจงมีความเจริญด้วยจตุรพิธพร ทำคุณประโยชน์ในด้านการสร้างสรรค์ปัญญา เพื่อพัฒนาประเทศสืบไป

(ดร.สุภัทร จำปาทอง)
เลขาธิการคณะกรรมการการอุดมศึกษา

(ศาสตราจารย์ ดร.วิชัย บุญแสง)
ผู้อำนวยการสำนักบริหารโครงการฯ

HERP CONGRESS V
UDONTHANI 2017

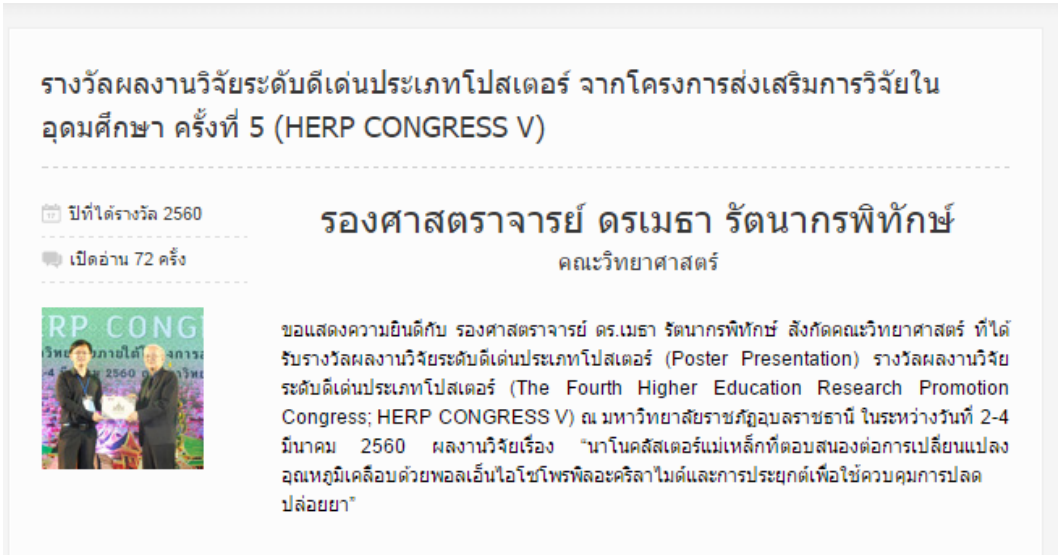

รางวัลผลงานวิจัยระดับดีเด่นประเภทโปสเตอร์ จากโครงการส่งเสริมการวิจัยในอุดมศึกษา ครั้งที่ 5 (HERP CONGRESS V)

ปีที่ได้รางวัล 2560

เปิดอ่าน 72 ครั้ง

รองศาสตราจารย์ ดรเมธา รัตนากรพิทักษ์

คณะวิทยาศาสตร์

ขอแสดงความยินดีกับ รองศาสตราจารย์ ดร.เมธา รัตนากรพิทักษ์ สังกัดคณะวิทยาศาสตร์ ที่ได้รับรางวัลผลงานวิจัยระดับดีเด่นประเภทโปสเตอร์ (Poster Presentation) รางวัลผลงานวิจัยระดับดีเด่นประเภทโปสเตอร์ (The Fourth Higher Education Research Promotion Congress; HERP CONGRESS V) ณ มหาวิทยาลัยราชภัฏอุบลราชธานี ในระหว่างวันที่ 2-4 มีนาคม 2560 ผลงานวิจัยเรื่อง "นาโนคลัสเตอร์แม่เหล็กที่ตอบสนองต่อการเปลี่ยนแปลงอุณหภูมิเคลือบด้วยพอลเอ็นไอโซโพรพิลอะคริลาไมด์และการประยุกต์เพื่อใช้ควบคุมการปลดปล่อยยา"

5.3) รางวัลนักวิจัยดีเด่น ด้านการวิจัยเชิงวิชาการพื้นฐาน ของมหาวิทยาลัยนเรศวร ประจำปี 2559

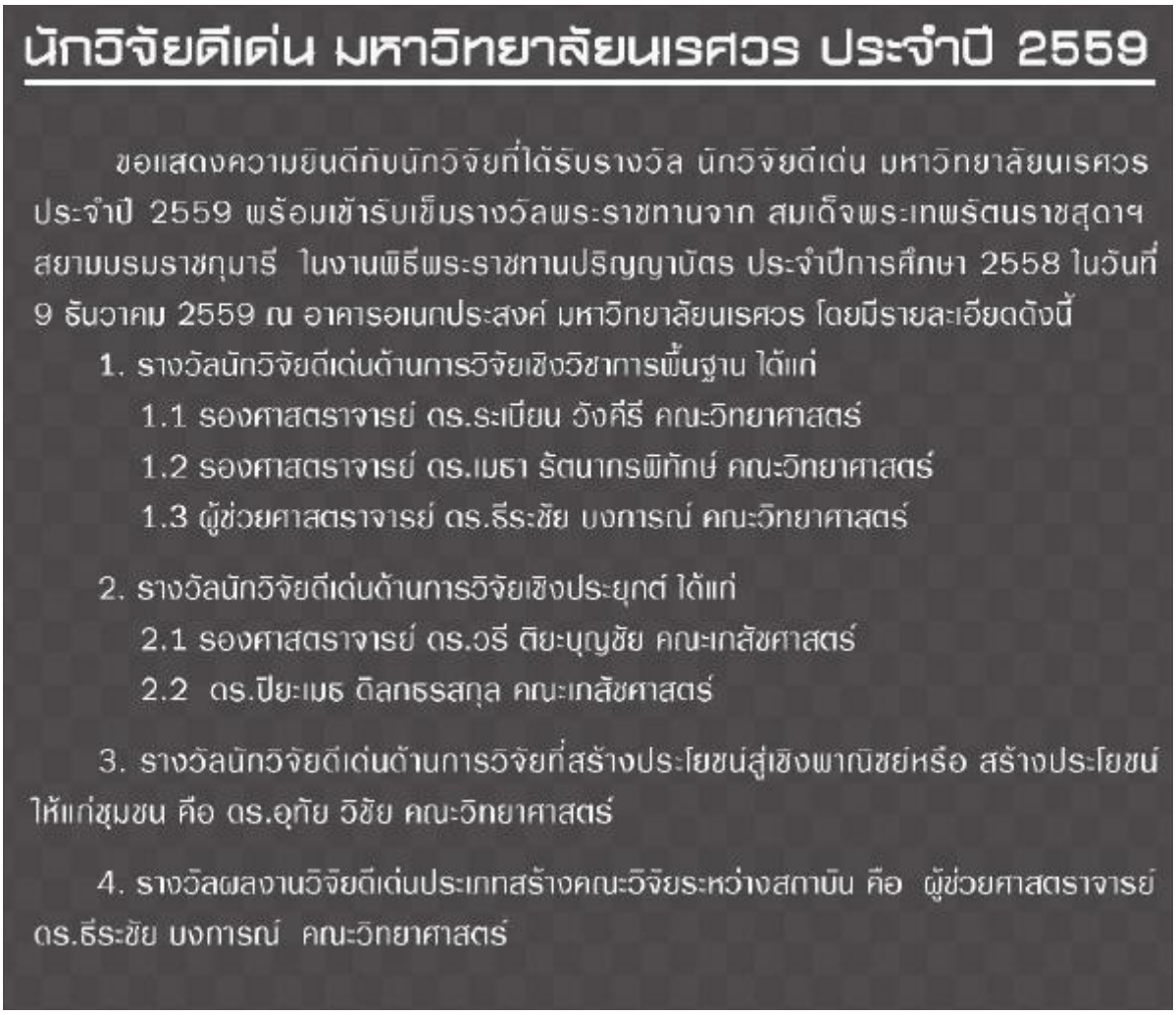

นักวิจัยดีเด่น มหาวิทยาลัยนเรศวร ประจำปี 2559

ขอแสดงความยินดีกับนักวิจัยที่ได้รับรางวัล นักวิจัยดีเด่น มหาวิทยาลัยนเรศวร ประจำปี 2559 พร้อมเข้ารับเข็มรางวัลพระราชทานจาก สมเด็จพระเทพรัตนราชสุดาฯ สยามบรมราชกุมารี ในงานพิธีพระราชทานปริญญาบัตร ประจำปีการศึกษา 2558 ในวันที่ 9 ธันวาคม 2559 ณ อาคารอเนกประสงค์ มหาวิทยาลัยนเรศวร โดยมีรายละเอียดดังนี้

1. รางวัลนักวิจัยดีเด่นด้านการวิจัยเชิงวิชาการพื้นฐาน ได้แก่
   1.1 รองศาสตราจารย์ ดร.ระเบียน อังคีรี คณะวิทยาศาสตร์
   1.2 รองศาสตราจารย์ ดร.เมธา รัตนากรพิทักษ์ คณะวิทยาศาสตร์
   1.3 ผู้ช่วยศาสตราจารย์ ดร.ธีระชัย บงการณ์ คณะวิทยาศาสตร์

2. รางวัลนักวิจัยดีเด่นด้านการวิจัยเชิงประยุกต์ ได้แก่
   2.1 รองศาสตราจารย์ ดร.วรี ติยะบุญชัย คณะเภสัชศาสตร์
   2.2 ดร.ปิยะเมธ ดิลกธรสกุล คณะเภสัชศาสตร์

3. รางวัลนักวิจัยดีเด่นด้านการวิจัยที่สร้างประโยชน์สู่เชิงพาณิชย์หรือ สร้างประโยชน์ให้แก่ชุมชน คือ ดร.อุทัย วิชัย คณะวิทยาศาสตร์

4. รางวัลผลงานวิจัยดีเด่นประเภทสร้างคณะวิจัยระหว่างสถาบัน คือ ผู้ช่วยศาสตราจารย์ ดร.ธีระชัย บงการณ์ คณะวิทยาศาสตร์

นักวิจัยดีเด่นด้านการวิจัยเชิงวิชาการพื้นฐาน

รองศาสตราจารย์ ดร.เมธา รัตนากรพิทักษ์
ภาควิชาเคมี คณะวิทยาศาสตร์ มหาวิทยาลัยนเรศวร

งานวิจัยนี้เป็นการศึกษาการออกแบบและสังเคราะห์ฟังก์ชันนอลพอลิเมอร์เพื่อดัดแปรพื้นผิวอนุภาคนาโนแมกนีไทท์ ด้วยเทคนิคที่หลากหลาย เช่น เทคนิคการพอลิเมอไรเซชันออกจากพื้นผิว ("grafting from") และการตรึงสายโซ่พอลิเมอร์ บนพื้นผิว ("grafting to") ด้วยพอลิเมอร์หลากหลายชนิด เช่น poly(N-isopropylacrylamide), poly(acrylic acid) เป็นต้น โดยเน้นการออกแบบพื้นผิวอนุภาคเพื่อให้มีสมบัติเฉพาะต่อการใช้งานทางด้านการแพทย์ เช่น

1) การออกแบบพื้นผิวเพื่อให้มีหมู่ฟังก์ชันที่ตอบสนองต่อการเปลี่ยนแปลงสภาวะความเป็นกรดเบส (pH) อุณหภูมิ หรือการกระตุ้นด้วยแสงยูวีเพื่อใช้เป็นตัวควบคุมในการปลดปล่อยยาที่กักเก็บไว้ (รูปที่ 1)

2) การออกแบบพื้นผิวอนุภาคเคลือบด้วยพอลิเมอร์แบบสองชั้นเพื่อการกักเก็บยาไว้ในพอลิเมอร์ชั้นใน เพื่อใช้ในการควบคุมการปลดปล่อยยา (รูปที่ 2A) และ

3) การออกแบบพื้นผิวให้มีหมู่ฟังก์ชันเพื่อใช้ในการตรึงสารชีวโมเลกุลบนพื้นผิวอนุภาค (รูปที่ 2B) เช่น ดีเอ็นเอ โปรตีน กรดอะมิโน โมเลกุลยา เป็นต้น โดยสามารถกำหนดอนุภาคให้อยู่ในตำแหน่งหรืออวัยวะที่ต้องการได้ (localization) โดยการเทียบนำด้วยสนามแม่เหล็กภายนอก ซึ่งจะทำยาถูกปลดปล่อยออกมา ณ อวัยวะเป้าหมายได้อย่างมีประสิทธิภาพ

รูปที่ 1A แสดงรูปตัวอย่างอนุภาคนาโนแมกนีไทท์ที่เคลือบด้วยพอลิเมอร์ ซึ่งถ่ายด้วยกล้องจุลทรรศน์อิเล็คตรอนแบบส่องผ่าน (TEM) แสดงถึงการกระจายตัวได้ดีในตัวกลางที่เป็นน้ำ นอกจากนี้ ตัวอย่างงานวิจัยที่เกี่ยวกับการเคลือบอนุภาคนาในแมกนีไทท์ด้วย poly(N-isopropylacrylamide) ซึ่งเป็นพอลิเมอร์ที่สามารถตอบสนองต่อการเปลี่ยนแปลงอุณหภูมิของสิ่งแวดล้อมได้ที่อุณหภูมิวิกฤติ (32oC) โดยในรูปที่ 1B และ 1C แสดงพฤติกรรมการตอบสนองของพอลิเมอร์เมื่อมีการเปลี่ยนแปลงอุณหภูมิของสิ่งแวดล้อม มีผลทำให้พอลิเมอร์ปลดปล่อยยาที่กักเก็บไว้ในอัตราที่แตกต่างกัน เนื่องจากเกิดการหดตัวของพอลิเมอร์ที่เคลือบไว้บนพื้นผิวอนุภาคเมื่ออุณหภูมิผ่านอุณหภูมิวิกฤติ

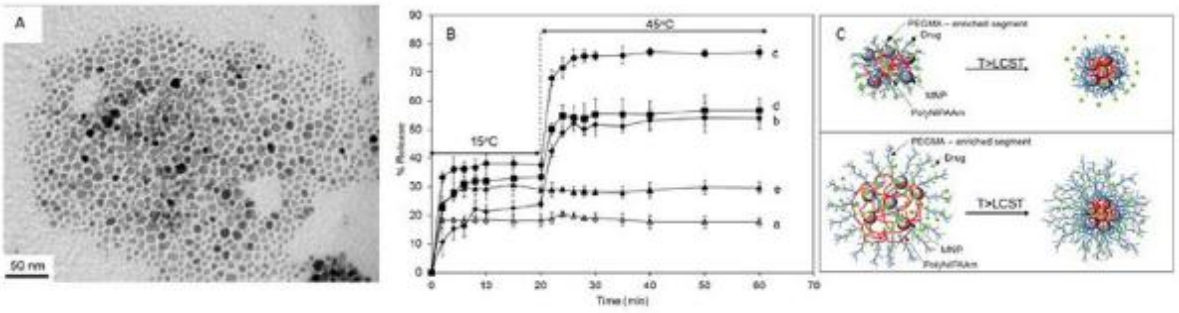

รูปที่ 1 (A) อนุภาคนาโนแมกนีไทท์ขนาดเส้นผ่าศูนย์กลาง 10 นาโนเมตร ถ่ายด้วยกล้องจุลทรรศน์อิเล็คตรอน แบบส่องผ่าน (TEM), (B) และ (C) การตอบสนองต่อการเปลี่ยนแปลงอุณหภูมิของสิ่งแวดล้อม ทำให้พอลิเมอร์ที่เคลือบบนอนุภาคปลดปล่อยยาที่กักเก็บไว้ในอัตราที่แตกต่างกัน เนื่องจากการหดตัวของพอลิเมอร์ที่เคลือบไว้บนพื้นผิวอนุภาคเมื่ออุณหภูมิผ่านอุณหภูมิวิกฤติ

รูปที่ 2A แสดงรูปอนุภาคนาโนแมกนีไทท์ที่เคลือบด้วยพอลิเมอร์แบบสองชั้นโดยมีพอลิเอสเตอร์เป็นพอลิเมอร์ชั้นใน เพื่อใช้ในการตรึงโมเลกุลยา และพอลิเอทิลีนไกลคอลเมทิลอีเทอร์เป็นพอลิเมอร์ชั้นนอกเพื่อการกระจายตัวได้ดีในน้ำ ส่วนรูปที่ 2B แสดงการออกแบบพอลิเมอร์บนพื้นผิวอนุภาคเพื่อใช้ในการตรึงโมเลกุลของกรดโฟลิคซึ่งใช้เป็นสารต้นแบบ

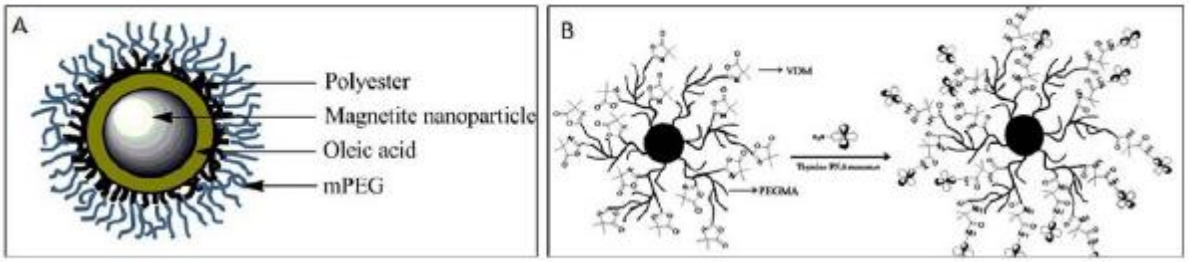

รูปที่ 2 (A) อนุภาคนาโนแมกนีไทท์ที่เคลือบด้วยพอลิเมอร์แบบสองชั้น และ (B) อนุภาคนาโนแมกนีไทท์ที่ดัดแปลงด้วยสารชีวโมเลกุลบนพื้นผิว

ผลกระทบขององค์ความรู้นี้ต่อความก้าวหน้าในเชิงวิชาการ ได้แก่ ได้แนวทางการออกแบบและการสังเคราะห์พอลิเมอร์ที่มีสมบัติจำเพาะบนพื้นผิวอนุภาคนาโนแมกนีไทท์ ซึ่งองค์ความรู้พื้นฐานเหล่านี้จะนำไปสู่การพัฒนาการสังเคราะห์และออกแบบโมเลกุลพอลิเมอร์บนพื้นผิวอนุภาคนาโนชนิดอื่นหรือโครงสร้างระดับโมเลกุลแบบอื่นๆที่ซับซ้อนมากขึ้น และตอบสนองความต้องการในการประยุกต์ใช้งานเฉพาะด้านต่อไป ซึ่งความรู้เหล่านี้จะสามารถประยุกต์ใช้และได้วัสดุที่มีประสิทธิภาพดีกว่าเทคโนโลยีที่ใช้ในปัจจุบัน ซึ่งจะนำไปสู่การพัฒนาทางด้านนาโนเทคโนโลยีของประเทศไทยให้สามารถแข่งขันได้ในระดับสากลได้

โดยงานวิจัยนี้ได้รับทุนสนับสนุนจาก สำนักงานกองทุนสนับสนุนการวิจัย (สกว.) ร่วมกับสำนักงานคณะกรรมการการอุดมศึกษา (สกอ.) และมหาวิทยาลัยนเรศวร ศูนย์นาโนเทคโนโลยีแห่งชาติ (นาโนเทค) ศูนย์ความเป็นเลิศด้านนวัตกรรมทางเคมี และโครงการปริญญาเอกกาญจนาภิเษก (คปก.)

รูปที่ 3 นักวิจัยจากซ้ายไปขวา ดร.ฐาปนพงศ์ เทพบุตร์ นายรฐนนท์ จันท์แก้ว ดร.ภาวิณี เทียนดี รศ.ดร.เมธา รัตนาภรพิทักษ์ นายบัณฑิต ทองอ่อน ดร.นันทรักษ์ รอดเกตุ ดร.ศิรประภา มีรอด และ นางสาวสุดารัตน์ ชัดสาย

งานวิจัยนี้ได้รับรางวัลระดับดี สาขาเคมีและเภสัช จากสำนักงานคณะกรรมการวิจัยแห่งชาติ (วช) ประจำปี 2555 และได้รับการตีพิมพ์ในวารสารระดับนานาชาติที่มีค่า impact factor แล้วมากกว่า 30 เรื่อง นอกจากนี้งานวิจัยนี้ยังทำให้เกิดความร่วมมือด้านงานวิจัย ระหว่างมหาวิทยาลัยนเรศวร และมหาวิทยาลัยที่มีชื่อเสียงจากต่างประเทศ เช่น University of Maine ประเทศฝรั่งเศส, University of New South Wales (UNSW) ประเทศออสเตรเลีย, Aston University ประเทศอังกฤษ โดยมีการแลกเปลี่ยนนิสิตปริญญาโทและเอกระหว่างสถาบันและมีผลงานวิจัยตีพิมพ์ร่วมกัน

5.4) นางสาวนันทิยา ดีบุบผาและนายวสวัตติ์ อินทรานุสรณ์ ได้รับรางวัลการนำเสนอผลงานวิจัยแบบบรรยายยอดเยี่ยม จากงานประชุมวิชาการ 9th Science Research Conference, 25-26 May 2017, Burapha University, Chonburi, Thailand

คณะวิทยาศาสตร์ มหาวิทยาลัยบูรพา

ขอมอบเกียรติบัตรฉบับนี้ให้ไว้เพื่อรับรองว่าผลงานวิจัย

เรื่อง การสังเคราะห์นาโนคอมโพสิตแม่เหล็กที่ตอบสนองต่อสิ่งกระตุ้นหลากหลายที่มีการเชื่อมโยงระหว่างโมเลกุล

โดย คุณนันทิยา ดีบุบผา

ได้ผ่านการพิจารณาจากคณะกรรมการผู้ทรงคุณวุฒิ ให้รับรางวัลระดับดีมาก การนำเสนอผลงานแบบบรรยาย กลุ่มสาขาเคมี เคมีเชิงวัสดุ และเคมีศึกษา ในการประชุมวิชาการระดับชาติ "วิทยาศาสตร์วิจัย" ครั้งที่ ๙ ระหว่างวันที่ ๒๕ - ๒๖ พฤษภาคม พ.ศ. ๒๕๖๐

(ผู้ช่วยศาสตราจารย์ ดร.เอกรัฐ ศรีสุข)
คณบดีคณะวิทยาศาสตร์ มหาวิทยาลัยบูรพา

คณะวิทยาศาสตร์ มหาวิทยาลัยบูรพา

ขอมอบเกียรติบัตรฉบับนี้ให้ไว้เพื่อรับรองว่าผลงานวิจัย

เรื่อง Surface modication of magnetite nanoparticles with poly (2-Acrylamido-2-methylpropane sulfonic acid, AMPS) for adsorption with antibody

โดย คุณวสวัตติ์ อินทรานุสรณ์

ได้ผ่านการพิจารณาจากคณะกรรมการผู้ทรงคุณวุฒิ ให้รับรางวัลระดับดีเด่น กลุ่มการนำเสนอผลงานแบบบรรยายภาคภาษาอังกฤษของนิสิตปริญญาตรี ในการประชุมวิชาการระดับชาติ "วิทยาศาสตร์วิจัย" ครั้งที่ ๙ ระหว่างวันที่ ๒๕ - ๒๖ พฤษภาคม พ.ศ. ๒๕๖๐

(ผู้ช่วยศาสตราจารย์ ดร.เอกรัฐ ศรีสุข)
คณบดีคณะวิทยาศาสตร์ มหาวิทยาลัยบูรพา

5.5) นางสาวสุดารัตน์ ขัดสาย ได้รางวัลการนำเสนอผลงานวิจัยแบบโปสเตอร์ยอดเยี่ยมจาก The First Materials Research Society of Thailand International Conference (1st MRS Thailand International Conference), Poster, 31 October-3 November 2017, Convention Center, The Empress Hotel, Chiang Mai, Thailand


MRS Thailand 2017

The First Materials Research Society of Thailand International Conference

Best Poster Presentation Award

presented to

Sudarat Khadsai, Boonjira Rutnakornpituk, Tirayut Vilaivan, Maliwan Nakkuntod and Metha Rutnakornpituk

Anionic magnetite nanoparticle conjugated with pyrrolidinyl PNA for real DNA pre concentration

31st October – 3rd November 2017, The Empress Hotel, Chiang Mai, Thailand

(Prof. Dr. Santi Maensiri)
President
Materials Research Society of Thailand

6) 5 International/National Collaborations

6.1) We have research collaboration with Prof.Dr.Martina Stenzel from the Department of Chemistry, The University of New South Wales (UNSW), Sydney, Australia. We have an exchange student, Mr.Bandit Thong-On, a PhD student awarded by a Royal Golden Jubilee PhD Program to do his research at Prof.Stenzel's laboratory for 9 months (March - November 2015). In addition, we now have an MOU between Naresuan University and The University of New South Wales (UNSW).

6.2) We had an exchange program for Miss Sudarat Khadssai, a PhD student awarded by a Royal Golden Jubilee PhD Program to do her research at Aston University during April 2016-March 2017 (1 year) under the supervision of Prof.Dr.Paul Topham, Department of Polymer Chemistry, Aston University. In addition, we have been granted for the Newton Fund for a Scholar and a supervisor. These fundings were sponsored by The Thailand Research Fund (TRF) and co-funded by the Newton Fund (the British Council). We also have an MOU between Naresuan University and Aston University.

6.3) We now have research collaboration with Prof.Dr.Philippe Daniel, a Professor at the Universite du Maine, Le Mans, France. With his proposal approved by the Region Pays de La Loire (France), he can now gather the researchers in many Universities in South East Asia to do research under the project entitled "New functional materials for food safety: the collaboration with South East Asia (InnovASIA)". Naresuan University is one of the collaborative institutes in this mega project. We believe that with the collaboration with the Universities in

South East Asia, we can extend our research interest and collaboration to the Universities in our neighbor countries in the future.

6.4) We now have research collaboration by exchanging a Ph.D. student to do research at Prof.Dr.Oliver Reiser's lab (the University of Regensburg, Germany). Miss Sujittra Paenkaew from my group is now joining Prof.Reiser's group during April 2018-March 2019 with the support from RGJ#16 with the research entitled "Polymer-coated magnetic nanoparticle for catalytic applications".

6.5) Professor Dr. Tirayut Vilaivan from the Department of Chemistry, Chulalongkron University, is a well-known chemist in the PNA research area. I have been honored to be a part of a TRF grant for a Distinguished Professor (2014-2018) having Prof.Vilaivan as a principal investigator.

7) การนำผลงานไปใช้ประโยชน์และการผลิตนักวิจัย

ผลงานวิจัยนี้ทำให้เกิดประโยชน์ในเชิงวิชาการ โดยการสร้างองค์ความรู้ที่เน้นการออกแบบโครงสร้างพอลิเมอร์ที่มีส่วนประกอบของกรดอะมิโนและพอลิเมอร์ที่ตอบสนองต่อสิ่งกระตุ้นภายนอกเพื่อเคลือบบนพื้นผิวอนุภาคนาโนแมกนีไทท์ เพื่อให้คุณสมบัติเหมาะสมต่อการประยุกต์ใช้งานเฉพาะทาง และมีผลิตผลงานวิจัยเพื่อตีพิมพ์ในวารสารระดับนานาชาติที่มีคุณภาพ จำนวน 5 เรื่อง นอกจากนี้ยังมีการสร้างนักวิจัยรุ่นใหม่ ระดับปริญญาโทและระดับปริญญาเอก สาขาเคมี ดังนี้

<u>ปริญญาโทจำนวน 1 คน</u>

นางสาวนันทิยา ดีบุบผา

<u>ปริญญาเอก จำนวน 5 คน</u>

1. ดร.สุดารัตน์ ขัดสาย
2. ดร.ยิ่งรัก พรายอินทร์
3. ดร.บัณฑิต ทองอ่อน
4. ดร.ศิรประภา มีรอด
5. นางสาวสุจิตรา แป้นแก้ว (คาดว่าจะจบการศึกษา ปี 2562)

ภาคผนวก

ผลงานวิจัยเรื่องที่ 1

Y. Prai-In, C. Boonthip, B. Rutnakornpituk, U. Wichai, V. Montembault, S. Pascual, L. Fontaine* and M. Rutnakornpituk*, “Recyclable magnetic nanocluster crosslinked with poly(ethylene oxide)-block-poly(2-vinyl-4,4-dimethylazlactone) copolymer for adsorption with antibody”, *Materials Science & Engineering C* (2016) 67, 285-293 (IF 5.085, year 2017)

Materials Science and Engineering C 67 (2016) 285–293

Contents lists available at ScienceDirect

Materials Science and Engineering C

journal homepage: www.elsevier.com/locate/msec

Recyclable magnetic nanocluster crosslinked with poly(ethylene oxide)-*block*-poly(2-vinyl-4,4-dimethylazlactone) copolymer for adsorption with antibody

Yingrak Prai-in [a], Chatchai Boonthip [a], Boonjira Rutnakornpituk [a], Uthai Wichai [a], Véronique Montembault [b], Sagrario Pascual [b], Laurent Fontaine [b,*], Metha Rutnakornpituk [a,*]

[a] Department of Chemistry and Center of Excellence in Biomaterials, Faculty of Science, Naresuan University, Phitsanulok 65000, Thailand
[b] Institut des Molécules et des Matériaux du Mans, UMR CNRS 6283, Equipe Méthodologie et Synthèse des Polymères, Université du Maine, Avenue Olivier Messiaen, 72085 Le Mans Cedex, France

ARTICLE INFO

Article history:
Received 18 December 2014
Received in revised form 23 February 2016
Accepted 6 May 2016
Available online 07 May 2016

Keywords:
Magnetite
Nanocluster
Azlactone
RAFT
Antibody
Adsorption

ABSTRACT

Surface modification of magnetic nanoparticle (MNP) with poly(ethylene oxide)-*block*-poly(2-vinyl-4,4-dimethylazlactone) (PEO-*b*-PVDM) diblock copolymers and its application as recyclable magnetic nano-support for adsorption with antibody were reported herein. PEO-*b*-PVDM copolymers were first synthesized *via* a reversible addition-fragmentation chain-transfer (RAFT) polymerization using poly(ethylene oxide) chain-transfer agent as a macromolecular chain transfer agent to mediate the RAFT polymerization of VDM. They were then grafted on amino-functionalized MNP by coupling with some azlactone rings of the PVDM block to form magnetic nanoclusters with tunable cluster size. The nanocluster size could be tuned by adjusting the chain length of the PVDM block. The nanoclusters were successfully used as efficient and recyclable nano-supports for adsorption with anti-rabbit IgG antibody. They retained higher than 95% adsorption of the antibody during eight adsorption-separation-desorption cycles, indicating the potential feasibility in using this novel hybrid nanocluster as recyclable support in cell separation applications.

1. Introduction

Magnetic nanoparticles (MNPs) have potential applications in a wide range of biomedical areas, such as hyperthermia treatment of tumor [1], contrast enhancement agents in magnetic resonance imaging (MRI) [2], immunoassay magnetic marker [3], site-specific drug delivery system [4] and magnetic separation [5]. However, there are limitations in applying external magnetic field to MNPs in biomedical uses because unmodified MNPs are not stable in physiological fluids, leading to their aggregation in aqueous dispersion due to attractive forces, *e.g.* dipole-dipole interaction and magnetic force [6]. Therefore, surface modification of MNPs is a crucial requirement to use these particles as biomedical materials. One of the most common useful methods for surface modification is grafting polymers onto the particle surface, not only to protect the particle against aggregation, but also to provide a platform for further surface functionalization.

In general, there are two approaches for attachment of polymers to particle surface, including the so-called "grafting-from" and "grafting-onto" strategies [7–10]. The "grafting-from" strategy involves the growth of polymer from particle surface [7,8], while in the "grafting-onto" strategy, a pre-synthesized polymer is first prepared in solution and then grafted onto particle surface [9,10]. The combination of these two strategies with controlled radical polymerization (CRP) techniques, such as atom transfer radical polymerization (ATRP) and reversible addition-fragmentation chain transfer (RAFT) polymerization, has been widely used to prepare well-defined polymers coated onto MNP surface [11–14]. RAFT polymerization is one of several types of CRP techniques that produce polymers with controllable molecular weights and narrow polydispersity indices (PDIs). Moreover, RAFT polymerization is applicable to a wide range of vinyl monomers without using metal catalysts. It can also be performed under mild condition reactions in various reaction systems, including aqueous solution, organic solvents, suspensions, emulsions and ionic liquids [15–23].

Another limitation of applications of MNPs in biomedical applications is the low magnetic sensitivity of single nanoparticles, resulting in difficulties concerning their targeted delivery of MNPs by using a permanent magnetic field. The particle size should be sufficiently large in order to yield high magnetization. However, the particles are unstable when their size is too large due to attractive forced among the particles, leading to macroscopic aggregation and thus loss in nano-scale related properties. Controllable formation of nanoclustering is another potential approach to enhance magnetic sensitivity of MNPs. High saturation magnetization of these magnetic nanoclusters is essential to efficiently separate them from dispersions or localize them to a target-organ.

* Corresponding author.
E-mail addresses: laurent.fontaine@univ-lemans.fr (L. Fontaine), methar@nu.ac.th (M. Rutnakornpituk).

http://dx.doi.org/10.1016/j.msec.2016.05.032
0928-4931/

In the present day, many works have reported the use of MNPs for separation of bio-entities such as DNA, RNA and proteins [24,25,5]. In addition, the potential of specific antibody-conjugated MNP for cell separation [26] and magnetic marker [3] was extensively studied. For example, Puertas et al. [27] have recently reported the synthesis of carboxylated MNP for ionic adsorption with antibodies through their richest positive charged regions. The adsorption of antibodies was applicable at the pH lower than its isoelectric point and the antibodies could be easily eluted by increasing the ionic strength and/or changing the net charge of the antibodies by changing the solution pH. Moreover, Xu et al. [26] have also synthesized antibody-conjugated MNPs for use as a platform to separate circulating tumor cells (CTCs) from fresh whole blood. MNPs having reactive carboxyl groups were conjugated with antibody against human epithelial growth factor receptor 2 (anti-HER2) through an amidation reaction. The particle was then used to isolate HER2 from human breast cancer cell line SK-BR3. It was found that the capture of the HER2 was obtained only when the MNP was conjugated with the specific antibody.

In this work, we used the "grafting-onto" strategy to modify MNP surface with poly(ethylene oxide)-*block*-poly(2-vinyl-4,4-dimethylazlactone) (PEO-*b*-PVDM) copolymers to form magnetic nanoclusters with tunable cluster size. The copolymers were synthesized *via* RAFT polymerization to produce well-defined diblock structures with controlled PVDM block lengths. PEO allows the particles to well disperse in aqueous medium and some azlactone rings in the PVDM block serve as reactive electrophilic sites for further coupling with amino groups grafted on MNP surface. It was hypothesized that the chain length of the reactive PVDM block should somewhat influence the nanoclustering formation, which essentially affected its magnetic properties and water dispersibility. Degree of nanoclustering and magnetic sensitivity of the MNP clusters were optimized such that water dispersible nanoclusters with high magnetic separation efficiency were obtained. In this study, the efficiency of the magnetic nanoclusters for separation of anti-rabbit IgG antibody from the dispersion and their recycling ability were also determined (Scheme 1).

2. Experimental

2.1. Materials

Unless otherwise noted, all reagents were used without further purification: iron (III) acetylacetonate ($Fe(acac)_3$, 99.9%, Acros), benzyl alcohol (98%, Unilab), oleic acid (90%, Fluka), (3-aminopropyl)triethoxysilane (APS, 99%, Sigma-Aldrich), triethylamine (TEA, ≥99%, Sigma-Aldrich), 4,4′-azobis(4-cyanovaleric acid) (ACVA, ≥98%, Aldrich), anti-rabbit IgG (antibody produced in goat, Sigma-Aldrich), IgG from rabbit serum (Sigma-Aldrich), *anti*-IgG-HRP (anti-rabbit IgG (whole molecule)-peroxidase (Sigma-Aldrich), 10% BSA diluents (KPL), ABTS® Peroxidase Substrate (KPL), Bradford reagent (Sigma), bovine gamma globulin (BGG, Thermo Scientific) and 2-(*N*-morpholino)ethanesulfonic acid (MES, 99%, Acros). 2-Dodecylsulfanylthiocarbonylsulfanyl-2-methylpropionic acid (DMP) [28], poly(ethylene oxide) chain transfer agent (PEO-CTA) [29] and 2-vinyl-4,4-dimethylazlactone (VDM) [30] were synthesized following the reported procedures. Pure water was obtained from a Millipore Direct Q system. 1,4-Dioxane (99.8%, Sigma-Aldrich), *n*-hexane (95%, Acros), *N*,*N*-dimethylformamide (DMF, 99.8%, Aldrich), toluene (99.8%, Sigma-Aldrich), ethanol (≥ 99.5%, Sigma-Aldrich), and dichloromethane (CH_2Cl_2, ≥99.5%, Sigma-Aldrich) were used as received.

2.2. Characterization

Fourier transform infrared (FTIR) spectroscopy was performed on a Perkin-Elmer Model 1600 Series FTIR Spectrophotometer. The solid samples were mixed with KBr to form pellets. Nuclear magnetic resonance (NMR) spectra were performed on a 400 MHz Bruker NMR spectrometer for ^1H NMR (400 MHz). Chemical shifts are reported in ppm relative to deuterated solvent resonances. Molar masses and molar mass distributions were determined *via* size exclusion chromatography (SEC) operating at 35 °C on a system equipped with a Spectra System AS1000 autosampler with a guard column (Polymer Laboratories, PL gel 5 μm guard, 50 × 7.5 mm) followed by two columns (Polymer Laboratories, two PL gel 5 μm Mixed–D columns, 2 × 300 × 7.5 mm) and a refractive index detector (SpectraSystem RI-150). Polystyrene standards (580–483 × 10^3 $g \cdot mol^{-1}$) were used to calibrate the SEC. Transmission electron microscopy (TEM) was performed on a Philips Tecnai 12 operated at 120 kV equipped with a Gatan model 782 CCD camera. Thermogravimetric analysis (TGA) was performed on SDTA 851 Mettler-Toledo at the temperature ranging between 25 and 600 °C at a heating rate of 20 °C/min under oxygen atmosphere. Vibrating sample magnetometer (VSM) measurements were performed at room temperature using a Standard 7403 Series, Lakeshore vibrating sample magnetometer. Hydrodynamic diameter (D_h) and zeta potential of the particles were measured *via* a photo correlation spectroscopy (PCS) using NanoZS4700 nanoseries Malvern instrument. The sample dispersions were sonicated for 30 min before the measurements at 25 °C without filtration. The ability of antibody adsorption to MNP was investigated with an ultraviolet-visible (UV–vis) spectrophotometer on Perkin Elmer model Lamda 20 at λ = 595 nm.

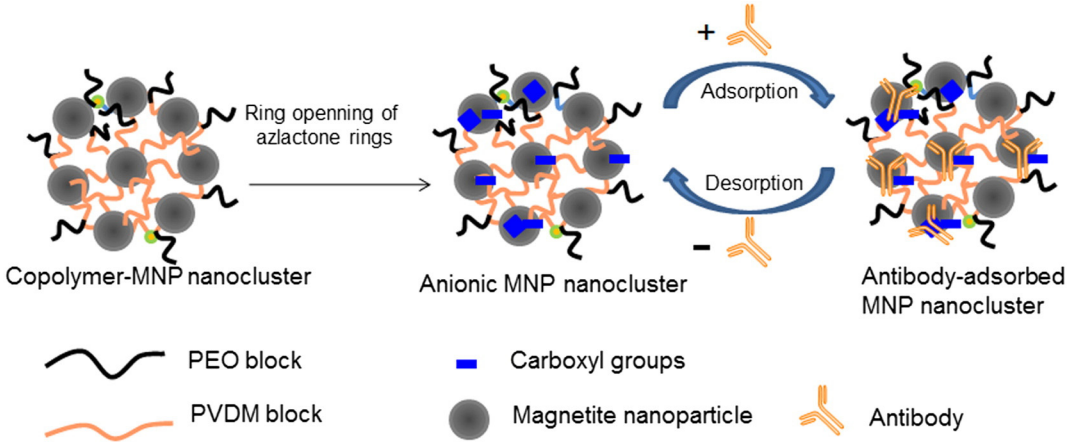

Scheme 1. Schematic illustration of PEO-*b*-PVDM diblock copolymer-MNP nanocluster for antibody adsorption and its recycling.

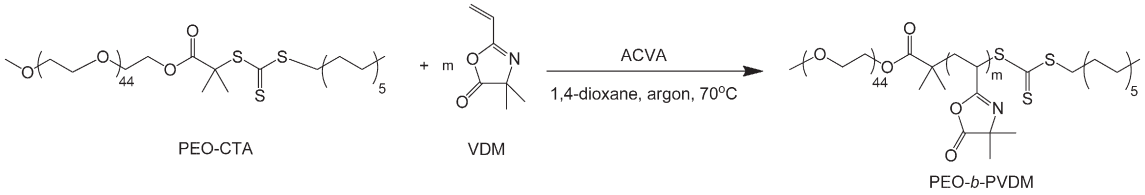

Scheme 2. Synthesis of PEO-*b*-PVDM diblock copolymers by RAFT polymerization.

2.3. Synthesis and properties of copolymers-MNP nanoclusters

2.3.1. Synthesis of PEO-b-PVDM diblock copolymers by RAFT polymerization (Scheme 2)

An example of the synthesis of PEO-*b*-PVDM block copolymer using a molar ratio of $[VDM]_0$:$[PEO\text{-}CTA]_0$:$[ACVA]_0$ equal to 100:1:0.2 M ratio is herein explained. VDM (0.74 g, 5.34×10^{-3} mol), PEO-CTA (0.126 g, 5.34×10^{-5} mol), ACVA (3 mg, 1.07×10^{-5} mol), 1,4-dioxane (3.0 mL) and DMF (0.2 mL) used as an internal reference were added to a Schlenk tube equipped with a stir bar. The mixture was deoxygenated by bubbling argon for 30 min. The solution was then immersed in an oil bath thermostated at 70 °C for 4 h to allow the polymerization to occur. Conversion of VDM was determined to be 41% by ^{1}H NMR spectroscopy by comparing the integration area value of the vinylic protons of VDM at 5.93 ppm with the integration area value of the CH proton of DMF at 8.01 ppm. After precipitation in *n*-hexane, the polymer was dried *in vacuo* at room temperature for 12 h to yield a yellow powder product. The final polymer was analyzed by SEC, FT-IR spectroscopy and ^{1}H NMR spectroscopy. $\overline{M_n}_{,SEC} = 8800\ g \cdot mol^{-1}$, PDI = 1.09. FTIR ($\nu$, cm^{-1}): $\nu_{(C=N;\ azlactone)} = 1201$, $\nu_{(C\_N;\ azlactone)} = 1699$ and $\nu_{(C\_O;\ azlactone)} = 1817$. ^{1}H NMR (400 MHz, $CDCl_3$, δ (ppm)): 0.86 ($CH_3(CH_2)_{10}CH_2S$), 1.40 ($OCOC(CH_3)_2N$), 1.80–2.80 ($CH_2CH)_n$, 3.38 ($CH_3O(CH_2CH_2O)_{44}$) and 3.65 ($CH_3O(CH_2CH_2O)_{44}CH_2CH_2OC(O)C(CH_3)_2$).

2.3.2. Synthesis of (3-aminopropyl)triethoxysilane-grafted MNP (APS-grafted MNP)

Amino-grafted MNPs were synthesized through a three-step process: (1) synthesis of MNP core, (2) grafting of oleic acid onto the MNP and (3) a ligand exchange reaction with APS. First, a thermal decomposition of $Fe(acac)_3$ (5 g, 14.05 mmol) in benzyl alcohol (90 mL) was performed at 180 °C for 48 h to obtain MNP core. The particle was magnetically separated from the dispersion and washed with ethanol and CH_2Cl_2 repetitively to remove benzyl alcohol and then dried *in vacuo*. Oleic acid (4 mL) was then dropped to a MNP-toluene dispersion (0.8 g of MNPs in 30 mL of toluene) previously sonicated, to form oleic acid-grafted MNPs. APS (0.6 g, 2.71×10^{-3} mol) was then added to the oleic acid-grafted MNP dispersed in toluene (0.8 g of the MNP in 30 mL of toluene) containing 2 M TEA (5 mL) to form APS-grafted MNPs. After stirring for 24 h, the particles were precipitated in ethanol and washed with toluene to remove oleic acid and ungrafted APS from the dispersion. FTIR (ν, cm^{-1}): $\nu_{(Fe-O)} = 586$, $\nu_{(Si-O\ stretching)} = 1103–1079$, $\nu_{(CH3\ stretching)} = 2974–2886$ and $\nu_{(N-H\ stretching)} = 3363$.

2.3.3. Formation of PEO-b-PVDM copolymers-MNP nanoclusters (Scheme 3)

APS-grafted MNP (100 mg) was dispersed in 10 mL 1,4-dioxane by sonication. Then, a PEO-*b*-PVDM diblock copolymer solution (100 mg of the copolymer in 10 mL of 1,4-dioxane) was added to the APS-grafted MNP dispersion under stirring at room temperature for 12 h. The copolymer-MNP nanocluster was magnetically separated from the dispersion and washed with 1,4-dioxane. This process was repeatedly performed to remove ungrafted copolymer from the MNP nanocluster. The copolymer-MNP nanocluster was then dried *in vacuo* at room temperature for 12 h.

2.3.4. Study in adsorption percentage of the copolymer-MNP nanoclusters with antibody

The copolymer-MNP nanocluster was first dispersed in water for 12 h to form carboxylated-enriched nanocluster due to the ring-opening reaction of the remaining azlactone rings in the copolymer on particle surface. After drying process, 10 mg of the copolymer-MNP nanoclusters were incubated in 1 mL of 10 mM MES pH 6 solution

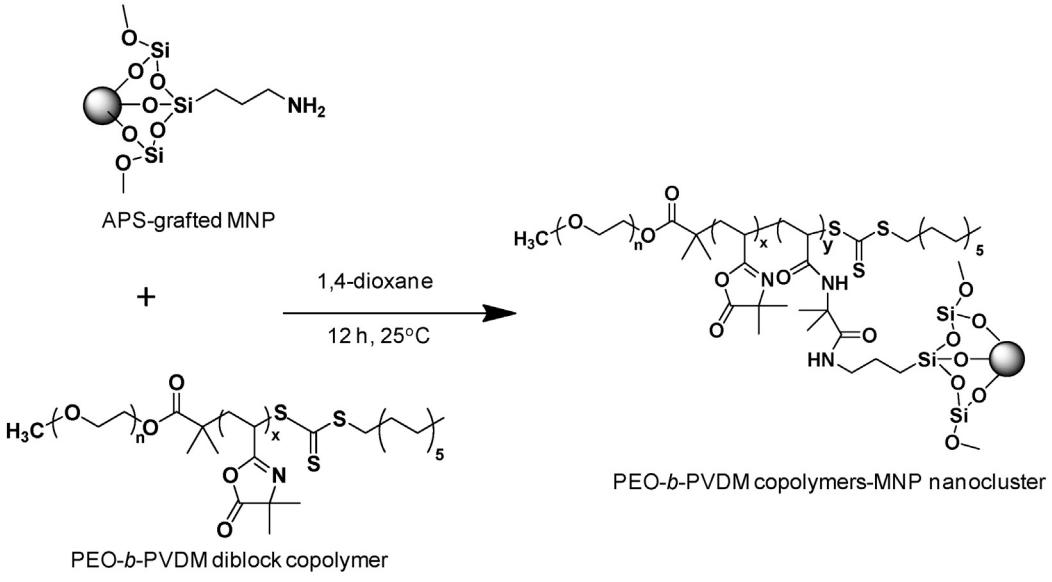

Scheme 3. Synthesis of PEO-*b*-PVDM copolymers-MNP nanocluster.

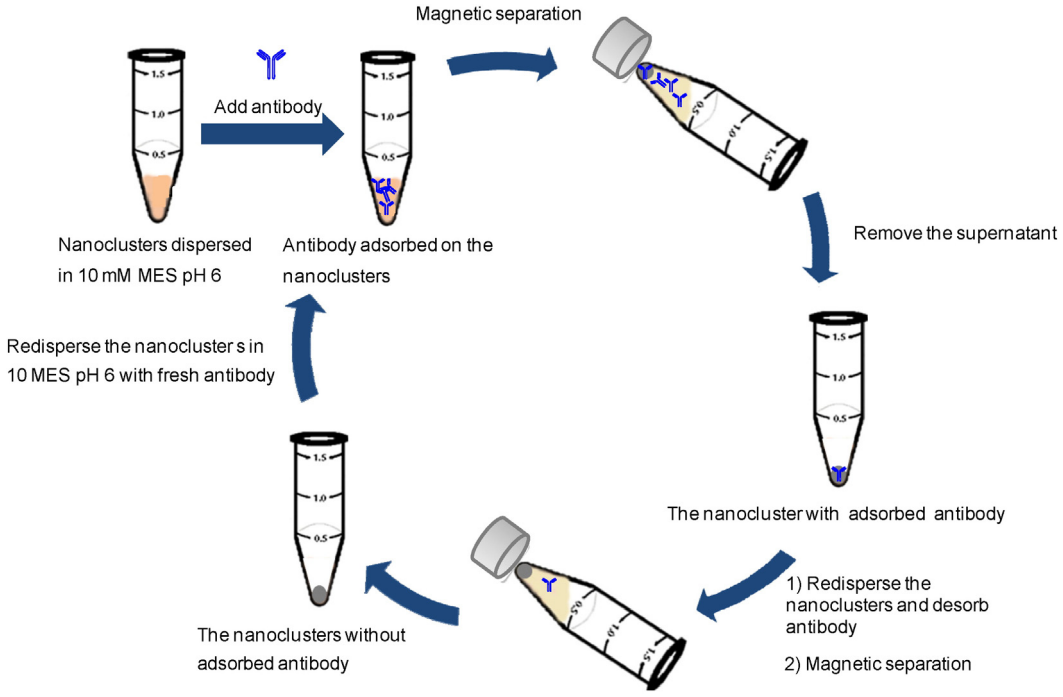

Scheme 4. Schematic illustration of an adsorption-separation-desorption cycle of the recyclable copolymer-MNP nanocluster in adsorption with antibody (anti-rabbit-IgG).

containing anti-rabbit IgG antibody for 2 h at room temperature. The Bradford assay [31] was used to determine antibody adsorption percentage of the particles with antibody. The protein concentration of all samples was determined using a calibration curve of BGG as a protein standard (in the Supporting information). The copolymer-MNP nanoclusters after adsorption with antibody were separated from the supernatant using an external magnet and characterized *via* FTIR, VSM and TGA (see the Supporting information). The absorption at 595 nm of the antibody solution before and after adsorption process was measured using the Bradford assay. The adsorption percentage of the antibody on the nanoclusters can be directly calculated using the following equation:

$$\text{Adsorption percentage} = [(A-B)/A] \times 100 \quad (1)$$

where A is the initial concentration of antibody and B is the concentration of antibody in the supernatant at time *t* (non-adsorbed antibody).

2.3.5. Determination of recycling ability of the PEO-b-PVDM copolymer-MNP nanoclusters in adsorption with anti-rabbit IgG antibody

Copolymer-MNP nanoclusters adsorbed with anti-rabbit IgG antibody were thoroughly washed with 1 mL of a washing solution to desorb the antibody on the nanocluster surface. Desorption percentage of the antibody on the nanoclusters was determined using the Bradford assay and calculated from the following equation:

$$\text{Desorption percentage} = (C/B) \times 100 \quad (2)$$

where C is the concentration of desorbed antibody and B is the concentration of adsorbed antibody. The adsorption-separation-desorption process was performed repeatedly to determine the recycling efficiency of the nanoclusters as illustrated in Scheme 4.

2.3.6. Antigen recognition capacity study of antibody-adsorbed magnetic nanoclusters

After antibody adsorption procedure, the remaining carboxyl groups of magnetic nanoclusters were blocked with 1 mL of 1% BSA in 10 mM MES pH 6 at 25 °C for 16 h. MNP nanoclusters were then washed with 10 mM MES pH 6 to remove an excess BSA. To detect the antigen recognition capacity of antibody-adsorbed MNP nanoclusters, an indirect detection method was used. First, 1 mL of 400 ppm of primary antigen (2.00 times molar excess) in 10 mM MES pH 6 was added into anti rabbit-IgG antibody-adsorbed MNP nanoclusters and incubated for 30 min. After washing the particles with 10 mM MES pH 6, they were incubated with 1 mL of 400 ppm of anti-rabbit-HRP antibody for another 30 additional min. The presence of antigen on the particle surface was visualized by adding 1 mL of ABTS-H_2O_2 solution into 10 μl of the MNP nanocluster dispersion.

Table 1
Diblock copolymers based on PEO and VDM synthesized by RAFT polymerization at 70 °C in 1,4-dioxane: experimental conditions and characterizations.

Run	Copolymer[a]	$[VDM]_0$: $[PEO\text{-}CTA]_0$: $[ACVA]_0$	Reaction time (h)	VDM conv.[b] (%)	$\overline{M_n}_{,th}$[c] (g/mol)	$\overline{M_n}_{,SEC}$[d] (g/mol)	PDI[d]
1	PEO_{44}-*b*-$PVDM_{21}$	25:1:0.2	4	84	5277	7400	1.04
2	PEO_{44}-*b*-$PVDM_{41}$	100:1:0.2	4	41	8060	8800	1.09
3	PEO_{44}-*b*-$PVDM_{84}$	100:1:0.2	8	84	14,083	14,500	1.06

[a] The number of monomer units determined by ^{1}H NMR spectroscopy.
[b] VDM conversion determined by ^{1}H NMR spectroscopy by comparing the integration area value of the vinylic protons of VDM at 5.93 ppm with the integration area value of the CH proton of DMF at 8.01 ppm.
[c] $\overline{M_{n,\,th}} = \overline{M_{n,\,NMR\ of\ PEO\text{-}CTA}} + (([VDM]_0 / [PEO\text{-}CTA]_0) \times VDM_{conv.} \times M_{VDM})$.
[d] Determined by SEC in THF using polystyrene standard.

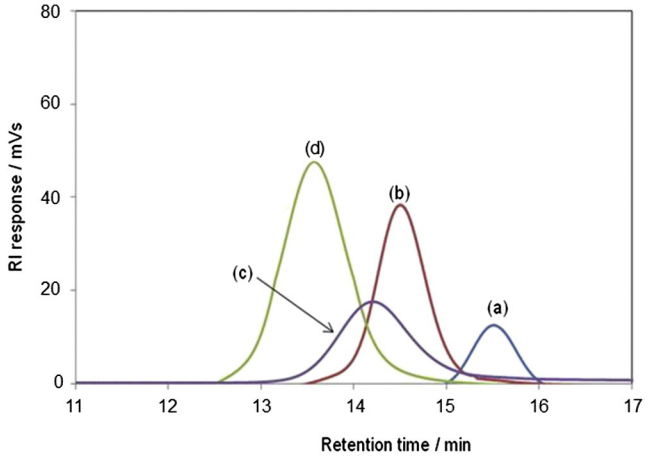

Fig. 1. Overlay SEC traces of (a) PEO_{44}-CTA, (b) PEO_{44}-*b*-$PVDM_{21}$ copolymer (Run 1, Table 1), (c) PEO_{44}-*b*-$PVDM_{41}$ copolymer (Run 2, Table 1) and (d) PEO_{44}-*b*-$PVDM_{84}$ copolymer (Run 3, Table 1).

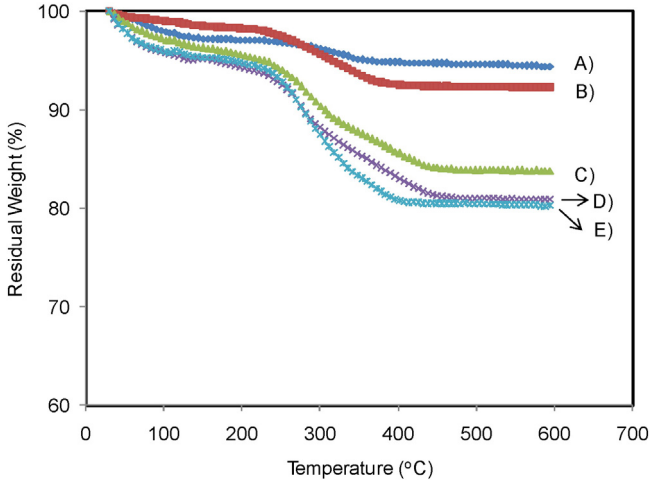

Fig. 3. TGA thermograms of A) bare MNPs, B) APS-grafted MNPs, C) PEO_{44}-*b*-$PVDM_{21}$-MNP nanoclusters, D) PEO_{44}-*b*-$PVDM_{41}$-MNP nanoclusters and E) PEO_{44}-*b*-$PVDM_{84}$-MNP nanoclusters.

3. Results and discussion

3.1. Synthesis of PEO-b-PVDM diblock copolymers by RAFT polymerization

PEO-*b*-PVDM copolymers-MNP nanoclusters were obtained by the reaction between primary amine groups coated on MNPs surface and azlactone groups within the backbone of PEO-*b*-PVDM diblock copolymers *via* a ring-opening reaction (Scheme 3). In the first step, PEO-*b*-PVDM diblock copolymers were synthesized using PEO-CTA as the macromolecular chain transfer agent to mediate the RAFT polymerization of VDM in the presence of ACVA used as initiator in 1,4-dioxane at 70 °C. The characteristics of the copolymers having three different PVDM block lengths are shown in Table 1. Theoretical number-average molecular weights ($\overline{M_{n,\mathrm{th}}}$) calculated from the monomer conversion increased as increasing the PVDM block length and this result is in good agreement with SEC results (Table 1). Fig. 1 shows that SEC traces of PEO-*b*-PVDM diblock copolymers shift to earlier retention times with respect to the SEC trace of PEO-CTA maintaining low polydispersity indices (PDIs ≤ 1.10). This result shows that the copolymerization is well controlled leading to well-defined diblock copolymer structures.

^{1}H NMR spectrum (Fig. 2A) of the PEO_{44}-*b*-$PVDM_{41}$ copolymer (Run 2, Table 1) shows the presence of signals at 3.38 ppm ($CH_3O(CH_2CH_2O)_{44}$, labeled *a*) and at 3.65 ppm ($CH_3O(CH_2CH_2O)_{44}CH_2CH_2OC(O)C(CH_3)$, labeled *b*), which are characteristics of the PEO block and the presence of a signal at 1.40 ppm (OCO–C(CH_3)–N, labeled *c*), which is characteristic of PVDM block. The other two block copolymers show similar ^{1}H NMR patterns to that of PEO_{44}-*b*-$PVDM_{41}$ block copolymer with different integration ratios of signals labeled *b* and *c*, depending on the block lengths of each copolymer. Moreover, the FTIR spectrum (Fig. 2B) of the PEO_{44}-*b*-$PVDM_{41}$ copolymer shows the characteristic bands of the azlactone rings at 1817 cm^{-1} ($\nu_{C=O}$), at 1699 cm^{-1} ($\nu_{C=N}$) and at 1201 cm^{-1} (ν_{C-O}).

3.2. Formation of PEO-b-PVDM copolymers-MNP nanoclusters

PEO-*b*-PVDM copolymers-MNP nanoclusters were obtained by reaction between amino groups grafted onto the surface of APS-grafted MNPs with azlactone rings of PVDM block of copolymers in 1,4-dioxane at room temperature. Resulting copolymers-MNP nanoclusters were characterized by TGA and FTIR spectroscopy. TGA technique was used

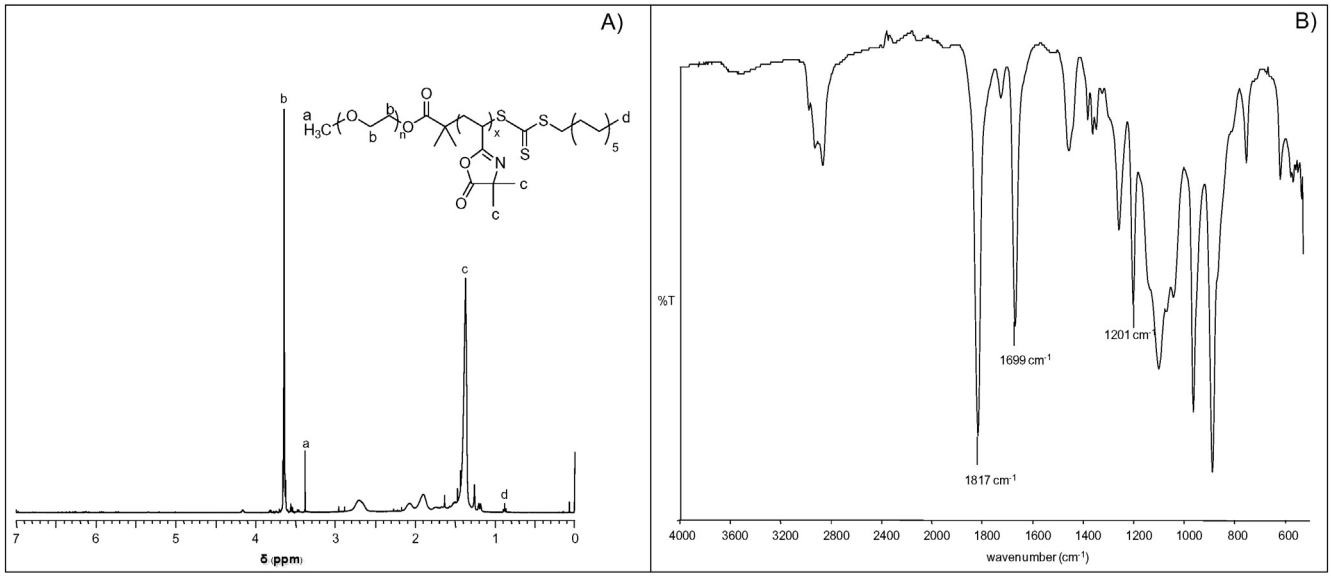

Fig. 2. A) ^{1}H NMR spectrum of the PEO_{44}-*b*-$PVDM_{41}$ block copolymer (Run 2, Table 1) in $CDCl_3$ and B) FTIR spectrum of the PEO_{44}-*b*-$PVDM_{41}$ block copolymer.

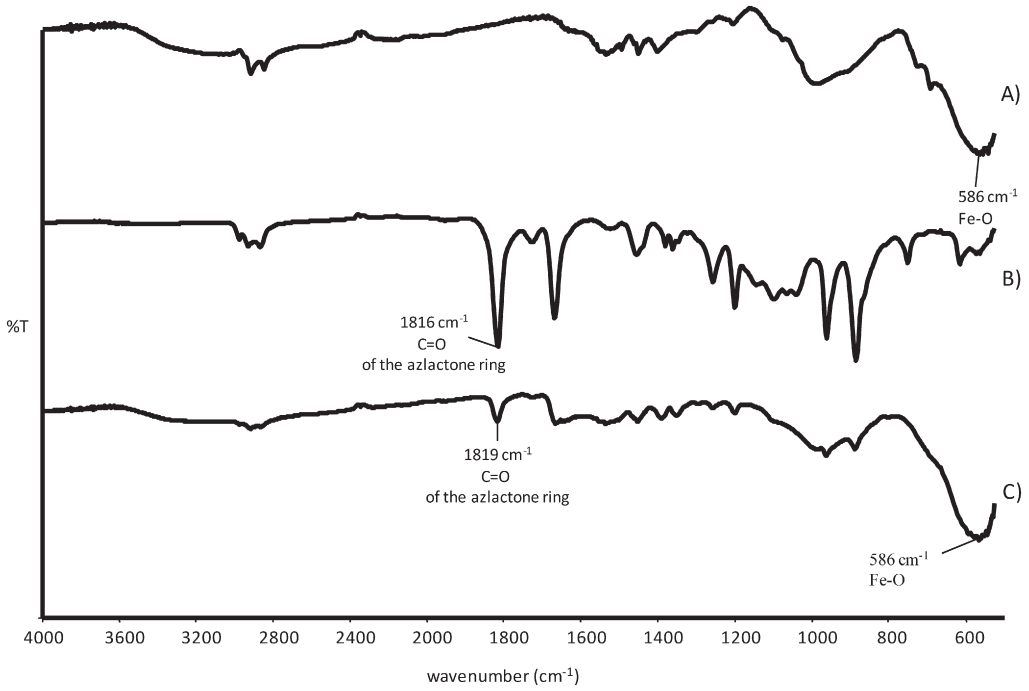

Fig. 4. FTIR spectra of A) APS-grafted MNPs, B) PEO_{44}-*b*-$PVDM_{41}$ block copolymers and C) PEO_{44}-*b*-$PVDM_{41}$-MNP nanoclusters.

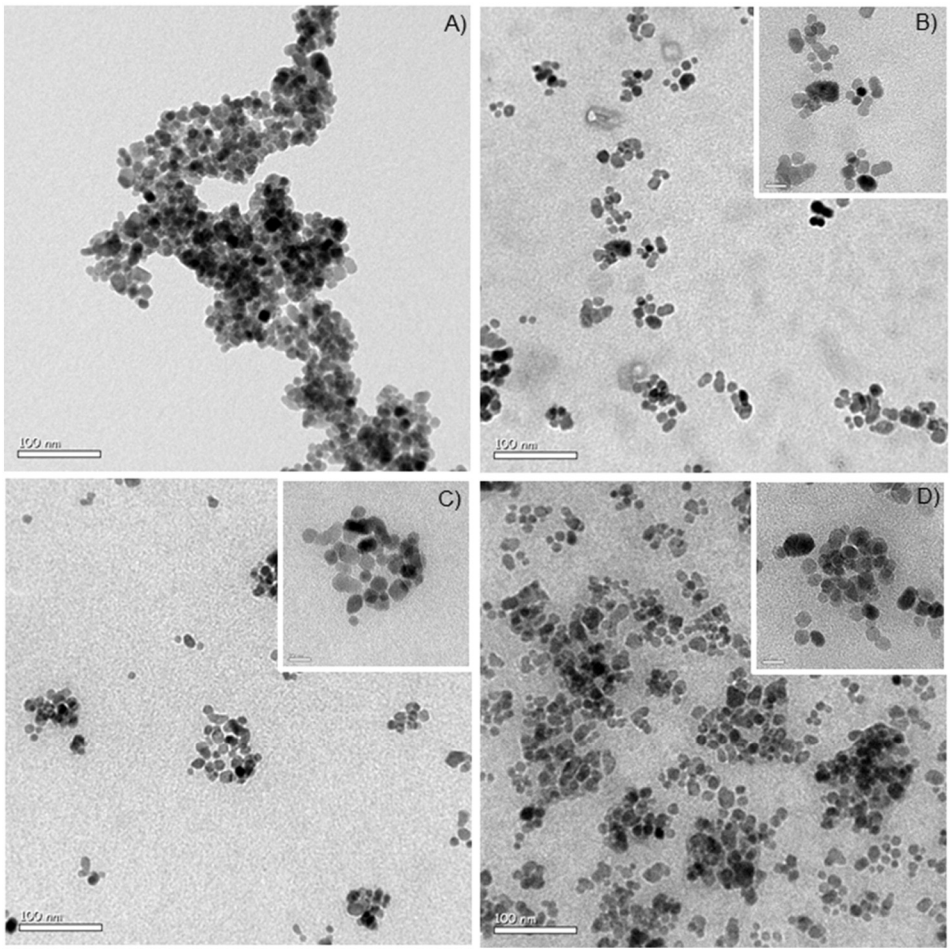

Fig. 5. TEM images of A) APS-grafted MNPs, B) PEO_{44}-*b*-$PVDM_{21}$-MNP nanoclusters, C) PEO_{44}-*b*-$PVDM_{41}$-MNP nanoclusters and D) PEO_{44}-*b*-$PVDM_{84}$-MNP nanoclusters. All TEM samples were prepared from aqueous dispersions. The expansion of some nanoclusters is shown in the inset.

to calculate the percentage of organic layers bound onto MNPs. It was assumed that the percent weight loss was attributed to the weight of organic components and the residual weight was due to completely oxidized iron oxide in the form of magnetite. It was found that APS content in the nanoclusters was about 2.2% and the copolymers in the nanoclusters were in the range of 8.4–11.9% (Fig. 3).

The FTIR spectrum of PEO_{44}-*b*-$PVDM_{41}$-MNP nanoclusters exhibits the left over C⌒O characteristic band of the azlactone ring at 1819 cm^{-1} after the coupling reaction (Fig. 4), indicating the availability of some azlactone rings for further hydrolysis with water to form the MNP containing carboxylated-enriched surface for ionic adsorption with antibody in the next step.

TEM images of APS-grafted MNPs and MNP nanoclusters coated with PEO-*b*-PVDM block copolymers containing different PVDM chain lengths are shown in Fig. 5. It was found that large aggregations of the particles were observed for APS-grafted MNPs (Fig. 5A). After PEO-*b*-PVDM block copolymer coating, the particle dispersibility was obviously improved due to hydrophilic PEO coating on its surface. In addition, the existence of carboxylic acid groups arising from the ring-opening reaction of azlactone rings in the PVDM block after exposure in water might also enhance water dispersibility of the particles. The ring-opening reaction between azlactone rings in the PVDM block of the copolymers and amino groups grafted on MNP surface led to the formation of the nanoclusters (Scheme 3). The size of these nanoclusters increased from 20 to 150 nm with increasing the PVDM chain lengths: approximately 10, 50 and 100 particles/cluster were obtained for PEO_{44}-*b*-$PVDM_{21}$, PEO_{44}-*b*-$PVDM_{41}$ and PEO_{44}-*b*-$PVDM_{84}$ block copolymers, respectively (Fig. 5B, 5C and 5D). Increasing reactive azlactone groups in the PVDM block by increasing the PVDM length increased numbers of the MNP participating in the nanoclustering, indicating that the size of these nanoclusters can be controlled by adjusting the number of reactive azlactone rings in the block copolymers.

Hydrodynamic diameter (D_h) of APS-grafted MNP estimated by PCS was significantly larger than those of the MNPs coated with PEO-*b*-PVDM block copolymers, indicating the improvement in water dispersibility of the particles after copolymer coating (Table 2) and are in good agreement with TEM results. Increasing PVDM block lengths in the copolymers led to the increase in D_h (97–166 nm) as ascertained by the TEM results. In addition, hydrodynamic size distributions of the copolymers-MNP nanoclusters were narrow as compared to that of APS-grafted MNP as a result of polymer coating and thus improving their water dispersibility. Zeta potential values of the nanoclusters were increased significantly after copolymer coating (−27.2 to −33.9 mV) due to the ring-opening of PVDM units in the copolymers, resulting in the formation of the nanoclusters with carboxylated-enriched surface. The negative charge of the carboxylated-coated nanoclusters was essential for magnetic separation of antibody through ionic adsorption mechanism in the next step.

Magnetic properties of bare MNP, APS-grafted MNP and MNP nanoclusters coated with PEO-*b*-PVDM block copolymers containing different PVDM chain lengths are shown in Fig. 6. Saturation magnetizations (M_s) of MNP nanoclusters ranged between 33 and 42 emu/g and these numbers were lower than their MNP precursors. This was attributed to the presence of organic components in the structure, leading to the lower percentage of magnetite content in the nanoclusters. Although there was some degree of MNP nanoclustering, these particles

Table 2
Hydrodynamic diameter (D_h), size distribution and zeta potential of the nanoclusters dispersed in 10 mM MES pH 6 solutions.

Run	Samples	D_h (nm)	Zeta potential (mV)
1	APS-coated MNP	984.1	−3.5
2	PEO_{44}-*b*-$PVDM_{21}$-MNP nanoclusters	96.7	−27.2
3	PEO_{44}-*b*-$PVDM_{41}$-MNP nanoclusters	117.5	−28.3
4	PEO_{44}-*b*-$PVDM_{84}$- MNP nanoclusters	166.1	−33.9

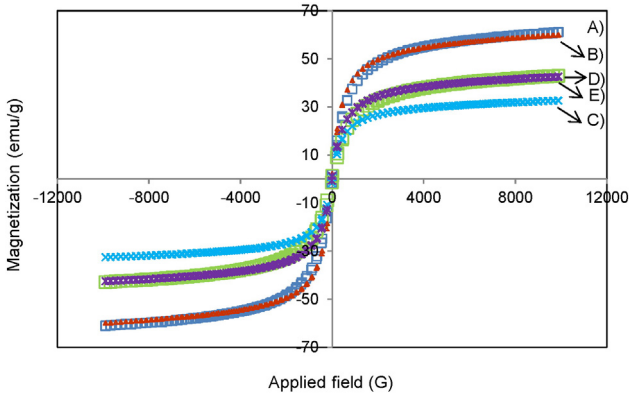

Fig. 6. *M-H* curves of A) bare MNPs, B) APS-grafted MNPs, C) PEO_{44}-*b*-$PVDM_{21}$-MNP nanoclusters, D) PEO_{44}-*b*-$PVDM_{41}$-MNP nanoclusters and E) PEO_{44}-*b*-$PVDM_{84}$-MNP nanoclusters.

exhibited superparamagnetism evidenced by the absence of magnetic remanence and coercivity in the *M-H* curves.

3.3. Adsorption percentage and recycling studies of the copolymer-MNP nanoclusters with antibody

To use them in antibody adsorption application, copolymers-MNP nanoclusters having carboxylated-enriched surface are desirable for ionic adsorption between negatively charged MNP and positive moiety in anti-rabbit IgG antibody. Residual azlactone rings on the MNP surface were thus hydrolyzed to form nanoclusters with negatively charged surface due to carboxylated groups coating before adsorption experiments. Nanoclusters having four different cluster sizes as shown in Table 2 were used as nano-solid supports in antibody adsorption experiments. It was found that APS-coated MNP was not dispersible in 10 mM MES pH 6 solution due to the absence of polymer coating on its surface. On the other hand, the nanoclusters grafted with carboxylated-functionalized PEO_{44}-*b*-$PVDM_{21}$ and PEO_{44}-*b*-$PVDM_{41}$ copolymers were well dispersible in the media but not completely separated from the media using an external magnet. Traces of MNP in the supernatant after magnetic separation and/or ultracentrifugation could therefore interfere with Bradford assay [27]. The presence of single nanoparticles or magnetic clusters with small size, hypothetically having low magnetic sensitivity, resulted in difficulty in removal from the dispersion [32]. A

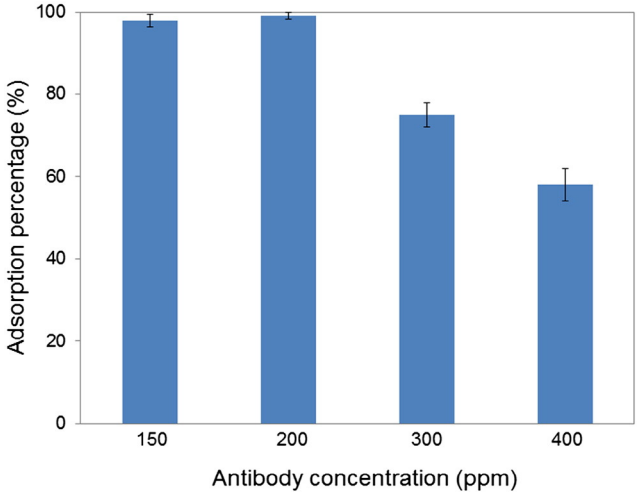

Fig. 7. Adsorption percentages of PEO_{44}-*b*-$PVDM_{84}$-MNP nanoclusters for ionic adsorption with anti-rabbit IgG antibody (Adsorption percentage = [(A − B) / A] × 100, where A is the initial concentration of antibody and B is the concentration of antibody in the supernatant at time *t* (non-adsorbed antibody)).

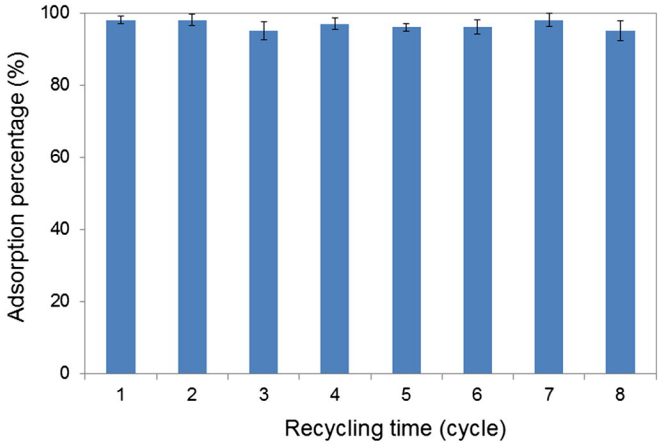

Fig. 8. Recycling efficiency of PEO_{44}-*b*-$PVDM_{84}$-MNP nanoclusters in the ionic adsorption of anti-rabbit IgG antibody after 8-recycling process.

compromise between good water dispersibility and magnetic sensitivity of MNP is crucial for use as a nano-solid support. Therefore, the nanoclusters grafted with these two copolymers were unable to be used as supports for antibody adsorption. Interestingly, nanoclusters grafted with PEO_{44}-*b*-$PVDM_{84}$ copolymer with D_h of 166 nm exhibited good dispersibility in the media and, more importantly, they facilitated separation by an external magnet without traces of MNP in the dispersion resulting in an absence of interference with Bradford assay. Therefore, the carboxylated-functionalized PEO_{44}-*b*-$PVDM_{84}$ copolymer-coated MNP nanoclusters were then subjected to the adsorption experiments with anti-rabbit-IgG antibody.

Adsorption percentage of the copolymer-MNP nanoclusters with anti-rabbit-IgG antibody was investigated after removing an excess antibody from the mixture. Fig. 7 shows that 200 ppm was the maximum concentration of antibody that can be used for binding on nanocluster surface. Increasing antibody concentration to 300 and 400 ppm resulted in the existence of non-adsorbed antibody in the dispersion. Therefore, 200 ppm antibody loading in 10 mg of PEO_{44}-*b*-$PVDM_{84}$-MNP nanoclusters will be used for further experiments. In addition, the M_s from VSM and the percent weight residual from TGA techniques of the antibody-adsorbed nanoclusters showed slight decreases as compared to those before the adsorption, implying that there was some antibody adsorbed on the complexes.

Because these nanoclusters possess magnetically guidable properties, which are great advantages in facilitating recycling process, the recycling ability of the copolymer-MNP nanoclusters was thus investigated. After 2 h adsorption of antibody, the nanoclusters were separated from dispersion using a permanent magnet. To prove the recycling concept, desorption of anti-rabbit IgG from nanocluster surface was examined by testing different washing solutions. The amount of antibody in supernatant after adsorption-desorption processes were quantitatively determined using Bradford assay and the desorption percentage was determined using Eq. (2). NaCl salt solutions at concentrations 300 mM, 1.0 and 2.5 M at pH 7, as well as 1.0 M NaCl solution at pH 12 were used for this purpose. These salt solutions at pH 7 were unable to desorb anti-rabbit IgG antibody from the nanocluster surface probably because the solution pH was in the range of isoelectric point (pI) of the antibody (6–9) [33]. The antibody can also be desorbed by changing the global net charge of the antibody by shifting the solution pH [27]. 1.0 M NaCl solution with pH 12 exhibited a complete removal of the antibody from the surface due to the suppression in ionic adsorption between carboxylated nanoclusters and the antibody as opposed to the case when the pH is in the pI range of the antibody. Therefore, 1 M NaCl pH 12 solution was used as the washing solution to investigate the adsorption recycling ability of the nanoclusters.

Fig. 8 shows the adsorption percentage of the nanoclusters with the antibody in each cycle. After each adsorption-separation process, the concentration of adsorbed antibody and desorbed antibody from each cycle was determined using Bradford assay. The results showed that the particles retained a higher than 96% adsorption of the antibody for eight adsorption-separation-desorption cycles, indicating the potential feasibility in using this novel hybrid nanocluster as recyclable support in cell separation applications.

3.4. Antigen recognition capacity study of antibody-adsorbed magnetic nanoclusters

The antigen recognition capacity of antibody-adsorbed MNP nanoclusters was determined from the development of a green-blue color product after the oxidation with ABTS, when reacted with horseradish peroxidase (HRP) labeled conjugates. Therefore, anti-rabbit IgG-adsorbed MNP nanoclusters were first immobilized with an IgG antigen, followed by anti-rabbit IgG-HRP as a secondary antibody for color development when reacted with ABTS. It was found that anti-rabbit IgG-adsorbed MNP nanoclusters exhibited the changing of color from light green to blue after the oxidation with ABTS (Fig. 9D), indicating the conjugation of IgG antigen with anti-rabbit IgG adsorbed on the nanocluster surface. The MNP nanoclusters without anti-rabbit IgG-HRP as the secondary antibody (Fig. 9E), without IgG antigen (Fig. 9F) and without anti-rabbit IgG (Fig. 9G) were used as control dispersions. These dispersions showed negative results as their solution color did not change upon the oxidation with ABTS. The dispersion media (10 mM MES pH 6) (Fig. 9A) and those with 1% BSA as a blocking reagent (Fig. 9B) were also testified to evaluate the negative results of the control solutions. In addition, the solution of anti-rabbit IgG-HRP as the secondary antibody (without MNP nanoclusters) was also used in the testing to evaluate the color change (positive result) due to the reaction between HRP and ABTS (Fig. 9C). It should be also noted that the MNP nanoclusters after eight recycling process also showed a positive result as illustrated in Fig. 9D. Therefore, these experiments confirm that the antigen recognition of the antibody-adsorbed MNP nanoclusters was preserved. These MNP nanoclusters could be used as a recyclable magnetic marker to immobilize with other specific antibody-antigen conjugates.

4. Conclusions

Surface modification of MNPs with well-defined PEO-*b*-PVDM diblock copolymers using “grafting-onto” strategy to form magnetic nanoclusters was described. The nanocluster size could be tuned by adjusting the amount of reactive azlactone rings in the PVDM block to obtain a controllable size below 150 nm. The obtained nanoclusters

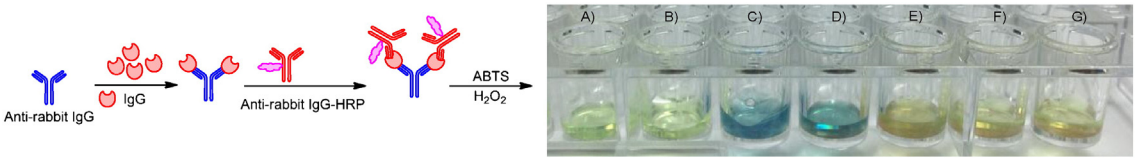

Fig. 9. Scheme showing the indirect method used to visualize the antigen recognition capability; A) 10 mM MES pH 6, B) 1% BSA in 10 mM MES pH 6, C) anti-rabbit IgG-HRP, D) anti-rabbit IgG-adsorbed MNP nanoclusters immobilized with IgG and anti-rabbit IgG-HRP, E) anti-rabbit IgG-adsorbed MNP nanoclusters immobilized with IgG, F) anti-rabbit IgG-adsorbed MNP nanoclusters without IgG (blocked with BSA) and G) MNP nanoclusters.

were well dispersed in water, have good magnetic sensitivity and negatively charged surface. These properties are required to use these particles in magnetic separation applications. The good magnetic sensitivity of the nanoclusters allowed facile manipulation using magnetic separation. Moreover, their negatively charged surface provided adsorption capability with positively charged bio-entities. These novel magnetic nanoclusters were successfully used as efficient and recyclable nano-solid supports for adsorption with anti-rabbit IgG antibody for at least 8-recycling process. The preliminary studies in the adsorption of the nanoclusters with IgG antigen were also demonstrated. The purity of the antigen after the adsorption and their efficiency for use in real sample separation are warranted for further exploration. These magnetic nanoclusters might be advantageous for use as nano-solid supports for efficient and facile separation of other positively charged molecules, especially antibody-antigen conjugates.

Acknowledgement

The authors thank the Thailand Research Fund (TRF) (RSA59-Metha Rutnakornpituk) for financial funding. We also thank the Franco-Thai Cooperation Program in Higher Education and Research 2009–2010, supported by the Ministry of Foreign Affairs, Ministry of Higher Education and Research of France and the Commission on Higher Education of Thailand and PHC grant (PHC 2009–2010 no. 20609UF). YP specially acknowledges the Royal Golden Jubilee for the scholarship (PHD/0207/2551) and the France Embassy for living expenses in France.

Appendix A. Supplementary data

Supplementary data to this article can be found online at http://dx.doi.org/10.1016/j.msec.2016.05.032.

References

[1] D.H. Kim, S.H. Lee, K.H. Im, K.N. Kim, K.M. Kim, I.B. Shim, et al., Curr. Appl. Phys. 6 (Suppl. 1) (2006) 242–246.
[2] R.Y. Hong, B. Feng, L.L. Chen, G.H. Liu, H.Z. Li, Y. Zheng, et al., Biochem. Eng. J. 42 (2008) 290–300.
[3] J.M. Moon, B.S. Kim, Y.S. Choi, J.O. Lee, T. Nakahara, K. Yoshinaga, Macromol. Res. 18 (2010) 793–799.
[4] Q. Yuan, R. Venkatasubramanian, S. Hein, R.D.K. Misra, Acta Biomater. 4 (2008) 1024–1037.
[5] F. Xu, J.H. Geiger, G.L. Baker, M.L. Bruening, Langmuir 27 (2011) 3106–3112.
[6] D.K. Kim, Y. Zhang, W. Voit, K.V. Rao, M. Muhammed, J. Magn. Magn. Mater. 225 (2001) 30–36.
[7] Y. Shen, W. Guo, L. Qi, J. Qiao, F. Wang, L. Mao, J. Mater. Chem. B. 1 (2013) 2260–2267.
[8] Y. Prai-in, K. Tankanya, B. Rutnakornpituk, U. Wichai, V. Montembault, S. Pascual, et al., Polymer 53 (2012) 113–120.
[9] T.T.T. N'Guyen, H.T.T. Duong, J. Basuki, V. Montembault, S. Pascual, C. Guibert, et al., Angew. Chem. Int. Ed. 52 (2013) 14152–14156.
[10] J.S. Basuki, H.T.T. Duong, A. Macmillan, R. Whan, C. Boyer, T.P. Davis, Macromolecules 46 (2013) 7043–7054.
[11] Y. Zhou, S. Wang, B. Ding, Z. Yang, Chem. Eng. J. 138 (2008) 578–585.
[12] N. Pothayee, S. Balasubramaniam, R.M. Davis, J.S. Riffle, M.R.J. Carroll, R.C. Woodward, et al., Polymer 52 (2011) 1356–1366.
[13] H. Wang, W. Luo, J. Chen., J. Mater. Sci. 47 (2012) 5918–5925.
[14] A. Aqil, S. Vasseur, E. Duguet, C. Passirani, J.P. Benoît, A. Roch, et al., Eur. Polym. J. 44 (2008) 3191–3199.
[15] C.L. McCormick, A.B. Lowe, Acc. Chem. Res. 37 (2004) 312–325.
[16] H. Mori, H. Iwaya, T. Endo, React. Funct. Polym. 67 (2007) 916–927.
[17] X. Zhang, J. Rieger, B. Charleux, Polym. Chem. 3 (2012) 1502–1509.
[18] C.N. Urbani, H.N. Nguyen, M.J. Monteiro, Aust. J. Chem. 59 (2006) 728–732.
[19] S. Puttick, D.J. Irvine, P. Licence, K.J. Thurecht, J. Mater. Chem. 19 (2009) 2679–2682.
[20] S. Pascual, T. Blin, P.J. Saikia, M. Thomas, P. Gosselin, L. Fontaine, J. Polym. Sci. A Polym. Chem. 48 (2010) 5053–5062.
[21] M.E. Levere, H.T. Ho, S. Pascual, L. Fontaine, Polym. Chem. 2 (2011) 2878–2887.
[22] H.T. Ho, M.E. Levere, D. Fournier, V. Montembault, S. Pascual, L. Fontaine, Aust. J. Chem. 65 (2012) 970–977.
[23] H.T. Ho, M.E. Levere, S. Pascual, V. Montembault, N. Casse, A. Caruso, et al., Polym. Chem. 4 (2013) 675–685.
[24] T. Theppaleak, B. Rutnakornpituk, U. Wichai, T. Vilaivan, M. Rutnakornpituk, J. Biomed. Nanotechnol. 9 (2013) 1509–1520.
[25] T.R. Sarkar, J. Irudayaraj, Anal. Biochem. 379 (2008) 130–132.
[26] H. Xu, Z.P. Aguilar, L. Yang, M. Kuang, H. Duan, Y. Xiong, et al., Biomaterials 32 (2011) 9758–9765.
[27] S. Puertas, P. Batalla, M. Moros, E. Polo, P. del Pino, J.M. Guisan, et al., ACS Nano 5 (2011) 4521–4528.
[28] J.T. Lai, D. Filla, R. Shea, Macromolecules 35 (2002) 6754–6756.
[29] Y. He, T.P. Lodge, Chem. Commun. 26 (2007) 2732–2734.
[30] L.D. Taylor, H.S. Kolesinski, A.C. Mehta, L. Locatell, P.S. Larson, Makromol. Chem. Rapid Comm. 3 (1982) 779–782.
[31] M.M. Bradford, Anal. Biochem. 72 (1976) 248–254.
[32] H. Amiri, M. Mahmoudi, A. Lascialfari, Nanoscale 3 (2011) 1022–1030.
[33] M.A. Clauss, R.K. Jain, Cancer Res. 50 (1990) 3487–3492.

J Nanopart Res (2018) 20:193
https://doi.org/10.1007/s11051-018-4295-2

RESEARCH PAPER

Effect of alkyl chain lengths on the assemblies of magnetic nanoparticles coated with multi-functional thiolactone-containing copolymer

Sujittra Paenkaew · Metha Rutnakornpituk

Received: 8 March 2018 / Accepted: 5 July 2018

Abstract This work presents the synthesis of magnetite nanoparticle (MNP) coated with poly(N,N-diethylaminoethyl methacrylate)-*b*-poly(N-isopropyl acrylamide-*st*-thiolactone acrylamide) (PDEAEMA-*b*-P(NIPAAm-*st*-TlaAm) copolymer and its use in controlled drug release and bio-conjugation. TlaAm units in the copolymer were ring-opened with various alkyl amines to form thiol groups (-SH), followed by thiol-ene coupling reactions with acrylamide-coated MNP and then quaternized to obtain cationic copolymer-MNP assemblies (the size < 200 nm/cluster). The use of alkyl amines having various chain lengths (e.g., 1-propylamine, 1-octylamine, or 1-dodecylamine) in the nucleophilic ring-opening reactions of the thiolactone rings affected their magnetic separation ability, water dispersibility, and release rate of doxorubicin model drug. In all cases, when increasing the temperature, they showed a thermo-responsive behavior as indicated by the decrease in hydrodynamic size and the accelerated drug release rate. These copolymer-MNP assemblies could be used as a novel platform with thermal-triggering controlled drug release and capability for adsorption with any negatively charged biomolecules.

Keywords Magnetic · Nanoparticle · Assembly · Thiolactone · Thermo-responsive · Polimer coating · Drug delivery

Introduction

In recent years, magnetite nanoparticle (MNP) has extensively attracted interest owing to their superparamagnetic properties and their potential applications in various fields. Incorporation of MNP into various organic nano-assemblies has been investigated by features of their intriguing biomedical applications, such as remotely controlled drug release, magnetically guidable drug delivery (Sahoo et al. 2013; Wang et al. 2013; Li et al. 2006), magnetic resonance imaging (MRI) (Mahmoud et al. 2013; Hu et al. 2013), and hyperthermia cancer treatment delivery (Qu et al. 2014; Chen et al. 2015; Singh et al. 2014). However, it tends to aggregate to each other mainly owing to dipole-dipole and magnetic attractive forces, leading the loss in nano-scale related properties and a decrease in the surface area/volume ratio (Lim et al. 2013). Grafting long-chain polymers onto MNP surface

Electronic supplementary material The online version of this article (https://doi.org/10.1007/s11051-018-4295-2) contains supplementary material, which is available to authorized users.

S. Paenkaew · M. Rutnakornpituk (✉)
Department of Chemistry and Center of Excellence in Biomaterials, Faculty of Science, Naresuan University, Phitsanulok 65000, Thailand
e-mail: methar@nu.ac.th

Published online: 13 July 2018

is currently one of the promising approaches to realize its dispersibility in the media due to charge repulsion of ionic surface or steric repulsion of long chain surfactant (Chen et al. 2012; Mekkapat et al. 2013). In addition, this polymeric coating can also serve as a platform for conjugation of biomolecules of interest on the MNP surface (Leung et al. 2013; Machida et al. 2014; Prabha and Raj 2016; Ulbrich et al. 2016).

Many works have now extensively reported in the MNP polymeric coating accomplished either via "grafting from" or "grafting to" strategies (Qin et al. 2004; Wang et al. 2008) with controlled radical polymerization (CRP) techniques. CRP technique produces well controllable polymer architecture on particle surface because it can control molecular weight, polydispersity, functionality, and composition distribution of polymers (Braunecker and Matyjaszewski 2007). Three general techniques of CRP include nitroxide-mediated polymerization (NMP) (Sciannamea et al. 2008), atom transfer radical polymerization (ATRP) (Matyjaszewski 2012; Huang et al. 2017), reversible addition fragmentation chain transfer polymerization (RAFT) (Moad et al. 2008; Hill et al. 2015). Being of our particular interest, RAFT as opposed to other CRP techniques can be performed in various kinds of solvent, wide range of temperature, no need of metals used for polymerization, and large range of monomer classes (Willcock and O'Reilly 2010).

This present work reports the synthesis of a multifunctional copolymer via RAFT for coating onto the surface of MNP and its use in drug-controlled release and bio-conjugation. This copolymer was well designed to have multi-functions including: (1) thermo-responsive poly(N-isopropylacrylamide) (PNIPAAm) serving as a drug reservoir with a temperature-triggering mechanism, (2) thiolactone moiety for covalent grafting with MNP surface and tuning degree of hydrophobicity of the copolymer, and (3) positively charged poly(N,N-diethylamino-2-ethylmethacrylate) (PDEAEMA) for improving its water dispersibility and ionic adsorption with anionic bio-entities. PNIPAAm responded to the change of the environmental temperature due to the phase separation when crossing its lower critical solution temperature (LCST = 30–34 °C) (Gandhi et al. 2015). When raising the temperature above its LCST, the copolymer was in the collapse state due to the formation of the intramolecular hydrogen bonding among the polymer chains. In contrast, it swelled at the temperature below its LCST owing to the intermolecular hydrogen bonding between water molecules and polymer chains (Du et al. 2010; Bischofberger and Trappe 2015; Patil and Wadgaonkar 2017; Rodkate and Rutnakornpituk 2016; Meerod et al. 2015).

The reactions involving thiol chemistry have now gain a great attention because thiols (-SH) are highly reactive nucleophiles for the reactions with epoxide, alkyl halides, and double or triple bonds (Espeel and Du Prez 2015; Stamenovi et al. 2011). However, the applications of thiols are rather limited because they have a short shelf life due to the oxidation reaction resulting in disulfide formation (Espeel et al. 2012). A promising approach to overcome this limitation is to use a reactive thiolactone, a cyclic thioester, as a latent thiol functional group. This reaction involves a ring-opening reaction of thiolactone moieties to obtain thiol functionality (-SH), subsequently reacting with electrophiles for the second modification in one-pot reaction (Espeel and Du Prez 2015; Chen et al. 2014; Reinicke et al. 2013; Espeel et al. 2011). Many works from Du Prez's research group have reported the use of thiolactone for the double modification purpose (Espeel and Du Prez 2015; Stamenovi et al. 2011; Espeel et al. 2012; Chen et al. 2014; Reinicke et al. 2013; Espeel et al. 2011).

In this report, we describe a synthesis of a thermo-responsive multifunctional diblock copolymer containing thiolactone acrylamide (TlaAm) units for coating on MNP surface and its use for drug-controlled release and bio-conjugation applications. PDEAEMA synthesized via RAFT polymerization was used as a macro chain transfer agent (CTA) for a chain extension of PNIPAAm-*st*-PTlAm second block. PTlAm units were ring opened by alkyl amines to form thiol groups, which were subsequently reacted with the acrylamide-coated MNP to obtain the copolymer-coated particle. PDEAEMA block was then quaternized to obtain cationic MNP to improve the water dispersibility of the particle and for ionic adsorption with negative bio-entities. The effect of alkyl chain lengths (C3, C8, and C12) on the assemblies of the copolymer-coated MNP, affecting their water dispersibility and magnetic separation ability, was investigated. Moreover, the temperature change and the effect of alkyl chain lengths on the rate of the drug release (doxorubicin as a model drug) were also studied (Fig. 1).

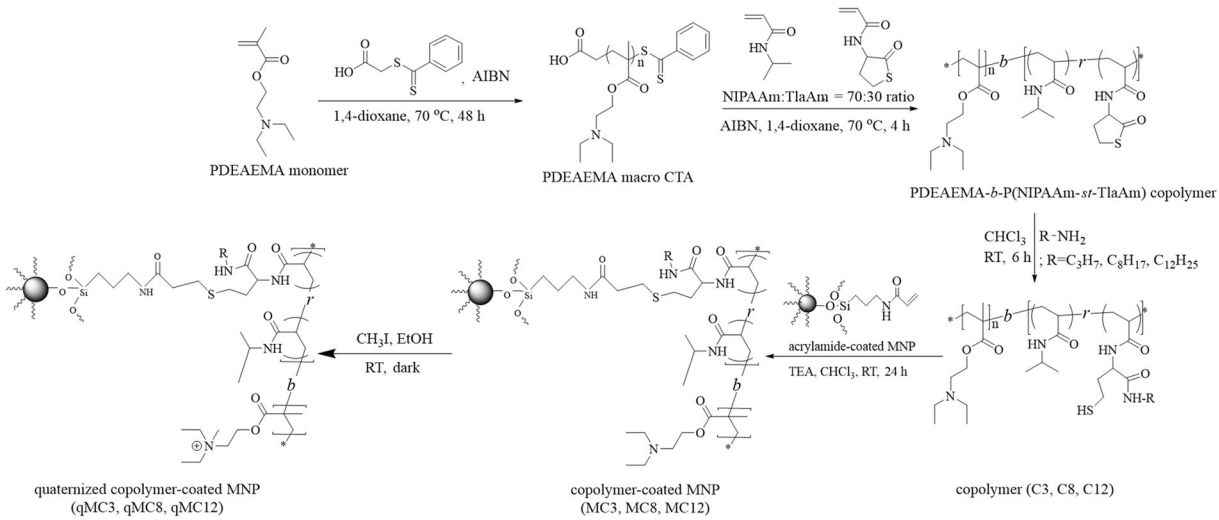

Fig. 1 Synthetic scheme of the copolymer-coated MNP (MC) and its quaternization (qMC)

Experimental

Materials

Unless otherwise stated, the reagents were used without purification: iron(III) acetylacetonate ($Fe(acac)_3$, 99%, Acros), aminopropyltriethoxysilane (APTES, 99%, Acros), *D,L*-homocysteine thiolactone hydrochloride (99%, Acros), oleic acid (Carlo Erba), (3-aminopropyl) triethoxysilane (APTES, 99%, Acros), triethylamine (TEA, 97%, Carlo Erba), 2,2′-azobis(2-methylpropionitrile) (AIBN, 98%, Sigma-Aldrich), s-(thiobenzoyl) thioglycolic acid as a chain transfer agent (99%, Aldrich), 2-(diethylamino) ethyl methacrylate (DEAEMA, 99% stabilized, Acros), and *N*-isopropylacrylamide (NIPAAm, 99%, Acros) were used as received. Acryloyl chloride was synthesized prior to use via a chloride exchange reaction between acrylic acid (98%, Acros) and benzoyl chloride (99%, Acros) to obtain a colorless liquid with 60% yield. 1-Propylamine (99%, Sigma-Aldrich), 1-octylamine (99%, Merck), 1-dodecylamine (98%, Acros), and iodomethane (2.0 M in tert-butyl methyl ether, Sigma-Aldrich) were used as received. Doxorubicin hydrochloride (DOX, 2 mg/ml, Pharmachemie BV) were used as received.

Synthesis of N-thiolactone acrylamide (TlaAm) monomer (Reinicke et al. 2013)

To the mixture of *D,L*-homocysteine thiolactone hydrochloride (7.05 g, 45.6 mmol) in a H_2O/1,4-dioxane solution (100 ml), $NaHCO_3$ (19.20 g, 227.9 mmol) was added and stirred for 30 min in an ice bath. Acryloyl chloride (8.3 g, 91.2 mmol) was then added dropwise and stirred at room temperature overnight. After the reaction completed, brine (100 ml) was added into the solution, followed by extracting with ethyl acetate (3 × 200 ml) to obtain TlaAm in an organic layer. Finally, TlaAm monomer was purified by recrystallization from CH_2Cl_2 and then dried in vacuo.

Synthesis of acrylamide-coated MNP

MNP was synthesized via a thermal decomposition method of $Fe(acac)_3$ (5 g, 14.1 mmol) in 90 ml benzyl alcohol at 180 °C for 48 h. Then, the particle was magnetically separated and washed with ethanol and then chloroform. Oleic acid (4 ml) was slowly added to the MNP-toluene dispersion (30 ml) with sonication to form oleic acid-coated MNP, followed by an addition of APTES (4 ml) containing TEA (2 ml) to form amino-coated MNP. After stirring for 24 h, the particles were precipitated in ethanol and washed with toluene. After re-dispersing the particles (0.1 g) in a NaOH solution (6.72 mmol in 10 ml DI), acryloyl chloride (3.36 g, 37.1 mmol) was then added to the dispersion and stirred for 24 h. The product was magnetically separated, repeatedly washed with water, and then stored in the form of dispersions in THF (0.1 g MNP/1 ml).

Synthesis of PDEAEMA macro chain transfer agent (PDEAEMA macro CTA)

DEAEMA monomer (1.9361 g, 10.4 mmol), S-(thiobenzoyl) thioglycolic acid (31.7 mg, 0.1 mmol) as CTA, and AIBN initiator (4.9 mg, 0.03 mmol) ($[DEAEMA]_0$:[CTA]:[AIBN] molar ratio of 70:1:0.2, respectively) were dissolved in 1,4-dioxane (7 ml) under N_2 atmosphere with stirring for 30 min. The RAFT polymerization was performed for 48 h at 70 °C to obtain ca. 50% monomer conversion with $\overline{M_n}$ of PDEAEMA about 6700 g/mol (Supplementary material Fig. S1). The polymerization was ceased by cooling at room temperature in air. The PDEAEMA macro CTA was purified by dialysis in methanol and dried in vacuo.

Synthesis of PDEAEMA-b-P(NIPAAm-st-TlaAm) block copolymer

PDEAEMA macro CTA (0.06 mmol), NIPAAm (4.24 mmol), TlaAm (1.82 mmol), and AIBN initiator (0.01 mmol) ($[NIPAAm]_0$:$[TlaAm]_0$:[PDEAEMA macro CTA]:[AIBN] molar ratio of 70:30:1:0.2, respectively) were dissolved in 1,4-dioxane (8.5 ml) under N_2 atmosphere with stirring for 30 min. The RAFT polymerization was performed at 70 °C for 4 h to obtain ca.50% NIPAAm conversion and 30% TlaAm conversion with $\overline{M_n}$ of the copolymer about 12,200 g/mol (Supplementary material Fig. S2). The polymerization was stopped by cooling at room temperature with air. The copolymer was purified by dialysis in methanol and dried in vacuo.

Synthesis of the copolymer-coated MNP by a double modification of PDEAEMA-b-P(NIPAAm-st-TlaAm) copolymer

The copolymer (0.16 mmol of TlaAm unit) was dissolved in chloroform (5 ml) followed by an addition of primary alkylamines (0.32 mmol, 2:1 M ratio of alkyl amine to TlaAm unit), e.g., 1-propylamine, 1-octylamine, and 1-dodecylamine, to obtain the C3, C8, and C12 copolymers, respectively. The solution was then mixed with the acrylamide-coated MNP (100 mg) and TEA (0.1 ml) and stirred for 24 h under N_2 gas. The copolymer-coated MNP was magnetically separated and washed with chloroform and designated as MC3, MC8, and MC12, respectively.

Quaternization of PDEAEMA in the copolymer-coated MNP

The copolymer-coated MNP (1.76 mmol of DEAEMA units) was re-dispersed in ethanol (40 ml), followed by dropwise addition of 2 M CH_3I solution (1.76 mmol). The mixture was stirred for 20 h in dark at room temperature. The quaternized products (qMC3, qMC8, and qMC12) were magnetically separated and washed with THF to remove an excess of CH_3I, followed by drying in vacuo to obtain black powder.

In vitro release studies of entrapped DOX from the copolymer-coated MNP

The drug solution (2 mg/ml of DOX) was added dropwise into the quaternized MNP dispersions (10 mg/2 ml in DI water) with stirring at 15 °C for 3 h. The DOX-entrapped MNP was separated from an excess DOX by magnetic separation for 30 min and washed with DI water for 4 times. The dispersion of DOX-entrapped MNP (10 mg in 3 ml DI water) was placed in a water bath at 25 °C (below LCST of PNIPAAm) for 1 h, and then, temperature was increased to 45 °C (above LCST of PNIPAAm) for another 80 min. During the experiment, 0.2 ml of the dispersions was withdrawn from the release media at a predetermined time until the released drug reached the equilibrium (the total time points ranging between 12 and 15). After 30-min magnetic separation, the concentrations of the released drug in the supernatant at a given time were determined via UV-visible spectrophotometry at $\lambda = 480$ nm and % drug release was calculated from the following equation;

$$\%\text{drug released} = \frac{\text{Weight of released drug at a given time}}{\text{Weight of the entrapped drug in the MNP}} \times 100$$

where the weight of the entrapped drug in the MNP was determined from the amount of the drug at the maximum point of the release profile combined with those remaining in the particles. To dissolve the remaining drug from the MNP, DI water (3 ml) was added to the particles and then the mixture was heated at 50 °C for 1 h. After 30-min magnetic separation, the drug concentration in the supernatant was then determined via UV-

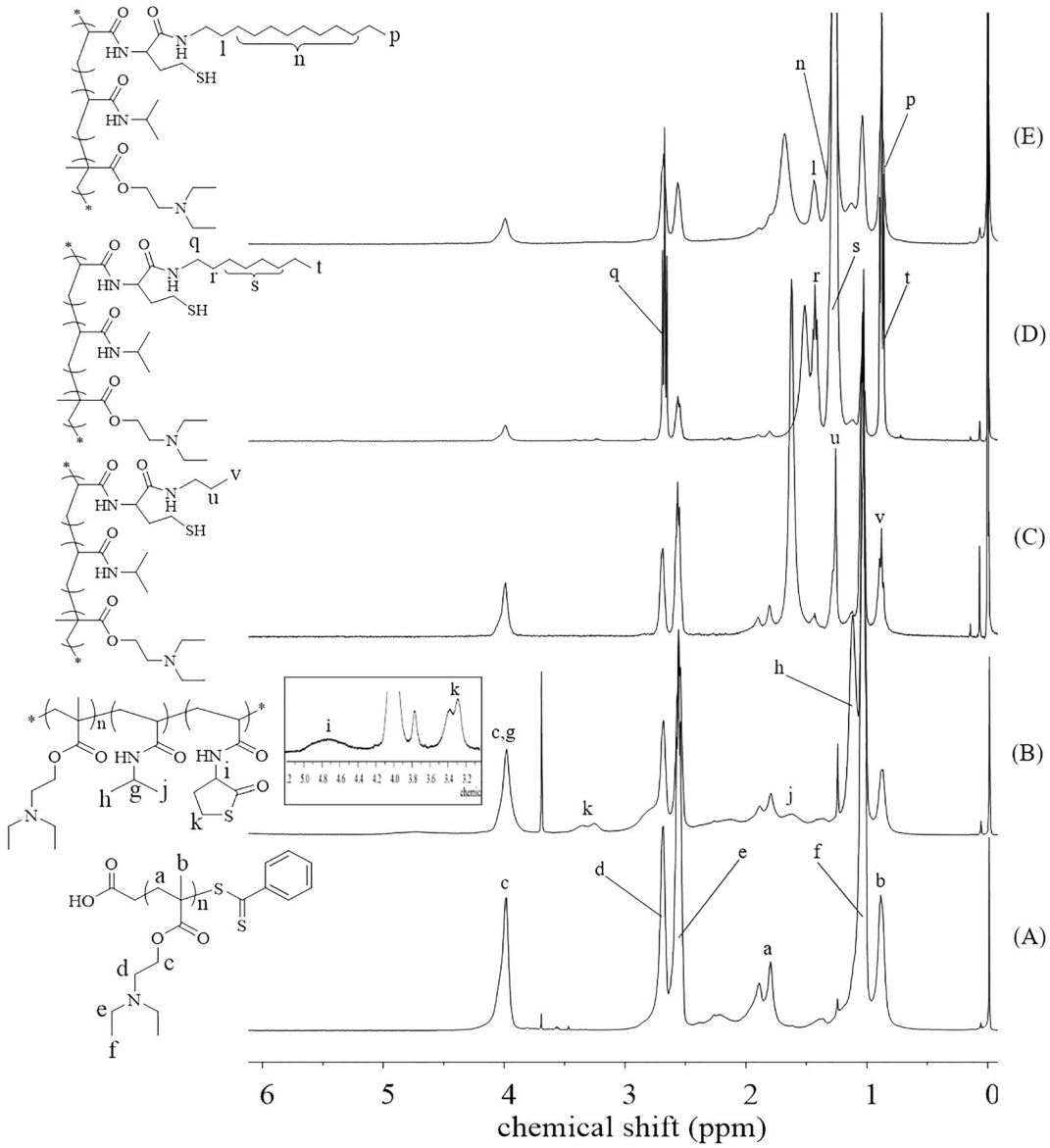

Fig. 2 ^{1}H NMR spectra of **a** PDEAEMA macro CTA, **b** PDEAEMA-*b*-P(NIPAAm-*st*-TlaAm) copolymers before the ring-opening reaction, and after the ring-opening reactions with **c** 1-propylamine, **d** 1-octylamine, and **e** 1-dodecylamine

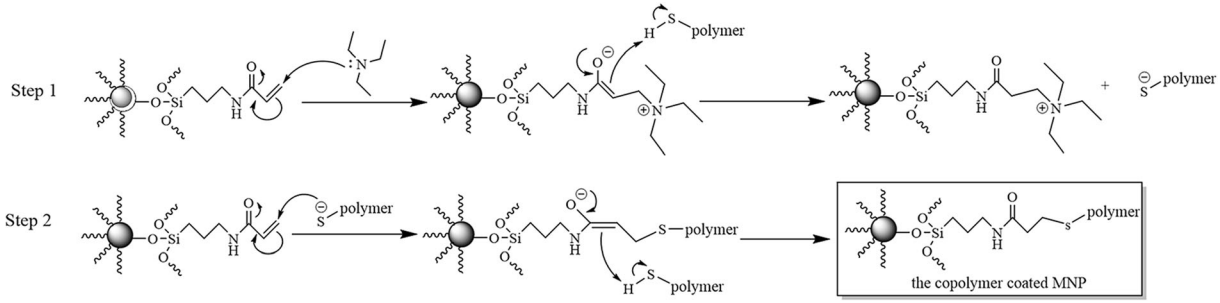

Fig. 3 The thiol-ene reaction mechanism between the acrylamide groups on the MNP surface and thiol groups of the copolymer

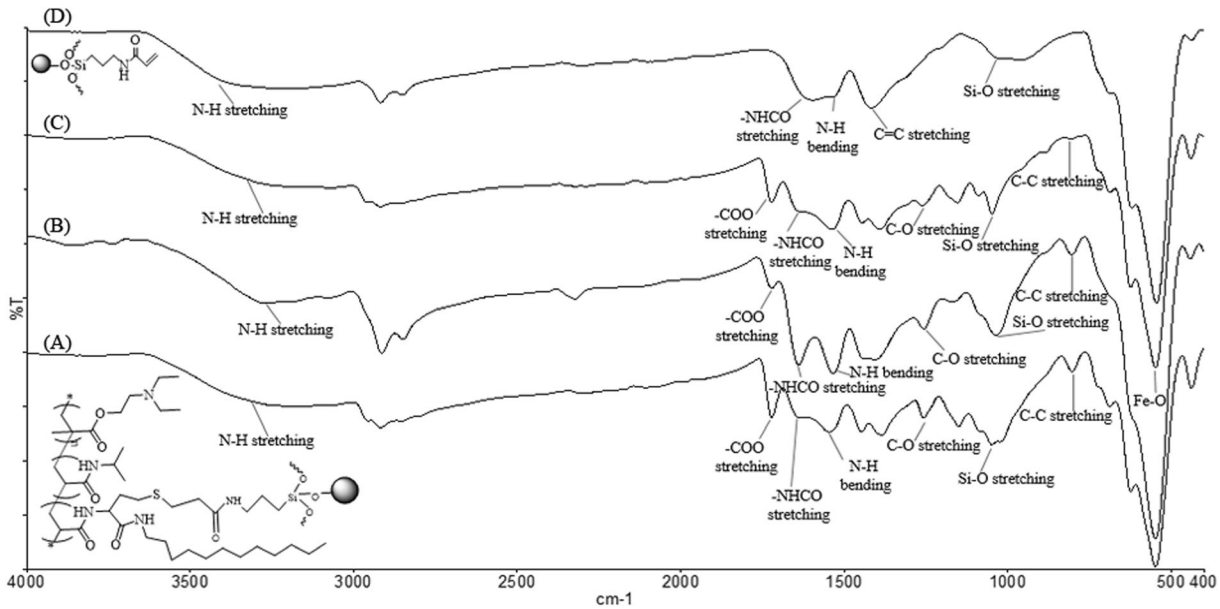

Fig. 4 FTIR spectra of **a** acrylamide-coated MNP, **b** MC3, **c** MC8, and **d** MC12

visible spectrophotometry. The drug entrapment efficiency was calculated from the following equation:

$$\text{Entrapment efficiency (\%EE)} = \frac{\text{weight of the entrapped drug in the MNP}}{\text{weight of the loaded drug}} \times 100$$

Characterization

FTIR spectrophotometry was operated on a Perkin–Elmer Model 1600 Series FTIR spectrophotometer. ^{1}H NMR spectroscopy was performed on a 400-MHz Bruker NMR spectrometer using DMSO-d_6 or $CDCl_3$ as solvents. The hydrodynamic diameter (D_h) and zeta potential of the particles were measured by PCS using NanoZS4700 nanoseries Malvern instrument. The sample dispersions were sonicated for 1 h before each measurement without filtration. The TEM images were conducted using a Philips Tecnai 12 operated at 120 kV equipped with Gatan model 782 CCD camera. The particles were re-dispersed in water and then sonicated before deposition on a TEM grid. TGA was performed on Mettler-Toledo's SDTA 851 at the temperature ranging between 50 and 800 °C and a heating rate of 20 °C/min under oxygen atmosphere. Magnetic properties of the particles were measured at room temperature using a Standard 7403 Series, Lakeshore vibrating sample magnetometer (VSM). UV-visible spectrophotometry was performed on microplate reader at λ = 480 nm.

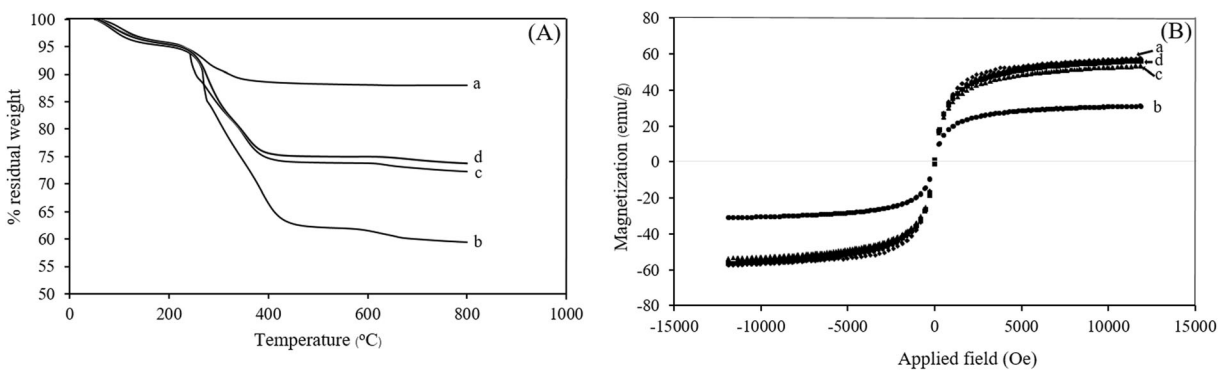

Fig. 5 **A** TGA thermograms and **B** *M-H* curves of (a) acrylamide-coated MNP, (b) MC3, (c) MC8, and (d) MC12

Table 1 Zeta potential values and hydrodynamic size (D_h) of the copolymer-coated MNP

Types of MNP	Zeta potential [mV]		D_h of quaternized particles [nm]	
	Before quaternization	After quaternization	at 25 °C	at 45 °C
Acrylamide-coated MNP	− 15.3 ± 0.5	− 15.3 ± 0.5	564 ± 63	506 ± 52
MC3	0	28.4 ± 1.0	1068 ± 197	396 ± 58
MC8	0	16.2 ± 0.6	836 ± 214	372 ± 103
MC12	0	26.3 ± 0.8	1426 ± 218	295 ± 0

Results and discussion

This work focused on the surface modification of MNP with multi-functional PDEAEMA-*b*-P(NIPAAm-*st*-TlaAm) copolymer to obtain magnetic nanocluster with thermo-responsive properties for drug-controlled release application. The copolymer was synthesized via RAFT polymerization to control architecture and the molecular weight of the block copolymer. PDEAEMA macro CTA was first synthesized, followed by the extension of P(NIPAAm-*st*-TlaAm) second block from PDEAEMA first block. It was envisioned that the quaternized PDEAEMA could form the corona, while P(NIPAAm-*st*-TlaAm) block self-assembled to be a core in aqueous media. (Supplementary material Fig. S3). PTlaAm in the P(NIPAAm-*st*-TlaAm) allowed for a double modification for (1) adjustment of the degree of the hydrophobicity of the polymeric core and (2) immobilization of the polymer on MNP surface. This P(NIPAAm-*st*-TlaAm) core was also used for entrapment of a therapeutic drug with a thermo-triggering release mechanism owing to the existence of PNIPAAm

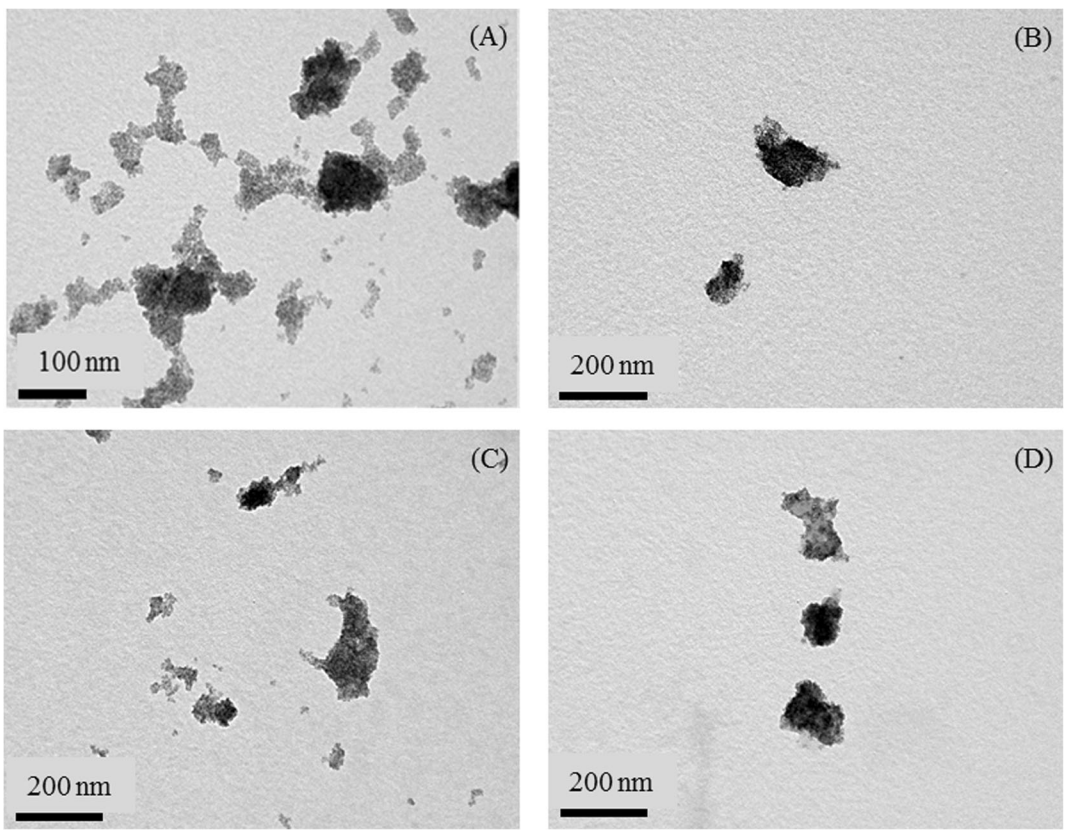

Fig. 6 TEM images of **a** acrylamide-coated MNP, **b** qMC3, **c** qMC8, and **d** qMC12 prepared from aqueous dispersions

in the structure. In addition, an optimal degree of hydrophilicity/hydrophobicity of the copolymer might be necessary for controlled release of the entrapped drug. Therefore, three different alkyl chain lengths (C3, C8, and C12) were used for tuning the degree of the hydrophobicity of the copolymer coated on the particle surface.

Synthesis and characterization of the copolymer-coated MNP

^{1}H NMR spectra of the purified products from each step are shown in Fig. 2. The signals corresponding to the methylene protons of PDEAEMA macro CTA (1.8–1.9 ppm) indicated the polymerization of PDEAEMA (Fig. 2a). This macro CTA was then used for the propagation of NIPAAm and TlaAm monomers. The new signals at δ 1.1 and 3.6 ppm of the NIPAAm units and at δ 3.2 and 4.7 ppm of TlaAm units indicated the propagation of both monomers from PDEAEMA macro CTA (Fig. 2b). After the ring-opening reactions of thiolactone units with various alkylamines (1-propylamine, 1-octylamine, and 1-dodecylamine), the strong signals of the protons of alkyl groups appeared in the range of δ 0.9–1.4 ppm (Fig. 2c–e). In good agreement with this result, the disappearance of TlaAm signals at δ 3.3–3.4 ppm (signal *k* in Fig. 2b) and δ 4.7 (signal *i* in Fig. 2b), indicating the successful ring-opening reactions of thiolactone moiety in the copolymers. In addition, the results from FTIR were also in good agreement with those obtained from ^{1}H NMR (Supplementary material Fig. S4).

After the ring-opening reaction of thiolactone rings in the copolymers with alkylamines to form thiol groups (-SH), the acrylamide-coated MNP was subsequently added to the mixture allowing for the thiol-ene reaction (Lowe 2010). The proposed thiol-ene reaction mechanism between the acrylamide on the MNP surface and thiol groups (-SH) of the copolymer is shown in Fig. 3. Figure 4 shows FTIR spectra of the acrylamide-coated MNP and the MNP coated with the copolymers after the thiol-ene reaction. The signal at 590 cm^{-1} corresponding to Fe–O bond in the MNP appeared in every sample (Fig. 4). Figure 4b, d shows the characteristic adsorption signals of C=O stretching (1730 cm^{-1}), C–O stretching (1260 cm^{-1}) of carboxyl groups, and C–C stretching (800 cm^{-1}) of the copolymer, signifying the existence of the copolymer on the particle surface through the thiol-ene reaction.

To study the organic/inorganic composition of the copoymer-coated MNP, TGA was used to determine the weight loss at 800 °C (Fig. 5a). It was hypothesized that the residue weight was the weight of iron oxide from oxidized MNP, while the loss weight was the organic conponents in the copolymer-MNP assemblies. The decrease of the residual weight in the samples corresponded to the increase in the organic contents in the MNP. It was found that there was about 12% organic content in acrylamide-coated MNP, while after coating with the copolymer, there were 26, 28, and 41% of the polymers in MC12, MC8, and MC3, respectively, signifying that MC3 had higher degree of alkyl substitution as compared to the other two. This was rationalized that the short alkyl chain length in the C3 copolymer might have less steric hindrance in the particle coating step, resulting in the better accessibility of the particles to react with the copolymers and thus higher amounts of the copolymers on the particles.

VSM technique was used to determine magnetic properties of the MNP before and after the copolymer coating (Fig. 5b). They well responded to an applied magnet and showed superparamagnetic behavior due to the absence of the coercitivity (H_c) and remanence (M_r)

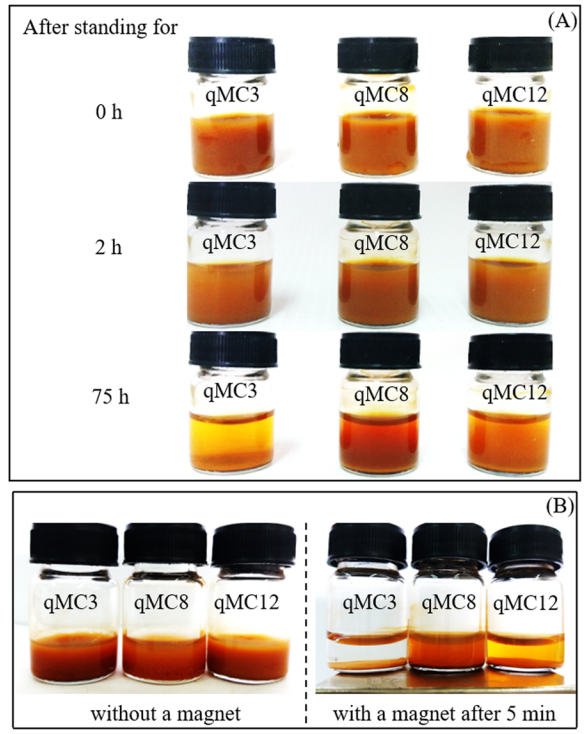

Fig. 7 **a** Water dispersibility and **b** magnetic separation ability of qMC3, qMC8, and qMC12

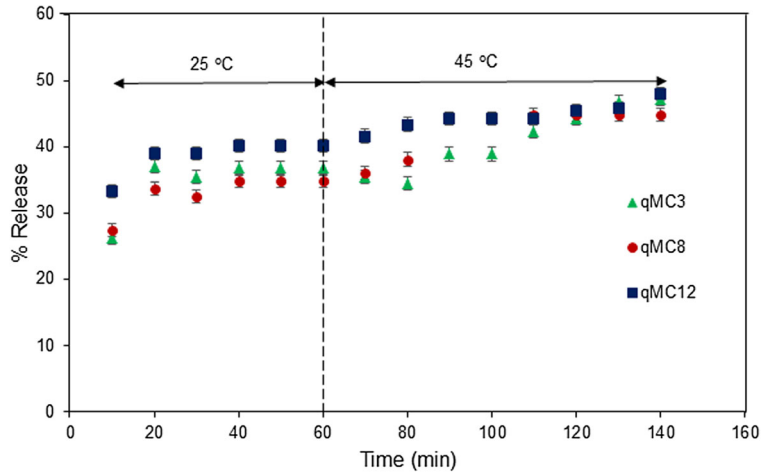

Fig. 8 DOX release profiles of the copolymer-coated MNP (qMC3, qMC6, and qMC12)

upon removal of an external magnetic field. The saturation magnetization (M_s) decreased from 58 emu/g of acrylamide-coated MNP to 56 emu/g of MC12, 54 emu/g of the MC8, and 31 emu/g of MC3, due to the presence of non-magnetic copolymer on the particle surface and thus the drop of their magnetic responsiveness. The decrease in the net magnetization corresponded well to the increase of the copolymers coated on the particles observed in TGA.

The copolymer-coated MNP was then quaternized to improve the particle dispersibility in water. Zeta potentials of the particle both before (MC3, MC8, and MC12) and after quaternization (qMC3, qMC8, and qMC12) were studied using PCS (Table 1). The zeta potentials of acrylamide-coated MNP before and after quaternization did not change because there was no copolymer coated on the MNP surface. After the copolymer coating, their zeta potential values of all copolymers significantly increased from 0 to 16–28 mV after quaternizations, owing to the formation of permanent positive charges of quaternary ammonium groups in the copolymer-coated MNP. It should be noted that these positive charges might facilitate the particles to be well dispersible in an aqueous media, which was necessary for the use in drug-controlled release applications discussed later in this report.

In addition, the preliminary studies in the use of the cationic MNP for ionic adsorption with negative bioentities were also investigated. DNA tagged with 6-carboxytetramethyl rhodamine (TAMRA-5′-TACC ACCATTC-3′) was selected as a model compound to proof the idea of ionic adsorption capability of the particles. qMC12 (2 mg) as a representative was dispersed in 0.4 μM DNA solution (2 ml) and then stirred for 2 h, followed by magnetic separation. It was found

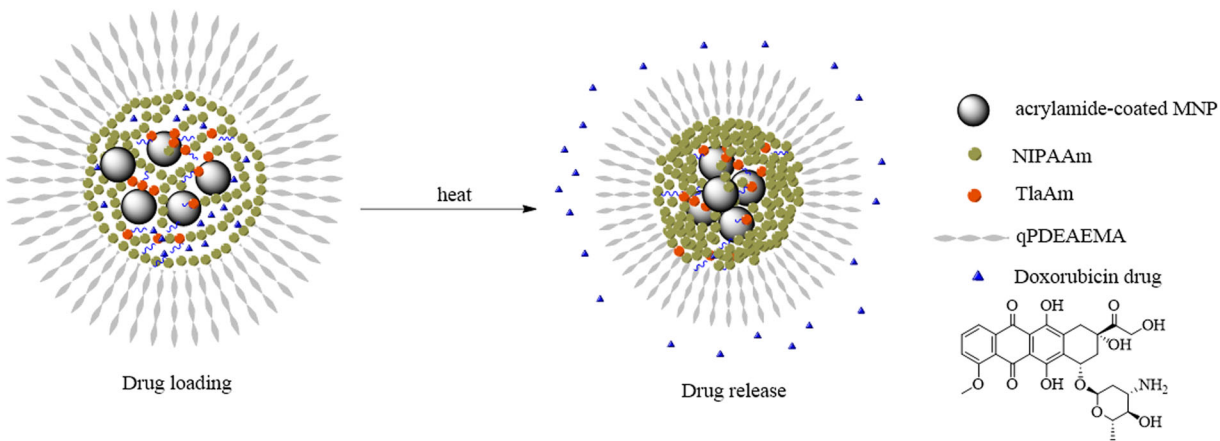

Fig. 9 The proposed mechanism of DOX release from the copolymer-coated MNP

that the concentrations of DNA in the solutions significantly decreased from 0.42 to 0.05 μM (Supplementary materials Fig. S5), indicating that the MNP can be used as a cationic platform for adsorption with DNA through the electrostatic interaction.

Representative TEM images of acrylamide-coated MNP and the quaternized copolymer-coated MNP (qMC) prepared from aqueous dispersions are shown in Fig. 6. Acrylamide-coated MNP showed macroscopic aggregation due to the lack of polymer coating resulting in the particles with poor water dispersibility (Fig. 6a). After coating with the copolymer and then quaternization, formation of the nanoclusters with the size below 200 nm/cluster was observed (Fig. 6b–d). They showed good dispersibility in water without noticeable aggregation after standing for 2 h (Fig. 7a). After 75 h, the qMC3 dispersion exhibited some aggregation, while those of qMC8 and qMC12 were insignificant. This was attributed to the higher degree of alkyl substitution of 1-propylamine in the copolymer due to less steric hindrance as compared to those of 1-octyl and 1-dodecylamines, resulting in the higher degree of hydrophobicity of the copolymer and consequently aggregating in water. The TGA result discussed above also supported this assumption that there was higher amount of the copolymer in qMC3, which might result in the higher degree of hydrophobicity as compared to qMC8 and qMC12.

The particle dispersibility in water shown in Fig. 7a was in good agreement with their magnetic separation ability in water. After 5 min of magnetic separation, qMC3 can be completely separated while there were some dispersible particles remaining in qMC8 and qMC12 dispersions (Fig. 7b). Importantly, the completely separated ability of particles from the dispersion with an assistance of a magnet was necessary for the determination of the drug-controlled release discussed later in this work.

Because the copolymer coated on the particles in this work comprised thermo-responsive moieties of PNIPAAm and PDEAEMA, the effect of the change in the temperature on their D_h was investigated. The experimental temperatures were set at 25 and 45 °C, which crosses their critical solution temperature (LCST of PNIPAAm = 30–34 °C and LCST of PDEAEMA = 31 °C) (Gandhi et al. 2015; Maeda and Mochiduki 2004). It was found that, in all cases, D_h of the particle coated with the copolymers at 45 °C was smaller than those at 25 °C (Table 1). The copolymers collapsed at the temperature above its critical solution temperature, resulting in the shrinkage of the nanocluster and thus the decrease in their D_h. It should be noted that the shrinkage of the copolymer when heated to 45 °C would be utilized as a triggering mechanism for drug-controlled release discussed in the later section.

In vitro release studies of entrapped DOX from the copolymer-coated MNP triggered by the temperature change

DOX, known as a chemotherapy medication used to treat cancer, was used as a model drug for entrapment in and then release from the copolymer-coated MNP. It was hypothesized that DOX was entrapped in the copolymer-coated particles due to the hydrogen bonding of DOX molecules with the copolymer. %EE of qMC3 was ca. 5.4%, while those of qMC8 and qMC12 ranged between 10.3 and 10.8%. The two-fold lower percentage of qMC3 as compared to those of the other two samples was probably due to the higher degree of hydrophobicity in qMC3 (higher degree of alkyl substitution), which might result in less entrapment of DOX on the particles.

DOX release studies were performed at 25 °C with a step-wise increase in the temperature to 45 °C after the equilibrium (Fig. 8). In all cases, the release of DOX from the particle at 25 °C reached their equilibrium within 40 min and they were held at this temperature for 1 h to ensure the equilibrium. Generally, when the temperature of dispersion is increased above room temperature, the preloaded drug should mainly be released via a diffusion mechanism (Liu et al. 2010). In this work, when increasing the temperature to 45 °C (above LCST of PNIPAAm), all samples (qMC3, qMC8, and qMC12) showed the same trend of the drug release. The increment of DOX release upon increasing the temperature was mainly attributed to "a diffusion mechanism". Interestingly, qMC8 and qMC12 showed the faster rate of DOX release with additional release of ca. 8–10% and reached the equilibrium within 40 min. This accelerated release rate was attributed to "a squeezing mechanism" due to the collapse of PNIPAAm chains at above its LCST (Trongsatitkul and Budhlall 2013). However, the release rate of DOX in qMC3 seemed to be retarded at the beginning of the elevated temperature and it was then slowly released afterward with additional DOX release of ca. 11%. The higher degree of hydrophobicity in qMC3 discussed above might inhibit the squeezing behavior of PNIPAAm in the copolymer, which thus initially retarded

the release of the entrapped drug from the particles at the elevated temperature (Fig. 9).

Conclusions

We herein reported the multi-responsive MNP modified with cationic PDEAEMA-*b*-P(NIPAAm-*st*-TlaAm) copolymer and its potential applications in controlled drug release and bio-conjugation. Degree of hydrophobicity of the copolymers coated on surface of particle can be tuned by using various alkyl chain lengths in thiolactone ring-opening reaction and this can influence the particle self-assemblies in water (e.g., D_h, dispersibility, nano-aggregation) and the drug release rate. These particles exhibited the temperature responsive behavior, which can be used as a triggering mechanism for controlled release of DOX. These versatile copolymer-MNP assemblies showed an enormous potential for use as a smart platform with thermal-triggering controlled drug release system and for conjugation with any negatively charged bio-entities.

Acknowledgements The authors acknowledge the Thailand Research Fund (TRF)(RSA5980002) for financial support. MR thanks the National Research Council of Thailand (NRCT) (R2561B086) for the supports. SP thanks The Royal Golden Jubilee PhD Program (PhD/0210/2556) for the scholarship.

Funding This study was funded by The Thailand Research Fund (TRF) (RSA5980002), the National Research Council of Thailand (NRCT) (R2561B086), and the Royal Golden Jubilee PhD Program (PhD/0210/2556).

Compliance with ethical standards

Conflict of interest The authors declare that they have no conflict of interest.

References

Bischofberger I, Trappe V (2015) New aspects in the phase behaviour of poly-N-isopropyl acrylamide: systematic temperature dependent shrinking of PNiPAM assemblies well beyond the LCST. Sci Rep 5:15520–15529

Braunecker WA, Matyjaszewski K (2007) Controlled/living radical polymerization: features, developments, and perspectives. Prog Polym Sci 32:93–146

Chen J-T, Ahmed M, Liu Q, Narain R (2012) Synthesis of cationic magnetic nanoparticles and evaluation of their gene delivery efficacy in Hep G2 cells. J Biomed Mater Res A 100A:2342–2347

Chen Y, Espeel P, Reinicke S, Du Prez FE, Stenzel MH (2014) Control of glycopolymer nanoparticle morphology by a one-pot, double modification procedure using thiolactones. Macromol Rapid Commun 35:1128–1134

Chen L, Zhang H, Li L, Yang Y, Liu X, Xu B (2015) Thermoresponsive hollow magnetic microspheres with hyperthermia and controlled release properties. J Appl Polym Sci 132:42617

Du H, Wickramasinghe R, Qian X (2010) Effects of salt on the lower critical solution temperature of poly (N-isopropylacrylamide). J Phys Chem 114:16594–16604

Espeel P, Du Prez FE (2015) One-pot multi-step reactions based on thiolactone chemistry: a powerful synthetic tool in polymer science. Eur Polym J 6:247–272

Espeel P, Goethals F, Du Prez FE (2011) One-pot multistep reactions based on thiolactones: extending the realm of thiol-ene chemistry in polymer synthesis. J Am Chem Soc 133:1678–1681

Espeel P, Goethals F, Stamenovi MM, Petton L, Du Prez FE (2012) Double modular modification of thiolactone-containing polymers: towards polythiols and derived structures. Polym Chem 3:1007–1015

Gandhi A, Paul A, Sen OS, Sen KK (2015) Studies on thermoresponsive polymers: phase behaviour, drug delivery and biomedical applications. Asian J Pharm Sci 10:99–107

Hill MR, Carmean RN, Sumerlin BS (2015) Expanding the scope of RAFT polymerization: recent advances and new horizons. Macromolecules 48:5459–5469

Hu Y, Meng L, Niu L, Lu Q (2013) Highly cross-linked and biocompatible polyphosphazene-coated superparamagnetic Fe_3O_4 nanoparticles for magnetic resonance imaging. Langmuir 29:9156–9163

Huang L, Liu M, Mao L, Xu D, Wan Q, Zeng G, Shi Y, Wen Y, Zhang X, Wei Y (2017) Preparation and controlled drug delivery applications of mesoporous silica polymer nanocomposites through the visible light induced surface-initiated ATRP. Appl Surf Sci 412:571–577

Leung KCF, Lee S, Wong C, Chak C, Lai JMY, Zhu X, Wang YJ, Wang YXJ, Cheng CHK (2013) Nanoparticle–DNA–polymer composites for hepatocellular carcinoma cell labeling, sensing, and magnetic resonance imaging. Methods 64:315–321

Li Y, Zhang X, Cheng H, Kim G, Cheng S, Zhuo R (2006) Novel stimuli-responsive micelle self-assembled from Y-shaped P(U-Y-NIPAAm) copolymer for drug delivery. Biomacromolecules 7:2956–2960

Lim J, Yeap SP, Che HX, Low SC (2013) Characterization of magnetic nanoparticle by dynamic light scattering. Nanoscale Res Lett 8:381–394

Liu P, Luo Q, Guan Y, Zhang Y (2010) Drug release kinetics from monolayer films of glucose-sensitive microgel. Polymer 51: 2668–2675

Lowe AB (2010) Thiol-ene "click" reactions and recent applications in polymer and materials synthesis. Polym Chem 1:17–36

Machida N, Inoue Y, Ishihara K (2014) Phospholipid polymer-coverd magnetic nanoparticles for tracking intracellular molecular reaction. Trans Mat Res Soc Japan 39:427–430

Maeda Y, Mochiduki H (2004) Hydration changes during thermosensitive association of a block copolymer consisting of LCST and UCST blocks. Macromol Rapid Commun 25: 1330–1334

Mahmoud WE, Bronstein LM, Al-Hazmi F, Al-Noaiser F, Al-Ghamdi AA (2013) Development of Fe/Fe_3O_4 core-shell nanocubes as a promising magnetic resonance imaging contrast agent. Langmuir 29:13095–13101

Matyjaszewski K (2012) Atom transfer radical polymerization (ATRP): current status and future perspectives. Macromolecules 45:4015–4039

Meerod S, Rutnakornpituk B, Wichai U, Rutnakornpituk M (2015) Hydrophilic magnetic nanoclusters with thermo-responsive properties and their drug controlled release. J Magn Magn Mater 392:83–90

Mekkapat S, Thong-On B, Rutnakornpituk B, Wichai U, Rutnakornpituk M (2013) Magnetic core–bilayer shell complex of magnetite nanoparticle stabilized with mPEG–polyester amphiphilic block copolymer. J Nanopart Res 15:2051–2062

Moad G, Rizzardo E, Thang SH (2008) Radical addition fragmentation chemistry in polymer synthesis. Polymer 49:1079–1131

Patil SS, Wadgaonkar PP (2017) Temperature and pH dual stimuli responsive PCL-*b*-PNIPAAm block copolymer assemblies and the cargo release studies. J Polym Sci A Polym Chem 55:1383–1396

Prabha G, Raj V (2016) Preparation and characterization of polymer nanocomposites coated magnetic nanoparticles for drug delivery applications. J Magn Magn Mater 408:26–34

Qin S, Qin D, Ford WT, Resasco DE, Herrera JE (2004) Functionalization of single-walled carbon nanotubes with polystyrene *via* grafting to and grafting from methods. Macromolecules 37:752–757

Qu Y, Li J, Ren J, Leng J, Lin C, Shi D (2014) Enhanced magnetic fluid hyperthermia by micellar magnetic nanoclusters composed of $Mn_xZn_{1-x}Fe_2O_4$ nanoparticles for induced tumor cell apoptosis. ACS Appl Mater Interfaces 6:16867–16879

Reinicke S, Espeel P, Stamenović MM, Du Prez FE (2013) One-pot double modification of P(NIPAAm): a tool for designing tailor-made multiresponsive polymers. ACS Macro Lett 2: 539–543

Rodkate N, Rutnakornpituk M (2016) Multi-responsive magnetic microsphere of poly(N-isopropylacrylamide)/carboxymethylchitosan hydrogel for drug controlled release. Carbohydr Polym 151:251–259

Sahoo B, Devi KSP, Banerjee R, Maiti TK, Pramanik P, Dhara D (2013) Thermal and pH responsive polymer-tethered multifunctional magnetic nanoparticles for targeted delivery of anticancer drug. ACS Appl Mater Interfaces 5:3884–3893

Sciannamea V, Jérôme R, Detrembleur C (2008) In-situ nitroxide-mediated radical polymerization (NMP) processes: their understanding and optimization. Chem Rev 108:1104–1126

Singh LP, Srivastava SK, Mishra R, Ningthoujam RS (2014) Multifunctional hybrid nanomaterials from water dispersible CaF_2:Eu^{3+}, Mn^{2+} and Fe_3O_4 for luminescence and hyperthermia application. J Phys Chem C 118:18087–18096

Stamenovi MM, Espeel P, Van Camp V, Du Prez FE (2011) Norbornenyl-based RAFT agents for the preparation of functional polymers *via* thiol-ene chemistry. Macromolecules 44: 5619–5630

Trongsatitkul T, Budhlall BM (2013) Microgels or microcapsules? Role of morphology on the release kinetics of thermoresponsive PNIPAm-co-PEGMa hydrogels. Polym Chem 4:1502–1516

Ulbrich K, Holá K, Šubr V, Bakandritsos A, Tuček J, Zbořil R (2016) Targeted drug delivery with polymers and magnetic nanoparticles: covalent and noncovalent approaches, release control, and clinical studies. Chem Rev 116:5338–5431

Wang B, Li B, Zhao B, Li CY (2008) Amphiphilic janus gold nanoparticles *via* combining "solid-state grafting-to" and "grafting-from" methods. J Am Chem Soc 130:11594–11595

Wang C, Xu H, Liang C, Liu Y, Li Z, Yang G, Cheng L, Li Y, Liu Z (2013) Iron oxide @ polypyrrole nanoparticles as a multifunctional drug carrier for remotely controlled cancer therapy with synergistic antitumor effect. ACS Nano 7:6782–6795

Willcock H, O'Reilly RK (2010) End group removal and modification of RAFT polymers. Polym Chem 1:149–157

Hindawi
Journal of Nanomaterials
Article ID 8252036

Research Article

Multiresponsive Poly(*N*-Acryloyl glycine)-Based Nanocomposite and Its Drug Release Characteristics

Nunthiya Deepuppha, Sudarat Khadsai, Boonjira Rutnakornpituk, Uthai Wichai, and Metha Rutnakornpituk

Department of Chemistry and Center of Excellence in Biomaterials, Faculty of Science, Naresuan University, Phitsanulok 65000, Thailand

Correspondence should be addressed to Metha Rutnakornpituk; methar@nu.ac.th

Received 22 May 2018; Accepted 29 October 2018

Academic Editor: Domenico Acierno

pH- and thermoresponsive nanocomposite composed of poly(*N*-acryloyl glycine) (PNAG) matrix and magnetite nanoparticle (MNP) was synthesized and then used for drug controlled release application. The effects of crosslinkers, e.g., ethylenediamine and *tris*(2-aminoethyl)amine, and their concentrations (1 and 10 mol%) on the size, magnetic separation ability, and water dispersibility of the nanocomposite were investigated. The nanocomposite crosslinked with *tris*(2-aminoethyl)amine (size ranging between 50 and 150 nm in diameter) can be rapidly separated by a magnet while maintaining its good dispersibility in water. It can respond to the pH and temperature change as indicated by the changes in its zeta potential and hydrodynamic size. From the in vitro release study, theophylline as a model drug was rapidly released when the pH changed from neutral to acidic/basic conditions or when increasing the temperature from 10°C to 37°C. This novel nanocomposite showed a potential application as a magnetically guidable vehicle for drug controlled release with pH- and thermotriggered mechanism.

1. Introduction

Magnetite nanoparticle (MNP) has attracted great attention in recent years in biomedical and biotechnological applications [1–5] owing to its magnetically guidable properties [2], high surface area-to-volume ratio [4], high saturation magnetization [6, 7], low toxicity, and high biocompatibility [8]. These intriguing properties make MNP as an ideal candidate for use in various biomedical fields such as drug delivery [5], diagnostics, therapeutics [2, 9, 10], and magnetic separation [11–13].

In the magnetic separation application, MNP should have high magnetic responsiveness, so that it should abruptly respond to a magnet and completely remove unadsorbed entities after decanting [14, 15]. Formation of nanocomposite containing multiparticles of MNP embedded in polymer matrix was another promising approach to enhance magnetic sensitivity while maintaining its good dispersibility in the media. When individual unique properties of both MNP and polymer matrix were combined, multifunctional nanocomposite serving as a platform for further conjugation with desirable bioentities can be obtained [16, 17]. Thus, this hybrid nanocomposite has been particularly used in the biological field such as drug delivery system [18, 19], controlled release [16, 20, 21], and magnetic separation [11–13]. Previous works have reported the synthesis of MNP-polymer nanocomposite having both good magnetic separation ability and good water dispersibility for drug controlled release [4, 16] and for conjugation with bioentities [17, 22].

Interestingly, polymer matrix having external stimuli-responsive properties in nanocomposite can be used as a handle in controlled release applications [23–27]. Previous works have presented the use of MNP coated with pH- and thermoresponsive polymers as a handle for triggered mechanisms for drug controlled release [26]. Among the pH- and thermo-responsive polymers, poly(*N*-acryloyl glycine) (PNAG) is of particular interest in this research because it can be facilely synthesized via a free radical polymerization

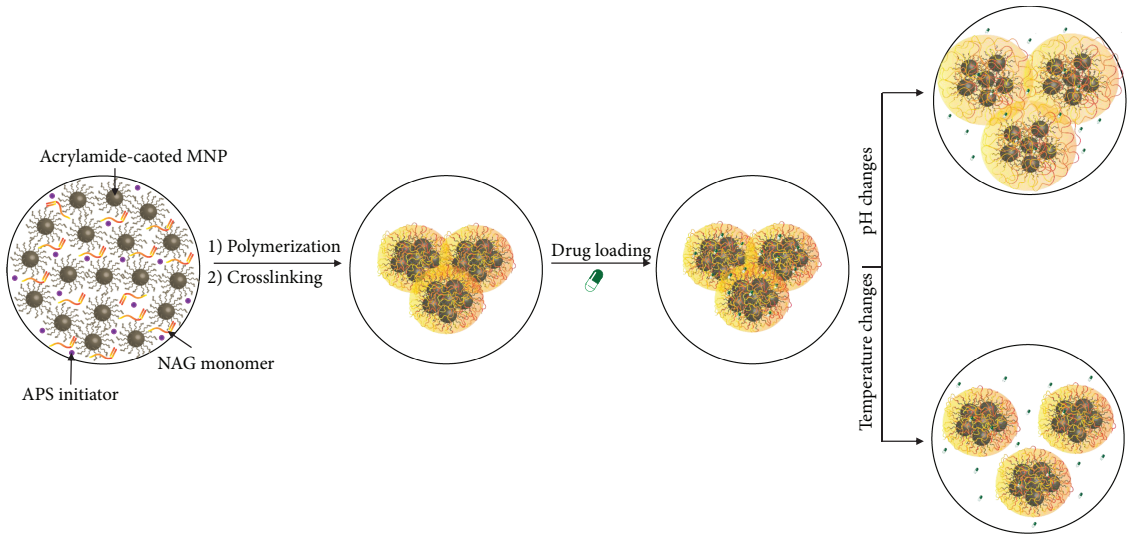

Figure 1: Schematic preparation of PNAG-coated MNP nanocomposite for drug controlled release applications.

of *N*-acryloyl glycine monomer in aqueous solutions [12, 28]. H-bonding network of carboxyl groups (-COOH) and amide groups (-CONH-) in PNAG chains with water molecules plays a crucial role in its pH- and temperature-responsive properties [29].

In a basic pH condition, the carboxylate groups (COO^-) of PNAG should be formed, resulting in the enhancement in water swelling due to negative-charge repulsion among the chains. On the other hand, when the polymer was protonated in an acidic pH condition, its collapsed structure should be formed [30]. PNAG also showed thermoresponsive properties when its environmental temperature changed due to H-bonding of amide bonds in the chains with water molecules [31, 32], similarly to the case of the amino acid-derived polymers, such as poly(*N*-acryloyl glycinamide) (PNAGA) [33], poly(acrylamide) (PAAm), and poly(acrylic acid) (PAA) [34–36]. However, the study in upper critical solution temperature (UCST) of PNAG homopolymer has never been reported, while that of PNAG-containing copolymer was very limited [37]. At the temperature below the UCST, PNAG should be stabilized by intramolecular H-bonding, resulting in the formation of solid hydrogels. At the temperature above its UCST, it can reversibly turn into fluid state because the intramolecular H-bonding is diminished and because of the simultaneous formation of intermolecular H-bonding between water molecules and chains of polymer [33].

This work reports the synthesis of MNP nanocomposite coated with pH-/thermoresponsive PNAG and its use in drug controlled release. Modification of MNP surface with PNAG was first prepared via a free radical polymerization, followed by a crosslinking reaction. Different types and concentrations of the crosslinkers (1 mol% and 10 mol% of *tris*(2-aminoethyl)amine or ethylenediamine) were used in the crosslinking in an attempt to tune the reaction condition to gain the nanocomposite with good water dispersibility and high magnetic separation ability. The effect of the crosslinking condition of the nanocomposite on the controlled release of theophylline as a model drug was also investigated. It was rationalized that PNAG can serve as a reservoir of the drug with both pH- and temperature-triggered drug release mechanisms (Figure 1). The effects of pH (pH 2.0, pH 7.4, and pH 11.0) and temperature (10°C and 37°C) on its drug release rate were also herein investigated.

2. Experimental

2.1. Materials. Ammonium hydroxide (NH_4OH) (28–30%, J.T. Baker), *N*-(3-dimethylaminopropyl)-*N*′-ethylcarbodiimide hydrochloride (EDC·HCl) (GL Biochem Shanghai Ltd.), ethylenediamine (Carlo Erba), glycine (AR grade), iron(II) chloride tetrahydrate ($FeCl_2.4H_2O$) (99%, Acros Organic), iron(III) chloride ($FeCl_3$) (98%, Acros), oleic acid (Carlo Erba), ammonium persulfate (APS) (98%, Carlo Erba), (3-aminopropyl) triethoxysilane (APTES) (99%, Acros), triethylamine (TEA) (97%, Carlo Erba), theophylline anhydrous (≥99%, Sigma-Aldrich), and *tris*(2-aminoethyl)amine (96%, Sigma-Aldrich) were used as received. Acryloyl chloride was prepared via a chloride exchange reaction between benzoyl chloride (Acros, 99%) and acrylic acid (98%, Acros) at 75°C to obtain a colorless liquid with 60% yield.

2.2. Characterization. Fourier-transform infrared spectrometry (FTIR) was conducted on a Perkin–Elmer Model 1600 series FTIR spectrometer. ^{1}H NMR spectroscopy was characterized via a 400 MHz Bruker NMR spectrometer. Transmission electron microscopy (TEM) was conducted on Philips Tecnai 12 operated at 120 kV. The dispersion of the particle in water was dropped on a carbon-coated copper grid at room temperature without filtration. Zeta potential and hydrodynamic size (D_h) of the particle were determined on NanoZS4700 nanoseries Malvern photocorrelation spectrometer (PCS). Magnetic properties were characterized via a Standard 7403 Series, Lakeshore vibrating sample magnetometer (VSM). UV-visible spectrophotometry was conducted on Analytik-Jena AG Specord 200 plus UV-Vis spectrophotometer at $\lambda = 272$ nm.

2.3. Preparation of N-Acryloyl Glycine (NAG) Monomer. Glycine (61.8 mmol, 4.64 g) was dissolved in a NaOH aqueous solution (123.6 mmol, 4.95 g). An acryloyl chloride solution in tetrahydrofuran (61.8 mmol, 5.0 mL) was added into the solution and then stirred at 0°C for 3 h. The mixture was washed with diethyl ether, and then the aqueous solution layer was adjusted to a pH 2 solution with conc. HCl. The extraction with ethyl acetate was carried out, and then the organic layer was dried with anh. Na_2SO_4, filtered, and evaporated in vacuo. Finally, white solid as a product was obtained: 2.41 g, 30% yield; ^{1}H NMR (400 MHz, D_2O): δ 4.08 ppm (*s*, 2H), 5.82–5.84 (*dd*, 1H), and 6.24–6.39 (*dd* and *t*, 2H).

2.4. Preparation of Acrylamide-Coated MNP. 30% NH_4OH solution (5.0 mL) was added into a solution mixture of $FeCl_2{\cdot}4H_2O$ (2.1 mmol, 0.83 g) and $FeCl_3$ (2.5 mmol, 0.50 g) with stirring at 25°C for 30 min. After being separated and washed with distilled water, an oleic acid solution (1.0 mL) in toluene (9.0 mL) was added into the MNP dispersion and then stirred at 25°C for 30 min. Oleic acid-coated MNP was precipitated in acetone, separated by a magnet, and then redispersed in toluene (10.0 mL). TEA (13.6 mmol, 1.0 mL) and APTES (11.9 mmol, 2.5 mL) were then added to the dispersion with stirring at 25°C under N_2 for 24 h to obtain amino-coated MNP.

After magnetic separation, washing, and evaporation until dryness, amino-coated MNP (0.05 g) was then dispersed in a NaOH solution (1.50 g) by ultrasonication. An acryloyl chloride (49.5 mmol, 5.0 mL) was slowly added into the MNP dispersion at 0°C in an ice bath for 1 h, and then the mixture was continuously stirred at 25°C for 24 h. After a reaction was completed, the particle was separated by a magnet and then repeatedly washed with distilled water and stored in the dispersion form (0.02 g MNP/mL H_2O).

2.5. Preparation of PNAG-Coated MNP Nanocomposite. NAG monomer (0.25 g, 1.94 mmol) was dissolved in distilled water (20.0 mL), followed by an addition of a dispersion of acrylamide-coated MNP (0.05 g MNP in 25.0 mL distilled water). An APS radical initiator solution (10% in distilled water, 0.04 mmol) was injected into the mixture, and the reaction was set allowed for 2 h at 70°C under N_2 gas to obtain PNAG-coated MNP nanocomposite. After magnetic separation and washing with distilled water to remove the unreacted monomers and uncoated polymer chains, the nanocomposite was then dried in vacuo. In the crosslinking reaction, the dispersion of the nanocomposite (0.05 g nanocomposite in 50.0 mL distilled water) was added with EDC·HCl (5% in distilled water) as a coupling agent and stirred at 25°C 1 h. After magnetic separation, the nanocomposite was redispersed in the crosslinker solutions (1 or 10 mol% of ethylenediamine or *tris*(2-aminoethyl)amine in a pH 11 buffer solution) and then stirred for 1 h. After the crosslinking reaction, the MNP nanocomposite was rinsed with distilled water with the use of a magnet to wash the unreacted crosslinking agents and then dried in vacuo.

2.6. The Release Studies of Entrapped Theophylline from the MNP Nanocomposite. The dispersion of the MNP nanocomposite (5 mg of the MNP nanocomposite in 1.0 mL aqueous dispersion) was dropwise added with a theophylline solution (1.0 mL, 10 mg/mL in distilled water). After stirring for 3 h at 40°C, the drug-loaded MNP nanocomposite was removed from an excess drug using an external magnet. In the *in vitro* release study, the theophylline-entrapped MNP nanocomposite (5 mg of the MNP nanocomposite) was dispersed in 5.0 mL buffer solutions (pH 2.0, pH 7.4, or pH 11.0). The dispersion was placed into a water bath at 10°C or 37°C. At a predetermined time interval, 100 μL of sample dispersion was withdrawn from the release media. After each sampling, the nanocomposite was magnetically separated and then the supernatant was analyzed via UV-visible spectrophotometer at 272 nm wavelength. Percent release (%) was estimated from the following equation;

$$\text{Percent release}\,(\%) = \frac{\text{weight of the release drug at a given time}}{\text{weight of the drug entrapped in the MNP nanocomposite}} \times 100. \quad (1)$$

To determine drug entrapment efficiency (EE) and drug loading efficiency (DLE), the weight of theophylline entrapped in the MNP nanocomposite was determined from the amount of the drug at the maximum point of the release profile combined with those remaining in the particles. The nanocomposite was extracted with a 0.1 M HCl solution to dissolve the leftover drug and then analyzed via UV-visible spectrophotometer. Therefore, EE and DLE were defined from the following equations:

$$\text{EE}\,(\%) = \frac{\text{weight of the drug entrapped in the MNP nanocomposite}}{\text{weight of the loaded drug}} \times 100, \quad (2)$$

$$\text{DLE}\,(\%) = \frac{\text{weight of the drug entrapped in the MNP nanocomposite}}{\text{weight of the MNP nanocomposite}} \times 100. \quad (3)$$

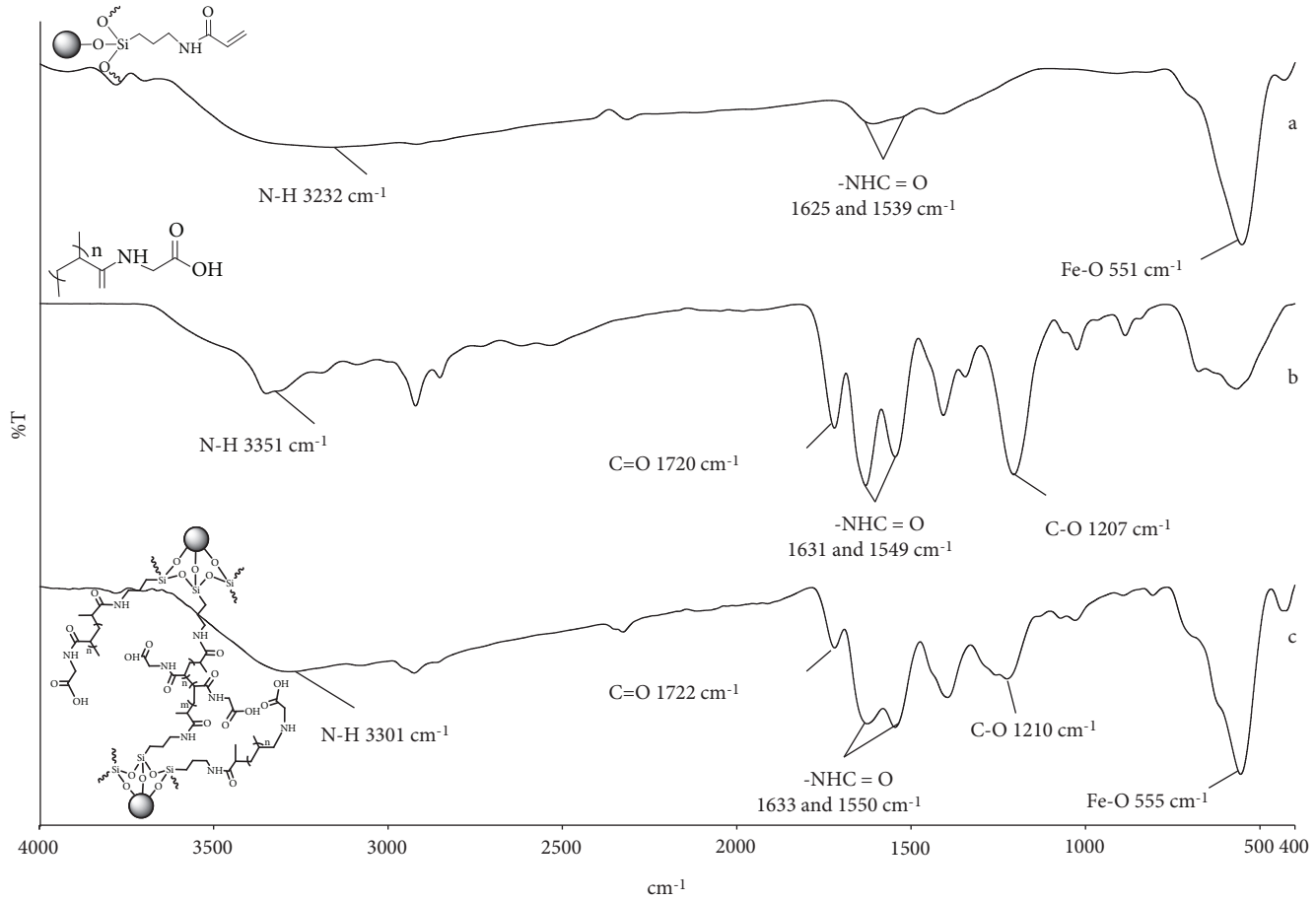

Figure 2: FTIR spectra of (a) acrylamide-coated MNP, (b) PNAG homopolymer, and (c) PNAG-coated MNP nanocomposite.

3. Results and Discussion

In this work, PNAG-coated MNP was first synthesized via a free radical polymerization to form a water dispersible magnetic nanocomposite. In addition to steric stabilization, PNAG also provided electrostatic repulsion stabilization to the nanocomposite due to the presence of carboxylate groups. Additional crosslinking of the MNP nanocomposite was conducted to obtain those with good magnetic separation ability while retaining its good water dispersibility. Two different crosslinkers (ethylenediamine and *tris*(2-aminoethyl)amine) were used in this work to study the effect of the crosslinkers and their concentrations on D_h, water dispersibility and magnetic separation ability of the MNP nanocomposite. pH- and thermoresponsive properties of PNAG coated on its surface provided dual triggering mechanisms for drug release. In this report, in vitro release profile of theophylline entrapped on the nanocomposite was investigated as a function of pH (2.0 7.4 and 11.0) and temperature (10°C and 37°C).

3.1. Characterization of the MNP Nanocomposite. FTIR spectra of the particles before and after coating with PNAG are displayed in Figure 2. The spectrum of acrylamide-coated MNP shows the weak signals of NHC=O stretching (1539 and 1625 cm^{-1}), N-H stretching (3232 cm^{-1}), and also those of the MNP core at 551 cm^{-1} (Fe-O stretching) (Figure 2(a)). Once the nanocomposite was formed by coating MNP with PNAG, the peaks attributed to C-O stretching (1221 cm^{-1}), NHC=O stretching (1550 and 1633 cm^{-1}), C=O stretching (1722 cm^{-1}), and N-H stretching (3301 cm^{-1}) were observed (Figure 2(c)). These signals corresponded well to those of PNAG homopolymer (Figure 2(b)), indicating the presence of PNAG coated on the MNP nanocomposite.

3.2. Effect of Crosslinking Reactions on the Properties of the MNP Nanocomposite. Ethylenediamine and *tris*(2-aminoethyl)amine with two different concentrations (1 and 10 mol%) were used as the crosslinkers in the nanocomposite. The goal of this work was to obtain the MNP nanocomposite with good magnetic separation ability while retaining its good water stability; the conditions in the crosslinking reactions (type of crosslinkers and concentrations) were thus optimized. Zeta potentials and D_h of the nanocomposites were investigated using the PCS technique (Figure 3).

As compared to acrylamide-coated MNP, PNAG-coated MNP nanocomposite did not show an increase in D_h while its zeta potential values significantly increased from −12 to −24 mV, and this was probably due to the existence of anionic carboxylate groups from PNAG. This result well corresponded to that observed from the conductometric

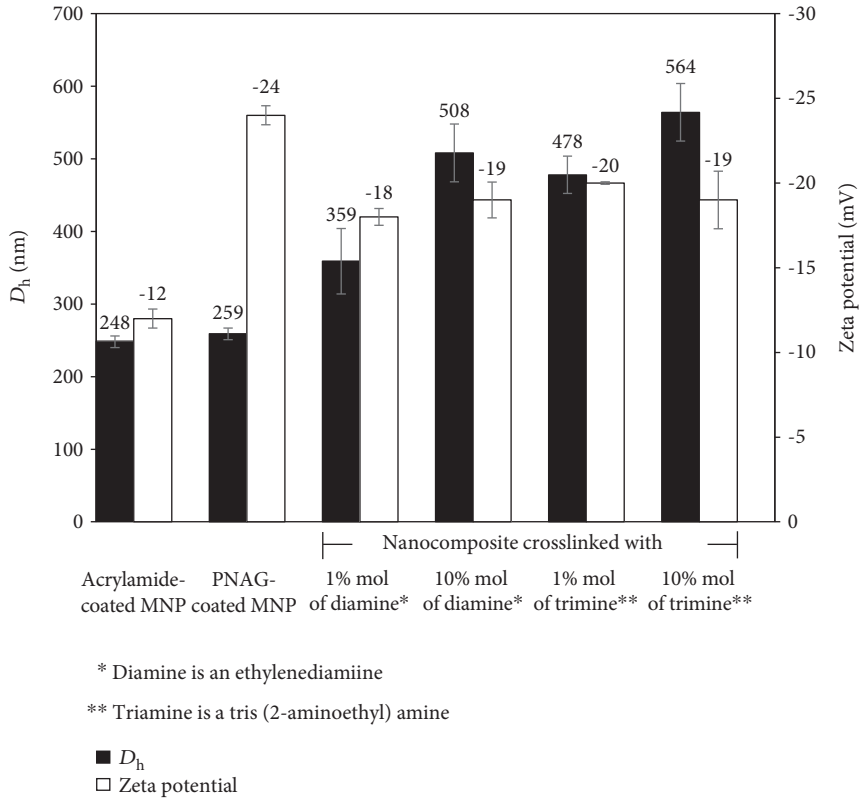

FIGURE 3: D_h and zeta potential values of acrylamide-coated MNP, the MNP nanocomposite (before crosslinking), the MNP nanocomposites after crosslinking with 1 mol% and 10 mol% of ethylenediamine, and 1 mol% and 10 mol% of *tris*(2-aminoethyl)amine.

titration shown in supporting information. After the crosslinking reactions, D_h of all samples significantly increased while its zeta potential values decreased. The coupling reactions between the carboxyl groups of PNAG coated on the particles and the amino groups of the crosslinkers induced the nanoaggregation of the individual particles, resulting in the formation of nanocomposite having multiple particles embedded and a slight drop in the degree of negative charge. The increase in the crosslinker concentration from 1% to 10% also promoted the formation of the crosslinked nanocomposite as indicated by the enlarged D_h. Interestingly, the use of *tris*(2-aminoethyl)amine seemed to enhance the degree of crosslinking as compared to that of ethylenediamine (at the same crosslinker concentrations), probably due to the higher number of the equivalent reactive amines in the reactions (Figure 4).

The size and the size distribution of the MNP nanocomposite in each step of the reactions were also observed via TEM (Figure 5). Acrylamide-coated MNP exhibited aggregation of the particles without the formation of nanoclusters owing to the lack of polymer coating (Figure 5(a)). When MNP surface was coated with PNAG, the particles showed an improvement in water dispersibility without significant aggregation (Figure 5(b)). After the crosslinking, the cluster feature of the nanocomposite with the size of ca. 50–150 nm in diameter was observed (Figures 5(c)–5(f)) and this corresponded to that observed in PCS results. However, there was no apparent difference in the size and the size distribution of the nanocomposite between those crosslinked with ethylenediamine and *tris*(2-aminoethyl)amine or with different concentrations.

Water dispersibility, stability, and magnetic separation ability of the particles in each step of the reactions were investigated. Acrylamide-coated MNP aggregated within a few minutes after the preparation due to a lack of polymeric stabilization. After coating with PNAG, the particles were well stabilized through both steric and electrostatic repulsion mechanisms, resulting in the stable MNP dispersions with insignificant aggregation even after 24 h of the preparation. However, they cannot be completely separated after applying with a magnet for 5 min, which would be troublesome when employed for magnetic separation applications. The crosslinking of these nanocomposites was conducted in an attempt to enhance the magnetic separation ability, while retaining its good water stability. *Tris*(2-aminoethyl)amine and ethylenediamine with two different concentrations (1 mol% and 10 mol%) were used as additional crosslinkers. According to the results in Table 1, the nanocomposites after crosslinking showed a fair dispersibility in water after 24 h standing with a slight aggregation. This was probably due to the formation of the nanoclusters with a larger size, which corresponded well to the results observed from the PCS technique discussed above. These nanocomposites can be separated within 5 min due to the increase in its size, resulting

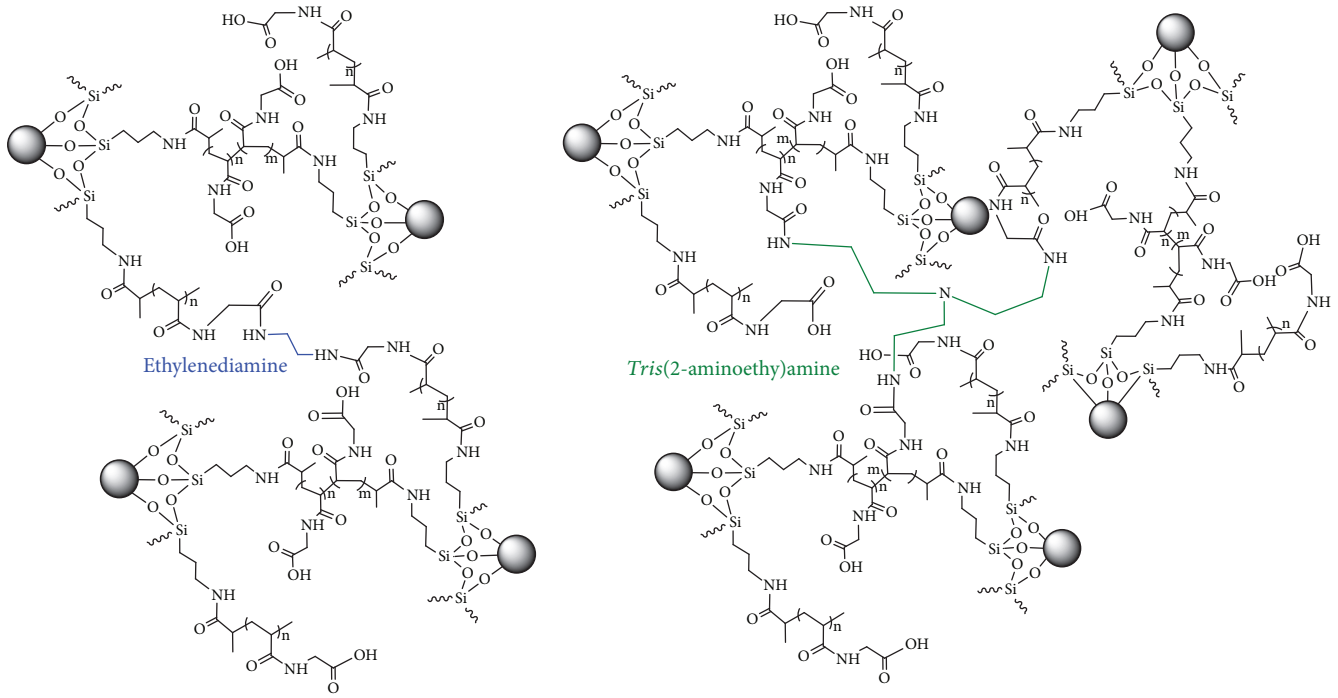

Figure 4: The proposed mechanism of the crosslinking amidations of PNAG-coated MNP with (a) ethylenediamine and (b) *tris*(2-aminoethyl)amine.

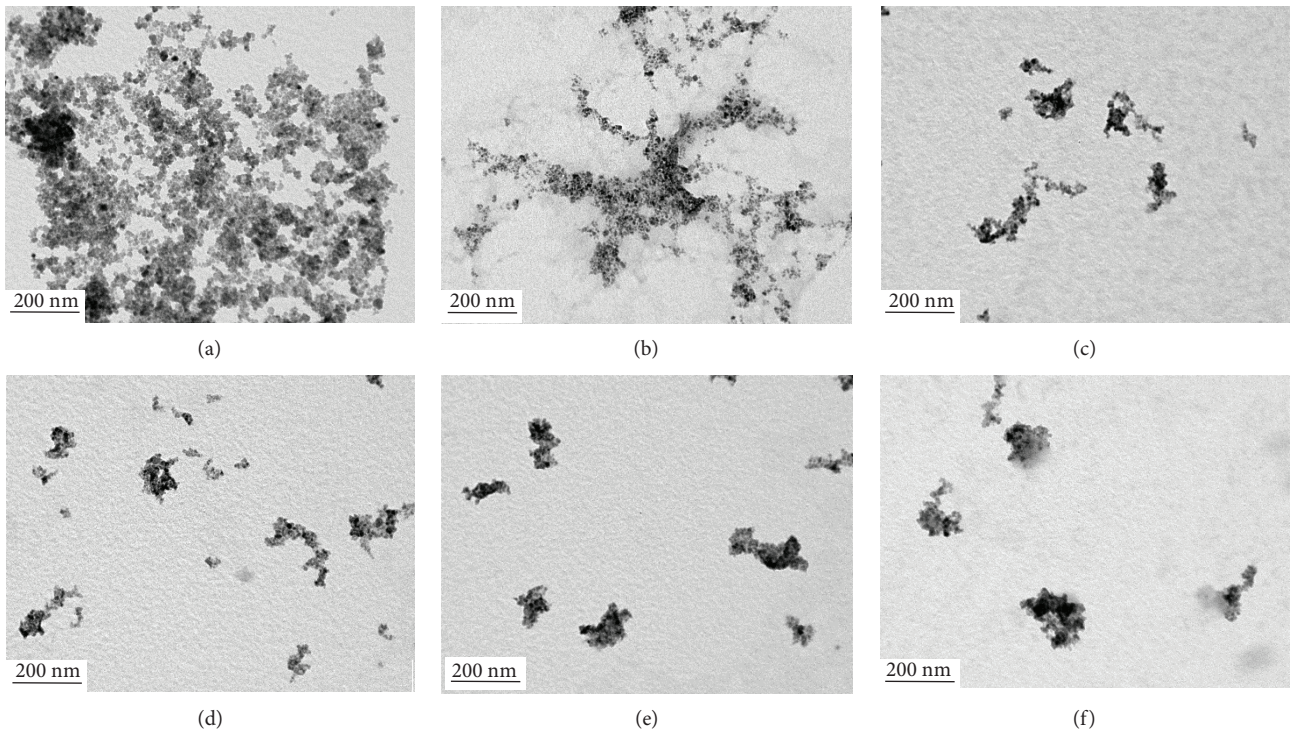

Figure 5: TEM of (a) acrylamide-coated MNP, (b) the MNP nanocomposite (before crosslinking), the MNP nanocomposite after crosslinking with (c) 1 mol% and (d) 10 mol% of ethylenediamine, and (e) 1 mol% and (f) 10 mol% of *tris*(2-aminoethyl)amine.

in an improved response to a magnet. Interestingly, as compared to the others, those crosslinked with 10 mol% *tris*(2-aminoethyl)amine can be completely separated from the dispersion and it would be used as a representative for other studies, e.g., magnetic properties, drug entrapment, and controlled release studies.

Table 1: The effect of crosslinking agents and their concentrations on water dispersibility and magnetic separation ability.

Acrylamide-coated MNP (no PNAG coating)	PNAG coating (before crosslinking)	After crosslinking with			
		1 mol% of diamine*	10 mol% of diamine*	1 mol% of triamine**	10 mol% of triamine**
At initial time					
Dispersibility in water *After 24* h					
Magnetic separation ability *After 5* min					

*Diamine is ethylenediamine. **Triamine is *tris*(2-aminoethyl)amine.

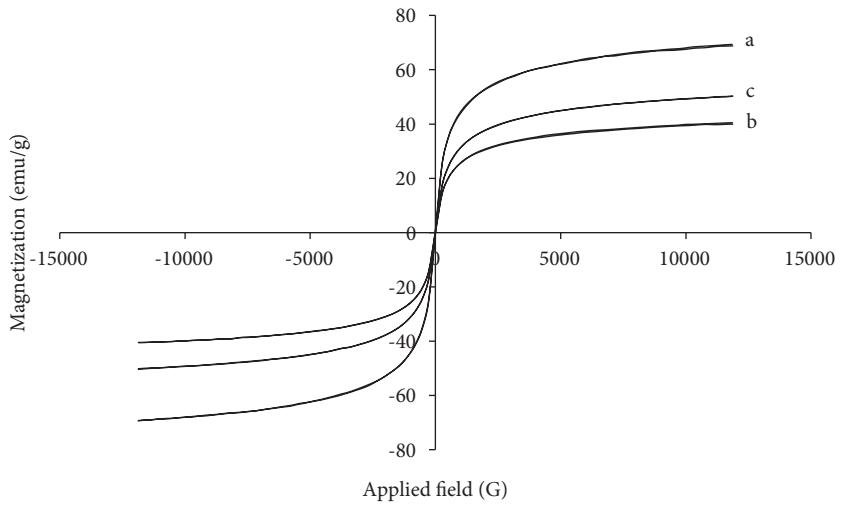

Figure 6: M-H curves of (a) acrylamide-coated MNP, (b) the MNP nanocomposite (before crosslinking), and (c) the MNP nanocomposites after crosslinking with 10 mol% of *tris*(2-aminoethyl)amine.

3.3. Multiresponsive Properties of the MNP Nanocomposite as a Function of Magnetic Field, Dispersion pH, and Temperature. Magnetic properties of acrylamide-coated MNP and PNAG-coated MNP nanocomposites before and after crosslinking with 10 mol% of *tris*(2-aminoethyl)amine were determined via the VSM technique. It was found that the saturation magnetization (M_s) of the particles decreased from 68 emu/g to 40 emu/g after coating with PNAG due to

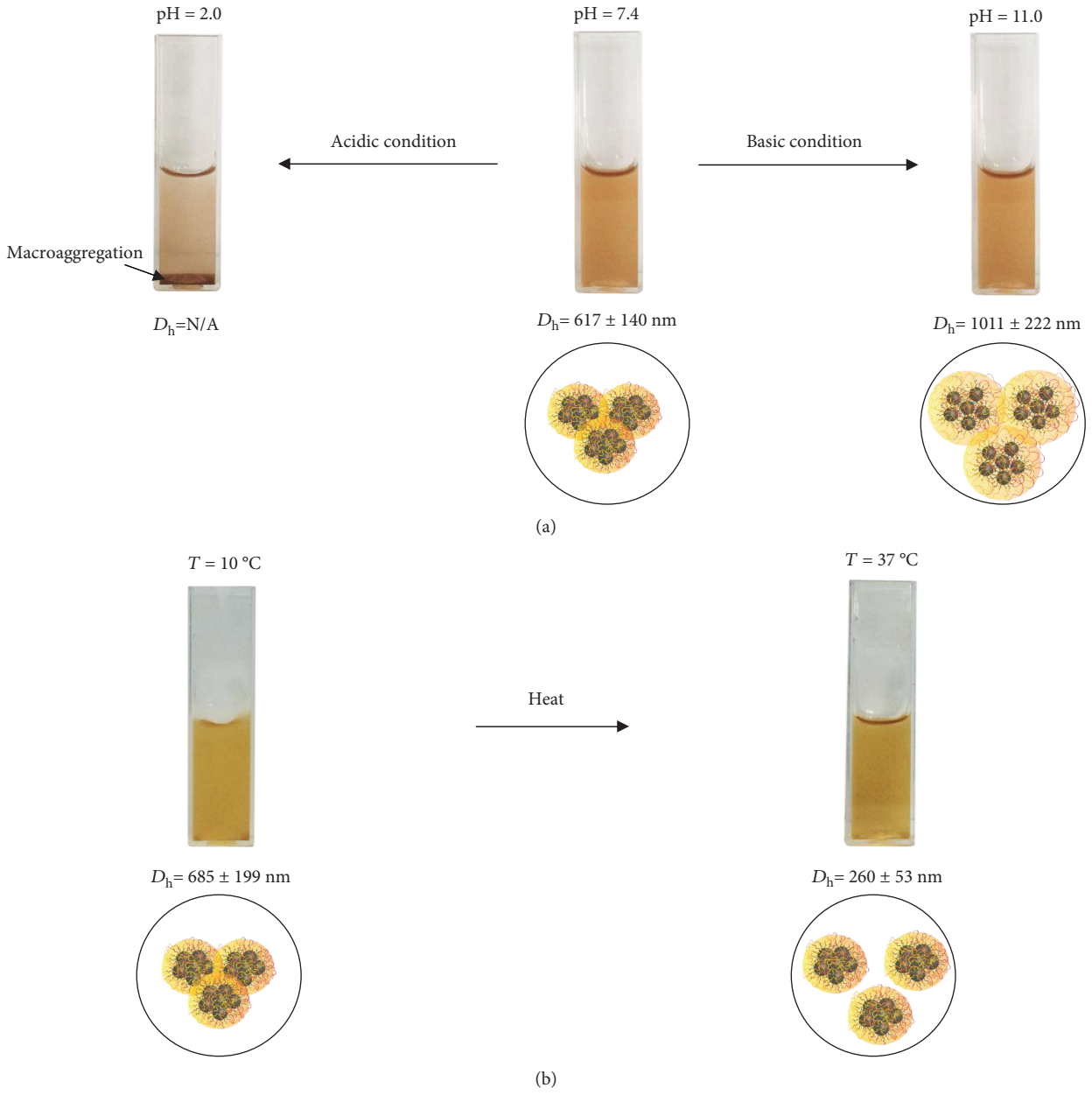

Figure 7: (a) pH- and (b) thermo-responsive properties of the MNP nanocomposite after crosslinking with 10 mol% of *tris*(2-aminoethyl)amine.

the presence of nonmagnetic organic polymer in the nanocomposite (Figure 6). After the crosslinking reaction, its M_s value increased to 50 emu/g and this was probably owing to the formation of MNP nanoclusters, leading to the increase in the magnetic sensitivity [15].

To confirm pH-responsive properties of the crosslinked MNP nanocomposite, its D_h was determined in pH 2.0, 7.4, and 11.0 buffer solutions. It was found that D_h in pH 2.0 cannot be measured due to macroaggregation of the particles (indicated by an arrow in the inset in Figure 7(a)). This was probably because PNAG was in the COOH form, resulting in the lack of anionic charged repulsion. In addition, its D_h increased from 617 nm to 1011 nm when the pH changed from pH 7.4 to pH 11.0 and this was attributed to presence of negatively charged repulsion of -COO^- from PNAG chains, resulting in the swelling of the nanocomposite. The change of D_h as a function of dispersion pH corresponded to the pK_a value of PNAG (pK_a 3.2) in terms of the protonated/deprotonated forms of the carboxyl groups [38]. D_h of the MNP nanocomposite was then investigated at 10°C and 37°C in pH 7.4 buffer solutions. D_h significantly dropped from 685 nm to 260 nm when the temperature was decreased from 10°C to 37°C (Figure 7(b)). It was rationalized that a number of the crosslinked MNP nanocomposites might be in the agglomerated form at 10°C due to the H-bonding among each nanocomposite.

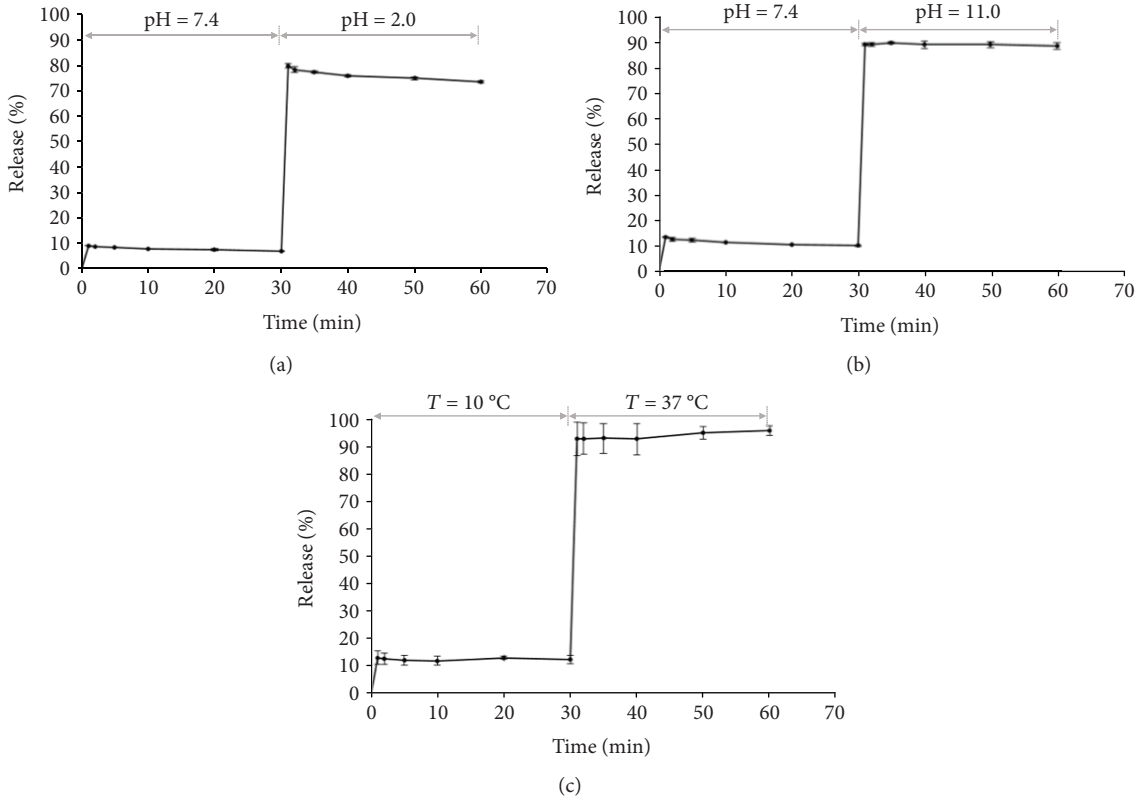

Figure 8: (a, b) The effect of pH and (c) temperature on the theophylline release profiles from the MNP nanocomposite crosslinking with 10 mol% of *tris*(2-aminoethyl)amine.

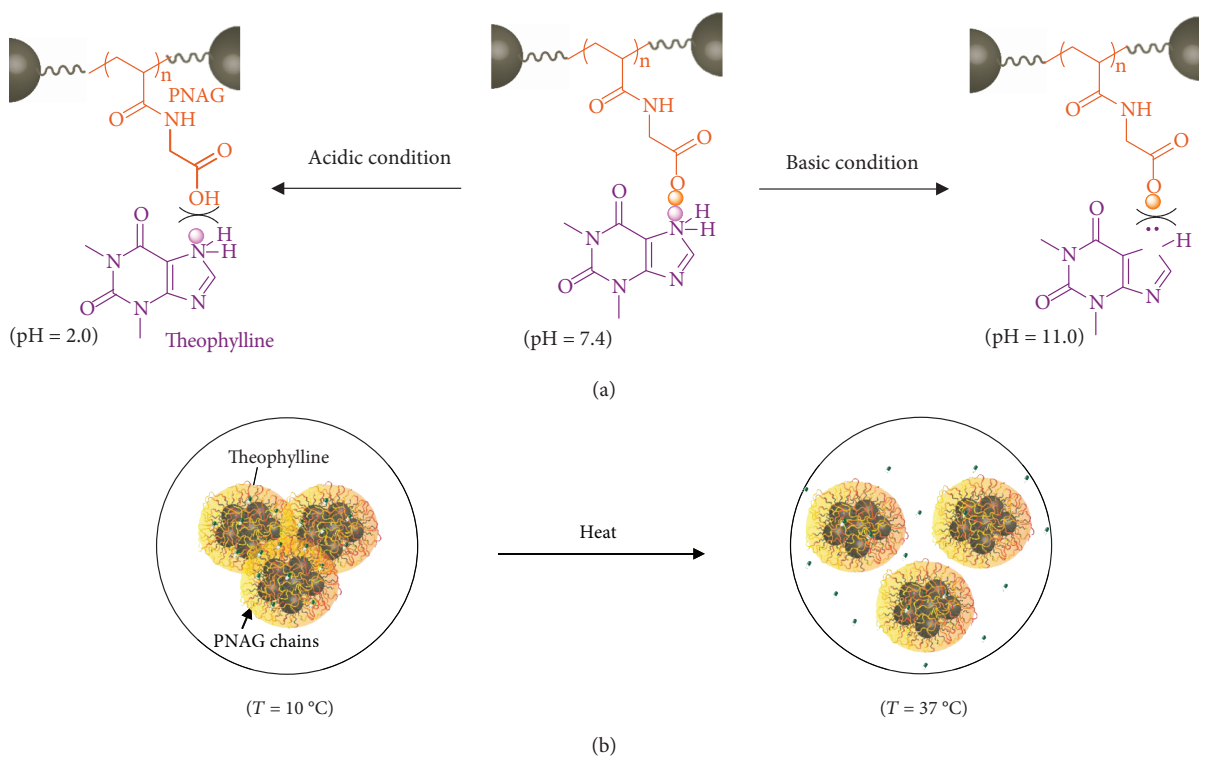

Figure 9: Proposed mechanisms of the theophylline release from the MNP nanocomposite triggered with (a) pH and (b) temperature changes.

At 37°C, the nanocomposite might be separated from each other due to the predominant interaction between PNAG on the nanocomposite surface and water molecules.

3.4. Drug Release Behavior. A showcase of the MNP nanocomposite for a drug controlled release application was also carried out in this work. Theophylline, a methylxanthine drug used in therapy for respiratory diseases, was selected as a model drug because it can be quantified via UV-vis spectrophotometry and possesses the amino groups in the structure. The protonation/deprotonation of the amino groups in theophylline leads to ionic adsorption/repulsion interactions with the carboxyl groups of PNAG, resulting in the drug release triggered by the change of the dispersion pH.

EE and DLE of the MNP nanocomposite crosslinked with 10 mol% of *tris*(2-aminoethyl)amine were first investigated. EE and DLE of the nanocomposite were 22–35% and 45–69%, respectively, depending on the pH and temperature of the dispersions. The effect of pH and temperature changes on the theophylline release rate from the MNP nanocomposite was then studied. The theophylline release studies were performed using stepwise pH changes from pH 7.4 to pH 2.0 and from pH 7.4 to pH 11.0 (Figures 8(a) and 8(b)). It should be noted that pK_a of PNAG was about 3.2 [38] and that of theophylline was 8.8 [39, 40]. It was found that the drug was rapidly released when the pH changed from neutral to acidic/basic conditions. This was attributed to the negatively charged repulsion of the deprotonated forms of PNAG (-COO^-) on the particle surface and theophylline in the basic condition (Figure 9(a)). Similarly, the positively charged repulsion of the protonated forms of these two components (-COOH of PNAG and $\equiv NH^+$ of theophylline) was rationalized for the abrupt release of the drug in the case of acidic condition.

The effect of the temperature change on the theophylline release behavior was also studied using a stepwise temperature change from 10°C to 37°C (Figure 8(c)). There was about 12% of the drug released at 10°C, and it was rapidly released for 92% when heated to 37°C. The abrupt release of the drug from the nanocomposite was attributed to the separation of the agglomerated nanocomposites at high temperature as indicated by the decrease in D_h (Figure 9(b)).

4. Conclusions

This work presented the preparation of pH- and thermoresponsive nanocomposite based on PNAG matrix and MNP and its application in drug controlled release. The MNP nanocomposite having good magnetic separation ability and water stability was obtained by tuning the types and concentrations of the crosslinkers. It exhibited dual-responsive properties as indicated by the change in its zeta potential and D_h when the environmental pH and temperature were changed. In addition, this novel nanocomposite was also demonstrated for use as a magnetically guidable vehicle for theophylline controlled release with pH- and thermotriggered mechanisms.

Data Availability

The data in the synthesis of PNAG-based magnetic nanocomposite and its drug release behavior used to support the findings of this study are included within the article and in the supplementary information file. All the raw data such as hydrodynamic size (D_h), zeta potential values, and drug release data used to support the findings of this study are available from the corresponding author upon request.

Conflicts of Interest

The authors declare that they have no conflicts of interest.

Acknowledgments

The authors thank the National Research Council of Thailand (NRCT) (R2562B093) for the support. MR especially acknowledges the Thailand Research Fund (TRF) (RSA5980002) for the financial funding. ND thanks the Science Achievement Scholarship of Thailand (SAST) for the scholarship.

Supplementary Materials

The supplementary file contains a ^1H NMR spectrum of NAG monomer, the calculations of the grafting density of carboxyl groups on PNAG-coated MNP after dispersing in water, and the calibration curves of theophylline in various conditions. *(Supplementary Materials)*

References

[1] A. Muñoz-Bonilla, J. Sánchez-Marcos, and P. Herrasti, "Conducting polymer hybrids," in *Springer Series on Polymer and Composite Materials*, V. Kumar, S. Kalia, and H. C. Swart, Eds., pp. 45–80, Springer International Publishing AG, Switzerland, 2017.

[2] J. Estelrich, E. Escribano, J. Queralt, and M. A. Busquets, "Iron oxide nanoparticles for magnetically-guided and magnetically-responsive drug delivery," *International Journal of Molecular Sciences*, vol. 16, no. 12, pp. 8070–8101, 2015.

[3] M. A. Willard, L. K. Kurihara, E. E. Carpenter, S. Calvin, and V. G. Harris, "Chemically prepared magnetic nanoparticles," *International Materials Review*, vol. 49, no. 3-4, pp. 125–170, 2013.

[4] B. Thong-On and M. Rutnakornpituk, "Controlled magnetite nanoclustering in the presence of glycidyl-functionalized thermo-responsive poly(*N*-isopropylacrylamide)," *European Polymer Journal*, vol. 85, pp. 519–531, 2016.

[5] S. Bucak, B. Yavuztürk, and A. D. Sezer, "Magnetic nanoparticles: synthesis, surface modifications and application in drug delivery," in *Recent Advances in Novel Drug Carrier Systems*, A. D. Sezer, Ed., pp. 165–200, IntechOpen, 2012.

[6] K. Petcharoen and A. Sirivat, "Synthesis and characterization of magnetite nanoparticles *via* the chemical co-precipitation method," *Materials Science & Engineering, B: Advanced Functional Solid-State Materials*, vol. 177, no. 5, pp. 421–427, 2012.

[7] M. Hetti, Q. Wei, R. Pohl et al., "Magnetite core-shell nanoparticles in nondestructive flaw detection of polymeric materials,"

ACS Applied Materials & Interfaces, vol. 8, no. 41, pp. 28208–28215, 2016.

[8] L. Xiao, J. Li, D. F. Brougham et al., "Water-soluble superparamagnetic magnetite nanoparticles with biocompatible coating for enhanced magnetic resonance imaging," *ACS Nano*, vol. 5, no. 8, pp. 6315–6324, 2011.

[9] N. N. Reddy, Y. M. Mohan, K. Varaprasad, S. Ravindra, P. A. Joy, and K. M. Raju, "Magnetic and electric responsive hydrogel-magnetic nanocomposites for drug-delivery application," *Journal of Applied Polymer Science*, vol. 122, no. 2, pp. 1364–1375, 2011.

[10] S. Panja, B. Saha, S. K. Ghosh, and S. Chattopadhyay, "Synthesis of novel four armed PE-PCL grafted superparamagnetic and biocompatible nanoparticles," *Langmuir*, vol. 29, no. 40, pp. 12530–12540, 2013.

[11] A. Pourjavadi, A. Abedin-Moghanaki, and S. A. Nasseri, "A new functionalized magnetic nanocomposite of poly(methylacrylate) for the efficient removal of anionic dyes from aqueous media," *RSC Advances*, vol. 6, no. 10, pp. 7982–7989, 2016.

[12] J.-M. Ringeard, P. Griesmar, E. Caplain et al., "Design of poly(*N*-acryloylglycine) materials for incorporation of microorganisms," *Journal of Applied Polymer Science*, vol. 130, no. 2, pp. 835–841, 2013.

[13] S. F. Medeiros, A. M. Santos, H. Fessi, and A. Elaissari, "Stimuli-responsive magnetic particles for biomedical applications," *International Journal of Pharmaceutics*, vol. 403, no. 1-2, pp. 139–161, 2011.

[14] J. Ge, Y. Hu, M. Biasini, W. P. Beyermann, and Y. Yin, "Superparamagnetic magnetite colloidal nanocrystal clusters," *Angewandte Chemie (International Ed. in English)*, vol. 46, no. 23, pp. 4342–4345, 2007.

[15] B. Luo, S. Xu, A. Luo et al., "Mesoporous biocompatible and acid-degradable magnetic colloidal nanocrystal clusters with sustainable stability and high hydrophobic drug loading capacity," *ACS Nano*, vol. 5, no. 2, pp. 1428–1435, 2011.

[16] S. Meerod, B. Rutnakornpituk, U. Wichai, and M. Rutnakornpituk, "Hydrophilic magnetic nanoclusters with thermo-responsive properties and their drug controlled release," *Journal of Magnetism and Magnetic Materials*, vol. 392, pp. 83–90, 2015.

[17] S. Khadsai, B. Rutnakornpituk, T. Vilaivan, M. Nakkuntod, and M. Rutnakornpituk, "Anionic magnetite nanoparticle conjugated with pyrrolidinyl peptide nucleic acid for DNA base discrimination," *Journal of Nanoparticle Research*, vol. 18, no. 9, 2016.

[18] C. Oka, K. Ushimaru, N. Horiishi, T. Tsuge, and Y. Kitamoto, "Core-shell composite particles composed of biodegradable polymer particles and magnetic iron oxide nanoparticles for targeted drug delivery," *Journal of Magnetism and Magnetic Materials*, vol. 381, pp. 278–284, 2015.

[19] S. Merino, C. Martín, K. Kostarelos, M. Prato, and E. Vázquez, "Nanocomposite hydrogels: 3D polymer-nanoparticle synergies for on-demand drug delivery," *ACS Nano*, vol. 9, no. 5, pp. 4686–4697, 2015.

[20] S. Davaran, S. Alimirzalu, K. Nejati-Koshki et al., "Physicochemical characteristics of Fe_3O_4 magnetic nanocomposites based on poly(*N*-isopropylacrylamide) for anti-cancer drug delivery," *Asian Pacific Journal of Cancer Prevention*, vol. 15, no. 1, pp. 49–54, 2014.

[21] S. Dutta, S. Parida, C. Maiti, R. Banerjee, M. Mandal, and D. Dhara, "Polymer grafted magnetic nanoparticles for delivery of anticancer drug at lower pH and elevated temperature," *Journal of Colloid and Interface Science*, vol. 467, pp. 70–80, 2016.

[22] Y. Prai-In, C. Boonthip, B. Rutnakornpituk et al., "Recyclable magnetic nanocluster crosslinked with poly(ethylene oxide)-*block*-poly(2-vinyl-4,4-dimethylazlactone) copolymer for adsorption with antibody," *Materials Science & Engineering. C, Materials for Biological Applications*, vol. 67, pp. 285–293, 2016.

[23] F. Li, J. Sun, H. Zhu, X. Wen, C. Lin, and D. Shi, "Preparation and characterization novel polymer-coated magnetic nanoparticles as carriers for doxorubicin," *Colloids and Surfaces. B, Biointerfaces*, vol. 88, no. 1, pp. 58–62, 2011.

[24] B. Koppolu, M. Rahimi, S. Nattama, A. Wadajkar, and K. T. Nguyen, "Development of multiple-layer polymeric particles for targeted and controlled drug delivery," *Nanomedicine*, vol. 6, no. 2, pp. 355–361, 2010.

[25] P. Theamdee, R. Traiphol, B. Rutnakornpituk, U. Wichai, and M. Rutnakornpituk, "Surface modification of magnetite nanoparticle with azobenzene-containing water dispersible polymer," *Journal of Nanoparticle Research*, vol. 13, no. 10, pp. 4463–4477, 2011.

[26] K. Kurd, A. A. Khandagi, S. Davaran, and A. Akbarzadeh, "Cisplatin release from dual-responsive magnetic nanocomposites," *Artificial Cells, Nanomedicine, and Biotechnology*, vol. 44, no. 3, pp. 1031–1039, 2016.

[27] N. Rodkate and M. Rutnakornpituk, "Multi-responsive magnetic microsphere of poly(*N*-isopropylacrylamide)/carboxymethylchitosan hydrogel for drug controlled release," *Carbohydrate Polymers*, vol. 151, pp. 251–259, 2016.

[28] I. M. El-Sherbiny, R. J. Lins, E. M. Abdel-Bary, and D. R. K. Harding, "Preparation, characterization, swelling and *in vitro* drug release behaviour of poly(*N*-acryloylglycine-chitosan) interpolymeric pH and thermally-responsive hydrogels," *European Polymer Journal*, vol. 41, no. 11, pp. 2584–2591, 2005.

[29] K. Deng, Q. Li, L. Bai et al., "A pH/thermo-responsive injectable hydrogel system based on poly(*N*-acryloylglycine) as a drug carrier," *Iranian Polymer Journal*, vol. 20, pp. 185–194, 2011.

[30] Z. M. O. Rzaev, S. Dinçer, and E. Pişkin, "Functional copolymers of *N*-isopropylacrylamide for bioengineering applications," *Progress in Polymer Science*, vol. 32, no. 5, pp. 534–595, 2007.

[31] W. Sun, Z. An, and P. Wu, "UCST or LCST? Composition-dependent thermoresponsive behavior of poly(*N*-acryloylglycinamide-*co*-diacetone acrylamide)," *Macromolecules*, vol. 50, no. 5, pp. 2175–2182, 2017.

[32] J. Seuring and S. Agarwal, "Polymers with upper critical solution temperature in aqueous solution," *Macromolecular Rapid Communications*, vol. 33, no. 22, pp. 1898–1920, 2012.

[33] J. Seuring, F. M. Bayer, K. Huber, and S. Agarwal, "Upper critical solution temperature of poly(*N*-acryloyl glycinamide) in water: a concealed property," *Macromolecules*, vol. 45, no. 1, pp. 374–384, 2012.

[34] B. A. Pineda-Contreras, H. Schmalz, and S. Agarwal, "pH dependent thermoresponsive behavior of acrylamide-acrylonitrile UCST-type copolymers in aqueous media," *Polymer Chemistry*, vol. 7, no. 10, pp. 1979–1986, 2016.

[35] A. Gandhi, A. Paul, S. O. Sen, and K. K. Sen, "Studies on thermoresponsive polymers: phase behaviour, drug delivery and biomedical applications," *Asian Journal of Pharmaceutical Sciences*, vol. 10, no. 2, pp. 99–107, 2015.

[36] M. A. Ward and T. K. Georgiou, "Thermoresponsive polymers for biomedical applications," *Polymer*, vol. 3, no. 3, pp. 1215–1242, 2011.

[37] Y. Zhang, S. Chen, M. Pang, and W. Zhang, "Synthesis and micellization of a multi-stimuli responsive block copolymer based on spiropyran," *Polymer Chemistry*, vol. 7, no. 45, pp. 6880–6884, 2016.

[38] K. L. Deng, H. B. Zhong, T. Tian, Y. Gou, Q. Li, and L. R. Dong, "Drug release behavior of a pH/temperature sensitive calcium alginate/poly(*N*-acryloylglycine) bead with core-shelled structure," *Express Polymer Letters*, vol. 4, no. 12, pp. 773–780, 2010.

[39] A. A. Elouzi, F. Abeid, M. Almegrhe, and M. El-Baseir, "Acidic beverage and the bioavailability of theophylline," *Journal of Chemical and Pharmaceutical Research*, vol. 4, pp. 3454–3459, 2012.

[40] M. Shalaeva, J. Kenseth, F. Lombardo, and A. Bastin, "Measurement of dissociation constants (pK_a values) of organic compounds by multiplexed capillary electrophoresis using aqueous and cosolvent buffers," *Journal of Pharmaceutical Sciences*, vol. 97, no. 7, pp. 2581–2606, 2008.

Author(s) Name(s)

It is very important to confirm the author(s) last and first names in order to be displayed correctly on our website as well as in the indexing databases:

Author 1
Given Names: Nunthiya
Last Name: Deepuppha
Author 2
Given Names: Sudarat
Last Name: Khadsai
Author 3
Given Names: Boonjira
Last Name: Rutnakornpituk
Author 4
Given Names: Uthai
Last Name: Wichai
Author 5
Given Names: Metha
Last Name: Rutnakornpituk

It is also very important for each author to provide an ORCID (Open Researcher and Contributor ID). ORCID aims to solve the name ambiguity problem in scholarly communications by creating a registry of persistent unique identifiers for individual researchers.

To register an ORCID, please go to the Account Update page (http://mts.hindawi.com/update/) in our Manuscript Tracking System and after you have logged in click on the ORCID link at the top of the page. This link will take you to the ORCID website where you will be able to create an account for yourself. Once you have done so, your new ORCID will be saved in our Manuscript Tracking System automatically.

European Polymer Journal 85 (2016) 519–531

Contents lists available at ScienceDirect

European Polymer Journal

journal homepage: www.elsevier.com/locate/europolj

Macromolecular Nanotechnology

Controlled magnetite nanoclustering in the presence of glycidyl-functionalized thermo-responsive poly(*N*-isopropylacrylamide)

Bandit Thong-On, Metha Rutnakornpituk *

Department of Chemistry and Center of Excellence in Biomaterials, Faculty of Science, Naresuan University, Phitsanulok 65000, Thailand

ARTICLE INFO

Article history:
Received 6 June 2016
Received in revised form 30 October 2016
Accepted 1 November 2016
Available online 9 November 2016

Keywords:
Magnetite
Nanoparticle
Nanocluster
Poly(*N*-isopropylacrylamide)
Thermo-responsive

ABSTRACT

Glycidyl-functionalized poly(*N*-isopropylacrylamide) (PNIPAAm), synthesized *via* a reversible addition-fragmentation transfer polymerization (RAFT), was used for controlling degree of nanoclustering of magnetite nanoparticle (MNP). The polymer was grafted onto MNP *via* the ring-opening reaction between glycidyl groups at the PNIPAAm chain terminal and amino groups on the MNP surface to obtain thermo-responsive MNP nanocluster. Hydrodynamic size (D_h) and colloidal stability of the nanocluster, corresponding to the degree of nanoclustering reaction, can be regulated either by adjusting the ratio of MNP to the polymer in the reaction or by introducing glycidyl groups to the polymers. The size of the nanocluster ranged between 20 and 150 nm in diameter with about 10–120 particles/cluster. Thermogravimetric analysis (TGA) and vibrating sample magnetometry (VSM) were used to confirm the presence of the polymer in the nanocluster. A study showing indomethacin controlled release of these MNP nanoclusters was also performed. This stable nanocluster with magnetically guidable properties might be potentially used for entrapment of other bio-entities or therapeutic drugs with temperature-responsive properties for controlled release applications.

1. Introduction

In recent years, much attention has been paid in the study in magnetite nanoparticle (MNP) particularly in developing facile and efficient synthetic approaches to control its size, magnetic properties and chemical reactivity. Because of its high surface area-to-volume ratio, many attempts have been made in conjugating bioentities such as deoxyribonucleic acid (DNA) [1,2], peptide nucleic acid (PNA) [3,4], protein [5,6], amino acid [7] and antibodies [8,9], on the surface for potential uses in biomedical applications. Due to strong inter-particle attractive interactions such as Van der Waals force and magnetic force, they tended to agglomerate to form uncontrollable aggregate, resulting in the loss in nanoscale-related properties [10] and thus limiting its biomedical applications [11]. Coating the particle with long chain polymer is one of a promising approach to prevent the particle aggregation through a steric stabilization mechanism, resulting in improvement in stability and dispersibility in the media. In addition, the polymer coated on the particle surface also served as a platform for conjugation with functional biomolecules [12,13].

* Corresponding author.
E-mail address: methar@nu.ac.th (M. Rutnakornpituk).

http://dx.doi.org/10.1016/j.eurpolymj.2016.11.002
0014-3057/

Many applications, such as controlled drug delivery and magnetic separation of cells and antibodies, take advantages of magnetically guidable properties of MNP. In these applications, drug-conjugated or bioentity-conjugated MNP should have good magnetic responsiveness, so that they can rapidly respond to an external magnetic field. One of the promising approaches in enhancing magnetic responsiveness of MNP without the formation of macroscopic particle aggregation was to assemble them into the form of nanocluster. MNP nanocluster is composed of many interconnected single particles of ≈3–20 nm in size and minor amount of organic components [14]. Unlike micron-sized particles, formation of MNP nanocluster significantly increased magnetic responsiveness [15,16] as opposed to individual MNP and also maintained its dispersibility and stability in the media [17,18]. Importantly, its superparamagnetic properties should also be maintained as long as individual MNP core can be distinguished from each other after nanocluster formation, meaning that there was no one polycrystalline particle but a nanocluster with distinguishable particles smaller than 20 nm [19]. Controlling the degree of MNP nanoclustering with reasonable size will result in the nanocluster with good magnetic responsiveness, good dispersibility and stability in the media. Many approaches have been investigated in controlling the formation of MNP nanocluster such as physical or physicochemical interaction between pre-synthesized MNP and polymer particle [16,20], *in-situ* polymerization of monomers in the presence of MNP [21–23] and *in-situ* precipitation of MNP in the presence of polymer microsphere [24,25].

The study in the synthesis of MNP nanocluster coated with responsive polymers was rather limited [26,27]. In this work, preparation of MNP nanocluster coated with poly(*N*-isopropylacrylamide) (PNIPAAm) is presented. PNIPAAm functionalized with glycidyl methacrylate (GMA) was first synthesized *via* Reversible Addition Fragmentation Chain Transfer (RAFT) polymerization and then grafted onto MNP surface. RAFT polymerization, one of several types of controlled radical polymerization (CRP) techniques, was used in this work because it can produce polymers with controllable molecular weights and narrow polydispersity indices (PDIs) and can be performed under mild condition reactions in various reaction systems without using metal catalysts [28]. PNIPAAm is the most studied thermo-responsive polymer owing to its physiologically relevant transition temperature and relative insensitivity to pH and salt content [29]. It has a lower critical solution temperature (LCST) at 32 °C, which is close to that of human body [30]. Below its LCST, PNIPAAm is well soluble in water due to the formation of hydrogen bonding of the chains with water molecules, resulting in the formation of a swollen state. When increasing the temperature above its LCST, PNIPAAm deswells to a collapsed state due to the formation of hydrogen bondings among the polymer chains. This process is generally reversible, making the polymer to behave as an on-off system when the temperature is changed across the LCST. Syntheses of the copolymers containing PNIPAAm have been widely reported [31–35]. However, the studies in surface modification of MNP with PNIPAAm-containing copolymers are rather limited [36,37].

In this report, PNIPAAm was first synthesized *via* RAFT polymerization, followed by the functionalization with GMA units at the chain terminal. The chemical structures and functional groups of the synthesized PNIPAAm were characterized *via* proton nuclear magnetic resonance spectroscopy (^{1}H NMR) and fourier transform infrared spectroscopy (FTIR), respectively. It was then grafted to MNP through the ring-opening reaction of the glycidyl groups at the chain terminal with amino groups grafted on MNP surface and essentially induced the formation of MNP nanocluster. Transmission electron microscopy (TEM) was conducted to determine the nanocluster size and photocorrelation spectroscopy (PCS) was performed to determine hydrodynamic size (D_h) and LCST of the nanoclusters. The effects of MNP-to-polymer ratio used in the reactions and the number of GMA units in the polymer on D_h and colloidal stability of the nanocluster were also investigated. Magnetic properties of the nanoclusters were investigated *via* vibrating sample magnetometry (VSM). The composition of MNP-polymer nanocluster was also determined *via* thermogravimetric analysis (TGA). In addition, a case study showing the drug controlled release application of these MNP nanoclusters was also investigated (see Fig. 1).

2. Experimental

2.1. Materials

Unless otherwise stated, all reagents were used without further purification: iron (III) acetylacetonate ($Fe(acac)_3$) (Acros, 99.9%), benzyl alcohol (Unilab, 98%), oleic acid (Fluka), triethylamine (Carto Erba, 97%), 3-aminopropyl triethoxysilane (APS) (Acros, 99%), glycidyl methacrylate (GMA) (Sigma-Aldrich, 97%), 2,2′-azobis (2-methylpropionitrile) (AIBN) (Sigma-Aldrich, 98%), *S*-(thiobenzoyl)thioglycolic acid (Sigma-Aldrich, 99%). *N*-isopropylacrylamide (NIPAAm) (Acros, 99%) was recrystallized twice in hexane before polymerization.

2.2. Synthesis

2.2.1. Synthesis of PNIPAAm macro RAFT agents

In a round bottom flask, NIPAAm (10 g, 88.370 mmol), S-(thiobenzoyl) thioglycolic acid RAFT agent (0.0924 g, 0.435 mmol) and an AIBN initiator (0.0182 g, 0.110 mmol) were dissolved in 50 mL of 1,4-dioxane under N_2 atmosphere with stirring for 30 min. RAFT polymerization of PNIPAAm was allowed for 48 h at 60 °C to achieve 60% monomer conversion. The mixture was then diluted with 1,4-dioxane to 100 mL and cooled to room temperature. The polymer was then purified by

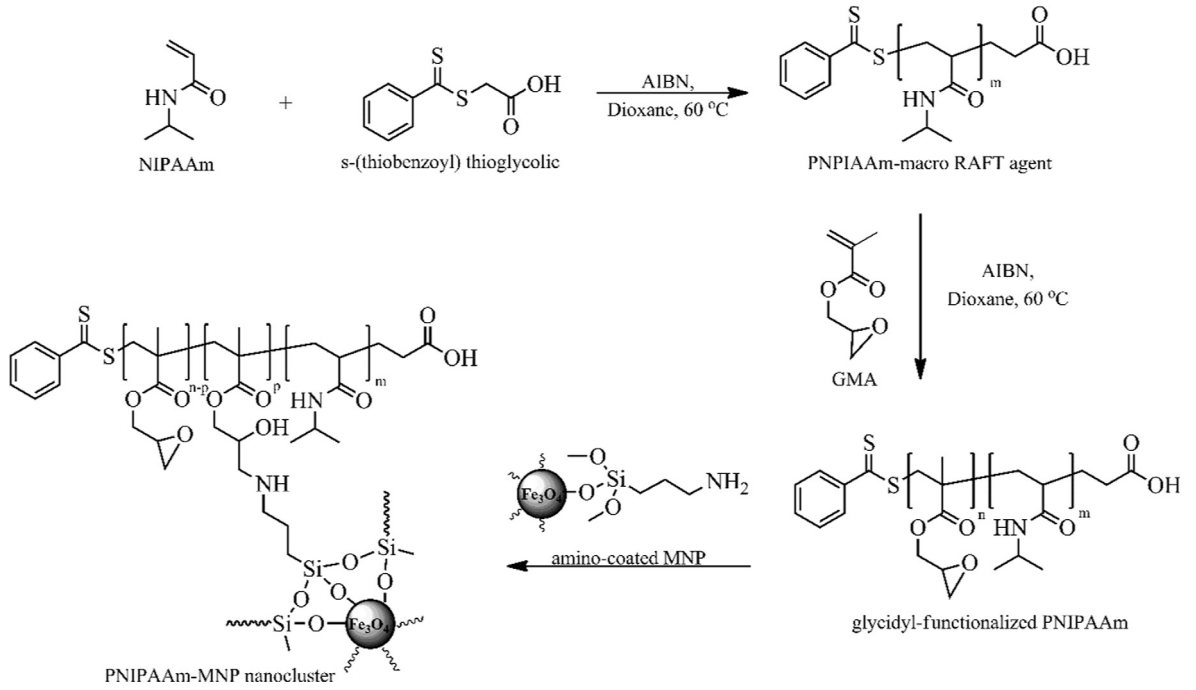

Fig. 1. Schematic representation for controlled nanoclustering of MNP with glycidyl-functionalized PNIPAAm.

precipitation in diethyl ether and dried *in vacuo*. Purified PNIPAAm macro RAFT agents were subsequently used for the synthesis of glycidyl-functionalized PNIPAAm.

2.2.2. Synthesis of glycidyl-functionalized PNIPAAm (PNIPAAm-GMA)

A procedure similar to aforementioned polymerization was used for the synthesis of PNIPAAm-GMA with the use of PNIPAAm macro RAFT agent. An example described here is for the synthesis of PNIPAAm-GMA with 8 repeating units of GMA (PNIPAAm-GMA_8). PNIPAAm-GMA with 18 repeating units of GMA (PNIPAAm-GMA_{18}) was synthesized using the similar procedure with appropriate amounts of GMA loaded. GMA (0.16 mL, 1.173 mmol), PNIPAAm macro RAFT agent (1.00 g, 0.077 mmol) and AIBN initiator (3.0 mg, 0.018 mmol) were dissolved in 1,4-dioxane (30 mL) with N_2 purging for 30 min. The reaction was set under N_2 atmosphere at 60 °C for 48 h to achieve about 60% reaction conversion. After the reaction, the product was purified by precipitation in methanol and dried *in vacuo*.

2.2.3. Synthesis of amino-coated MNP

MNP was synthesized *via* a thermal decomposition of $Fe(acac)_3$ (5 g, 14.05 mmol) in benzyl alcohol (90 mL) at 180 °C for 48 h under N_2 atmosphere. After the reaction, the precipitant was removed from the mixture using an applied magnetic field and repetitively washed with ethanol and then CH_2Cl_2. The resultant product was obtained as fine black powder after drying under reduced pressure. Oleic acid (4 ml) was then added to the MNP dispersion (0.6 g MNP in 30 ml toluene) with sonication for 3 h under N_2 atmosphere. MNP aggregate was removed from the oleic acid-coated MNP by centrifugation at 5000 rpm for 15 min. To prepare amino-coated MNP, APS (1 ml, 4.517 mmol) was added to a mixture of oleic acid-coated MNP (0.1g) and TEA (0.01 ml, 0.075 mmol) in dried toluene (6 ml). The dispersion was sonicated for 4 h at room temperature under N_2 atmosphere. Amino-coated MNP was retrieved using a magnet, washed twice with ethanol and toluene and finally dried *in vacuo*.

2.2.4. Synthesis of MNP-polymer nanoclusters

The polymer solution (0.001–10 mg in 1 mL of DI water) was added dropwise to amino-coated MNP dispersion (1 mg MNP in 2 mL pH 10-aqueous solution). The mixture was stirred at 65 °C for 12 h under N_2 atmosphere. The product was isolated using a magnet, washed twice with DI water and acetone and then dried *in vacuo*.

2.3. Characterization

2.3.1. Characterization of the polymers and nanoparticles

^1H NMR spectra were performed on a 400 MHz Br.uker NMR spectrometer using $CDCl_3$ as a solvent. FTIR was performed on a Perkin-Elmer Model 1600 Series FTIR Spectrophotometer in the wavenumber range of 4000–400 cm^{-1}. The samples

were mixed and pressed with KBr to form disc samples. TEM was performed on Philips Tecnai 12, operated at 120 kV equipped with Gatan model 782 CCD camera. MNP dispersions in water were directly cast onto carbon-coated copper grids and allowed to slowly evaporate at room temperature. Magnetic properties of the particles were measured at room temperature using a Standard 7403 Series, Lakeshore vibrating sample magnetometer. Magnetic moment of each sample was investigated over a range of ±10,000 G of applied magnetic fields using 30 min sweep time. TGA was performed on SDTA 851 Mettler-Toledo at the temperature ranging between 25 and 600 °C at a heating rate of 20 °C/min under oxygen atmosphere. Hydrodynamic size (D_h) of the particles was measured by PCS using NanoZS4700 nanoseries Malvern instrument.

2.3.2. Determination of indomethacin entrapment (EE) and loading efficiency (DLE) of the polymer-coated MNP nanoclusters

The indomethacin solution (1 mL, 5 mg/mL in ethanol) was added dropwise with stirring to an aqueous dispersion of the nanoclusters (3 mL, 5 mg of MNP nanocluster). The mixture was stirred at 20 °C for 120 min. The weight of the entrapped drug in the complex was determined from the difference of the weights of the loaded drug and the excess of the drug remaining dispersible in the solution. After centrifugation to remove agglomerated particles, the drug concentration in the supernatant, reflecting the amount of the entrapped drug in the MNP nanoclusters, was determined using UV–Visible spectrophotometer at λ_{max} = 320 nm. EE and DLE were calculated from the following equations:

$$\text{Entrapment efficiency (EE)} = \frac{\text{Weight of the entrapped drug in the MNP nanocluster}}{\text{Weight of the loaded drug}} \times 100 \quad (1)$$

$$\text{Drug loading efficiency (DLE)} = \frac{\text{Weight of the entrapped drug in the MNP nanocluster}}{\text{Weight of the MNP nanocluster}} \times 100 \quad (2)$$

2.3.3. The cumulative release studies of entrapped indomethacin from the polymer-coated MNP nanoclusters

Indomethacin-loaded MNP nanoclusters (5 mg of MNP nanocluster) were dispersed in a 2 mL phosphate buffer solution (PBS) (pH 7.4). The dispersion of indomethacin-loaded MNP nanoclusters was placed in a water bath at 20 °C (below LCST) or 45 °C (above LCST). At a predetermined time interval, 200 μL aliquots of the dispersions were withdrawn from the release media and 200 μL of PBS (pH 7.4) was replaced. After separation of the MNP nanoclusters using an external magnet, the concentrations of the released drug in the supernatant were determined *via* UV–Visible spectrophotometer at λ_{max} = 320 nm.

$$\textit{Cumulative release} = \frac{\text{weight of released drug at a given time}}{\text{Weight of the entrapped drug in the MNP nanocluster}} \times 100 \quad (3)$$

3. Results and discussion

The main objective of this work is to control degree of nanoclustering of MNP using glycidyl-functionalized PNIPAAm (PNIPAAm-GMA) *via* a "grafting onto" approach. PNIPAAm-GMA was first synthesized *via* a RAFT polymerization by a sequential addition of NIPAAm monomer and then GMA monomer to form reactive glycidyl-functionalized PNIPAAm. It was envisioned that reactive amino groups on the particle surface can readily open the epoxy rings in PNIPAAm-GMA and then induce MNP nanoclustering due to the presence of multi-functional groups on MNP surface and also in the polymer structure. PNIPAAm-GMA_8 and PNIPAAm-GMA_{18} (Table 1) were used in MNP nanoclustering reactions to investigate the effect of numbers of GMA on D_h, dispersibility and stability of MNP nanocluster in aqueous dispersions. In addition, effect of the polymer concentrations used in the nanoclustering reaction on D_h was also determined.

3.1. Synthesis of glycidyl-functionalized PNIPAAm (PNIPAAm-GMA)

PNIPAAm macro RAFT agent was synthesized *via* a RAFT polymerization of NIPAAm using S-(thiobenzoyl)thioglycolic acid as a chain-transfer agent. In Fig. 2A, the presence of the signals at 1.5 ppm (peak *d*) and 2.0 ppm (peak *c*) corresponding to methylene and methine protons, respectively, indicated the formation of PNIPAAm. In addition, the C$\underline{H}_3$ signals at 1.1 ppm (peak *a*) and C$\underline{H}$ signals at 3.85 ppm (peak *b*) of the repeating units without the signals of vinyl groups of NIPAAm monomers

Table 1
RAFT polymerizations of PNIPAAm and PNIPAAm-GMA.

Polymer name	[Monomer]:[RAFT]: [AIBN][a]	Conversion (%) after 48 h	($\overline{M_n}$ 1H NMR[b] (g/mol)	($\overline{M_n}$ GPC (g/mol)	PDI
PNIPAAm	[200]:[1]:[0.25]	64	11,000	13,000	1.30
PNIPAAm-$PGMA_8$	[15]:[1]:[0.25]	60	12,000	14,000	1.24
PNIPAAm-$PGMA_{15}$	[30]:[1]:[0.25]	61	14,000	16,000	1.41

[a] The monomers are NIPAAm or GMA.
[b] ($\overline{M_n}$, 1H NMR = $\frac{[\text{monomer}]}{[\text{RAFT agent}]} \times$ %conversion × molecular weight of monomer.

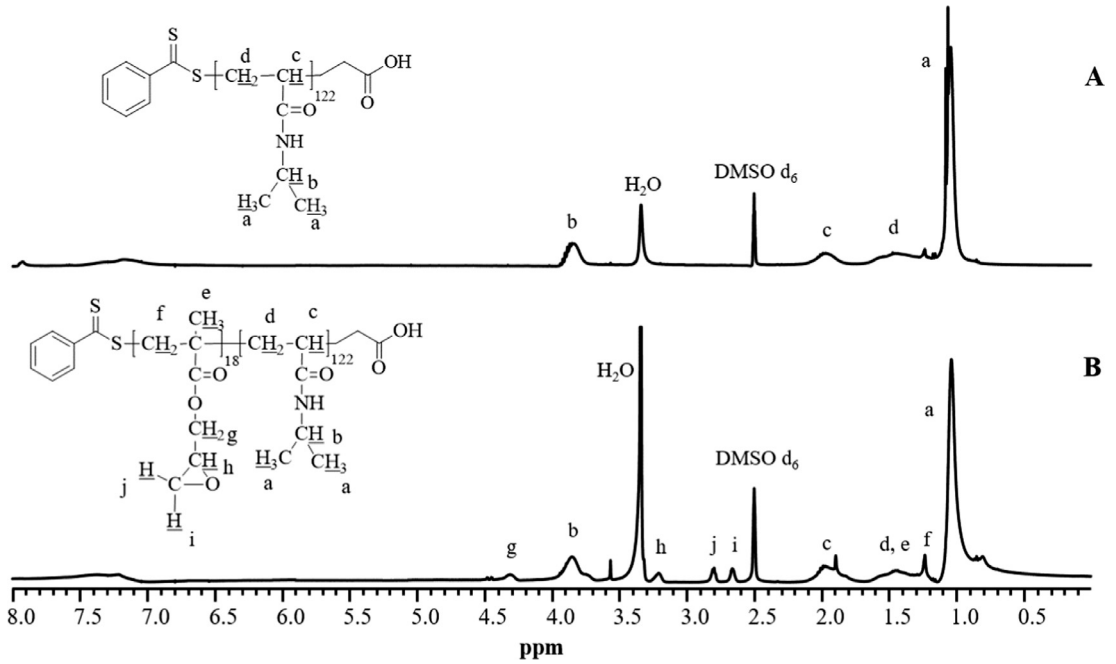

Fig. 2. ^{1}H NMR spectra of (A) PNIPAAm macro RAFT agent and (B) PNIPAAm-GMA$_{18}$ (solvent: DMSO D_6).

(5.6, 6.0 and 6.2 ppm of C$\underline{H}_2$=C$\underline{H}$—) also signified the formation of the PNIPAAm macro RAFT agent. The molecular weight ($\overline{M}_n$) of the polymer calculated from the reaction conversion (64% conversion) was about 11,000 g/mol corresponding to 122 NIPAAm repeating units. This polymer was then used as a macro RAFT agent for further functionalization with GMA to obtain PNIPAAm with different numbers of glycidyl units.

Fig. 2B shows an example of ^{1}H NMR spectrum of PNIPAAm-GMA$_{18}$. The signals of glycidyl groups, such as 2.6, 2.8 and 3.2 ppm (peak *i*, *j* and *h*) of epoxy rings and 4.3 ppm (peak *g*) of methylene protons adjacent to the ester groups, were observed indicating the formation of PNIPAAm-GMA. According to the reaction conversion (60%), PNIPAAm with two different numbers of GMA units (8 and 18 units) was obtained, and the polymer was thus designated as PNIPAAm-GMA$_8$ and PNIPAAm-GMA$_{18}$, respectively (Table 1). ^{1}H NMR spectrum of PNIPAAm-GMA$_8$ is similar to that of Fig. 2B and shown in the supporting information.

From the results in Table 1, both $\overline{M}_n$, GPC and $\overline{M}_n$, 1H NMR of the polymers gradually increased when increasing the numbers of GMA units (8 and 18 repeating units) in PNIPAAm chains. In all cases, the $\overline{M}_n$, GPC values were slightly higher than $\overline{M}_n$, 1H NMR and their PDIs were in the range of 1.24–1.41.

In good agreement with ^{1}H NMR, FTIR spectrum of PNIPAM shows N-H stretching at 3437 cm^{-1} and the characteristic signals of amide groups at 1647 cm^{-1} and 1550 cm^{-1} ((O=C)—N—H) (Fig. 3A). After functionalization of PNIPAAm with glycidyl groups, FTIR spectrum shows the characteristic signals of epoxy rings of GMA at 841 cm^{-1} and 909 cm^{-1} (Fig. 3B) [38,39]. In addition, the signals at 1730 cm^{-1} ((C=O)—O) and 1173 cm^{-1} (C—O) also indicated the presence of ester linkages of GMA units in the polymer chains.

3.2. Synthesis of MNP-PNIPAAm-GMA nanocluster

FTIR spectrum of the amino-coated MNP shows the signals at 998 cm^{-1} (Si—O stretching), 1537 cm^{-1} (N—H bending), 3369 cm^{-1} (N—H stretching) and 583 cm^{-1} (Fe—O) of the MNP core (in the Supporting information). To form the nanocluster, glycidyl-functionalized PNIPAAm solutions in water having various polymer concentrations were added to the amino-coated MNP dispersions in basic condition (pH 10) and the reaction was set at 65 °C for 12 h. Epoxy functional groups of PNIPAAm-GMA can readily react with amino groups on MNP surface *via* a ring-opening reaction. FTIR spectrum of the nanocluster shows characteristic signals of both MNP core at 583 cm^{-1} (Fe—O stretching) and PNIPAAm-GMA at 1719 cm^{-1} ((C=O)—O stretching of glycidyl groups), 3393 cm^{-1} (N—H stretching), 1623 cm^{-1} and 1548 cm^{-1} ((O=C)—N—H of the amide groups) (Fig. 3C). In addition, the characteristic peaks of the epoxy groups (841 cm^{-1} and 909 cm^{-1}) disappeared after the MNP nanoclustering due to the ring-opening reactions of glycidyl units.

D_h of the polymers including PNIPAAm, PNIPAAm-GMA$_8$ and PNIPAAm-GMA$_{18}$ (without MNPs) and those of MNP-polymers nanoclusters were investigated as a function of the polymer concentrations *via* PCS (Fig. 4A). Without MNP, D_h tended to consistently increase when increasing polymer concentrations from 0.001 to 10 mg/ml. Interestingly, PNIPAAm-

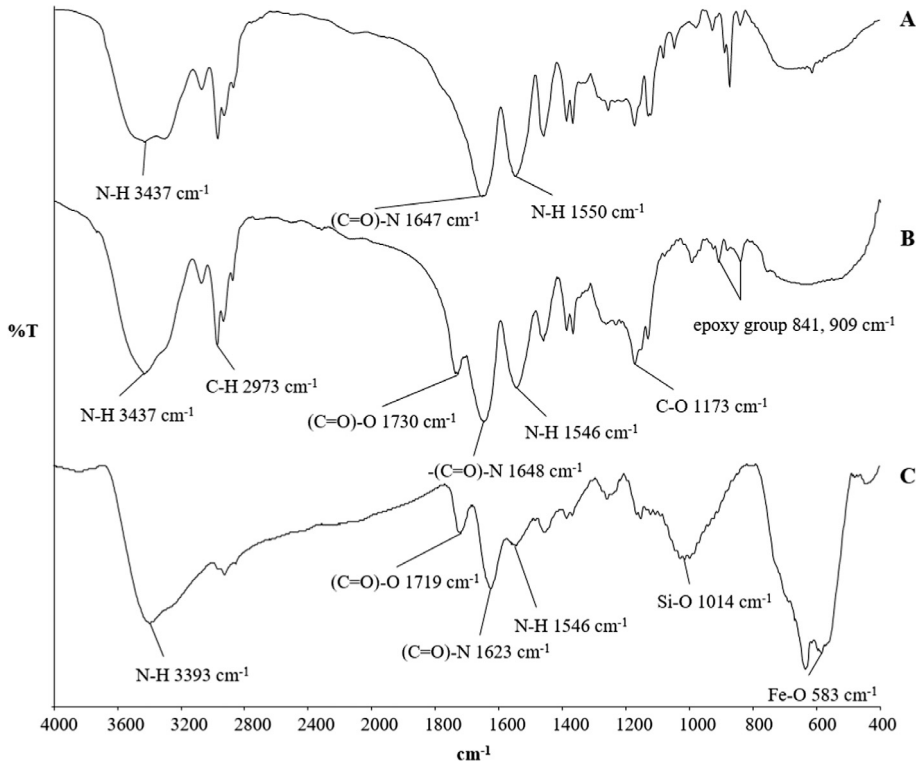

Fig. 3. FTIR spectra of (A) PNIPAAm, (B) PNIPAAm-GMA$_{18}$ and (C) MNP-PNIPAAm-GMA$_{18}$ nanocluster.

GMA$_{18}$ showed significantly larger D_h (up to 820 nm at 10 mg/ml polymer concentration) than those of the other two polymers (PNIPAAm and PNIPAAm-GMA$_8$). This result suggested that PNIPAAm-GMA$_{18}$ might have some polymer agglomeration in water due to the relatively long hydrophobic GMA segments in the structure.

After the naoclustering reaction, ungrafted polymer was removed from the MNP dispersion *via* a magnetic separation and washing process. MNP-polymer nanocluster was then redispersed in water and its D_h was investigated as a function of the polymer concentration (Fig. 4B). MNP-PNIPAAm (without GMA unit) apparently aggregated, regardless of the ratio of MNP to the polymer used, due to the absence of glycidyl group in the polymer chain for covalent coating on the MNP surface, and thus its D_h did not measured. The presence of glycidyl groups in PNIPAAm-GMA provided covalent bonding of the polymers with MNP *via* ring-opening reactions, resulting in the improved dispersibility of the particles in water due to the polymer coating. D_h tended to increase (from 100 nm to 400 nm) when the ratio of the polymer in the reactions increased and this was attributed to the formation of MNP nanoclustering. In addition, it should be mentioned that D_h of these MNP nanoclusters seemed to be smaller than those of their corresponding polymers at the same polymer concentrations (Fig. 4A), signifying the formation of nanoclustering between the MNP and the functionalized polymers. The proposed mechanism of the formation of the nanoclusters is shown in Fig. 5. Because MNP coated with multifunctional groups of primary amino groups, these particles can serve as nano-crosslinkers and thus induced the formation of MNP nanoclusters, which were evidenced by TEM technique. These results implied that D_h of the nanoclusters, reflecting the degree of nanoclustering reactions, can be regulated either by adjusting the ratio of the polymers to MNP in the reactions or by introducing GMA units to the polymers.

TEM images of amino-coated MNP and the nanoclusters using 1:0.1 and 1:10 ratio of MNP to PNIPAAm-GMA$_{18}$ are shown in Fig. 6. These particles were dispersed in water and directly cast on copper grids for the TEM sample preparation. Before the reactions between MNP and the polymers, amino-coated MNP showed large aggregate of the particles without nanoclusters due to the lack of polymeric stabilization to the particles (Fig. 6A). When introducing amino-coated MNP into PNIPAAm-GMA$_{18}$ solutions, MNP nanoclusters were thoroughly observed in TEM images (Fig. 6B and C). The size of these nanoclusters ranged between 20 and 150 nm in diameter with about 10–120 particles/cluster. These TEM results supported the proposed mechanism of MNP nanoclustering shown in Fig. 5. TEM images of the MNP nanoclusters grafted with PNIPAAm-GMA$_8$ exhibit the formation of the nanoclusters similarly to those of PNIPAAm-GMA$_{18}$ without significant difference in their size (in the Supporting information).

It should be noted that a compromise between colloidal stability in water and magnetic responsiveness of the nanoclusters is crucial for use in magnetic separation applications. It was hypothesized that the formation of MNP nanoclusters with a controllable degree of clustering should retain its nano-scale related properties but having sufficient magnetic responsiveness. Therefore, the stability in water and magnetic responsiveness of the MNP nanoclusters coated with PNIPAAm-GMA$_8$ or

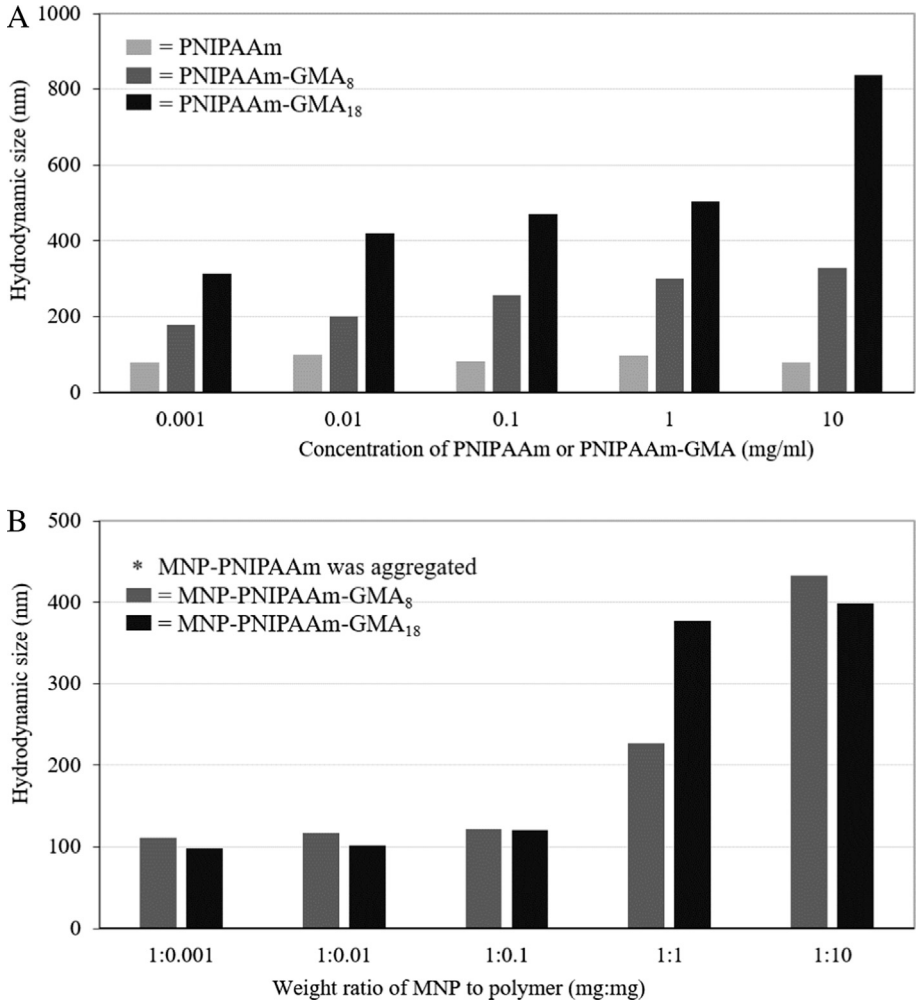

Fig. 4. (A) D_h of PNIPAAm and PNIPAAm-GMA (without MNP) and (B) D_h of MNP nanocluster grafted with PNIPAAm or PNIPAAm-GMA in various polymer concentrations. 1 mg MNP in 1 ml polymer solution was used in these reactions.

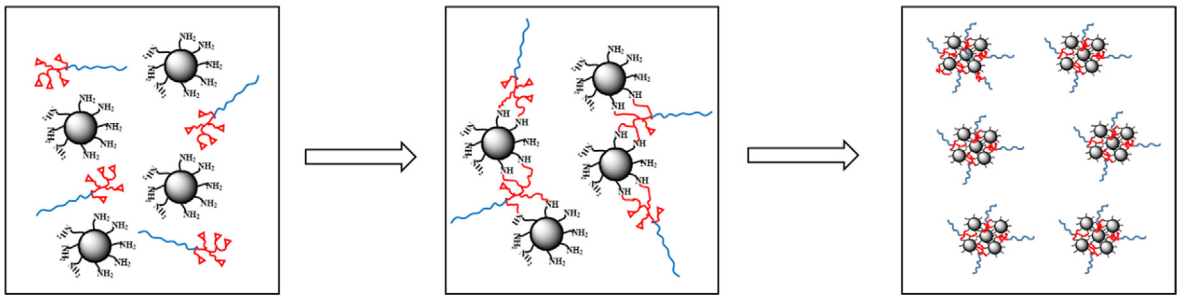

Fig. 5. Schematic mechanism of the formation of MNP-PNIPAAm nanoclusters.

PNIPAAm-GMA_{18} were investigated. This experiment was performed with the use of MNP:PNIPAAm-GMA ratio of 1:10 because PCS results indicated that there was some degree of MNP-polymer nanoclustering as opposed to those having 1:0.1 MNP:polymer (Fig. 4B). Therefore, 1:10 ratio of MNP to the polymers would be focused for the studies in the effect of the number of GMA units (PNIPAAm-GMA_8 and PNIPAAm-GMA_{18}) on the particle stability, magnetic responsiveness and thermo-responsive properties.

The MNP nanoclusters coated with PNIPAAm-GMA_8 or PNIPAAm-GMA_{18} showed a good dispersibility in water without aggregation after 3 days and some slight aggregation after 7 days of the preparations (Fig. 7a and b), while those coated with

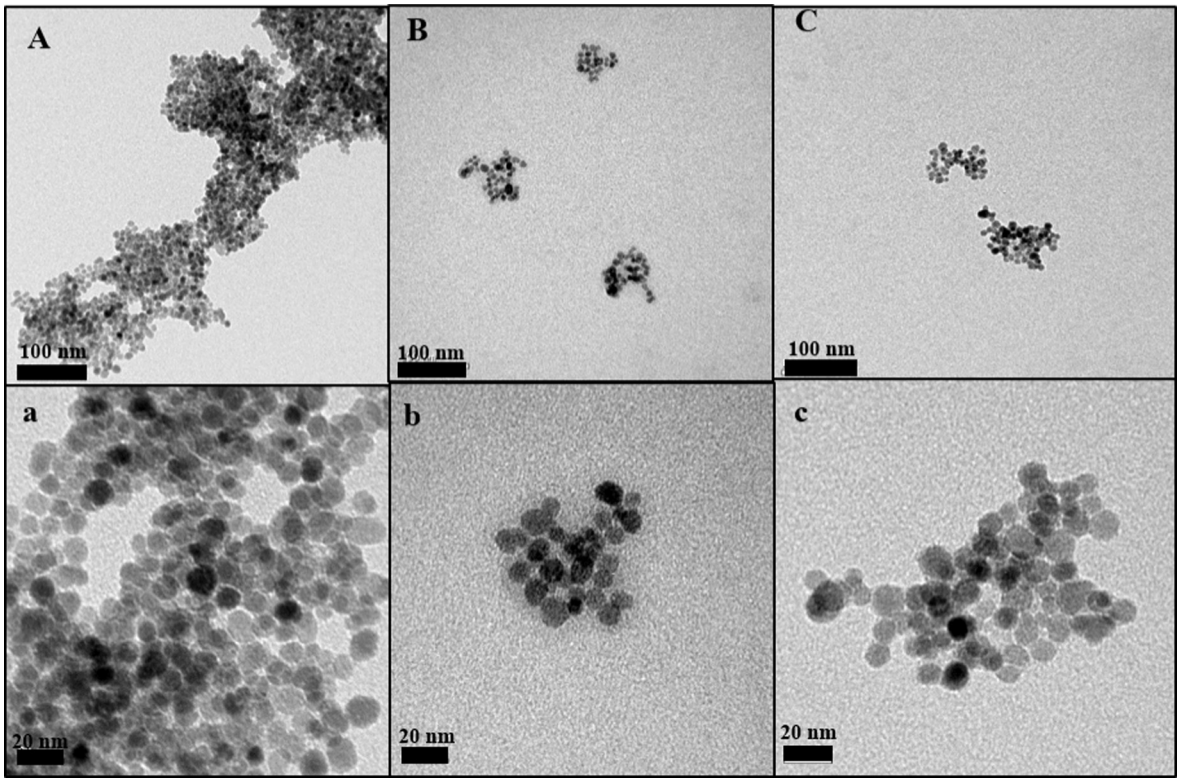

Fig. 6. Representative TEM images of MNP before and after nanoclustering reactions dispersed from water. (A, a) amino-coated MNP, (B, b) MNP-PNIPAAm-GMA_{18} nanocluster with MNP:polymer ratio of 1:0.1 and (C, c) MNP-PNIPAAm-GMA_{18} nanocluster with MNP:polymer ratio of 1:10.

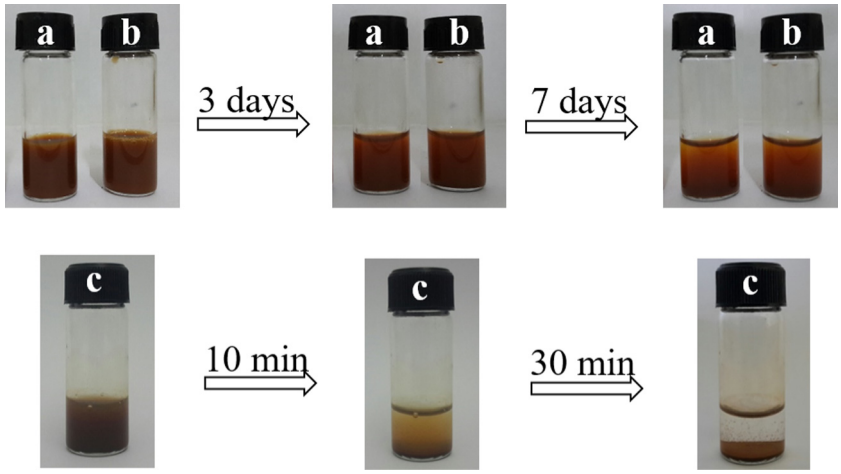

Fig. 7. Water dispersibility of MNP nanoclusters coated with (a) PNIPAAm-GMA_8, (b) PNIPAAm-GMA_{18} and (c) PNIPAAm.

PNIPAAm (without GMA units) exhibited macroscopic aggregation within 30 min (Fig. 7c). This result confirmed the reactions between GMA units in the polymers and the amino groups on the particle surface, resulting in the polymer coating and thus improved dispersibility in water.

Colloidal stability of MNP nanoclusters coated with the polymers in water when subjected to an applied magnetic field was investigated. The particles coated with PNIPAAm-GMA were able to be completely separated from the dispersions within 120 min with an assistance of a permanent magnet (Fig. 8a and b). This was attributed to the formation of MNP nanoclusters, resulting in an improvement in magnetic responsiveness. It should be mentioned that individual MNP cannot be magnetically separated from its carrier fluid because the particle and the solvent can move as a whole [40]. When PNIPAAm

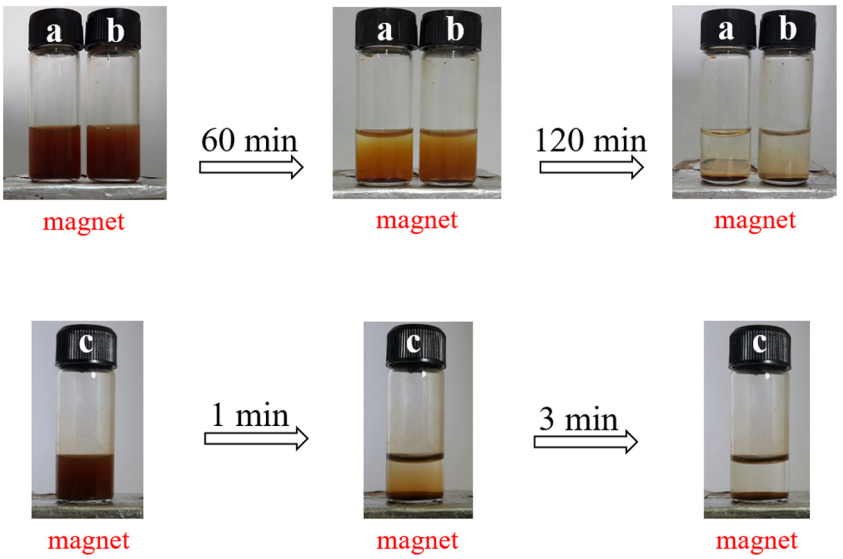

Fig. 8. Magnetic separation in water of MNP nanoclusters coated with (a) PNIPAAm-GMA_8, (b) PNIPAAm-GMA_{18} and (c) PNIPAAm.

(without GMA) was used instead of PNIPAAm-GMA, the particles were magnetically separated from the dispersion within 3 min (Fig. 8c). The much shorter separation time was again attributed to the large aggregation of the particles due to a lack of polymer coating, which was in good agreement with the PCS and water dispersibility results. These results indicated that coating the polymers on MNP is necessary in order to obtain stable nanoclusters with ability to be separated from their dispersions. However, the magnetic responsiveness and water dispersibility of the nanoclusters coated with PNIPAAm-GMA_8 and PNIPAAm-GMA_{18} were not different from each other.

Percentage of organic components in the nanoclusters was determined *via* TGA technique. It was assumed that the percent weight loss was attributed to the weight of organic components and the residual weight was those of iron oxide in the nanoclusters (Fig. 9A). The organic component in amino-coated MNP (without the polymer) was about 5%, while those in MNP-polymer nanoclusters were about 37% and 47%, depending on the type of the polymer (PNIPAAm-GMA_8 or PNIPAAm-GMA_{18}) used in the nanoclustering reactions. The MNP nanoclusters coated with the polymers with higher number of GMA units (PNIPAAm-GMA_{18}) showed higher percentage of the organic component in the structure.

The results from VSM experiments were also in good agreement with those from TGA. The nanoclusters having low MNP contents (high organic components) exhibited low magnetic responsiveness, as indicated by the low saturation magnetization (M_s) in the *M-H* curves (Fig. 9B). These nanoclusters showed superparamagnetic behavior as indicated by the absence of coercivity and remanence when there was no applied magnetic field.

Fig. 10 shows D_h of MNP nanoclusters coated with PNIPAAm-GMA_8 and PNIPAAm-GMA_{18} as a function of dispersion temperature. D_h values did not significantly change at the temperature below 34 °C and drastically increased at the temperature between 34 °C and 40 °C, indicating the LCST of the MNP nanoclusters of 34 °C for both samples. The observed LCST was slightly higher than those of PNIPAAm homopolymer (32°) [41] and this was attributed to the existence of GMA moiety in the structure, resulting in the formation of hydroxyl groups in the structure after the ring-opening reactions. The increase in LCST of PNIPAAm due to the presence of hydrophilic components in the polymer structure has been previously reported [31].

At the temperature above the LCST (34 °C), PNIPAAm in the nanoclusters became more hydrophobic due to hydrogen bonding among the polymer chains, leading to the enhancement in the particle agglomeration in water and thus increasing their D_h. These results well corresponded to their aggregation when standing at the temperature above the LCST for 30 min (the inset in Fig. 10). They can be re-dispersible at the temperature below the LCST and this behavior was reversible. When considering the effect of the number of GMA units in the polymer chains on D_h of the nanoclusters, the increase in GMA units further improved their water swellability due to the increased formation of hydrophilic hydroxyl groups as indicated by the larger D_h at the temperature above the LCST.

A case study showing the drug controlled release application of these MNP nanoclusters was also performed. EE and DLE of the nanoclusters were first investigated. It was found that EE and DLE of the nanoclusters were rather high (45–48% of EE and 75–85% of DLE). Indomethacin release profiles of the MNP nanoclusters coated with PNIPAAm-GMA_8 and PNIPAAm-GMA_{18} in PBS (pH 7.4) at the temperature below (20 °C) and above (45 °C) its LCST were then investigated. In all cases, indomethacin releases from the samples reached their equilibrium within 30 min.

In the case of MNP nanoclusters coated with PNIPAAm-GMA_8, 74% indomethacin was released at the temperature above its LCST (44 °C), while 44% indomethacin released when the temperature was below its LSCT (20 °C). The significantly higher

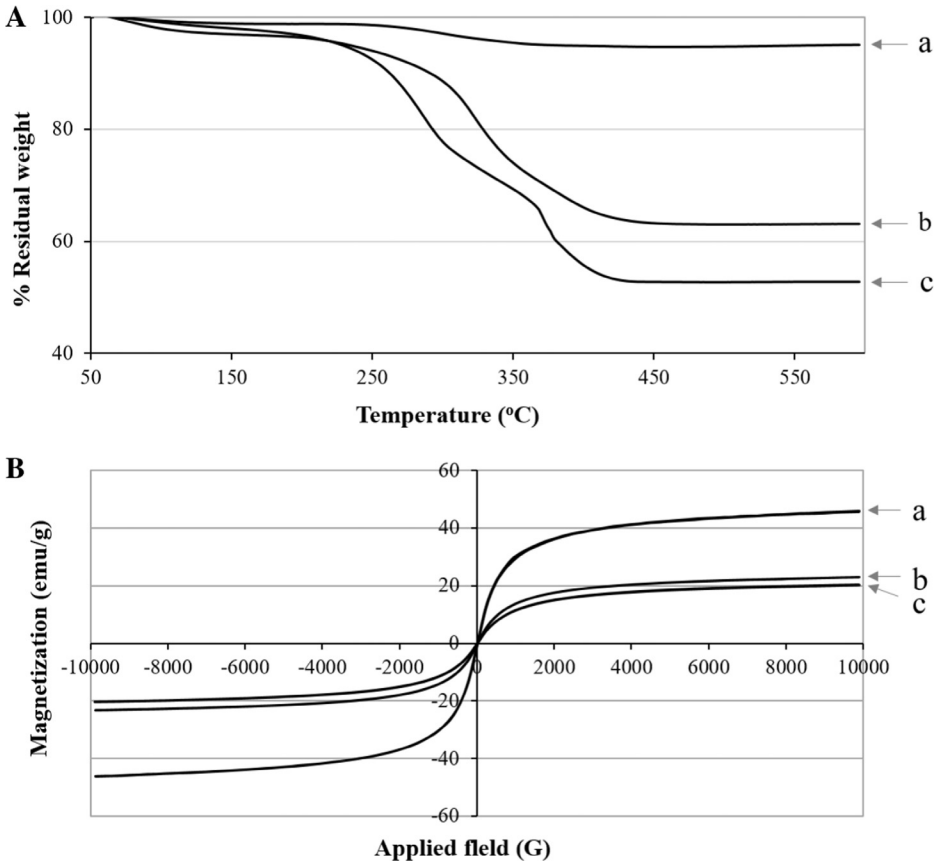

Fig. 9. (A) TGA thermograms and (B) *M-H* curves of (a) amino-coated MNP, (b) MNP-PNIPAAm-GMA_8 and (c) MNP-PNIPAAm-GMA_{18}, when 1:10 ratio of MNP to the polymer was used in the nanoclustering reactions.

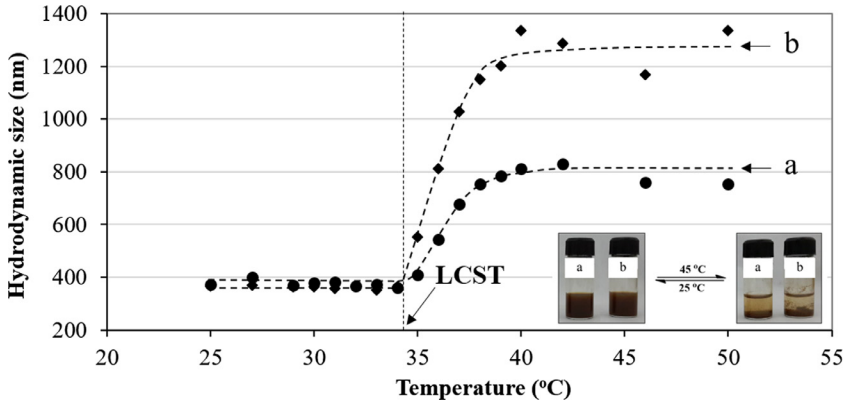

Fig. 10. D_h of MNP nanoclusters coated with (a) PNIPAAm-GMA_8 and (b) PNIPAAm-GMA_{18} as a function of temperatures, when 1:10 ratio of MNP to the polymers was used in the nanoclustering reactions.

percent drug release (ca. 30%) at the temperature above its LCST was owing to the squeezing mechanism of the collapsed PNIPAAm coated on the MNP nanoclusters at 45 °C (Fig. 11A), resulting in an increased amount of indomethacin being released. A similar result was also observed when the nanoclusters coated with PNIPAAm-GMA_{18} were used in the experiment (Fig. 11B). However, less difference in the indomethacin being released of (ca.5%) when the temperature passed the LCST in this case was attributed to the presence of higher hydrophilic hydroxyl groups after the ring-opening reaction as discussed in PCS results (Fig. 10). As a result, loosely packed structure of PNIPAAm-GMA_{18} on the particles was formed and influenced the shrinkage of PNIPAAm and the release of the entrapped indomethacin.

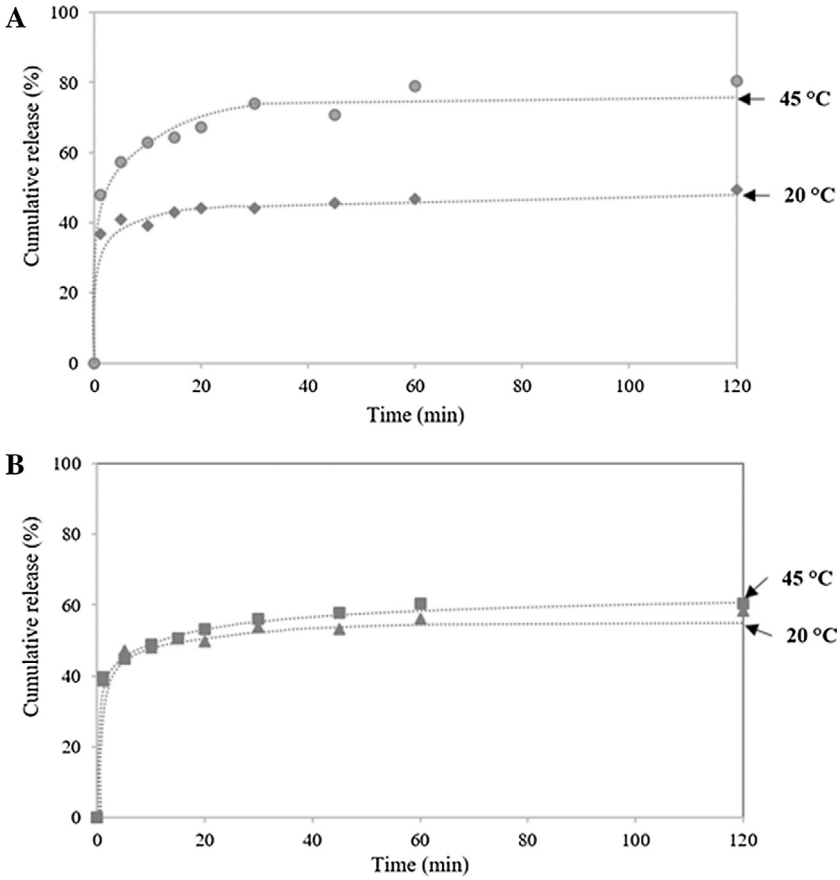

Fig. 11. Indomethacin release profiles of MNP nanoclusters coated with (A) PNIPAAm-GMA$_8$ and (B) PNIPAAm-GMA$_{18}$ at 20 °C and 45 °C.

4. Conclusions

Controlled nanoclustering of MNP using PNIPAAm-GMA *via* a "grafting onto" approach was presented in this work. PNIPAAm provided thermo-responsive properties to the nanoclusters while GMA units allowed for the formation of nanocluster structure through the glycidyl ring-opening reactions. RAFT polymerization was used to control the molecular weight of PNIPAAm and the number of GMA units in the polymer. The particles with good colloidal stability in water with good magnetic responsiveness were much desirable. The degree of nanoclustering can be controlled either by tuning the ratio of MNP to the polymers in the reactions or by introducing GMA units to the polymer. Increasing the ratio of the polymer to MNP in the reaction seemed to increase D_h and improved their water dispersibility. The temperature change crossing its LCST can be used as a triggering mechanism for controlled release of entrapped drugs on the nanoclusters. These novel MNP nanoclusters with thermo-responsive properties, good magnetic sensitivity and good water dispersibility might be good candidates for advanced technologies such as controlled release applications.

Acknowledgement

The authors thank the Thailand Research Fund (TRF) (RSA5980002) for financial support. MR acknowledges the funding from the Office of the Commission on Higher Education of Thailand (R2559A012). BT specially acknowledges the Royal Golden Jubilee Ph.D. Program for the scholarship (PHD/0362/2552).

Appendix A. Supplementary material

Supplementary data associated with this article can be found, in the online version, at http://dx.doi.org/10.1016/j.eurpolymj.2016.11.002.

References

[1] H.H.P. Yiu, S.C. McBain, Z.A.D. Lethbridge, M.R. Lees, J. Dobson, Preparation and characterization of polyethylenimine-coated Fe_3O_4-MCM-48 nanocomposite particles as a novel agent for magnet-assisted transfection, J. Biomed. Mater. Res. A 92A (1) (2010) 386–392.
[2] M. Chorny, B. Polyak, I.S. Alferiev, K. Walsh, G. Friedman, R.J. Levy, Magnetically driven plasmid DNA delivery with biodegradable polymeric nanoparticles, FASEB J. 21 (10) (2007) 2510–2519.
[3] T. Theppaleak, B. Rutnakornpituk, U. Wichai, T. Vilaivan, M. Rutnakornpituk, Magnetite nanoparticle with positively charged surface for immobilization of peptide nucleic acid and deoxyribonucleic acid, J. Biomed. Nanotechnol. 9 (9) (2013) 1509–1520.
[4] T. Theppaleak, M. Rutnakornpituk, U. Wichai, T. Vilaivan, B. Rutnakornpituk, Anion-exchanged nanosolid support of magnetic nanoparticle in combination with PNA probes for DNA sequence analysis, J. Nanopart Res. 15 (12) (2013).
[5] M. Bayrakci, O. Gezici, S.Z. Bas, M. Ozmen, E. Maltas, Novel humic acid-bonded magnetite nanoparticles for protein immobilization, Mater. Sci. Eng., C 42 (2014) 546–552.
[6] W. Jiang, K. Lai, Y. Wu, Z. Gu, Protein corona on magnetite nanoparticles and internalization of nanoparticle–protein complexes into healthy and cancer cells, Arch. Pharmacal. Res. 37 (1) (2013) 129–141.
[7] S. Karamipour, M.S. Sadjadi, N. Farhadyar, Fabrication and spectroscopic studies of folic acid-conjugated Fe_3O_4@Au core–shell for targeted drug delivery application, Spectrochim. Acta Part A Mol. Biomol. Spectrosc. 148 (2015) 146–155.
[8] T.J. Li, C.C. Huang, P.W. Ruan, K.Y. Chuang, K.J. Huang, D.B. Shieh, et al, In vivo anti-cancer efficacy of magnetite nanocrystal - based system using locoregional hyperthermia combined with 5-fluorouracil chemotherapy, Biomaterials 34 (32) (2013) 7873–7883.
[9] Y. Zhang, N. Kohler, M. Zhang, Surface modification of superparamagnetic magnetite nanoparticles and their intracellular uptake, Biomaterials 23 (7) (2002) 1553–1561.
[10] H. Dong, J. Huang, R.R. Koepsel, P. Ye, A.J. Russell, K. Matyjaszewski, Recyclable antibacterial magnetic nanoparticles grafted with quaternized poly(2-(dimethylamino)ethyl methacrylate) brushes, Biomacromolecules 12 (4) (2011) 1305–1311.
[11] X. Yang, L. Chen, B. Han, X. Yang, H. Duan, Preparation of magnetite and tumor dual-targeting hollow polymer microspheres with pH-sensitivity for anticancer drug-carriers, Polymer 51 (12) (2010) 2533–2539.
[12] L.M. Rossi, A.D. Quach, Z. Rosenzweig, Glucose oxidase-magnetite nanoparticle bioconjugate for glucose sensing, Anal. Bioanal. Chem. 380 (4) (2004) 606–613.
[13] A.F. Reynolds, J.Z. Hilt, Poly(n-isopropylacrylamide)-based hydrogel coatings on magnetite nanoparticles via atom transfer radical polymerization, Nanotechnology 19 (17) (2008) 175101.
[14] S. Sun, H. Zeng, D.B. Robinson, S. Raoux, P.M. Rice, S.X. Wang, et al, Monodisperse MFe2O4 (M = Fe Co, Mn) nanoparticles, J. Am. Chem. Soc. 126 (1) (2004) 273–279.
[15] B. Luo, S. Xu, A. Luo, W.R. Wang, S.L. Wang, J. Guo, et al, Mesoporous biocompatible and acid-degradable magnetic colloidal nanocrystal clusters with sustainable stability and high hydrophobic drug loading capacity, ACS Nano. 5 (2) (2011) 1428–1435.
[16] H. Amiri, M. Mahmoudi, A. Lascialfari, Superparamagnetic colloidal nanocrystal clusters coated with polyethylene glycol fumarate: a possible novel theranostic agent, Nanoscale 3 (3) (2011) 1022–1030.
[17] J. Ge, Y. Hu, M. Biasini, W.P. Beyermann, Y. Yin, Superparamagnetic magnetite colloidal nanocrystal clusters, Angew. Chem. Int. Ed. 46 (23) (2007) 4342–4345.
[18] J. Gao, X. Ran, C. Shi, H. Cheng, T. Cheng, Y. Su, One-step solvothermal synthesis of highly water-soluble, negatively charged superparamagnetic Fe_3O_4 colloidal nanocrystal clusters, Nanoscale 5 (15) (2013) 7026–7033.
[19] J.-F. Berret, N. Schonbeck, F. Gazeau, D. El Kharrat, O. Sandre, A. Vacher, et al, Controlled clustering of superparamagnetic nanoparticles using block copolymers: design of new contrast agents for magnetic resonance imaging, J. Am. Chem. Soc. 128 (5) (2006) 1755–1761.
[20] J. Dou, Q. Zhang, L. Jian, J. Gu, Magnetic nanoparticles encapsulated latexes prepared with photo-initiated miniemulsion polymerization, Colloid Polym. Sci. 288 (18) (2010) 1751–1756.
[21] T. Fan, M. Li, X. Wu, M. Li, Y. Wu, Preparation of thermoresponsive and pH-sensitivity polymer magnetic hydrogel nanospheres as anticancer drug carriers, Colloids Surf. B Biointerf. 88 (2) (2011) 593–600.
[22] A. Khan, A.M. El-Toni, M. Alhoshan, Preparation of thermo-responsive hydrogel-coated magnetic nanoparticles, Mater. Lett. 89 (2012) 12–15.
[23] S. Meerod, B. Rutnakornpituk, U. Wichai, M. Rutnakornpituk, Hydrophilic magnetic nanoclusters with thermo-responsive properties and their drug controlled release, J. Magn. Magn. Mater. 392 (2015) 83–90.
[24] K.Y. Yoon, C. Kotsmar, D.R. Ingram, C. Huh, S.L. Bryant, T.E. Milner, et al, Stabilization of superparamagnetic iron oxide nanoclusters in concentrated brine with cross-linked polymer shells, Langmuir 27 (17) (2011) 10962–10969.
[25] S. Chaleawlert-umpon, N. Pimpha, Morphology-controlled magnetite nanoclusters via polyethyleneimine-mediated solvothermal process, Mater. Chem. Phys. 135 (1) (2012) 1–5.
[26] T. Isojima, M. Lattuada, J.B. Vander Sande, T.A. Hatton, Reversible clustering of pH- and temperature-responsive janus magnetic nanoparticles, ACS Nano. 2 (9) (2008) 1799–1806.
[27] H. Wakamatsu, K. Yamamoto, A. Nakao, T. Aoyagi, Preparation and characterization of temperature-responsive magnetite nanoparticles conjugated with N-isopropylacrylamide-based functional copolymer, J. Magn. Magn. Mater. 302 (2) (2006) 327–333.
[28] N. Micic, A. Young, J. Rosselgong, C. Hornung, Scale-up of the reversible addition-fragmentation chain transfer (RAFT) polymerization using continuous flow processing, Processes 2 (1) (2014) 58–70.
[29] W. Wei, X. Hu, X. Qi, H. Yu, Y. Liu, J. Li, et al, A novel thermo-responsive hydrogel based on salecan and poly(N-isopropylacrylamide): synthesis and characterization, Colloids Surf. B Biointerf. 125 (2015) 1–11.
[30] H.S. Abandansari, E. Aghaghafari, M.R. Nabid, H. Niknejad, Preparation of injectable and thermoresponsive hydrogel based on penta-block copolymer with improved sol stability and mechanical properties, Polymer 54 (4) (2013) 1329–1340.
[31] P. Théato, R. Zentel, α, ω-Functionalized poly-N-isopropylacrylamides: controlling the surface activity for vesicle adsorption by temperature, J. Colloid Interf. Sci. 268 (1) (2003) 258–262.
[32] M. Constantin, M. Cristea, P. Ascenzi, Lower critical solution temperature versus volume phase transition temperature in thermoresponsive drug delivery systems, Exp. Polym. Lett. 5 (10) (2011) 839–848.
[33] F. Eeckman, A.J. Moës, K. Amighi, Synthesis and characterization of thermosensitive copolymers for oral controlled drug delivery, Eur. Polym. J. 40 (4) (2004) 873–881.
[34] S.P. Rwei, Y.Y. Chuang, T.F. Way, W.Y. Chiang, Thermosensitive copolymer synthesized by controlled living radical polymerization: phase behavior of diblock copolymers of poly(N-isopropyl acrylamide) families, J. Appl. Polym. Sci. 133 (13) (2016) 43224–43231.
[35] V. Zeighamian, M. Darabi, A. Akbarzadeh, M. Rahmati-Yamchi, N. Zarghami, F. Badrzadeh, et al, PNIPAAm-MAA nanoparticles as delivery vehicles for curcumin against MCF-7 breast cancer cells, Artificial Cells, Nanomed., Biotechnol. 44 (2) (2016) 735–742.
[36] K. Yamamoto, D. Matsukuma, K. Nanasetani, T. Aoyagi, Effective surface modification by stimuli-responsive polymers onto the magnetite nanoparticles by layer-by-layer method, Appl. Surf. Sci. 255 (2) (2008) 384–387.
[37] Y.H. Lien, T.M. Wu, Preparation and characterization of thermosensitive polymers grafted onto silica-coated iron oxide nanoparticles, J. Colloid Interf. Sci. 326 (2) (2008) 517–521.
[38] P. Li, R. Xu, W. Wang, X. Li, Z. Xu, K.W.K. Yeung, et al, Thermosensitive poly(N-isopropylacrylamide-co-glycidyl methacrylate) microgels for controlled drug release, Colloids Surf. B Biointerf. 101 (2013) 251–255.
[39] Y. Tang, L. Liu, J. Wu, J. Duan, Synthesis and self-assembly of thermo/pH-responsive double hydrophilic brush–coil copolymer with poly(l-glutamic acid) side chains, J. Colloid Interf. Sci. 397 (2013) 24–31.

[40] R. Sondjaja, T. Alan Hatton, M.K.C. Tam, Clustering of magnetic nanoparticles using a double hydrophilic block copolymer, poly(ethylene oxide)-b-poly (acrylic acid), J. Magn. Magn. Mater. 321 (16) (2009) 2393–2397.
[41] H.-Y. Chin, D. Wang, D.K. Schwartz, Dynamic molecular behavior on thermoresponsive polymer brushes, Macromolecules 48 (13) (2015) 4562–4571.

Journal of Applied Polymer Science

Reusable magnetic nanocluster coated with poly(acrylic acid) and its adsorption with an antibody and an antigen

Siraprapa Meerod,[1] Nunthiya Deepuppha,[2] Boonjira Rutnakornpituk,[2] Metha Rutnakornpituk [2]

[1]Department of Chemistry, Faculty of Science and Technology, Kampaeng Phet Rajabhat University, Kampaeng Phet 62000, Thailand

[2]Department of Chemistry and Center of Excellence in Biomaterials, Faculty of Science, Naresuan University, Phitsanulok 65000, Thailand

Correspondence to: M. Rutnakornpituk (E-mail: methar@nu.ac.th)

ABSTRACT: The synthesis of negatively charged magnetite nanoclusters grafted with poly(acrylic acid) (PAA) and their application as reusable nanosupports for adsorption with antibodies and antigens are presented in this article. They were facilely prepared via the free-radical polymerization of PAA in the presence of functionalized magnetite nanoparticles to obtain highly negative charged nanoclusters with a high magnetic responsiveness and good dispersibility and stability in water. According to transmission electron microscopy, the sizes of the nanoclusters ranged between 200 and 500 nm, without large aggregation visually observed in water. The hydrodynamic size of the nanocluster consistently increased with increasing pH of the dispersion; this indicated its pH-responsive properties, which was due to the repulsion of the anionic carboxylate groups in the structure. This nanocluster was successfully used as an efficient and reusable support for adsorption with anti–horseradish peroxidase antibody. It preserved higher than a 97% adsorption ability of the antibody after eight reuse cycles; this signified the potential of this novel nanocluster as a reusable support in the magnetic separation applications of other bioentities. © 2017 Wiley Periodicals, Inc. J. Appl. Polym. Sci. **2018**, *135*, 46160.

KEYWORDS: biomedical applications; hydrophilic polymers; magnetism and magnetic properties; nanoparticles; nanowires and nanocrystals; separation techniques

Received 28 July 2017; accepted 9 December 2017

DOI: 10.1002/app.46160

INTRODUCTION

Magnetite nanoparticles (MNPs) have recently shown great potential for use in biotechnology because of their ability to get close to biological entities, such as cells, viruses, proteins, and genes, with heating abilities when exposed to magnetic fields.[1] However, bare MNPs without surface modification are not practical for these applications because they are not stable in physiological fluids. Their use would result in particle agglomeration in aqueous media because of the many attractive forces, such as magnetic and dipole–dipole attractions.[2] Therefore, the challenge for the preparation of stable magnetic fluids is to prevent agglomeration during the nanoparticle synthesis process. Promising methods to prevent particle agglomeration include the use of electrostatic and steric stabilizers. Long-chain and/or charged polymers are usually coated on the MNP surface to provide steric and/or charge-repulsion-stabilization mechanisms to improve their stability and dispersibility in media[3–5] and also serve as a platform for conjugation with functional bioentities.[6,7]

Previous researchers have presented the application of MNPs for the magnetic separation of bioentities, including DNA,[8–10] RNA,[10,11] proteins,[12] and enzymes.[13] In particular, researchers have widely focused on the specific conjugation of MNPs with antibodies for magnetic separation. MNPs conjugated with antibodies against human epithelial growth factor receptor 2 were used for the immunomagnetic separation of tumor cells from fresh whole blood[14] and for tumor targeting and hyperthermia.[15] By taking advantage of the ionic reversible interactions, researchers synthesized highly active antibody-conjugated MNPs.[16] MNPs conjugated with dengue specific immunoglobulin M antibody were proven to have better analytical responses than those of traditional enzyme-linked immunosorbent assay.[17] MNPs bound with ScFv (fragment antibody) and anti-CD73 antibody magnetically separated 5′-nucleotidase enzyme used as a bioindicator for diagnosing diseases.[18] Anti–glypican 3 antibody-conjugated MNPs can be used to detect glypican 3 liver cancer cells with enzyme-linked immunosorbent assay.[19] In addition, MNPs coated with poly(ethylene oxide)-*block*-poly(2-vinyl-4,4-dimethylazlactone) diblock

Additional Supporting Information may be found in the online version of this article.

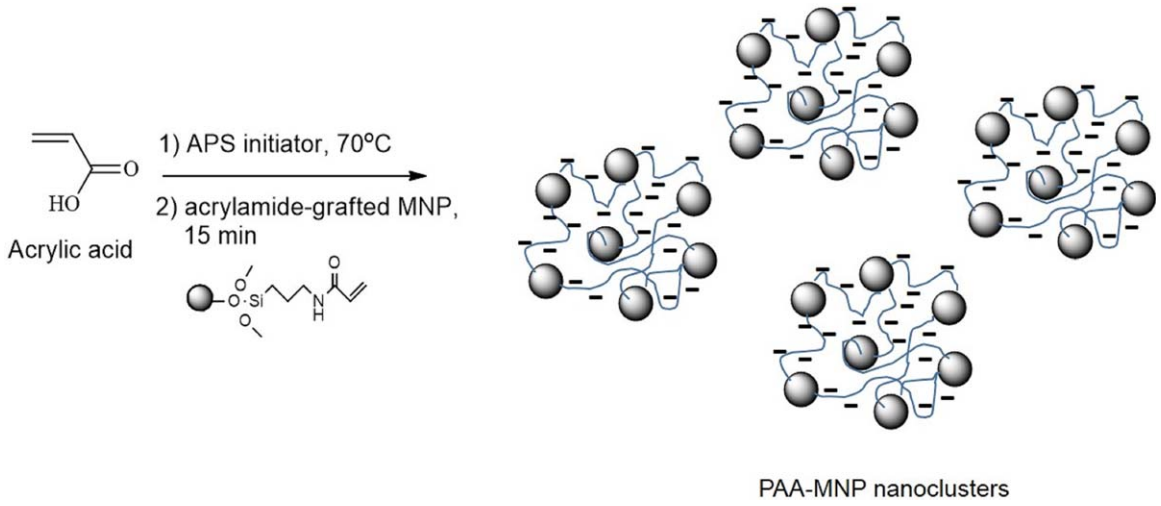

Figure 1. Synthesis of PAA–MNP nanoclusters via free-radical polymerization in the presence of acrylamide-functionalized MNPs. [Color figure can be viewed at wileyonlinelibrary.com]

copolymers were used as a recyclable magnetic nanosupport for adsorption with anti–rabbit immunoglobulin G antibody.[20]

However, the weak magnetic responsiveness of the very dispersible MNPs might be a main limitation in the magnetic separation and targeted-delivery applications.[21,22] To increase the magnetic sensitivity of MNPs, the particle size should be suitably large to produce a high magnetic responsiveness. Nonetheless, the particles are not stable when their size is too large because of particle attractive forces; this yields an unstable colloidal dispersion of the particles, which can rapidly agglomerate.[23,24] The formation of MNP nanoclusters in a controllable fashion is a promising approach for improving their magnetic responsiveness.

MNP nanoclusters are composed of many interconnected single particles (ca. 3–20 nm in diameter) and minor amounts of organic components.[25] The formation of MNP nanoclusters with a proper size gave rise to those with good dispersibility and stability in media[26,27] and also good magnetic responsiveness.[21] Also, their superparamagnetic properties were also retained as long as each MNP core could be distinguished from one another after a nanoclustering reaction.[28] Many researchers have investigated for the control of the formation of MNP nanocluster via many approaches, for example, physicochemical or physical interactions between presynthesized MNPs and polymer particles,[29] the *in situ* precipitation of MNPs in the presence of polymeric microspheres,[30,31] and the *in situ* polymerization of monomers in the presence of functional MNPs.[32–34]

In our previous studies, we attempted to prepare magnetic nanoclusters via the *in situ* precipitation of MNPs in the presence of presynthesized functional polymers. Water-dispersible MNP nanoclusters prepared via a ring-opening reaction of poly(ethylene oxide)-*block*-poly(2-vinyl-4,4-dimethylazlactone) diblock copolymers were used as reusable magnetic solid supports for antibody adsorption.[20] They showed a high adsorption ability (>95%) with anti–rabbit immunoglobulin G antibody even after eight adsorption–separation–desorption cycles. Other functional polymers used to control the degree of MNP nanoclustering, for example, diacrylate-terminated polydimethylsiloxane–disiloxane[35] and glycidyl-functionalized poly(*N*-isopropyl acrylamide),[36] have also been demonstrated with some potential applications, such as drug controlled release. The *in situ* polymerization of thermoresponsive poly(*N*-isopropyl acrylamide) in the presence of acrylamide-coated MNPs has been reported as a facile method for preparing magnetic nanoclusters for temperature-triggered controlled drug-release applications.[32]

In this article, a radical polymerization of poly(acrylic acid) (PAA) in the presence of functionalized MNPs to obtain anionic magnetic nanoclusters for adsorption with antibodies and antigens is reported (Figure 1). The loading ratio of acrylic acid (AA) monomer and MNPs in the polymerization was varied such that water-dispersible nanoclusters with good magnetic sensitivity were gained. PAA was of great interest in this study because it could provide good water dispersibility to the particles because of its electrostatic and steric repulsion mechanisms. In addition, anionic PAA on the nanocluster surface also allowed for electrostatic adsorption with positively charged bioentities; antibodies and antigens produced from rabbits were used as representatives in this study. The adsorption ability and reuse efficiency of the anionic MNP nanoclusters with the antibodies were also investigated.

EXPERIMENTAL

Materials

Unless otherwise indicated, the following reagents were used without purification: anhydrous iron(III) chloride ($FeCl_3$; 98%, Acros), iron(II) chloride tetrahydrate ($FeCl_2{\cdot}4H_2O$; 99%, Acros organic), oleic acid (68%, Carlo Erba), (3-aminopropyl)trimethoxysilane (98%, Acros), ammonium persulfate (APS; 98%, Carlo Erba), ammonium hydroxide (NH_4OH; 28–30%, J. T. Baker), and triethylamine (97%, Carlo Erba). AA (99.5%, Acros) was distilled under reduced pressure. Acryloyl chloride was synthesized via a coupling reaction between AA and benzoyl chloride (99%, Acros) at 75 °C to give a colorless liquid

Table I. Summary of the Preparation of the PAA–MNP Nanoclusters

	Initiator (APS)[a]		Monomer (AA)[b]		
Nanocluster	g	mol	g	mol	Molar ratio (initiator/monomer)
PAA100-MNP	0.002	8.76×10^{-5}	0.068	8.76×10^{-3}	1:100
PAA300-MNP	0.002	8.76×10^{-5}	0.21	2.61×10^{-2}	1:300

[a] Dissolved in 0.05 mL of deionized water
[b] Dissolved in 5.0 mL of deionized water.

with about a 60–65% yield. Anti-peroxidase antibody produced in rabbits [anti–horseradish peroxidase (anti-HRP)], horseradish peroxidase (HRP), 10% bovine serum albumin (BSA) diluents (KPL), 2,2′-azino-bis(3-ethylbenzothiazoline-6-sulfonic acid) (ABTS) peroxidase substrate (KPL), Bradford reagent (Sigma), bovine γ globulin (Thermo Scientific), and 2-(*N*-morpholino)ethane sulfonic acid (MES; 99%; Acros) were used as received.

Characterization

Fourier transform infrared (FTIR) spectrophotometry was conducted on a PerkinElmer model 1600 series FTIR spectrophotometer. Transmission electron spectroscopy (TEM) was performed on a Philips Tecnai12 TEM instrument operated at 120 kV with a Gatan charge coupled device (CCD) camera (model 782). Aqueous dispersions were sonicated and then cast on carbon-coated copper grids. High-resolution TEM and energy-dispersive X-ray (EDX) mapping were performed on a JEOL JEM 2010 200 kV TEM–EDX instrument. Photocorrelation spectroscopy was performed on a NanoZS4700 Nanoseries Malvern instrument. Dispersing media (water) was filtered through nylon syringe filters (0.2 μm pore size) before use. The dispersion was sonicated for about 20 min before each experiment. Thermogravimetric analysis (TGA) was conducted on a TGA/DSC1 Mettler Toledo instrument with a 20 °C/min heating rate under an O_2 atmosphere. Vibrating sample magnetometry (VSM) was performed at room temperature with a Standard 7403 Series instrument (Lakeshore). Antibody adsorption and nanocluster desorption were investigated via a Synergy HT microplate reader (BioTek) with an ultraviolet–visible (UV–vis) at λ of 595 nm.

Synthesis of Acrylamide-Grafted MNPs as a Crosslinker

The synthesis of acrylamide-grafted MNPs was reported previously.[32] Briefly, MNPs were synthesized via the coprecipitation of $FeCl_3$ (0.83 g in 10 mL of deionized water) and $FeCl_2{\cdot}4H_2O$ (0.5 g in 10 mL of deionized water) in 25% NH_4OH (10 mL) solutions. After the dispersion was stirred for 30 min, the particles were precipitated by centrifugation for 10 min (5000 rpm), and the aqueous layer was discarded. A volume of 15 mL of toluene was added to the particles without dryness. An oleic acid solution in hexane (2 mL in 20 mL of hexane) was then slowly introduced into MNP–toluene dispersion (ca. 0.4 g of MNP in 15 mL of toluene) with sonication; this was followed by reprecipitation in acetone to obtain oleic acid coated MNPs, which were then dried *in vacuo*.

(3-Aminopropyl)trimethoxysilane (0.3 g, 1.36×10^{-3} mol) was then added to the MNP dispersion (0.4 g of the MNPs in 15 mL of toluene) containing 2 *M* triethylamine (2.5 mL) to form amino-grafted MNP. After 24 h of stirring, the particles were repeatedly precipitated in EtOH and washed with toluene. After the particles were redispersed (0.05 g) in a 7.5 *M* NaOH solution (5 mL), acryloyl chloride (2.0 mL, 0.022 mol) was slowly added to the dispersion at 0 °C in an ice–water bath. After 24 h of stirring, the product was magnetically separated, repetitively washed with water, and then kept in the form of aqueous dispersions with 0.01 g of MNPs/mL of water.

Synthesis of the PAA–MNP Nanoclusters

PAA100–MNP nanoclusters and PAA300–MNP nanoclusters were synthesized via free-radical polymerization with 1 mol equivalent of APS as the initiator with 100 and 300 molar equivalents of AA, respectively. Table I summarizes the details of the sample preparation used in this study. First, APS solution was added to the AA solutions. The polymerization was performed at 70 °C under an N_2 atmosphere for 30 min. An acrylamide-grafted MNP dispersion (0.01 g of MNP, 0.5 mL of water) was slowly dropped into the mixture, and the mixture was stirred for another 10 min to form PAA–MNP nanoclusters. This was repeatedly washed with water with the assistance of a magnet to remove the unreacted monomer and ungrafted polymer chain from the nanoclusters.

Adsorption Efficiency of the PAA–MNP Nanoclusters with Anti-HRP Antibodies

PAA–MNP nanoclusters (10 mg) were incubated in a 10 m*M* MES solution at pH 5 (1 mL) containing 400 ppm anti-HRP antibodies for 2 h. A Bradford assay was used as an indirect method to study the antibody adsorption efficiency. The protein concentrations of all of the samples were investigated with a calibration curve of bovine γ globulin as a protein standard. After adsorption with anti-HRP antibodies, the PAA–MNP nanoclusters were separated from the supernatant with a permanent magnet. The absorptions at 595 nm of the antibody solutions before and after adsorption were determined with the Bradford assay. The adsorption efficiency was calculated from the amount of the antibodies adsorbed on the nanoclusters (milligrams of antibody per milligrams of MNPs; Figure 2). So, it was calculated from the following equation:

$$\text{Adsorption efficiency} = [(A-B/A)]\times 100 \quad (1)$$

where *A* is the loaded amount of anti-HRP antibody and *B* is the amount of anti-HRP antibody remaining in the supernatant.

Reuse Efficiency of the PAA–MNP Nanoclusters in Adsorption with Anti-HRP Antibodies

PAA–MNP nanoclusters (10 mg) were mixed with anti-HRP antibodies in a 10 *M* MES buffer solution at pH 5 (1 mL). The nanoclusters adsorbed with anti-HRP were magnetically separated

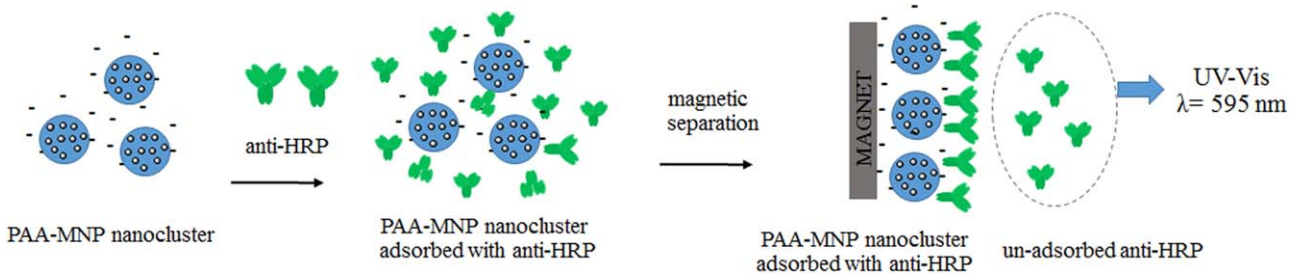

Figure 2. Schematic representation of PAA–MNP nanoclusters for adsorption with an anti-HRP antibody. [Color figure can be viewed at wileyonlinelibrary.com]

with a magnet, and excess anti-HRP in the solution was decanted. Anti-HRP on the nanocluster surface was then desorbed by repeated washing with a 2 *M* NaCl solution at pH 12. The amount of the antibodies after desorption was investigated with the Bradford assay described previously. The desorption efficiency was estimated from the following equation:

$$\text{Desorption efficiency} = (C/B) \times 100 \quad (2)$$

where C is the amount of desorbed anti-HRP antibodies.

The anti-HRP-free nanoclusters were then retrieved from the mixture with a permanent magnet. The adsorption–desorption process was performed repetitively to study the reuse efficiency in adsorption with the anti-HRP antibodies of the nanocluster, as illustrated in Figure 3.

Capacity for Antigen Recognition of the PAA–MNP Nanoclusters Adsorbed with Antibodies

After the adsorption with antibodies, the residue carboxyl groups of the PAA–MNP nanoclusters were blocked with 1 mL of 1% BSA in 10 m*M* MES at pH 7 and 25 °C for 16 h. The nanocluster was then washed with 10 m*M* MES at pH 6 to remove excess BSA. An indirect detection method was used to

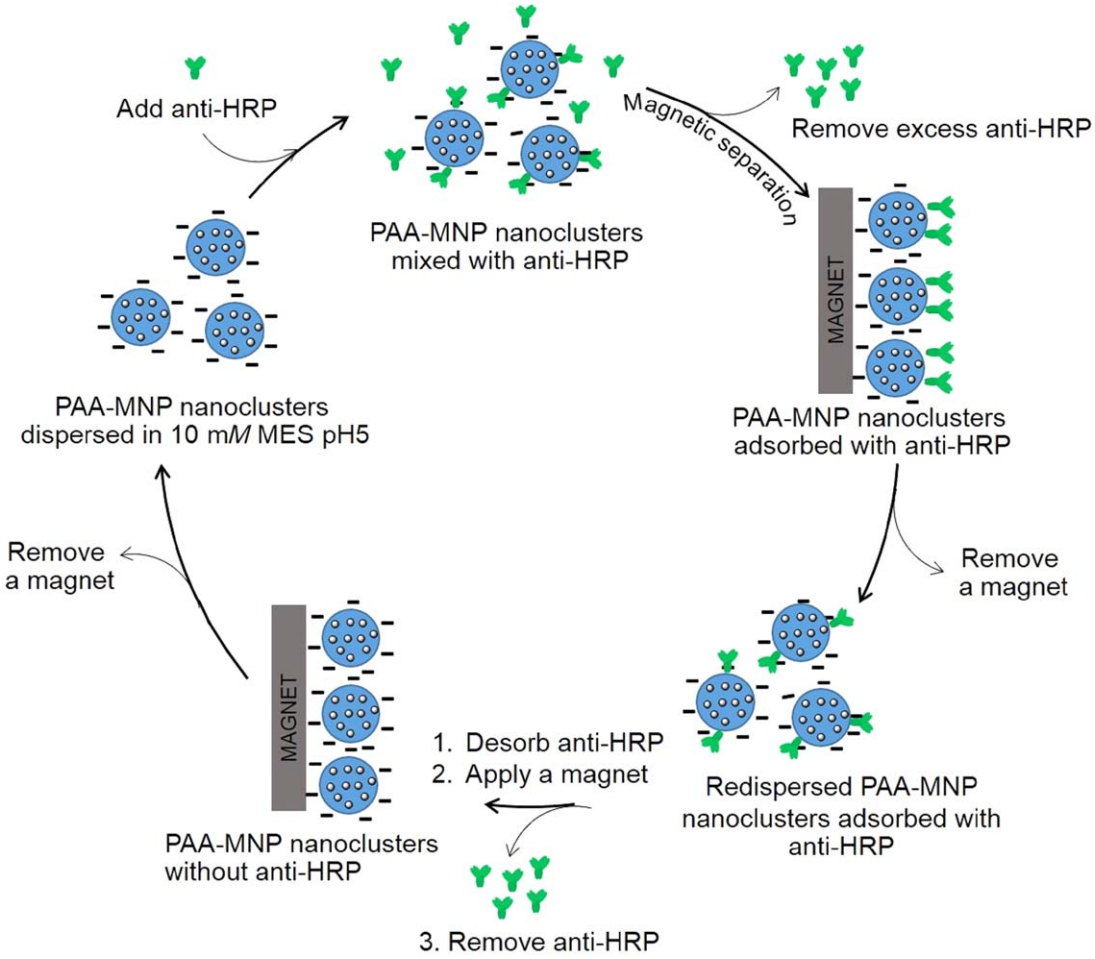

Figure 3. Illustration of an adsorption–desorption cycle of PAA–MNP nanoclusters in adsorption with an anti-HRP antibody. [Color figure can be viewed at wileyonlinelibrary.com]

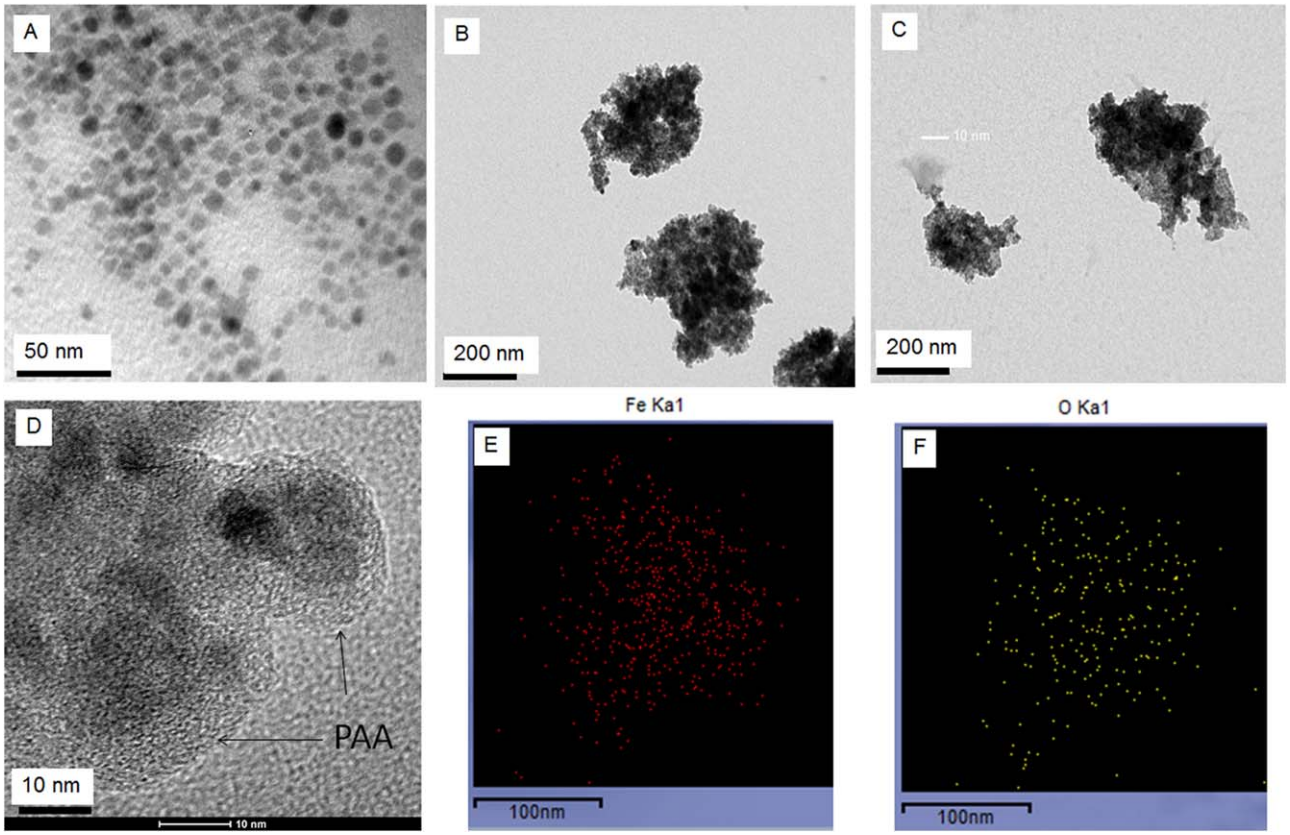

Figure 4. TEM images of (A) oleic acid coated MNPs, (B) PAA100–MNP nanoclusters, and (C) PAA300–MNP nanoclusters; (D) high-resolution TEM image of PAA100–MNP nanoclusters; and EDX mapping of PAA100–MNP nanoclusters showing the distribution of (E) iron (presented as red dots) and (F) oxygen (presented as yellow dots). [Color figure can be viewed at wileyonlinelibrary.com]

determine the antigen-recognition capacity of the nanocluster adsorbed with antibody. First, 1 mL of 400 ppm of HRP antigen in a 10 m*M* MES solution at pH 7 was added to the anti-HRP antibody-adsorbed nanoclusters and incubated for 30 min. The nanoclusters were repeatedly washed with a 10 m*M* MES solution at pH 7. The existence of antigens on the particle surface was apparently observed through the addition of 1 mL of ABTS–H_2O_2 solution to 10 μL of the nanocluster dispersion. The UV absorbance at a λ of 414 nm of the mixtures was then measured.

RESULTS AND DISCUSSION

The objective of this study was to synthesize negatively charged magnetic nanoclusters via a facile single-step free-radical polymerization of PAA in the presence of functionalized MNPs to obtain nanoclusters with high antibody adsorption abilities. The ratio of AA monomer to the MNPs was fine-tuned such that nanoclusters with good water dispersibility, good magnetic responsiveness, and highly negatively charged surfaces were obtained. These nanoclusters with negatively charged surfaces were demonstrated for use as magnetic nanosupports for adsorption with anti-HRP antibodies, and their adsorption abilities were also investigated. In addition, the reuse efficiency of the nanoclusters in adsorption with anti-HRP antibodies and its antigen-recognition capacity were also studied.

To prepare the PAA–MNP nanoclusters, acrylamide-coated MNPs were first synthesized via a coupling reaction between amino groups coated on the MNP surface and acryloyl chloride. These functionalized MNPs could serve as active nanocrosslinkers during the free-radical polymerization of AA and, thus, induced MNP nanoclustering because of the presence of multifunctional acrylamide groups on the particle surface (Figure 1). We observed that PAA homopolymer might also be formed during the polymerization in competition with the formation of PAA–MNP nanoclusters. The PAA homopolymer was then removed from the nanoclusters via repetitive magnetic separation and washing processes.

TEM images of oleic acid coated MNPs and PAA100–MNP and PAA300–MNP nanoclusters are shown in Figure 4. The TEM samples of oleic acid coated MNPs were prepared from toluene dispersion, whereas those of both PAA–MNP nanocluster samples were prepared from pH 7 aqueous dispersions. The oleic acid coated MNPs were spherical in shape with sizes 8–10 nm in diameter, without any sign of nanoclustering [Figure 4(A)]. After the polymerization, the formation of MNP nanoclusters was thoroughly observed from the TEM images [Figure 4(B,C)]. High-resolution TEM clearly evidenced the presence of a PAA layer (as indicated by an arrow) coated on the particles with a thickness of approximately 5–8 nm [Figure 4(D)]. EDX mapping of the nanoclusters showing iron (Fe) and oxygen (O) distributions also confirmed that the MNPs (Fe_3O_4) were in the

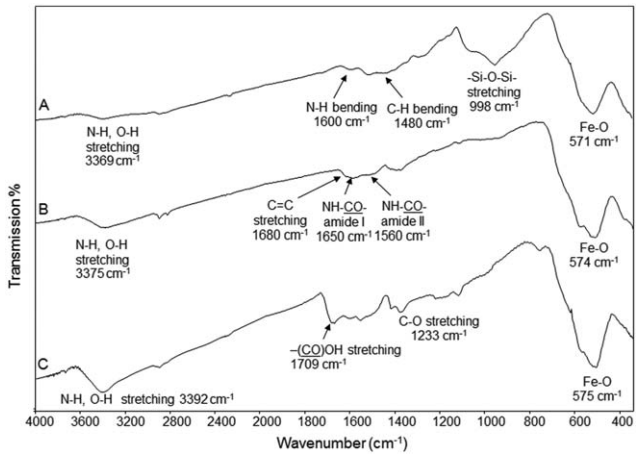

Figure 5. FTIR spectra of (A) amino-grafted MNPs, (B) acrylamide-grafted MNPs, and (C) PAA100–MNP nanoclusters.

form of nanoclusters [Figure 4(E,F)]. These results support the proposed mechanism of the formation of PAA–MNP nanoclusters illustrated in Figure 1. The size of the PAA100–MNP nanoclusters ranged between 200 and 300 nm in diameter, whereas the PAA300–MNP nanoclusters were broader and slightly larger (200–500 nm in diameter). The slightly larger size of the PAA300–MNP nanoclusters was attributed to the relatively higher amounts of PAA in the PAA300–MNP nanoclusters available to react with the reactive MNPs in the clustering reaction.

The FTIR spectra of the samples from each step of the reactions are shown in Figure 5. The spectrum of the amino-grafted MNPs showed the signals of an amino-coated silica layer at 3369 cm^{-1} (N—H stretching), 1600 cm^{-1} (N—H bending), 1480 cm^{-1} (C—H bending), and 998 cm^{-1} (Si—O stretching) and that of the MNP core at 571 cm^{-1} [Fe—O stretching; Figure 5(A)].[37] After functionalization with acrylamide groups, the FTIR spectrum exhibited characteristic signals of amide I and II stretching bands at 1650 and 1560 cm^{-1} and C=C stretching at 1680 cm^{-1} [Figure 5(B)].[38] After the polymerization and nanoclustering reactions, the spectrum of the PAA–MNP nanoclusters showed characteristic signals of O=CO stretching (1709 cm^{-1}) and O—H stretching bands (3392 cm^{-1}) of carboxylic acid groups; this signified the presence of PAA units in their structure [Figure 5(C)].

The ζ-potential values of the nanocluster as a function of the dispersion pH are shown in Figure 6(A). The presence of the ionizable carboxylic acid groups of PAA in the structure should have made them a polyelectrolyte in aqueous dispersion. In addition to functioning as a stabilizer that was both electrostatic and steric, the polyelectrolyte PAA also provided advantageous pH-responsive properties to the nanoclusters because of its large electrostatic potentials (pK_a of AA = 4.25).[39] The results in Figure 6 suggest that this nanocluster was pH responsive. The ζ-potential values of these nanoclusters in water continuously decreased with increasing dispersion pH and became highly negatively charged in basic pH. This was attributed to the formation of protonated carboxylic acid groups (—COOH) and deprotonated carboxylate groups ($—COO^-$) and depended on the solution pH. Figure 6(A) indicates that the isoelectric point (PI) of these particles was at a pH of about 2.5. This number was about two orders of magnitude lower than the pK_a of AA (pK_a of AA = 4.25).[39] The polymeric nature of PAA could have decreased the pK_a by one or more units because of the potential electrostatic repulsion of many adjacent carboxylate groups. At pH 7, the surface charge of the nanoclusters was highly negative (−35 mV); this was necessary for the magnetic separation of

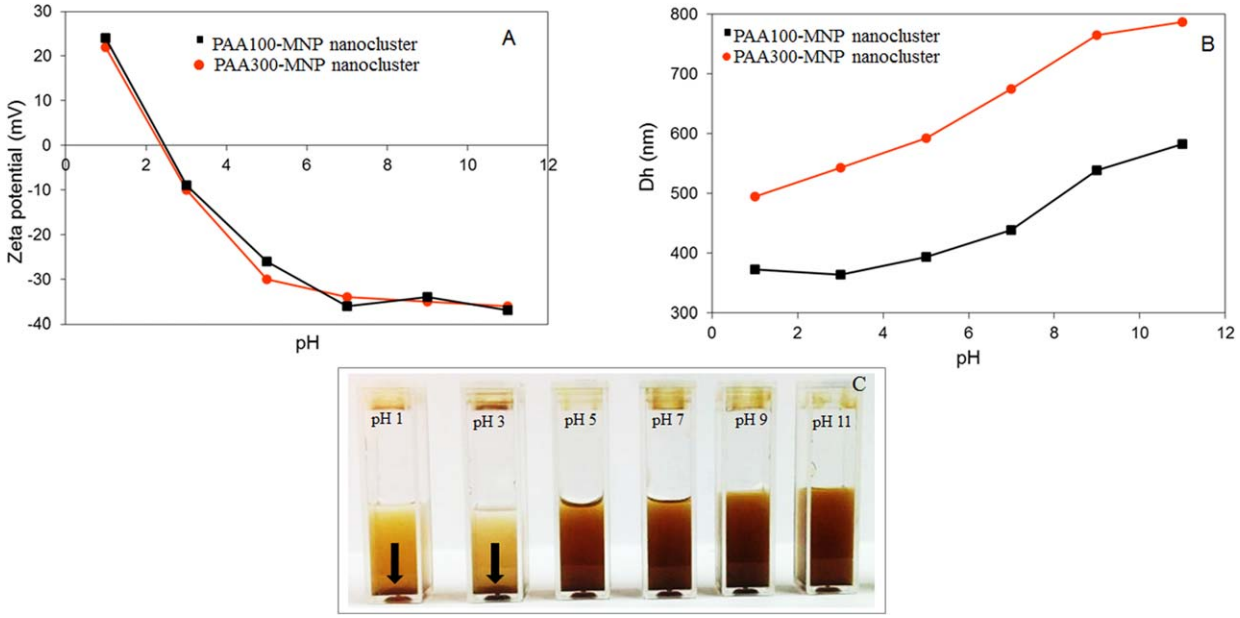

Figure 6. (A) ζ potentials of PAA100–MNP and PAA300–MNP nanoclusters, (B) D_h values of PAA100–MNP and PAA300–MNP nanoclusters as a function of the dispersion pH, and (C) appearance of PAA100–MNP nanoclusters dispersed in water at various pHs. The arrows in panel C indicate the aggregation of the nanoclusters in pH 1 and 3 dispersions after 1 h of preparation. [Color figure can be viewed at wileyonlinelibrary.com]

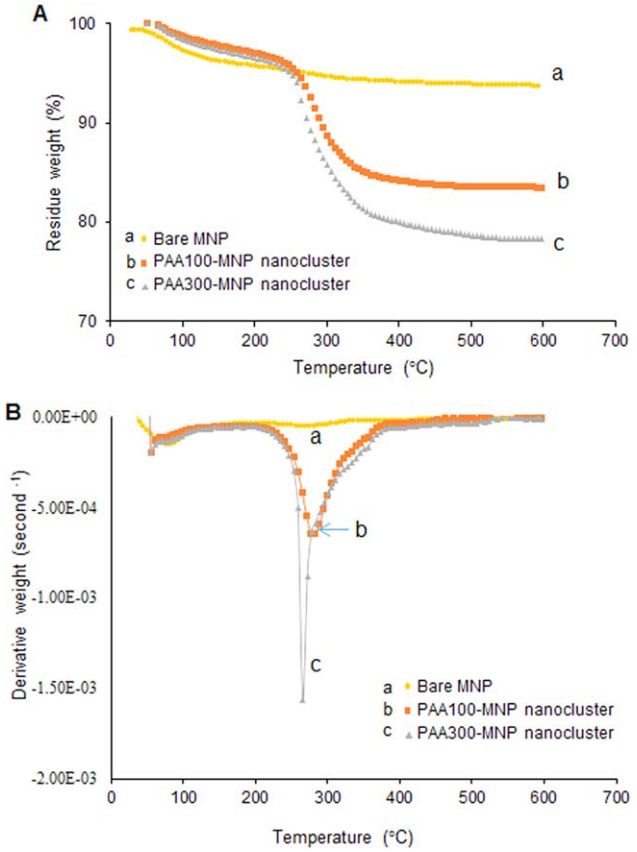

Figure 7. (A) TGA thermograms and (B) plots of the derivative weight loss of (a) bare MNPs, (b) PAA100–MNP nanoclusters, and (c) PAA300–MNP nanoclusters. [Color figure can be viewed at wileyonlinelibrary.com]

the antibodies via an electrostatic adsorption mechanism later discussed in this article.

The hydrodynamic size (D_h) of the nanoclusters was studied as a function of the solution pH [Figure 6(B)]. We found that D_h increased with increasing pH of the dispersion. At pHs below its PI, the PAA chain in the nanoclusters was in a protonated form (—COOH); this made it have no or less electrostatic repulsion among the chains and eventually shrink. An increase in the pH of the dispersion above its PI further increased the degree of negative charge of the nanoclusters and resulted in an enhancement in polymer swelling and thus an increase in its D_h. This explanation agreed well with the ζ-potential plots as a function of pH shown in Figure 6(A). In addition, pH-responsive properties of the nanoclusters were also evidenced by their dispersibility and stability as a function of pH in water [Figure 6(C)]. The nanoclusters were stable and very dispersible in pH 5–11 dispersions because of the existence of additional electrostatic repulsion stabilization.

However, some aggregation of the nanoclusters was observed when they were suspended in pH 1–3 dispersions. This might have been the result of some detachment of PAA from the nanoclusters under highly acidic conditions because of the hydrolysis of the amide linkages on their surface. The FTIR spectra of the nanoclusters showing the relatively lower intensity of PAA signals after treatment under acidic conditions (pH 1) are provided in the Supporting Information.

Effect of PAA compositions on D_h of the nanocluster was also investigated [Figure 6(B)]. PAA300–MNP nanocluster showed higher D_h values than that of PAA100–MNP nanocluster at the same dispersion pH. This was attributed to the higher amount of PAA in the PAA300–MNP nanocluster; this resulted in a higher degree of water swelling and a higher D_h. The results also support the slightly larger size of the PAA300–MNP nanoclusters observed in the TEM images (Figure 4).

To determine the composition of PAA grafted in the MNP nanocluster, TGA was performed to measure the weight loss at 600 °C [Figure 7(A)]. The ungrafted species, including PAA homopolymer and residue monomer, were removed from the MNP nanoclusters via a repetitive washing–magnetic separation process. We assumed that the residue weight was the weight of iron oxide from the MNP core remaining at 600 °C; the weight loss was attributed to the organic PAA content in the nanoclusters. We found that the PAA content in the PAA100–MNP nanoclusters was 10%, and that in the PAA300–MNP nanoclusters was about 16%. These results corresponded well with the high D_h and the high degree of water swelling of the PAA300–MNP nanoclusters observed in the photon correlation spectroscopy (PCS) experiment because of the high percentage of PAA in the structure as compared to the PAA100–MNP nanoclusters. The derivative weight loss was also plotted to clearly show the onset and maximum thermal degradation points of each sample [Figure 7(B)]. Bare MNPs showed an insignificant loss in their weight because of the lack of a polymer coating. Both PAA–MNP nanoclusters exhibited onset points of weight loss at 200 °C and maximum points at 280–290 °C, which corresponded to the degradation of organic PAA on the particle surface.

The magnetic properties of the bare MNPs, PAA100–MNP nanoclusters, and PAA300–MNP nanoclusters were investigated via a VSM technique (Figure 8). Saturation magnetization decreased from 62 emu/g for bare MNPs to 22–40 emu/g for the nanoclusters. This was again attributed to the presence of nonmagnetic PAA in the structure, which resulted in a lowered

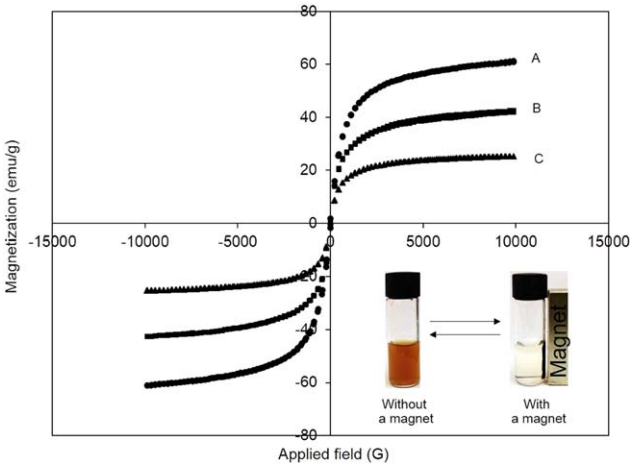

Figure 8. Magnetization curves of (A) bare MNPs, (B) PAA100–MNP nanoclusters, and (C) PAA300–MNP nanoclusters. The inset shows the capture of PAA100–MNP nanoclusters with a magnet. [Color figure can be viewed at wileyonlinelibrary.com]

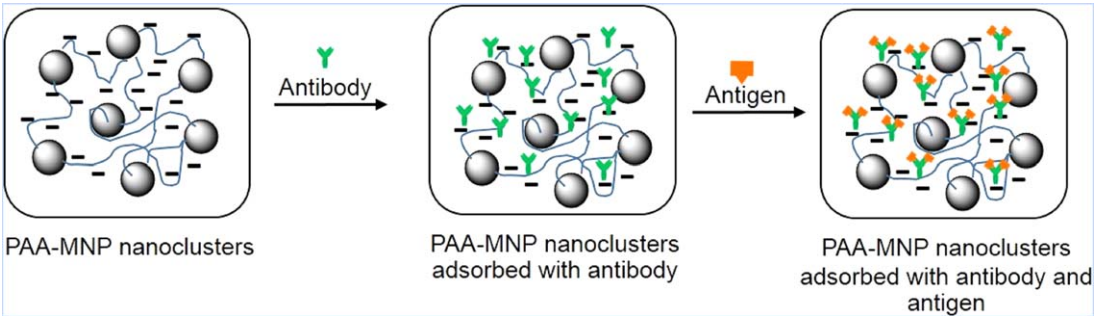

Figure 9. Schematic illustration of PAA–MNP nanoclusters adsorbed with an antibody and an antigen. [Color figure can be viewed at wileyonlinelibrary.com]

percentage of magnetite in the nanoclusters. The PAA300–MNP nanoclusters showed a lower saturation magnetization value than the others because of the higher PAA content in the structure. This result was in good agreement with that observed from the TGA experiment; this indicated a higher PAA content in the PAA300–MNP nanoclusters than in the other samples. Even though there was some drop in the saturation magnetization value because of the presence of PAA in the structure, it was still very responsive to an applied magnetic field, as shown in the inset in Figure 8. This figure shows that the PAA100–MNP nanoclusters dispersed in deionized water and showed magnetically assisted separation. Without an external magnetic field, the colloidal dispersion was brown in color and homogeneous, without any sign of precipitation. When a magnetic field was applied, the nanoclusters were enriched; this led to transparent dispersion. The dispersing–magnetically separating process of the nanoclusters was reversible for a number of cycles, without any sign of precipitation when they were stored at room temperature. This dispersing–magnetically separating behavior was not observed in the very dispersible individual MNPs.[40] In addition, these nanoclusters still retained their superparamagnetic properties, as evidenced by the lack of coercivity and remanence after the removal of the magnetic field.

For adsorption with antibodies, it was desirable to have nanoclusters with carboxylated–enriched surfaces for ionic adsorption with positively charged anti-HRP (Figure 9). To determine the antibody adsorption ability of the nanoclusters, various concentrations of anti-HRP antibody were loaded into the nanoclusters (10 mg) in 1 mL of 10 m*M* MES solutions at pH 5. We found that the maximum concentration of antibodies that could bind on the nanocluster surface while retaining 100% adsorption efficiency was 400 ppm (Figure 10). An increase in the antibody concentration from 400 to 500–1000 ppm resulted in remaining unadsorbed antibodies in the dispersions. Hence, 400 ppm antibodies loaded in 10 mg of PAA–MNP nanocluster were used for the following experiments. However, the antibody adsorption efficiencies of both samples (PAA100–MNP nanoclusters and PAA300–MNP nanoclusters) were not significantly different. Therefore, in the next experiments, the PAA100–MNP nanoclusters were chosen as representative because they exhibited a higher magnetic responsiveness than the PAA300–MNP nanoclusters, as evidenced via the VSM technique. In addition, the PAA100–MNP nanoclusters also showed better stability as they were very dispersible in water, without any sign of precipitation, even after 24 h of preparation.

Figure 11 shows the reuse efficiency of the PAA100–MNP nanoclusters for the adsorption with anti-HRP antibodies after eight reuse processes. After each adsorption–separation process, the concentrations of the adsorbed and desorbed antibodies from each cycle were investigated with the Bradford assay. The results indicate that the nanoclusters preserved a greater than 97% adsorption ability for the antibodies for eight reuse cycles; this signified the capability of these novel nanoclusters to serve as reusable solid supports in magnetic separation applications of bioentities. After the nanoclusters were reused for more than

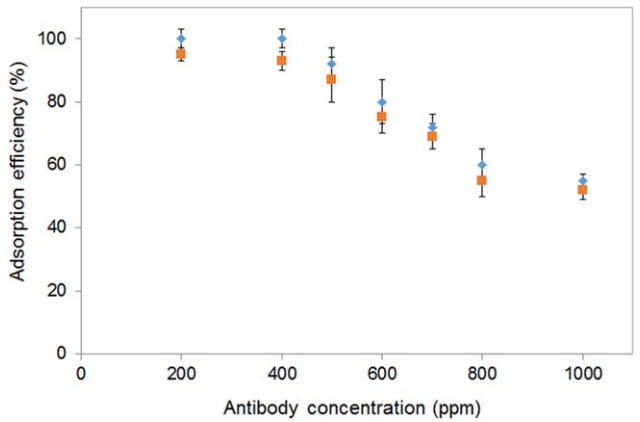

Figure 10. Adsorption efficiencies of (◆) PAA100–MNP nanoclusters and (■) PAA300–MNP nanoclusters with an anti-HRP antibody as a function of the antibody concentrations. [Color figure can be viewed at wileyonlinelibrary.com]

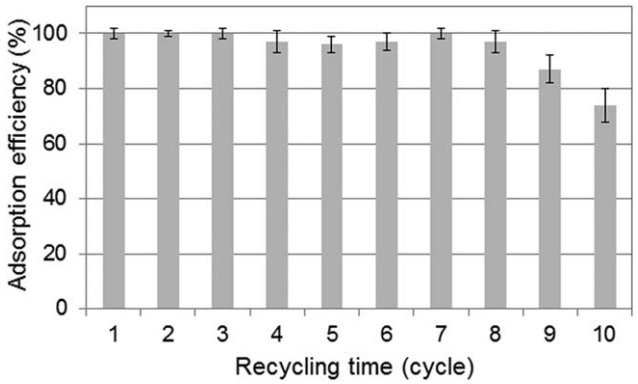

Figure 11. Adsorption efficiency of the PAA100–MNP nanoclusters with an anti-HRP antibody after 10 reuses.

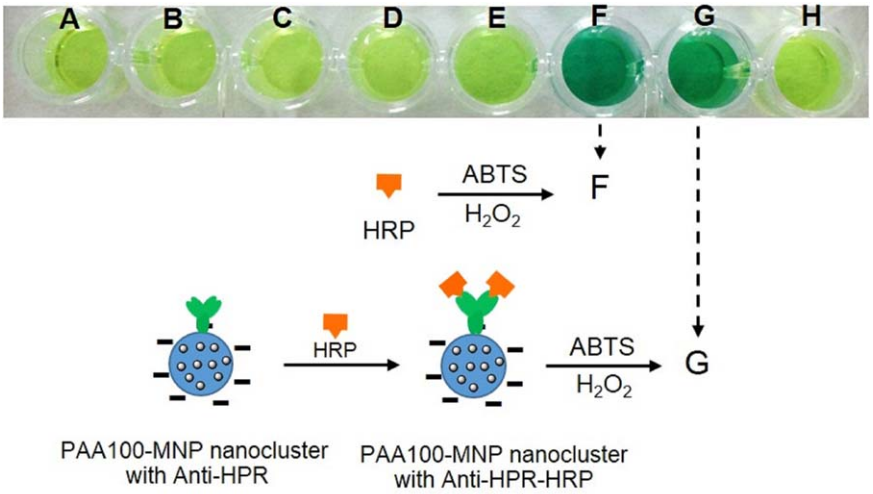

Figure 12. Visualization of the antigen-recognition capability with an indirect method. The appearance of the samples after the addition of an ABTS oxidizing agent is shown: (A) 10 m*M* MES buffer at pH 7, (B) 1% BSA in a 10 m*M* MES buffer at pH 7, (C) anti-HRP, (D) nanocluster without anti-HRP and HRP, (E) nanocluster adsorbed with anti-HRP, (F) HRP antigen (the positive control), (G) nanocluster adsorbed with anti-HRP and HRP (the sample), and (H) ABTS. [Color figure can be viewed at wileyonlinelibrary.com]

eight cycles, the adsorption efficiency tended to decrease, and this was attributed to the detachment of PAA from the particles because some macroscopic aggregation of the particles was observed after repeated washing with 2 *M* NaCl solutions in the antibody desorption step.

The capacity of the antigen recognition of the nanoclusters adsorbed with antibodies was observed from the change to a greenish product after oxidation with an ABTS oxidizing agent once it was reacted with HRP-labeled conjugates. Hence, the nanoclusters adsorbed with anti-HRP were conjugated with HRP for color development once they were reacted with ABTS. The PAA100–MNP nanoclusters adsorbed with anti-HRP and HRP exhibited a color change from light green to blue once they were oxidized with ABTS [Figure 12(G)]; this signified a positive result because of the conjugation of HRP with anti-HRP on the nanocluster surface. The nanoclusters without anti-HRP and HRP [Figure 12(D)] and those solely adsorbed with anti-HRP [without HRP; Figure 12(E)] were used as the controls. These dispersions showed no changes in the color development after they were oxidized with ABTS. Other control dispersions, including the pH 7 MES buffer solution [the dispersing media; Figure 12(A)] and those with 1% BSA [a blocking reagent; Figure 12(B)], anti-HRP [Figure 12(C)], and ABTS [Figure 12(H)], were also investigated to confirm their negative results. Moreover, the solution of HRP antigens (without MNP nanoclusters) was also tested to confirm the color change (positive testing) because of the reaction of HRP with ABTS [Figure 12(F)]. More importantly, after eight reuse processes, the nanoclusters adsorbed with anti-HRP and HRP showed the color change (the positive result) after the addition of ABTS; this indicated that the antigen recognition of the MNP nanoclusters adsorbed with antibodies was still preserved, even after repeated use. These results signify that the nanoclusters with good adsorption efficiency could be used as reusable magnetic supports for immobilization with other conjugates, such as aptamers and their target molecules. Also, a comparison of these nanoclusters with other related works focusing on the adsorption with antibodies and their critical properties is provided in the Supporting Information.

CONCLUSIONS

Magnetic nanoclusters grafted with PAA were synthesized via a free-radical polymerization in the presence of MNPs to obtain particles with a highly negative charge for use as supports for adsorption with anti-HRP. The degree of nanoclustering was optimized such that a good dispersibility and stability in neutral water were obtained with maintenance of a good magnetic sensitivity. The nanoclusters showed pH-responsive behavior because of their coating with anionic PAA. They were effectively used as reusable supports for adsorption with anti-HRP for eight cycles without a significant drop in their adsorbing efficiency; this indicated their potential for use as nanosupports for efficient and facile separation of other positively charged bioentities.

ACKNOWLEDGMENTS

Metha Rutnakornpituk acknowledges the Thailand Research Fund (contract grant number RSA5980002) for financial funding. All of the authors thank the National Research Council of Thailand (contract grant number R2560B091) for their support. They also thank Jutatip Namahoot (Department of Chemistry, Naresuan University) for their valuable discussion about the EDX results.

REFERENCES

1. Tartaj, P.; Morales, M. D.; Veintemillas-Verdaguer, S.; González-Carreño, T.; Serna, C. J. *J. Phys. D* **2002**, *36*, 182.
2. Dong, H.; Huang, J.; Koepsel, R. R.; Ye, P.; Russell, A. J.; Matyjaszewski, K. *Biomacromolecules* **2011**, *12*, 1305.

3. Ramesan, M. T. *J. Appl. Polym. Sci.* **2014**, *131*, DOI: 10.1002/app.40116.
4. Khadsai, S.; Rutnakornpituk, B.; Vilaivan, T.; Nakkuntod, M.; Rutnakornpituk, M. *J. Nanopart. Res.* **2016**, *18*, 263.
5. Rutnakornpituk, M.; Puangsin, N.; Theamdee, P.; Rutnakornpituk, B.; Wichai, U. *Polymer* **2011**, *52*, 987.
6. Ramesan, M. T.; Surya, K. *J. Appl. Polym. Sci.* **2016**, *133*, DOI: 10.1002/app.43496.
7. Uygun, D. A.; Ozturk, N.; Akgol, S.; Denizli, A. *J. Appl. Polym. Sci.* **2012**, *123*, 2574.
8. Theppaleak, T.; Rutnakornpituk, B.; Wichai, U.; Vilaivan, T.; Rutnakornpituk, M. *J. Biomed. Nanotechnol.* **2013**, *9*, 1509.
9. Theamdee, P.; Rutnakornpituk, B.; Wichai, U.; Rutnakornpituk, M. *J. Nanopart. Res.* **2014**, *16*, 2494.
10. Sarkar, T. R.; Irudayaraj, J. *Anal. Biochem.* **2008**, *379*, 130.
11. Xiong, L.; Bi, J.; Tang, Y.; Qiao, S. Z. *Small* **2016**, *12*, 4735.
12. Honarmand, D.; Ghoreishi, S. M.; Habibi, N.; Nicknejad, E. T. *J. Appl. Polym. Sci.* **2016**, *133*, DOI: 10.1002/app.43335.
13. Kalkan, N. A.; Aksoy, S.; Aksoy, E. A.; Hasirci, N. *J. Appl. Polym. Sci.* **2012**, *123*, 707.
14. Xu, H.; Aguilar, Z. P.; Yang, L.; Kuang, M.; Duan, H.; Xiong, Y.; Wei, H.; Wang, A. *Biomaterials* **2011**, *32*, 9758.
15. Ito, A.; Kuga, Y.; Honda, H.; Kikkawa, H.; Horiuchi, A.; Watanabe, Y.; Kobayashi, T. *Cancer Lett.* **2004**, *212*, 167.
16. Puertas, S.; Batalla, P.; Moros, M.; Polo, E.; del Pino, P.; Guisan, J. M.; Grazú, V.; de la Fuente, J. M. *ACS Nano* **2011**, *5*, 4521.
17. Ortega, G. A.; Zuaznabar-Gardona, J. C.; Morales-Tarre, O.; Reguera, E. *RSC Adv.* **2016**, *6*, 98457.
18. Gonzalez, C. C.; Perez, C. A. M.; Martinez, A. M.; Armendáriz, I. O.; Tapia, O. Z.; Martel-Estrada, A.; García-Casillas, P. E. *J. Nanomater.* **2014**, *21*, 978284.
19. Trung, T. B.; Hung, V. P.; Hoang, H. T.; Tung, L. M.; Lee, J. *Geosyst. Eng.* **2015**, *18*, 219.
20. Prai-In, Y.; Boonthip, C.; Rutnakornpituk, B.; Wichai, U.; Montembault, V.; Pascual, S.; Fontaine, L.; Rutnakornpituk, M. *Mater. Sci. Eng. C* **2016**, *67*, 285.
21. Luo, B.; Xu, S.; Luo, A.; Wang, W. R.; Wang, S. L.; Guo, J.; Lin, Y.; Zhao, D. Y.; Wang, C. C. *ACS Nano* **2011**, *5*, 1428.
22. Sun, Q.; Kandalam, A. K.; Wang, Q.; Jena, P.; Kawazoe, Y.; Marquez, M. *Phys. Rev. B* **2006**, *73*, 134409.
23. Amiri, H.; Mahmoudi, M.; Lascialfari, A. *Nanoscale* **2011**, *3*, 1022.
24. Mahmoudi, M.; Simchi, A.; Imani, M.; Stroeve, P.; Sohrabi, A. *Thin Solid Films* **2010**, *518*, 4281.
25. Sun, S.; Zeng, H.; Robinson, D. B.; Raoux, S.; Rice, P. M.; Wang, S. X.; Li, G. *J. Am. Chem. Soc.* **2004**, *126*, 273.
26. Ge, J.; Hu, Y.; Biasini, M.; Beyermann, W. P.; Yin, Y. *Angew. Chem. Int. Ed.* **2007**, *46*, 4342.
27. Gao, J.; Ran, X.; Shi, C.; Cheng, H.; Cheng, T.; Su, Y. *Nanoscale* **2013**, *5*, 7026.
28. Berret, J. F.; Schonbeck, N.; Gazeau, F.; Kharrat, D. E.; Sandre, O.; Vacher, A.; Airiau, M. *J. Am. Chem. Soc.* **2006**, *128*, 1755.
29. Dou, J.; Zhang, Q.; Jian, L.; Gu, J. *Colloid Polym. Sci.* **2010**, *288*, 1751.
30. Fan, T.; Li, M.; Wu, X.; Li, M.; Wu, Y. *Colloids Surf. B* **2011**, *88*, 593.
31. Khan, A.; El-Toni, A. M.; Alhoshan, M. *Mater. Lett.* **2012**, *89*, 12.
32. Meerod, S.; Rutnakornpituk, B.; Wichai, U.; Rutnakornpituk, M. *J. Magn. Magn. Mater.* **2015**, *392*, 83.
33. Yoon, K. Y.; Kotsmar, C.; Ingram, D. H.; Huh, C.; Bryant, S. L.; Milner, T. E.; Johnston, K. P. *Langmuir* **2011**, *27*, 10962.
34. Chaleawlert-Umpon, S.; Pimpha, N. *Mater. Chem. Phys.* **2012**, *135*, 1.
35. Thong-On, B.; Rutnakornpituk, B.; Wichai, U.; Rutnakornpituk, M. *J. Nanopart. Res.* **2015**, *17*, 261.
36. Thong-On, B.; Rutnakornpituk, M. *Eur. Polym. J.* **2016**, *85*, 519.
37. Silverstein, R. M.; Webster, F. X. Spectrometric Identification of Organic Compounds, 6th ed.; Wiley: New York, **1998**; Chapter 3, p 81.
38. Khan, I. U.; Stolch, L.; Serra, C. A.; Anton, N.; Akasov, R.; Vandamme, T. F. *Int. J. Pharm.* **2015**, *478*, 78.
39. Tjipangandjara, K. F.; Somasundaran, P. *Adv. Powder Technol.* **1992**, *3*, 119.
40. Chen, K.; Zhu, Y.; Li, L.; Lu, Y.; Guo, X. *Macromol. Rapid Commun.* **2010**, *31*, 1440.